

**Synthesis, Coordination Chemistry and Reactivity
of 1H-pyridin-(2*E*)-ylidenes and Application of
Their Transition Metal Complexes**

by

Qi Shi

A thesis submitted for the degree of
Doctor of Philosophy

University of York
Department of Chemistry

April 2010

Abstract

This thesis describes the synthesis of 1*H*-pyridin-(2*E*)-ylidenes (PYE) ligands, their coordination chemistry with late transition metals and the application of their metal complexes in selected catalytic reactions and anticancer activity.

The preparation of mono- and bidentate PYE ligands was achieved from reactions between pyridinium salts and primary amines in the presence of a base. A variety of PYE ligands including chiral and bulky examples were fully characterised by a number of techniques, including single crystal X-ray diffraction.

A range of transition metal precursors were tested with PYE ligands and the resulting metal complexes including Rh(I), Pd(II), Ni(II) and Ru(II) were characterised by methods including single-crystal X-ray diffraction and NMR spectroscopy to examine metal-ligand bonding and ligand dynamics. Data comparison of the solid-state structures, NMR spectroscopy and DFT calculations with respect to neutral ligands, protonated salts and metal complexes indicates that charge redistribution occurs within the PYE heterocyclic ring to give a contribution from a pyridinium-amido-type resonance structure. Strong donor character of PYE ligands was supported by IR spectroscopy and supplemented by DFT calculations.

Selective cyclopalladation, directed by various ligand structural motifs was studied and steric effects were found to be dominant. A series of cationic derivatives were prepared from coordination of small molecules, e.g. CO, NH₃ and pyridine and it was found that steric hindrance from the PYE *N*-methyl group prevents side-on coordination of ligands such as alkenes and alkynes.

Application of PYE ligands in the Suzuki-Miyaura cross-coupling and enantioselective addition of diethylzinc to aldehydes was carried out. A reasonable yield (88%) was obtained for the coupling of 4-bromotoluene with phenylboronic acid using one chelating PYE derivative. Enantioselectivities of up to 21% *ee* for the ethyl addition of benzaldehyde were also obtained.

The biological activity of two types of Ru(II) complexes derived from alkyl and aryl linked di-PYE ligands and a cationic palladacycle **31** were tested against three cancer cell lines. Complexes **31** and **40** showed promising cytotoxicity results compared with *cis*-platin.

Overall it has been found that PYE ligands are amongst the strongest donors and that the lack of rotation about the formally exocyclic imine bond locates the *N*-methyl group in the vicinity of the metal. Whilst this allows the steric environment to be controlled, there are other consequences such as cyclometallation and a weakening of the M-PYE bond due to steric pressure.

Contents

1.0 Introduction	1
1.1 'Neutral amido' ligands	1
1.2 α -Diimine ligands	3
1.2.1 Synthesis of 1,4-Diaza-1,3-butadiene (DAB-R) ligands	3
1.2.2 Electronic properties and bonding of DAB-R metal complexes	4
1.2.3 Coordination of DAB-R ligands	5
1.2.4 Application of DAB-R ligands	6
1.3 Amidine and guanidine ligands	8
1.3.1 Amidines	9
1.3.2 Guanidines	12
1.3.2.1 Electron delocalisation property through guanidine framework	13
1.3.2.2 Coordination of guanidines and their application	15
1.3.2.2.1 Monodentate guanidines	16
1.3.2.2.2 Polydentate guanidines with organic bridges	18
1.3.2.2.3 Bicyclic guanidines	21
1.4 Imidazolin-2-imine ligands	23
1.4.1 Imidazolin-2-imine ligands – carbene analogues	23
1.4.2 Synthesis and theoretical investigation of imidazolin-2-imines	25
1.4.3 Transition metal complexes incorporating imidazolin-2-imines	27
1.4.3.1 Copper complexes	28
1.4.3.2 Molybdenum and ruthenium half-sandwich complexes	29
1.4.3.3 Other metal complexes and their application	30
1.5 Isopropyl(1-methyl-1H-pyridin-4-ylidene)amine	31
1.6 Aims of the project	32
1.7 References	33
2.0 Synthesis of 1H-pyridin-(2E)-ylidenes (PYE) ligands	40
2.1 Introduction	40
2.2 Synthesis and characterisation of mono- and bidentate 1H-pyridin-(2E)-ylidenes (PYE) ligands	43
2.2.1 Monodentate PYE ligands	43

2.2.2 Bidentate PYE ligands	45
2.3 UV-vis and IR spectroscopic studies of bidentate PYE ligands	52
2.3.1 UV-vis absorption studies	52
2.3.2 Infra-red studies	54
2.4 Reactivity tests of PYE ligands	56
2.5 NBO calculations for neutral and protonated PYE ligands	57
2.6 Conclusions and the future work	58
2.7 References	59
3.0 Transition metal complexes with PYE ligands and their catalytic applications	61
3.1 Introduction	61
3.2 Rhodium complexes with monodentate PYE ligands	61
3.3 Nickel complexes with PYE ligands	65
3.3.1 Introduction	65
3.3.2 Synthesis and properties of nickel(II) complexes with PYE ligands	66
3.4 Palladium (II) complexes of PYE ligands	70
3.4.1 Introduction	70
3.4.2 Attempts to prepare palladium complexes with mono-PYE ligands	71
3.4.3 Preparation of palladium(II) dihalide complexes using chelating PYE ligands	72
3.4.3.1 Synthesis of $[\text{PdCl}_2(\text{MeN}^{\text{C}_6\text{H}_4}\text{N}^{\text{Me}})]$ (22)	73
3.4.3.2 Synthesis and dynamic study of $[\text{PdCl}_2(\text{BnN}^{(\text{CH}_2)_2}\text{N}^{\text{Bn}})]$ (23)	76
3.4.3.3 $[\text{PdCl}(\text{NCCH}_3)(\text{MeN}^{\text{Quino}})]^+\text{Cl}^-$ (24)	79
3.4.3.3.1 Synthesis of $[\text{PdCl}(\text{NCCH}_3)(\text{MeN}^{\text{Quino}})]^+\text{Cl}^-$ (24)	79
3.4.3.3.2 Reactivity studies of $[\text{PdCl}(\text{NCCH}_3)(\text{MeN}^{\text{Quino}})]^+\text{Cl}^-$ (24)	81
3.4.3.4 Synthesis and reactivity of $[\text{Pd}(\text{CH}_3)_2(\text{MeN}^{\text{Quino}})]$ (25)	84
3.5 Attempts to synthesis of other transition metal complexes with PYE ligands	86
3.5.1 Gold	86
3.5.2 Platinum	87
3.6 Palladium-catalysed Suzuki-Miyaura cross-coupling reactions	89
3.6.1 Introduction	89
3.6.1.1 Advanced development of Pd- and Ni-catalysed SMC reaction	90

3.6.1.2 Nitrogen donor ligands in SMC reaction	92
3.6.2 Application of PYE ligands in the SMC reaction	93
3.7 Enantioselective addition of diethylzinc to aldehydes	97
3.7.1 Introduction	97
3.7.2 Enantioselective addition of diethylzinc to aldehydes with PYE ligands	98
3.8 Theoretical comparison of donor properties between PYE and NHC	100
3.9 Conclusions and future work	102
3.10 References	104
4.0 Palladacycles and their derivatives	109
4.1 Introduction	109
4.2 Synthesis of palladacycles with PYE ligands	110
4.2.1 Monocyclopalladated complexes (26)-(29)	111
4.2.2 Dicyclopalladated complex (30)	118
4.2.3 Comparison and discussion of noncyclo- and cyclopalladated behaviour	119
4.3 Synthesis and reactivity of cationic derivatives	122
4.3.1 $[\text{Pd}(\text{MeCN})(\eta^3\text{-CH}_2\text{N}^{\text{C}_6\text{H}_{10}}\text{N}^{\text{Me}})] [\text{BAR}_4^{\text{F}}]$ (31)	123
4.3.2 Reactivity of cationic derivatives	124
4.3.3 $\{[\text{Pd}(\eta^3\text{-CH}_2\text{N}^{\text{C}_6\text{H}_{10}}\text{N}^{\text{Me}})]_2\text{Cl}\}(\text{BF}_4)$ (35)	129
4.3.4 $[\text{Pd}(\text{C}_6\text{H}_5)(\eta^3\text{-CH}_2\text{N}^{\text{C}_6\text{H}_{10}}\text{N}^{\text{Me}})]$ (36)	131
4.4 Reactivity of palladacycles with H^+ , H^- , and H_2	134
4.5 Conclusions	138
4.6 References	139
5.0 Anticancer activity of metal complexes with PYE ligands	142
5.1 Introduction	142
5.1.1 Development of ruthenium complexes as anticancer agents	144
5.1.2 Development of palladacycles as anticancer agents	146
5.2 Synthesis and characterisation of Ru(II)-DMSO complexes with PYE ligands	147
5.2.1 $[\text{RuCl}_2(\text{DMSO})_3(\text{MeN}^{\text{tBu}})]$ (38) and $[\text{RuCl}_2(\text{DMSO})_2(\text{MeN}^{\text{C}_6\text{H}_4}\text{N}^{\text{Me}})]$ (39)	150
5.2.2 $[\text{RuCl}(\text{DMSO})_3(\text{L}_2)](\text{Cl})$ (40-42)	151
5.2.3 Electrical conductivity measurement of 39 and 40	154

5.2.4 Stability of ruthenium complexes in neutral and low pH water	155
5.2.5 Attempts to synthesis of Ru(II)-arene complexes with PYE ligands	155
5.3 Investigation of anticancer activity	156
5.3.1 Introduction of MTT assay	156
5.3.2 <i>In vitro</i> cytotoxicity tests	157
5.4 Conclusions and future work	159
5.5 References	161
6.0 Experimental	165
6.1 General Procedures	165
6.2 Compounds and complexes preparation and characterisation data	166
6.3 Suzuki-Miyaura cross-coupling catalysed by a Pd/PYE-ligand system	209
6.4 Enantioselective addition of diethylzinc to aldehyde	210
6.5 Cell culture and MTT assay	211
6.6 References	212
Appendix 1	213
Single crystal X-ray structure data for [^{Me} N ^{C6H10} N ^{Me}] (7)	213
Single crystal X-ray structure data for [^{Me} N ^(C6H4) N ^{Me}] (12)	217
Single crystal X-ray structure data for [^{Me} N ^{(CH2)2} N ^{Me}][H ⁺] ₂ (16)	223
Single crystal X-ray structure data for [NiCl ₂ (^{Me} N ^{C6H10} N ^{Me})] (18)	228
Single crystal X-ray structure data for [NiCl ₂ (^{Me} N ^{C6H4} N ^{Me})] (21)	236
Single crystal X-ray structure data for [PdCl ₂ (^{Me} N ^{C6H4} N ^{Me})] (22)	244
Single crystal X-ray structure data for [PdCl ₂ (^{Bn} N ^{(CH2)2} N ^{Bn})] (23)	254
Single crystal X-ray structure data for [PdCl(η ³ -CH ₂ N ^{C6H10} N ^{Me})] (26)	269
Single crystal X-ray structure data for [PdCl(η ³ -CH ₂ N ^{(C(Me)2)2} N ^{Me})] (28)	276
Single crystal X-ray structure data for {[Pd(η ³ -CH ₂ N ^{C6H10} N ^{Me})] ₂ Cl}(BF ₄) (35)	285
Single crystal X-ray structure data for [Pd(C ₆ H ₅)(η ³ -CH ₂ N ^{C6H10} N ^{Me})] (36)	302
Appendix 2	319
Compounds	319

List of figures

Figure 1-1. Generic structures of metal complexes with amido, neutral amido, amine and imine ligands.	2
Figure 1-2. Possible resonance structures of ‘neutral amido’ ligands on coordination to a metal fragment.	2
Figure 1-3. Generic structures of α -diimine examples.	3
Figure 1-4. Examples of metal complexes with DAB-R ligands, illustrating the various coordination possibilities.	6
Figure 1-5. First example of a stable boryl anion with α -diimines ligand.	8
Figure 1-6. Generic structures of neutral amidines and guanidines.	9
Figure 1-7. Examples of various amidines.	10
Figure 1-8. Isomeric and tautomeric forms for tri-substituted amidines.	10
Figure 1-9. Examples of metal complexes with amidine ligands.	11
Figure 1-10. Molecular structure of $\text{Mo}(\text{CO})_5(\text{MeC}\{\text{DipN}\}\{\text{NHDip}\})$.	12
Figure 1-11. Generic representations for guanidines, guanidates and guanidinium salts.	13
Figure 1-12. Delocalization of the positive charge over all N-atoms in the guanidine unit upon protonation.	13
Figure 1-13. Possible resonance structures of the guanidine motif on coordination to a metal fragment.	14
Figure 1-14. 1,3-bis(<i>N,N,N',N'</i> -tetramethylguanidino)propane (btmgp), its protonated salt and metal complexes.	14
Figure 1-15. Molecular structure of $[(\text{H-hpp})_2\text{CuCl}]$.	15
Figure 1-16. Examples of metal complexes incorporating monodentate guanidine ligands.	16
Figure 1-17. Alkoxide-bridged zinc aryloxide dimer stabilised by 1,1,3,3-tetramethylguanidine.	17
Figure 1-18. Examples of metal complexes with high oxidation states incorporating biguandines.	18
Figure 1-19. Generic structure of two different classes of linked bis- and tris-guanidines.	19

Figure 1-20. Examples of high-valent oxoferryl complexes.	20
Figure 1-21. Generic structure of bicyclic guanidines.	22
Figure 1-22. Examples of metal complexes incorporating mono- and bis- (bicyclic guanidine), and tris-(bicyclic guanidine) compounds.	23
Figure 1-23. Relative contributions from the ylidic mesomeric structures B and NBO charges of the exocyclic nitrogen atom for 2- iminoimidazoline, 2-iminoimidazolidine and guanidine model systems.	27
Figure 1-24. Examples of metal complexes of 2-iminoimidazolines.	27
Figure 1-25. Examples of 16-electron half-sandwich complexes incorporating imidazolin-2-imines.	30
Figure 1-26. Examples of half-sandwich complexes of cyclopentadienyl-amido (left) and cyclopentadienyl-imidazolin-2-imino (right) ligands.	31
Figure 1-27. Zinc complexes of bis(guanidine) and bis(imidazolin-2-imine) ligands.	31
Figure 1-28. Generic structure of PYE ligands studied in this thesis.	32
Figure 2-1. ¹ H NMR spectrum of 2 in CDCl ₃ and the numbering scheme of 2 .	44
Figure 2-2. ¹ H NMR spectrum of compound 8 in CDCl ₃ and numbering scheme for compound 8 .	47
Figure 2-3. Molecular structure of compound 7 .	48
Figure 2-4. Bond lengths (Å) in 2-aminopyridine.	48
Figure 2-5. Molecular structure of compound 12 .	49
Figure 2-6. Molecular structure of compound 16 .	51
Figure 2-7. The molecular structures of 1-MIP and 2-MIP.	52
Figure 2-8. UV-vis spectrum of 7 in acetonitrile.	53
Figure 2-9. Beer's law plots for 7 in acetonitrile at 240 nm (left) and 314 nm (right).	53
Figure 2-10. UV-vis spectrum of 16 in acetonitrile.	54
Figure 2-11. Beer's law plots for 16 in acetonitrile at 240 nm (left) and 310 nm (right).	54

Figure 2-12. IR spectra of compound 7 (above) and protonated ligand 16 (below).	55
Figure 2-13. PYE compound 1 and its protonated form.	57
Figure 3-1. A plot of $\nu(\text{CO})$ (cm^{-1}) vs. $d(\text{CO})$ (\AA) for the $\text{IrCp}(\text{CO})\text{L}$ complexes studied.	64
Figure 3-2. Examples of nitrogen donor ligands utilized in polymerisation and cross-coupling.	66
Figure 3-3. Molecular structure of complex 18 .	67
Figure 3-4. Molecular structure of complex 21 .	68
Figure 3-5. Palladacycle with N,N-dimethyl-1-naphthylamine ligand.	72
Figure 3-6. Molecular structure of complex 22 (<i>cis</i> -isomer left and <i>trans</i> -isomer right).	73
Figure 3-7. Comparison of ^1H NMR spectra of 12 (top) and 22 (bottom) in CDCl_3 .	75
Figure 3-8. Molecular structure of complex 23 .	77
Figure 3-9. Proposed isomer exchanging of 23 through a C_{2v} intermediate.	78
Figure 3-10. Variable temperature ^1H NMR spectra of palladium complex 23 in CD_2Cl_2 .	79
Figure 3-11. Examples of palladium complexes structurally analogous to 24 .	81
Figure 3-12. Examples of gold(I) and gold(III) complexes with N-donor or N,O-donor ligands.	86
Figure 3-13. Examples of platinum complexes incorporating nitrogen ligands.	88
Figure 3-14. General catalytic cycle for Suzuki-Miyaura cross-coupling reaction.	91
Figure 3-15. Examples of N-donor ligands utilised in SMC reaction.	93
Figure 3-16. Concept of asymmetric activation.	97
Figure 3-17. Molecular models of $(\text{BINOLate})\text{Zn}(\text{PYE-7})$.	100
Figure 3-18. Model complexes of chelating di-NHC and di-PYE ligands.	101
Figure 4-1. Two primary types of palladacycles.	110
Figure 4-2. ^1H NMR spectrum of complex 26 in CD_2Cl_2 .	113
Figure 4-3. Molecular structure of complex 26 .	116

Figure 4-4. Molecular structure of complex 28 .	117
Figure 4-5. Examples of five-membered palladacycles with C(sp ³)-Pd bond and their corresponding Pd-C bond lengths (Å).	118
Figure 4-6. Selective cyclopalladation directed by various backbones.	119
Figure 4-7. Plausible isomerisation of 22 .	120
Figure 4-8. Plausible explanation of cyclopalladation steric prevention for 22 .	120
Figure 4-9. ¹ H NMR spectrum of 31 in CDCl ₃ .	124
Figure 4-10. Infra-red spectrum of 32 .	126
Figure 4-11. Comparison of infra-red spectra of 33 -NH ₃ (red colour) and 33 -ND ₃ (blue colour).	126
Figure 4-12. Spacefill structure of 26 . Chlorine atom has been omitted for clarity.	128
Figure 4-13. Examples of bimetallic complexes with an unsupported single halide bridge.	129
Figure 4-14. Molecular structure of complex 35 .	131
Figure 4-15. Molecular structure of complex 36 .	133
Figure 4-16. Product from degradation of grease by phenyl Grignard reagent.	134
Figure 4-17. Molecular structure of complex 37 .	135
Figure 4-18. Example of dechelated palladium complex via protonation.	137
Figure 5-1. Marketed platinum anticancer drugs.	142
Figure 5-2. Diverse metal compounds with anticancer activity.	144
Figure 5-3. Examples of palladacycles with differential response among various cell lines.	146
Figure 5-4. Examples of palladacycles with potential anticancer activity and their different targets from <i>cis</i> -platin.	147
Figure 5-5. Molecular structure of complex X .	148
Figure 5-6. Possible isomers for compound 39 .	151
Figure 5-7. ¹ H NMR spectrum of 40 in CD ₃ OD.	153
Figure 5-8. Pictures of conducting MTT assay.	157
Figure 5-9. Cytotoxic activity of 31 on DLD-1 and 40 on various cell lines with a 4 days exposure.	158

List of schemes

Scheme 1-1. Synthetic route for DAB-R ligands.	4
Scheme 1-2. Synthetic route to Ar-BIAN, a rigid DAB-R derivative.	4
Scheme 1-3. Example of $[\text{Ni}\{\text{Ph-DAB}(\text{Me})\}_2]$ and DAB-R ligands in different oxidation states.	5
Scheme 1-4. Stoichiometric arene C-H activation at cationic platinum complexes with DAB-R ligands.	6
Scheme 1-5. Proposed catalytic cycle for hydrogenation of alkynes.	8
Scheme 1-6. Suzuki-Miyaura cross-coupling reaction catalysed by $\text{Pd}(\text{OAc})_2/\text{guanidine}$ system.	17
Scheme 1-7. Asymmetric nitroaldol reaction mediated by chiral guanidine complexes.	18
Scheme 1-8. C-H activation mediated by a copper superoxo complex.	19
Scheme 1-9. Reactivity comparison between bis-guanidine, guanidine-amine hybrid and bis-amine ligands on phenolate hydroxylation reaction.	21
Scheme 1-10. Generation of stable N-heterocyclic carbenes and their aromatic resonance structures.	23
Scheme 1-11. Formation of imidazole-based ligands and their mesomeric structures.	24
Scheme 1-12. Synthesis of titanium complexes incorporating imidazolin-2-iminato ligands.	25
Scheme 1-13. Two limiting mesomeric structures of poly(imidazolin-2-imine) ligands.	25
Scheme 1-14. A novel synthetic route to multidentate imidazolin-2-imine ligands by Tamm and co-workers.	26
Scheme 1-15. Reactivity of copper complexes of 2,6-bis(imidazolin-2-imino)pyridine pincer ligand.	28
Scheme 1-16. Oxygen activation by copper(I) diimine complexes.	29
Scheme 1-17. Selective C-F activation mediated by Ni(0) with a nitrogen ligand isopropyl(1-methyl-1H-pyridin-4-ylidene)amine.	32

Scheme 2-1. Possible resonance structures of the 1H-pyridin-(2E)-ylidene motif on coordination to a metal fragment.	41
Scheme 2-2. Various routes to PYE motif.	42
Scheme 2-3. Imination of 2-chloro pyridinium salt.	42
Scheme 2-4. Synthetic route to monodentate PYE ligands.	43
Scheme 2-5. Synthetic route to bidentate PYE ligands.	45
Scheme 2-6. Products resulting from synthesis of ligand 9 using potassium carbonate as base determined by ¹ H NMR spectroscopy.	46
Scheme 2-7. Synthetic route to bulky isoquinolin analogue 15 .	50
Scheme 2-8. Synthesis of protonated ligand 16 and possible representations A and B .	50
Scheme 2-9. Stability test of compound 7 and 9 .	57
Scheme 3-1. Synthesis of rhodium complex 17 .	62
Scheme 3-2. Synthesis of nickel(II) complexes of PYE ligands.	67
Scheme 3-3. Attempt to synthesis of palladium complexes.	71
Scheme 3-4. Attempt to synthesis of palladium complex with compound 4 .	72
Scheme 3-5. Synthesis of palladium complex 22 .	73
Scheme 3-6. Preparation of palladium complex 23 .	76
Scheme 3-7. Synthesis of complex 24 .	80
Scheme 3-8. Proposed mechanism for reaction between 24 , NaBAr ^F ₄ and C ₆ D ₆ .	83
Scheme 3-9. Reactions involving with B-C bond cleavage of BAr ^F ₄ anion.	84
Scheme 3-10. Synthesis of dimethyl palladium complex 25 .	85
Scheme 3-11. Attempted C-H activation of benzene mediated by 25 .	85
Scheme 3-12. Attempts to synthesis of gold complexes with PYE ligands.	87
Scheme 3-13. Attempts to synthesis of platinum complexes with PYE ligands.	88
Scheme 3-14. First example of Suzuki-Miyaura cross-coupling.	89
Scheme 3-15. Examples of active ligand families in SMC reaction.	90
Scheme 3-16. First asymmetric SMC reaction of racemic non-activated secondary alkyl halides.	92
Scheme 4-1. Cyclopalladation of azobenzene.	109
Scheme 4-2. Proposed synthetic route of cyclometallated palladium complexes.	111

Scheme 4-3. Preparation of palladacycle via C-H activation method.	111
Scheme 4-4. Synthesis of monocyclopalladated complexes 26-29 .	112
Scheme 4-5. Synthesis of complex 30 .	118
Scheme 4-6. Oxidative addition and electrophilic substitution mechanism for C-H activation.	121
Scheme 4-7. Preparation of complex 31 .	123
Scheme 4-8. Synthesis of 32 , 33 and 34 .	125
Scheme 4-9. CO insertion in sulphur- and nitrogen-derived palladacycles.	127
Scheme 4-10. Attempted N-H activation reaction of 33 -ND ₃ .	128
Scheme 4-11. Synthesis of dimer complex 35 and the attempt to an agostic complex.	130
Scheme 4-12. Postulated C-H activation mediated by PYE phenyl Pd complex.	132
Scheme 4-13. Synthesis of complex 36 .	132
Scheme 4-14. Synthesis of 37 via protonation to imine nitrogens.	135
Scheme 4-15. Transcyclopalladation reaction between dialkylbenzylamine and phenylpyridine in acetic acid solvent.	136
Scheme 4-16. Reactivity of 26 and 32 with H ⁻ and H ₂ .	137
Scheme 5-1. Synthetic routes to new types of Ru(II)-DMSO complexes with PYE ligands.	149
Scheme 5-2. Reaction between <i>cis</i> -RuCl ₂ (DMSO) ₄ and nitrogen ligands.	150
Scheme 5-3. Synthetic route to <i>cis</i> (Cl,S), <i>trans</i> (O,S)-[RuCl(Hdpa)(DMSO-O)(DMSO-S) ₂](OTf).	152
Scheme 5-4. Conversion of MTT via mitochondrial reductase.	156
Scheme 5-5. Ring open of palladacycle 26 via protonation.	159
Scheme 5-6. Formation of a proposed more active species from 31 under acidic condition.	160

List of tables

Table 2-1 The ^1H and ^{13}C NMR chemical shifts (ppm) of PYE moiety of 1-5 .	44
Table 2-2. Selected bond lengths (\AA) and angles ($^\circ$) for compound 7 .	48
Table 2-3. Selected bond lengths (\AA) and angles ($^\circ$) for compound 12 .	49
Table 2-4. Selected bond lengths (\AA) and angles ($^\circ$) for compound 16 .	51
Table 3-1. IR carbonyl frequencies (cm^{-1}) of cis-[(L)Rh(CO) $_2$ Cl] complexes.	62
Table 3-2. ^1H and ^{13}C NMR chemical shifts (ppm) of 1 and 17 in $\text{CD}_3\text{C}_6\text{D}_5$.	63
Table 3-3. Selected bond lengths and angles for complex 18 .	67
Table 3-4. Selected bond lengths (\AA) and angles ($^\circ$) for complex 21 .	68
Table 3-5. Comparison of bond lengths (\AA) between 7 , 16 , 18 and 21 .	69
Table 3-6. Selected bond lengths and angles for complex 22 .	74
Table 3-7. Selected bond lengths and angles for complex 23 .	77
Table 3-8. Comparison of ^1H NMR chemical shifts (ppm) of 5 , the protonated form and 24 .	80
Table 3-9. Influence of PYE ligands and palladium precursors on the SMC reaction.	94
Table 3-10. Pd(OAc) $_2$ /PYE(12)-catalysed SMC reaction of aryl halides with phenylboronic acid.	95
Table 3-11. SMC reaction of aryl halides with phenylboronic acid using Fe, Mn and Ni systems.	96
Table 3-12. Results of screening chiral and achiral bidentate PYE ligands with BINOL.	99
Table 4-1. Selected ^1H and ^{13}C NMR chemical shifts (ppm) of 26-29 in CD_2Cl_2 and CDCl_3 .	114
Table 4-2. Selected bond lengths and angles for complex 26 .	116
Table 4-3. Selected bond lengths and angles for complex 28 .	117
Table 4-4. ^1H and ^{13}C NMR chemical shifts (ppm) comparison of PdCH $_2$ for 26 and 31-34 .	127
Table 4-5. Selected bond lengths and angles for complex 36 .	133
Table 4-6. Selected bond lengths and angles for complex 37 .	136

Table 5-1. A variety of metal complexes with anticancer activity and their relative biological targets.	143
Table 5-2. Selected ^1H NMR Chemical Shifts (ppm) of 40 , 7 , $7(\text{H}^+)$ and $7(\text{H}^+)_2$ in CD_3OD .	153
Table 5-3. Selected ^{13}C NMR Chemical Shifts (ppm) of 40 , 7 , $7(\text{H}^+)_2(\text{Cl}^-)_2$ in CD_3OD .	154
Table 5-4. Results of electrical conductivity measurement.	154
Table 5-5. IC_{50} values (μM) on the HT-29, MCF-7 and DLD-1 cell lines after 96 hr incubation.	158

Declaration

Except where specific reference has been made to other sources, the work in this thesis is the original work of the author. It has not been submitted for any other degree. A number of the results have subsequently been published.

Qi Shi

Acknowledgements

I would like to thank my supervisor Dr. Richard E. Douthwaite for constantly giving me kind support and encouragement over the past four years and for the opportunity of discovering and improving myself.

I would also like to thank Dr. Patrick McGowan at the University of Leeds for the guidance and discussion on this project, Dr. Roger Phillips and Hafiz Makeen at the University of Bradford for the generous support and training during the biological experiment, and Dr. John Slattery for the kind contribution to the theoretical calculations.

Thanks to all the past and present members of Team Douthwaite, who gave me a lot of help and an enjoyable time. Thanks to Steve, JC, Gav, Swamp and Deep for letting me blend in the group and realise my potential of playing football and talking cold jokes. Thanks also to Hasan, Cindy and Rob for every moment of working together and the really exciting time of playing laser quest. I will miss all of you!

Thanks to all the technical staff: Steve Hau, Mike Keogh and Val Patrick (Stores); Brian Smith (Glass Workshop); Terry Chamberlain, Chris Mortimer and Jonathan Hamstead (Mechanical Workshop); Roy Noakes (Electronics Workshop) and Trevor Dransfield and Ben Glennie (Mass Spectrometry). Special thanks to Heather Fish and Amanda Dixon for NMR training and help, to Adrian Whitwood and Robert Thatcher for X-ray structure determinations and to Iman Khazal for experimental support.

I wish to acknowledge the White Rose University Consortium (White Rose) and the Wild Fund for their financial support.

Finally, I would like to thank the closest people to me for their support and love. Thanks, Mum and Dad, for your raise, encouragement and understanding. Thanks to Fang for your support, belief and consolation. This thesis is dedicated to my Grandpa, who is bravely fighting against cancer. Last, but not least, I extend thanks and appreciation to everyone who helped directly or indirectly to get this work done.

1.0 Introduction

1.1 'Neutral amido' ligands

During the last fifty years the development of organometallic chemistry and homogeneous catalysis, particularly involving the transition metals, has been progressively established and attracted much attention. Consequently, the formation, stability and reactivity of transition metal complexes with a variety of different ligands have been extensively investigated. The discovery of efficient and selective catalytic systems is one of the most important applications in this area. Numerous ligands have been designed and widely investigated for their electronic properties, coordination chemistry and chemical applications. As one of the most ubiquitous classes of ligands, nitrogen donors have been of great interest as their transition metal complexes exhibit many of the most interesting stoichiometric and useful catalytic transformations across synthetic and biological chemistry.^{1,2}

Recently, much attention has been devoted to coordinatively and electronically unsaturated transition metal complexes due to the involvement of many of them in catalytic cycles. To stabilise these relatively reactive species, ligands with strong donating ability are useful, such as amido donors ($\text{RR}'\text{N}$) (Figure 1-1). As both σ -donor and π -donor ligands,³ the hard donor features of amido donors adequately match the electronic demands of high-oxidation-state early-transition-metal complexes and interesting reactivity of the resulting complexes has been observed. Similarly, amido donors should be potentially capable of promoting oxidative addition reactions with the late transition metals by favourably boosting electron density of the metal centre. However, for low-valent soft metals, amido complexes are generally too reactive due to the excessively hard donor features of amido ligands and the strongly π -antibonding interactions between the occupied metal d orbitals and the nitrogen-based lone pair.^{4,5} Also, neutral ligands are preferentially utilised over anionic ones to support active species in catalysis mediated by late transition metals. In comparison with amido donor, common neutral nitrogen ligands like amine ($\text{NRR}'\text{R}''$) or imine ($\text{RNCR}'\text{R}''$) (Figure 1-1) are pure σ -donor ligands which are unable to promote oxidative addition reactions.

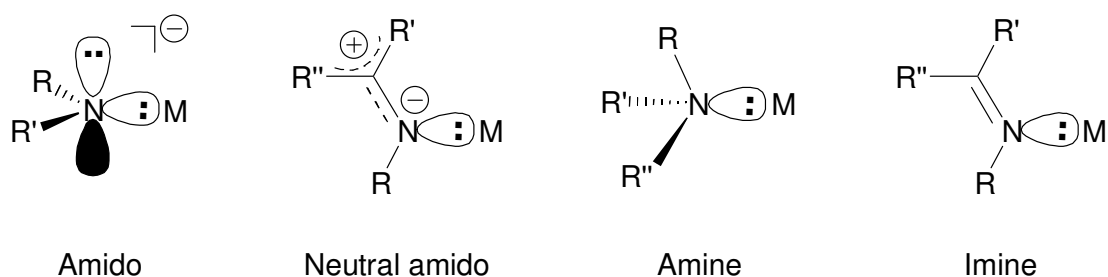


Figure 1-1. Generic structures of metal complexes with amido, neutral amido, amine and imine ligands.

Notably, a compromise nitrogen-donor ligand with amido-donor-like properties but a net neutral charge could potentially address the challenges stated above. Toward this end, the ligand needs to be capable of redistributing electronic charge through π bonding to enhance the electronic density of the coordinated nitrogen atom within the ligand framework (Figure 1-1) and a π interaction between the nitrogen atom and a moiety which can stabilise a positive charge is required. Based on these requirements, a series of compounds containing a conjugated imine moiety meet the required criteria including amidines and guanidines, imidazolin-2-imines and isopropyl(1-methyl-1H-pyridin-4-ylidene)amine. Their possible charge redistribution resonance structures (**B**) resembling a conjugated zwitterionic form (Figure 1-2) could increase π -donation of the ligand to the metal centre.

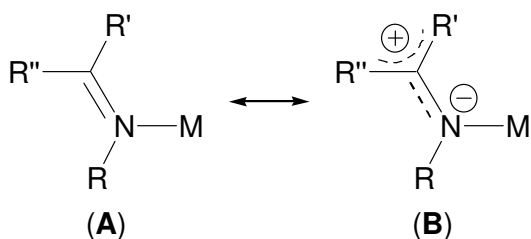


Figure 1-2. Possible resonance structures of 'neutral amido' ligands on coordination to a metal fragment.

A different but related type of nitrogen ligand called α -diimines will also be discussed in this chapter. Unlike those 'neutral amido' ligands above, α -diimines act as amido-like ligands via oxidation of metal centres. The strong π -acidic property is fundamentally different from the electronic properties of the other ligands here. However, in order to give a fuller context to 'neutral amido' type ligands and their applications, α -diimines are included in this Chapter. In the following sections, we will introduce their coordination chemistry, electronic properties and catalytic applications.

1.2 α -Diimine ligands

Molecules containing the 1,4-diaza-1,3-butadiene skeleton fall into the α -diimine category, including polypyridyl (bpy, phen, etc), pyridine-2-carbaldehyde (R-PyCa) and 1,4-diaza-butadiene (DAB-R) (Figure 1-3). In the past decades, α -diimines have been widely investigated in organometallic chemistry due to their interesting structural and electronic properties and well-known ability to stabilise organometallic complexes. Furthermore, as non-innocent ligands,^{6, 7} their metal complexes can have an ambiguous oxidation state and be redox active (*vide infra*), which is favourably applied in catalytic transformations associated with redox process.

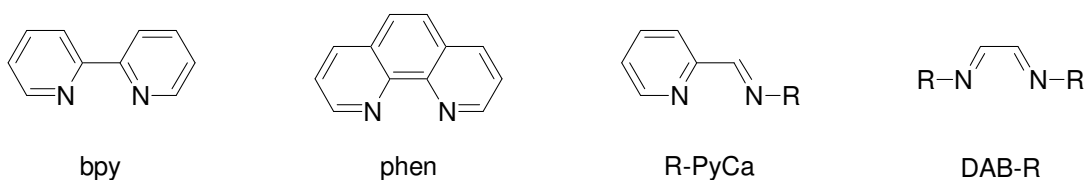
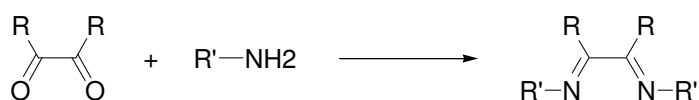


Figure 1-3. Generic structures of α -diimine examples.

Although α -diimines cover a variety of compounds, DAB-R with a flexible framework is the most popular. Commonly in the literature, DAB-R ligands are referred to as α -diimines.⁸ Herein, the focus will be on the coordination chemistry and catalytic application of DAB-R ligands as a representative of α -diimines. The bonding of their metal complexes also will be discussed.

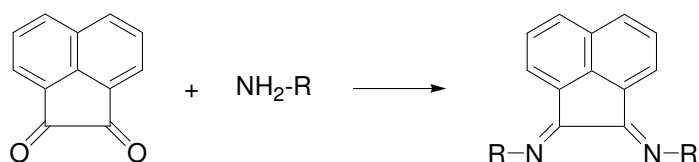
1.2.1 Synthesis of 1,4-Diaza-1,3-butadiene (DAB-R) ligands

DAB-R ligands have been known for a long time.^{9, 10} The synthesis of DAB-R ligands is derived from a condensation reaction between one equivalent of a diketone with two equivalents of alkyl or aryl amine in the presence of a Lewis or Brønsted acid as a catalyst (Scheme 1-1). The backbone and the aryl substituent can be modified to give different steric and electronic effects at the metal center. The reports of metal complexes with DAB-R ligands date back to 1953 when Krumholz¹¹ described the synthesis of some ferrous complexes. Since then numerous examples of metal complexes incorporating DAB-R ligands have been synthesised and the bonding studied by spectroscopic and theoretical methods.¹²



Scheme 1-1. Synthetic route for DAB-R ligands.

Compared with the flexible skeleton of the common DAB-R ligands, relatively rigid derivatives are expected to give some different chemical behaviour. Elsevier *et al.*¹³ reported the synthesis and full characterization of the rigid nitrogen ligands bis(aryl)acenaphthenequinonediimine (Ar-BIAN) by condensation of the rigid acenaphthenquinone with a primary amine (Scheme 1-2).



Scheme 1-2. Synthetic route to Ar-BIAN, a rigid DAB-R derivative.

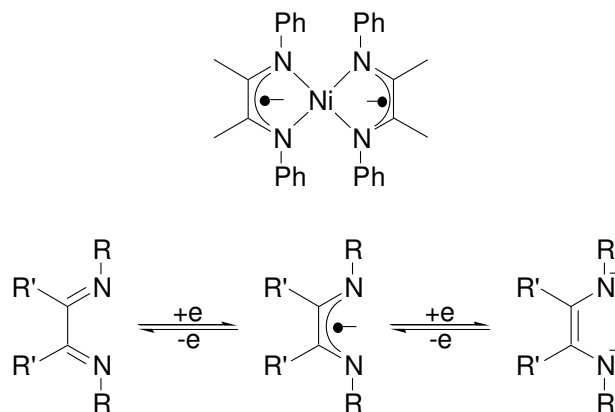
1.2.2 Electronic properties and bonding of DAB-R metal complexes

Along with spectroscopic techniques and improving theoretical calculations, the electronic properties of DAB-R ligands have been widely and intensively studied in detail. Several model systems of metal complexes containing α -diimines have been established to understand the electronic structure and relevant reactivity of organometallic compounds.¹⁴⁻

16

For example, homoleptic complexes of substituted DAB-R ligands with late transition metals $[M(\text{DAB-R})_2]$ are well known. In 1966, Balch and Holm¹⁷ first synthesized the extremely oxygen-sensitive complex $[\text{Ni}\{\text{Ph-DAB}(\text{Me})\}_2]$ and proposed the electronic structure as a Ni^{II} centre with two radical monoanionic $(\text{DAB-R})^{1-}$ ligands (Scheme 1-3). At that stage, the electron transfer behaviour was not fully understood. However, since spectroscopic oxidation state of the non-innocent ligand can be elegantly determined using a high-quality single-crystal X-ray analysis and theoretical calculation can give a comprehensive understanding of electronic structures of metal complexes, nowadays, it is clearly established that the $(\text{DAB-R})^0$ ligand possessing a low-lying antibonding π^* orbital is able to accept one or two electrons giving an open-shell

monoanion (DAB-R)¹⁻ or closed-shell dianion (DAB-R)²⁻, respectively.¹⁴ In other words, owing to its non-innocent nature DAB-R can form complexes with different ligand and metal oxidation states.



Scheme 1-3. Example of [Ni{Ph-DAB(Me)}₂] and DAB-R ligands in different oxidation states.

Another well-established model is tetracarbonyl-diimine complexes [M(CO)₄(α -diimine)] (M = Cr, Mo and W), which are found to be electrochemically reduced in several successive steps and oxidized in a single one-electron step.¹⁵ For the reduction, the observation is in agreement with the [M(DAB-R)₂] system, showing α -diimines can accommodate electrons to maintain the oxidation state of the metal. Upon oxidation, the charge redistribution occurs via π -backdonation from CO and, to a lesser extent, the diimine ligands to the metal. Therefore DAB-R ligands can be considered as highly π -acidic and/or weakly π -donor ligands.

1.2.3 Coordination of DAB-R ligands

Molecules containing the 1,4-diaza-1,3-butadiene skeleton have attracted much attention because of both their versatile coordination behaviour and the interesting properties of the resulting metal complexes. DAB-R compounds are particularly interesting since they have a flexible N=C-C=N skeleton, and they appear to have unusual electron donor and acceptor properties and can potentially act in a variety of coordination modes. The latter bonding modes involve not only the lone pairs of the N atoms but also the π -C=N bonds.¹⁸ Various coordination modes between metals and DAB-R ligands have been studied revealing the fascinating and versatile coordination behaviour of this class of ligand.

DAB-R has the unusual property that it enables the metal centre to adjust its electron density by modifying ligand coordination, and formally donating either 2, 4, 6 or 8 electrons (Figure 1-4).¹⁸

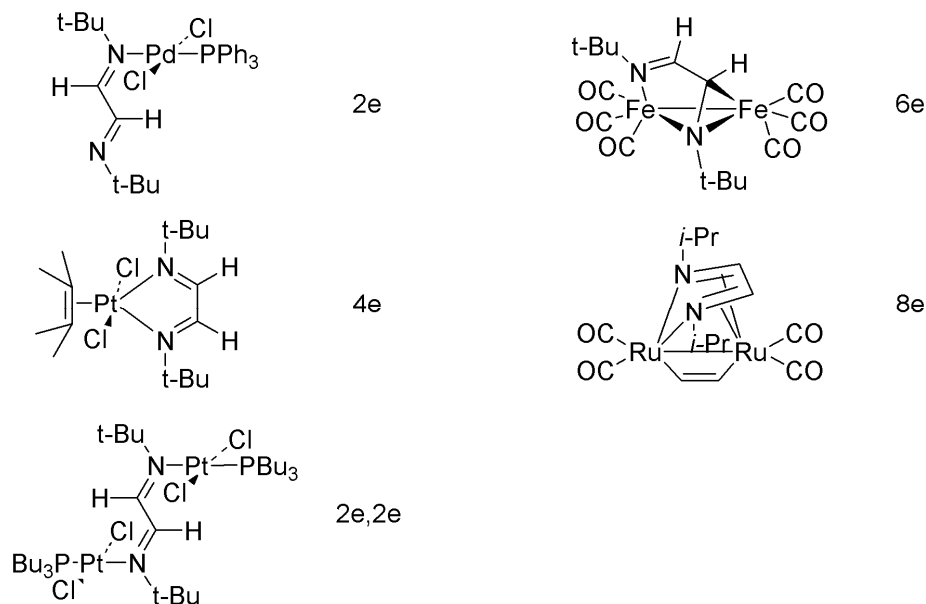
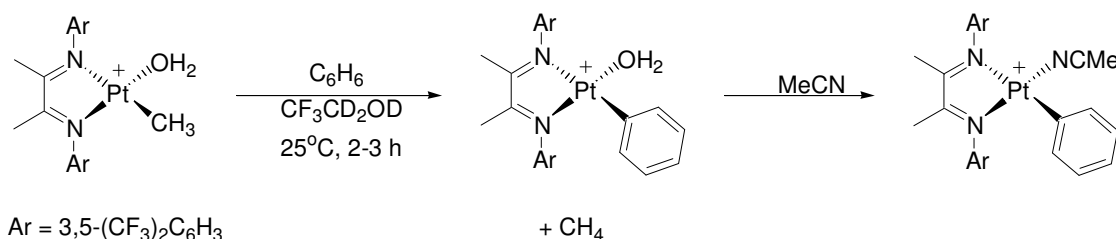


Figure 1-4. Examples of metal complexes with DAB-R ligands, illustrating the various coordination possibilities.

1.2.4 Application of DAB-R ligands

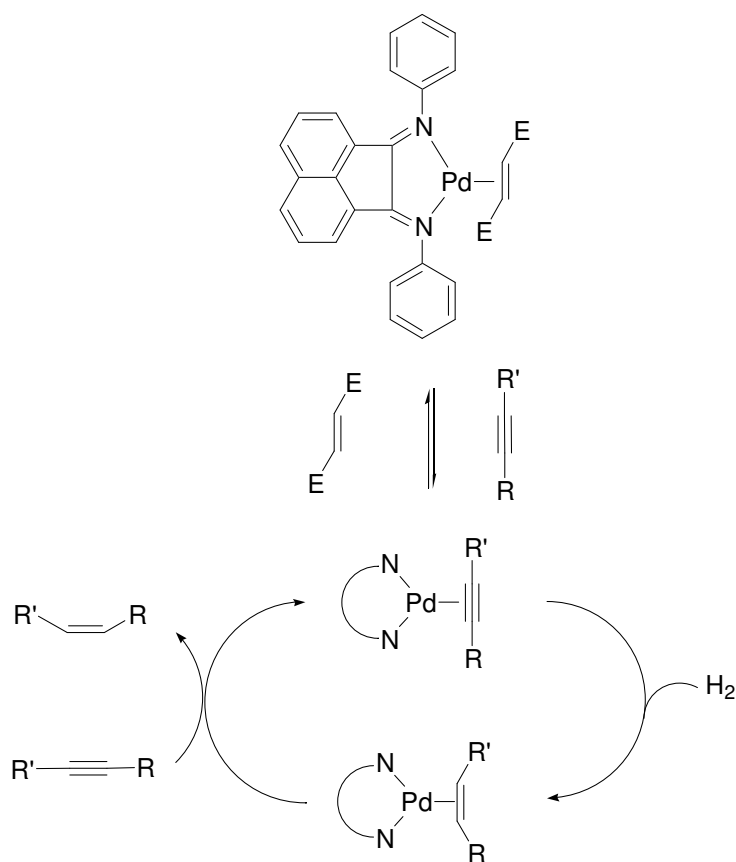
Besides coordination chemistry, complexes of DAB-R ligands have also exhibited a range of stoichiometric and catalytic reactivity. Platinum complexes with DAB-R ligands have been utilized in stoichiometric methane and arene C-H activation (Scheme 1-4). Importantly, it has been pointed out that the nitrogen-based ligands stabilize complexes with higher oxidation state to a greater extent than do phosphine ligands.¹⁹



Scheme 1-4. Stoichiometric arene C-H activation at cationic platinum complexes with DAB-R ligands.

In 1995, Brookhart and his group reported a new Pd(II)- and Ni(II)-based catalytic system for polymerisation of ethylene and α -olefins affording high molecular weight polymer and high catalytic activity.²⁰ Since then, a number of particular complexes of palladium and nickel bearing α -diimine ligands have been synthesised and investigated for the polymerization of ethylene, α -olefins, cyclic olefins and the copolymerization of nonpolar olefins with a variety of functionalized olefins.^{21, 22} Furthermore, Brookhart and coworkers proposed that the incorporation of sterically bulky axial substituents in the α -diimine ligand is essential in the generation of high molecular weight polymer because the bulky axial substituents dramatically retard the rates of chain transfer.^{20, 23}

Elsevier and co-workers²⁴ reported a series of palladium complexes with rigid bidentate nitrogen ligands Ar-BIAN which were shown to be efficient catalysts for the selective homogeneous hydrogenation of alkynes to alkenes (Scheme 1-5). The effect of the N-substituents of BIAN on the selectivity was briefly addressed. The selectivity significantly decreases when the electron-donor character of the N-substituents are reduced or the N-substituents become more sterically demanding.



Scheme 1-5. Proposed catalytic cycle for hydrogenation of alkynes.

Nozaki and co-workers²⁵ in 2006 reported the preparation of the first example of a stable boryl anion stabilized by α -diimine ligands (Figure 1-5). Furthermore, it was successfully demonstrated that the compound behaves as an efficient base and nucleophile in its reactions with a range of electrophiles.

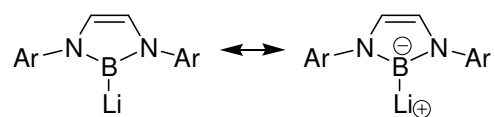


Figure 1-5. First example of a stable boryl anion with α -diimines ligand.

1.3 Amidine and guanidine ligands

As two closely related classes of N-donor ligands, neutral amidines and guanidines (Figure 1-6) are formed from a central sp^2 -hybridized carbon atom to which an imine and one or two amine groups are bonded. Structurally, by modifying the substituents on the nitrogen atoms, a variety of amidine and guanidine derivatives with different steric and

electronic properties can be obtained. This modularity provides great benefit to the investigation of their coordination chemistry and catalytic application. Furthermore, owing to the contribution of possible resonance structures, the presence of the lone-pairs of formal amine nitrogens in the “CN₂ or CN₃” framework potentially affects the electron donation ability of the imine nitrogen to a metal.²⁶ For nearly three decades of development, neutral amidines and guanidines have been gradually studied in coordination chemistry. As ligands these simple organic molecules coordinate metals from across the periodic table, resulting in the discovery of their various coordination modes.²⁷ Herein, and particularly relevant to the topic of this thesis, the coordination chemistry of amidines and guanidines with transition metals will be emphasised.

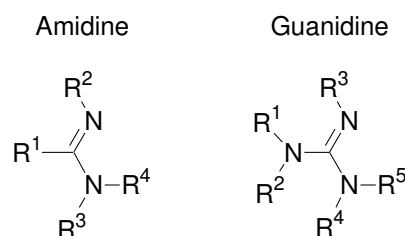


Figure 1-6. Generic structures of neutral amidines and guanidines.

1.3.1 Amidines

Due to developments in synthetic methodology, libraries of amidine ligand systems with a wide variety of substituents, such as silyl,²⁸ fluorinated aryl²⁹ and extremely bulky groups can be prepared.^{27, 30} Also, chirality has been successfully introduced into some systems.³¹ Several examples of amidines with different functional groups are shown in Figure 1-7. For non-symmetrical amidines, different isomers are afforded depending on the positions of the N-substituents. In addition, the presence of secondary amino groups can lead to the generation of different tautomers (Figure 1-8). Boéré and co-workers^{32, 33} conducted a study of bulky amidines showing the existence of different isomers and tautomers associated with the steric and electronic properties of the carbon substituents. However, a correlation between isomerisation and tautomerisation and steric and electronic tuning is unclear.

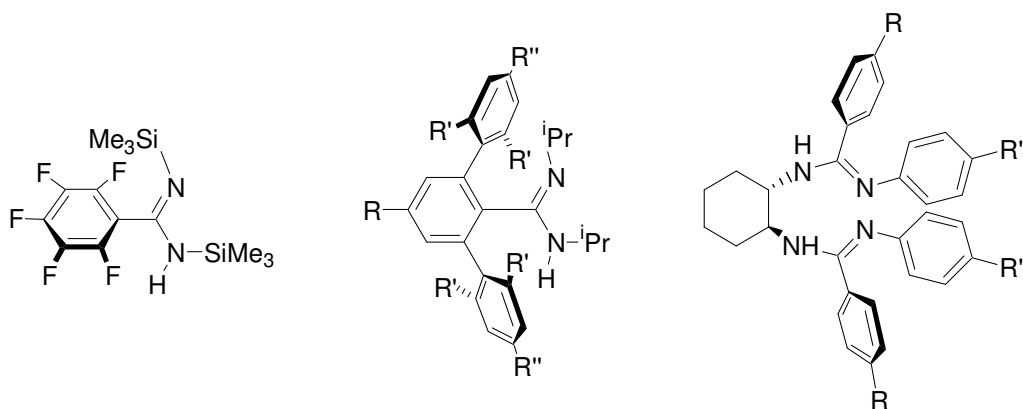


Figure 1-7. Examples of various amidines.

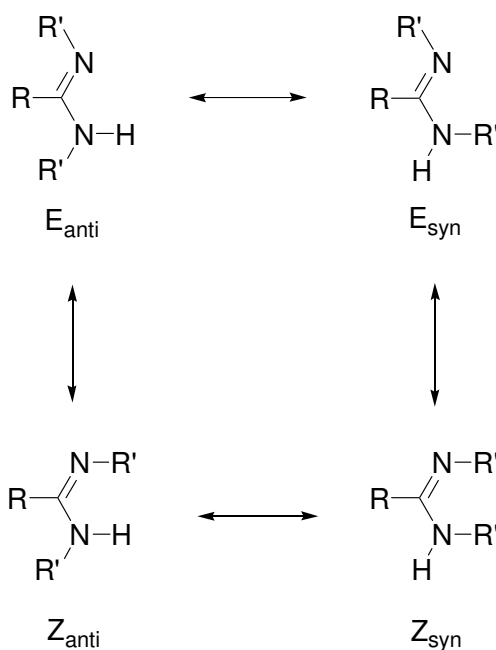


Figure 1-8. Isomeric and tautomeric forms for tri-substituted amidines.

Amidines generally act as two-electron donors via the more basic and less sterically crowded imino lone-pair. Compared with their anionic form amidinates, neutral amidines have drawn limited attention.³⁴ Nevertheless, amidines have exhibited the capacity for stabilising various transition metals from early metals in high oxidation state to late metals in lower oxidation state. A variety of coordination geometries have been obtained, including tetrahedral,³⁵⁻³⁷ trigonal-planar,³⁸ square planar,³⁵ square-pyramidal³⁷ and octahedral³⁹ (Figure 1-9). As mentioned above, due to the interest of coordination of amidinates, secondary amino groups are always present in the neutral amidines for

conversion to the anionic form via deprotonation. The presence of the *NH* groups makes intra- and intermolecular hydrogen bonds quite common within metal complexes of amidines.

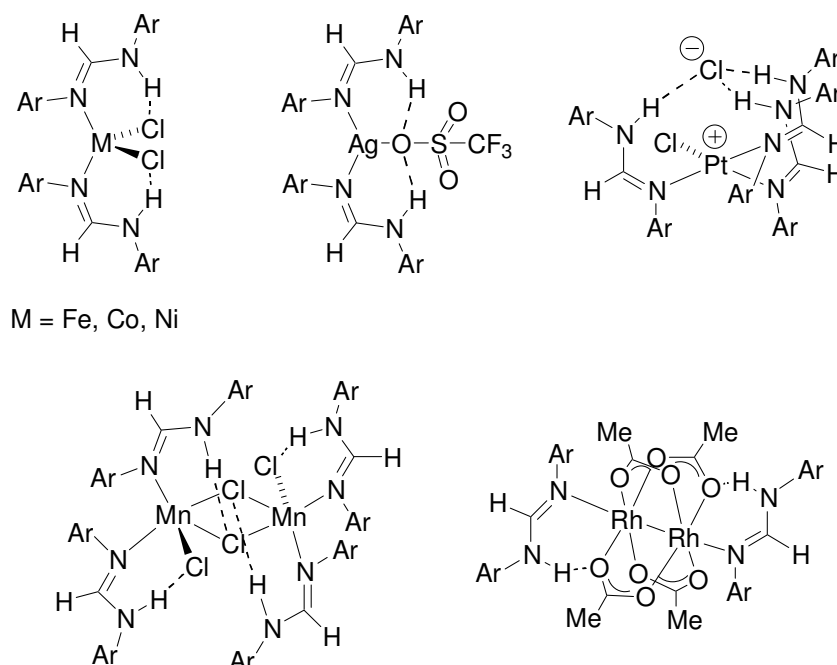


Figure 1-9. Examples of metal complexes with amidine ligands.

To distinguish the coordination mode of the ligand, IR spectroscopy is commonly utilised to investigate the coordination compounds of amidines. A diagnostic shift to lower wavenumbers occurs for the $\nu(\text{C}=\text{N})$ band when bonding to a metal occurs through the N_{imine} atom.^{27, 40} Also, in the ^{13}C NMR spectra, the chemical shift of the central carbon in the ‘ CN_2 ’ framework appears significantly downfield compared to other resonances when coordination occurs.²⁷ For assessing the extent of delocalisation of metal complexes within the ‘ CN_2 ’ component, the Δ_{CN} parameter is considered which measures the difference between the formally C-N and the C=N bond length. For example, Boéré and co-workers³² prepared a pentacarbonyl molybdenum complex with an amidine ligand $\text{Mo}(\text{CO})_5(\text{MeC}\{\text{DipN}\}\{\text{NHDip}\})$ shown in Figure 1-10. Evidently, the character of the C(1)-N(1) and C(1)-N(2) bonds are retained as single and double bonds respectively. However, comparing the Δ_{CN} value of the Mo complex and a related derivative 4-MePhC{DipN}{NHDip} (comparison with ligand itself is prevented due to the bond length distortion caused by intermolecular hydrogen-bonding), shows a decreasing trend of the

Δ_{CN} value in metal complexes,³⁷ indicating possible electronic contribution of the amine nitrogen via resonance upon coordination (*vide supra*).

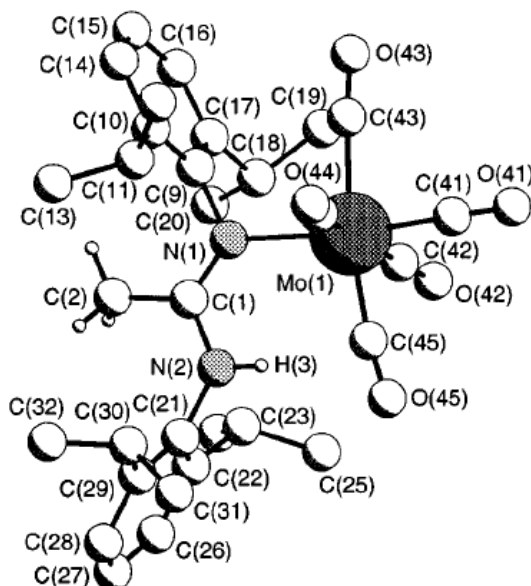


Figure 1-10. Molecular structure of $\text{Mo}(\text{CO})_5(\text{MeC}\{\text{DipN}\}\{\text{NHDip}\})$.

Metal complexes incorporating amidines have been investigated in catalytic applications. Eberhardt and co-workers⁴¹ prepared a series of N-acylamidines with different substituents to study the influence of the reactivity of these ligands in Pd-catalysed Suzuki-Miyaura reactions. Palladium complexes with N-acylamidine ligands in a 1:2 ratio were characterised by X-ray diffraction, showing a *trans* arrangement of amidines about the square-planar metal. High turnover number and yield were obtained using these complexes as precatalysts in the reaction between aryl bromide and phenylboronic acid. However, very low yield was achieved when aryl chlorides were employed.

1.3.2 Guanidines

As a product of protein metabolism found in urine, guanidines and their derivatives have generated widespread interest due to their biological activity,⁴² high proton affinity⁴³ and coordination chemistry with a wide range of metal ions.^{27, 44} The corresponding anionic and cationic forms, known as guanidinate and guanidinium respectively (Figure 1-11), represent another two types of popular compounds in a range of research areas. For

example, cationic guanidinium salts have been extensively utilised in noncovalent binding and molecular recognition to understand biological processes.⁴⁵ In coordination chemistry, anionic guanidates show electronic flexibility and compatibility with transition metals in a range of oxidation states.⁴⁴

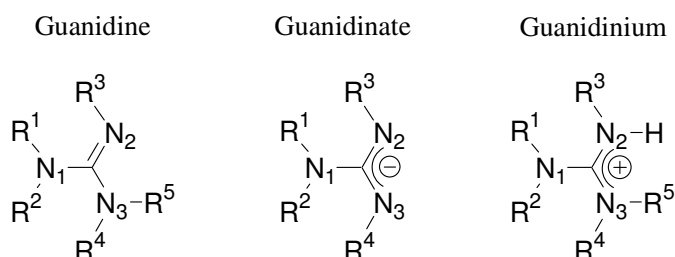


Figure 1-11. Generic representations for guanidines, guanidates and guanidinium salts.

1.3.2.1 Electron delocalisation property through guanidine framework

In contrast to amidines, guanidines are expected to have an enhanced basicity and nucleophilicity due to the presence of the second amino nitrogen atom. The ‘CN₃’ framework is capable of distributing positive charge throughout the molecule when the imine nitrogen is protonated (Figure 1-12).⁴⁶ Based on this concept, a series of guanidine compounds with superbasicity were discovered, and experimentally and theoretically studied in detail.^{47, 48}

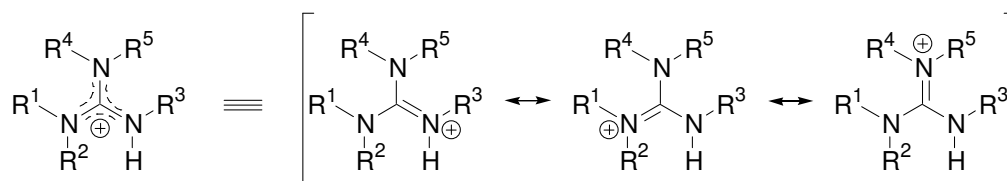


Figure 1-12. Delocalization of the positive charge over all N-atoms in the guanidine unit upon protonation.

Similarly, due to the ability of stabilising positive charge of the ‘CN₃’ framework, coordination to metal centres could result in electron delocalisation throughout coordinated guanidine ligands to some extent and consequently enhance nucleophilicity of coordinated nitrogen atoms (Figure 1-13). From a simple orbital description, this is determined by the extent of overlap between the nitrogen lone-pairs and the empty p-orbital of the sp²-carbon within the ‘CN₃’ framework.⁴⁸

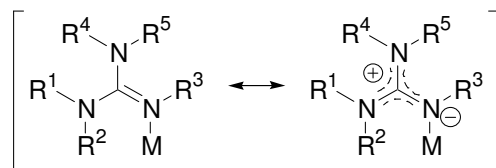


Figure 1-13. Possible resonance structures of the guanidine motif on coordination to a metal fragment.

Delocalisation is generally reflected by perturbation of spectroscopic and X-ray diffraction data (*vide supra*). For instance, Pohl *et al.*⁴⁶ compared the ¹H NMR data of the neutral chelating bis-guanidine ligand 1,3-bis(*N,N,N',N'*-tetramethylguanidino)propane (btmgp), its diprotonated salt and metal complexes, showing the signals of the metal complexes lie between neutral ligand and protonated salt (Figure 1-14). Also, comparison between the uncomplexed state, its metal complexes and diprotonated salt in terms of the C=N_{imine} and C-N_{amine} bond lengths in the solid state indicates remaining double-bond character for the C=N_{imine} of the metal complexes and a greater π delocalisation for the protonated salt. Presumably, the restricted delocalisation within the 'CN₃' framework of the metal complexes is due to the steric demands of the NMe₂ fragments, which prevent a better overlap between the nitrogen lone-pair and the empty p-orbital of the sp²-carbon.⁴⁹ Furthermore, the N_{imine}-M bond order for Fe^{II} and Cu^{II} was concluded to be evidently larger than that for lower oxidation state Cu^I complex, indicating the ability of guanidines to stabilise high metal oxidation states.⁵⁰

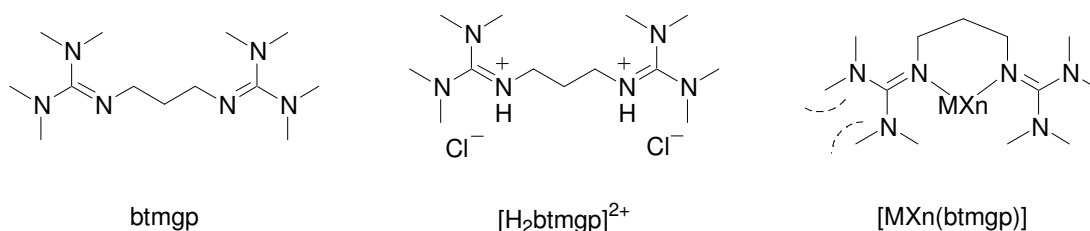


Figure 1-14. 1,3-bis(*N,N,N',N'*-tetramethylguanidino)propane (btmgp), its protonated salt and metal complexes.

To reduce rotational freedom about the C-N_{amine} bonds, a bicyclic guanidine system was introduced into coordination chemistry by Coles and co-workers.⁵¹⁻⁵³ The nitrogen substituents are formally constrained into the ring system to generate a rigid framework. Consequently, an enhanced delocalisation within the 'CN₃' framework is expected. Coles and co-workers prepared bis-(H-hpp) copper complexes and their molecular structures were

determined using X-ray crystallography (Figure 1-15). Inspection of the Δ_{CN} parameter of those complexes shows a better delocalisation of π -electron density within the constrained 'CN₃' framework as expected.

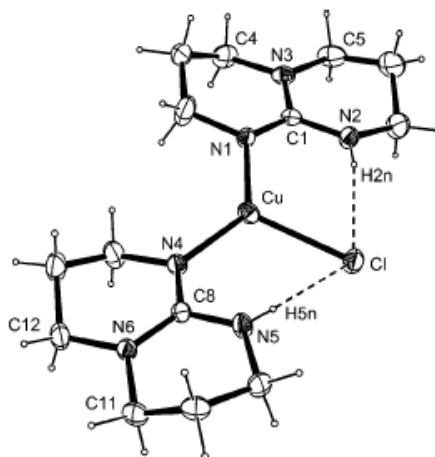


Figure 1-15. Molecular structure of [(H-hpp)₂CuCl].

1.3.2.2 Coordination of guanidines and their application

Although neutral guanidines have received relatively less attention in studies of coordination chemistry compared with anionic guanidates in the past decades, recent studies based on neutral guanidine functionality have developed the field rapidly. Monodentate,^{44, 54, 55} polydentate with organic bridges^{27, 46, 50, 56} and bicyclic^{27, 57} guanidine systems have been introduced into coordination chemistry and some resulting complexes have exhibited interesting reactivity.⁵⁸

Along with the need for better control over metal mediated catalytic transformations, the synthetic routes to guanidines have been further developed to yield many new derivatives with a variety of substituents,⁵⁹ including silyl,⁶⁰ extremely bulky,^{53, 61} chiral⁶² and mixed donor groups.^{63, 64} However, here the synthetic methodology of guanidines will not be described in detail. Herein, only complexes containing guanidine moieties directly bound to transition metals are considered, and the coordination chemistry and relevant applications will be described.

1.3.2.2.1 Monodentate guanidines

In guanidine complexes, coordination occurs almost exclusively through the donation of the lone-pair electrons of the N_{imine} atom to an appropriate acceptor orbital of the metal complex fragment. Such ligands have been successfully used in the stabilisation of different coordination geometries, including linear,⁶⁵ trigonal-planar,⁵³ tetrahedral,⁵⁵ square planar^{66,67} and octahedral⁶⁸ species (Figure 1-16). The first report of transition metal complexes incorporating guanidines was published by Drago and co-workers in 1965.⁵⁴ Complexes of Co(II), Cu(II), Zn(II), Pd(II), Ni(II) and Cr(III) were prepared with the tetracoordinate cobalt, copper, and zinc perchlorate complexes characterised by spectroscopy, magnetic measurements and X-ray powder diffraction. However, until the 1990s, further development of coordination chemistry was lacking.

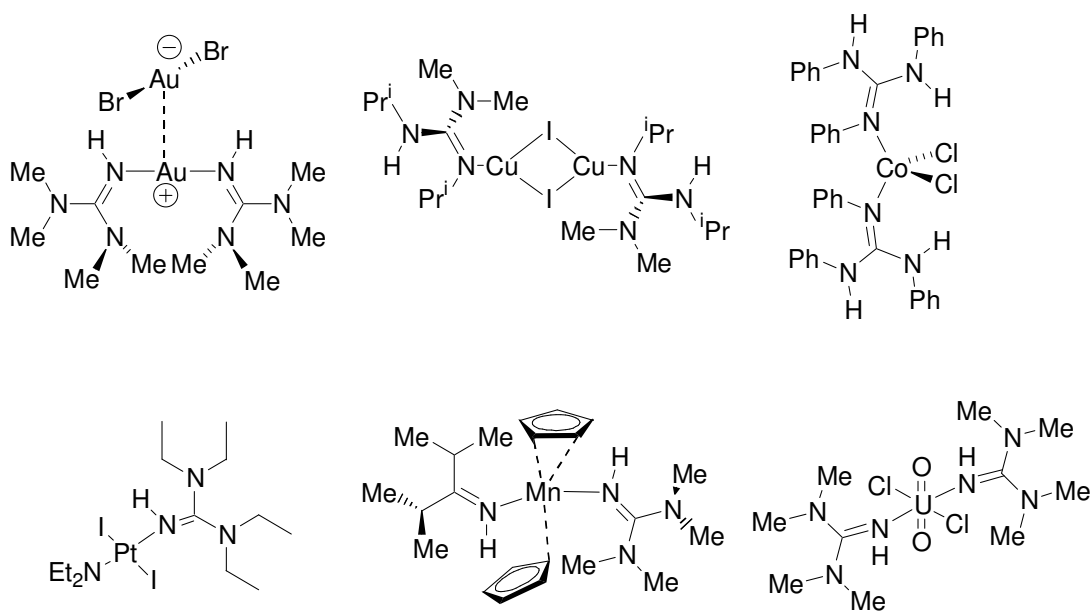
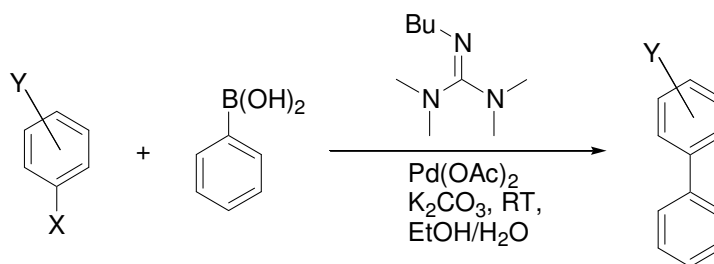


Figure 1-16. Examples of metal complexes incorporating monodentate guanidine ligands.

Recently, due to their versatile coordination chemistry, guanidines are emerging as a potentially useful class of ligand in some catalytic transformations, in particular cross-coupling and polymerisation reactions.

Li *et al.*⁶⁹⁻⁷¹ reported a highly efficient $\text{Pd}(\text{OAc})_2/\text{guanidine}$ aqueous system for the Suzuki cross-coupling reaction. A wide range of aryl halides, including aryl iodides, aryl

bromides, and even activated aryl chlorides, could couple with arylboronic acids smoothly at room temperature under aerial conditions by using a water-soluble catalyst $\text{Pd}(\text{OAc})_2/[\text{BuNC}(\text{NMe})_2]$ (Scheme 1-6) which was determined by X-ray diffraction showing a *trans* arrangement of guanidines about the square-planar metal. It is worth noting that the results of the coupling reactions between benzene chloride and phenylboronic acid to evaluate of the steric bulk effect of the ligands are questionable as homocoupling reaction can give the same product.



Scheme 1-6. Suzuki-Miyaura cross-coupling reaction catalysed by $\text{Pd}(\text{OAc})_2$ /guanidine system.

Bunge *et al.*⁷² studied the reactivity between 1,1,3,3-tetramethylguanidine and diethyl zinc and prepared a series of zinc alkoxide and aryloxy complexes in the presence of the alcohol. Ring-opening polymerisation tests of the resultant complexes showed an alkoxide-bridged zinc aryloxy dimer stabilised by guanidines (Figure 1-17) which exists as a monomer in solution and is an active catalyst.

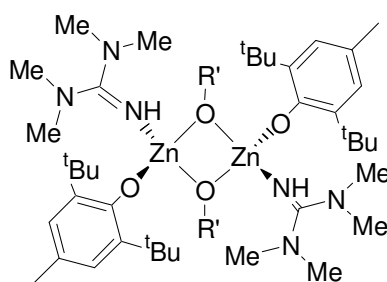
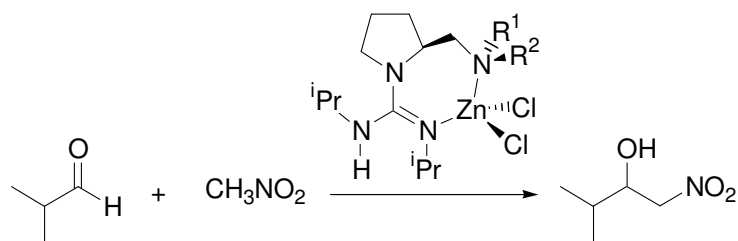


Figure 1-17. Alkoxide-bridged zinc aryloxy dimer stabilised by 1,1,3,3-tetramethylguanidine.

A chiral zinc complex containing a guanidine fragment prepared by Köhn and co-workers⁶² was tested in an asymmetric nitroaldol reaction between 2-methylpropanal and nitromethane (Scheme 1-7). Though high yields were obtained in selected cases, the ee values were quite poor and further work is apparently ongoing.



Scheme 1-7. Asymmetric nitroaldol reaction mediated by chiral guanidine complexes.

1.3.2.2 Polydentate guanidines with organic bridges

The coordination chemistry of bis-, tris-, and oligoguanidines has become of interest partially because of the marked tendency of biguanides to stabilize unusually high oxidation states of metals, such as Ag^{III} and Ni^{III} complexes (Figure 1-18).^{73, 74} Also, their control of donor strength and steric demand by variation of the substituents at the guanidine function has potentially played an important role in coordination chemistry and catalytic application.

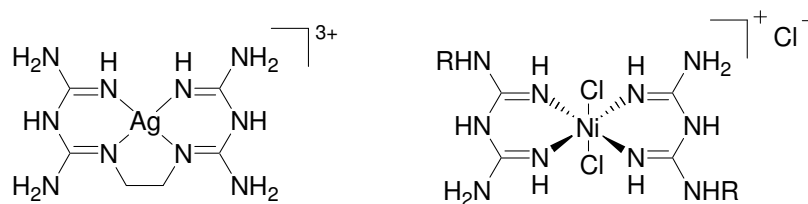


Figure 1-18. Examples of metal complexes with high oxidation states incorporating biguanidines.

The first complexes of chelating bis(guanidine)s were reported by Kuhn⁷⁵ and Sundermeyer.⁷⁶ Since then, a variety of polyguanidine derivatives with organic bridges have been prepared. Not only can the linking unit be modified, but also the position of the linking unit can be chosen either through the N_{imine} atoms or the N_{amine} atoms. The former class is quite common and has been successfully exploited in coordination chemistry (Top, Figure 1-19), whereas the later one has only recently been described (Bottom, Figure 1-19).²⁷

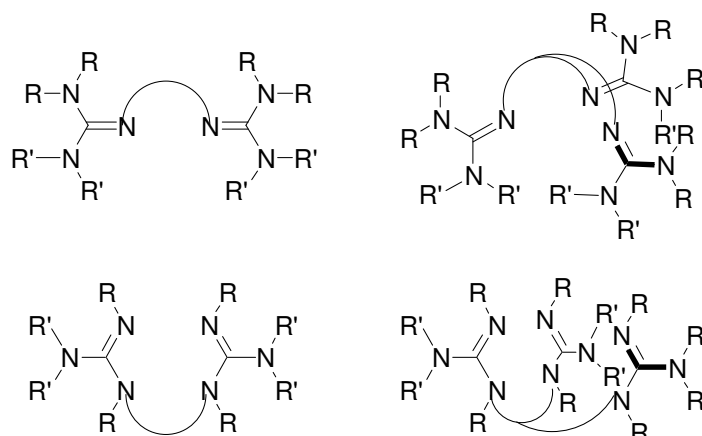
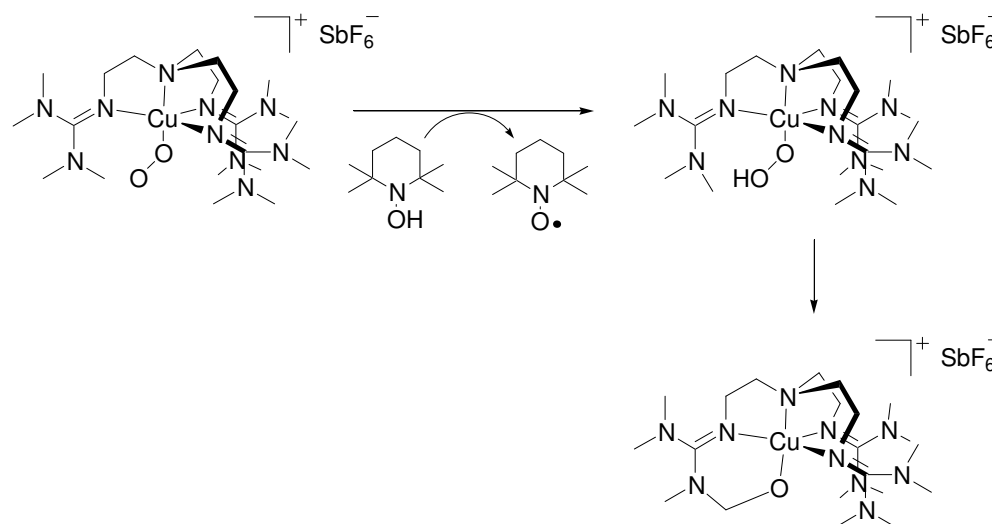


Figure 1-19. Generic structure of two different classes of linked bis- and tris-guanidines.

Similar to monodentate guanidines, polyguanidines have exhibited the ability to stabilise a range of transition metals²⁷ with a variety of coordination geometries including trigonal-planar,⁴⁹ tetrahedral,⁷⁷ square-planar^{75, 78} and trigonal-bipyramidal.⁵⁶ Considering the structural tuning and strong σ -donating properties, polyguanidines have been recently investigated as mimics for biological processes. Sundermeyer and co-workers prepared the cationic Cu complex $[(\text{tmg})_3\text{trenCu}]^+\text{Cl}^-$ ⁷⁹ and found the tendency of the complex to bind O_2 at low temperature in an end-on fashion.⁸⁰ Subsequently, it has been shown that this Cu^{II} superoxo complex is capable of C-H activation (Scheme 1-8).⁸¹



Scheme 1-8. C-H activation mediated by a copper superoxo complex.

Applying the same ligand (tmg)₃tren to stabilise high-valent oxoferryl complexes, Que and co-workers⁸² reported the synthesis in a high yield of the first long lifetime S=2 oxoiron(IV) complex [Fe^{IV}(O)(tmg)₃tren]²⁺ that was fully characterized by spectroscopy. The oxidation reactivity of the oxoiron(IV) complex with selected substrates was observed to be attenuated compared with that of the S=1 oxoiron(IV) complex [Fe^{IV}(O)(N4Py)]²⁺ (N4Py=bis(2-pyridylmethyl)bis(2-pyridyl)methylamine) probably due to the protection of the high-spin oxoiron(IV) moiety afforded by the sterically bulky (tmg)₃tren ligand (Figure 1-20).

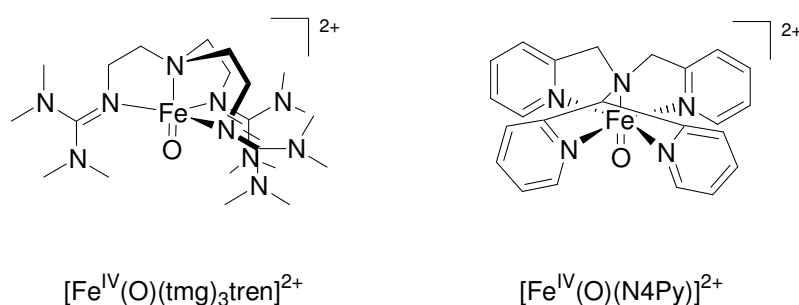
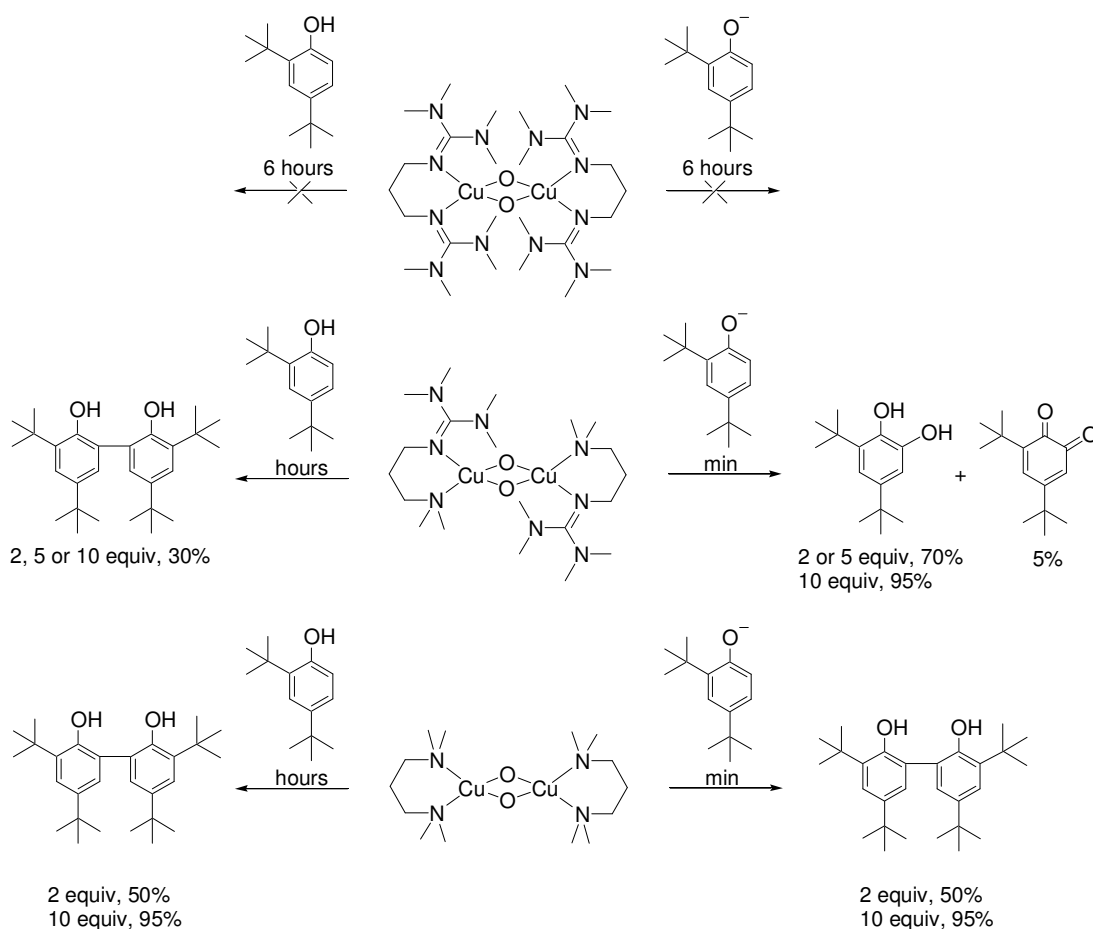


Figure 1-20. Examples of high-valent oxoferryl complexes.

Very recently, Stack and co-workers⁵⁸ compared three bis(μ -oxo)dicopper(III) complexes incorporating bis-guanidine, guanidine-amine hybrid and bis-amine ligands (Scheme 1-9) in a phenolate hydroxylation reaction and found only the complex with the hybrid ligand shows the desired activity. Comparison showed the most congested complex is the bis-guanidine and the most oxidative complex the bis-amine, thus the complex with the hybrid ligand contains less steric demanding amine moiety and stronger σ -donating guanidine moiety and has reasonable core accessibility in oxidation and electron donation to attenuate the one-electron outer-sphere oxidizing strength. In contrast the bis-amine ligand yields exclusively the C-C radical coupled bis-phenol product with both phenols and phenolates, a reactivity observed for most bis(μ -oxo)dicopper^{III} complexes.



Scheme 1-9. Reactivity comparison between bis-guanidine, guanidine-amine hybrid and bis-amine ligands on phenolate hydroxylation reaction.

1.3.2.2.3 Bicyclic guanidines

As mentioned above, in order to reduce the flexibility of amine groups to construct a better delocalisation through the 'CN₃' framework of guanidines, a bicyclic guanidine system was introduced to coordination chemistry (Figure 1-21). Constraining the substituents of the amine nitrogen atoms into the ring system generates a favourable alignment for the lone-pairs of the atoms to be included in the delocalisation scheme. In addition, within the rigid framework of the ring system, the rotation about the C-N bonds is reduced and possible isomerisation is prevented about the C=N double bond. A comprehensive review published by Coles⁵⁷ very recently gives full introduction of the

recent developments of this bicyclic system, where nomenclatures and synthesis of bicyclic guanidines are given in detail, and will therefore not be presented here.

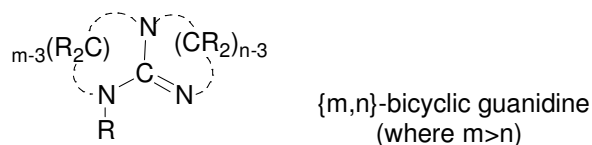


Figure 1-21. Generic structure of bicyclic guanidines.

So far, coordination chemistry of neutral bicyclic guanidines has been almost exclusively developed using the parent {6,6} derivative, H-hpp. It is partially because the presence of the five-membered ring in other bicyclic examples^{83, 84} prevents the tertiary amine nitrogen from achieving a planar configuration, reducing the extent of delocalisation of the 'CN₃' framework. However, the consequence of delocalisation attenuation has yet been explored, so some different chemical behaviour may be expected.

Similar to acyclic guanidines, coordination of bicyclic examples to metals exclusively occurs through the N_{imine} lone-pair, supporting a range of different coordination geometries including linear,^{51, 52} trigonal-planar,^{53, 85} tetrahedral,⁸⁶⁻⁸⁹ square-planar⁹⁰ and octahedral.^{78, 91, 92} For the ligands with NH groups, intramolecular hydrogen bonding to additional ligands may occur in some cases to favourably stabilise the metal complexes (Figure 1-22). Cotton and co-workers⁸⁸ in 1999 reported the first metal complexes incorporating neutral bicyclic guanidines. Tetrahedral iron(II) and cobalt(II) complexes were readily prepared from reactions between metal dichlorides and the H-hpp ligand. Since then, the H-hpp ligand has been widely studied in coordination chemistry. Furthermore, Coles and co-workers introduced a series of N_{amine}-linked bis- and tris-guanidine containing H-hpp as the guanidine functionality. For bis-guanidine examples, CH₂ and SiMe₂ linking unit are accessible to date, and SiMe and SiPh for tris-guanidine ones (Figure 1-22). However, coordination complexes of the later examples have not been accessible, possibly a consequence of cleavage of the N-Si linkage. Several examples containing bicyclic guanidines are shown in Figure 1-22.

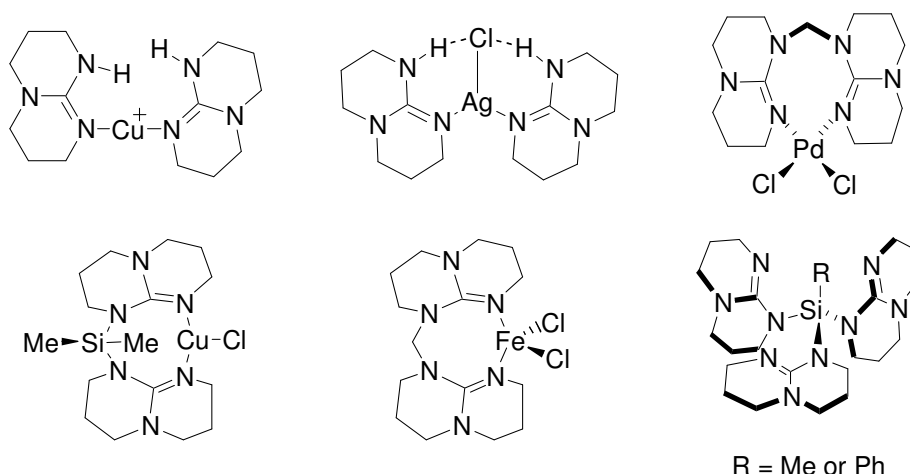
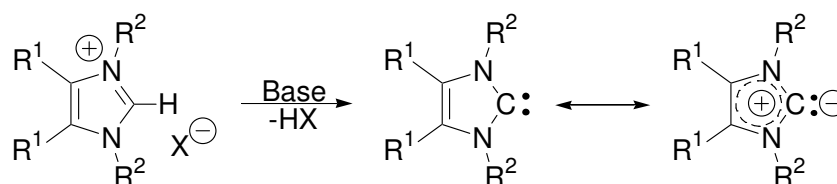


Figure 1-22. Examples of metal complexes incorporating mono- and bis-(bicyclic guanidine), and tris-(bicyclic guanidine) compounds.

1.4 Imidazolin-2-imine ligands

1.4.1 Imidazolin-2-imine ligands – carbene analogues

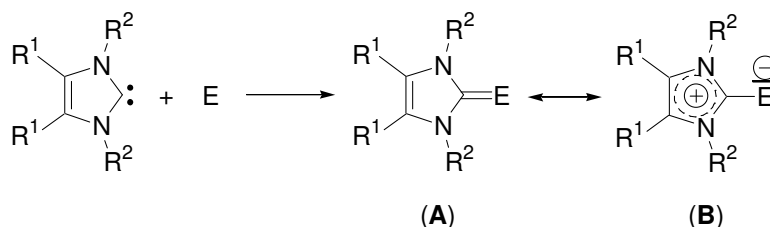
Since the first successful isolation of stable carbenes in 1991,⁹³ N-heterocyclic carbenes of the imidazolin-2-ylidene type (Scheme 1-10) have successfully been investigated and emerged in a range of diverse research areas such as homogeneous catalysis,⁹⁴ materials science⁹⁵ and medicinal chemistry.⁹⁶ The stability of these carbenes can be attributed to the capability of the imidazolium ring to effectively stabilize a positive charge (Scheme 1-10) leading to strongly basic and highly nucleophilic ligands.



Scheme 1-10. Generation of stable N-heterocyclic carbenes and their aromatic resonance structures.

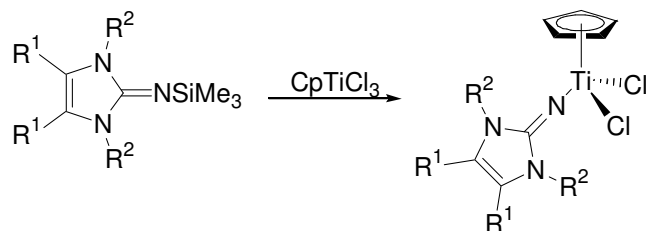
Owing to their highly nucleophilic character, not only can N-heterocyclic carbenes behave as ancillary ligands to stabilize transition metal complexes, but also they react with electrophilic centres (E = CR₂, NR, O, etc) of most main group elements to form stable adducts (Scheme 1-11).⁹⁷ The resulting compounds **A** with doubly bound substituents at the 2-position were considered to have a similarly enhanced basicity and nucleophilicity to

carbenes due to a strong contribution from the ylidic mesomeric structure **B**. On the basis of this concept, the performance of transition metal catalysts incorporating type **A** ligands can be potentially enhanced, in particular, the oxidative addition step due to strong donation.



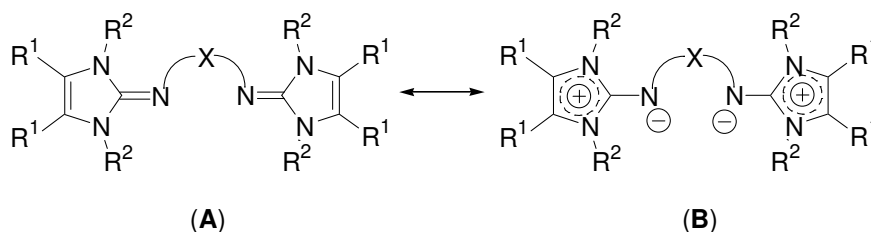
Scheme 1-11. Formation of imidazole-based ligands and their mesomeric structures.

Another concept that intrigued chemists to investigate these carbene analogue ligands is called the pseudo-isolobal phenomenon,^{98, 99} that is, pairs of compounds of both ligand types with the same metal atom show analogies in structure and bonding modes. For example, due to the capability to act as 2σ , 4π -electron donors, phosphaneimides (R_3PN^-) can be regarded as monodentate analogues to cyclopentadienides (C_5R_5^-). Such ideas were successfully transplanted by Stephan *et al.* into olefin polymerisation catalysts design. A series of titanium complexes incorporating phosphinimides ligands that sterically and electronically mimic metallocenes to some extent have shown high activity.¹⁰⁰⁻¹⁰³ Inspired by this work, imidazolin-2-iminato ($\text{E} = \text{N}^-$) ligands were considered to be in a pseudo-isolobal relationship with phosphaneimides ligands (R_3PN^-). Kuhn and co-workers first prepared imidazolin-2-iminato transition metal complexes^{104, 105} with the use of the ligand precursor 2-imino-1,3-dimethylimidazoline.¹⁰⁶ A few years later, Tamm and co-workers modified the preparation route of imidazolin-2-iminato titanium complexes by using the precursor 2-(trimethylsilylimino)imidazolines (Scheme 1-12) and the resulting complexes show moderate to high activities in olefin polymerisation.¹⁰⁷⁻¹⁰⁹ Furthermore, tungsten alkylidyne complexes of the type $[\text{RC}\equiv\text{W}(\text{ImN})(\text{OR}^t)_2]$ bearing imidazolin-2-imides have exhibited efficiently catalytic ability in alkyne metathesis at room temperature.¹¹⁰



Scheme 1-12. Synthesis of titanium complexes incorporating imidazolin-2-iminato ligands.

The related neutral ligands imidazolin-2-imines were extensively studied shortly afterwards with the additional feature of forming polydentate ligands.¹¹¹⁻¹¹⁴ Similarly, imidazolin-2-imine ligands are characterized by a strong donating ability due to a considerable transfer of negative charge to the exocyclic nitrogen at the 2-position of the N-heterocycle, resulting from the contribution of the mesomeric form **B** (Scheme 1-13). This behaviour is considered to become even more pronounced upon metal complexation.¹¹¹



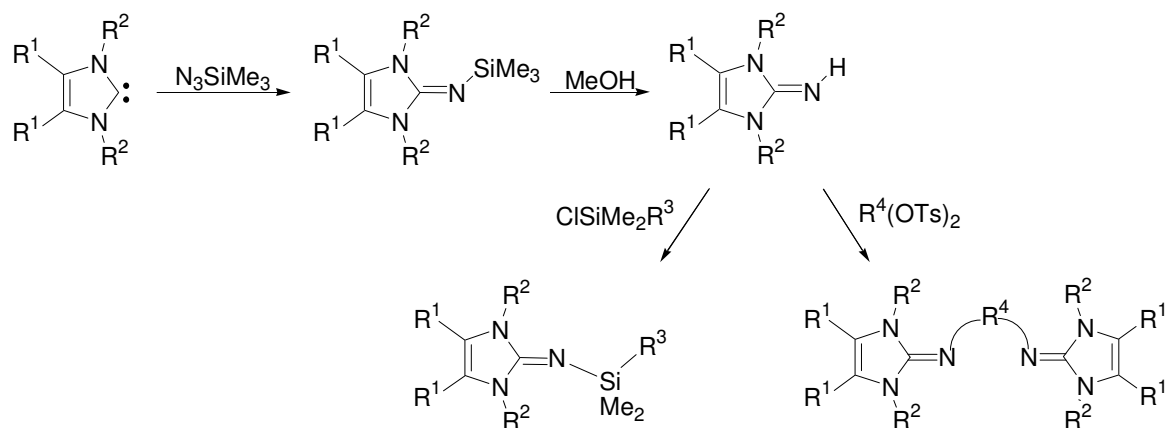
Scheme 1-13. Two limiting mesomeric structures of poly(imidazolin-2-imine) ligands.

1.4.2 Synthesis and theoretical investigation of imidazolin-2-imines

The first poly(imidazolin-2-imine) ligand was synthesised by Kuhn *et al.* in 1998 from reaction between the ligand precursor 2-imino-1,3-dimethylimidazoline and 1,2-ethyleneditosylate in the presence of a base.⁷⁵ However, the modularity of this type of ligand was restricted by a multistep synthetic route to the ligand precursor.¹⁰⁶

In 2007, Tamm *et al.* reported a modified synthesis protocol *via* silylation of free carbenes, desilylation and detosylation.^{26, 114} This novel method allows convenient access to the desired compounds with various substituents in high yield. The coordination modes and steric and electronic environment can be adjusted through modification of R¹, R² and R³ groups (Scheme 1-14). It is noteworthy that the primary imine compounds attained from

desilylation can be utilised as a building block to prepare bifunctional ligands (Scheme 1-14).¹¹⁵



Scheme 1-14. A novel synthetic route to multidentate imidazolin-2-imine ligands by Tamm and co-workers.

To aid the understanding of imidazolin-2-imine ligands with respect to their electronic properties, systematic DFT calculations were conducted by Tamm *et al.* on 2-imino-1,3-dimethylimidazoline (X = CH), 2-imino-1,3-dimethylimidazolidine (X = CH₂) and tetramethylguanidine (X = CH₃) as shown in Figure 1-23.²⁶ Initially, the proton affinities (PAs) of all three compounds were measured as the basicity can reflect their reactivity towards transition metals to some extent. However, no significant differences were obtained for three compounds regarding the computed values of the proton affinities. Nevertheless, NBO (natural bond orbital) and NRT (natural resonance theory) calculations were applied on three compounds to investigate the nucleophilicity differences. Clearly, as shown in Figure 1-22, 2-iminoimidazoline ligands (-0.822) exhibit higher Lewis basicity compared with the other two types of ligands (-0.781 and -0.755) according to NBO calculation. The results from NRT calculation reveal that relative contributions of the mesomeric structures **B** account for the enhanced nucleophilicity. Due to a stronger capability of the imidazole ring to stabilise positive charge, 2-iminoimidazolines (20.6%) exhibit a greater contribution from the zwitterionic structure **B**.

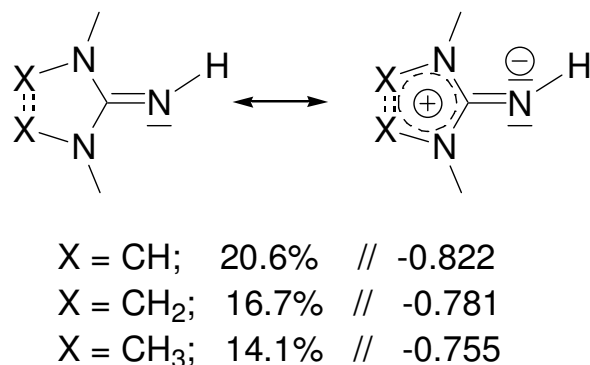


Figure 1-23. Relative contributions from the ylidic mesomeric structures **B** and NBO charges of the exocyclic nitrogen atom for 2-iminoimidazoline, 2-iminoimidazolidine and guanidine model systems.²⁶

1.4.3 Transition metal complexes incorporating imidazolin-2-imines

The first transition metal complex containing imidazolin-2-imine was reported by Kuhn and co-workers in 1998 from reaction between 1,2-bis(1',3'-dimethylimidazolin-2'-iminato)ethane and $\text{PdCl}_2(\text{PhCN})_2$ (Figure 1-24).⁷⁵ After that, several late transition metal complexes incorporating bifunctional ligands containing imidazolin-2-imine (Figure 1-24) were also prepared by Kuhn *et al.*,¹¹⁶ however, there was no further report of their reactivity or catalytic application.

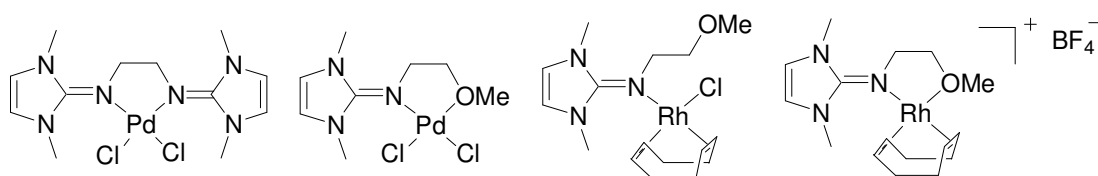


Figure 1-24. Examples of metal complexes of 2-iminoimidazolines.

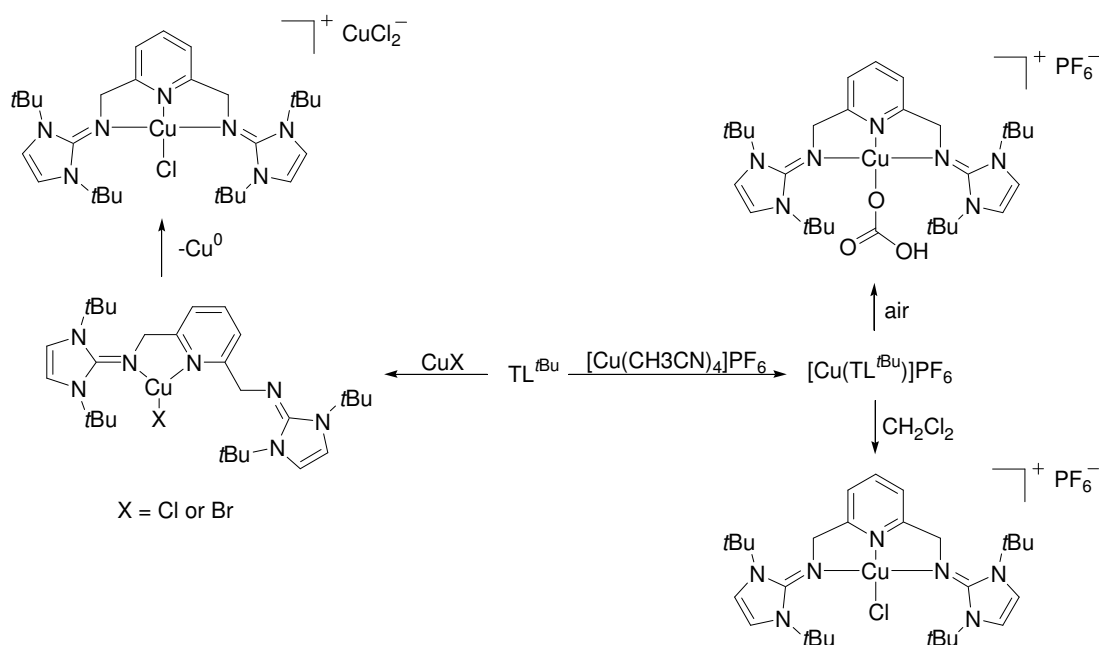
Later, along with the discovery of a new synthetic route (*vide supra*), Tamm and co-workers carried out a series of investigations of transition metal complexes incorporating imidazolin-2-imines with respect to their coordination chemistry, reactivity and catalytic application.^{26, 111-115, 117-120}

For the transition metal complexes of imidazolin-2-imines, more imidazolium-amide character needs to be considered, which is generally reflected by a pronounced elongation

of the C-N_{imine} bond and a more obtuse N-C-N (imidazole ring) angle of metal complexes compared with those of neutral ligands (*vide infra*).

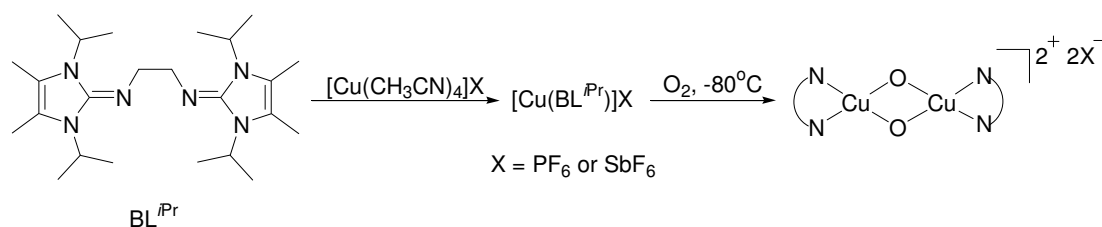
1.4.3.1 Copper complexes

Initially, copper complexes incorporating ethylene- or pyridine-bridged bis(imidazolin-2-imine) ligands were investigated due to their potential oxygen activation and polymerisation activity. The copper(I) complexes of the 2,6-bis(imidazolin-2-imino)pyridine pincer ligand (TL^{tBu}) are highly reactive and exhibit a pronounced tendency to form stable, square-planar copper(II) complexes, allowing effective aerobic CO₂ fixation, C-Cl bond activation and Cu(I) disproportionation (Scheme 1-15).¹¹⁴ Those activities were considerably attributed to the strong electron-donating property of the TL^{tBu} ligand. For example, the C-Cl bond activation was observed generally for the copper(I) complexes with electron-rich N-donors. The mechanism of that transformation was believed to involve a copper(III) intermediate generated from oxidative addition of halide substrates.¹²¹ Ligand effects on the redox reactivity of copper(I) complexes are very important, and ligands with stronger electron-donating properties, such as imidazolin-2-imines, are more likely to support the intermediate with a high oxidation state.



Scheme 1-15. Reactivity of copper complexes of 2,6-bis(imidazolin-2-imino)pyridine pincer ligand.

Furthermore, a low coordinated copper(I) complex incorporating the ethylene-bridged bis(imidazolin-2-imine) ligand (BL^{iPr}) was prepared to study oxygen activation where N-functionalised ligands have been extensively utilised. Due to the enhanced electron-donating ability of imidazolin-2-imines, a thermally sensitive bis(μ -oxo)dicopper(III,III) intermediate was detected by UV-vis spectroscopy at low temperature (Scheme 1-16).¹¹¹ The powerful electron donating capability of this type of ligand was also supported by very low oxidation potentials and these copper(I) imine complexes exhibit promising catalytic activity in atom transfer radical polymerisations (ATRP) due to their ease of oxidation.¹¹¹



Scheme 1-16. Oxygen activation by copper(I) diimine complexes.

1.4.3.2 Molybdenum and ruthenium half-sandwich complexes

Half sandwich d^6 complexes are ubiquitous in organometallic chemistry, and typically adhere to the 18e rule. However, there is a growing interest in relatively stable 16-electron complexes, so-called coordinatively unsaturated complexes.¹²² Since such unsaturated complexes are considered intermediates in homogeneous transition metal-catalysed reactions, it is highly desirable to understand in more detail the parameters that are related to stability, reactivity and structure. In general, π -donor ligands are more capable of stabilising this coordinative unsaturation even without the use of noncoordinating counteranions like $[\text{B}\{3,5\text{-C}_6\text{H}_3(\text{CF}_3)_2\}_4]^-$.¹¹³

Not surprisingly, the strong electron donating property of imidazolin-2-imines favours the stabilisation of half-sandwich 16-electron ruthenium complexes of the type $[(\eta^5\text{-C}_5\text{Me}_5)\text{Ru}(\text{BL}^{\text{R}})]^+$, $[(\eta^6\text{-C}_6\text{H}_6)\text{Ru}(\text{BL}^{\text{R}})]^{2+}$ and $[(\eta^6\text{-C}_{10}\text{H}_{14})\text{Ru}(\text{BL}^{\text{R}})]^{2+}$ (Figure 1-25).^{113, 120} The coordination of π -basic ligands, such as chloride, is resisted in the above systems, whereas π -acid ligands such as CO or isocyanides show high reactivity towards these

coordinatively unsaturated complexes. Moreover, 16-electron half sandwich cycloheptatrienyl-molybdenum complexes which are analogous to 16-electron cyclopentadienyl-ruthenium complexes were first prepared (Figure 1-25),¹¹² although the similarity between the isoelectronic and isolobal fragments $[(\eta^5\text{-C}_5\text{R}_5)\text{Ru}]$ and $[(\eta^7\text{-C}_7\text{H}_7)\text{Mo}]$ has been well recognised for quite a while.¹²³ Both molybdenum and ruthenium complexes were tested in the transfer hydrogenation of acetophenone and several ruthenium complexes show reasonable activity.

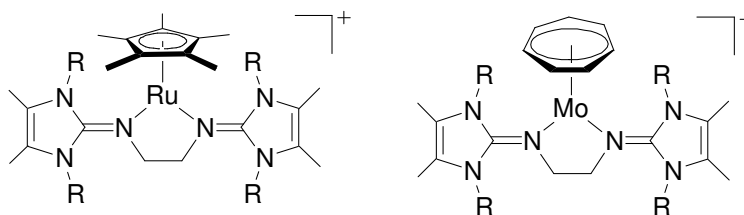


Figure 1-25. Examples of 16-electron half-sandwich complexes incorporating imidazolin-2-imines.

1.4.3.3 Other metal complexes and their application

Analogous to “constrained-geometry” *ansa*-cyclopentadienyl-amido ligands (Figure 1-26) which have been studied as homogeneous model systems for industrially applied heterogeneous catalysis,¹²⁴ cyclopentadienyl-imidazolin-2-imine ligands were prepared by tethering an imidazolin-2-imine unit to a cyclopentadienyl ring via a Me_2Si group. Rare earth metal (Sc, Y and Lu) complexes¹¹⁸ and chromium complexes¹¹⁵ containing cyclopentadienyl-imidazolin-2-imine ligands were isolated and short metal-nitrogen bonds were observed due to the strong electron-donating ability of the imidazolin-2-imine moiety (Figure 1-26). Preliminary catalytic activity studies on both systems showed that chromium complexes can be used as precatalysts for ethylene polymerization at room temperature and rare earth metal complexes are active catalysts for the hydroamination/cyclization of aminoalkenes and aminoalkynes. However, the decreasing performance of the chromium catalysts along with the increasing reaction time suggests the imine donor suffers faster degradation than the amine or N-heterocyclic analogues.

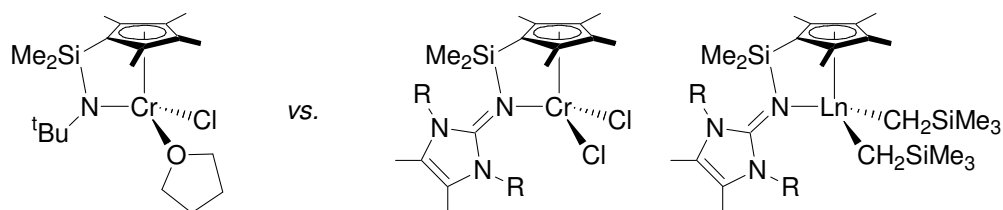


Figure 1-26. Examples of half-sandwich complexes of cyclopentadienyl-amido (left) and cyclopentadienyl-imidazolin-2-imino (right) ligands.

Inspired by the promising observation from zinc guanidine complexes in the ring-opening polymerisation of lactides, zinc complexes of ethylene-bridged bis(imidazolin-2-imine) ligands were also prepared, and experimentally and theoretically studied in the lactide polymerisation compared with a related guanidine system (Figure 1-27).¹¹⁷ The results showed the activity of the imidazolin-2-imine system is slightly higher than that of the guanidine system, which is consistent with a slightly enhanced Lewis acidity of the zinc atoms coordinated with imidazolin-2-imine compared with guanidine in NBO charge calculations.

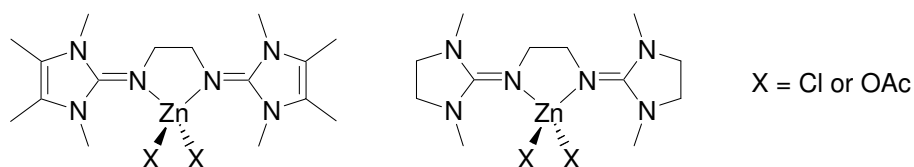
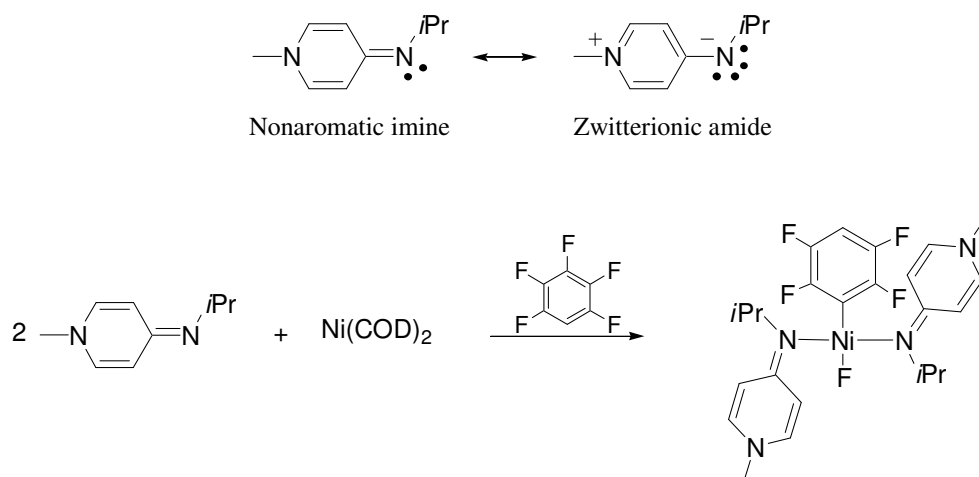


Figure 1-27. Zinc complexes of bis(guanidine) and bis(imidazolin-2-imine) ligands.

1.5 Isopropyl(1-methyl-1H-pyridin-4-ylidene)amine

Toward the end of the work described in this thesis, Johnson and co-workers¹²⁵ reported a structurally similar compound to our ligand system 1H-pyridin-(2E)-ylidenes (PYE) ligands, isopropyl(1-methyl-1H-pyridin-4-ylidene)amine (Scheme 1-17). Owing to a contribution of the zwitterionic amide resonance structure to the metal-ligand bond, the neutral nitrogen ligand exhibits a strong donating ability. This compound can be used in the selective nickel-mediated C-F activation of aryl fluorides, which was attributed to the strong σ -donating nitrogen ligand with the ability to selectively facilitate a difficult oxidative addition, as observed similarly for N-heterocyclic-carbene (NHC) ligands.¹²⁶ Compared with the reactivity of phosphine and NHC systems with polyfluorobenzenes,

isopropyl(1-methyl-1H-pyridin-4-ylidene)amine with Ni(0) shows a higher selectivity towards C-F bond activation of polyfluorobenzenes and it was the first time that tetrafluorobenzenes can be selectively activated. Collectively, the perceived interesting features and related published work suggested investigation of PYE type ligands was warranted, which has been partially justified by the report by Johnson.



Scheme 1-17. Selective C-F activation mediated by Ni(0) with a nitrogen ligand isopropyl(1-methyl-1H-pyridin-4-ylidene)amine.

1.6 Aims of the project

The aims of this research project are to synthesise chelating nitrogen ligands containing 1H-pyridin-(2E)-ylidene (PYE) moieties including achiral and chiral examples (Figure 1-28). These compounds will be complexed to a variety of transition metals to study their coordination chemistry including potential coordination modes and geometries. Electronic properties and bonding character of the resulting metal complexes will be investigated to understand the possible ‘neutral amido’ character of PYE type ligands. In select cases, some complexes will be tested for potential applications including catalysis and biological activity.

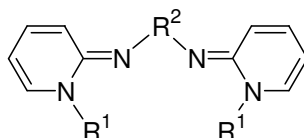


Figure 1-28. Generic structure of PYE ligands studied in this thesis.

1.7 References

1. F. Fache, E. Schulz, M. L. Tommasino and M. Lemaire, *Chem. Rev.*, 2000, **100**, 2159-2232.
2. C. A. Caputo and N. D. Jones, *Dalton Trans.*, 2007, 4627.
3. L. H. Gade, *Chem. Commun.*, 2000, 173.
4. E. D. Blue, A. Davis, D. Conner, T. B. Gunnoe, P. D. Boyle and P. S. White, *J. Am. Chem. Soc.*, 2003, **125**, 9435.
5. J. R. Fulton, A. W. Holland, D. J. Fox and R. G. Bergman, *Acc. Chem. Res.*, 2002, **35**, 44.
6. M. D. Ward and J. A. McCleverty, *J. Chem. Soc., Dalton Trans.*, 2002, 275-288.
7. C. K. Jørgensen, *Coord. Chem. Rev.*, 1966, **1**, 164.
8. V. Rosa, T. Aviles, G. Aullon, B. Covelo and C. Lodeiro, *Inorg. Chem.*, 2008, **47**, 17.
9. M. Dvolaitzky, *Acad. Sci. Paris, Ser. C*, 1969, **268**, 1811.
10. I. Matei and T. Lixandru, *Bull. Ist. Politeh. Iasi*, 1967, **13**, 245.
11. P. Krumholz, *J. Am. Chem. Soc.*, 1953, **75**, 2163-2166.
12. S. Greulich, W. Kaim, A. F. Strange, H. Stoll, J. Fiedler and S. Zalis, *Inorg. Chem.*, 1996, **35**, 3998-4002.
13. R. van Asselt, C. J. Elsevier, J. J. W. Smeets, A. L. Spek and R. Benedix, *Recl. Trav. Chim. Pays-Bas.*, 1994, **113**, 88-98.
14. M. M. Khusniyarov, K. Harms, O. Burghaus and J. Sundermeyer, *Eur. J. Inorg. Chem.*, 2006, 2985-2996.
15. A. Vlček Jr., *Coord. Chem. Rev.*, 2002, **230**, 225-242.
16. F. Hartl, P. Rosa, L. Ricard, P. L. Floch and S. Zalis, *Coord. Chem. Rev.*, 2007, **251**, 557-576.
17. A. L. Balch and R. H. Holm, *J. Am. Chem. Soc.*, 1966, **88**, 5201-5209.
18. G. van Koten and K. Vrieze, *Adv. Organomet. Chem.*, 1982, **21**, 151-239.
19. M. Lersch and M. Tilset, *Chem. Rev.*, 2005, **105**, 2471-2526.
20. L. K. Johnson, C. M. Killian and M. Brookhart, *J. Am. Chem. Soc.*, 1995, **117**, 6414-6415.
21. S. D. Ittel, L. K. Johnson and M. Brookhart, *Chem. Rev.*, 2000, **100**, 1169-1203.

22. Z. Guan and C. S. Popeney, *Top. Organomet. Chem.*, 2009, **26**, 179-220.
23. D. P. Gates, S. K. Svejda, E. Onate, C. M. Killian, L. K. Johnson, P. S. White and M. Brookhart, *Macromolecules*, 2000, **33**, 2320-2334.
24. M. W. van Laren and C. J. Elsevier, *Angew. Chem. Int. Ed.*, 1999, **38**, 3715.
25. Y. Segawa, M. Yamashita and K. Nozaki, *Science*, 2006, **314**, 113-115.
26. M. Tamm, D. Petrovic, S. Randoll, S. Beer, T. Bannenberg, P. G. Jones and J. Grunenberg, *Org. Biomol. Chem.*, 2007, **5**, 523-530.
27. M. P. Coles, *Dalton Trans.*, 2006, 985-1001.
28. A. R. Sanger, *Inorg. Nucl. Chem. Lett.*, 1973, **9**, 351.
29. C. Knapp, E. Lork, P. G. Watson and R. Mews, *Inorg. Chem.*, 2002, **41**, 2014.
30. J. A. R. Schmidt and J. Arnold, *J. Chem. Soc., Dalton Trans.*, 2002, 2890.
31. G. D. Whitener, J. R. Hagadorn and J. Arnold, *J. Chem. Soc., Dalton Trans.*, 1999, 1249.
32. R. T. Boéré, V. Klassen and G. Wolmershauser, *J. Chem. Soc., Dalton Trans.*, 1998, 4147.
33. R. T. Boéré, V. Klassen and G. Wolmershauser, *Can. J. Chem.*, 2000, **78**, 583.
34. J. Barker and M. Kilner, *Coord. Chem. Rev.*, 1994, **133**, 219.
35. F. A. Cotton, L. M. Daniels, C. A. Maloney, J. H. Matonic and C. A. Murillo, *Polyhedron*, 1994, **13**, 815.
36. F. A. Cotton, L. M. Daniels and C. A. Murillo, *Inorg. Chim. Acta*, 1994, **224**, 5.
37. D. I. Arnold, F. A. Cotton, D. J. Maloney, J. H. Matonic and C. A. Murillo, *Polyhedron*, 1997, **16**, 133.
38. D. I. Arnold, F. A. Cotton, J. H. Matonic and C. A. Murillo, *Polyhedron*, 1997, **16**, 1837.
39. F. Nicolo, G. Bruno, S. L. Schiavo, M. S. Sinicropa and P. Piraino, *Inorg. Chim. Acta*, 1994, **223**, 145.
40. R. Longhi and R. S. Drago, *Inorg. Chem.*, 1965, **4**, 11.
41. J. K. Eberhardt, R. Frohlich and E.-U. Wurthwein, *J. Org. Chem.*, 2003, **68**, 6690.
42. R. G. S. Berlinck, *Nat. Prod. Rep.*, 1996, 377.
43. Z. B. Maksic and B. Kovacevic, *J. Org. Chem.*, 2000, **65**, 3303-3309.
44. P. J. Bailey and S. Pace, *Coord. Chem. Rev.*, 2001, **214**, 91.

45. K. A. Schug and W. Lindner, *Chem. Rev.*, 2005, **105**, 67-113.
46. S. Pohl, M. Harmjanz, J. Schneider, W. Saak and G. Henkel, *J. Chem. Soc., Dalton Trans.*, 2000, 3473-3479.
47. V. Raab, J. Kipke, R. M. Gschwind and J. Sundermeyer, *Chem. Eur. J.*, 2002, **8**, 7.
48. M. P. Coles, P. J. Aragon-Saez, S. H. Oakley, P. B. Hitchcock, M. G. Davidson, Z. B. Maksic, R. Vianello, I. Leito, I. Kaljurand and D. C. Apperley, *J. Am. Chem. Soc.*, 2009, **131**, 16858-16868.
49. S. Pohl, M. Harmjanz, J. Schneider, W. Saak and G. Henkel, *Inorg. Chim. Acta*, 2000, **311**, 106-112.
50. S. Herres-Pawlis, A. Neuba, O. Seewald, T. Seshadri, H. Egold, U. Florke and G. Henkel, *Eur. J. Org. Chem.*, 2005, 4879-4890.
51. S. H. Oakley, M. P. Coles and P. B. Hitchcock, *Inorg. Chem.*, 2003, **42**, 3154-3156.
52. S. H. Oakley, M. P. Coles and P. B. Hitchcock, *Inorg. Chem.*, 2004, **43**, 5168-5170.
53. S. H. Oakley, D. B. Soria, M. P. Coles and P. B. Hitchcock, *J. Chem. Soc., Dalton Trans.*, 2004, 537-546.
54. R. S. Drago and R. Longhi, *Inorg. Chem.*, 1965, **4**, 11.
55. P. J. Bailey, K. J. Grant, S. Pace, S. Parsons and L. J. Stewart, *J. Chem. Soc., Dalton Trans.*, 1997, 4263-4266.
56. H. Wittmann, V. Raab, A. Schorm, J. Plachmeyer and J. Sundermeyer, *Eur. J. Inorg. Chem.*, 2001, 1937-1948.
57. M. P. Coles, *Chem. Commun.*, 2009, 3659-3676.
58. S. Herres-Pawlis, P. Verma, R. Haase, P. Kang, C. T. Lyons, E. C. Wasinger, U. Florke, G. Henkel and T. D. P. Stack, *J. Am. Chem. Soc.*, 2009, **131**, 1154-1169.
59. W.-X. Zhang and Z. Hou, *Org. Biomol. Chem.*, 2008, **6**, 1720-1730.
60. M. P. Coles and P. B. Hitchcock, *Eur. J. Inorg. Chem.*, 2004, 2662.
61. R. E. Boéré, R. T. Boéré, J. Masuda and G. Wolmershauser, *Can. J. Chem.*, 2000, **78**, 1613.
62. U. Köhn, W. Günther, H. Görls and E. Anders, *Tetrahedron: Asymmetry*, 2004, **15**, 1419.
63. K. Kincaid, C. P. Gerlach, G. R. Giesbrecht, J. R. Hagadorn, G. D. Whitener, A. Shafir and J. Arnold, *Organometallics*, 1999, **18**, 5360.

64. F. A. Cotton, P. Lei, C. A. Murillo and L.-S. Wang, *Inorg. Chim. Acta*, 2003, **349**, 165.
65. W. Schneider, A. Bauer, A. Schier and H. Schmidbaur, *Chem. Ber.*, 1997, **130**, 1417.
66. W. P. Fehlhammer, R. Metzner and W. Sperber, *Chem. Ber.*, 1994, **127**, 829.
67. E. M. A. Ratilla and N. M. Kostic, *J. Am. Chem. Soc.*, 1988, **110**, 4427.
68. J. A. Bertke and S. D. Bunge, *Dalton Trans.*, 2007, 4647-4649.
69. S.-H. Li, H.-B. Xie, S.-B. Zhang, Y.-J. Lin, J.-N. Xu and J.-G. Cao, *Synlett*, 2005, **12**, 1885.
70. S.-H. Li, Y.-J. Lin, H.-B. Xie, S.-B. Zhang and J.-N. Xu, *Org. Lett*, 2006, **8**, 391.
71. S.-H. Li, Y.-J. Lin, J.-G. Cao and S.-B. Zhang, *J. Org. Chem.*, 2007, **72**, 4067-4072.
72. S. D. Bunge, J. M. Lance and J. A. Bertke, *Organometallics*, 2007, **26**, 6320-6328.
73. M. L. Simms, J. L. Atwood and D. A. Zlatko, *J. Chem. Soc., Chem. Commun.*, 1973, 46.
74. D. Sen and C. Saha, *J. Chem. Soc., Dalton Trans.*, 1976, 776.
75. N. Kuhn, M. Grathwohl, M. Steimann and G. Henkel, *Z. Naturforsch., B*, 1998, **53**, 997-1003.
76. H. Wittmann, A. Schorm and J. Sundermeyer, *Z. Anorg. Allg. Chem.*, 2000, **626**, 1583-1590.
77. D. Domide, C. Neuhauser, E. Kaifer, H. Wadepohl and H. Himmel, *Eur. J. Inorg. Chem.*, 2009, 2170-2178.
78. A. Peters, U. Wild, O. Hubner, E. Kaifer and H. Himmel, *Chem. Eur. J.*, 2008, **14**, 7813-7821.
79. V. Raab, J. Kipke, O. Burghaus and J. Sundermeyer, *Inorg. Chem.*, 2001, **40**, 6964-6971.
80. C. Wurtele, E. Gaoutchenova, K. Harms, M. C. Holthausen, J. Sundermeyer and S. Schindler, *Angew. Chem. Int. Ed.*, 2006, **45**, 3867-3869.
81. D. Maiti, D. Lee, K. Gaoutchenova, C. Wurtele, M. C. Holthausen, A. A. N. Sarjeant, J. Sundermeyer, S. Schindler and K. D. Karlin, *Angew. Chem. Int. Ed.*, 2008, **47**, 82-85.

82. J. England, M. Martinho, E. R. Farquhar, J. R. Frisch, E. L. Bominaar, E. Münck and L. Que Jr., *Angew. Chem. Int. Ed.*, 2009, **48**, 3622-3626.
83. F. A. Cotton, C. A. Murillo, X. Wang and C. C. Wilkinson, *Inorg. Chem.*, 2006, **45**, 5493-5500.
84. F. A. Cotton, C. A. Murillo, X. Wang and C. C. Wilkinson, *Dalton Trans.*, 2006, 4623-4631.
85. M. P. Coles and P. B. Hitchcock, *Polyhedron*, 2001, **20**, 3027-3032.
86. S. H. Oakley, M. P. Coles and P. B. Hitchcock, *Inorg. Chem.*, 2004, **43**, 7564-7566.
87. S. H. Oakley, D. B. Soria, M. P. Coles and P. B. Hitchcock, *Polyhedron*, 2006, **25**, 1247-1255.
88. F. A. Cotton, C. A. Murillo and D. J. Timmons, *Polyhedron*, 1999, **18**, 423-428.
89. M. P. Coles and P. B. Hitchcock, *Chem. Commun.*, 2005, 3165-3167.
90. U. Wild, P. Roquette, E. Kaifer, J. Mautz, O. Hubner, H. Wadepl and H. Himmel, *Eur. J. Inorg. Chem.*, 2008, 1248-1257.
91. F. A. Cotton, J. P. Donahue, N. E. Gtuhn, D. L. Lichtenberger, C. A. Murillo, D. J. Timmons, L. O. Van Dorn, D. Villagran and X. Wang, *Inorg. Chem.*, 2006, **45**, 201-213.
92. J. F. Berry, F. A. Cotton, P. Huang, C. A. Murillo and X. Wang, *Dalton Trans.*, 2005, 3713-3715.
93. A. J. Arduengo III, R. L. Harlow and M. Kline, *J. Am. Chem. Soc.*, 1991, **113**, 361.
94. H. Clavier and S. P. Nolan, *Annu. Rep. Prog. Chem. Sect. B*, 2007, **103**, 193-222.
95. A. J. Boydston, K. A. Williams and C. W. Bielawski, *J. Am. Chem. Soc.*, 2005, **127**, 12496-12497.
96. M.-L. Teyssot, A.-S. Jarrousse, M. Manin, A. Chevry, S. Roche, F. Norre, C. Beaudoin, L. Morel, D. Boyer, R. Mahiou and A. Gautier, *Dalton Trans.*, 2009, 6894-6902.
97. N. Kuhn and A. Al-Sheikh, *Coord. Chem. Rev.*, 2005, **249**, 829-857.
98. A. Diefenbach and F. M. Bickelhaupt, *Z. Anorg. Allg. Chem.*, 1999, **625**, 892.
99. K. Dehnicke and A. Greiner, *Angew. Chem. Int. Ed.*, 2003, **42**, 12.

100. D. W. Stephan, J. C. Stewart, F. Guerin, S. Courtenay, J. Kickham, E. Hollink, C. Beddie, A. Hoskin, T. Graham, P. Wie, R. E. v. H. Spence, W. Xu, L. Koch, X. Gao and D. G. Harrison, *Organometallics*, 2003, **22**, 1937.
101. N. L. S. Yue and D. W. Stephan, *Organometallics*, 2001, **20**, 2303.
102. D. W. Stephan, J. C. Stewart, R. E. v. H. Spence, L. Koch, X. Gao, S. J. Brown, J. W. Swabey, Q. Wang, W. Xu, P. Zoricak and D. G. Harrison, *Organometallics*, 1999, **18**, 2046.
103. D. W. Stephan, J. C. Stewart, F. Guerin, R. E. v. H. Spence, W. Xu and D. G. Harrison, *Organometallics*, 1999, **18**, 1116.
104. N. Kuhn, M. Gohner, M. Grathwohl, J. Wiethoff, G. Frenking and Y. Chen, *Z. Anorg. Allg. Chem.*, 2003, **629**, 793.
105. N. Kuhn, R. Fawzi, M. Steinmann and J. Wiethoff, *Z. Anorg. Allg. Chem.*, 1997, **623**, 769.
106. N. Kuhn, R. Fawzi, M. Steinmann, J. Wiethoff, D. Blaser and R. Boese, *Z. Naturforsch., B*, 1995, **50**, 1779.
107. M. Tamm, S. Randoll, T. Bannenberg and E. Herdtweck, *Chem. Commun.*, 2004, 876-877.
108. M. Tamm, S. Beer and E. Herdtweck, *Z. Naturforsch., B: Chem. Sci.*, 2004, **59**, 1497-1504.
109. M. Tamm, S. Randoll, E. Herdtweck, N. Kleigrewe, G. Kehr, G. Erker and B. Rieger, *Dalton Trans.*, 2006, 459-467.
110. S. Beer, C. G. Hrib, P. G. Jones, K. Brandhorst, J. Grunenberg and M. Tamm, *Angew. Chem. Int. Ed.*, 2007, **46**, 8890-8894.
111. D. Petrovic, L. M. R. Hill, P. G. Jones, W. B. Tolman and M. Tamm, *Dalton Trans.*, 2008, 887-894.
112. D. Petrovic, C. G. Hrib, S. Randoll, P. G. Jones and M. Tamm, *Organometallics*, 2008, **27**, 778-783.
113. D. Petrovic, T. Gloge, T. Bannenberg, C. G. Hrib, S. Randoll, P. G. Jones and M. Tamm, *Eur. J. Inorg. Chem.*, 2007, 3472-3475.
114. D. Petrovic, T. Bannenberg, S. Randoll, P. G. Jones and M. Tamm, *Dalton Trans.*, 2007, 2812-2822.

115. S. Randoll, P. G. Jones and M. Tamm, *Organometallics*, 2008, **27**, 3232-3239.
116. N. Kuhn, M. Grathwohl, C. Nachtigal and M. Steimann, *Z. Naturforsch., B*, 2001, **56**, 704.
117. J. Borner, U. Florke, T. Gloge, T. Bannenberg, M. Tamm, M. D. Jones, A. Doring, D. Kuckling and S. Herres-Pawlis, *J. Mol. Catal. A: Chem.*, 2010, **316**, 139-145.
118. T. K. Panda, C. G. Hrib, P. G. Jones, J. Jenter, P. W. Roesky and M. Tamm, *Eur. J. Inorg. Chem.*, 2008, 4270-4279.
119. T. K. Panda, D. Petrovic, T. Bannenberg, C. G. Hrib, P. G. Jones and M. Tamm, *Inorg. Chim. Acta*, 2008, **361**, 2236-2242.
120. T. Gloge, D. Petrovic, C. Hrib, P. G. Jones and M. Tamm, *Eur. J. Inorg. Chem.*, 2009, 4538-4546.
121. T. Osako, K. D. Karlin and S. Itoh, *Inorg. Chem.*, 2005, **44**, 410-415.
122. R. Poli, *Chem. Rev.*, 1996, **96**, 2135.
123. M. L. H. Green and D. K. P. Ng, *Chem. Rev.*, 1995, **95**, 439.
124. K. H. Theopold, *Eur. J. Inorg. Chem.*, 1998, 15.
125. M. E. Doster and S. A. Johnson, *Angew. Chem. Int. Ed.*, 2009, **48**, 2185-2187.
126. E. A. B. Kantchev, C. J. O'Brien and M. G. Organ, *Angew. Chem. Int. Ed.*, 2007, **46**, 2768.

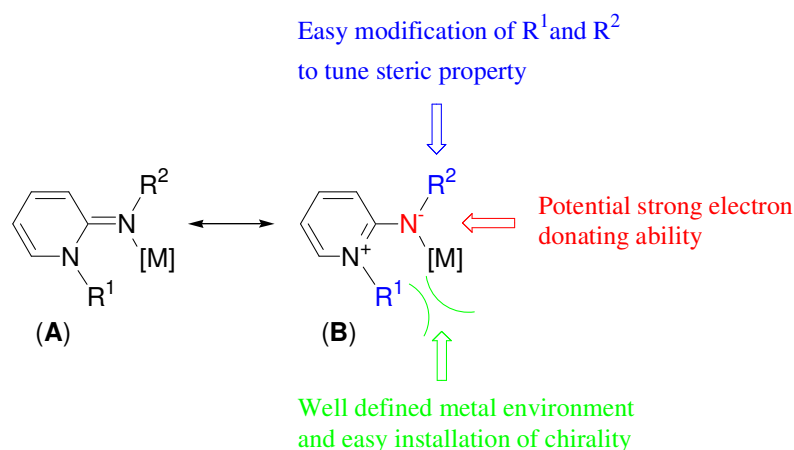
2.0 Synthesis of 1H-pyridin-(2E)-ylidenes (PYE) ligands

2.1 Introduction

During past decades, transition metal complexes have contributed enormously to a wide range of chemical and biological areas. A variety of ancillary ligands have been developed, with a wide range of stereoelectronic properties for use in catalysis, therapeutic and diagnostic medicine, biomimetics and molecular devices. Of the large array of different ligands coordinating to a metal centre the vast majority are drawn from a few *p*-block elements including C, N, O, S and P, with arguably nitrogen donor ligands having the greatest diversity across synthetic and biological chemistry. However, there is still a constant demand for new ligand systems to overcome identified challenges and develop new chemical processes.

Inspired by the versatile coordination behaviour and interesting properties of nitrogen ligands, in particular robust catalytic activity¹⁻⁴ and extensive biological properties,⁵ we decided to exploit new potential nitrogen donor ligands. A potentially interesting class of molecules that we identified are based on the 1H-pyridin-(2E)-ylidene (PYE) motif (Scheme 2-1). We perceived there to be several interesting features with respect to steric and electronic influence as follows:

- (i) a library of structural analogues can be easily accessible based on the PYE motif;
- (ii) a well-defined steric environment with respect to the metal centre can be achieved by introducing variable steric bulk at the R¹ and R² groups and because rotation is restricted about the double bond of the imine moiety;
- (iii) strong donation due to a contribution of the pyridinium–amido resonance (**B**) structure to the metal–ligand bond.

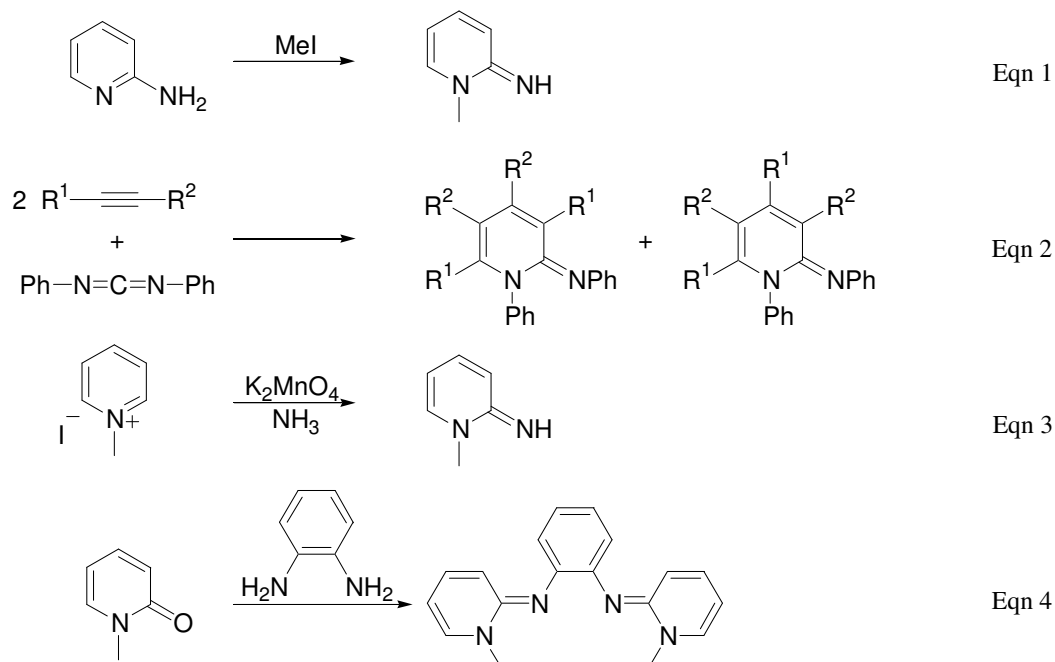


Scheme 2-1. Possible resonance structures of the 1H-pyridin-(2E)-ylidene motif on coordination to a metal fragment.

Before the commencement of this research, PYE-type compounds had been known for over 80 years.⁶ Since then, their organic and biological chemistry⁷⁻¹⁷ and spectroscopy¹⁸⁻²² have been studied, whereas there was only one report describing the coordination chemistry of a single PYE derivative.²³

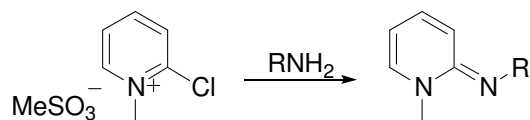
Although limited, there are several reported different methods for the preparation of 1H-pyridin-(2E)-ylidenes (PYEs). The first example of a PYE motif was reported by Tschitschibabin *et al.*⁶ in 1921, using methylation of 2-aminopyridine with methyl iodide to yield N-methyl-2-pyridoneimide (Eqn 1, Scheme 2-2). This N-alkylation of 2-aminopyridine method was proved later to be unselective.⁷ After a few decades, a cyclotrimerisation methodology was discovered by Hong *et al.*⁸ using two equivalents of an acetylene and one equivalent of a carbodiimide (Eqn 2, Scheme 2-2). Although this methodology was developed by several groups^{10-13, 16} and occurs under mild conditions with a good chemo- and regioselectivity, substrate scope and unconventional reactors limited its general synthetic application. In 1986, Buurman *et al.*²⁴ reported a new method derived from imination of *N*-methylpyridinium salts in the presence of liquid ammonia and potassium permanganate (Eqn 3, Scheme 2-2), but the yield was poor. In 2003, the first and also the only chelating PYE ligand before we started this research was reported from reaction between pyridone and *o*-phenylene diamine by Gaur *et al.*²³ (Eqn 4, Scheme 2-2), although no characterising data was presented and our attempts to repeat this reaction failed.

Unfortunately, all of these routes are generally incompatible with the synthesis of compounds containing multiple PYE motifs selectively and therefore in high yield.



Scheme 2-2. Various routes to PYE motif.

An alternative route which derives from the imination of 2-chloro pyridinium salts in the presence of a base was reported by Tanaka *et al.*²⁵ in 1976 (Scheme 2-3). It was found that the 2-chloro pyridinium ion is sufficiently activated to undergo nucleophilic aromatic substitution by an addition-elimination mechanism due to the presence of the quaternary nitrogen atom in the aromatic ring.²⁶ Compared with other routes shown in Scheme 2-2, we thought this method to PYE ligands should give easy access to target compounds in good yield. Furthermore, the synthetic method can be modular and generate various members of a ligand family using the same reaction by varying the combination of starting materials including multiple stereocentres using a variety of different chiral amines.¹



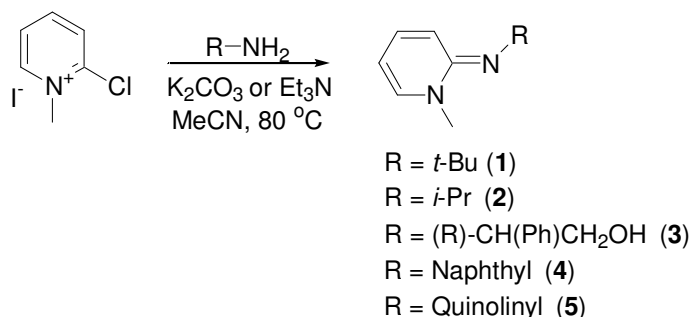
Scheme 2-3. Imination of 2-chloro pyridinium salt.

2.2 Synthesis and characterisation of mono- and bidentate 1H-pyridin-(2E)-ylidenes (PYE) ligands

A modified procedure from the route described in Scheme 2-3 was found to be straightforward and to generally give good yield. Reaction between 2-chloro pyridinium salts and primary amines in the presence of a base in acetonitrile at 80 °C gave access to a range of substitution patterns. In this chapter, we will discuss mono- and bidentate types of PYE ligands.

2.2.1 Monodentate PYE ligands

Applying the modified procedure to the synthesis of monodentate PYE ligands, a variety of substituent groups can be incorporated into the PYE motif as shown in Scheme 2-4. 2-Chloro-1-methyl pyridinium iodide was selected as a starting material because it is commercially available and inexpensive. Compounds **1-5** were isolated in high yield (75-93 %) as a hygroscopic, yellow oil for **1-2**, a yellow solid for **3-4** and a dark brown solid for **5** respectively. Compounds **1-2** are soluble in most organic solvents. **3-5** are quite soluble in chlorinated solvents, alcoholic solvents, THF and acetonitrile but poor in ether and aromatic solvents.



Scheme 2-4. Synthetic route to monodentate PYE ligands.

Compounds **1-5** were characterised by NMR spectroscopy, mass spectrometry and elemental analysis and all the data is consistent with the proposed formulations. The ¹H and ¹³C assignments are based on NoeSY, ¹H-¹H COSY and ¹³C HSQC experiments. The ¹H NMR spectra of **1-5** all showed a set of distinctive signals derived from the PYE moiety and other signals from the R groups (Scheme 2-4). Taking compound **2** as a representative

example and using the numbering scheme shown in Figure 2-1, the ^1H NMR spectra of **2** in CDCl_3 shows a set of signals for the PYE moiety at δ 3.23 (NCH_3), 5.45 (H^4), 6.31 (H^2), 6.75 (H^3) and 6.87 ppm (H^5), and the ^{13}C NMR shows δ 39.0 (NCH_3), 99.5 (C^4), 112.1 (C^2), 134.0 (C^3), 139.0 (C^5), 151.8 (C^1) ppm respectively. The ^1H and ^{13}C NMR chemical shifts of PYE moiety of compounds **1-5** are given in Table 2-1.

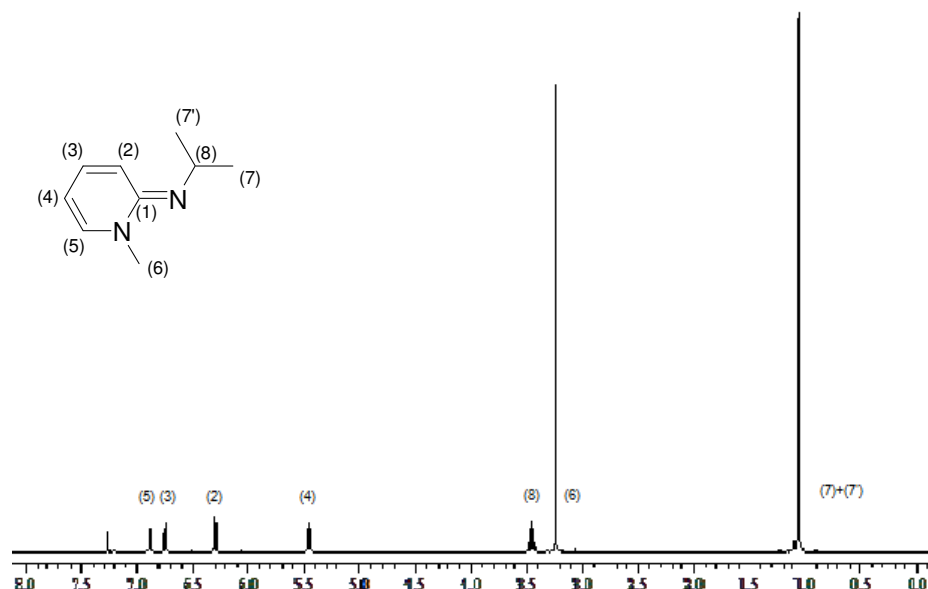
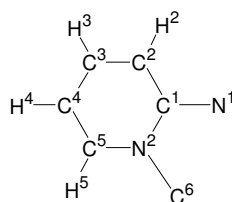


Figure 2-1. ^1H NMR spectrum of **2** in CDCl_3 and the numbering scheme of **2**.

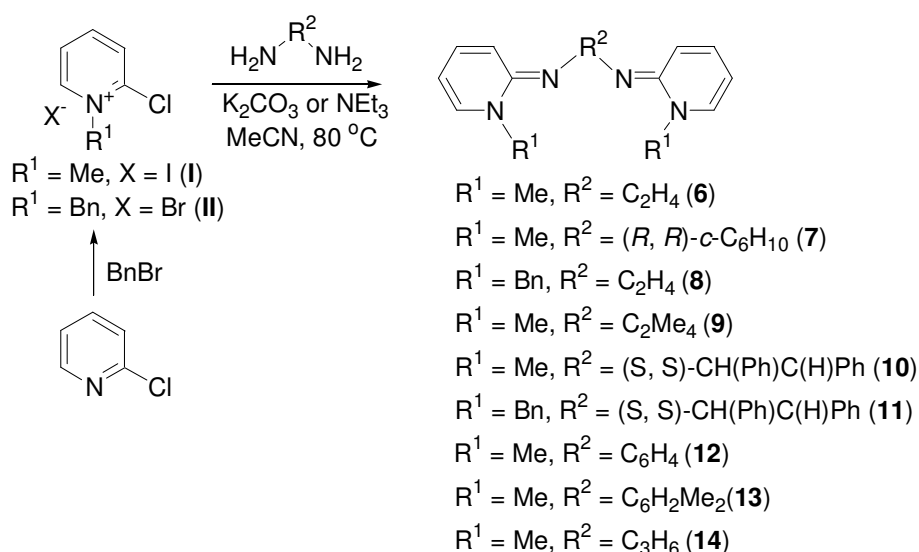
Table 2-1 The ^1H and ^{13}C NMR chemical shifts (ppm) of PYE moiety of **1-5**.



	NCH_3	H^2	H^3	H^4	H^5	NCH_3	C^1	C^2	C^3	C^4	C^5
1	3.27	6.42	6.73	5.48	6.97	39.6	150.4	115.6	133.1	99.0	139.8
2	3.23	6.31	6.75	5.45	6.87	39.0	151.8	112.1	134.0	99.5	139.0
3	3.49	6.14	6.79	5.66	7.05	39.7	155.2	113.6	135.3	101.6	138.9
4	3.68	6.20	6.79	5.76	7.12	40.2	153.0	114.3	135.7	103.4	138.8
5	3.78	6.20	6.87	5.94	7.26	41.1	153.4	115.1	136.3	105.5	139.2

2.2.2 Bidentate PYE ligands

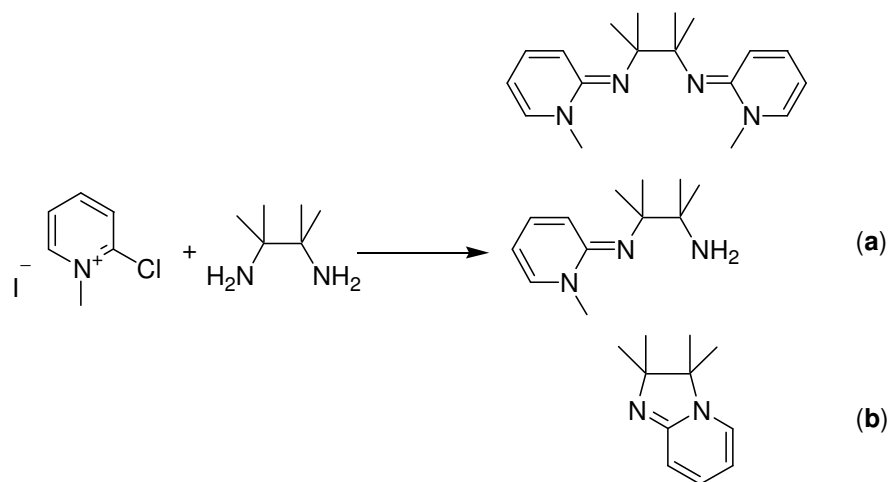
Considering that bidentate nitrogen ligands have been applied extensively, in particular to homogeneous catalysis,¹⁻⁴ we decided to develop bidentate PYE ligands (Scheme 2-5) from 2-chloro-1-methyl pyridinium iodide (**I**). Another pyridinium salt, 2-chloro-1-benzyl pyridinium bromide (**II**) was prepared by a one-step reaction between benzyl bromide and 2-chloro pyridine.²⁷ A variety of chiral and achiral diamines were selected, thus enabling the modification on the backbone of PYE ligands to tune the steric and electronic effect at the metal centre, which will be discussed further in Chapter 3.



Scheme 2-5. Synthetic route to bidentate PYE ligands.

Initially, potassium carbonate, which can be removed easily after a reaction by filtration, was used as the base for synthesis of compounds **1-3**, **6-8**, and **12-13**. However, attempts to synthesise ligand **9** were problematic suffering from long reaction times and low yields and significant by-product formation, including (**a**) and cyclisation by-product (**b**) as shown in Scheme 2-6. Potentially, problems occurred because the solubility of potassium carbonate in organic solvents is poor leading to slow deprotonation, therefore triethyl amine was used because it can be easily removed under reduced pressure and is miscible with acetonitrile. Comparatively, a shorter reaction time, good yield and easy work-up (recrystallization) were possible. This method was utilized for ligands **4-5**, **9-11** and **14** where good yields are obtained in 66 – 92 %. Apart from **6** which shows poor solubility in all organic solvents, all the other compounds **7-14** are quite soluble in

chlorinated, alcoholic solvents, THF and acetonitrile, but poor in hydrocarbon, aromatic solvents and water.



Scheme 2-6. Products resulting from synthesis of ligand **9** using potassium carbonate as base determined by ^1H NMR spectroscopy.

All the compounds were characterised by elemental analysis, mass spectrometry and ^1H and ^{13}C NMR spectroscopy and in select cases single crystal X-ray diffraction. The ^1H and ^{13}C assignments are based on NoeSY, ^1H - ^1H COSY and ^{13}C HSQC experiments. A set of symmetrical signals were shown in NMR spectra indicating C_2 symmetry of bidentate PYE ligands. Taking compound **8** as a representative example and using the numbering scheme shown in Figure 2-2, ^1H NMR spectroscopy shows distinctive signals for the PYE moiety at 5.46 (H^4), 6.45 (H^2), 6.70 (H^3), and 6.80 (H^5) ppm and corresponding ^{13}C NMR signals at 101.1 (C^4), 113.6 (C^2), 134.3 (C^3), 137.9 (C^5) and 153.3 (C^1) ppm respectively.

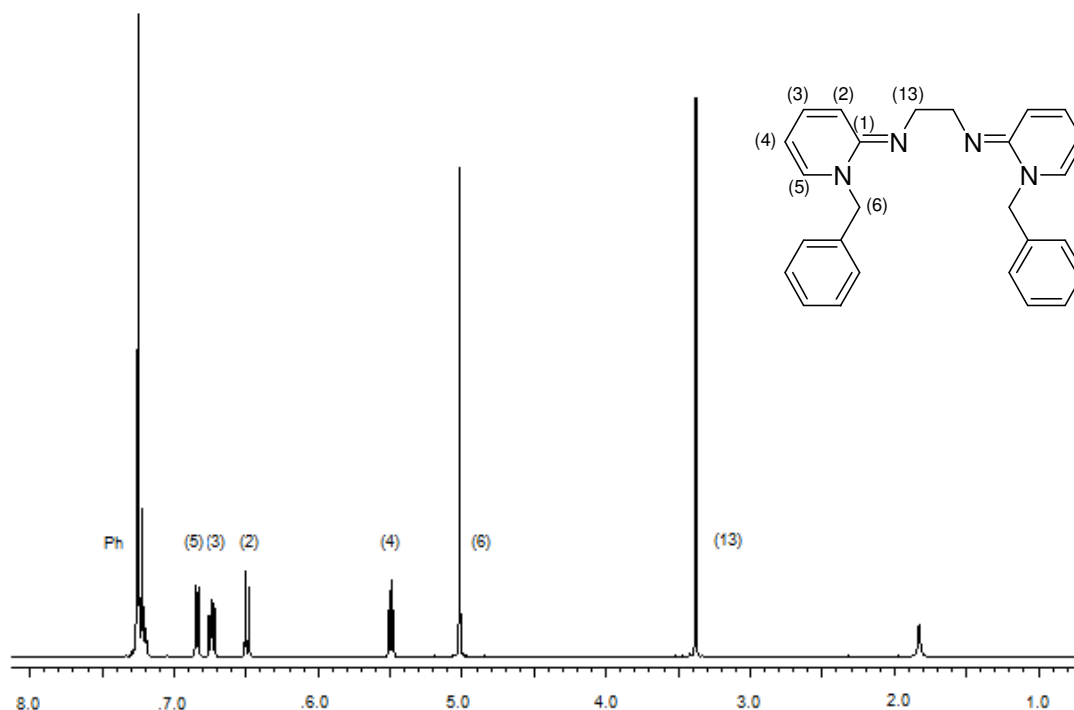


Figure 2-2. ^1H NMR spectrum of compound **8** in CDCl_3 and numbering scheme for compound **8**.

Single crystals of **7** suitable for X-ray diffraction were grown from acetone and diethyl ether. The molecular structure is shown in Figure 2-3 and selected bond lengths and angles are given in Table 2-2. The asymmetric unit contains one half of **7** with coincident crystallographic and molecular C_2 axes. Examination of C-C and C-N bond lengths and comparison with the single crystal X-ray structure of 2-amino pyridine^{28, 29} gives some information regarding the electron distribution of the PYE ligand system (Figure 2-3 and Table 2-2). In 2-aminopyridine, the bond lengths inside and outside the the ring suggest an aromatic structure where all the C-N bonds are ca. 1.345 Å (Figure 2-4), which is a typical $\text{C}(\text{sp}^2)\text{-N}$ bond.³⁰ In contrast, a localised multiple bond structure shown in Scheme 2-5 is a good representation for **7** (and for all PYE compounds), where for example C(1)-C(2) and C(2)-C(3) are 1.4496(16) and 1.3527(16) Å respectively and the exo-imine bond C(1)-N(1) = 1.2960(15) Å. The atoms about the C(1)-N(1) bond are also essentially planar with planes defined by C(2)-C(1)-N(2) and C(7)-N(1)-C(1) only ca. 6.5° from coplanarity. The lone pairs of electrons on atoms N(1) and N(1') are pointing in opposite directions.

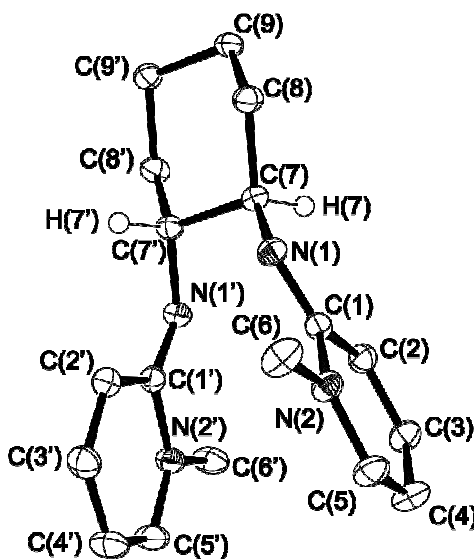


Figure 2-3. Molecular structure of compound 7. Ellipsoids are shown at 50 % probability. Hydrogen atoms have been removed for clarity.

Table 2-2. Selected bond lengths (Å) and angles (°) for compound 7.

bond	lengths (Å)	bond	angles (°)
C(1) – N(1)	1.2960(15)	C(1) – N(1) – C(7)	119.29(9)
C(1) – C(2)	1.4496(16)	C(2) – C(1) – N(1)	113.83(10)
C(2) – C(3)	1.3527(16)	C(1) – N(2) – C(5)	122.70(10)
C(1) – N(2)	1.4078(14)	C(2) – C(1) – N(1) – C(7)	6.60(18)

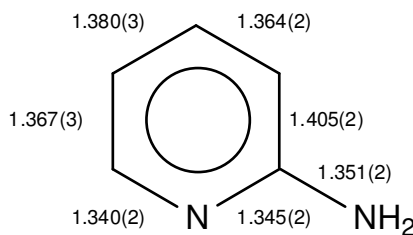


Figure 2-4. Bond lengths (Å) in 2-aminopyridine.

Single crystals of **12** suitable for X-ray diffraction were also grown from acetone and diethyl ether. The molecular structure is shown in Figure 2-5 and selected bond lengths and angles are given in Table 2-3. In the solid state the compound does not exhibit C_2 symmetry. For example, the planes defined by C(2)-C(1)-N(2) and C(8)-C(7)-N(1) give ca. 88.08° from coplanarity, whereas the planes defined by C(14)-C(13)-N(4) and C(8)-C(7)-

N(1) give a significant different angle ca. 60.35 °. Furthermore, the bond lengths of the aryl ring reflect electrons that are delocalised, whereas the PYE moieties exhibit bond lengths indicative of a localised system. There is no structural evidence for conjugation between the PYE and phenyl groups. Comparison of bond lengths between **7** and **12** within the PYE ring and exo imine does not show any significant differences.

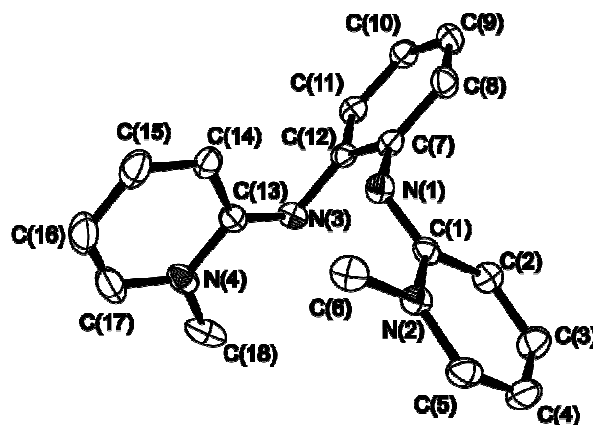


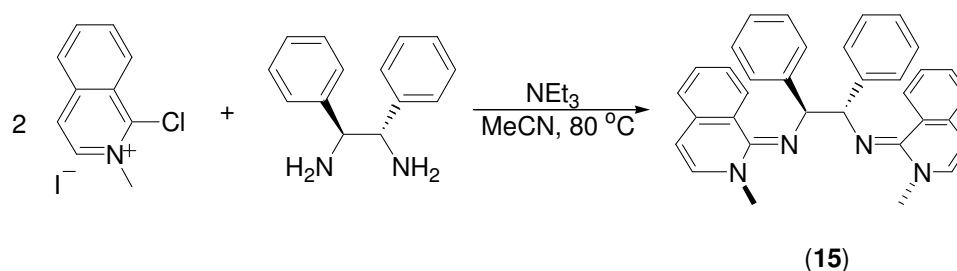
Figure 2-5. Molecular structure of compound **12**. Ellipsoids are shown at 50 % probability. Hydrogen atoms have been removed for clarity.

Table 2-3. Selected bond lengths (Å) and angles (°) for compound **12**.

bond	lengths (Å)	bond	angles (°)
C(1) – N(1)	1.2960(17)	C(1) – N(1) – C(7)	118.25(11)
C(1) – C(2)	1.4371(18)	C(2) – C(1) – N(1)	128.11(12)
C(2) – C(3)	1.3547(19)	C(1) – N(2) – C(5)	122.32(12)
C(1) – N(2)	1.4012(16)	N(1) – C(7) – C(8) – C(9)	175.68(12)
C(13) – N(3)	1.2997(17)	C(1) – N(1) – C(7) – C(8)	87.13(15)
C(7) – N(1)	1.4161(16)		

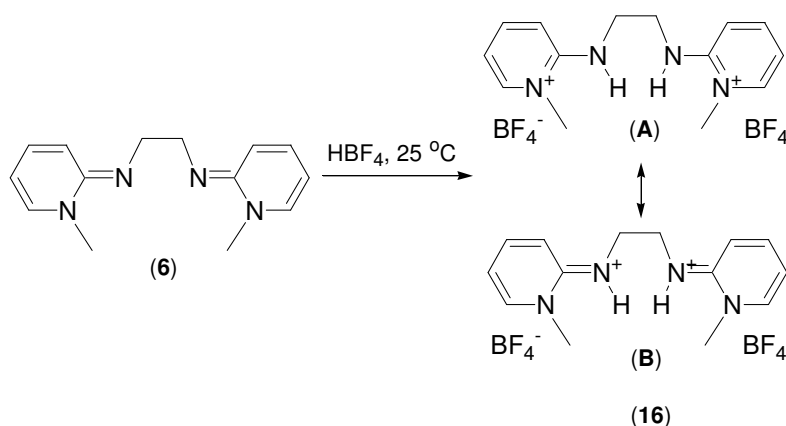
Importantly, compounds **1-14** all show single *E*-isomer conformation and there is no evidence for rotation or significant libration about the exocyclic C-N bond in any of the compounds at the temperatures studied. It appears the observed *E*-isomer is thermodynamically dominant, presumably for steric reasons. To study the steric tolerance and whether the *Z*-isomer exists, an analogue **15** with more bulky isoquinolin group and biphenyl ethylene backbone was prepared using similar condition as for **1-14** (Scheme 2-7).

The ESI mass spectrum of **15** recorded in positive-ion mode contains a strong peak at m/z 495.2 due to the $[M+H]^+$ ion. The ^1H NMR spectrum of **15** shows a single set of symmetrical signals indicating formation of only one isomer. There is no correlation between either isoquinolin or *N*-methyl and phenyl protons in NoeSY experiment. At this stage, it is not clear if **15** is the *E* or *Z* isomer. This work was conducted at the end of project and due to lack of time, further investigation will be carried out in the group at a later stage.



Scheme 2-7. Synthetic route to bulky isoquinolin analogue **15**.

As one of aims of this project, in order to understand electronic and structural features of PYE containing complexes and identify potential decomposition products, the protonation of PYE compounds was examined. Addition of 2 equivalents of acid gave similar behaviour and spectroscopic data but to date only single crystals of protonated **6** have been obtained as compound **16**. Addition of two equivalents of $\text{HBF}_4 \cdot \text{Et}_2\text{O}$ to **6** gave **16** (Scheme 2-8) that could be recrystallised as the bromide salt from methanol as colourless crystals. The molecular structure is shown in Figure 2-6 and selected bond lengths and angles are given in Table 2-4.



Scheme 2-8. Synthesis of protonated ligand **16** and possible representations **A** and **B**.

One half of the molecular formula is contained in the asymmetric unit with a methanol molecule of crystallisation for each PYE moiety. Comparison of bond lengths between **7** and **16** within the PYE ring and exo imine show that the significant differences are a lengthening of C(1)-N(1) (0.04 Å) and shortening of C(1)-N(2) (0.03 Å) with little change in the remaining C-C and C-N bonds. The bond lengths C(1)-N(1) = 1.334(4) and C(1)-N(2) = 1.374(4) Å of **16**, and planarity of the atoms about the C(1)-N(2) bond, suggest that representation **B** in Scheme 2-8 is perhaps a more accurate description of the bonding than **A**, which is occasionally presented for these molecules.³¹

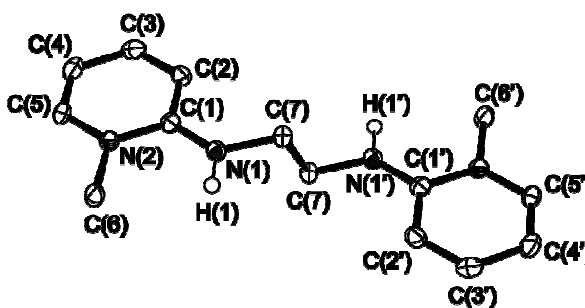


Figure 2-6. Molecular structure of compound **16**. Ellipsoids are shown at 50 % probability. Hydrogen atoms except H(1) and H(1') been removed for clarity.

Table 2-4. Selected bond lengths (Å) and angles (°) for compound **16**.

bond	lengths (Å)	bond	angles (°)
C(1) – N(1)	1.334(4)	C(1) – N(1) – C(7)	124.2(3)
C(1) – C(2)	1.413(4)	C(2) – C(1) – N(1)	123.9(3)
C(2) – C(3)	1.366(5)	C(1) – N(2) – C(5)	121.6(3)
C(1) – N(2)	1.374(4)	C(2) – C(1) – N(1) – C(7)	2.8(5)

Furthermore, the exocyclic C=N bond is very resistant to hydrolysis. Taking compound **6** as an example, no decomposition was observed after **6** was refluxing in D₂O as determined by using ¹H NMR spectroscopy. In addition, there is no occurrence of acid-catalysed *E/Z* isomerisation for the protonated form of PYE ligands, which is a well-known process for imine type compounds.³²

2.3 UV-vis and IR spectroscopic studies of bidentate PYE ligands

As mentioned in section 2.1, PYE type compounds have been studied by UV-vis and IR spectroscopy for many decades, however, previous literature only describes simple monodentate PYE molecules designated as 1-MIP or 1-MPI (1-methyl-2(1H)-pyridinimine) and 2-MIP (1,2-dimethylpyridinimine) as shown in Figure 2-7.¹⁸⁻²¹ There are no descriptions and discussion on the spectroscopic studies of bidentate PYE compounds. In the following, we will report the spectroscopic studies of bidentate PYE compounds, including ultraviolet-visible absorption and infra-red spectroscopy, and compare those with previously reported data.

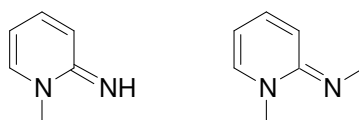


Figure 2-7. The molecular structures of 1-MIP and 2-MIP.

2.3.1 UV-vis absorption studies

Owing to solubility issues and no additional chromophores apart from the PYE moiety, we took compound **7** as a representative example. The UV-vis absorption spectrum of **7** in acetonitrile (Figure 2-8) shows the first prominent absorption centred at about 314 nm extending to approximately 440 nm and a second, stronger absorption with a maximum at about 240 nm. The structure at wavelengths less than 220 nm is due to instrumental artifacts. Beer's law plots were generated at a wavelength of 240 and 314 nm, and the results are shown in Figure 2-9. Compound **7** was found to have a molar absorption coefficient of $\epsilon = 17551 (166) \text{ M}^{-1} \text{ cm}^{-1}$ at 240 nm and $9756 (143) \text{ M}^{-1} \text{ cm}^{-1}$ at 314 nm. The spectrum of 2-MIP recorded in water shows a short-wavelength and a long-wavelength band maximum at approximately the same wavelength, 235 and 312 nm respectively, as for **7**.

In contrast, the UV-vis absorption spectrum of protonated form **16** in acetonitrile (Figure 2-10) is similar to the corresponding spectrum of **7** except that the long-wavelength absorption band exhibits a slight blue-shift to approximately 310 nm. The short-wavelength

band is at approximately the same, 240 nm, as in **7**. This observation is consistent with what Traore *et al.*²¹ found for 1-MIP and 2-MIP that there are no virtually distinguishable absorption spectra between the neutral and protonated form. A molar absorption coefficient of $\epsilon = 20371 (19) \text{ M}^{-1} \text{ cm}^{-1}$ at 240 nm and $13299 (66) \text{ M}^{-1} \text{ cm}^{-1}$ at 310 nm (Figure 2-11) for **16** is significantly higher than **7**, suggesting that electron redistribution occurs on protonation.

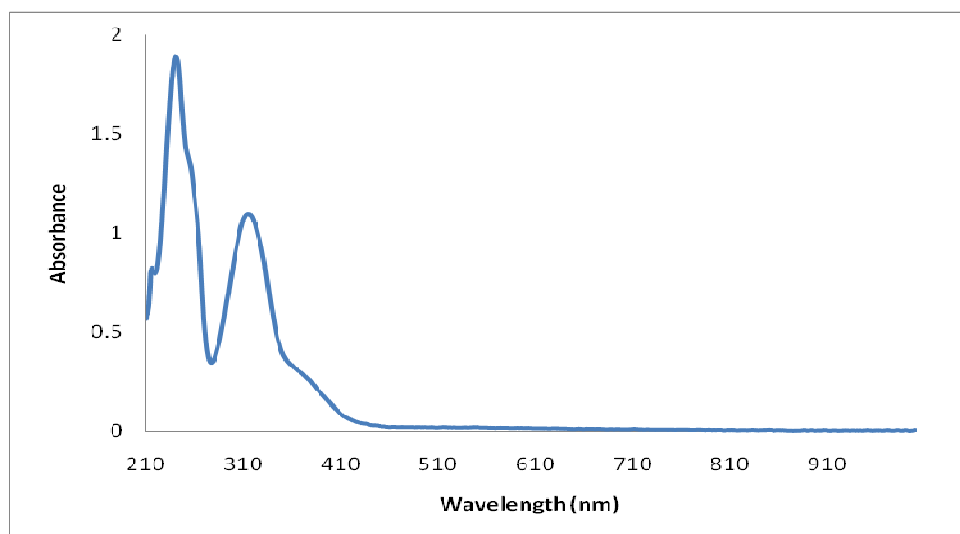


Figure 2-8. UV-vis spectrum of **7** in acetonitrile.

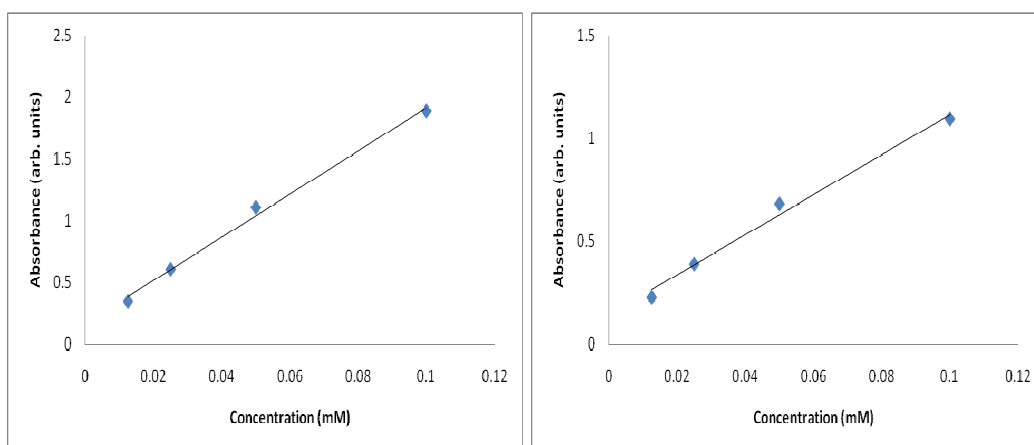


Figure 2-9. Beer's law plots for **7** in acetonitrile at 240 nm (left) and 314 nm (right).

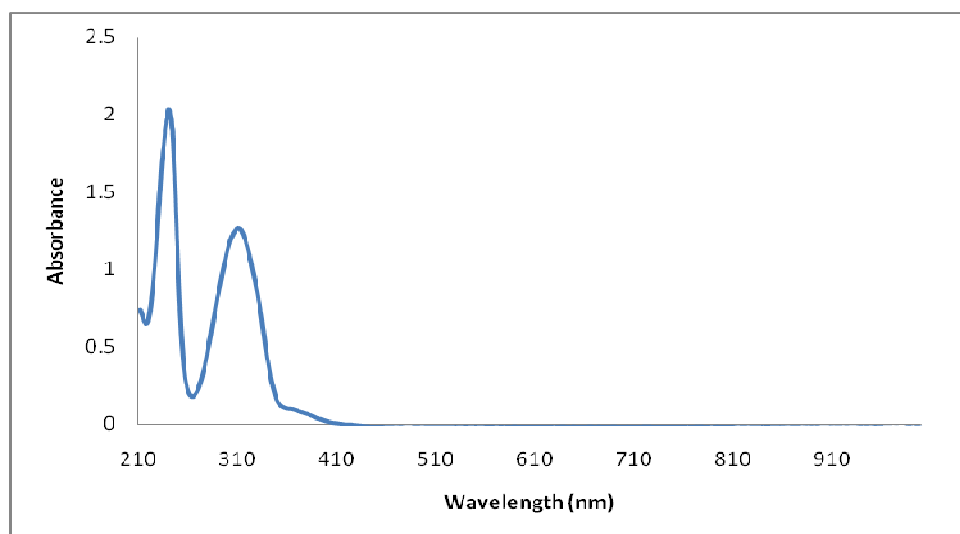


Figure 2-10. UV-vis spectrum of **16** in acetonitrile.

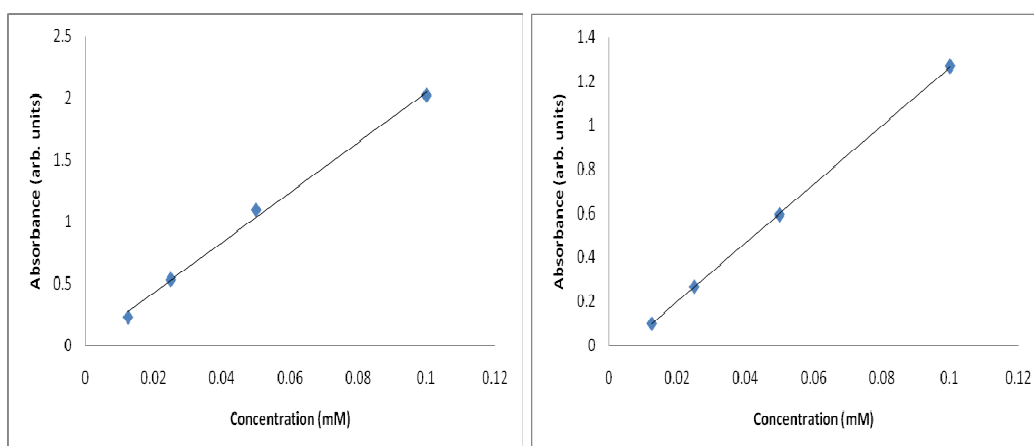


Figure 2-11. Beer's law plots for **16** in acetonitrile at 240 nm (left) and 310 nm (right).

2.3.2 Infra-red studies

Inuzuka and co-workers¹⁸ reported that three prominent strong bands corresponding to C=C group and C=N groups of the PYE moiety are characteristic of the IR spectra of PYE type compounds. For 1-MIP (Figure 2-7), three strong bands at 1647, 1572 and 1533 cm^{-1} in CCl_4 and 1644, 1563 and 1529 cm^{-1} in the neat liquid respectively were observed in the IR spectra. Taking compound **7** and protonated ligand **16** as examples (Figure 2-12), we found three similar strong bands as 1-MIP at 1638, 1575 and 1539 cm^{-1} for **7**, and four strong bands at 1642, 1592, 1555 and 1535 cm^{-1} for **16** in KBr.

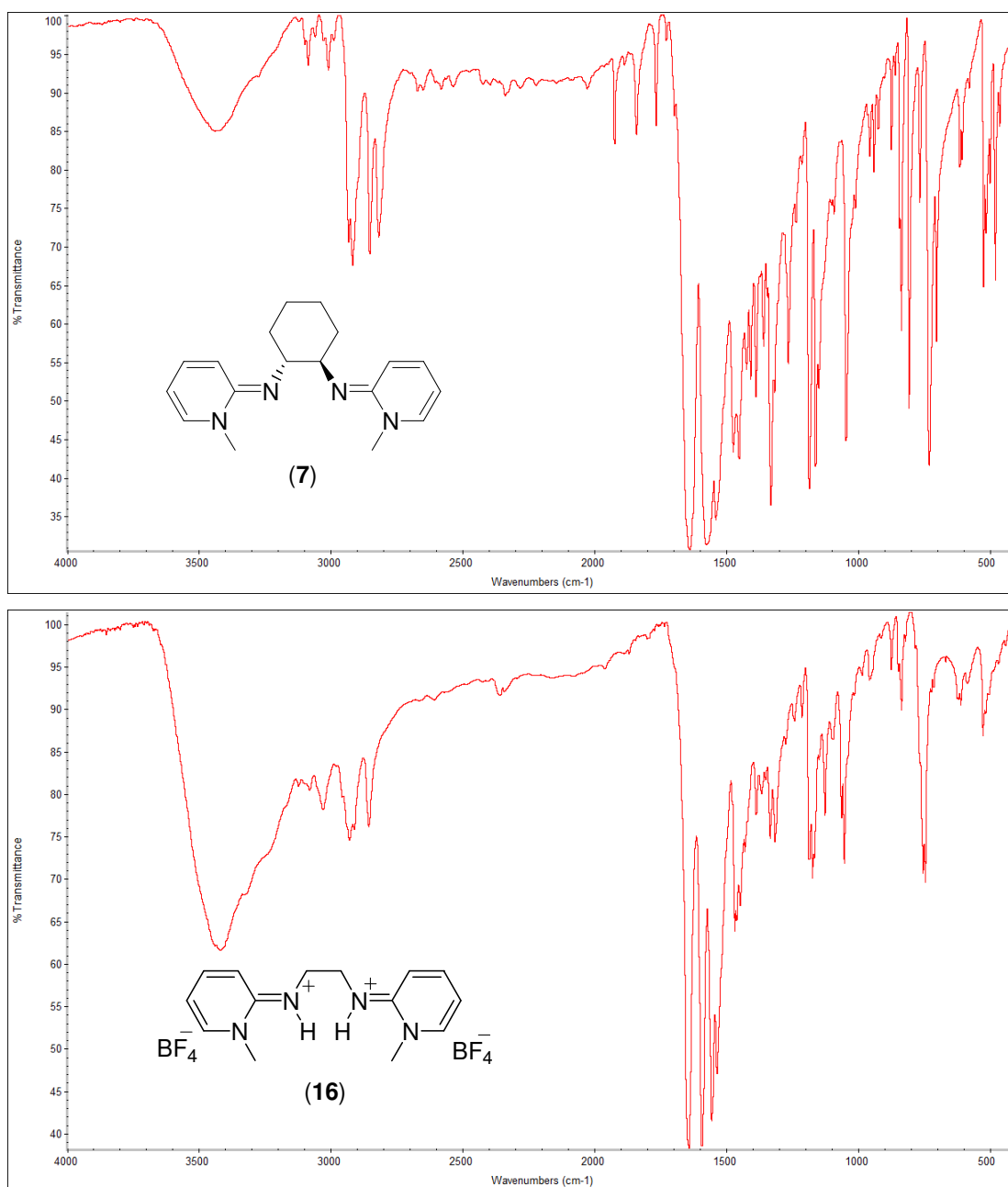


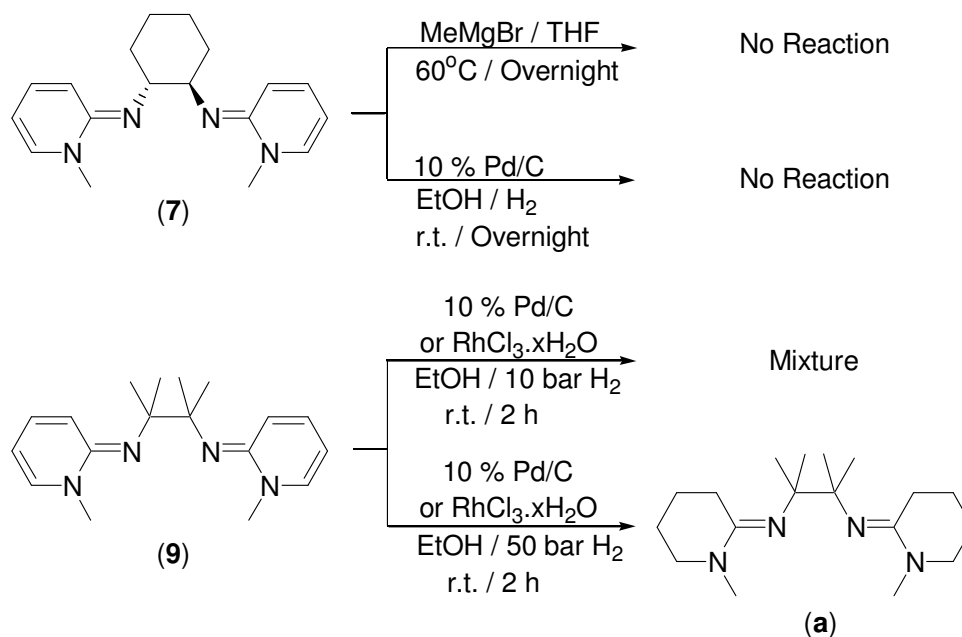
Figure 2-12. IR spectra of compound **7** (above) and protonated ligand **16** (below).

In comparison with three bands attributed to the stretching vibrations of the C=N and C=C bonds of **7**, the appearance of one more band in the IR spectrum of **16** indicates a significant delocalisation change within the heterocycle ring and exocyclic C=N bond.

2.4 Reactivity tests of PYE ligands

Considering the potential future study of PYE compounds and complexes, some reactivity has been explored to determine the stability and possible decomposition routes. Firstly, the reactivity of compound **7** toward the Grignard reagent MeMgBr was tested at 60 °C. According to ¹H NMR spectroscopy, the tolerance of ligand **7** toward Grignard reagents is high and nearly quantitative starting material was recovered without any products of nucleophilic addition (Scheme 2-9).

Secondly, a series of hydrogenation tests were conducted with compound **7** and **9** catalysed by 10 % Pd/C or RhCl₃.xH₂O. Compound **7** was examined using 10 % Pd/C in ethanol at 25 °C (Scheme 2-9). After stirring overnight under 1 atm H₂, no change occurred as judged by ¹H NMR spectroscopy and compound **7** was recovered essentially quantitatively. Furthermore, increasing the pressure of H₂ to 10 bar, an ethanolic solution of compound **9** was stirred for 2 h at room temperature with 10 % Pd/C or RhCl₃.xH₂O. A mixture of starting material and hydrogenated products was detected by ¹H NMR spectroscopy for both conditions. Increasing the pressure of H₂ to 50 bar gave a single hydrogenated product **a** determined by ¹H and ¹³C NMR spectroscopy, and mass spectrometry where a single mass peak 307.2 corresponding to cation [a+H]⁺ was observed. The failure to hydrogenate the exocyclic C=N double bonds is probably due to the steric hindrance of the tetramethyl ethylene group and the heterocyclic rings.



Scheme 2-9. Stability test of compound **7** and **9**.

2.5 NBO calculations for neutral and protonated PYE ligands

To aid the understanding of the electronic properties of PYE ligands, NBO calculation has been conducted by Dr. John Slattery.

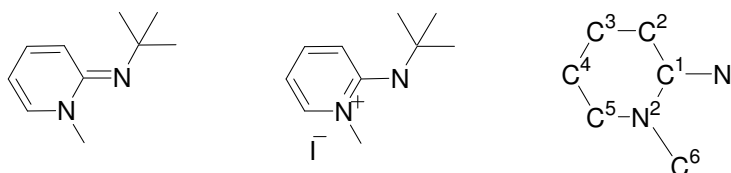


Figure 2-13. PYE compound **1** and its protonated form.

NBO calculations were performed at the PBE1PBE/TZVP level using GAUSSIAN03. For **1** the NBO results are based on the imine resonance form with substantial delocalisation of the N(2) lone pair into the C(1)-N(1) and C(4)-C(5) π BD* orbitals (with the formation of N(2)-C(1) and N(2)-C(5) π interactions). The magnitude of these can be gauged from the resulting occupation of the N(2) lone pair (1.555 e^-) and the stabilisation energy of these interactions (176 and 213 kJ mol^{-1} respectively). In addition, the C(4)-C(5), C(2)-C(3) and C(1)-N(1) π bonding orbitals are also delocalised around the aromatic system, but to a lesser extent. The C(1)-N(1) π bonding orbital has an occupation

of 1.950 e⁻ suggesting a large degree of double bond character. In contrast, the NBO results for protonated form of **1** (Figure 2-13) are based on the aminopyridinium resonance form with delocalisation of the N(1) lone pair into the C(1)-N(2) π BD* orbital (the N(1) lone pair occupation is 1.656 e⁻ and stabilisation energy for this interaction is 397 kJ mol⁻¹) to give a system with significant C(1)-N(1) double bond character. In addition to this, the π system around the ring is significantly delocalised. These results suggest, along with the structural evidence, that protonation leads to a considerably more amidopyridinium-like structure, but that the C(1)-N(1) bond retains significant double bond character.

2.6 Conclusions and the future work

A modified procedure of the synthesis of PYE ligands was found and a series of monodentate PYE ligands **1-5** and bidentate PYE ligands **6-14** including achiral and chiral examples were synthesised and fully characterised. The method has shown good functional group tolerance including alcohol (**3**) and bulky (**15**) groups. According to the comparison of X-ray structures between PYE compounds and 2-aminopyridine, the electronic structure of PYE may more strongly resemble a conjugated polyene as shown in Scheme 2-5 than the delocalised aromatic structure of pyridine. In contrast, the protonated ligand shows that the heterocycle moiety exhibits increased pyridinium character, although there is always significant double-bond character in the exocyclic C-N bond. UV-vis absorption spectra of **7** show a $\pi\pi^*$ electronic transition and the slight bathochromic shifts in absorption relative to 2-MIP could be due to the donation of electron density to the π -bonding system by the cyclohexyl ring. Moreover, the resistance to hydrolysis and hydrogenation under mild conditions will benefit the catalytic reactions tested in the future. Finally, the modularity of PYE ligands will allow us to investigate the coordination chemistry and reactivity of transition metal complexes with respect to steric and electronic properties.

2.7 References

1. C. A. Caputo and N. D. Jones, *Dalton Trans.*, 2007, 4617-4740.
2. A. Togni and L. M. Venanzi, *Angew. Chem. Int. Ed.*, 1994, **33**, 497-526.
3. F. Glorius, *Angew. Chem. Int. Ed.*, 2008, **47**, 8347-8349.
4. F. Fache, E. Schulz, M. L. Tommasino and M. Lemaire, *Chem. Rev.*, 2000, **100**, 2159-2231.
5. L. Ronconi and P. J. Sadler, *Coord. Chem. Rev.*, 2007, **251**, 1633-1648.
6. A. E. Tschitschibabin, R. A. Konowalowa and A. A. Konowalowa, *Ber. Dtsch. Chem. Ges.*, 1921, **54**, 814-822.
7. R. Adams and J. B. Campbell, *J. Am. Chem. Soc.*, 1949, **71**, 3539-3540.
8. P. Hong and H. Yamazaki, *Tetrahedron Lett.*, 1977, **18**, 1333-1336.
9. J. Rokach, P. Hamel, N. R. Hunter, G. Reader, C. S. Rooney, P. S. Anderson, E. J. Cragoe and L. R. Mandel, *J. Med. Chem.*, 1979, **22**, 237-247.
10. G. Ege, H. O. Frey and E. Schuck, *Synthesis*, 1979, 376-378.
11. H. Hoberg and G. Burkhardt, *Synthesis*, 1979, 525-526.
12. P. Diversi, G. Ingrosso, A. Lucherini and S. Malquori, *J. Mol. Catal.*, 1987, **40**, 267-280.
13. T. Takahashi, F. Y. Tsai, Y. Z. Li, H. Wang, Y. Kondo, M. Yamanaka, K. Nakajima and M. Kotora, *J. Am. Chem. Soc.*, 2002, **124**, 5059-5067.
14. Y. M. Elkholy and A. W. Erian, *Heteroat. Chem.*, 2003, **14**, 503-508.
15. A. Elassar, *Heteroat. Chem.*, 2004, **15**, 293-299.
16. D. D. Young and A. Deiters, *Angew. Chem. Int. Ed.*, 2007, **46**, 5187-5190.
17. I. Hachiya, Y. Minami, T. Aramaki and M. Shimizu, *Eur. J. Org. Chem.*, 2008, 1411-1417.
18. K. Inuzuka, A. Fujimoto and H. Ito, *Bull. Chem. Soc. Jpn.*, 1993, **66**, 2871-2876.
19. M. A. Young, G. DeBoer, A. Fujimoto, N. Iwasaki, H. Traore and I. Yourshaw, *Bull. Chem. Soc. Jpn.*, 1997, **80**, 561-569.
20. A. Fujimoto, N. Iwasaki, Y. Hikiba, M. A. Young, K. Homma and K. Inuzuka, *Spectrochim. Acta Part A*, 1998, **54**, 1779-1792.
21. H. Traore, M. Saunders and S. Blasiman, *Aust. J. Chem.*, 2000, **53**, 951-957.
22. N. Akai, K. Ohno and M. Aida, *J. Photochem. Photobiol. A*, 2007, **187**, 113-118.

23. S. Gaur, *Asian J. Chem.*, 2003, **15**, 250-254.
24. D. J. Buurman and H. C. Vanderplas, *J. Heterocycl. Chem.*, 1986, **23**, 1015-1018.
25. T. Tanaka and T. Mukaiyama, *Chem. Lett.*, 1976, 1259-1262.
26. E. C. S. Brenelli and P. J. S. Moran, *J. Chem. Soc., Perkin Trans. 2*, 1989, 1219-1222.
27. Y. T. Park, C. H. Joo and L. H. Lee, *Bull. Korean Chem. Soc.*, 1990, **11**, 270-271.
28. M. Chao, E. Schempp and R. D. Rosenstein, *Acta. Crystallogr. Sect. B*, 1975, **31**, 2922-2924.
29. M. Chao, E. Schempp and R. D. Rosenstein, *Acta. Crystallogr. Sect. B*, 1975, **31**, 2924-2926.
30. F. H. Allen, *Acta. Crystallogr. Sect. B*, 2002, **58**, 380-388.
31. J. Lokaj, V. Kettmann, V. Milata, R. Kada and J. Ulrich, *Acta. Cryst.*, 1998, **54**, 785.
32. J. M. Johnson, N. M. Morales, A. M. Gorczyca, D. D. Dolliver and M. A. McAllister, *J. Org. Chem.*, 2001, **66**, 7979-7985.

3.0 Transition metal complexes with PYE ligands and their catalytic applications

3.1 Introduction

PYE derivatives have been known for a long time, however there is very little chemistry describing their coordination chemistry and application. As proposed in Section 2.1, one important feature resulting from metal coordination of PYE ligands is strong donation due to a contribution of the pyridinium–amido resonance structure to the metal–ligand bond. The resulting strong donation could potentially facilitate oxidative addition reactions making PYE ligands useful ancillary ligands in catalysis. Furthermore, the modular synthetic route to PYE ligands allows installation of various substituents including bulky and stereogenic groups. Study of the steric effects on the reactivity of PYE metal complexes could be very interesting.

Herein, coordination chemistry of PYE ligands with a range of transition metals will be described and the characterising data of the resulting metal complexes, including spectroscopy and X-ray diffraction will be carefully interpreted to understand the stereoelectronic properties of PYE ligands. The reactivity of the complexes with a series of substrates will be studied and some select catalytic reactions will be described.

3.2 Rhodium complexes with monodentate PYE ligands

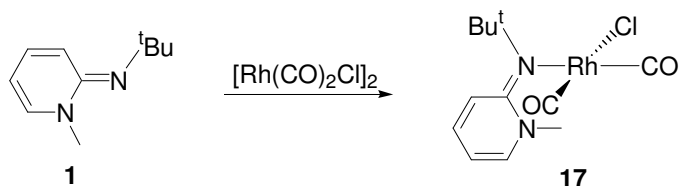
The measurement of the carbonyl IR stretching frequencies of dicarbonyl rhodium complexes $(L)Rh(CO)_2Cl$ has been commonly used to determine the donating properties of a two electron neutral ligand, L. The corresponding data of various selected ligands including nitrogen, phosphine, and carbene types are illustrated in Table 3-1.

Table 3-1. IR carbonyl frequencies (cm⁻¹) of cis-[(L)Rh(CO)₂Cl] complexes.

ligands	$\nu(\text{CO})$ I	$\nu(\text{CO})$ II	average
pyridine ¹	2089	2015	2052
PPh ₃ ²	2087	2009	2048
PMe ₂ Ph ²	2089	2002	2046
1, 3-dimethyl imidazol-2-ylidene ³	2076	2006	2041
1, 3-dimesitylimidazolidin-2-ylidene ⁴	2081	1996	2039
isopropyl-(1-methyl-1H-pyridin-4-ylidene)-amine ⁵	2077	1998	2038
(<i>tert</i> -butyl)-(diisopropylamino)carbene ⁶	2070	1989	2030

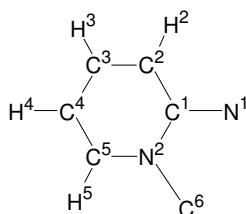
In order to have a knowledge of the donating ability of PYE ligands, a (L)Rh(CO)₂Cl type complex was isolated from reaction between ligand **1** and [RhCl(CO)₂]₂ in toluene giving the complex [(^{Me}N^{tBu})Rh(CO)₂Cl] **17** (Scheme 3-1) as an air sensitive white solid in 95 % yield. For complex **17**, IR spectroscopy in toluene shows two CO peaks at 2071 and 1992 cm⁻¹, and in a KBr matrix 2071 and 1989 cm⁻¹ (average 2030 cm⁻¹). By this measure, **1** is a significantly stronger donor than most of the selected ligands shown in Table 3-1. Remarkably, the average $\nu(\text{CO})$ value of **17** is similar to acyclic carbene (*tert*-butyl)-(diisopropylamino)carbene which is one of the most strongly donating carbenes currently known, indicating that using the (L)Rh(CO)₂Cl probe, **1** is a strongly donating ligand. An analogous complex of isopropyl-(1-methyl-1H-pyridin-4-ylidene)-amine⁵ gave stretching frequencies at 2077 and 1998 cm⁻¹ indicating **1** may be a marginally better donor.

With respect to the donating properties of PYE containing ligands, comparison of the IR data of **17** with literature data would suggest that these compounds are strong donor ligands. However, some caution should be applied when interpreting data of this type in which multiple π -acceptor ligands are present and steric factors may be important.

**Scheme 3-1.** Synthesis of rhodium complex **17**.

Comparison of ^1H and ^{13}C NMR spectroscopy between **17** and ligand **1** (Table 3-2) in $\text{CD}_3\text{C}_6\text{D}_5$ shows downfield chemical shifts for all signals, with the most significant changes in the ^1H NMR for H^4 (5.15 to 5.63 ppm) and H^2 (6.35 to 6.81 ppm). In addition to two signals at 182.0 ($^1J_{\text{Rh-C}} = 78$ Hz) and 183.8 ($^1J_{\text{Rh-C}} = 66$ Hz) ppm assigned to the carbon monoxide ligands, the most significant changes in the ^{13}C NMR spectrum are for C^1 (149.6 to 164.5 ppm), C^2 (115.0 to 122.4 ppm), and C^4 (98.1 to 108.0 ppm). Unfortunately poor solubility of protonated ligand **16** in toluene prevented comparison of **1** and **17**.

Table 3-2. ^1H and ^{13}C NMR chemical shifts (ppm) of **1** and **17** in $\text{CD}_3\text{C}_6\text{D}_5$.



	H^2	H^3	H^4	H^5	C^1	C^2	C^3	C^4	C^5
1	6.35	6.45	5.15	6.26	149.6	115.0	132.7	98.1	139.4
17	6.81	6.58	5.63	6.40	164.5	122.4	134.6	108.0	140.2

To provide some further insight into the metal-PYE bond, a theoretical analysis was conducted by Dr. John Slattery to place PYE ligands in the context of other donors.⁷ Two models $\text{Ni}(\text{CO})_3\text{L}$ and $\text{IrCp}(\text{CO})\text{L}$ (L = neutral two electron ligands) have been used to evaluate the donor properties of the selected ligands by correlating the calculated $\nu(\text{CO})$ with the calculated CO bond length $\{d(\text{CO})\}$ in complexes. Herein, a better correlation result from calculated $\text{IrCp}(\text{CO})\text{L}$ complexes compared with $\text{Ni}(\text{CO})_3\text{L}$ is shown in Figure 3-1. Ligands lying to the left hand side of Figures 3-1, with lower frequency $\nu(\text{CO})$ bands can be considered to be strong net donors and those lying to the right hand side weak donors with significant acceptor character. An expected ranking of donor strength for known ligands is shown within a class e.g. $\text{PMe}_3 > \text{PH}_3 > \text{PF}_3$. $\text{IrCp}(\text{CO})\text{L}$ model shows pure σ -donor ligands such as NMe_3 as being very strong donors. The PYE ligand **1** is found in the region of very strong N-donor ligands and on this scale is ranked as a stronger donor than for example, the NHCs included in the study. In fact, the complex $\text{IrCp}(\text{CO})(\mathbf{1})$ is found to have the second lowest $\nu(\text{CO})$ of all the ligands studied, which supports the experimental IR data for analogous $\text{RhCl}(\text{CO})_2\text{L}$ complexes.

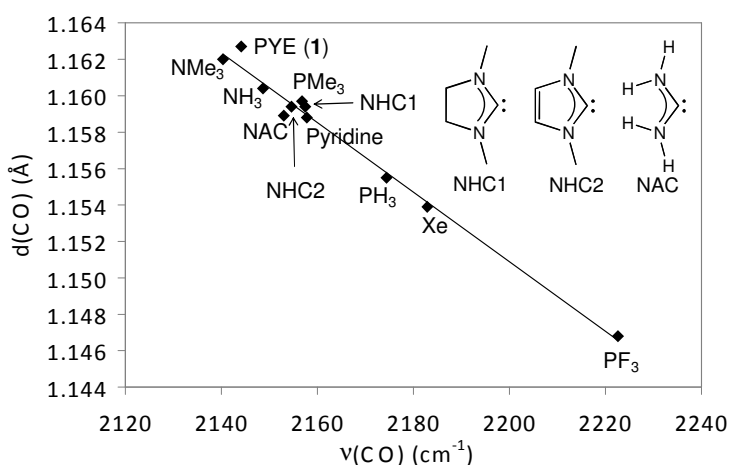


Figure 3-1. A plot of $\nu(\text{CO})$ (cm^{-1}) vs. $d(\text{CO})$ (\AA) for the $\text{IrCp}(\text{CO})\text{L}$ complexes studied.

3.3 Nickel complexes with PYE ligands

3.3.1 Introduction

Nickel chemistry of nitrogen donor ligands has been extensively investigated with respect to catalytic applications in the last few decades. In particular, remarkable success has been obtained for polymerisation^{8,9} and C-C cross-coupling.¹⁰⁻¹² In 1995 Brookhart and co-workers reported nickel and palladium complexes with α -diimine ligands can catalyse olefin polymerization.¹³ This system was unique from other late metal catalysts due to the ability of producing high molar mass materials, rather than oligomers, from both ethylene and higher α -olefins. Since then, much effort has been done on modification of α -diimine and design of new nitrogen ligands to explore potential various polymer features.⁸

Due to the versatility of cross-coupling to build new carbon-carbon bonds in organic molecules, metal-catalysed cross-coupling has been of special interest for decades. Numerous instances of transition metal complexes catalysing C-C cross coupling of both C_{sp2} and C_{sp3} centres have been investigated. However, for alkyl-alkyl cross-coupling reactions, side reactions led by β -hydride elimination and/or dimerization of radicals from reduction of alkyl halides are the main obstacles to expand the scope of implementation of this methodology, which requires the exploration of new ligands and conditions. In recent years, nickel complexes incorporating nitrogen ligands have exhibited interesting reactivity in this area. In 2004, Vicic and co-workers demonstrated that Ni(I) species with a terpyridine ligand can be catalytically active in the cross-coupling of unactivated alkyl halides.¹⁴ In 2005, Fu *et al.* reported the first examples of asymmetric Negishi cross-couplings of alkyl halides using C_2 -symmetric pybox ligands.¹⁵ More recently, Hu *et al.* reported that a new pincer-type amido bis(amine) ligand ($^{Me}NN_2$) coordinated to a Ni(II) centre can be applicable in selective C-C bond formation resulting from multi C-Cl bonds activation.¹² Some examples of nitrogen ligands are summarised in Figure 3-2.

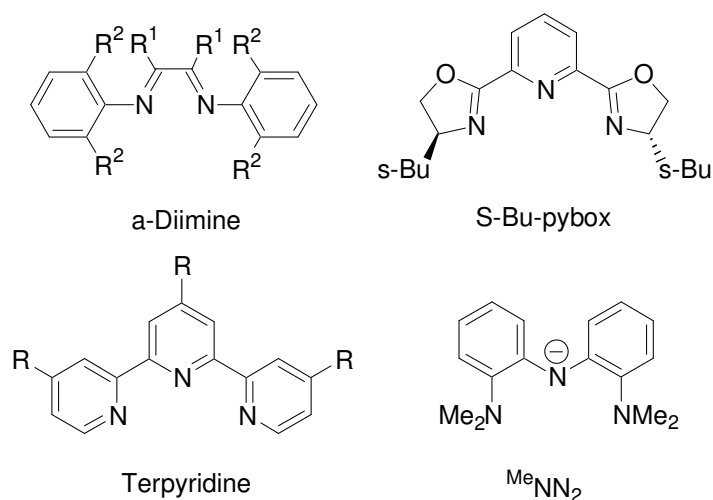
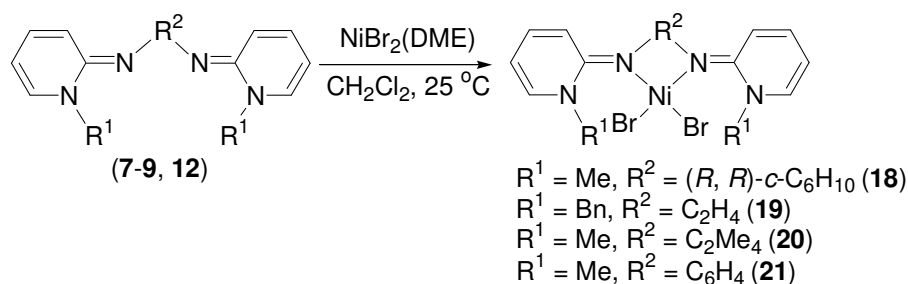


Figure 3-2. Examples of nitrogen donor ligands utilized in polymerisation and cross-coupling.

Due to the high activity of α -diimine and pybox ligand nickel (II) complexes in polymerisation and cross coupling respectively, we decided to synthesise nickel complexes of ligands **7-9** and **12**, and investigate the potential electronic properties of PYE ligands.

3.3.2 Synthesis and properties of nickel(II) complexes with PYE ligands

Reaction between the precursor $NiBr_2(DME)$ and ligands **7-9** and **12** in dichloromethane at room temperature gave the complexes $[NiCl_2(MeN^{C_6H_{10}}N^{Me})]$ (**18**), $[NiCl_2(BnN^{(CH_2)_2}N^{Bn})]$ (**19**), $[NiCl_2(MeN^{(C(Me)_2)_2}N^{Me})]$ (**20**) and $[NiCl_2(MeN^{C_6H_4}N^{Me})]$ (**21**) as paramagnetic dark green (**18-19**) or dark red (**20-21**) solids respectively (Scheme 3-2). Mass spectrometry, elemental analysis and in select cases single crystal x-ray diffraction are consistent with the proposed formulations. Complexes **18-21** are very soluble in $CHCl_3$, CH_2Cl_2 and MeCN but poorly soluble in other common organic solvents. Complexes **18-21** are quite moisture and air sensitive, being stable as solids for hours and decomposing within minutes in solution in air. The decomposed products are the corresponding protonated ligands and what is presumed to be nickel(II) hydroxide.



Scheme 3-2. Synthesis of nickel(II) complexes of PYE ligands.

Single crystals of **18** suitable for X-ray diffraction were grown from acetonitrile and diethyl ether at $-40\text{ }^\circ\text{C}$. The molecular structure is shown in Figure 3-3 and selected bond lengths and angles are given in Table 3-3.

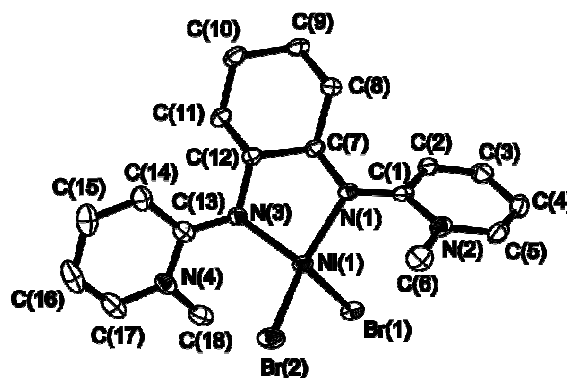


Figure 3-3. Molecular structure of complex **18**. Ellipsoids are shown at 50 % probability. Hydrogen atoms have been omitted for clarity.

Table 3-3. Selected bond lengths and angles for complex **18**.

bond	lengths (Å)	bond	angles ($^\circ$)
Ni(1) – Br(1)	2.4106(4)	N(1) – Ni(1) – N(3)	86.85(7)
Ni(1) – Br(2)	2.3934(3)	Br(1) – Ni(1) – Br(2)	107.433(12)
N(1) – Ni(1)	1.9931(16)	C(2) – C(1) – N(1) – C(7)	13.1(3)
N(3) – Ni(1)	1.9990(16)	C(14) – C(13) – N(3) – C(12)	11.8(3)

The complex **18** exhibits pseudo C_2 symmetry. The geometry at the nickel atom is close to tetrahedral, where the angle between the planes defined by N(1)-Ni(1)-N(2) and Br(1)-Ni(1)-Br(2) is ca. 74.05 ° . Compared with **7** and **18**, the nitrogen atoms N(1) and

N(3) show distinct pyramidal geometry, where the sum of the angles about atoms N(1) and N(3) are ca. 342.6 and 343.68 ° respectively. The ligand bite angle N(1)-Ni(1)-N(3) = 86.85(7) ° is approximately four to seven degrees greater than the structurally related 2, 2'-bipyridine and α -diimine bidentate nitrogen ligands.^{16, 17}

Single crystals of **21** suitable for X-ray diffraction were grown from dichloromethane and diethyl ether at -40 °C. There are two molecules with a slight difference in bond lengths and angles in the asymmetric unit. Both molecules are symmetrical about the Br-Ni-Br plane. The molecular structure is shown in Figure 3-4 and selected bond lengths and angles are given in Table 3-4.

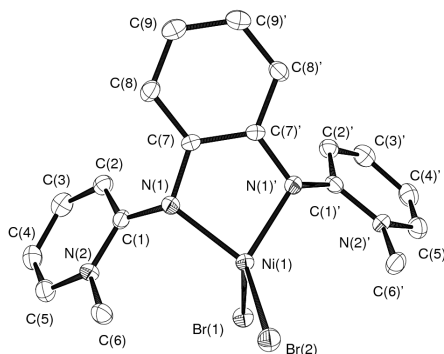


Figure 3-4. Molecular structure of complex **21**. Ellipsoids are shown at 50 % probability. Hydrogen atoms have been omitted for clarity.

Table 3-4. Selected bond lengths (Å) and angles (°) for complex **21**.

21(A)			
bond	lengths (Å)	bond	angles (°)
Ni(1) – Br(1)	2.3988(9)	N(1) – Ni(1) – N(1)	84.49(18)
Ni(1) – Br(2)	2.3853(8)	Br(1) – Ni(1) – Br(2)	107.10(3)
N(1) – Ni(1)	1.998(3)	C(2) – C(1) – N(1) – C(7)	22.4(5)
21(B)			
bond	lengths (Å)	bond	angles (°)
Ni(2) – Br(3)	2.3989(9)	N(3) – Ni(2) – N(3)	84.63(18)
Ni(2) – Br(4)	2.3894(8)	Br(3) – Ni(2) – Br(4)	105.09(3)
N(3) – Ni(2)	2.005(3)	C(2) – C(1) – N(1) – C(7)	24.6(5)

The complex **21** exhibits pseudo C_s symmetry with a mirror plane through the plane defined by Br-Ni-Br. Similarly, the geometry at the nickel atom is close to tetrahedral, where the angle between the planes defined by N(1)-Ni(1)-N(2) and Br(1)-Ni(1)-Br(2) is ca. 90° . The two N-methyl groups are pointing in the same direction. In comparison with **18**, the bite angle N-Ni-N in **21** is slightly smaller which is attributed to the rigid aryl backbone, however the N-Ni bond lengths are quite similar. The slightly difference of Ni-Br bond lengths within the individual molecule is partly accounted for by different packing effects at individual bromine atoms as a result of the absence of crystallographic symmetry for the molecules.¹⁸ The Ni-N and Ni-Br bond lengths of both **18** and **21** are in the typical range for bidentate nitrogen ligands.¹⁷

Comparison of bond lengths (Table 3-5) within the PYE moieties between **7**, **16**, **18** and **21** shows the structure of PYE moieties of **18** and **21** are close to the protonated salt **16**. Therefore the structure drawn in Scheme 3-2 is a more accurate representation of the bonding, where electron density in the PYE moiety tends to be localised.

Table 3-5. Comparison of bond lengths (Å) between **7**, **16**, **18** and **21**.

	$[\text{MeN}^+(\text{C}_6\text{H}_{10})\text{N}^{\text{Me}}]$ (7)	$[\text{MeN}(\text{H})^{(\text{CH}_2)_2}\text{N}(\text{H})^{\text{Me}}]$ (16)	$[\text{NiBr}_2(\text{MeN}^+\text{C}_6\text{H}_{10}\text{N}^{\text{Me}})]$ (18)	$[\text{NiBr}_2(\text{MeN}^+\text{C}_6\text{H}_4\text{N}^{\text{Me}})]$ (21)
C(1) – N(1)	1.2960(15)	1.334(4)	1.332(3)	1.357(5) 1.347(5)
C(1) – C(2)	1.4496(16)	1.413(4)	1.424(3)	1.427(5) 1.421(5)
C(2) – C(3)	1.3527(16)	1.366(5)	1.360(3)	1.337(6) 1.382(6)
C(1) – N(2)	1.4078(14)	1.374(4)	1.388(3)	1.355(5) 1.378(5)

Magnetic moments were determined at room temperature in CD_2Cl_2 using the Evans method.¹⁹ The values for complexes **18-21** are 3.01(0.19), 3.18(0.12), 2.58(0.07) and 2.70(0.10) μ_B respectively, which is slightly different from the spin-only value of 2.83 μ_B for high spin tetrahedral d^8 complexes.

As mentioned in section 3.2.1, remarkable success has been exhibited in polymerisation and cross-coupling catalysed by nickel complexes with nitrogen ligands. So some initial test of catalytic activity was inspired to explore the potential reactivity, if possible, with nickel complex with PYE ligands. Polymerisation tests were carried using samples of complex **18-20** in the group of Prof. P. T. Gomes, Institute Superior Tecnico, Lisbon, Portugal. Unfortunately, the complexes did not show polymerisation activity. Furthermore, Suzuki cross-coupling between bromobenzene and phenylboronic acid was attempted with complex **18** under standard reaction conditions, however no cross-coupling product was obtained (*vide infra*).

3.4 Palladium (II) complexes of PYE ligands

3.4.1 Introduction

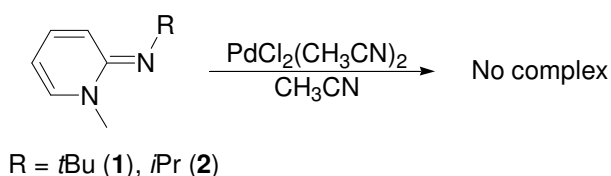
During the last few decades, palladium complexes incorporated with nitrogen donor ligands have attracted much attention from academia and industry as they show a variety of interesting features, in particular catalytic²⁰⁻²² and biological activity.^{23, 24} Due to the stability and versatility of nitrogen ligands, a number of palladium complexes with various nitrogen ligands have been synthesised and investigated in a variety of catalytic reactions including cross-coupling,²⁵ oxidation,²⁶ hydroamination²⁷ and asymmetric variants. Along with the continuous development, those original “small scale” methods in laboratory have been practically utilized in fine chemical and pharmaceutical industry on a larger scale.²⁸ Similarly, Pd complexes with nitrogen ligands have shown great potential for biological activity, especially as antitumor agents due to the similarity between the coordination chemistry of palladium(II) and platinum(II).

In order to understand the influence of the steric and electronic effect of PYE ligands on the reactivity of metal complexes and further investigation of catalytic applications, we decided to synthesise palladium complexes with PYE ligands.

3.4.2 Attempts to prepare palladium complexes with mono-PYE ligands

The first attempts to synthesise palladium complexes incorporating PYE ligands was commenced using monodentate PYE ligands **1** and **2** with the precursor $\text{PdCl}_2(\text{CH}_3\text{CN})_2$, which contains two acetonitrile ligands which are very labile. According to the literature, complexes of the type $\text{Pd}(\text{L})(\text{MeCN})\text{Cl}_2$ (where L = nitrogen ligands) have not been isolated, whereas *cis*- $\text{Pt}(\text{Py})(\text{MeCN})\text{Cl}_2$ is stable.²⁹ This difference between two metals from the same group could be derived from the variation of the dissociation energy due to stronger Pt-L bonds. Unsurprisingly, complexes of the type $\text{Pd}(\text{L})_2\text{Cl}_2$ (where L = nitrogen ligands) such as *trans*- $\text{Pd}(\text{Py})_2\text{Cl}_2$ have been recognised for very long time.³⁰

Reactions between PYE ligands and $\text{PdCl}_2(\text{CH}_3\text{CN})_2$ in 1:1 and 2:1 ratio were carried out at room temperature in acetonitrile, where the reaction colour became red instantaneously (Scheme 3-3). However, in both cases (1:1 and 2:1 ratio), ^1H NMR spectrum shows an extra broad peak around 8 ppm indicating formation of a protonated ligand species after reaction. The chemical shifts derived from the ligand are close to those of the protonated form generated from addition of 1 eq. of $\text{HBF}_4(\text{Et}_2\text{O})$ into a solution of ligand. Refluxing the reaction mixture made no change. The steric interference of N-methyl groups of PYE ligands is probably responsible for the failure to coordinate resulting in a relatively weak Pd-N bond (*vide infra*).



Scheme 3-3. Attempt to synthesis of palladium complexes.

Considering the instability resulted from rapid dissociation observed above, compound **4** with a naphthyl group was introduced to act as a bidentate ligand via orthopalladation to stabilise Pd(II). An analogous ligand was used by Dupont *et al.* to synthesise a dimeric palladacycle complex as shown in Figure 3-5.

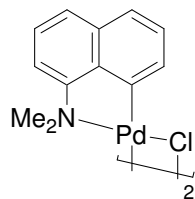
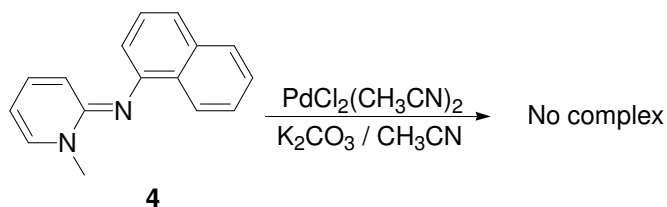


Figure 3-5. Palladacycle with N,N-dimethyl-1-naphthylamine ligand.

However, reaction between compound **4** and $\text{PdCl}_2(\text{CH}_3\text{CN})_2$ in the presence of potassium carbonate as base on refluxing gave no complex as judged by ^1H NMR spectroscopy and shows a series of complicated broad signals, indicating possible decomposition or intermolecular metallation has occurred.



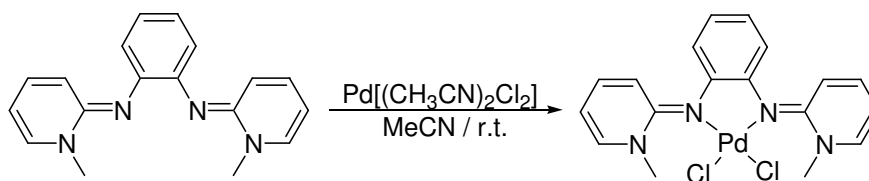
Scheme 3-4. Attempt to synthesis of palladium complex with compound **4**.

3.4.3 Preparation of palladium(II) dihalide complexes using chelating PYE ligands

As palladium complexes incorporating bidentate nitrogen donor ligands have been utilized in a variety of catalytic transformations, we decided to study the reactivity of bidentate PYE ligands with palladium precursors. Again, $\text{Pd}(\text{CH}_3\text{CN})_2\text{Cl}_2$ was first chosen as the palladium precursor. Initial tests were carried out in a Youngs-type NMR tube where free ligand (compound **6** was unsuccessful to test due to poor solubility in organic solvent), $\text{Pd}(\text{CH}_3\text{CN})_2\text{Cl}_2$ and acetonitrile- d_3 were added. After shaking the tube for a few minutes, all the starting materials were dissolved in the solvent giving a deep green (**12**) or a deep red (**7-11**) coloured solution. The ^1H NMR spectra show chemical shifts significantly downfield from free ligands, indicating complexation has occurred. However, the ^1H NMR spectra of compound **7-11** with $\text{Pd}(\text{CH}_3\text{CN})_2\text{Cl}_2$ show beside the expected signals, which can be attributed to a C_2 symmetric palladium complex, several other signals reflective of extra species. Alternative reaction temperatures and solvents did not give a pure material. This chemistry will be discussed in Chapter 4.

3.4.3.1 Synthesis of $[\text{PdCl}_2(\text{MeN}^{\text{C}_6\text{H}_4\text{N}^{\text{Me}})]$ (**22**)

Reaction between compound **12** and $\text{Pd}(\text{CH}_3\text{CN})_2\text{Cl}_2$ in acetonitrile at room temperature (Scheme 3-5) gave the complex $[\text{PdCl}_2(\text{MeN}^{\text{C}_6\text{H}_4\text{N}^{\text{Me}})]$ **22** as a dark green solid. Complex **22** is air and moisture stable, and moderately soluble in chlorinated solvents, acetone, acetonitrile and ethyl acetate. ^1H and ^{13}C NMR spectroscopy, mass spectrometry and elemental analysis are consistent with the proposed formulation.



Scheme 3-5. Synthesis of palladium complex **22**.

Single crystals of **22** suitable for X-ray diffraction were grown from acetone and pentane at room temperature. There are two molecules with *trans* and *cis* conformation in the asymmetric unit. The *trans*-isomer shows C_2 symmetry with one half of the molecule in the asymmetric unit. Unlike the *trans*-isomer, the *cis*-isomer shows C_s symmetry with a slight difference between both halves of the molecule. The molecular structures are shown in Figure 3-6 and selected bond lengths and angles are given in Table 3-6.

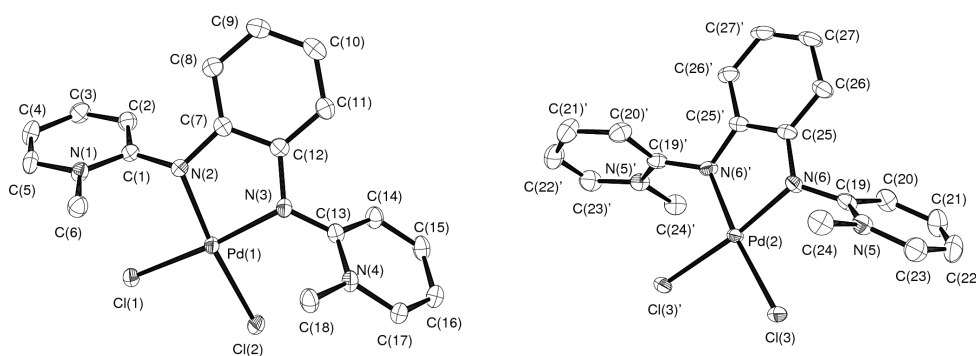


Figure 3-6. Molecular structure of complex **22** (*cis*-isomer left and *trans*-isomer right). Ellipsoids are shown at 50 % probability. Hydrogen atoms have been omitted for clarity.

Table 3-6. Selected bond lengths and angles for complex **22**.

<i>Cis-isomer</i>			
bond	lengths (Å)	bond	angles (°)
C(1) – N(2)	1.364(3)	N(2) – Pd(1) – N(3)	80.23(9)
C(13) – N(3)	1.357(3)	Cl(1) – Pd(1) – Cl(2)	89.09(2)
Pd(1) – N(2)	2.037(2)	C(2) – C(1) – N(2) – C(7)	42.9(4)
Pd(1) – N(3)	2.041(2)	C(16) – C(15) – N(3) – C(14)	45.4(4)
Pd(1) – Cl(1)	2.3319(7)		
Pd(1) – Cl(2)	2.3260(7)		
<i>Trans-isomer</i>			
bond	lengths (Å)	bond	angles (°)
C(19) – N(6)	1.366(3)	N(6) – Pd(2) – N(6)	82.47(12)
Pd(2) – N(6)	2.038(2)	Cl(3) – Pd(2) – Cl(3)	90.83(3)
Pd(2) – Cl(3)	2.3185(6)	C(20) – C(19) – N(6) – C(25)	50.9(4)

Compared with the structure of free ligand **12**, the PYE moieties of **22** show a relatively delocalised structure, arguably greater than the protonated salt **16** probably due to the existence of the aryl backbone. The rigid backbone gives rise to a larger torsion angle ca. 42.9° and 45.4° for *cis*-isomer and ca. 50.9° for *trans*-isomer, where ca. 0.33° is found for free ligand **12**. In comparison with structurally related 2,2'-bipyridine,¹⁸ the Pd-N bond lengths in **22** are close to that in an analogous 2,2'-bipyridine complex (2.03 Å), whereas the Pd-Cl bond lengths in *cis*-isomer of **22** are longer than that in 2,2'-bipyridine (2.277 and 2.317 Å) possibly indicating a higher trans effect for the PYE ligand.

In solution, a single set of signals for **22** was observed in the ¹H and ¹³C NMR spectra, for example, where a singlet signal was observed for the CH₃ group at 4.24 ppm. In comparison to **12**, the signals attributable to the PYE moiety are downfield but upfield for the aryl linker (Figure 3-7). Although there were no indications of dynamic behavior through line-broadening or resolution of signals even at temperatures down to -60 °C (CD₂Cl₂), a flipping motion of the PYE rings is very likely according to the conformers observed in the structure of **22**.

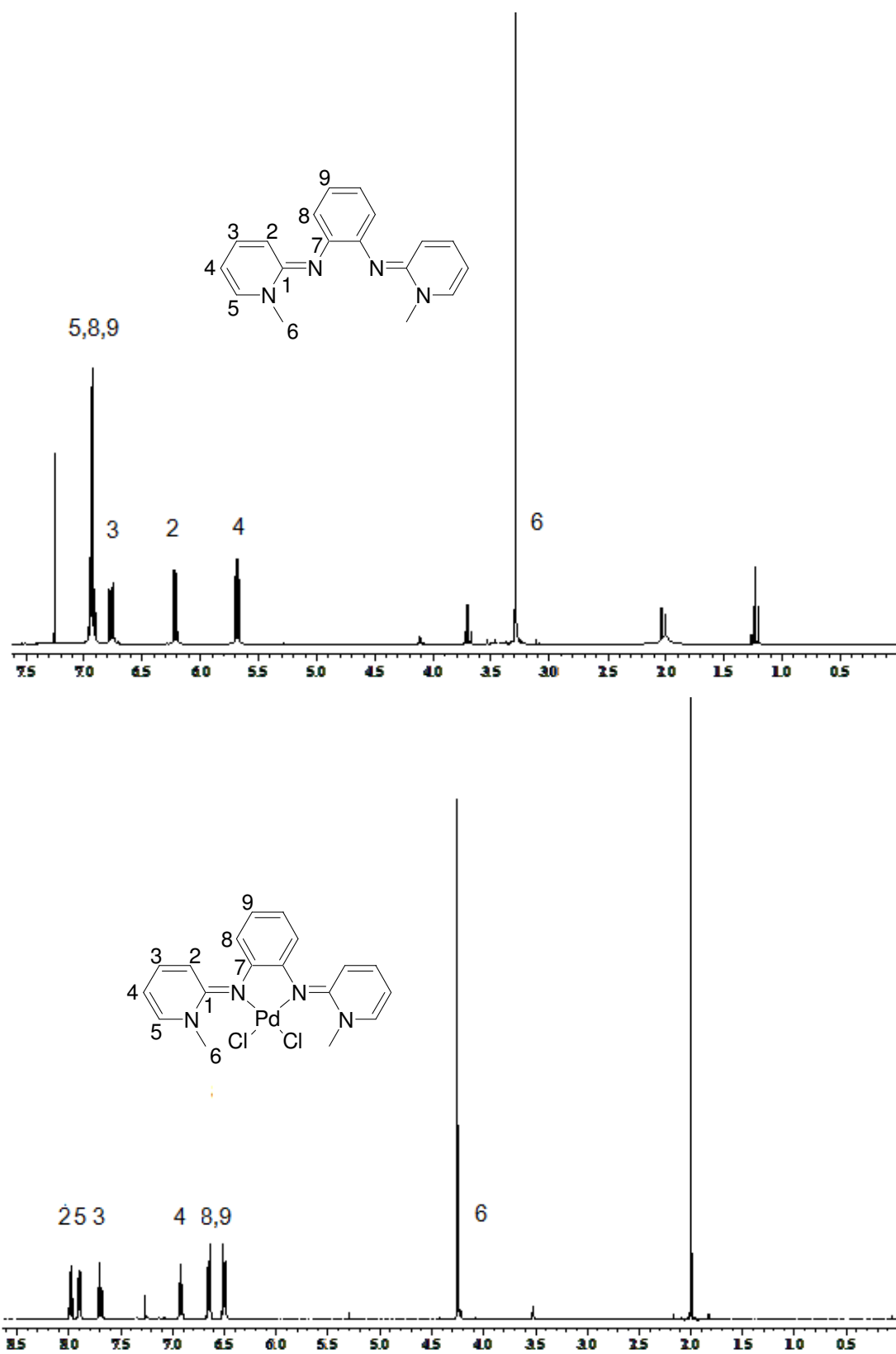
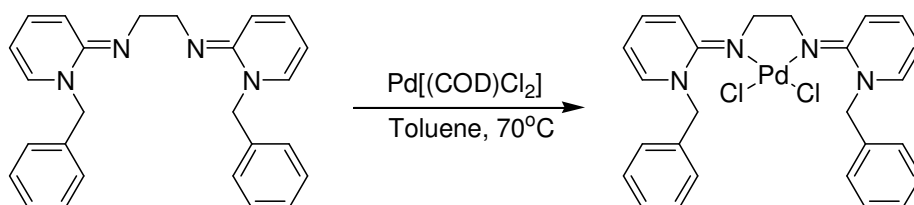


Figure 3-7. Comparison of ¹H NMR spectra of **12** (top) and **22** (bottom) in CDCl₃.

3.4.3.2 Synthesis and dynamic study of $[\text{PdCl}_2(\text{BnN}^{(\text{CH}_2)_2\text{N}^{\text{Bn}})]$ (**23**)

An alternative precursor $\text{Pd}(\text{COD})\text{Cl}_2$ was chosen. After screening this precursor with ligands (**7-11**), complex $[\text{PdCl}_2(\text{BnN}^{(\text{CH}_2)_2\text{N}^{\text{Bn}})]$ **23** derived from **8** was obtained in toluene at 70°C and stirring for 2 hours (Scheme 3-6). Other ligands **7** and **9-11** did not allow the preparation of pure complexes analogous to **23**, due to formation of other species. This will be discussed in Chapter 4.



Scheme 3-6. Preparation of palladium complex **23**.

Single crystals of **23** were grown from acetonitrile at -40°C . The molecular structure is shown in Figure 3-8 and selected bond lengths and angles are given in Table 3-7. There are two molecules with only a slight difference in bond lengths and angles in the asymmetric unit. The geometry at the palladium atom is close to square planar with a ligand bite angle $\text{N}(1)\text{-Pd}(1)\text{-N}(3) = 79.18(9)^\circ$ and Pd-N bond lengths identical at $2.041(2) \text{ \AA}$. However, the Pd-Cl bond lengths differ where $\text{Pd}(1)\text{-Cl}(1) = 2.2944(7)$ and $\text{Pd}(1)\text{-Cl}(2) = 2.3347(7) \text{ \AA}$ respectively, which is induced by the asymmetry observed in the ligand. Orientation of the benzyl substituents to minimise non-covalent interactions also results in a short $\text{Pd}(1)\text{-H}(20\text{a})$ distance of ca. 2.38 \AA . The complex exhibits pseudo- C_s symmetry and bond lengths within the PYE ring moieties are similar to **18**, and between free ligand **7** and protonated salt **16**.

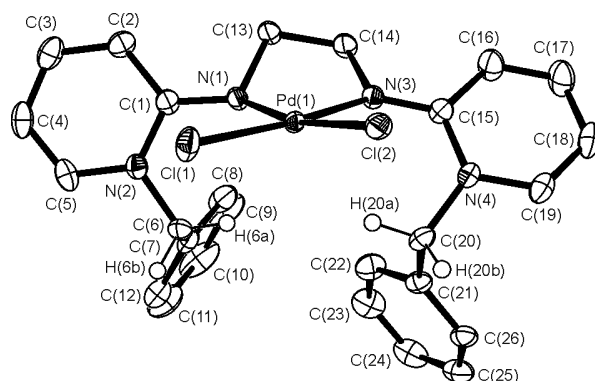


Figure 3-8. Molecular structure of complex **23**. Ellipsoids are shown at 50 % probability. Hydrogen atoms except for H(6a), H(6b), H(20a) and H(20b) have been omitted for clarity.

Table 3-7. Selected bond lengths and angles for complex **23**.

Bond	lengths (Å)	Bond	Angles (°)
Pd(1) – Cl(1)	2.2944(7)	N(1) – Pd(1) – N(3)	79.18(9)
Pd(1) – Cl(2)	2.3347(7)	Cl(1) – Pd(1) – Cl(2)	91.12(3)
N(1) – Pd(1)	2.041(2)	C(2) – C(1) – N(1) – C(13)	15.0(4)
N(3) – Pd(1)	2.041(2)	C(16) – C(15) – N(3) – C(14)	21.0(4)

In the solid state the two benzyl groups of complex **23** are on the same side of the palladium square plane giving approximate C_s symmetry, however ^1H NMR spectroscopy gave signals consistent with C_{2v} symmetry or exchanging C_2 or C_s isomers (Figure 3-9) as singlet signals at 3.67 and 6.49 ppm were observed for the linker CH_2 and benzyl CH_2 groups respectively at 300 K in CD_2Cl_2 . Variable temperature NMR down to 163 K (Figure 3-10) shows some significant changes to both the linker and benzyl CH_2 groups, which resolve into pairs of signals at 163 K. It can be interpreted as a flipping motion of the PYE moieties above and below the palladium square plane through a C_{2v} intermediate arising from a complex with C_s or C_2 symmetry. Coalescence was observed at 213 K giving an activation free energy (ΔG^\ddagger) = 37.9 (± 0.2) kJ mol^{-1} . Non-covalent interactions between benzyl groups and chlorine atoms could be additional contributions to the motion activation energies.

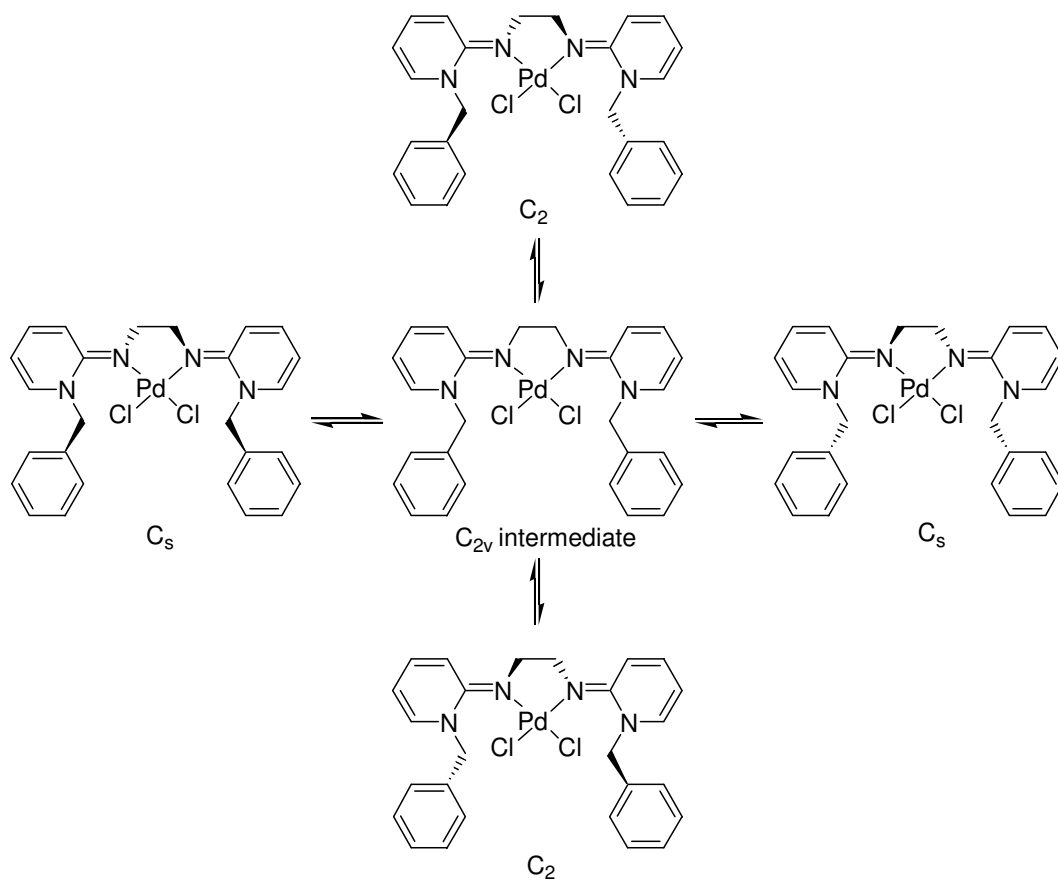


Figure 3-9. Proposed isomer exchanging of **23** through a C_{2v} intermediate.

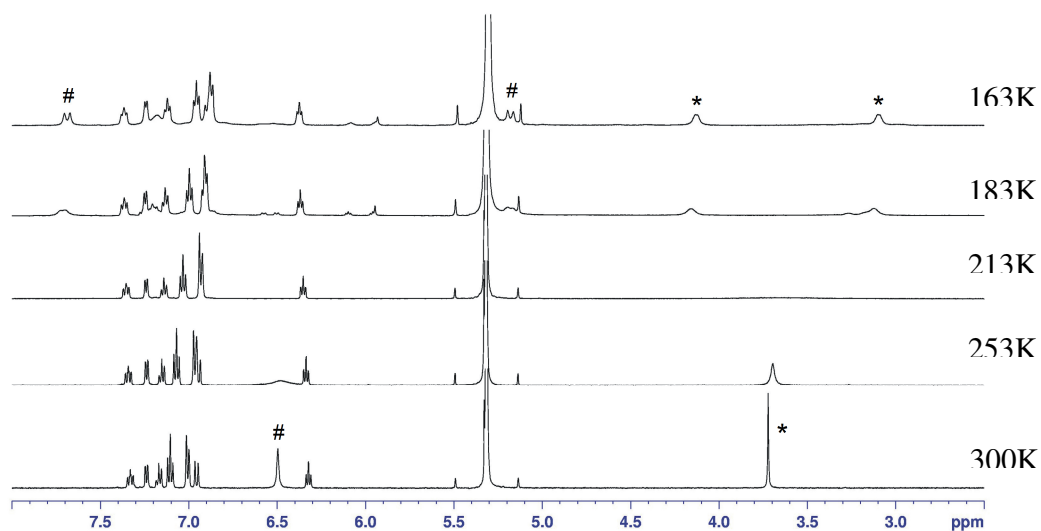


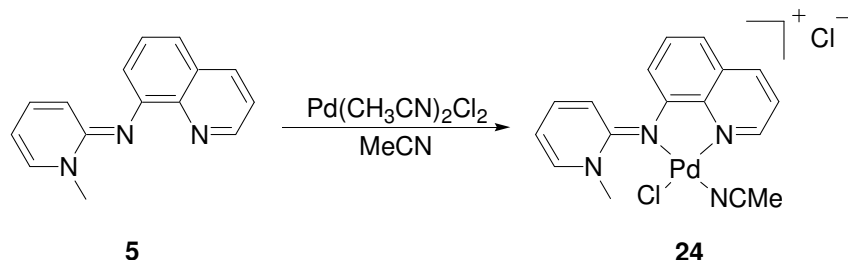
Figure 3-10. Variable temperature ^1H NMR spectra of palladium complex **23** in CD_2Cl_2 . (CH_2 -linker (*) and benzylic signals (#)).

3.4.3.3 $[\text{PdCl}(\text{NCCH}_3)(^{\text{Me}}\text{N}^{\text{Quino}})]^+\text{Cl}^-$ (**24**)

3.4.3.3.1 Synthesis of $[\text{PdCl}(\text{NCCH}_3)(^{\text{Me}}\text{N}^{\text{Quino}})]^+\text{Cl}^-$ (**24**)

Considering the poor selectivity of reaction between **4** and $\text{Pd}[(\text{CH}_3\text{CN})_2\text{Cl}_2]$, analogue **5** with a quinoliny substituent was prepared with two nitrogen atoms to coordinate to a metal centre. This unsymmetrical hybrid ligand potentially could give different reactivity from the C_2 symmetrical PYE ligands. Unlike the PYE moiety that was proved to be a strong σ -donor, the conjugation system of the quinoliny ring is able to act as an electronic “buffer” to probably favour the stabilisation of the resulting complex. Interestingly, reaction between **5** and $\text{Pd}[(\text{CH}_3\text{CN})_2\text{Cl}_2]$ in acetonitrile at room temperature yielded a cationic complex **24** (Scheme 3-7). The proposed formulation is confirmed by ^1H and ^{13}C NMR spectroscopy, mass spectrometry and elemental analysis. The solubility of **24**

is moderate in chlorinated solvents and good in DMSO, but quite poor in other common organic solvents.



Scheme 3-7. Synthesis of complex **24**.

In comparison with neutral ligand **5** and the protonated form $\text{L}(\text{H}^+)$ (comparison with $\text{L}(\text{H}^+)_2$ was prevented due to poor solubility), the ^1H NMR spectrum of **24** shows significant downfield signals in both PYE and quinolinyll moieties indicating both nitrogen atoms are coordinated. The ^1H NMR chemical shifts of the selected resonances are shown in Table 3-8. The integration of the coordinated acetonitrile signal is less than 3H in the spectrum probably due to a rapid exchange with solvents.³¹ Similarly, the downfield shift and the disappearance of the acetonitrile signal were exhibited in the ^{13}C spectrum as well. The ESI mass spectrum of **24** recorded in positive-ion mode contains a strong peak at m/z 417 due to the $[\text{M}-\text{Cl}]^+$ ion.

Table 3-8. Comparison of ^1H NMR chemical shifts (ppm) of **5**, the protonated form and **24**.

	L (5) ^a	L(H⁺) ^a	[PdLCl(NCCH₃)]⁺Cl⁻ (24) ^b
NCH ₃	3.78	4.25	4.34
H ₂	6.20	6.67	6.83
H ₃	6.87	7.50	8.05
H ₄	5.94	6.76	7.34
H ₅	7.26	7.99	8.14
^a in CDCl ₃ , ^b in CD ₂ Cl ₂ .			

Previously, several hybrid ligands were reported to yield palladium complexes with a core structure $[\text{PdL}(\text{MeCN})\text{Cl}]^+$ including the pyrazole derivative 4-(2-hydroxybenzoyl)-2-(pyridin-2-yl)-1*H*-pyrazol-3-ol (**A**),³² the Schiff base N-(benzoyl)-N'-(2,4-dimethoxybenzylidene)hydrazine (**B**)³³ and the iminocarbene [3-methyl-1-{2-(2,6-

diisopropylphenylimino)-propyl}imidazolium] chloride (**C**)³¹ (Figure 3-11). For complex **A**, the Cl-atom occupies the *trans* site with respect to the N-atom of pyrazol ring which has a lower *trans* directing ability than the pyridine N-atom, evidenced by X-ray structure data of platinum dihalide complexes incorporating the same ligand.³² For complex **B**, the Cl ligand is *trans* to the aryl C-atom, although generally a σ -bonded carbon has a higher *trans* influence than an imine or amine N-atom.^{34, 35} However, Crociani *et al.* reported that for C,N chelating ligands, the *trans* site of halide is switchable depending on the nature of the ligands.³¹ In the case of complex **C**, a possible exchange of the chloride and acetonitrile ligands was observed.

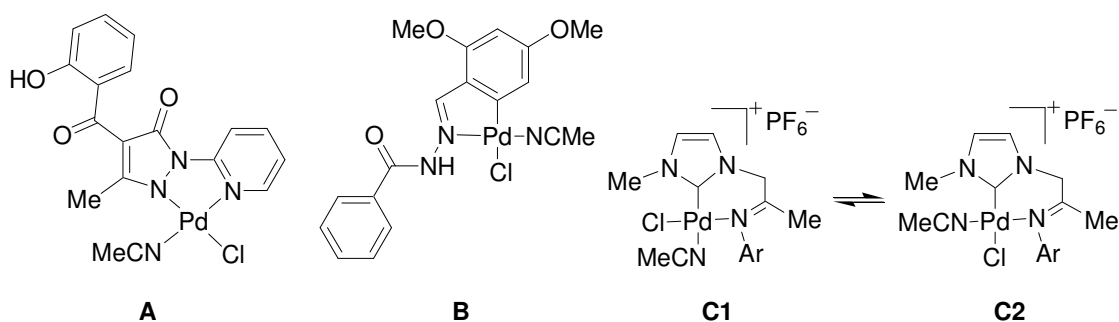


Figure 3-11. Examples of palladium complexes structurally analogous to **24**.

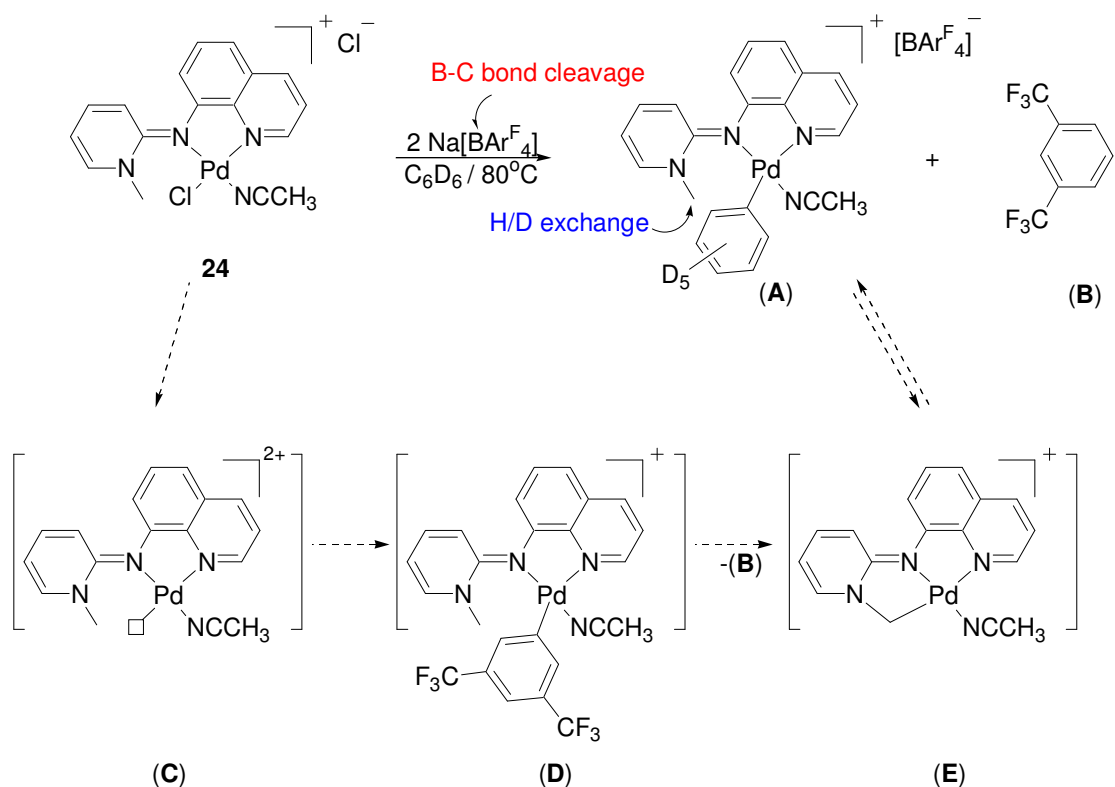
Due to the lack of an X-ray crystal structure, the conformation of **24** was unable to be confirmed. However, taking all the description above into account, due to the stronger donating ability of the PYE moiety than that of the quinolinyl N-atom (see Chapter 2), we presumed the acetonitrile ligand is more likely *trans* to the N-atom of the PYE moiety as drawn in Scheme 3-7.

3.4.3.3.2 Reactivity studies of $[\text{PdCl}(\text{NCCH}_3)(\text{MeN}^{\text{Quino}})]^+\text{Cl}^-$ (**24**)

A project aim was to examine the reactivity of transition metal PYE complexes and investigate the influence of steric factors and the strong donating ability of PYE ligands. One area of initial interest was C-H bond activation, an important research area with application to functionalisation of fine and bulk chemicals.³⁶ Mechanistically, Bercaw *et al.* proposed five different classes for C-H bond activation, on the basis of reaction stoichiometries, including oxidative addition, σ -bond metathesis, electrophilic substitution, 1,2-addition, and metalloradical activation.³⁷ The oxidative addition mechanism usually

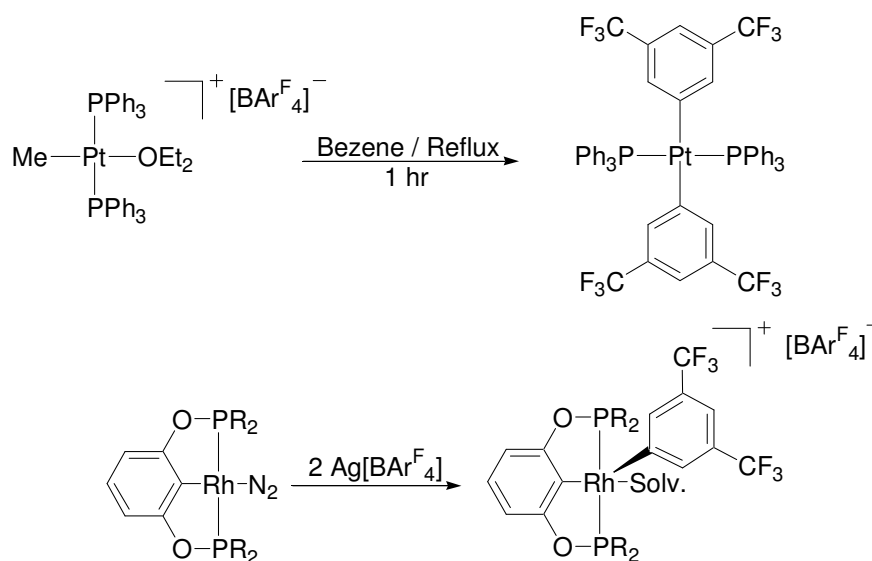
operates for reactions at electron-rich, low-oxidation-state complexes, which involves two steps, the association of the hydrocarbon at the metal and the oxidative cleavage of the C-H bond of the coordinated hydrocarbon. To make the first step happen, a coordination site is required by displacing the coordinated ligand with hydrocarbon via an associative or dissociative step.

A common method for introducing a 'vacant' coordination site to increase reactivity for C-H bond activation, is halide abstraction in the presence of a noncoordinating anion by using compounds such as Na[B{3,5-(CF₃)₂C₆H₂}₄] (NaBAr^F₄). The poor coordinating ability of the [BAr^F₄]⁻ anion decreases the anion interference during reaction and also improves the solubility of charged products. Reaction between **24** and 2 eq. NaBAr^F₄ in benzene-d₆ at 80 °C (Scheme 3-8) initially showed a significant colour change from red to green after very short heating, followed by a yellow coloured solution on continuous heating. The ¹H NMR spectrum of the reaction mixture after one day shows the complete consumption of **24** and the presence of several new species. A single set of coordinated acetonitrile and ligand signals indicates the reaction proceeded selectively via ligand metathesis from chloride to a new ligand. Prolonging the heating gave no further formation of new species but a disappearance of the ligand *N*-methyl signal. Furthermore, free 1,3-bis(trifluoromethyl)benzene was characterised in the ¹H NMR spectrum. In addition, the ¹⁹F NMR spectrum shows several signals close to each other at ca. -62 ppm.



Scheme 3-8. Proposed mechanism for reaction between **24**, $\text{NaBAR}_4^{\text{F}}$ and C_6D_6 .

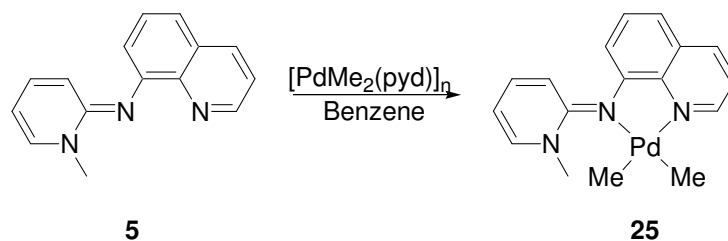
Taking all the above observations into account, B-C bond cleavage of BAR_4^{F} anion and H/D exchange of N-methyl group are proposed to take place in the reaction above (Scheme 3-8). The observation of B-C bond cleavage is very rare and only two cases have been reported for Pt and Rh complexes respectively^{38, 39} (Scheme 3-9). Herein, the B-C cleavage of BAR_4^{F} anion occurred as a result of an electrophilic attack of an unsaturated Pd(II) cationic center (**C**) to generate an intermediate **D**. A cyclometallation reaction was followed to yield the free aryl compound **B** and a palladacycle intermediate **E** which contains a reactive Pd-C bond. Then C_6D_6 was activated to generate a more stable phenyl complex **A**. The disappearance of N-methyl signal indicates step **E** to **A** is reversible under heating.



Scheme 3-9. Reactions involving with B-C bond cleavage of BARF_4^- anion.

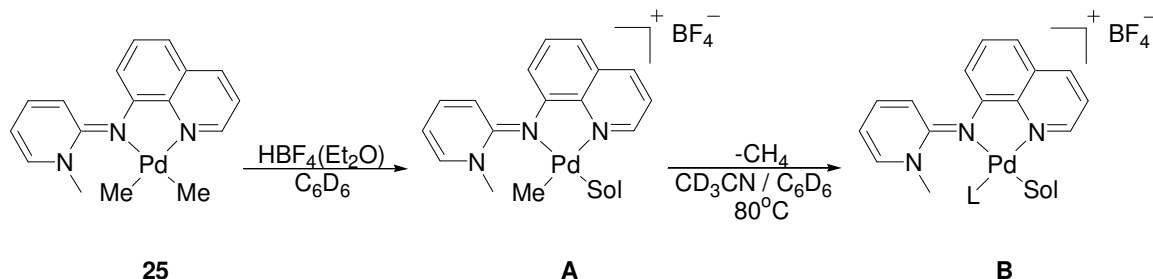
3.4.3.4 Synthesis and reactivity of $[\text{Pd}(\text{CH}_3)_2(\text{MeN}^{\text{Quino}})]$ (**25**)

Inspired by the discovery of the unique reaction in Scheme 3-8, a dimethyl palladium complex **25** was synthesised to gain insight into the C-H bond activation mediated by PYE ligands. Complex **25** was obtained as an orange solid from reaction between **5** and $[\text{PdMe}_2(\text{pyd})]_n$, a common dimethyl precursor,⁴⁰ in benzene at room temperature, followed by recrystallisation in hexane at $-40\text{ }^\circ\text{C}$ (Scheme 3-10). The data of ^1H and ^{13}C NMR spectroscopy, mass spectrometry and elemental analysis is consistent with the proposed formulation. As expected, the solubility of **25** is very good in most common organic solvents. The ^1H NMR spectrum of **25** shows chemical shifts downfield in comparison to the free ligand and significant separation of two methyl ligand signals at 0.21 and 1.31 ppm recorded in C_6D_6 , and -0.66 and 0.19 ppm in CD_3CN respectively. Similarly, the ^{13}C NMR spectrum displays two methyl signals at -10.1 and -3.5 ppm recorded in C_6D_6 . This separation reflects the significant difference of the *trans* influence of PYE (corresponding to higher field PdMe signal) and quinolinyl moieties. The chemical shifts of the methyl ligand (PdMe) in ^1H and ^{13}C NMR spectroscopy are comparable with that of bipyridyl analogue (1.11 ppm for ^1H and -6.6 ppm for ^{13}C).⁴¹



Scheme 3-10. Synthesis of dimethyl palladium complex **25**.

To initiate C-H bond activation, 1 eq. $\text{HBF}_4(\text{Et}_2\text{O})$ was added into the C_6D_6 solution of **25** instantaneously leading to the formation of methane gas and an insoluble yellow precipitate which was separately characterised to be a monocationic palladium complex **A** (Scheme 3-11) by ^1H NMR spectroscopy recorded in CD_2Cl_2 . The resulting complex **A** in C_6D_6 was heated at 80°C . However, the poor solubility of **A** prevented the proceeding of the activation of benzene in benzene. So a combination solvent of CD_3CN and C_6D_6 (3:1) was filled into the tube after the removal of C_6D_6 . After heating for three days, ^1H NMR spectroscopy shows the formation of methane gas and a new species, and also a slow consumption of C_6D_6 . The reaction was extremely slow, even after heating for 24 days, the reaction was still not complete. Although the formation of methane and the consumption of C_6D_6 were observed, no significant reduction of the N-methyl signal due to H/D exchange was observed (Scheme 3-11). Unlike the reaction in Scheme 3-9, a different reaction pathway that is not through a cyclometallated intermediate but involving the Pd-Me bond could be possible due to substrates and solvent variation. The new species **B** could be the product of aromatic C-H activation. However, at this stage, no conclusion can be drawn. This work was conducted at the end of project and due to lack of time, further investigation was not carried out.



Scheme 3-11. Attempted C-H activation of benzene mediated by **25**.

3.5 Attempts to synthesis of other transition metal complexes with PYE ligands

3.5.1 Gold

Recently, gold chemistry has become fashionable as the so-called “gold rush” in organometallic chemistry, has progressed, with the development of efficient and selective Au-catalysed transformations.⁴² The vast majority of Au-catalysed reactions involve substrates containing unsaturated carbon-carbon bonds as nucleophiles which can be activated by gold. Gold has been regarded as an exceedingly mild, relatively carbophilic Lewis acid similar to a ‘soft proton’.^{42, 43} To date, phosphine and NHC carbene ligands have been extensively investigated and utilised in Au-catalysed homogeneous catalysis, but there is little known about nitrogen ligands in this area. Before we look into the potential of PYE ligands as ancillary ligands in Au-catalysed catalysis, a knowledge of the coordination chemistry of gold with PYE ligands needs to be obtained.

The most common oxidation states of gold catalysts are Au(I) and Au(III). For Au(I), there are not too many examples of gold complexes incorporating sp^2 -nitrogen ligands. For example, AuCl(Py) as shown in Figure 3-12 was synthesised by Ray *et al.* in 1930.⁴⁴ The precursor, AuCl(SMe₂), is commonly used to yield linear Au(I) complexes. For Au(III), it has been concluded that nitrogen ligands can greatly improve the stability of Au(III) catalysts.⁴³ Compared with Au(I), Au(III) complexes with mono-,⁴⁵ bi-dentate nitrogen ligands⁴⁶ and N,O chelating ligands⁴⁷ (Figure 3-12) are more common in catalysis and show excellent activity.

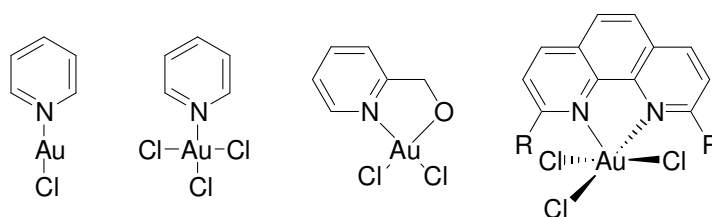
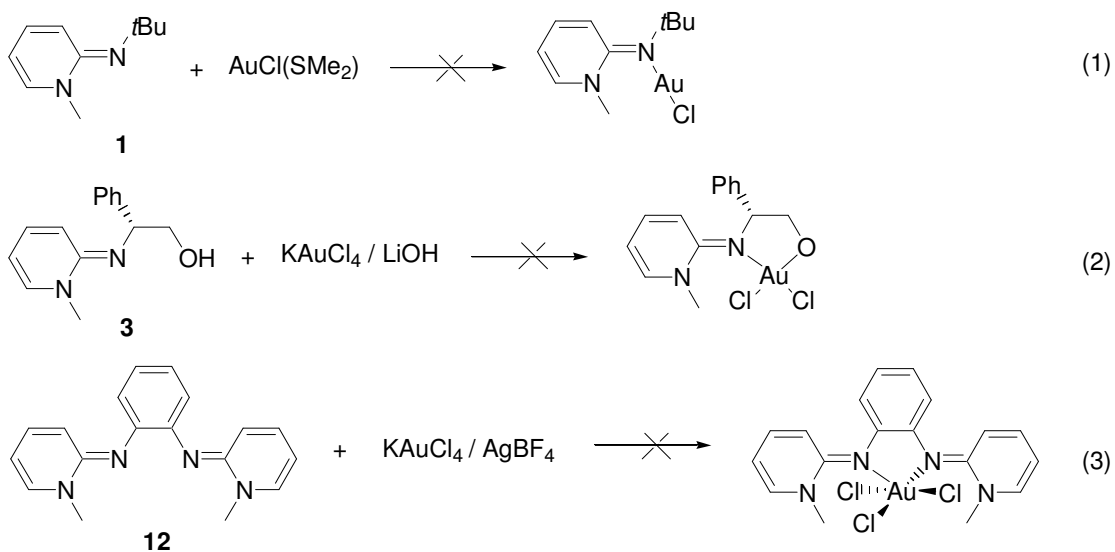


Figure 3-12. Examples of gold(I) and gold(III) complexes with N-donor or N,O-donor ligands.

Initially, we attempted to synthesis the gold complexes with PYE ligands from the reaction between compound **1** and AuCl(SMe₂) in acetonitrile at room temperature (Scheme 3-12, eqn 1). ¹H NMR spectroscopy shows a series of broad signals which are not

consistent with the expected complex. After refluxing for 72 hours, free SMe_2 signal was observed but the rest of the signals were still complicated. Furthermore, due to the interest of asymmetric catalysis, the chiral compound **3** was introduced and mixed with KAuCl_4 in MeOH in the presence of LiOH as base at room temperature (Scheme 3-12, eqn 2). Again, a series of broad signals were observed in the ^1H NMR spectrum. Similarly, reaction between bidentate ligand **12** and KAuCl_4 in acetonitrile followed by halide abstraction with AgBF_4 did not give any products that could be isolated (Scheme 3-12, eqn 3).



Scheme 3-12. Attempts to synthesis of gold complexes with PYE ligands.

3.5.2 Platinum

As shown in sections 3.3 and 3.4, the coordination chemistry of nickel and palladium with PYE ligands occurs readily. As platinum is in the same group as nickel and palladium, platinum was obviously considered to be the next target to investigate. There is no doubt that platinum complexes with nitrogen ligands have played a very important role in a wide range of chemistry. A number of platinum complexes with various type of nitrogen ligands have been designed and applied extensively in catalytic transformations⁴⁸ and medicinal chemistry.⁴⁹ A few examples of platinum dichloride complexes incorporating sp^2 -nitrogen ligands (bipyridyl,⁵⁰ phenanthroline⁵¹ and 1,4-diaza-1,3-butadiene³⁶) are shown in Figure 3-13.

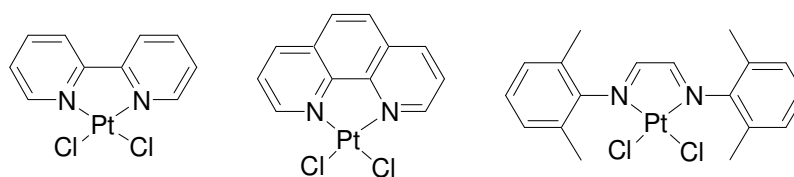
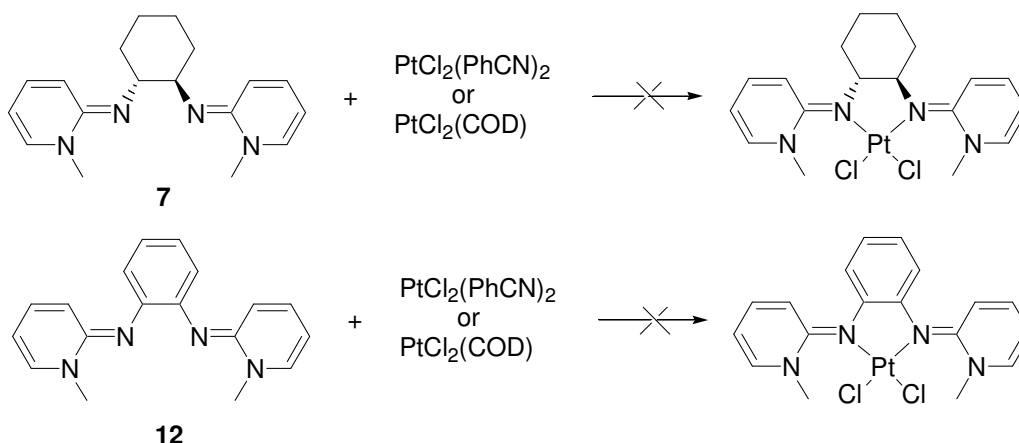


Figure 3-13. Examples of platinum complexes incorporating nitrogen ligands.

We chose two common platinum precursors $\text{PtCl}_2(\text{PhCN})_2$ and $\text{PtCl}_2(\text{COD})$ to attempt to synthesise the platinum complexes with PYE ligands. Ligand **7** and **12** were chosen due to their previous success in nickel and palladium chemistry. All the reactions for both ligands were carried out in acetonitrile or THF by heating for 40 hours (Scheme 3-13). For reaction between **7** and both platinum precursors, ^1H NMR spectroscopy shows complicated broad signals, indicating possibly intra- and intermolecular metallation has occurred. Increasing or decreasing reaction time made no difference. Similar results were obtained for reaction between **12** and $\text{PtCl}_2(\text{PhCN})_2$. A clean NMR spectrum was achieved from reaction between **12** and $\text{PtCl}_2(\text{COD})$, however the chemical shifts due to the ligand are close to those of the protonated form of **12** and there are no signals of coordinated or free cyclooctadiene. Mass spectrometry did not show any peaks expected of Pt-PYE complexes.



Scheme 3-13. Attempts to synthesis of platinum complexes with PYE ligands.

Although the failure of preparing Au and Pt complexes with PYE ligands is quite disappointing, some lessons have been learned to allow us to understand more about PYE ligands. First, the electronegativity of nitrogen probably makes PYE ligands too hard for

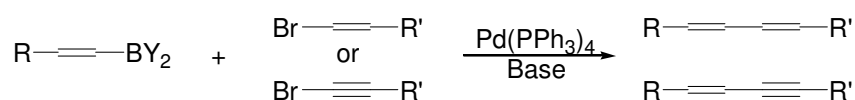
some ‘softer’ late transition metals. Second, the broad signals observed in the ^1H NMR spectra of the attempted reactions indicate additional reactions could be occurring and preventing the isolation of the expected complexes.

3.6 Palladium-catalysed Suzuki-Miyaura cross-coupling reactions

3.6.1 Introduction

Along with the rapid development of medicine, polymeric materials and fine chemicals, the requirement of compounds containing biaryl and substituted aromatic structures is vigorously growing. In that context, modern transition-metal catalysed cross-coupling reactions have been extensively investigated and utilised to construct the carbon-carbon bonds including Kumada, Negishi, Stille, Sonogashira, Heck, Hiyama and Suzuki type cross-coupling reactions. Among these methodologies, Suzuki-Miyaura cross-coupling (SMC) reaction⁵²⁻⁵⁶ has risen in popularity and become one of the most powerful tools in synthetic chemistry due to several advantages over others, *e.g.* mild reaction conditions, high tolerance towards functional groups, the commercial availability and stability of its reagents, and the ease of handling and separation of by-products from reaction mixtures.⁵⁷

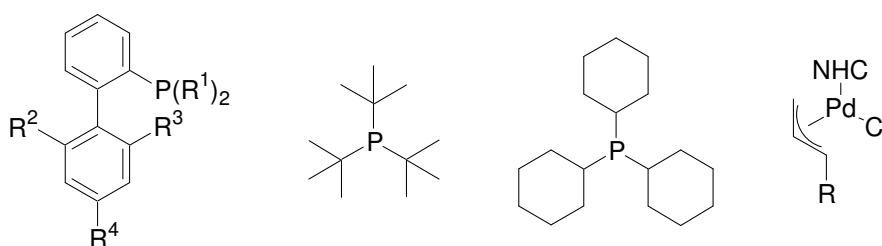
The SMC reaction was first established in 1979 by Suzuki, Miyaura and co-workers.⁵⁸ Alkenylboranes were found to be coupled with alkenyl halides or alkynyl halides in the presence of a catalytic amount of tetrakis(triphenylphosphine)palladium and bases with high regio- and stereospecificity in good yields (Scheme 3-14). A few years later, Suzuki *et al.* reported the palladium-catalyzed coupling of phenylboronic acid with haloarenes resulting in the corresponding biaryls in excellent yields.⁵⁹ Since then, a variety of transition metals, such as palladium,^{57, 60, 61} nickel,^{10, 62-64} iron⁶⁵ and copper,⁶⁶ have been used to mediate the SMC reaction. Herein, owing to our own interest of palladium and nickel chemistry, we only take palladium- or nickel-catalysed SMC reaction into account and introduce their advanced development.



Scheme 3-14. First example of Suzuki-Miyaura cross-coupling.

3.6.1.1 Advanced development of Pd- and Ni-catalysed SMC reaction

In the last three decades, with the wide expansion of the substrates scope and the deep investigation of the reaction mechanism, a number of different catalytic systems have been discovered. However, aryl chlorides with lower cost and wider diversity were rarely utilised due to the lower reactivity relative to other halides caused by higher bond dissociation energies (95 for Cl; 80 for Br; 65 kcal/mol for I).⁶⁷ Of those various systems, three ligand families reported by Buchwald (dialkylbiaryl phosphine),⁵⁷ Fu (tri-*tert*-butylphosphine and tricyclohexylphosphine)⁶⁰ and the Nolan group ($[(\text{NHC})\text{Pd}(\text{allyl})\text{Cl}]$)⁶¹ have shown active catalytic behaviour towards aryl chlorides including electronically deactivated, heterocyclic and hindered compounds under mild conditions (Scheme 3-15). The steric bulk and rich electronic donating ability of these ligands contribute to stabilizing active species under the reaction conditions and facilitating the oxidative addition step of aryl chlorides.⁶⁸



Scheme 3-15. Examples of active ligand families in SMC reaction.

As in other coupling reactions, the mechanism of SMC reaction involves three key steps, including the oxidative addition of an aryl halide to the Pd(0) complex, transmetalation with a boronic acid and reductive elimination to give the corresponding biaryl product and regenerate the Pd(0) species.⁶⁸ Each step has been investigated in mechanistic detail.⁶⁹⁻⁷¹ As shown in Figure 3-14, the role of the base has been proposed differently into two paths. In path A, a more reactive boronate species generated from the interaction of the base with the boronic acid subsequently interacts with the Pd centre and transmetalation in an intramolecular fashion.⁷¹ Alternatively, the halide is replaced by the base in the coordination sphere of the palladium complex to generate a new species that transmetalates with boronic acid intramolecularly (path B).⁷² The truly catalytically active palladium species is still unclear. Although considering the existing evidence, added donor

ligands such as phosphines, phosphites, NHCs and others can be a component of truly active, soluble palladium complexes (L_1Pd species) in SMC reaction, the possibility of Pd(0) nanoparticles liberated from precatalysts is not excluded.⁶⁸

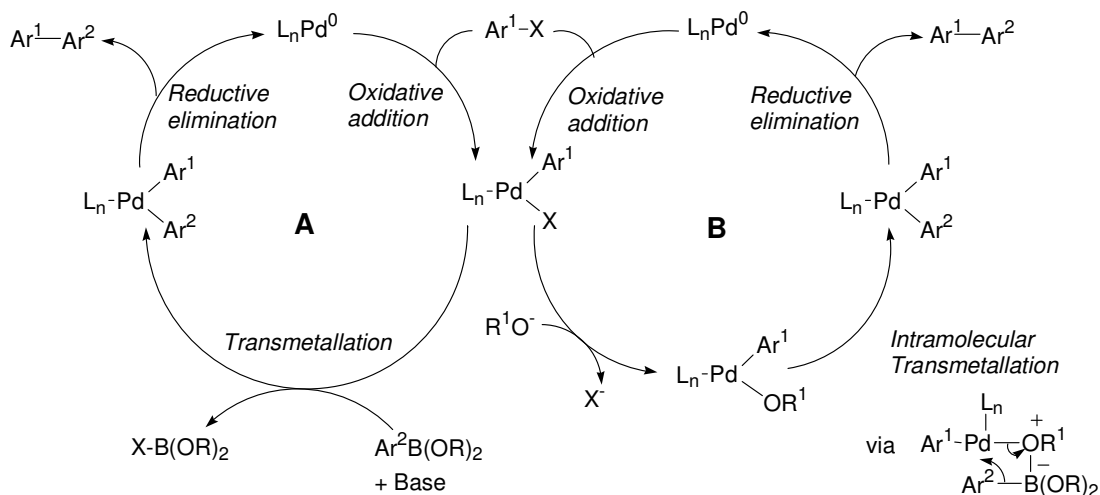


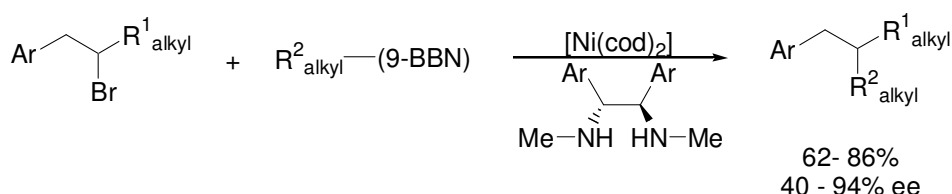
Figure 3-14. General catalytic cycle for Suzuki-Miyaura cross-coupling reaction.⁵⁷

Recently, the development of SMC reaction has been emphasised on the utility of secondary alkyl halides⁷³ and alkylboronic acid derivatives,⁷⁴ and the investigation of asymmetric SMC reaction.⁷⁵ Alkyl halides, in particular those containing β -hydrogen atoms that easily undergo β -hydride elimination pathway, were previously considered to be an unsuitable class for coupling reactions, not only because the stronger $C(sp^3)-X$ bonds compared with the $C(sp^2)-X$ bonds make the oxidative addition step more difficult, but also the lack of π electrons to interact with the empty metal d orbitals leads to the instability of reaction intermediates. In comparison with primary alkyl halides that have been exploited in a wide range,⁷⁶ secondary alkyl halides with more steric hindrance are still a challenge for organometallic chemists. Nevertheless, recent studies have taken this area a step forward using palladium⁷⁷ and nickel complexes,^{10, 62-64} however, the substrates scope and the yield remain the challenging task.

Alkyl boron derivatives are another challenging class of coupling partner due to their lower reactivity, and usually give lower yield than arylboronic acids. Since the groundbreaking work using $PdCl_2(dppf)$ and Tl_2CO_3 to couple alkylboronic esters and aryl halides was reported by Miyaura, Suzuki and co-workers in 1989,⁷⁸ the development of this

area has been widely expanded to alkylation of aryl, alkenyl halides or triflates and alkyl halides with alkyl boron derivatives. Although there have been developments, some limitations like harsh conditions, long reaction time, low turnover number and limited substrates scope still require more effort into this area.

As discussed above, secondary alkyl halides are a very challenging class for SMC reaction, however potential installation of a new stereogenic centres makes those very attractive for asymmetric SMC reaction. The first and also only highly enantioselective SMC reaction of alkyl electrophiles coupled with primary alkyl boranes was reported by Fu and co-workers using nickel precursor and several chiral diaryl-substituted diamines (Scheme 3-16).⁶⁴ This work opened the door to the development of general methods for asymmetric coupling of non-activated secondary alkyl halides. In addition, asymmetric SMC reaction also looks insight into the synthesis of axially chiral biaryls that are ubiquitous structural motifs in biologically active natural products or ligands for homogeneous catalysis.⁷⁹



Scheme 3-16. First asymmetric SMC reaction of racemic non-activated secondary alkyl halides. (BBN = 9-borabicyclo[3.3.1]nonane; cod = 1,5-cyclooctadiene)

3.6.1.2 Nitrogen donor ligands in SMC reaction

Although phosphine and N-heterocyclic carbenes are normally utilised in SMC reaction as discussed in section 3.6.1.1, these catalysts are often sensitive to air and/or moisture and therefore require air-free handling. A recent report from Hong *et al.*⁸⁰ has shown that the SMC reaction employing diimine as the ligand is more favourable than those with diamine or diphosphine. Having been developed for many decades, a number of various nitrogen donor ligands were designed to catalyse the coupling of aryl halides with aryl boronic acids, however, aryl chlorides are still a challenge for N-donor ligands. In Figure 3-15, several examples of N-donor ligands are shown including α -diimine,²⁵ simple

amine,⁸¹ guanidine,⁸² heterocyclic imine⁸³ and rigid diamine.⁸⁴ In 2001, Nolan *et al.* reported diazabutadiene (α -diimine) can be used to mediate the SMC reaction at 80 °C. High yields were obtained for aryl bromides and activated aryl chlorides but very poor for deactivated aryl chlorides. Similarly, Boykin *et al.* demonstrated that electron rich amine Cy_2NH can be an effective ligand for Pd-catalysed SMC reaction. Reactions can be conducted at room temperature for those electron-deficient aryl bromides, whereas high temperature is required for electron-rich ones. Recently, the reaction condition has been improved from high temperature, air-free condition to room temperature, aerobic condition using new catalytic systems including guanidine and benzimidazolium-pyrazole type ligands, but the yield of those coupling reactions is not ideal. Interestingly, Süß-Fink *et al.* designed a new type of *trans* geometrical complexes with a rigid diamine backbone that shows at temperatures above 60 °C the catalytic performance is increased in the SMC reaction of sterically hindered and deactivated bromides.

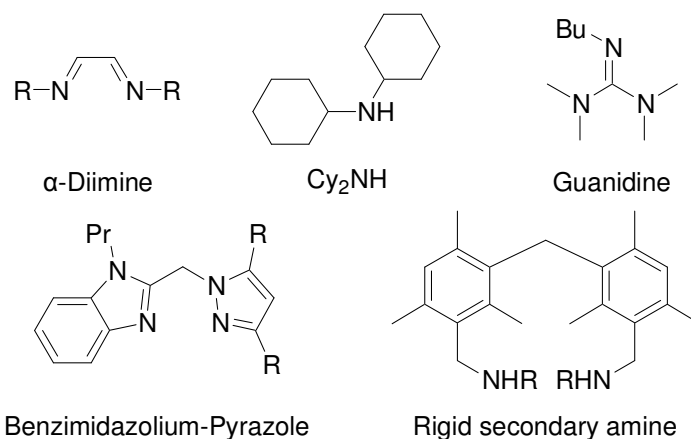


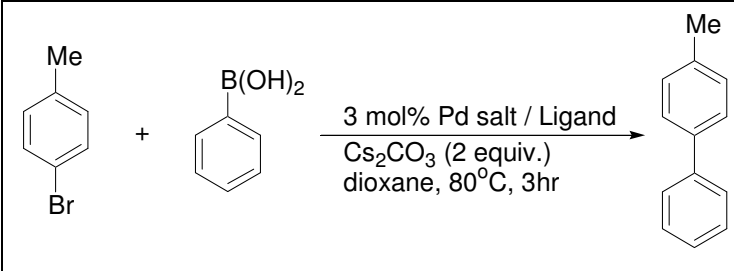
Figure 3-15. Examples of N-donor ligands utilised in SMC reaction.

3.6.2 Application of PYE ligands in the SMC reaction

As we discussed in Chapter 2, PYE ligands have a very strong donating ability that can facilitate the oxidative addition step of the SMC reaction. Furthermore, the modularity of PYE ligands allows us to tune the steric and electronic properties to investigate the influence of those on the SMC reaction.

Initially, we commenced the test with the coupling of 4-bromotoluene and phenylboronic acid in the presence of 3 mol % Pd precursor, 3 mol % ligand, and Cs₂CO₃ in dioxane, at 80 °C. Effect investigation of palladium precursors and ligands led to the observation which Pd(OAc)₂ is a better precursor than others (Table 3-9, entries 2-4) and aryl linked ligand **12** shows a more efficiently catalytic activity (88 %) than alkyl linked ligands **7** and **8**, and electron-rich derivative **13** (Table 3-9, entries 5-7). The poor activity given by alkyl linked ligands **7** and **8** is opposite to the higher activity obtained from electron-rich alkyl-diazabutadiene ligands reported by Nolan and co-workers.²⁵ This unusual behaviour was probably attributed to the interruption by cyclometallation for alkyl linked PYE ligands which will be discussed in Chapter 4.

Table 3-9. Influence of PYE ligands and palladium precursors on the SMC reaction.

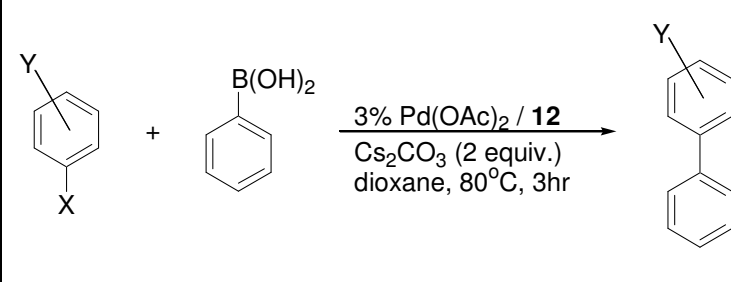
			
entry	ligand	precursor	yield (%) ^a
1	No ligand	Pd(OAc) ₂	32
2	12	Pd(OAc) ₂	88
3	12	PdCl ₂ (CH ₃ CN) ₂	78
4	12	Pd ₂ (dba) ₃	54
5	7	Pd(OAc) ₂	32
6	8	Pd(OAc) ₂	30
7	13	Pd(OAc) ₂	72

^a Isolated yields.

Moreover, the substrates scope was investigated including activated, deactivated and steric hindered bromides, and aryl chlorides using **12** as ancillary ligand in the Pd-catalysed SMC reaction. Surprisingly, the coupling of activated bromides (Table 3-10, entry 3) gave a lower yield (only 42 %) than that of 4-bromotoluene. Probably, the *meta*-substituted groups caused a steric problem, similar to the *ortho*-substituted substrate that

only gave a trace of product (Table 3-10, entry 2). For deactivated bromides, reaction proceeded slowly to give the corresponding product in a very low yield (34 %) (Table 3-10, entry 4). Unfortunately, this Pd(OAc)₂/PYE(**12**) catalytic system was unable to activate aryl chlorides (Table 3-10, entry 5).

Table 3-10. Pd(OAc)₂/PYE(**12**)-catalysed SMC reaction of aryl halides with phenylboronic acid.

		
entry	aryl halide	yield (%) ^a
1	Me-C ₆ H ₄ -Br	88
2	2,4,6-trimethylphenyl-Br	Trace
3	3,5-bis(trifluoromethyl)phenyl-Br	42
4	4-aminophenyl-Br	34
5	Me-C ₆ H ₄ -Cl	Trace

^a Isolated yields.

Although Pd-catalysed SMC reaction has achieved great success, palladium still is a quite expensive metal that consequently limits the expansion of this methodology in industry. Less expensive metals like nickel, iron and manganese have drawn much attention in this area.^{64, 65, 85} For those reasons, we decided to test PYE ligands in Ni, Fe or Mn-catalysed SMC reaction. However, all the reactions conducted with iron or manganese salts,

and ligand **1**, **5** or **12** only gave homocoupled product biphenyl instead of cross-coupled product 4-methylbiphenyl (Table 3-11, entries 1-6). Attempts to utilise nickel complex **18** was unsuccessful (Table 3-11, entry 7).

Table 3-11. SMC reaction of aryl halides with phenylboronic acid using Fe, Mn and Ni systems.

entry	catalyst		yield ^a
1	1	FeCl ₂	Homocoupling
2	1	MnCl ₂	Homocoupling
3	5	FeCl ₂	Homocoupling
4	5	MnCl ₂	Homocoupling
5	12	FeCl ₂	Homocoupling
6	12	MnCl ₂	Homocoupling
7	18		No reaction
^a Determined by ¹ H NMR.			

As shown above, for SMC reaction, PYE ligands seem not to exhibit as high catalytic activity as expected. Two possible reasons are proposed for the observed activity of PYE ligands. First, the steric hindrance caused by *N*-substituent hampers the oxidative addition step in the catalytic cycle, which is proved by the low yields obtained for bulky substrates (Table 3-10, entries 2 and 3). Second, PYE ligands were observed to be incapable of stabilising Pd(0) (*vide supra*). This observation indicates the potential deactivation of catalytic species within the catalytic cycle (Figure 3-13).

3.7 Enantioselective addition of diethylzinc to aldehydes

3.7.1 Introduction

Enantiomerically enriched organic products are of great importance to organic synthesis and the pharmaceutical industry. To obtain the products, much effort has been given into designing or modifying resolved chiral ligands that play an essential role in asymmetric catalysis, however to date there are no definitive rules for designing chiral ligands and complicated synthetic work is required in many cases.^{22, 86} Alternatively, promising approaches have been established including: i) chiral poisoning,^{87, 88} and ii) chiral⁸⁹ and achiral activation⁹⁰ (Figure 3-16). Those two methods require the addition of additives to deactivate or activate one enantiomer of a racemic catalyst, or activate an enantiopure catalyst. The advantage of the activation strategy over deactivation is that the activated catalyst can produce a greater enantiomeric excess in the products than can the enantiomerically pure catalyst on its own.⁹¹

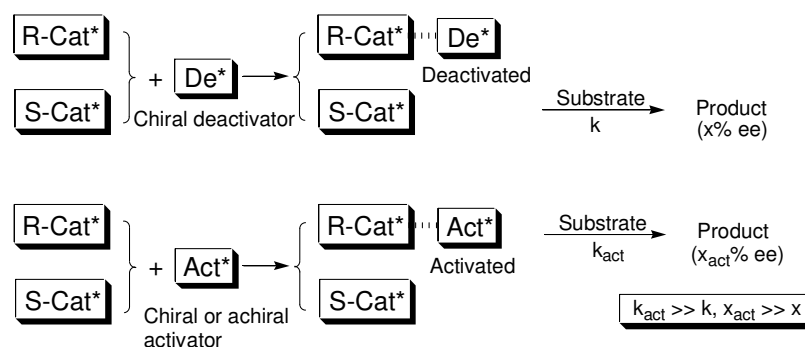
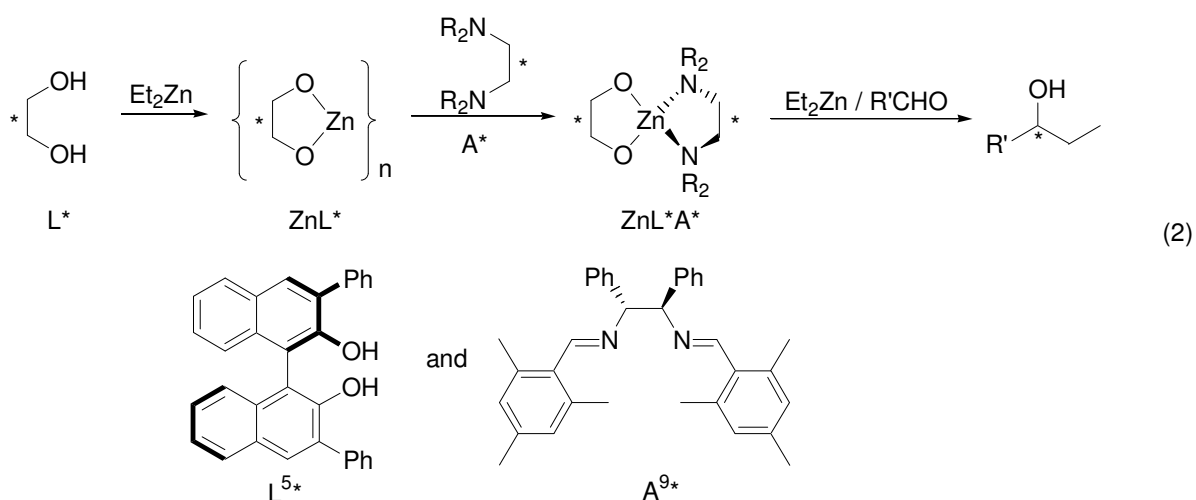
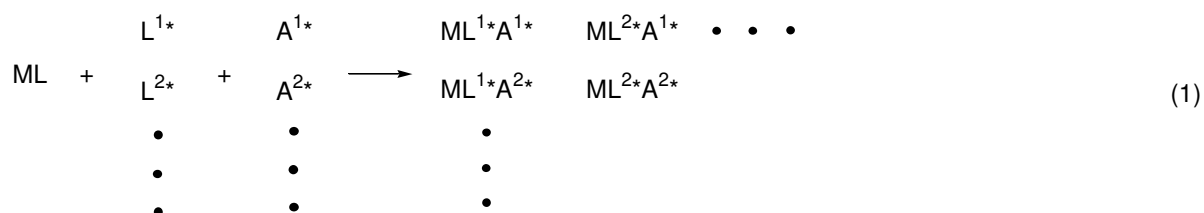


Figure 3-16. Concept of asymmetric activation.

By using the asymmetric activation method that was introduced by Mikami and co-workers, the efficiency and enantioselectivity of several asymmetric catalytic reactions have been enhanced including the carbonyl-ene reaction,⁹¹ hydrogenation reaction,⁹² Diels-Alder reaction⁹³ and addition of alkyl groups to aldehydes.^{90, 94} For example, Mikami *et al.*⁹⁴ screened a series of catalytic systems of chiral catalyst obtained from ligand exchange with chiral ligands (L^{1*}, L^{2*}, etc.) in parallel combination with chiral activator (A^{1*}, A^{2*}, etc.) through high-throughput screening method for alkyl addition of aldehydes (Scheme 3-17, eqn 1). They proposed that the zinc alkoxide aggregates from complexation of chiral diol ligands with diethyl zinc, which can be activated by chiral nitrogen activators to form a

monomeric zinc catalyst for the enantioselective alkyl transfer. The combination of L^{5*} and A^{9*} gave the best results in 100% yield and 97% ee which are massively higher than that of using L^{5*} alone (Scheme 3-17, eqn 2).



Scheme 3-17. Method of asymmetric alkyl addition to aldehydes by Mikami.

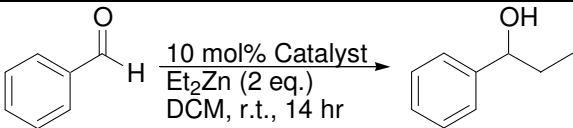
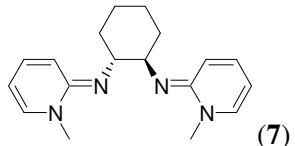
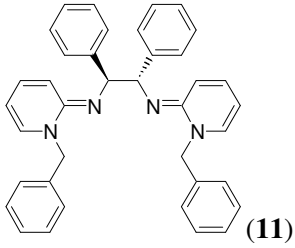
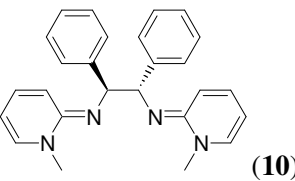
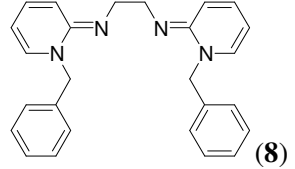
Later, Walsh *et al.*⁹⁰ established the achiral activation process for alkyl addition to aldehydes using achiral and meso activator to activate an enantiopure catalyst and the resulting catalyst exhibits enhanced efficiency and enantioselectivity. The existence of four-coordinate $(\text{Ph}_2\text{-BINOLate})\text{Zn}(\text{diimine})$ and $(\text{Ph}_2\text{-BINOLate})\text{Zn}(\text{diamine})$ complexes were evidenced by X-ray crystal structures.

3.7.2 Enantioselective addition of diethylzinc to aldehydes with PYE ligands

Inspired by the work of Mikami and Walsh, we decided to screen our bidentate chiral and achiral PYE ligands in combination with chiral BINOL and diethyl zinc for alkyl addition to aldehydes. First, we established the control experiment of (S)-BINOL and PYE ligands by running reactions separately in dichloromethane at room temperature for 14 hours. Unsurprisingly, low enantioselective excess of the products in those reactions is

obtained but in high yields (Table 3-12, entries 1-3). Combination of chiral ligands **7** or **11** with (S)-BINOL resulted in decline of ee value compared with using BINOL itself giving only 19% and 5% respectively (entries 4 and 7). Decreasing the reaction temperature to 0 °C gave only slight improvement (entry 5). Similarly, the utilisation of achiral ligands **8** and **12** showed no asymmetric amplification at all (entries 8 and 9).⁹⁵

Table 3-12. Results of screening chiral and achiral bidentate PYE ligands with BINOL.

				
entry	ligand	chiral diol	conversion (%) ^a	ee (%) (config.) ^b
1	N/A	(S)-BINOL	100	49 (S)
2	 (7)	N/A	90	12 (R)
3	 (11)	N/A	95	15 (R)
4	(7)	(S)-BINOL	100	19 (S)
5	(7)	(S)-BINOL	36	21 (R) ^c
6	(7)	(R)-BINOL	100	11 (S) ^c
7	 (10)	(S)-BINOL	100	5 (S)
8	 (8)	(S)-BINOL	100	3 (R)

9	 (12)	(S)-BINOL	100	12 (R)
^a Based on the consumed aldehydes. ^b Determined by HPLC on a OD column.				
^c Run at 0 °C for 4 hr.				

A monomeric tetrahedral zinc that can coordinate the aldehyde to give a 5-coordinate zinc centre was proposed generally for this type of reaction. By modelling the tetrahedral zinc complex, we found the combination of **7** with (S)-BINOL is likely to be more sterically encumbered than with (R)-BINOL (Figure 3-17). To detect the effect of this steric difference, a parallel reaction was run with a combination of **7** with (R)-BINOL (entry 6). Interestingly, significantly higher ligand acceleration was obtained with a 100% yield, however, a lower ee (11%) was quite disappointing. This interesting observation indicates that with less steric alkyl addition to aldehyde was significantly accelerated but the enantioselectivity was not improved.

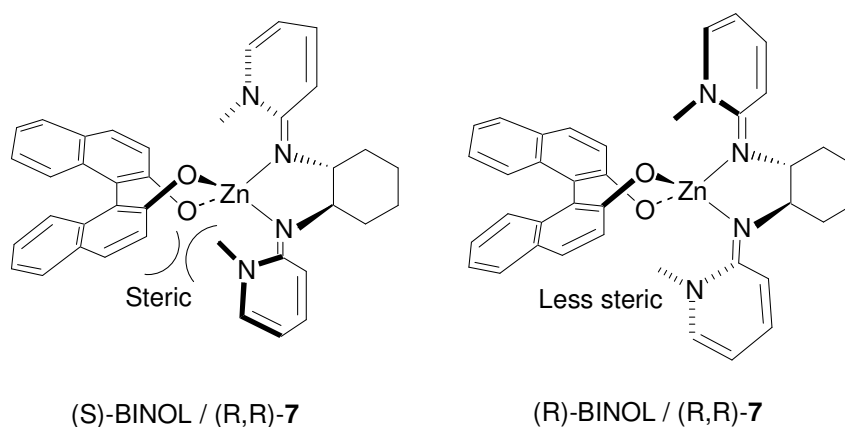


Figure 3-17. Molecular models of (BINOLate)Zn(PYE-7).

3.8 Theoretical comparison of donor properties between PYE and NHC

Evidently, the reactivity of the palladium complexes of PYE in Suzuki-Miyaura reaction is not as expected. In order to gain some greater insight into the comparative bonding of NHC and PYE palladium complexes, DFT calculations were performed by Dr. John Slattery.

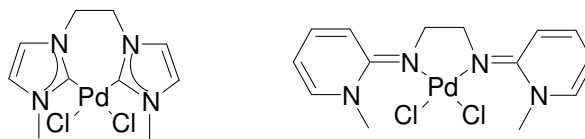


Figure 3-18. Model complexes of chelating di-NHC and di-PYE ligands.

DFT calculations have been performed on the complexes shown in Figure 3-18 to compare the bonding of NHC and PYE ligands coordinated to palladium. Analysis of the average partial charges of the Pd and C atoms in the NHC complex and Pd and N atoms in the PYE complex shows, as expected based on the electronegativities of the elements, a much greater polarization of the Pd-N bond (av. $\delta_{charge} = 0.53$ PABOON, 0.74 NBO) in the PYE complex than the Pd-C bond (av. $\delta_{charge} = 0.30$ PABOON, 0.36 NBO) in the NHC complex.

Analysis of the molecular orbitals (PBE0/def2-TZVPP level) for the two complexes also highlights differences in bonding between the PYE ligands and NHCs. The M-N σ -bonding orbitals of the PYE complex lie at significantly higher energy (-8.0 and -8.1 eV) than the M-C σ -bonding orbitals of the NHC complex (-10.9 and -11.0 eV) suggesting an increased stability of the NHC σ -bond towards electrophiles. In addition, the LUMO of the PYE complex lies at lower energy (-1.7 eV) than that of the NHC complex (-0.4 eV) suggesting a greater stability towards nucleophilic attack. The extent of M-L back bonding in these complexes can be estimated by analysis of the Pd “lone pair” orbitals in the NBO calculations, which hold the 8 d-electrons in this model. In the PYE complex, the average occupation of these Pd orbitals is 1.984 electrons and does not vary a great deal between the four orbitals (although one is a little lower than average at 1.977 electrons). In contrast, in the NHC complex one of the Pd lone pairs has a much lower occupation of 1.920 electrons. This is involved in back donation to the carbene and suggests that there is some π -back donation in this complex, whereas little π -back donation is suggested in the PYE system as would be expected. Essentially, the greater spread of orbital energies for the Pd-NHC complex in comparison to the Pd-PYE is indicative of greater metal-ligand orbital interaction and stronger bonding.

3.9 Conclusions and future work

A variety of transition metal complexes (Rh, Ni, Pd) incorporating PYE ligands have been synthesised and fully characterised. According to the comparison of X-ray structures, the electronic distribution across the PYE moiety of metal complexes with PYE ligands is close to that of the protonated salt. The CO stretching frequencies of $[(^{\text{Me}}\text{N}^{\text{tBu}})\text{Rh}(\text{CO})_2\text{Cl}]$ **16** indicate that PYE ligands are strong donor ligands with no significant π -backdonation, which is also inferred from the geometry of the nickel(II) complexes **18-21**.

The line-broadening and coalescence observed in variable temperature NMR of **23** evidently reveals the fluxionality of the complexes, also evidenced by the observation of *trans* and *cis* isomers in the solid state of **22**. However, there was no evidence for rotation about the imine bond.

A unique B-C bond cleavage of BAr^{F_4} anion by complex **24** was found probably through an electrophilic attack of an unsaturated Pd(II) cationic centre. The H/D exchange of the N-methyl group implies possible existence of a reactive cyclometallated intermediate. This observation would allow us to look into the activation of other types of inert bonds (e.g. N-H) with **24** or related complexes in future. To achieve a clear clue of C-H bond activation mediated by PYE ligands, dimethyl palladium complex **25** was prepared. Direct evidence such as methane formation and H/D exchange in benzene was observed, nevertheless, absence of H/D exchange of N-methyl group indicates a different reaction pathway and future investigation is required.

A series of Pd-catalysed Suzuki cross-coupling reactions with PYE ligands were carried out. A reasonable yield (88%) was obtained for the coupling of 4-bromotoluene with phenylboronic acid using **12**, however, this **12**/Pd(OAc)₂ system was unsuccessfully employed in the deactivated and steric bulky aryl bromides, and aryl chlorides. This could be partly attributable to the steric effect of the *N*-substituent. Also, DFT calculation shows Pd-PYE bonding is characterized by a high-lying Pd-PYE bond and significantly more ionic character because of the greater electronegativity difference between palladium and

nitrogen. The lack of acidity also accentuates the polarization of the Pd-N bond. Consequently, the Pd-PYE bond is susceptible to electrophilic and nucleophilic attack resulting in PYE ligand loss or substitution during a catalytic cycle.

Asymmetric alkyl addition to aldehydes with a combination of chiral binol and bidentate chiral or achiral PYE ligands did not give high enantioselective excess. Opposite results from two parallel reactions indicate that strict steric control is very crucial for this type of reaction.

Collectively, the results suggest that the *N*-substituent may be weakening coordination of PYE ligands to some metals or that the *N*-substituent is exhibiting reaction chemistry. It is surprising that PYE complexes of gold and especially platinum cannot be isolated or even observed spectroscopically, whereas nickel and palladium are easily prepared and stable. The initial aim of controlling the space at the metal, via restricted rotation about the imine bond, may in fact be detrimental to strong metal-ligand bonding.

3.10 References

1. B. T. Heaton, C. Jacob and J. T. Sampanthar, *J. Chem. Soc. Dalton Trans.*, 1998, 1403-1410.
2. E. Rotondo, G. Battaglia, G. Giordano and F. P. Cusmano, *J. Organomet. Chem.*, 1993, **450**, 245-252.
3. W. A. Herrmann, M. Elison, J. Ficscher, C. Kocher and G. R. J. Artus, *Chem. Eur. J.*, 1996, **2**, 772-780.
4. K. Denk, P. Sirsch and W. A. Herrmann, *J. Organomet. Chem.*, 2002, **649**, 219-224.
5. M. E. Doster and S. A. Johnson, *Angew. Chem. Int. Ed.*, 2009, **48**, 2185-2187.
6. V. Lavallo, J. Mafhouz, Y. Canac, B. Donnadiou, W. W. Schoeller and G. Bertrand, *J. Am. Chem. Soc.*, 2004, **126**, 8670-8671.
7. Q. Shi, R. J. Thatcher, J. Slattery, P. S. Sauari, A. C. Whitwood, P. C. McGowan and R. E. Douthwaite, *Chem. Eur. J.*, 2009, **15**, 11346-11360.
8. S. D. Ittel, L. K. Johnson and M. Brookhart, *Chem. Rev.*, 2000, **100**, 1169-1203.
9. G. J. Domski, J. M. Rose, G. W. Coates, A. D. Bolig and M. Brookhart, *Prog. Polym. Sci.*, 2007, **32**, 30-92.
10. J. Zhou and G. C. Fu, *J. Am. Chem. Soc.*, 2004, **126**, 1340-1341.
11. G. D. Jones, J. L. Martin, C. McFarland, O. R. Allen, R. E. Hall, A. D. Haley, R. J. Brandon, T. Konovalova, P. J. Desrochers, P. Pulay and D. A. Vivic, *J. Am. Chem. Soc.*, 2006, **128**, 13175-13183.
12. Z. Csok, O. Vechorkin, S. B. Harkins, R. Scopelliti and X. L. Hu, *J. Am. Chem. Soc.*, 2008, **130**, 8156.
13. L. K. Johnson, C. M. Killian and M. Brookhart, *J. Am. Chem. Soc.*, 1995, **117**, 6414-6415.
14. T. J. Anderson, G. D. Jones and D. A. Vivic, *J. Am. Chem. Soc.*, 2004, **126**, 8100-8101.
15. F. O. Arp and G. C. Fu, *J. Am. Chem. Soc.*, 2005, **127**, 10482-10483.
16. F. H. Allen, *Acta Crystallogr. Sect. B*, 2002, **58**, 380-388.
17. T. Kinnunen, M. Haukka, T. T. Pakkanen and T. A. Pakkanen, *J. Organomet. Chem.*, 2000, **613**, 257-262.

18. A. J. Canty, B. W. Skelton, P. R. Traill and A. H. White, *Aust. J. Chem.*, 1992, **45**, 417-422.
19. E. M. Schubert, *J. Chem. Educ.*, 1992, **69**, 62-62.
20. A. Togni and L. M. Venanzi, *Angew. Chem. Int. Ed. Engl.*, 1994, **33**, 497-526.
21. J. Durand and B. Milani, *Coord. Chem. Rev.*, 2006, **250**, 542-560.
22. F. Fache, E. Schulz, M. L. Tommasino and M. Lemaire, *Chem. Rev.*, 2000, **100**, 2159-2232.
23. A. S. Abu-Surrah, H. H. Al-Sa'doni and M. Y. Abdalla, *Cancer Therapy*, 2008, **6**, 1.
24. A. Garoufis, S. K. Hadjikakou and N. Hadjiliadis, *Coord. Chem. Rev.*, 2009, **253**, 1384-1397.
25. G. A. Grasa, A. C. Hillier and S. P. Nolan, *Org. Lett.*, 2001, **3**, 1077-1080.
26. J. A. Mueller, D. R. Jensen and M. S. Sigman, *J. Am. Chem. Soc.*, 2002, **124**, 8202.
27. M. Kawatsura and J. F. Hartwig, *J. Am. Chem. Soc.*, 2000, **122**, 9546.
28. A. Zapf and M. Beller, *Top. Catal.*, 2002, **19**, 101.
29. F. D. Rochon and P. Kong, *Can. J. Anal. Sci. Spectros.*, 2003, **48**, 30-47.
30. C. Liao and H. M. Lee, *Acta. Cryst.*, 2006, **E62**, m680.
31. M. Froseth, A. Dhindsa, H. Roise and M. Tilset, *Dalton Trans.*, 2003, 4516-4524.
32. E. Budzisz, M. Malecka, B. K. Keppler, V. B. Arion, G. Andrijewski, U. Krajewska and M. Rozalski, *Eur. J. Inorg. Chem.*, 2007, 3728-3735.
33. S. Das and S. Pal, *J. Organomet. Chem.*, 2004, **689**, 352-360.
34. B. Crociani, T. Boschi, R. Pietropaolo and U. Belluco, *J. Chem. Soc.*, 1970, 531.
35. B. J. Coe and S. J. Glenwright, *Coord. Chem. Rev.*, 2000, **203**, 5-80.
36. M. Lersch, A. Krivokapic and M. Tilset, *Organometallics*, 2007, **26**, 1581-1587.
37. S. S. Stahl, J. A. Labinger and J. E. Bercaw, *Angew. Chem. Int. Ed.*, 1998, **37**, 2180.
38. W. V. Konze, B. L. Scott and G. J. Kubas, *Chem. Commun.*, 1999, 1807-1808.
39. H. Salem, L. J. W. Shimon, G. Leitus, L. Weiner and D. Milstein, *Organometallics*, 2008, **27**, 2293-2299.
40. P. K. Byers and A. J. Canty, *Organometallics*, 1990, **9**, 210-220.
41. Y. Pan and B. Young, *J. Organomet. Chem.*, 1999, **577**, 257-264.
42. A. S. K. Hashmi, *Chem. Rev.*, 2007, **107**, 3108-3211.
43. D. J. Gorin, B. D. Sherry and F. D. Toste, *Chem. Rev.*, 2008, **108**, 3351-3378.

44. P. C. Ray and D. S. Sen, *J. Indian. Chem. Soc.*, 1930, **7**, 67.
45. H.-N. Adams and J. Strahle, *Z. Anorg. Allg. Chem.*, 1982, **485**, 65-80.
46. Z. D. Hudson, C. D. Sanghvi, M. A. Rhine, J. J. Ng, S. D. Bunge, K. I. Hardcastle, M. R. Saadein, C. E. MacBeth and J. F. Eichler, *Dalton Trans.*, 2009, 7473-7480.
47. L. Canovese, L. Cattalini and G. Marangoni, *J. Chem. Soc. Dalton Trans.*, 1985, 731.
48. M. Lersch and M. Tilset, *Chem. Rev.*, 2005, **105**, 2471-2526.
49. Y. Jung and S. J. Lippard, *Chem. Rev.*, 2007, **107**, 1389.
50. G. T. Morgan and F. H. Burstall, *J. Chem. Soc.*, 1934, 965-971.
51. F. P. Fanizzi, G. Natile, M. Lanfranchi, A. Tiripicchio, F. Laschi and P. Zanello, *Inorg. Chem.*, 1996, **35**, 3173-3182.
52. N. Miyaura and A. Suzuki, *Chem. Rev.*, 1995, **95**, 2457-2483.
53. A. J. Suzuki, *J. Organomet. Chem.*, 1999, **576**, 147-168.
54. J. Hassan, M. Sevignon, C. Gozzi, E. Schulz and M. Lemaire, *Chem. Rev.*, 2002, **102**, 1359-1470.
55. S. Kotha, K. Lahiri and D. Kashinath, *Tetrahedron*, 2002, **58**, 9633-9695.
56. N. Miyaura, *Top. Curr. Chem.*, 2002, **219**, 11-59.
57. R. Martin and S. L. Buchwald, *Acc. Chem. Res.*, 2008, **41**, 1461-1473.
58. N. Miyaura, K. Yamada and A. Suzuki, *Tetrahedron Lett.*, 1979, 3437.
59. T. Yanagi, N. Miyaura and A. Suzuki, *Synth. Comm.*, 1981, **11**, 513.
60. G. C. Fu, *Acc. Chem. Res.*, 2008, **41**, 1555-1564.
61. H. Clavier and S. P. Nolan, *Annu. Rep. Prog. Chem. Sect. B*, 2007, **103**, 193-222.
62. F. Gonzalez-Bobes and G. C. Fu, *J. Am. Chem. Soc.*, 2006, **128**, 5360.
63. B. Saito and G. C. Fu, *J. Am. Chem. Soc.*, 2007, **129**, 9602.
64. B. Saito and G. C. Fu, *J. Am. Chem. Soc.*, 2008, **130**, 6694.
65. D. Bezier and C. Darcel, *Adv. Synth. Catal.*, 2009, **351**, 1732.
66. J. H. Li and D. P. Wang, *Eur. J. Org. Chem.*, 2006, 2063-2066.
67. Y. R. Luo, in *Handbook of Bond Dissociation Energies in Organic Compounds*, CRC Press, New York, 2003.
68. N. T. S. Phan, M. Van Der Sluys and C. W. Jones, *Adv. Synth. Catal.*, 2006, **348**, 609-679.

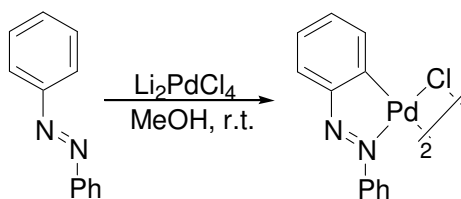
69. H. M. Senn and T. Ziegler, *Organometallics*, 2004, **23**, 2980.
70. V. P. Ananikov, D. G. Musaev and K. Morokuma, *J. Am. Chem. Soc.*, 2002, **124**, 2839.
71. A. A. C. Braga, N. H. Morgon, G. Ujaque and F. Maseras, *J. Am. Chem. Soc.*, 2005, **127**, 9298.
72. N. Miyaura, *J. Organomet. Chem.*, 2002, **653**, 54-57.
73. A. Rudolph and M. Lautens, *Angew. Chem. Int. Ed.*, 2009, **48**, 2656-2670.
74. H. Doucet, *Eur. J. Org. Chem.*, 2008, 2013-2030.
75. F. Glorius, *Angew. Chem. Int. Ed.*, 2008, **47**, 8347-8349.
76. A. C. Frisch and M. Beller, *Angew. Chem. Int. Ed.*, 2005, **44**, 674-688.
77. N. Rodriguez, C. Ramirez de Arellano, G. Asensio and M. Medio-Simon, *Chem. Eur. J.*, 2007, **13**, 4223-4229.
78. M. Sato, N. Miyaura and A. Suzuki, *Chem. Lett.*, 1989, 1405-1408.
79. O. Baudoin, *Eur. J. Org. Chem.*, 2005, 4223-4229.
80. Y. L. Huang, C. M. Weng and F. E. Hong, *Chem. Eur. J.*, 2008, **14**, 4426-4434.
81. B. Tao and D. W. Boykin, *J. Org. Chem.*, 2004, **69**, 4330-4335.
82. S. Li, Y. Lin, J. Cao and S. Zhang, *J. Org. Chem.*, 2007, **72**, 4067-4072.
83. F. Li and T. S. Andy Hor, *Adv. Synth. Catal.*, 2008, **350**, 2391-2400.
84. L. Chahen, B. Therrien and G. Suss-Fink, *Eur. J. Inorg. Chem.*, 2007, 5045-5051.
85. S.-K. Kang, J.-S. Kim and S.-C. Choi, *J. Org. Chem.*, 1997, **62**, 4208.
86. H. Kwong, H. Yeung, C. Yeung, W. Lee, C. Lee and W. Wong, *Coord. Chem. Rev.*, 2007, **251**, 2188.
87. N. W. Alcock, J. M. Brown and P. J. Maddox, *J. Chem. Soc. Chem. Commun.*, 1986, 1532-1533.
88. J. Faller, M. Mazzieri, J. Nguyen, J. Parr and M. Tokunaga, *Pure Appl. Chem.*, 1994, **66**, 1463-1469.
89. K. Mikami, M. Terada, T. Korenaga, Y. Matsumoto, M. Ueki and R. Angelaud, *Angew. Chem. Int. Ed.*, 2000, **39**, 3532-3556.
90. A. M. Costa, C. Jimeno, J. Gavenonis, P. J. Carroll and P. J. Walsh, *J. Am. Chem. Soc.*, 2002, **124**, 6929-6941.
91. K. Mikami and S. Matsukawa, *Nature*, 1997, **385**, 613-615.

92. T. Ohkuma, H. Doucet, Y. Pham, K. Mikami, T. Korenaga, M. Terada and R. Noyori, *J. Am. Chem. Soc.*, 1998, **120**, 1086-1087.
93. S. Matsukawa and K. Mikami, *Tetrahedron: Asymmetry*, 1997, **8**, 815-816.
94. K. Ding, A. Ishii and K. Mikami, *Angew. Chem. Int. Ed.*, 1999, **38**, 497-501.
95. J. Balsells and P. J. Walsh, *J. Am. Chem. Soc.*, 2000, **122**, 1802-1803.

4.0 Palladacycles and their derivatives

4.1 Introduction

As one of the most popular classes of organopalladium derivatives, palladacycles have been extensively developed in the past few decades.¹ Advantages like facile synthesis, easy handling and the possibility of modulating the electronic and steric properties make palladacycles useful in organic synthesis, organometallic catalysis, new molecular materials and medicinal applications.¹⁻⁴ Palladacycles or cyclopalladated compounds are defined as palladium complexes containing at least one metal-carbon bond intramolecularly stabilised by at least one donor atom (N, P, As, O, Se or S). The first palladacycle example was reported by Cope *et al.* in the 1960s using azobenzene derivatives to yield chloride-bridged palladacycle dimers (Scheme 4-1).⁵



Scheme 4-1. Cyclopalladation of azobenzene.

Since that breakthrough, a number of various palladacycles have been synthesised and characterised to allow chemists to investigate their synthesis, structural features, reactivity and applications. A primary classification divides palladacycles into two types: anionic four-electron donor (CY) or six-electron donor (YCY) as shown in Figure 4-1. The former type can be sub-categorised into neutral, cationic or anionic types depending on the nature of the X ligands. Metallated aromatic sp^2 carbon is more common than sp^3 or vinylic sp^2 carbon. The metallated ring of CY-type palladacycles has been found to vary from 3 to 11 members,⁶⁻¹¹ however, five- or six-membered rings are the most common structure. The latter type (YCY), so-called pincer type, contains symmetrical and unsymmetrical sub-categories generally with five- or six-membered rings.

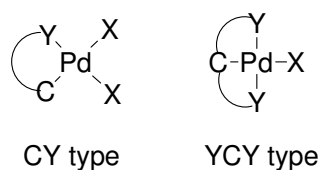


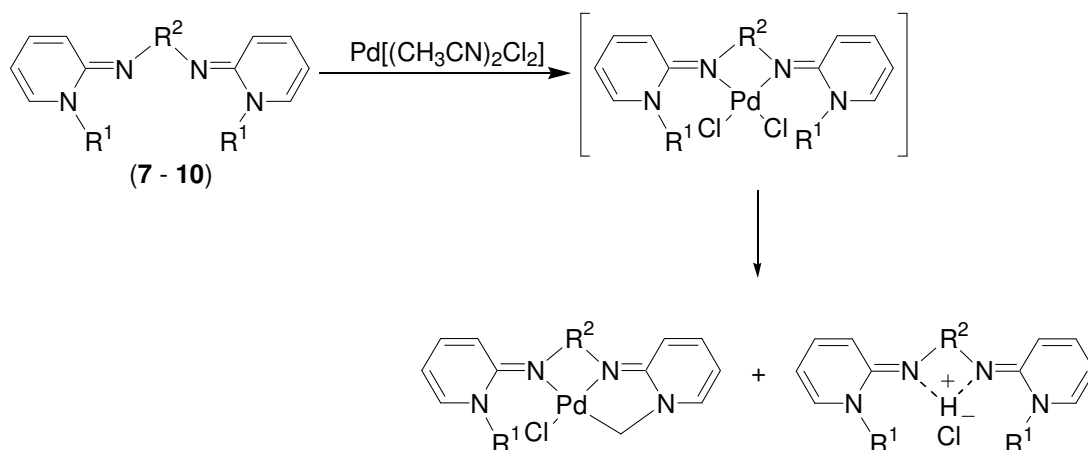
Figure 4-1. Two primary types of palladacycles.

Interesting stoichiometric or catalytic functionalisation of Pd-C bonds with a variety of small molecules including CO, isocyanides, allenes, alkenes and alkynes has been investigated in the past few decades. The insertion of those molecules into Pd-C bonds, followed by depalladation, subsequently yields various organic molecules with complicated heterocyclic rings which are really difficult to synthesis directly using conventional methods (*vide infra*). Furthermore, palladacycles as catalyst precursors in a range of catalytic reactions was initiated by the discovery of a cyclometallated triphenyl phosphite catalysed hydrogenation of C=C bonds in the 1980's.¹² Since then, palladacycles have occupied a central position in catalysis especially in cross-coupling¹³ and oxidation reactions.^{14, 15}

4.2 Synthesis of palladacycles with PYE ligands

As stated in section 3.4.3, extra species were observed in the ¹H NMR spectrum in the initial reactions between compounds **7-11** and [Pd(CH₃CN)₂Cl₂] or [Pd(COD)Cl₂]. For example, the addition of acetonitrile-d₃ into a NMR tube containing [Pd(CH₃CN)₂Cl₂] and compound **7** gave a deep red solution. After heating the tube, the colour of the solution became yellow and palladium black formed in the tube. ¹H NMR spectroscopy shows that the target complex was being consumed along with formation of an unknown species. A pair of roofed doublets indicative of two diastereotopic protons was observed at 4.14 and 4.34 ppm, and also a distinctive broad peak at 8.53 ppm appeared. To aid the interpretation of the latter peak, a control experiment by addition of one equivalent of HBF₄·Et₂O into the solution of **7** was carried out. The ¹H NMR spectrum shows a broad signal at δ 8.83 ppm corresponding to a proton coordinated to chelating nitrogen atoms. Considering the data as a whole, a base-driven cyclometallation reaction was suspected. A plausible explanation is shown in Scheme 4-2. As the coordination of the imine to the Pd centre is comparatively

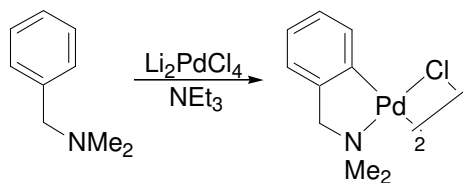
fast in relation to the cyclometallation reaction,¹⁶ reaction between alkyl linked PYE ligand and $[\text{Pd}(\text{CH}_3\text{CN})_2\text{Cl}_2]$ gives a dichloride palladium intermediate complex¹⁷ which cannot be isolated, and intramolecular C-H activation occurs to give a cyclopalladated complex. Evolved HCl is trapped by ligand present in solution either in excess or from decomposition of a complex formed in situ.



Scheme 4-2. Proposed synthetic route of cyclometallated palladium complexes.

4.2.1 Monocyclopalladated complexes (26)-(29)

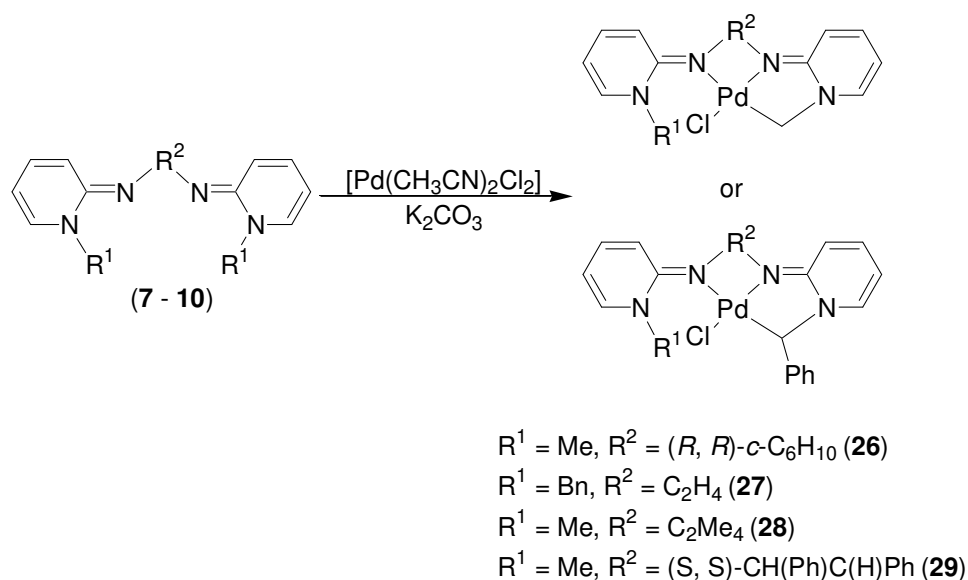
As one of the most common preparation methods for palladacycles including oxidative addition, transmetalation and nucleophilic addition onto an unsaturated bond, C-H activation is perhaps the most simple and direct method for the construction of palladacycles. Goel *et al.*¹⁸ reported an example of palladacycle preparation using tetrachloropalladated salt with a base to drive the formation of the desired product (Scheme 4-3).



Scheme 4-3. Preparation of palladacycle via C-H activation method.

To increase the yield of cyclopalladated complexes the Brønsted base potassium carbonate was added to the reaction as a proton scavenger^{17, 19} to prevent the formation of

ligand salt. Using this methodology cyclometallated $[\text{PdCl}(\eta^3\text{-CH}_2\text{N}^{\text{C}_6\text{H}_{10}}\text{N}^{\text{Me}})]$ **26**, $[\text{PdCl}(\eta^3\text{-CHPhN}^{\text{(CH}_2)_2}\text{N}^{\text{Bn}})]$ **27**, $[\text{PdCl}(\eta^3\text{-CH}_2\text{N}^{\text{(C(Me)}_2)_2}\text{N}^{\text{Me}})]$ **28** and $[\text{PdCl}(\eta^3\text{-CH}_2\text{N}^{\text{(CHPh)}_2}\text{N}^{\text{Me}})]$ **29** could be prepared (Scheme 4-4). In addition, complex **27** also can be prepared from reaction between dichloride palladium complex **23** and potassium carbonate. ^1H and ^{13}C NMR spectroscopy, mass spectrometry, elemental analysis and in selected cases X-ray crystallography are consistent with the proposed formulations. Complexes **26-29** are very soluble in chlorinated solvents, and exhibit a range of solubility in THF and acetonitrile, but are very poorly soluble in aromatic solvents and hydrocarbons. Complexes **26-29** are also air and water stable as solids and in solution at 25 °C for days.



Scheme 4-4. Synthesis of monocyclopalladated complexes **26-29**.

The unsymmetrical structure of **26-29** is confirmed by all the spectroscopies showing differentiated signals from noncyclo- or cyclopalladated PYE heterocycle rings. For example, distinctive signals are observed in the ^1H NMR spectrum of **26** (Figure 4-2), where a pair of doublet signals at 4.42 and 4.66 ppm are assigned to the diastereotopic NCH_2 group in addition to the downfield shift of the eight signals for the PYE ring hydrogen atoms compared to the neutral ligand.

Selected ^1H and ^{13}C NMR data of **26-29** are listed in Table 4-1. The noncyclometallated ring in both ^1H and ^{13}C NMR chemical shifts are generally downfield of the cyclometallated ring. It is probably due to diminished delocalisation of the N(2) lone pair into the heterocycle ring resulting from cyclopalladation. This can be indirectly proved by elongation of the $_{\text{c-met}}\text{C}(6)\text{-N}(2)$ bond compared with the corresponding noncyclopalladated bond length (*vide infra*). Comparison of ^1H and ^{13}C NMR spectroscopy between palladium dichloride **23** and cyclopalladated **27** in CDCl_3 shows upfield chemical shifts for most signals, with the most significant changes in the ^1H NMR for PhCH_2 (converted to PhCH in **27**) (6.49 to 6.06 ppm), H^2 (6.95 to 6.39 and 6.52 ppm) and H^4 (6.31 to 5.87 and 5.95 ppm). The most significant change in the ^{13}C NMR spectrum is for PhCH_2 (converted to PhCH in **27**) (57.9 to 66.9 ppm).

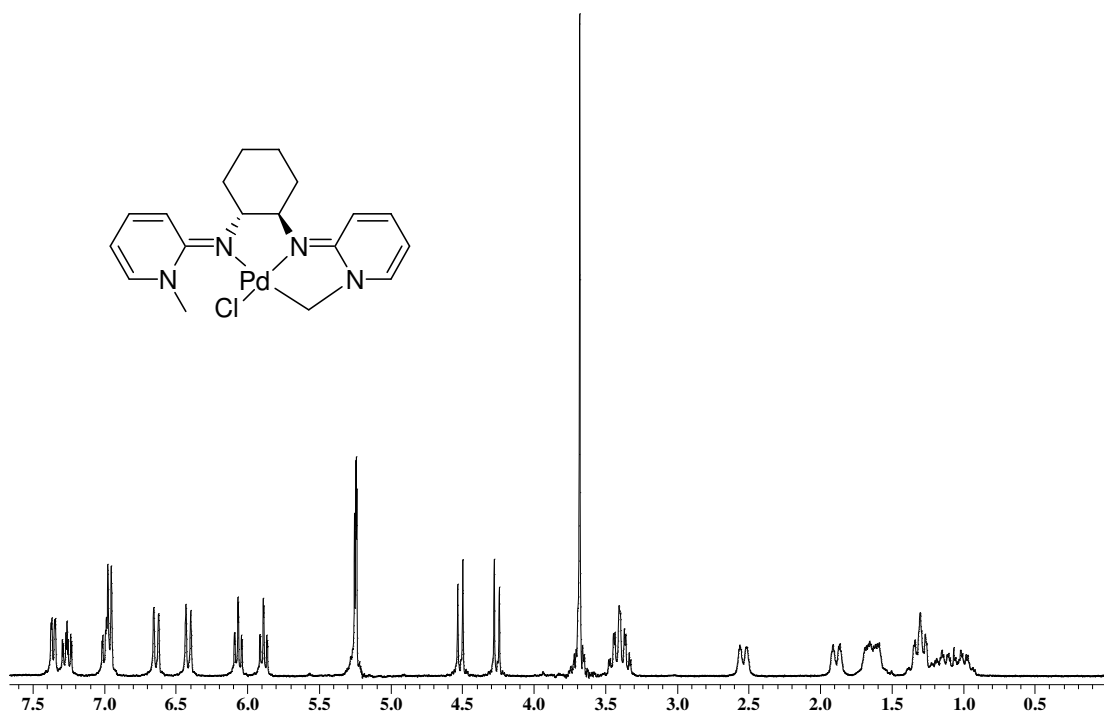
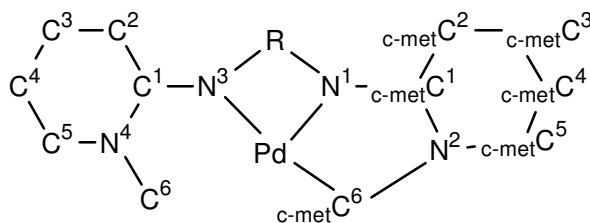


Figure 4-2. ^1H NMR spectrum of complex **26** in CD_2Cl_2 .

Table 4-1. Selected ^1H and ^{13}C NMR chemical shifts (ppm) of **26-29** in CD_2Cl_2 and CDCl_3 .



	26^a	27^b	28^b	29^b
PdCH ₂ or PdCHPh	4.22, 4.66	6.06	4.38, 4.64	4.71
<i>H</i> ²	6.65	6.52	6.83	5.85
<i>H</i> ³	7.24	7.10	7.10	6.75
<i>H</i> ⁴	6.07	5.95	6.03	5.85
<i>H</i> ⁵	7.36	7.03	7.29	7.08
c-met <i>H</i> ²	6.42	6.39	6.55	5.85
c-met <i>H</i> ³	6.95	7.03	6.97	6.75
c-met <i>H</i> ⁴	5.87	5.87	5.87	5.85
c-met <i>H</i> ⁵	6.95	6.88	6.97	6.90
c-met <i>C</i> ⁶	46.2	66.9	49.3	49.0
^a Recorded in CD_2Cl_2 , ^b in CDCl_3 .				

For **26** and **29** that were synthesised from enantiopure ligands, there is no change in ligand stereochemistry. For **27** that was generated from prochiral ligand, the cyclopalladated benzylic carbon becomes a new stereocentre. Two resulting enantiomers give the same NMR spectroscopic feature. The ^1H NMR spectra of **26-29** are consistent with a rigid structure and thermal stability, and there is no evidence to suggest rotation about the imine PYE bond or a second cyclometallation of the remaining NCH_3 or PhCH_2 group. Furthermore, heating **26** to 80 °C in the presence of K_2CO_3 or other bases including NaH and Et_3N also did not induce further cyclometallation, and this topic will be expanded upon in section 4.2.3.

Single crystals of **26** and **28** were grown from THF and hexane, and molecular structures are shown in Figures 4-3 and 4-4, and selected bond lengths and angles are given in Tables 4-2 and 4-3. The geometry is maintained at both palladium atoms as pseudo

square planar. There is no significant distortion in the bond lengths and angles of the PYE moieties of **26** and **28** caused by cyclopalladation in comparison to **23**. In contrast, due to the presence of different backbones, the difference between **26** and **28** with respect to bond lengths and angles can be examined in the solid state. For example, the bond lengths of C(6)-Pd(1) and N(3)-Pd(1) for **26** are both longer than those for **28** by ca. 0.012 and 0.08 Å respectively. The torsion angle C(2)-C(1)-N(1)-C(7) for **26** is greater than that for **28** by ca. 6.1 °. Conversely, the noncyclopalladated side torsion angle C(14)-C(13)-N(3)-C(12) for **26** is significantly smaller than C(14)-C(13)-N(3)-C(10) for **28** by ca. 9.6 °. The nitrogen atoms N(1) of **26** and **28** both exhibit planar geometry, whereas the nitrogen atoms N(3) both show distinct pyramidal geometry, where the sum of the angles about the atoms N(3) for **26** and **28** are ca. 333.48 and 351.26 ° respectively. Collectively, due to more flexibility of backbone of **28** compared with **26**, two PYE moieties of **28** can rotate more easily to fit for cyclopalladation, whereas such rotation for **26** is limited to some extent.

In comparison with C(18)-N(4) bond, cyclopalladation causes significant elongation of the corresponding C(6)-N(2) bond for both **26** and **28** by ca. 0.018 and 0.024 Å respectively. In the solid state, the closest distance between the Pd centre and a proton on the non-cyclopalladated N-methyl group is ca. 2.79 Å for **26** and 2.68 Å for **28** potentially explaining why a second cyclopalladation does not occur.

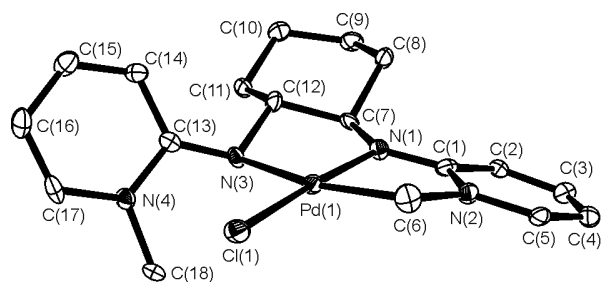


Figure 4-3. Molecular structure of complex **26**. Ellipsoids are shown at 50 % probability. Hydrogen atoms have been omitted for clarity.

Table 4-2. Selected bond lengths and angles for complex **26**.

Bond	lengths (Å)	Bond	Angles (°)
Pd(1) – Cl(1)	2.3457(12)	N(1) – Pd(1) – N(3)	80.60(14)
N(1) – Pd(1)	1.972(3)	N(1) – Pd(1) – C(6)	81.92(17)
N(3) – Pd(1)	2.236(4)	C(6) – Pd(1) – Cl(1)	91.79(13)
C(6) – Pd(1)	1.990(4)	N(3) – Pd(1) – Cl(1)	105.69(10)
C(1) – N(1)	1.318(5)	C(1) – N(1) – C(7)	124.4(4)
C(1) – C(2)	1.439(5)	C(13) – N(3) – C(12)	115.5(3)
C(2) – C(3)	1.352(6)	N(2) – C(6) – Pd(1)	107.7(3)
C(6) – N(2)	1.491(6)	C(2) – C(1) – N(1) – C(7)	6.3(7)
C(13) – N(3)	1.323(5)	C(14) – C(13) – N(3) – C(12)	14.2(6)
C(13) – C(14)	1.439(6)		
C(14) – C(15)	1.350(5)		
C(18) – N(4)	1.473(6)		

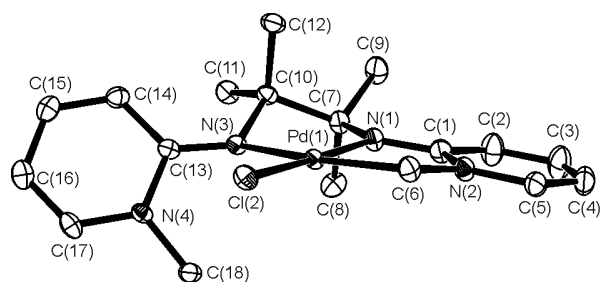


Figure 4-4. Molecular structure of complex **28**. Ellipsoids are shown at 50 % probability. Hydrogen atoms have been omitted for clarity.

Table 4-3. Selected bond lengths and angles for complex **28**.

Bond	lengths (Å)	Bond	Angles (°)
Pd(1) – Cl(1)	2.3550(4)	N(1) – Pd(1) – N(3)	80.45(6)
N(1) – Pd(1)	1.9714(14)	N(1) – Pd(1) – C(6)	83.45(7)
N(3) – Pd(1)	2.1560(14)	C(6) – Pd(1) – Cl(1)	91.07(5)
C(6) – Pd(1)	1.9781(17)	N(3) – Pd(1) – Cl(1)	105.04(4)
C(1) – N(1)	1.325(2)	C(1) – N(1) – C(7)	126.10(15)
C(1) – C(2)	1.435(3)	C(13) – N(3) – C(10)	121.52(14)
C(2) – C(3)	1.364(3)	N(2) – C(6) – Pd(1)	107.29(11)
C(6) – N(2)	1.487(2)	C(2) – C(1) – N(1) – C(7)	0.2(3)
C(13) – N(3)	1.319(2)	C(14) – C(13) – N(3) – C(10)	23.8(3)
C(13) – C(14)	1.439(2)		
C(14) – C(15)	1.357(3)		
C(18) – N(4)	1.463(2)		

In comparison with analogous five-membered palladacycles with C(sp³)-Pd bond (2,2'-bipyridine,²⁰ endo-cyclopalladated oxazoline²¹ and exo-cyclopalladated oxazoline²²) shown in Figure 4-5, the Pd-C bond lengths for complex **26** and **28**, 1.99 and 1.9781 Å respectively, are shorter and fall in the shorter end of narrow range reported for related palladacycles with C(sp³)-Pd (1.97-2.05 Å).²²

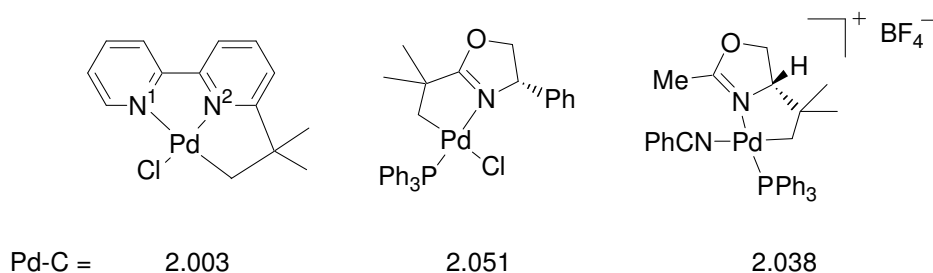
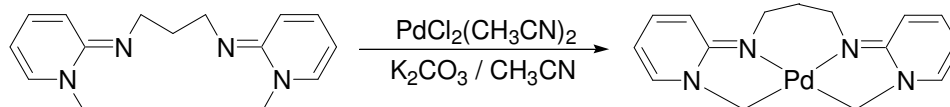


Figure 4-5. Examples of five-membered palladacycles with C(sp³)-Pd bond and their corresponding Pd-C bond lengths (Å).

4.2.2 Dicyclopalladated complex (30)

The discovery of monocyclopalladated complexes derived from PYE ligands led us to be curious about the possibility of cyclopalladation of the second remaining N-methyl group. Although the attempts to reach that goal by using C2 linked PYE ligands failed, compound **14** with a C3 backbone was considered to be more suitable for fulfilling the goal due to a more flexible molecular structure to shorten the distance between the Pd centre and the second NCH₃ group.

Initially, reaction between ligand **14** with excess potassium carbonate as base under similar reaction conditions as used for cyclopalladated complexes **26-29** did not give any desired product. However, by decreasing the reaction temperature to room temperature, a dicyclopalladated complex **30** was isolated as a creamy yellow solid in 36% yield (Scheme 4-5). Complex **30** is soluble in most common organic solvents, and air and moisture stable as a solid at 25 °C for days.



Scheme 4-5. Synthesis of complex **30**.

Complex **30** was characterised by ¹H and ¹³C NMR, mass spectrometry and elemental analysis. The dicyclopalladated structure was confirmed by symmetrical signals and intensity change of NCH₃ groups to four protons in the ¹H NMR spectrum. In

comparison with **14**, the ^1H NMR spectrum of **30** exhibited significant changes of chemical shifts and multiplicity of backbone signals. For example, the signals due to the protons of PYE moieties moved downfield from 5.57 (H^4), 6.44 (H^2), 6.84 (H^3), 6.96 (H^5) for free ligand **14** to 5.83 (H^4), 6.40 (H^2), 7.00 (H^3), 7.22 (H^5). Similarly, downfield tendency is generally observed comparing the ^{13}C NMR spectra of **14** and **30**, with the most significant changes for PdC (39.4 to 46.4 ppm) and C^1 (153.7 to 160.2 ppm). The ^1H and ^{13}C NMR chemical shift of PdCH₂ for **30** (4.20 for ^1H and 46.4 for ^{13}C) are comparable to those for **26** (4.22 and 4.66 for ^1H and 46.2 for ^{13}C). The FD mass spectrum of **29** recorded in positive-ion mode contains a strong peak at m/z 360 due to the $[\text{M}]^+$ ion.

4.2.3 Comparison and discussion of noncyclo- and cyclopalladated behaviour

The selective cyclopalladation apparently directed by various backbones spurred us to investigate the influence of steric and electronic aspects (Figure 4-6). Since the discovery of cyclopalladated complex **26**, many attempts to cyclopalladate **22** as a structural analogue of **26** were conducted using different bases like NaH, K_2CO_3 and Et_3N to drive the reaction. However, no desired product has been successfully isolated and complex **22** appears thermally stable to at least 80 °C in acetonitrile.

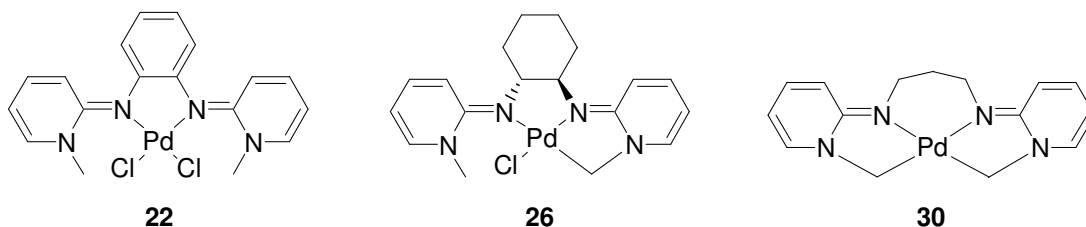


Figure 4-6. Selective cyclopalladation directed by various backbones.

Examining the structures of the free ligands **7** and **12** which are incorporated into the resulting complexes **26** and **22** respectively, they are clearly similar except for the hybridisation of the carbon atoms in the backbone ring which induces some extra flexibility in **7** and a greater NCCN torsion angle. The X-ray crystal structure of **22** shows the closest distance between the Pd atom and proton of N-methyl groups is ca. 2.89 Å, which is close to that (2.79 Å) between the Pd atom and the nonpalladated N-methyl group in complex **26**. The C-H activation could therefore be prevented by such long distance if there is no

significant libration motion of PYE rings in the solution state. However, the presence of *trans* and *cis* isomers of **22** in the solid state structure and only one set of NMR signals indicates the existence of a low energy C_{2v} transition state resulted from motion of two PYE rings (Figure 4-7) as observed in **22** (Section 3.4.3.2). A conformer approaching the C_{2v} transition state would increase the Pd-H interaction potentially promoting cyclopalladation. Why then does cyclopalladation not occur?

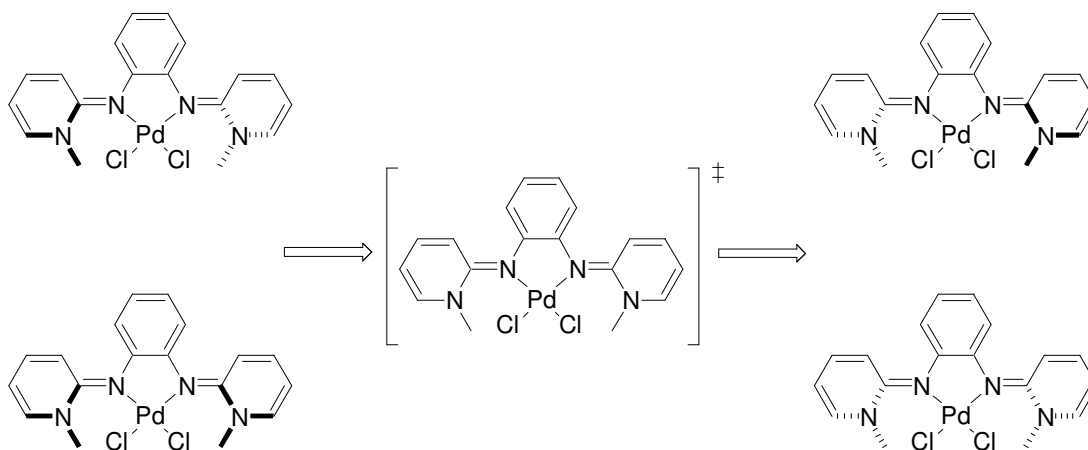


Figure 4-7. Plausible isomerisation of **22**.

From a steric point of view, due to more rigidity as a result of replacement of cyclohexyl (**26**) to aryl backbone (**22**), metallacyclic ring strain increases and any structural twist becomes difficult. Consequently, PYE moiety bending to reach close to the Pd centre is likely to have a high activation energy. Also, in order for cyclopalladation, the noncyclopalladated PYE moiety needs compromisingly to twist about the C=N bond (see X-ray structures of **26** and **28**). However, the rigidity of aryl backbone severely hampers that (Figure 4-8).

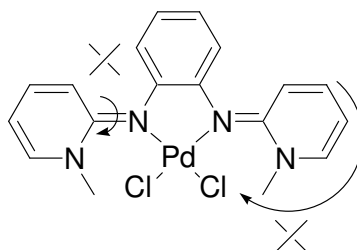
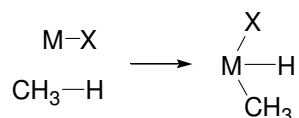


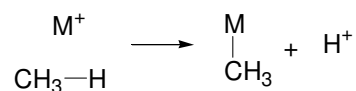
Figure 4-8. Plausible explanation of cyclopalladation steric prevention for **22**.

Before considering the electronic influence, the mechanism of C-H activation for Pd^{II} complexes should be mentioned. Generally, electrophilic substitutions are operative for Pd^{II} complexes, while oxidative additions are preferred for Pt^{II} complexes (Scheme 4-6).²³ Several examples have shown regioselective intramolecular cyclopalladation of arenes can be predicted on the basis of the electronic properties of the arene substituents.²⁴⁻²⁹

Oxidative addition:



Electrophilic substitution:



Scheme 4-6. Oxidative addition and electrophilic substitution mechanism for C-H activation.

If the cyclopalladation reactions of PYE complexes undergo the electrophilic substitution pathway, then cyclopalladation of complex **22** should be more likely to occur owing to more electrophilicity of the Pd centre derived from the aryl backbone. However, the experimental data shows contrary results, where complex **26** with more electron donating substituents underwent cyclopalladation. Whereas, taking oxidative addition pathway into account, the experimental data is more properly explained from an electronic standpoint because complex **26** will be more electron rich. It is noteworthy that some hydride complexes of Pd^{IV} have been postulated as intermediates in some processes.³⁰ For example, Larock *et al.*³¹ proposed that an organopalladium(IV) hydride intermediate was involve in a novel consecutive vinylic to aryl to allylic Pd migration reaction.

The formation of dicyclopalladated complex **30** was considered to be favoured from both steric and electronic standpoints, but more crucial are the steric features. Elongation of the backbone gives more flexibility to the second PYE ring after the completion of the first cyclopalladation.

Collectively, for the selective cyclopalladation of PYE ligands directed by various backbones, we think the influence of both steric and electronic effect should be taken into

account. However, increased flexibility from backbones enhances the feasibility of cyclopalladation, so the steric effect is more dominant. Furthermore, the presence of the phenyl group for **27** results in more steric hindrance of C-H bond on *N*-CH₂Ph group in comparison with **26**, **28-30** containing *N*-methyl substituents. Those changes hamper the process of cyclopalladation to some extent, which explains why only palladium dichloride **23** can be isolated for bidentate PYE ligands (Section 3.4.3.2).

Structural comparison between complexes **22**, **24** and **26** shows steric aspect dominantly accounts for the formation of the reactive cyclometallated intermediate **E** and the resulting H/D exchange via the C-H activation of C₆D₆ on the *N*-methyl group of the quinolinyl ligand proposed in Section 3.4.3.3.2. By building up a ball-stick model with a chemistry model kit, a closer distance between the Pd atom and the *N*-methyl group in complex **24** is observed in comparison with complex **22**, indicating less constraint resulted from the quinolinyl backbone than the aryl one. In contrast, the planar aromatic ring in **24** is less flexible than the *sp*³-carbon ring in **26**, which allows the formation of the stable monocyclometallated complex **26**. As the distance between the Pd atom and the *N*-methyl in **24** displays between those of **22** and **26** (cyclometallated side), the weakly cyclometallated intermediate **E** can be accessible to favour the C-H activation process.

Collectively, this selective cyclometallation influenced by various backbones could be useful for reactivity tuning via controlling steric environment of metal centres.

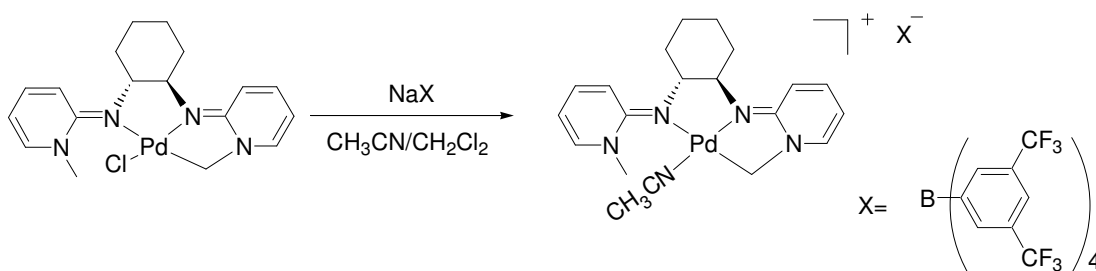
A theoretical calculation work is under way to attempt to find out the main factor in this selective cyclopalladation.

4.3 Synthesis and reactivity of cationic derivatives

Considering further study and potential catalytic applications, we decided to investigate the reactivity of cyclometallated palladium complexes with a range of molecules including small gas molecules, alkenes and alkynes. Initially CH₃CN was chosen to replace the chloride ligand because CH₃CN is a labile ligand and can potentially provide a vacant site for facile addition of other substrates.

4.3.1 [Pd(MeCN)(η^3 -CH₂N^{C6H10}N^{Me})] [BAr^F₄] (**31**)

Reaction between **26** and Na[B{3,5-(CF₃)₂C₆H₂}₄] (Na[BAr^F₄]) in a combination solvent of acetonitrile and dichloromethane gave the acetonitrile coordinated cationic derivative [Pd(MeCN)(η^3 -CH₂N^{C6H10}N^{Me})] [BAr^F₄] **31** as a yellow solid, as shown in Scheme 4-7.



Scheme 4-7. Preparation of complex **31**.

Complex **31** is very soluble in chlorinated solvents and acetonitrile, but displays a range of solubility in aromatic solvents and THF. ¹H and ¹³C NMR spectroscopy, mass spectrometry, and elemental analysis are consistent with the proposed formulation. An ion peak (20%) of m/z 442.1 mass units in the mass spectrum corresponds to the [M-BAr^F₄]⁺ ion. A distinctive singlet signal for CH₃CN at 1.77 ppm and two signals for [BAr^F₄]⁻ anion at 7.45 and 7.62 ppm were observed in the ¹H NMR spectrum (Figure 4-9). In comparison to **26**, a general downfield trend in chemical shift is shown in both the ¹H and ¹³C NMR spectra of **31**. The chemical shift of PdCH₂ in ¹³C NMR for **31** changes to 48.0 ppm compared to **26** (46.2 ppm).

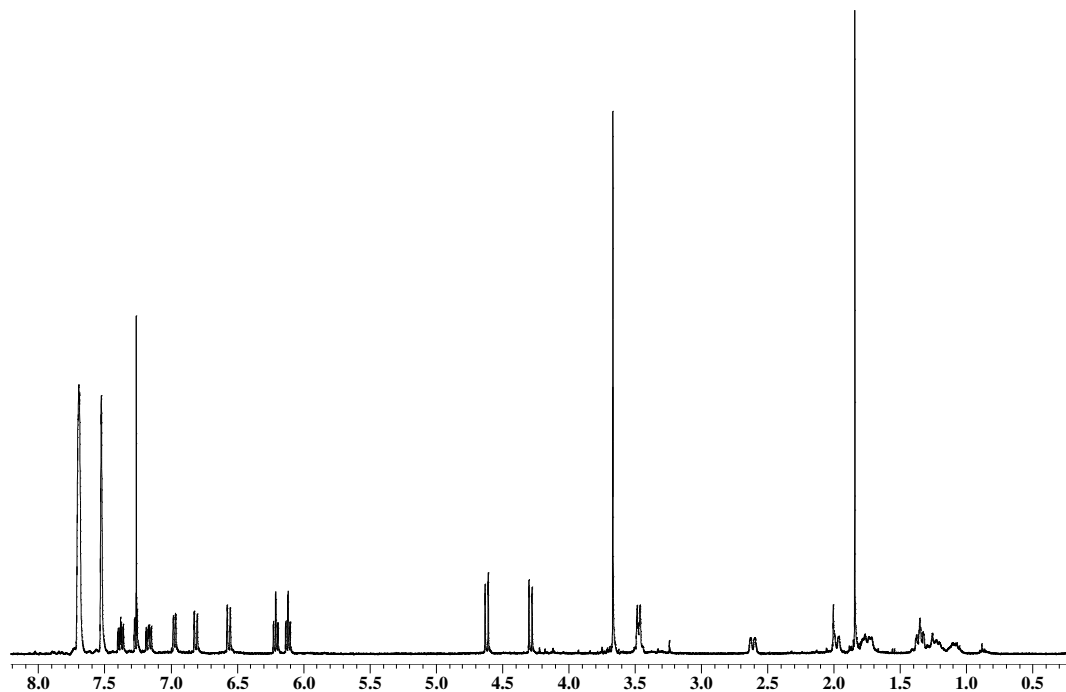
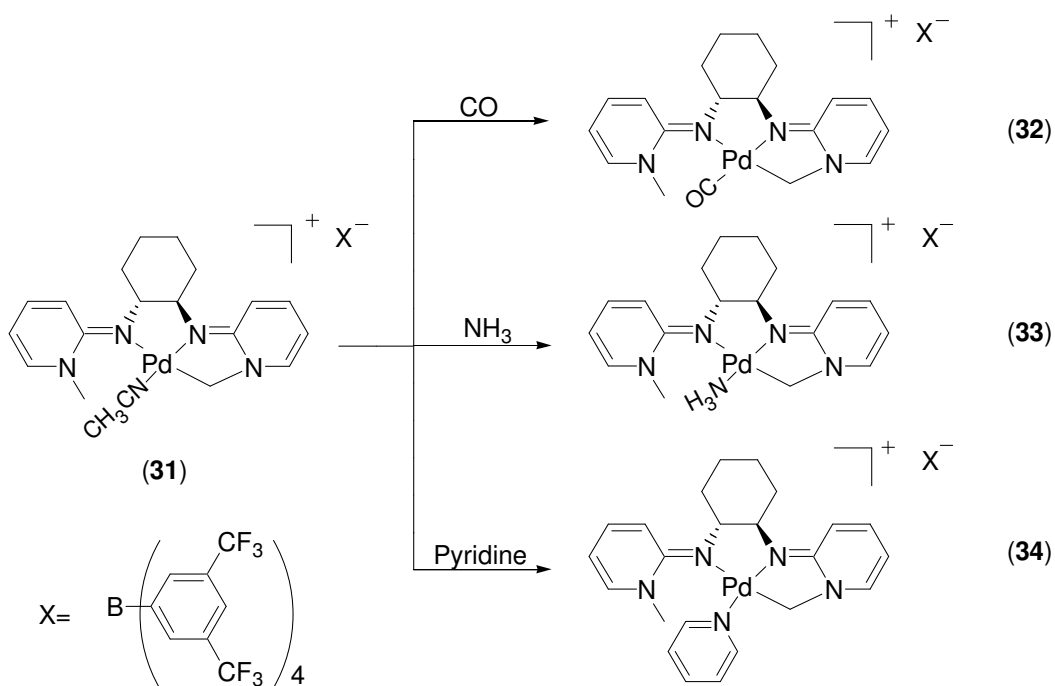


Figure 4-9. ^1H NMR spectrum of **31** in CDCl_3 .

4.3.2 Reactivity of cationic derivatives

The reactivity of palladium cationic derivatives with a range of molecules was investigated using **31** as a starting material. As shown in Scheme 4-8, carbon monoxide, ammonia and pyridine can coordinate to the palladium atom by replacing the acetonitrile molecule, giving $[\text{Pd}(\text{CO})(\eta^3\text{-CH}_2\text{N}^{\text{C}_6\text{H}_{10}}\text{N}^{\text{Me}})][\text{BAr}^{\text{F}}_4]$ **32** as a light green solid, $[\text{Pd}(\text{NH}_3)(\eta^3\text{-CH}_2\text{N}^{\text{C}_6\text{H}_{10}}\text{N}^{\text{Me}})][\text{BAr}^{\text{F}}_4]$ **33** as a yellow solid and $[\text{Pd}(\text{C}_6\text{H}_5\text{N})(\eta^3\text{-CH}_2\text{N}^{\text{C}_6\text{H}_{10}}\text{N}^{\text{Me}})][\text{BAr}^{\text{F}}_4]$ **34** as a yellow solid respectively.



Scheme 4-8. Synthesis of **32**, **33** and **34**.

All the characterising data are consistent with the proposed formulations. For example, a distinctive signal corresponding to CO at 177.5 ppm was observed in the ^{13}C NMR spectrum of **32**. Infra-red spectroscopy shows a sharp peak at 2103 cm^{-1} attributable to the CO vibration as shown in Figure 4-10. It is worth pointing out that this value (2103 cm^{-1}) is significant lower than the CO vibration observed for similar types of palladium complex like $[(\text{NN})\text{PdCOMe}]$ used in CO-alkene copolymerisation,³² indicating PYE ligands are relatively strong donating ligands. A broad peak at 1.18 ppm due to coordinated NH_3 was obtained in the ^1H NMR spectrum of **33**. Infra-red spectroscopy of **33-NH₃** shows a peak at 3380 cm^{-1} attributable to the NH_3 vibration, which was confirmed by the infra-red spectrum of the isotopomer **33-ND₃** with a new peak at 2490 cm^{-1} . Comparison of both spectra is shown in Figure 4-11.

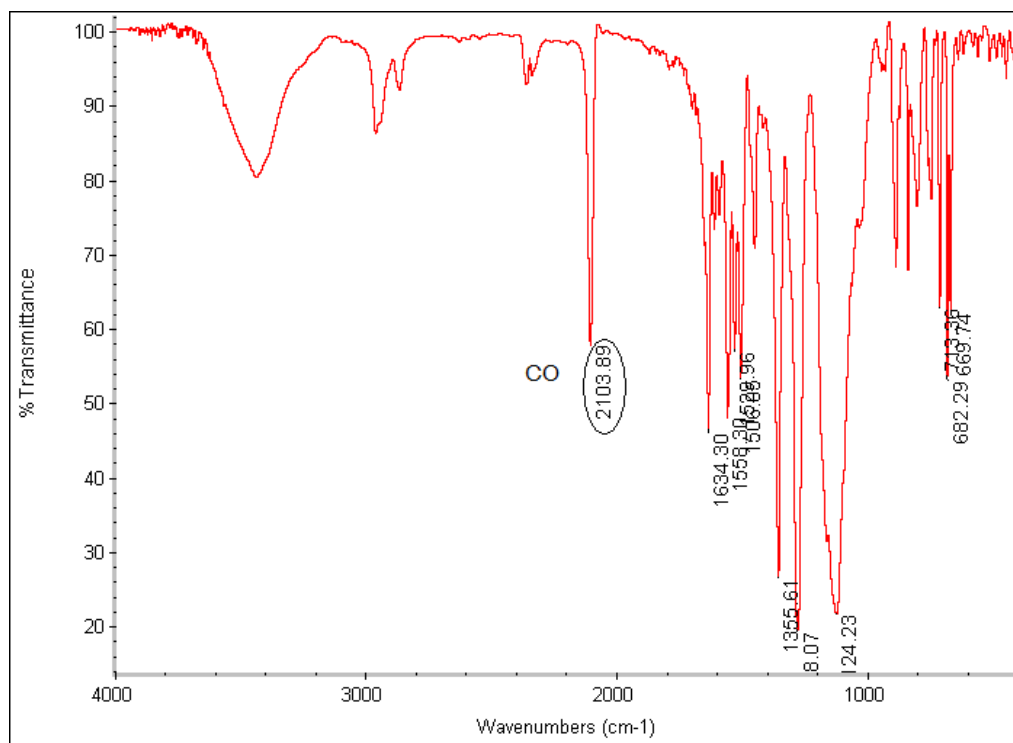


Figure 4-10. Infra-red spectrum of 32.

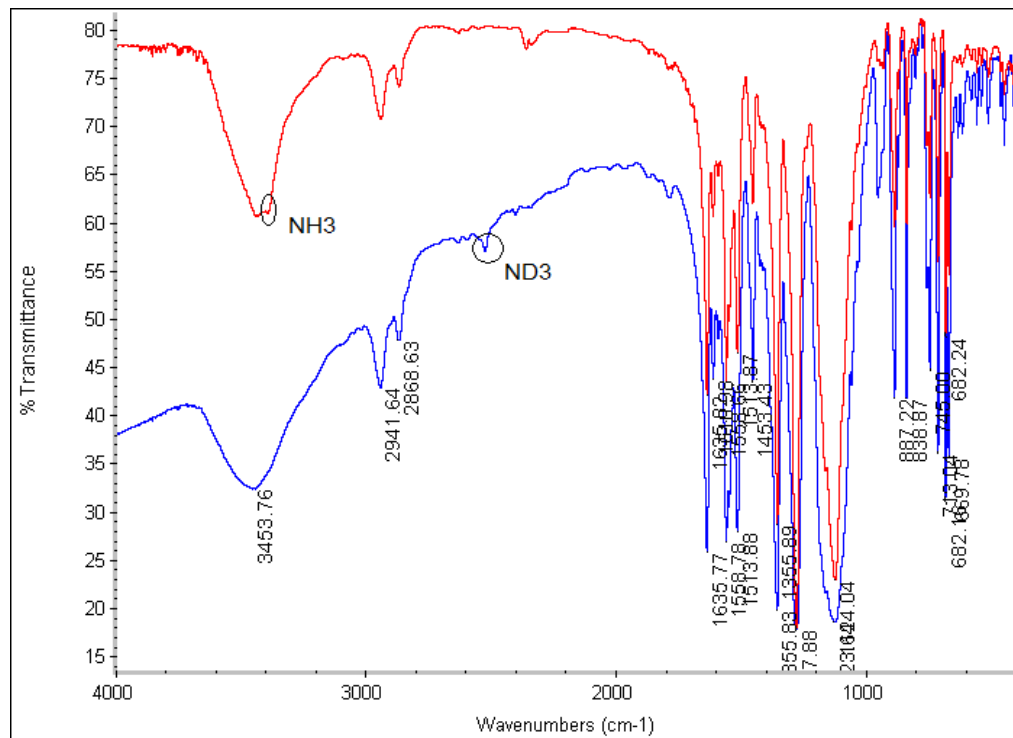


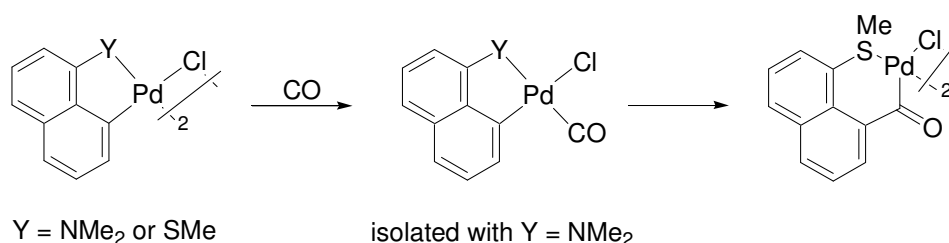
Figure 4-11. Comparison of infra-red spectra of 33-NH₃ (red colour) and 33-ND₃ (blue colour).

Diagnostic signals in ^1H and ^{13}C NMR spectroscopy for identifying PYE monopalladacycles are derived from comparing PdCH₂ data for **26** and **31-34** as shown in Table 4-4. Various coordination ligands *cis* to PdCH₂ do not result in significant changes with respect to chemical shifts of the PdCH₂ moiety. The pyridine coordinated complex **34** gives the largest difference of two doublets attributed to the two diastereotopic protons of the PdCH₂ group.

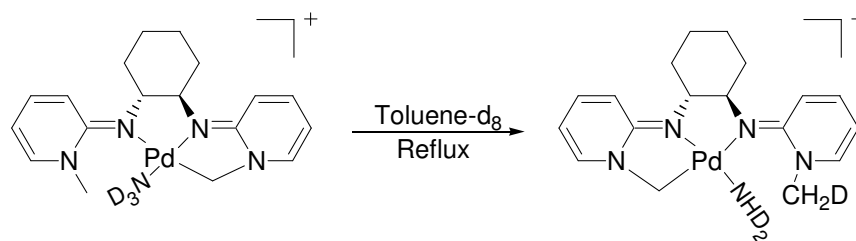
Table 4-4. ^1H and ^{13}C NMR chemical shifts (ppm) comparison of PdCH₂ for **26** and **31-34**.

	26	31	32	33	34
PdCH ₂	4.42, 4.66	4.22, 4.55	4.36, 4.75	4.10, 4.59	4.09, 4.62
PdCH ₂	46.2	48.0	50.4	46.5	50.6

The stoichiometric insertion of carbon monoxide into the Pd-C bond has been extensively observed and investigated for palladacycles. The mechanism generally involves coordination of CO to palladium *trans* to the donor group, insertion in the Pd-C bond, and depalladation (in some cases). Although we successfully isolated terminally bound carbonyl complex **32**, subsequent CO insertion does not occur. Dupont *et al.*³³ reported a series of reactions between carbon monoxide and naphthyl analogues (Scheme 4-9). Similarly, a terminally bound carbonyl complex was obtained for the nitrogen-bound palladacycle, whereas the enlarged palladacycle was isolated in the case of the sulphur analogue. It was concluded that CO insertion into the sulphur-containing palladacycle is more facile than that for the corresponding amine congeners. In the case of **32**, the constraint of the palladacycle ring was possibly responsible for the prevention of CO insertion, which is supported by a molecular model built from a molecular model kit.



Scheme 4-9. CO insertion in sulphur- and nitrogen-derived palladacycles.



Scheme 4-10. Attempted N-H activation reaction of **33-ND₃**.

In order to seek potential N-H bond activation, isotopomer **33-ND₃** was refluxed in toluene-d₈ for days (Scheme 4-10). However, no H/D exchange between the cyclopalladated or noncyclopalladated NCH₂ and NCH₃, and ND₃ was observed by ¹H NMR spectroscopy. Other molecules such as O₂, ethylene, cyclopentene, styrene and 1-hexyne were also investigated with **31**. Addition of those molecules into solution of **31** did not give new coordinated complexes. Even chloride abstraction of **26** in the presence of cyclopentene without any other coordinating substrates did not give an alkene product. Such a selectivity of coordinating ligand in the PYE monopalladacycle is probably due to the steric hindrance of the *N*-methyl group which allows end-on ligand coordination but prevents coordination of ligands with significant ‘lateral’ bulk. A spacefilling structure of **26** (Figure 4-12) clearly shows that the *N*-methyl group occupies some axial space of the potential coordination site for side-on ligands.

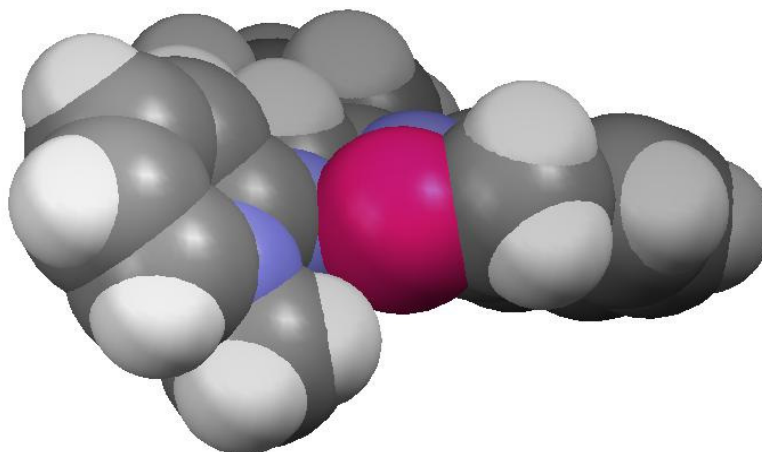


Figure 4-12. Spacefill structure of **26**. Chlorine atom has been omitted for clarity.

Furthermore, in the presence of alcohol, **31** decomposed giving palladium black and a stoichiometric amount of aldehyde as observed by ^1H NMR spectroscopy, indicating Pd(II) was reduced to Pd(0) through an unstable hydride intermediate.³⁴

4.3.3 $\{[\text{Pd}(\eta^3\text{-CH}_2\text{N}^{\text{C}_6\text{H}_{10}}\text{N}^{\text{Me}})]_2\text{Cl}\}(\text{BF}_4)$ (**35**)

In the 1980s, the study of stable bimetallic species with an unsupported single halide atom bridge became of growing interest as halide-bridged bimetallic intermediates are proposed in many redox or electron ligand transfer reactions of d^8 metal-halide complexes. Their structure and chemical behaviour were investigated in order to gain more information about the mechanism of halide-bridge cleavage reactions and halogen transfer processes.³⁵ The first example of dinuclear Pd(II) complexes with a single unsupported halide bridge was reported by Grove *et al.* using a pincer NCN ligand.³⁶ Since then, a number of monobridged bimetallic Pd(II) or Pt(II) complexes were isolated and studied in terms of their structure and reactivity (Figure 4-13).^{35, 37-43}

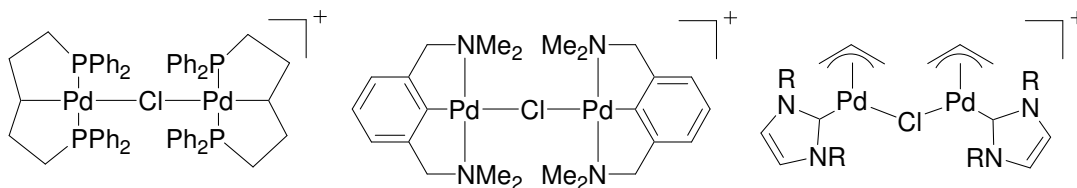
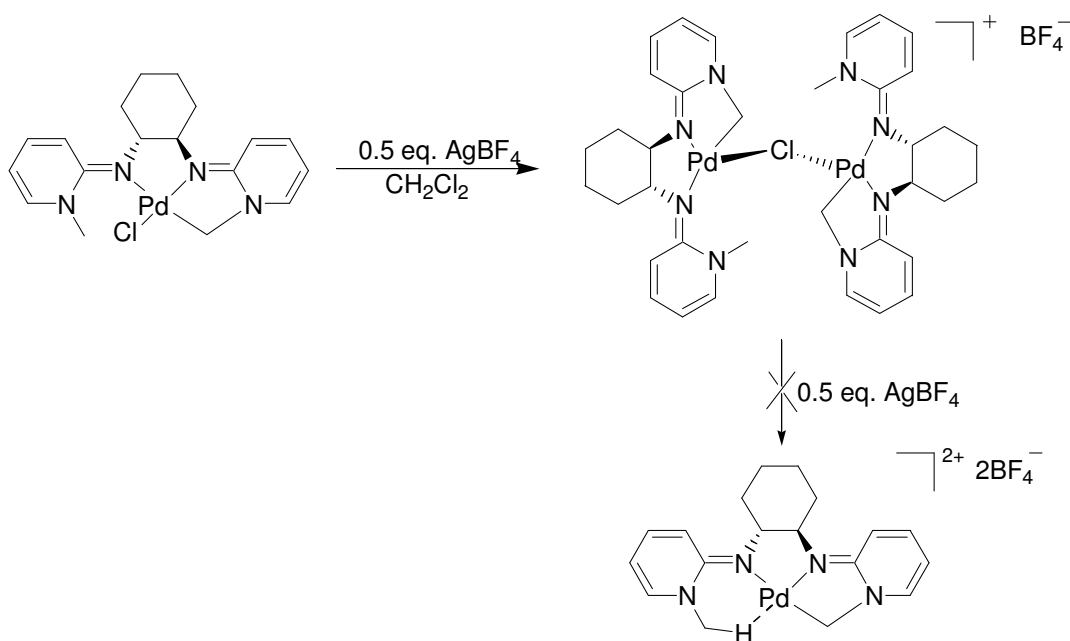


Figure 4-13. Examples of bimetallic complexes with an unsupported single halide bridge.

Reaction between **26** and 0.5 eq. AgBF_4 was carried out in dichloromethane at room temperature. As expected, a chlorine bridged dimer complex **35** was isolated as a yellow solid (Scheme 4-11). Unlike the example of NHC analogue obtained from addition of excess Tl salt,⁴² the bridging chloride atom was unable to remain stable on addition of excess silver salt which leads to the decomposition of **35**. No stable product such as a palladium agostic complex with vacant site was observed (Scheme 4-11). Complex **35** was thermodynamically stable in dichloromethane solution and on refluxing.



Scheme 4-11. Synthesis of dimer complex **35** and the attempt to an agostic complex.

All the characterising data are consistent with the proposed formulation. The chemical shift difference of two doublet signals due to PdCH_2 at 3.82 and 4.61 ppm in the ^1H NMR spectrum of **35** became significantly enlarged when compared with **26** and other derivatives, whereas the chemical shift of the PdCH_2 signal in the ^{13}C NMR spectrum (48.2 ppm) is comparable to **26** and other derivatives. A cation peak at m/z 837.1598 was found in a high resolution mass spectrometer due to the $[\text{M-BF}_4]^+$ ion (calc. 837.1603). Single crystals of **35** were grown from dichloromethane and diethyl ether at room temperature. While the structure could be solved, the refinement was problematic resulting in a low quality structure. However, the constitution of **35** is unambiguous and is shown in Figure 4-14.

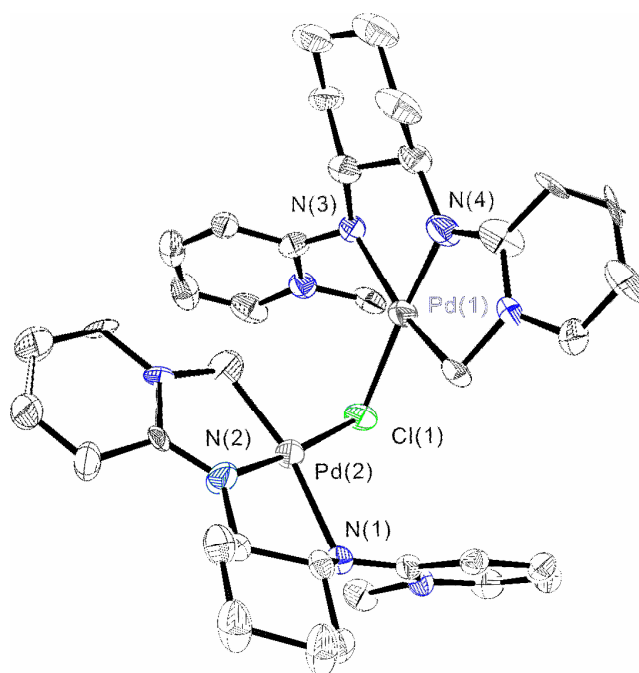
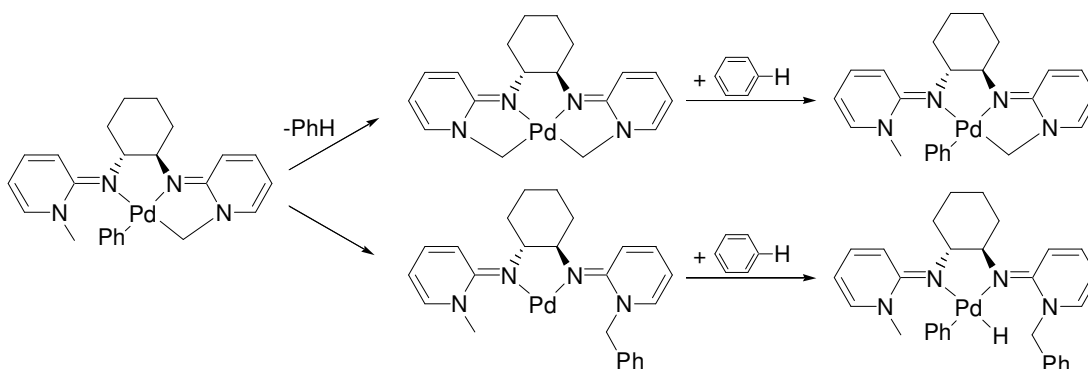


Figure 4-14. Molecular structure of complex **35**. Ellipsoids are shown at 50 % probability. Hydrogen atoms and the BF_4 anion have been omitted for clarity.

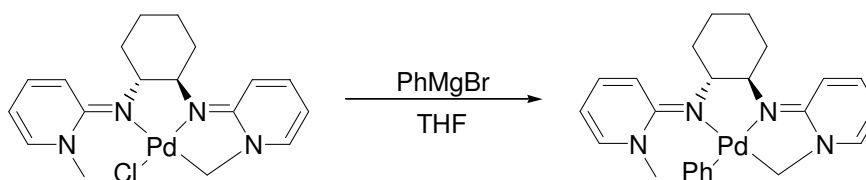
4.3.4 $[\text{Pd}(\text{C}_6\text{H}_5)(\eta^3\text{-CH}_2\text{N}^{\text{C}_6\text{H}_{10}}\text{N}^{\text{Me}})]$ (**36**)

Due to the interest in C-H bond activation, we decided to synthesise the aryl substituted Pd complex **36**, with **26** as the precursor, to look into the potential reactivity of this type of organometallic PYE complex. A motivation for preparing complex **36** which was synthesised from reaction between **26** and phenyl Grignard reagent is to examine the potential intermolecular C-H activation of arenes via elimination of benzene from **36** and subsequent addition of an arene to an intermediate dicyclopalladated complex. Alternatively, migration of the phenyl group to give a Pd(0) complex containing a N-benzyl group could also occur that may oxidatively add an arene (Scheme 4-12).



Scheme 4-12. Postulated C-H activation mediated by PYE phenyl Pd complex.

The phenyl substituted complex $[\text{Pd}(\text{C}_6\text{H}_5)(\eta^3\text{-CH}_2\text{N}^{\text{C}_6\text{H}_{10}}\text{N}^{\text{Me}})]$ **36** was isolated as a yellow solid via chloride abstraction from reaction between **26** and phenyl Grignard in THF at 0 °C as shown in Scheme 4-13.



Scheme 4-13. Synthesis of complex **36**.

The ^1H NMR spectrum of **36** shows a similar resonance pattern as **26** and an additional coordinated phenyl signals. In comparison with **26**, the most significant changes in ^1H NMR spectrum of **36** are $c\text{-met}H^3$ (6.95 to 6.55 ppm), H^3 (7.24 to 6.95 ppm), $c\text{-met}H^5$ (6.95 to 6.73 ppm) and H^5 (7.36 to 6.95 ppm). The ^1H and ^{13}C NMR chemical shifts of PdCH_2 for **36** (4.42 and 4.46 ppm for ^1H and 46.2 ppm for ^{13}C) are comparable to those of **26**. There is no significant change between **36** and **26** with respect to ^{13}C NMR data. A cation peak at m/z 479.0 was found using ESI mass spectrometry and is attributable to the $[\text{M}+\text{H}]^+$ ion. The solubility of **36** is much better than **26** in organic solvents, even in aromatic and hydrocarbon solvents, which will give benefit to the further investigation with respect to C-H activation. Single crystals of **36** were grown from toluene and hexane at room temperature. The molecular structure of **36** is shown in Figure 4-15 and selected bond lengths and angles are given in Table 4-5.

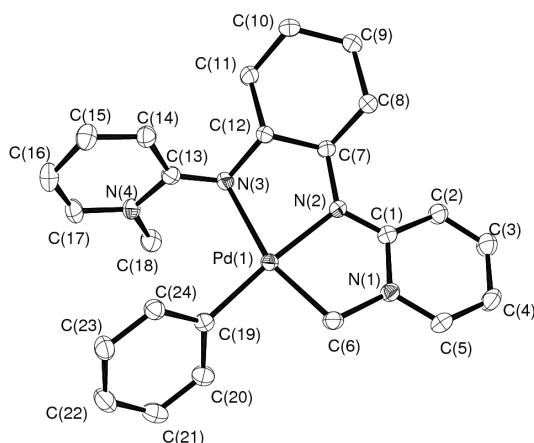


Figure 4-15. Molecular structure of complex **36**. Ellipsoids are shown at 50 % probability. Hydrogen atoms have been omitted for clarity.

Table 4-5. Selected bond lengths and angles for complex **36**.

Bond	lengths (Å)	Bond	Angles (°)
Pd(1) – N(2)	2.0213(15)	N(2) – Pd(1) – N(3)	79.49(6)
Pd(1) – N(3)	2.2287(16)	N(2) – Pd(1) – C(6)	81.87(7)
C(6) – Pd(1)	1.9986(19)	C(2) – C(1) – N(1) – C(7)	5.7(3)
C(19) – Pd(1)	2.0437(18)	C(14) – C(13) – N(3) – C(12)	15.6(3)
C(1) – N(2)	1.301(2)		
C(13) – N(3)	1.325(3)		

The bond lengths and angles in **36** are similar to those in **26**. The metal geometry is pseudo square planar with the sum of angles *ca.* 360.02 ° at the Pd atom. The phenyl plane is not perpendicular to the Pd square plane and the angle between planes defined by C24-C19-C20 and C6-N2-N3 is *ca.* 52.01 °, which possibly results from steric repulsion between the phenyl and N-methyl group (*vide supra*). This distortion may also reflect why alkene and alkyne substrates were not observed to coordinate (Section 4.3.2) and is presumably structurally similar to the pyridine adduct **34**. Due to the steric repulsion of the N-methyl group, an ideal orbital overlap between alkene/alkyne and Pd atom can not be established. Comparing to **26**, the Pd(1)-N(2) bond length for **36** is *ca.* 0.049 Å longer probably due to the replacement of chloride ligand to stronger trans effect phenyl ligand. The C(19)-Pd(1) bond of **36** is *ca.* 0.074 Å longer than the C(sp²)-Pd bond in [PdCl(Ph)(2,2'-bipy)] (1.970(7) Å)⁴⁴.

To study if complex **36** can activate C-H bonds, a solution of complex **36** in $C_6D_5CD_3$ was refluxed for 12 hours without observing any H/D exchange. However, prolonging the refluxing time slowly resulted in the formation of several new species and a significant signal change of the residual vacuum grease observed in the 1H NMR spectrum. A possible explanation for that observation is decomposition of **36** mediated by vacuum grease. Vacuum grease involved reactions are quite rare and obviously not usually targeted. Previously, Lennartson *et al.*⁴⁵ successfully isolated a dinuclear complex from reaction between silicone grease and phenylmagnesium bromide in diethyl ether (Figure 4-16). In any event **36** does not appear to undergo intermolecular C-H exchange under the conditions investigated.

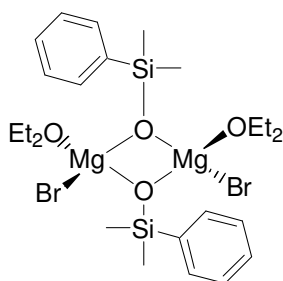


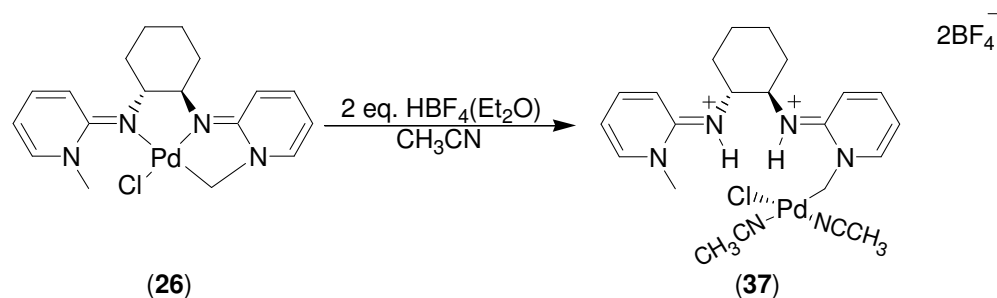
Figure 4-16. Product from degradation of grease by phenyl Grignard reagent.

4.4 Reactivity of palladacycles with H^+ , H^- , and H_2

In order to provide some insight into potential catalytic applications of PYE ligands and the possibility of Pd-C bond activation, the reactivity of **26** and **32** with different hydrogen sources H^+ , H^- and H_2 was investigated.

Addition of 2 eq. of $HBf_4 \cdot (Et_2O)$ to an acetonitrile solution of **26** led to selective protonation of two imine nitrogen atoms to give the *cis*-bis-acetonitrile palladium complex $[Pd(MeCN)_2Cl(\eta^1-CH_2N^{C_6H_{10}}N^{Me})(H^+)_2](BF_4)_2$ **37** as shown in Scheme 4-14. 1H and ^{13}C NMR spectroscopy, mass spectrometry, and elemental analysis are consistent with the proposed formulation. An unsymmetrical pattern was observed in the 1H and ^{13}C NMR spectra of **37** associated with disappearance of two doublets due to diastereotopic $PdCH_2$ protons. Instead, a singlet signal for $PdCH_2$ appeared at 4.11 ppm in the 1H NMR spectrum and 33.4 ppm in the ^{13}C NMR spectrum. Two distinctive broad signals derived from two

protonated *NH* were observed at 6.51 and 7.55 ppm respectively. A general downfield shift for **37** with respect to PYE moieties was shown in ^1H and ^{13}C NMR spectroscopy in comparison to **26**, except for $c\text{-met}C^1$ (159.7 to 153.3) and C^1 (162.9 to 154.4) with a significant upfield change.



Scheme 4-14. Synthesis of **37** via protonation to imine nitrogens.

Single crystals of **37** were grown from acetonitrile and diethyl ether at -40°C . The molecular structure is shown in Figure 4-17 and selected bond lengths and angles are given in Table 4-6. The bond lengths and angles with respect to the PYE moieties are close to the protonated salt **16**. The geometry at the palladium is pseudo square planar with two *cis* acetonitrile ligands. The Pd(1)-C(6) bond of **37** is 0.023 \AA longer than **26** and the Pd(1)-Cl(1) bond is 0.0447 \AA shorter. Furthermore, in comparison with structurally related complexes, the Pd-C bond of **37** is really close to the Pd-C(sp^3) bond of $[\text{PdCl}(\text{CH}_3)(\text{N-N})]$ ($2.020(11) \text{ \AA}$; N-N: $\text{ArN}=\text{C}(\text{H})\text{C}(\text{H})=\text{NAr}$, Ar: 2,6- $(i\text{Pr})_2\text{C}_6\text{H}_3$).⁴⁶

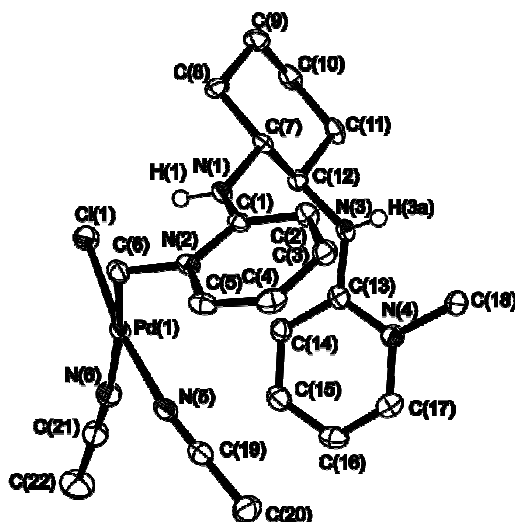
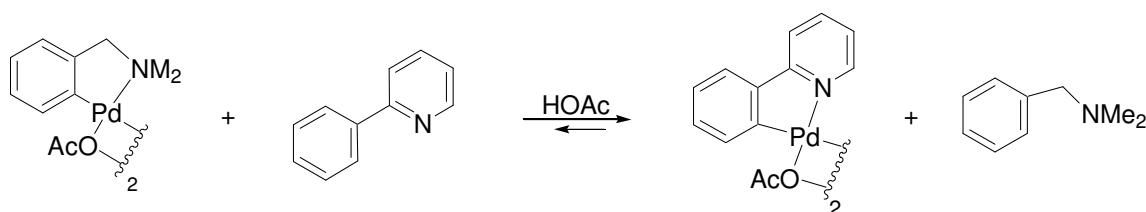


Figure 4-17. Molecular structure of complex **37**. Ellipsoids are shown at 50 % probability. Hydrogen atoms except for H(1) and H(3b) have been omitted for clarity.

Table 4-6. Selected bond lengths and angles for complex **37**.

Bond	lengths (Å)	Bond	Angles (°)
Pd(1) – Cl(1)	2.3010(7)	N(5) – Pd(1) – N(6)	90.44(9)
Pd(1) – C(6)	2.013(3)	Cl(1) – Pd(1) – C(6)	89.49(8)
N(5) – Pd(1)	2.026(2)	N(2) – C(6) – Pd(1)	114.11(16)
N(6) – Pd(1)	2.139(2)	C(2) – C(1) – N(1) – C(7)	7.6(4)
C(1) – N(1)	1.337(3)	C(14) – C(13) – N(3) – C(12)	3.1(4)
C(13) – N(3)	1.341(3)		
C(18) – N(4)	1.465(3)		
C(6) – N(2)	1.465(3)		

Protonation and decoordination of the supporting nitrogen atoms in palladacycles has been observed previously as one important step for transcyclopalladation. Ryabov *et al.*⁴⁷ reported the first transcyclopalladation reaction between dialkylbenzylamine and phenylpyridine in acetic acid solvent in 1984 (Scheme 4-15). Transcyclopalladation contains two steps which are (i) decoordination and protonation of the donor group to give a monodentate C-bound complex which is highly susceptible to acidolysis; (ii) recyclopalladation either through an inorganic intermediate or through a diorgano metal complex.^{48, 49}



Scheme 4-15. Transcyclopalladation reaction between dialkylbenzylamine and phenylpyridine in acetic acid solvent.

An *N*-protonated dechelated intermediate was isolated showing the existence of the Pd-C bond (Figure 4-18). The formation of **37** can be attributed to strain in the 5-membered palladacycle and strong basicity of the PYE imine-like nitrogen.

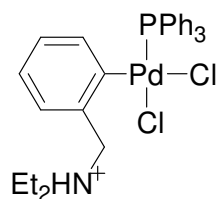
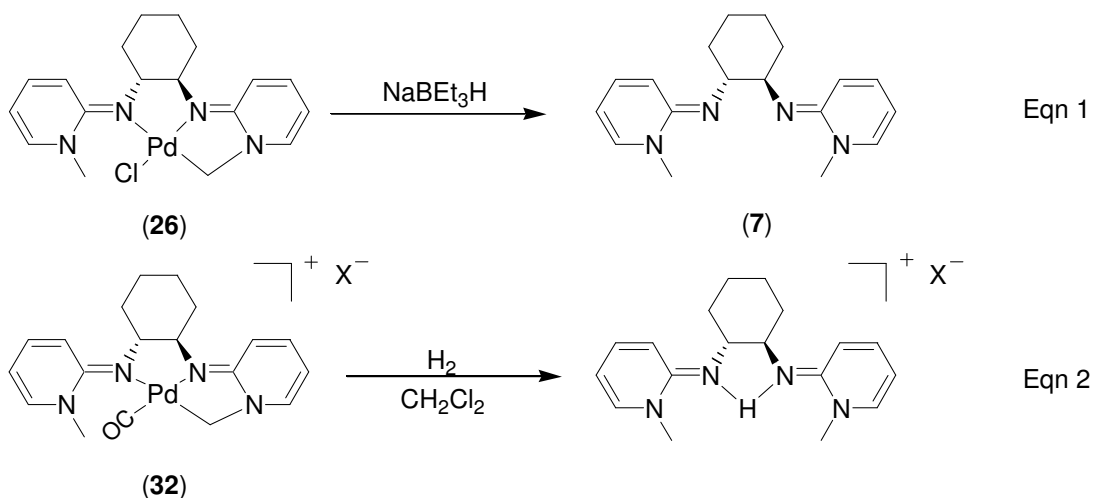


Figure 4-18. Example of dechelated palladium complex via protonation.

Furthermore, a palladium hydride cannot be isolated from reaction between **26** and “super hydride” NaBEt_3H , which ultimately gives neutral ligand based on the ^1H NMR spectrum of the reaction mixture (Eqn 1, Scheme 4-16). Interestingly, the addition of dihydrogen gas into a solution of **32** gave protonated product, whose ^1H NMR data is consistent with that of monoprotonated **7**. This indicates that the Pd-C bond can be hydrogenated presumably after oxidative addition or perhaps more likely addition of dihydrogen across the Pd-C bond (Eqn 2, Scheme 4-16). Eqn 1 and 2 imply the formation of a reactive palladium hydride intermediate.



Scheme 4-16. Reactivity of **26** and **32** with H^- and H_2 .

Those above observations suggest that the application of palladacycles incorporating PYE ligands in any catalytic reactions involving a proton transfer step may be problematic. The instability of palladacycles and their derivatives with PYE ligands in the presence of any hydrogen atom source is accounted for the previous catalytic testing failure including alcohol oxidation, hydrogenation, transfer hydrogenation and hydroamination.

4.5 Conclusions

Selective cyclopalladation influenced by various backbones (alkyl and aryl) for PYE ligands was observed and a series of mono- and dipalladacycles were successfully isolated in the presence of Brønsted base. Steric and electronic effects were taken into account for this selective cyclopalladation. However, steric effects are considered to be more dominant. In comparison with *N*-Me cyclopalladation, the presence of *N*-Bn group increases the energy barrier of cyclopalladation to allow the isolation of palladium dichloride intermediate **23**.

The reactivity of palladacycles was investigated with a variety of substrates including CO, NH₃, alkenes, alkynes and Grignard reagents (PhMgBr). The strong donating ability of the PYE moiety was confirmed by a lower CO stretching frequency of carbonyl complex **32** in comparison to very similar complexes. Owing to the steric constraint of the cyclopalladated ring, CO insertion into the Pd-C bond was prevented. Furthermore, there was no observation of any H/D exchange in isotopomer **33**-ND₃ and phenyl substituted complex **36** refluxed in C₆D₅CD₃ indicating the cyclopalladated Pd-C bond is relatively strong. The remaining second *N*-methyl group causes a steric repulsion to selectively direct coordination at the Pd atom. Due to this repulsion, alkenes and alkynes are unable to form good orbital overlap with the Pd atom.

Catalytic applications including oxidation, hydrogenation, transfer hydrogenation and hydroamination were carried out, unfortunately without any success. A systematic study to understand the problem identified a possible reason, which is the instability of palladacycles and their derivatives with PYE ligands in the presence of different hydrogen atom sources. The cyclopalladated Pd-C bond was found to be cleaved by hydride migration. The formation of the ligand-dangling complex **37** via protonation is consistent with a previous study of transcyclopalladation.

4.6 References

1. J. Dupont, C. S. Consorti and J. Spencer, *Chem. Rev.*, 2005, **105**, 2527-2571.
2. R. B. Bedford, C. S. J. Cazin and D. Holder, *Coord. Chem. Rev.*, 2004, **248**, 2283.
3. I. Omae, *Coord. Chem. Rev.*, 2004, **248**, 995.
4. M. E. van der Boom and D. Milstein, *Chem. Rev.*, 2003, **103**, 1759.
5. A. C. Cope and R. W. Siekman, *J. Am. Chem. Soc.*, 1965, **87**, 3272.
6. H. M. McPherson and J. L. Wardell, *Inorg. Chim. Acta.*, 1983, **75**, 37.
7. D. Sole, L. Vallverdu, X. Solans, M. Font-Bardia and J. Bonjoch, *J. Am. Chem. Soc.*, 2003, **125**, 1587.
8. J. C. Gaunt and B. L. Shaw, *J. Organomet. Chem.*, 1975, **102**, 511.
9. D. Zim and S. L. Buchwald, *Org. Lett.*, 2003, **5**, 2413.
10. F. Maassarani, M. Pfeffer and G. LeBorgne, *Organometallics*, 1987, **6**, 2029.
11. J. Dupont, M. Pfeffer, M. A. Rotteveel, A. Decian and J. Fischer, *Organometallics*, 1989, **8**, 1116.
12. L. N. Lewis, *J. Am. Chem. Soc.*, 1986, **108**, 743.
13. I. P. Beletskaya and A. V. Cheprakov, *J. Organomet. Chem.*, 2004, **689**, 4055.
14. K. Hallman and C. Moberg, *Adv. Synth. Catal.*, 2001, **343**, 260.
15. S. Paavola, K. Zetterberg, T. Privalov, I. Csoregh and C. Moberg, *Adv. Synth. Catal.*, 2004, **346**, 237.
16. M. Gomez, J. Granell and M. Martinez, *Organometallics*, 1997, **16**, 2539-2546.
17. M. Crespo, M. Font-Bardia, J. Granell, M. Martinez and X. Solans, *Dalton Trans.*, 2003, 3763-3769.
18. A. B. Goel and M. Pfeffer, *Inorg. Synth.*, 1989, **26**, 211.
19. A. D. Ryabov, *Chem. Rev.*, 1990, **90**, 403-424.
20. A. Zucca, M. Agostina, M. V. Pinna, S. Stoccoro and G. Minghetti, *Organometallics*, 2000, **19**, 4295-4304.
21. R. Y. Mawo, S. Mustakim, V. G. Young Jr., M. R. Hoffmann and I. P. Smoliakova, *Organometallics*, 2007, **26**, 1801-1810.
22. K. J. Keuseman and I. P. Smoliakova, *Organometallics*, 2005, **24**, 4159-4169.
23. G. Aullon, R. Chat, I. Favier, M. Font-Bardia, M. Gomez, J. Granell, M. Martinez and X. Solans, *Dalton Trans.*, 2009, 8292-8300.

24. H. Takahashi and J. Tsuji, *J. Organomet. Chem.*, 1967, **10**, 511.
25. M. I. Bruce, B. L. Goodall and F. G. A. Stone, *J. Chem. Soc., Chem. Commun.*, 1973, 558.
26. M. I. Bruce, B. L. Goodall and F. G. A. Stone, *J. Chem. Soc., Dalton Trans.*, 1978, 687.
27. K. Hiraki, Y. Fuchita and Y. Kage, *J. Chem. Soc., Dalton Trans.*, 1984, 99.
28. A. D. Ryabov, V. A. Polyakov, I. K. Taleborovskaya, V. A. Katkova, A. K. Yatsimirskii and I. V. Berezin, *Russ. Chem. Bull*, 1988, 162.
29. M. Hugentobler, A. J. Klaus, H. Mettler, P. Rys and G. Wehrle, *Helv. Chim. Acta*, 1982, **65**, 1202.
30. A. J. Canty, *Acc. Chem. Res.*, 1992, **25**, 83-90.
31. J. Zhao, M. Campo and R. C. Larock, *Angew. Chem. Int. Ed.*, 2005, **44**, 1873-1875.
32. C. Carfagna, G. Gatti, D. Martini and C. Pettinari, *Organometallics*, 2001, **20**, 2175-2182.
33. J. Dupont, M. Pfeffer, J. C. Daran and Y. Jeannin, *Organometallics*, 1987, **6**, 899.
34. I. D. Hills and G. C. Fu, *J. Am. Chem. Soc.*, 2004, **126**, 13178-13179.
35. J. Terheijden, G. van Koten, D. M. Grove and K. Vrieze, *J. Chem. Soc., Dalton Trans.*, 1987, 1359.
36. D. M. Grove, G. van Koten and H. J. C. Ubbels, *J. Am. Chem. Soc.*, 1982, **104**, 4285-4286.
37. O. Renn, A. Albinati and B. Lippert, *Angew. Chem., Int. Ed. Engl.*, 1990, **29**, 84.
38. C. R. Baar, H. A. Jenkins, M. C. Jennings, G. P. A. Yap and R. J. Puddephatt, *Organometallics*, 2000, **19**, 4870.
39. L. Dahlenburg and S. Mertel, *J. Organomet. Chem.*, 2001, **630**, 221.
40. V. G. Albano, M. D. Serio, M. Monari, I. Orabona, A. Panunzi and F. Ruffo, *Inorg. Chem.*, 2002, **41**, 2672.
41. N. Oberbeckmann-Winter, P. Braunstein and R. Welter, *Organometallics*, 2004, **23**, 6311.
42. Y. Ding, R. Goddard and K.-R. Porschke, *Organometallics*, 2005, **24**, 439.
43. K. E. Neo, H. V. Huynh, L. L. Koh, W. Henderson and T. S. Andy Hor, *J. Organomet. Chem.*, 2008, **693**, 1628-1635.

44. A. Mendes, R. D. W. Kemmitt, J. Fawcett and D. R. Russell, *Polyhedron*, 1999, **18**, 1141-1145.
45. A. Lennartson and M. Hakansson, *Acta Cryst.*, 2008, **C64**, m8-m9.
46. D. J. Tempel, L. K. Johnson, R. L. Huff, P. S. White and M. Brookhart, *J. Am. Chem. Soc.*, 2000, **122**, 6686-6700.
47. A. D. Ryabov and A. K. Yatsimirsky, *Inorg. Chem.*, 1984, **23**, 789-790.
48. A. D. Ryabov, *Inorg. Chem.*, 1987, **26**, 1252.
49. M. Albrecht, *Chem. Rev.*, 2010, **110**, 576-623.

5.0 Anticancer activity of metal complexes with PYE ligands

5.1 Introduction

For a long time, organic compounds have dominated the medicinal therapeutic area and transition metal ions were initially regarded as toxic “heavy metals”, making them potentially unsuitable for anticancer research. However, since the landmark discovery of the biological activity of cisplatin,¹ medicinal inorganic chemistry has attracted increasing attention. Cisplatin has shown extensive activity against a range of cancers, in particular testicular cancer. Once tumors are discovered early, a cure rate of nearly 100% can be achieved.² However, the clinical use of cisplatin and its platinum-based analogues are limited by dose-limiting side effects, which include nephrotoxicity, emetogenesis and neurotoxicity. Also, inherent and acquired resistance of many tumour cells to platinum-based drugs causes further problems.² To solve these problems, much effort has been put into developing new platinum-based drugs. However, only fewer than 30 compounds out of over 3000 synthesised and tested platinum compounds entered clinical trials and only 4 platinum-based drugs are officially registered as marketed drugs - cisplatin, carboplatin, oxaliplatin and nedaplatin (Figure 5-1).³⁻⁵ Relative to the substantial and urgent demands of patients, focusing only on platinum compounds will retard the development of anticancer agents. New types of metal complexes, which can be clinically utilized, are definitely required.

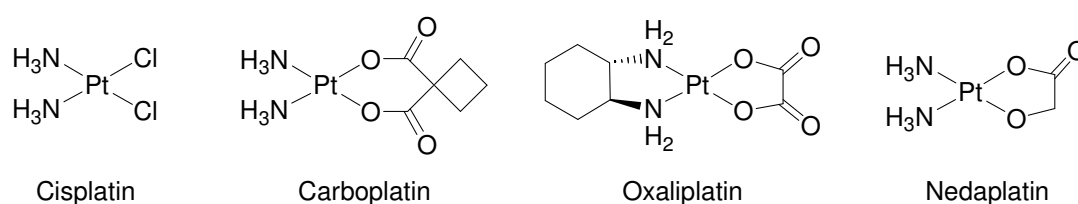


Figure 5-1. Marketed platinum anticancer drugs.

Inspired by cisplatin, research interest has been expanded into a wide range of other metal ions, eg. gold, copper, ruthenium, palladium, iron and titanium.^{6, 7} This wide investigation of other metal ions has not only introduced many possibilities for overcoming the drawbacks of platinum-based drugs, but also offered other novel anticancer targets. A variety of metal complexes and their relative biological targets are illustrated in Table 5-1

and Figure 5-2 to exhibit recent development of medicinal organometallic chemistry.

Table 5-1. A variety of metal complexes with anticancer activity and their relative biological targets.

Compounds	Anticancer targets
Cisplatin ^{2,6}	Binding to DNA and interacting with DNA to form inter- and intra-strand cross-links.
Ru(II)-arene (RM175) ⁸	Unique binding modes to duplex DNA in a bifunctional manner by both intercalation and direct metallation, and different structural distortions in DNA compared to cisplatin
KP1019 ⁹	Cellular transduction pathways
NAMI-A ¹⁰ and [Ru(II)(arene)Cl ₂ (PTA)] (RAPTA) ¹¹	Metastasis inhibition
Ni(II)-salphen ¹² and Mn porphrin ¹³	Interaction with the grooves and loops of the quadruplex to induce a high degree of quadruplex DNA stabilisation and telomerase inhibition
DW1 ¹⁴	Mimicking the protein kinase inhibitor as scaffold
Phosphole-Au(I) ¹⁵	Inhibition of hTrxR (human thioredoxin reductase) and hGR (human glutathione reductase)

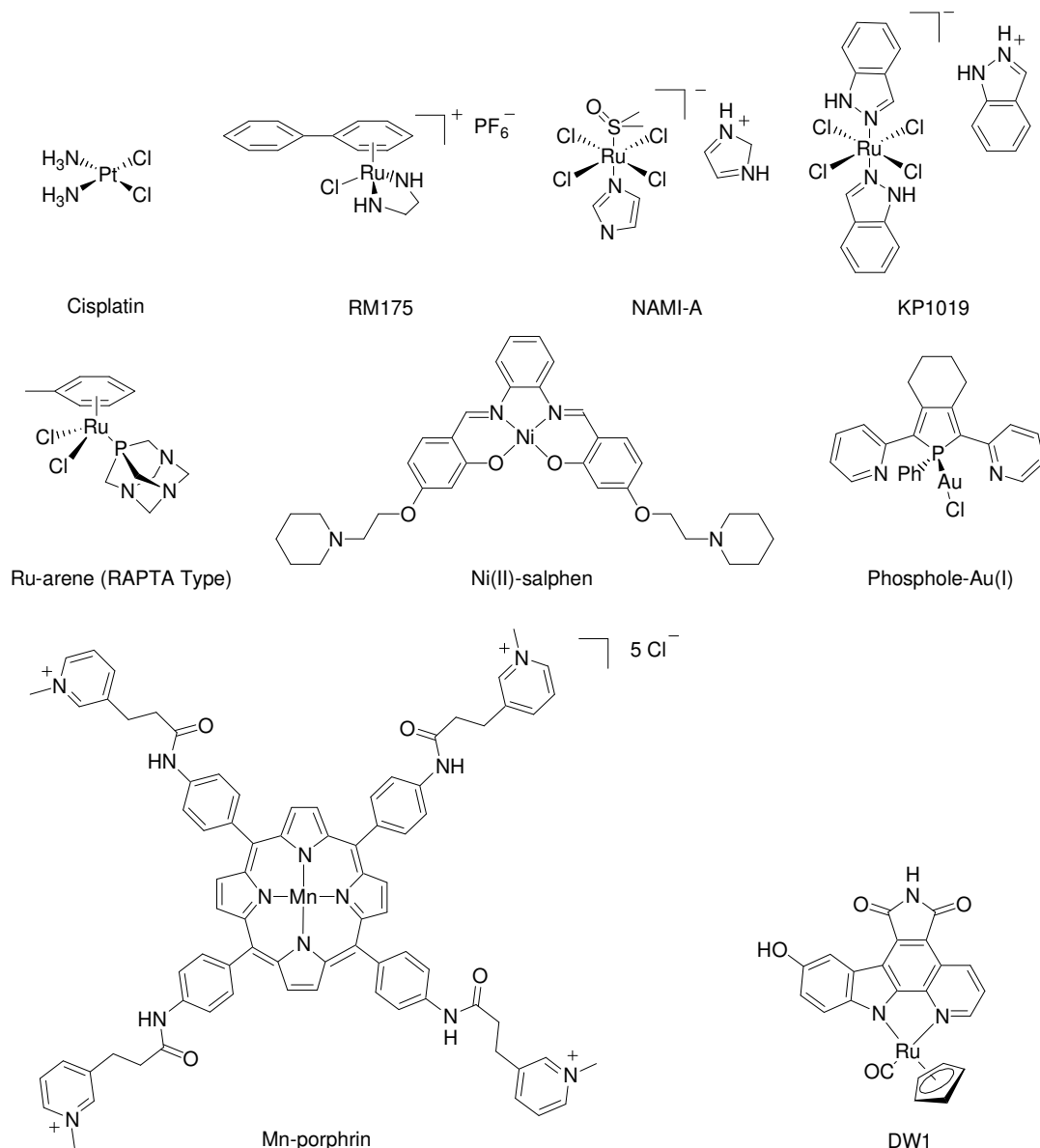


Figure 5-2. Diverse metal compounds with anticancer activity.

5.1.1 Development of ruthenium complexes as anticancer agents

As seen above, ruthenium-based compounds have drawn much attention in the last decade owing to several advantages as indicated by the following:¹⁶

- 1) Stable complexes with predictable structures which can be synthesised by reliable methods;
- 2) Capability of tuning ligand affinities, electron transfer and substitution rates, and

reduction potentials;

- 3) An increasing knowledge of biological activity and the mechanism of ruthenium complexes.

Early interest in investigating ruthenium complexes as anticancer agents stemmed from the discovery of Ru(III) ammines $[\text{Cl}(\text{NH}_3)_5\text{Ru}]^{2+}$ by Clarke *et al.*¹⁷ almost thirty years ago. Subsequently, a variety of neutral or cationic Ru(II)/(III) complexes have been synthesised and tested for anticancer activity. It has been found that ruthenium complexes provide novel targets of cancer treatment and consequently show positive effects against cancers that platinum drugs can not treat as well and there can also be a lower toxicity compared to platinum drugs.¹⁸

There are now several promising ruthenium complexes undergoing clinical trials. NAMI-A ($[\text{Him}]trans\text{-}[\text{RuCl}_4(\text{DMSO-}S)(\text{im})]$, where im = imidazole) and KP1019 ($[\text{Hind}]trans\text{-}[\text{RuCl}_4(\text{ind})_2]$, where ind = 1*H*-indazole) (Figure 5-2) are the first ruthenium-based anticancer drugs transferred into clinical trials and have successfully completed phase I.^{9,19} Alessio *et al.*¹⁰ reported that NAMI-A, a complex which failed the traditional *in vitro* cytotoxicity test, surprisingly is effective against metastatic solid tumors *in vivo*. Proof of its selectivity for metastatic tumor cells over primary tumor cells provides a new target for drug therapy. As a structurally related complex, KP1019 developed by Dyson *et al.*¹¹ exhibits a different mechanism of anticancer activity, which is proposed as, i) accumulation in transferrin receptor-(over)expressing tumor cells via the transferrin receptor; ii) reduction to Ru(II) species; iii) interaction with DNA and iv) induction of apoptosis via the intrinsic mitochondrial pathway.

It is believed, as anionic ruthenium(III) complexes, NAMI-A and KP1019 actually play a prodrug role, whereas reduced Ru(II) species are suggested as responsible for tumor reduction.⁹ Accordingly, a variety of ruthenium(II) complexes have been designed and synthesized for anticancer investigation. Of those active ruthenium(II) complexes, increasing attention has been drawn to two families of ruthenium(II)-arene complexes developed by Sadler *et al.*⁸ and Dyson *et al.*¹¹ respectively. Cationic ruthenium(II)-arene

complexes (e.g. RM175 in Figure 5-2), exhibit excellent *in vitro* and *in vivo* anticancer activity. In contrast to other types of ruthenium complexes (absence of arene) and cisplatin, additional interactions of this class, such as intercalative binding of arene ligand and specific hydrogen bonding interaction of amine group result in unique binding modes to duplex DNA. The other neutral class, RAPTA (Figure 5-2), shows pH dependent DNA binding features and selectivity towards metastatic tumors *in vivo* like NAMI-A, where the pta phosphine ligand is believed to be responsible for selectivity. Interestingly, the RAPTA complex also failed the traditional drug screening test *in vitro* displaying very poor IC₅₀ values as did NAMI-A. Failure of both promising potential drugs in primary screening test *in vitro* makes new assays urgently required to look beyond traditional *in vitro* cytotoxicity tests.

5.1.2 Development of palladacycles as anticancer agents

The development of palladacycles seems not to be as rapid as that of other organometallic complexes, especially platinum- and ruthenium-based, although some reports have highlighted the potential anticancer properties of palladacycles.^{20, 21} The advantages of utilizing palladacycles as attractive targets of anticancer agents are plenty, including ease of synthesis, stability, potential for rapid library generation for structural activity studies and modifications of the physiochemical properties (e.g. solubility and lipophilicity).²⁰ In 1993, Higgins III *et al.*²² synthesized and tested a selection of palladacycles for cytotoxicity on various cell lines. Most complexes were quite cytotoxic towards the tumor panel, having IC₅₀ values in the 10 mg/mL range. Interestingly, the two complexes shown in Figure 5-3 displayed a 3-5 fold differential response between the HT1376 (invasive bladder transitional cell carcinoma cell line) and the SW6020 (colon carcinoma line) cell lines.

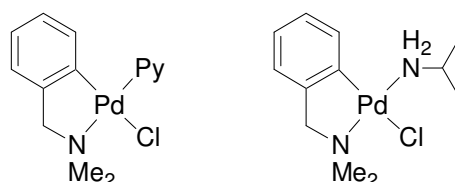
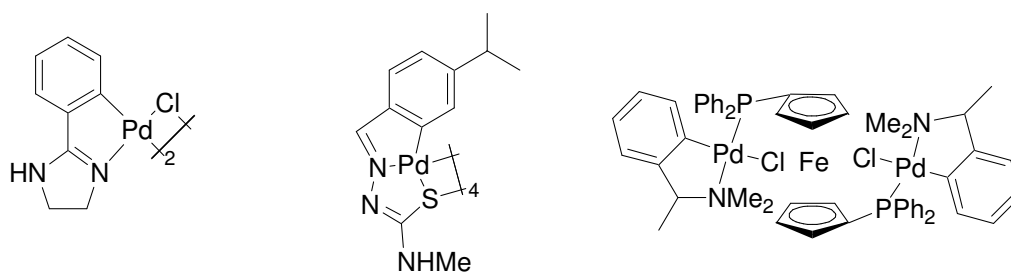


Figure 5-3. Examples of palladacycles with differential response among various cell lines.

Subsequently, a number of various palladacycles^{21, 23-27} have attracted attention in this area, showing cytotoxic effects against tumor cells *in vitro* and different binding modes of targets from that of *cis*-platin described above. For example, compounds **A-C** with micromolar activity against human cancer cell lines and their novel targets are illustrated in Figure 5-4.²⁸⁻³¹ Compound **A** was found to slightly increase the T_m (melting temperature) of DNA probably due to a predominantly intercalative mode of binding to DNA. Compound **B** induced DNA interhelical cross-links, a type of DNA adduct that is not formed by *cis*-platin, and shows the possibility of circumventing *cis*-platin resistance. In addition, compound **C** exhibited similar anticancer activity as NAMI-A and RAPTA complexes. Notably, these differential anticancer targets might lead to an entirely new phase of anticancer research to provide new choices to the therapy of *cis*-platin-resistant tumors.



(A) Intercalative DNA lesion (B) DNA interhelical cross-links (C) Matastatic tumors

Figure 5-4. Examples of palladacycles with potential anticancer activity and their different targets from *cis*-platin.

5.2 Synthesis and characterisation of Ru(II)-DMSO complexes with PYE ligands

As shown in section 5.1.1, ruthenium (II) or (III) complexes have exhibited very interesting biological properties, particularly in the field of anticancer treatment. Within those active organometallic molecules, imine or amine fragments play an important role in regard to interaction modes with anticancer targets⁸ and the stability and activity of the complexes.¹⁰ Furthermore, PYE ligands have shown some interesting biological activity.³² With these in mind, we decided to synthesise a new class of ruthenium(II) complexes with PYE ligands and subsequently test them for anticancer activity.

Cis-RuCl₂(DMSO)₄ is a widely used starting material for synthesizing ruthenium

complexes^{33, 34} through substitution of the labile chloro and DMSO ligands which have shown effective activity against solid tumor metastasis.³⁵ Therefore we chose *cis*-RuCl₂(DMSO)₄ as the precursor to start our ruthenium chemistry.

Before we began this project, we were aware of presence of a variety of neutral ruthenium(II)-DMSO complexes with different chelating imine ligands.³⁴ Following this precedent, a series of reaction condition tests were carried out. Solubility problems limited the use of hydrocarbon solvents (e.g. toluene). Chlorinated solvents (e.g. dichloromethane) were found to cause undesired side-reactions possibly due to addition of active C-Cl bonds to products and / or oxidation of Ru(II) to Ru(III) by chlorinated solvents. Attempts to use acetonitrile as the reaction solvent, either at room temperature or by refluxing, led to the formation of protonated ligand (**X**), which was confirmed by a solved but unrefined X-ray crystal structure (Figure 5-5) obtained from an acetonitrile solution. The reason for such a transformation is at present unclear. Finally, methanol and ethanol were found to be suitable choices. We chose to use methanol due to a relative shorter reaction time. The N-substituents of bidentate PYE ligands proved to be important in this type of reaction as no isolation of metal complexes with ligand **8** containing bulky benzyl group was successful.

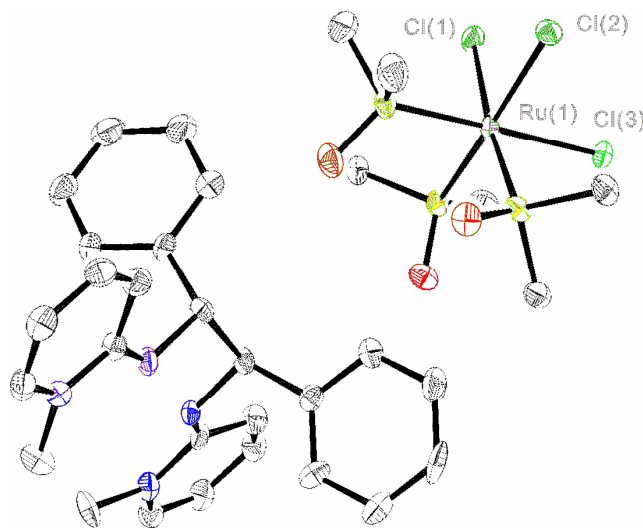
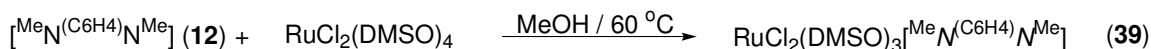
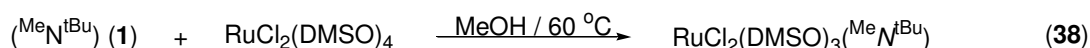
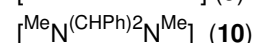
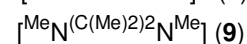
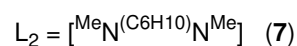
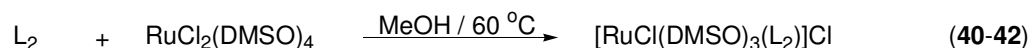


Figure 5-5. Molecular structure of complex **X**. Ellipsoids are shown at 50 % probability. Hydrogen atoms have been omitted for clarity.

Neutral type:



Cationic type:



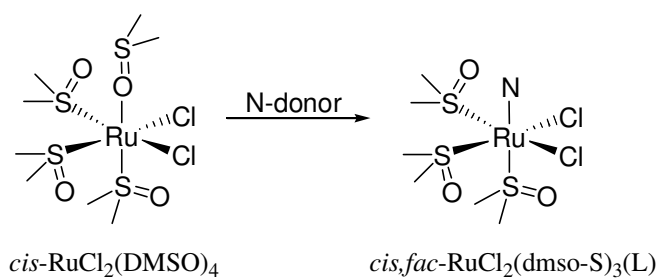
Scheme 5-1. Synthetic routes to new types of Ru(II)-DMSO complexes with PYE ligands.

As shown in Scheme 5-1, reactions between compounds **1**, **7**, **9**, **10** and **12** and the starting complex *cis*-RuCl₂(DMSO)₄ in 1:1 mole ratio with heating at 60°C in methanol gave products **38-42** in high yield (>90%). The solubility of all the compounds is very good in alcoholic solvents, DMSO and water but very poor in aromatic, ether and hydrocarbon solvents. These compounds are very hygroscopic and gradually degraded on exposure to air. All the complexes were characterised by NMR and infra-red spectroscopies and elemental analysis, which are consistent with the proposed formulas. Mass spectrometry is unable to provide desired evidence, which has been encountered commonly for this type of compound.³⁶⁻³⁹

Taking all the available characterising data into account, compounds **38** and **39** were formulated as neutral of the type [RuCl₂(DMSO)₃(L)] and [RuCl₂(DMSO)₂(L₂)] respectively which are typical formulas with respect to monodentate^{40, 41} and bidentate nitrogen ligands.^{33, 34, 39, 42} Interestingly, reaction between *cis*-RuCl₂(DMSO)₄ and alkyl linked ligands **7**, **9** and **10** gave a novel formula type [RuCl(DMSO)₃(L₂)](Cl) (**40-42**) respectively with replacement of O-bonded DMSO and one Cl ligand. The diverse behaviour of these complexes will be discussed in the following sections. It is worth noting that, due to the lack of X-ray crystal structure, geometries of all the compounds are not completely clear, so the structures drawn below only represent one of possible geometrical isomers (*vide infra*).

5.2.1 [RuCl₂(DMSO)₃(^{Me}N^{tBu})] (38) and [RuCl₂(DMSO)₂(^{Me}N^(C6H4)N^{Me})] (39)

As reported previously, the labile O-bonded DMSO ligand of *cis*-RuCl₂(DMSO)₄ is selectively replaced by stronger σ and/or π donor ligands of monodentate type to give *cis, fac*-RuCl₂(DMSO-S)₃(^{Me}N^{tBu}) derivatives (Scheme 5-2). The ¹H NMR spectrum of **38** recorded in methanol-d₄, in comparison with the spectra of the precursor *cis*-RuCl₂(DMSO)₄, shows a group of signals in a range of δ 3.10-3.50 ppm with an intensity of 18H attributed to three S-bonded DMSO groups and signals at δ 7.00, 7.49, 8.02 and 8.16 assigned to coordinated ligand protons. The lack of a peak at δ 2.72 ppm for the new complexes indicated the absence of O-bonded DMSO in the complexes, which was also reflected in the IR spectra of **38** by the presence of strong S=O stretching bands at 1084 cm⁻¹ for S-bonded DMSO and the absence of any strong bands in the region of 890-950 cm⁻¹ for O-bonded DMSO.³⁴ The resonance signals at δ 46.0 and 46.3 ppm in the ¹³C NMR spectrum of **38** are attributed to the DMSO *trans* to N-ligand and chloro respectively, which is comparable to the data reported by Taqui Khan *et al.*⁴¹ for pyrazole analogue (δ 46.12 *trans* to pyrazole and δ 47.19 and 47.83 *trans* to chloro). Although a *cis, mer* isomer is not expected from the known reactivity of *cis*-RuCl₂(DMSO)₄, the possibility of *cis, mer* isomer or their mixture is not completely excluded due to the ambiguity of multiple DMSO signals in the ¹H NMR spectra of **38**.



Scheme 5-2. Reaction between *cis*-RuCl₂(DMSO)₄ and nitrogen ligands, where L = NH₃,⁴³ Py,⁴⁰ imidazole,⁴³ Me₃Bzm.⁴⁰

For the chelating nitrogen ligands, many examples have shown that reactions between chelating N-ligands and *cis*-RuCl₂(DMSO)₄ preferentially yield *cis*(Cl),*cis*(S)-RuCl₂(DMSO)₂(L₂) complexes.⁴⁴⁻⁴⁹ However, it has been demonstrated recently that other isomers are accessible by alternative synthesis or thermal isomerizations. Koizumi *et al.*⁵⁰ and Schmid *et al.*⁵¹ reported the selective synthesis of *tran*(Cl),*cis*(S)-isomer for 1,8-

naphthyridine (napy) and paullone type ligands respectively. Interestingly, Llobet and co-workers³⁸ reported reaction of equimolecular amounts of *cis*-RuCl₂(DMSO)₄ and the neutral ligand (3,5-bis(2-pyridyl)pyrazole) (hbpp) in methanol at reflux for 45 min produces the *trans*(Cl),*cis*(S)-isomer, while prolonged reflux yielded the thermodynamically more stable *cis*(Cl),*cis*(S)-isomer completely. In some cases, reaction between chelating ligands and *cis*-RuCl₂(DMSO)₄ ended up with a mixture of two isomers, which was demonstrated by Suzuki *et al.*⁵² for bipyridine (bpy) and Cingi *et al.*⁵³ for 4-amino-5-methylthio-3-(2-pyridyl)-1,2,4-triazole.

The ¹H NMR spectrum of **39** shows a group of signals in the range δ 3.15-3.50 ppm with an intensity of 12H attributed to two S-bonded DMSO ligands and signals at δ 6.30, 6.44, 7.15, 7.28 and 7.57 assigned to the protons of the coordinated ligand. The ¹³C NMR spectrum also shows symmetrical signals attributed to coordinated ligand and DMSO ligands. These symmetrical NMR patterns reflect C_{2v} symmetry from which was inferred the possibility of symmetrical isomer **A** and/or **B** but not unsymmetrical isomer **C** (Figure 5-6). IR spectra shows strong S=O stretching bands at 1093 cm⁻¹ attributed to S-bonded DMSO and no sign of O-bonded DMSO.

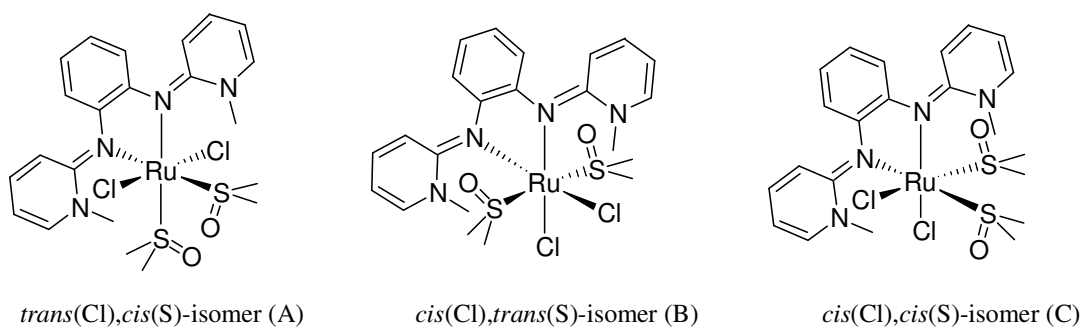
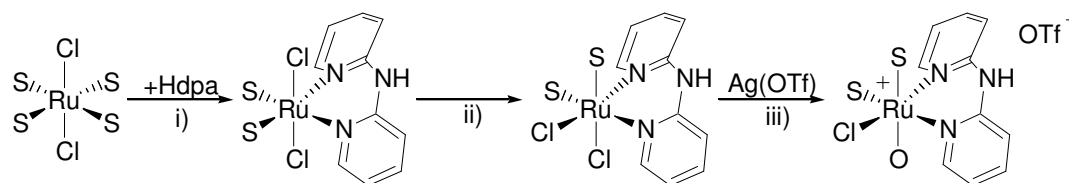


Figure 5-6. Possible isomers for compound **39**.

5.2.2 [RuCl(DMSO)₃(L₂)](Cl) (**40-42**)

Cationic [RuCl(DMSO)₃(L₂)](Cl) complexes with chelating nitrogen ligands are rare, and to our knowledge only one example has been published by Nagao and co-workers³⁹ to date. The synthetic route to that complex involved three steps: i) synthesis of *trans*(Cl),*cis*(S)-isomer by reaction between *trans*-RuCl₂(DMSO)₄ and di-2-pyridylamine

(Hdpa); ii) thermal isomerisation of *trans*(Cl),*cis*(S)-isomer to *cis*(Cl),*cis*(S)-isomer; iii) salt metathesis of *cis*(Cl),*cis*(S)-isomer with Ag(OTf) to give a *cis*(Cl,S),*trans*(O,S)-[RuCl(Hdpa)(DMSO-O)(DMSO-S)₂](OTf) complex as shown in Scheme 5-3.



- i) EtOH/H₂O (1:1), 0 °C, 40 hr;
- ii) EtOH/DMSO (14:1), refluxing, 5 min;
- iii) DMSO, 100 °C, 5 min.

Scheme 5-3. Synthetic route to *cis*(Cl,S),*trans*(O,S)-[RuCl(Hdpa)(DMSO-O)(DMSO-S)₂](OTf).

Elemental analysis provides evidence for the isolation of the cationic complexes [RuCl(DMSO)₃(L₂)](Cl). All three samples of **40-42** gave a satisfactory fit for the proposed formula, which is unlikely to be coincidence. The ¹H NMR spectra of those compounds show similar group signals around δ 3.1-3.6 ppm due to S-bonded DMSO ligands and corresponding coordinated *N*-ligand signals (Figure 5-7). Similarly, the ¹³C NMR spectra gave symmetrical signals for coordinated *N*-ligands and two separate DMSO signals attributed to axial and equatorial positions. The whole NMR pattern indicated that **40-42** exhibit C_s symmetry and S-bonded coordination mode which was also inferred from IR spectra ($\nu_{S=O}$ = 1085 cm⁻¹, **40**; 1083 cm⁻¹, **41**; 1077 cm⁻¹, **42**).

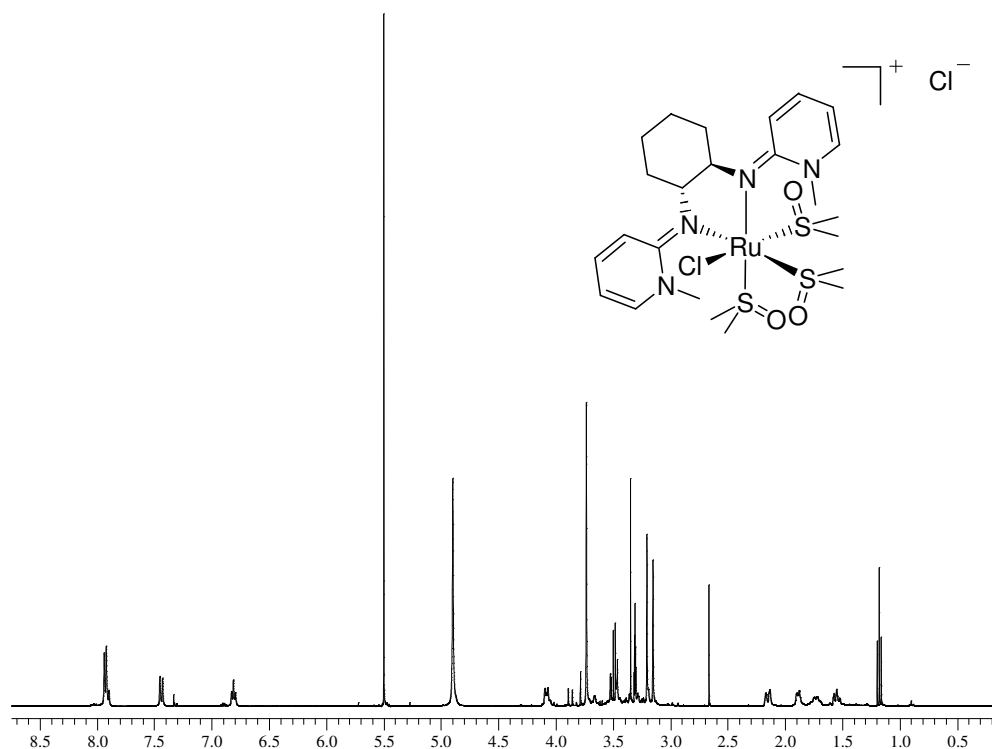


Figure 5-7. ^1H NMR spectrum of **40** in CD_3OD .

In order to compare the spectroscopic data of ruthenium complexes, neutral ligands and their protonated salts, we added one or two equivalent of $\text{HBF}_4(\text{OEt})_2$ into the methanol solution of complexes **40-42** to observe the change of chemical shifts. Taking compound **40** as an example, chemical shifts in the ^1H and ^{13}C NMR spectra of compound **40**, neutral ligand **7** and its protonated salts are compared in Table 5-2 and 5-3. ^1H and ^{13}C NMR chemical shifts of **40** show significant difference from **7** and its single protonated salt $7(\text{H}^+)(\text{BF}_4)$ but similar signals to the double protonated salt **43** and $7(\text{H}^+)_2(\text{BF}_4)_2$.

Table 5-2. Selected ^1H NMR Chemical Shifts (ppm) of **40**, **7**, $7(\text{H}^+)$ and $7(\text{H}^+)_2$ in CD_3OD .

	40	7	$7(\text{H}^+)(\text{BF}_4)$	$7(\text{H}^+)_2(\text{BF}_4)_2$	43 [$7(\text{H}^+)_2(\text{Cl}^-)_2$]
$H_{(\text{NCH}_3)}$	3.74	3.26	3.51	3.76	3.86
H_2	7.43	6.80	7.14	7.41	7.66
H_3	7.92	7.06	7.57	7.97	8.03
H_4	6.81	5.85	6.42	6.92	6.93
H_5	7.92	7.20	7.57	7.97	8.03

Table 5-3. Selected ^{13}C NMR Chemical Shifts (ppm) of **40**, **7**, **7**(H^+) $_2$ (Cl^-) $_2$ in CD_3OD .

	40	7	43 [7 (H^+) $_2$ (Cl^-) $_2$]
$\text{C}_{(\text{NCH}_3)}$	42.8	40.6	43.7
C_1	154.6	155.7	154.3
C_2	113.4	114.6	114.4
C_3	142.9	136.9	142.7
C_4	113.0	104.2	112.9
C_5	143.8	140.9	144.5

5.2.3 Electrical conductivity measurement of **39** and **40**

In order to obtain further comparison between neutral complex **39** and cationic complex **40**, electrical conductivity measurements were carried out. Before measuring compounds **39** and **40**, tetrabutylammonium chloride and *cis*- $\text{RuCl}_2(\text{DMSO})_4$ were measured as benchmarks and the results (Table 5-4) are consistent with the previous reports.^{33, 54} Taqui Khan *et al.*⁴¹ isolated several cationic ruthenium complexes and measured their molar conductance. Complex $[\text{RuCl}(\text{PzH})_2(\text{CO})(\text{DMSO})_2]\text{Cl}$ showed 88 μS in methanolic solution which indicates a 1:1 electrolyte (1 mM).⁵⁵ Similarly, as shown in Table 5-4, we achieved 106.4 μS for compound **40** in the reasonable range of 80 - 115 μS for a 1:1 electrolyte. While the measurement value 52.6 μS of compound **39** is somewhat higher than expected for neutral complex possibly due to the solvation of methanol but nonetheless much lower than **40**.⁵⁶

Table 5-4. Results of electrical conductivity measurement.

Compounds	Molar conductance (μS)
$[\text{RuCl}(\text{PzH})_2(\text{CO})(\text{DMSO})_2]\text{Cl}$	88
$(\text{Bu})_4\text{NHCl}$	99.2
<i>cis</i> - $\text{RuCl}_2(\text{DMSO})_4$	4.3
39	52.6
40	106.4

5.2.4 Stability of ruthenium complexes in neutral and low pH water

Before we began the test of *in vitro* cytotoxicity, stability of the tested complexes in water (the media to be used) was investigated. Utilizing ^1H NMR spectroscopy, the stability of the complexes was investigated by comparing the spectra over several days. It was found that complexes can still be observed within 96 h in D_2O while degradation was happening gradually. Interestingly, addition of 1 equivalent of $\text{HBF}_4(\text{Et}_2\text{O})$ into D_2O solution of compound **39** and **40** respectively caused a downfield change of chemical shifts of **39** from δ 6.4 (H_2), 6.5 (H_4), 7.4 (H_3) and 7.55 (H_5) to δ 6.7 (H_2), 6.85 (H_4), 7.7 (H_3) and 7.8 (H_5) but no change for **40**. The change of **39** could be derived from equilibrium between protonation of nitrogen atoms and their coordination to the metal centre. Cingi *et al.*⁵³ reported Ru(II) complexes with 4-amino-3-methyl-1,2,4- Δ^2 -triazoline-5-thione and 4-amino-3-ethyl-1,2,4- Δ^2 -triazoline-5-thione were oxidized by DMSO in acidic conditions to Ru(III) complexes. Similar observation was obtained for 1,10-phenanthroline⁴⁴ and *N,N,N,N*-tetramethylethylenediamine.⁵⁷ However, we did not observe any paramagnetic shift or line broadening for both compounds **39** and **40** over the course of the experiment.

5.2.5 Attempts to synthesis of Ru(II)-arene complexes with PYE ligands

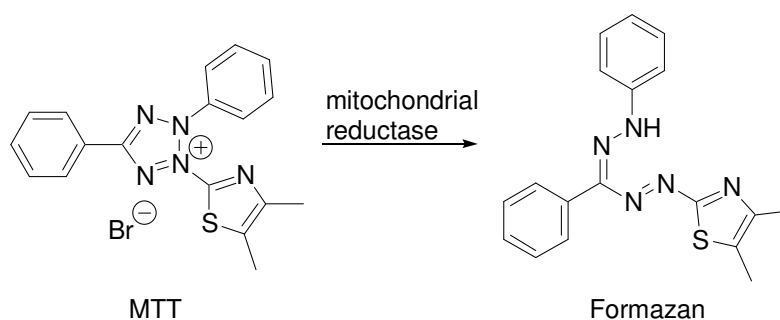
As discussed in section 5.1.1, Ru(II)-arene and RAPTA types of complexes have gained a significant progress in anticancer research. Following this work, we planned to synthesise similar types of complexes using precursor $[\text{RuCl}_2(\eta^6\text{-}p\text{-cymene})]_2$ and the bromide analogue $[\text{RuBr}_2(\eta^6\text{-}p\text{-cymene})]_2$, which is a typical starting material used,⁵⁸ and the monodentate ligand **1** and bidentate ligands **7** and **12**. Reactions were carried out in chloroform, methanol and acetonitrile under heating in or without the presence of NH_4PF_6 . The ^1H NMR spectra showed very broad signals for **1** and **7** which also was seen in platinum chemistry of PYE ligands. For **12**, after heating for days, a distinct spectrum was obtained, however, more than two new species appeared and *p*-cymene seems not to be coordinating to the metal centre probably due to a steric problem. Owing to shortage of time, we did not investigate further.

5.3 Investigation of anticancer activity

In order to evaluate the efficacy of our ruthenium complexes and cyclopalladated complexes as anticancer agents, we carried out cytotoxicity tests on a range of cell lines to deduce the cytotoxicity values using the MTT (3-(4,5-Dimethylthiazol-2-yl)-2,5-diphenyltetrazolium bromide) assay.⁵⁹

5.3.1 Introduction of MTT assay

The MTT assay, a standard colorimetric assay, routinely used to determine the cytotoxicity of potential medicinal compounds. The basis of this assay is the ability of viable cells to convert a yellow, water soluble dye (MTT) to a purple, water insoluble crystal (formazan) (Scheme 5-4). This conversion process occurs in the mitochondria and therefore, it only takes place in viable cells with functional mitochondria. After exposure the purple crystals are dissolved in an organic solvent (e.g. DMSO), and the absorbance of the resulting purple solution can be read on a spectrophotometer at 540 nm. IC₅₀ values can be deduced through a dose-response curve. The detail of conducting an MTT assay is described in the experimental. In Figure 5-8, pictures are shown after plating viable cells into a 96-well plate, after adding DMSO solution of drugs into a plate and after complete conversion of MTT to formazan.



Scheme 5-4. Conversion of MTT via mitochondrial reductase.

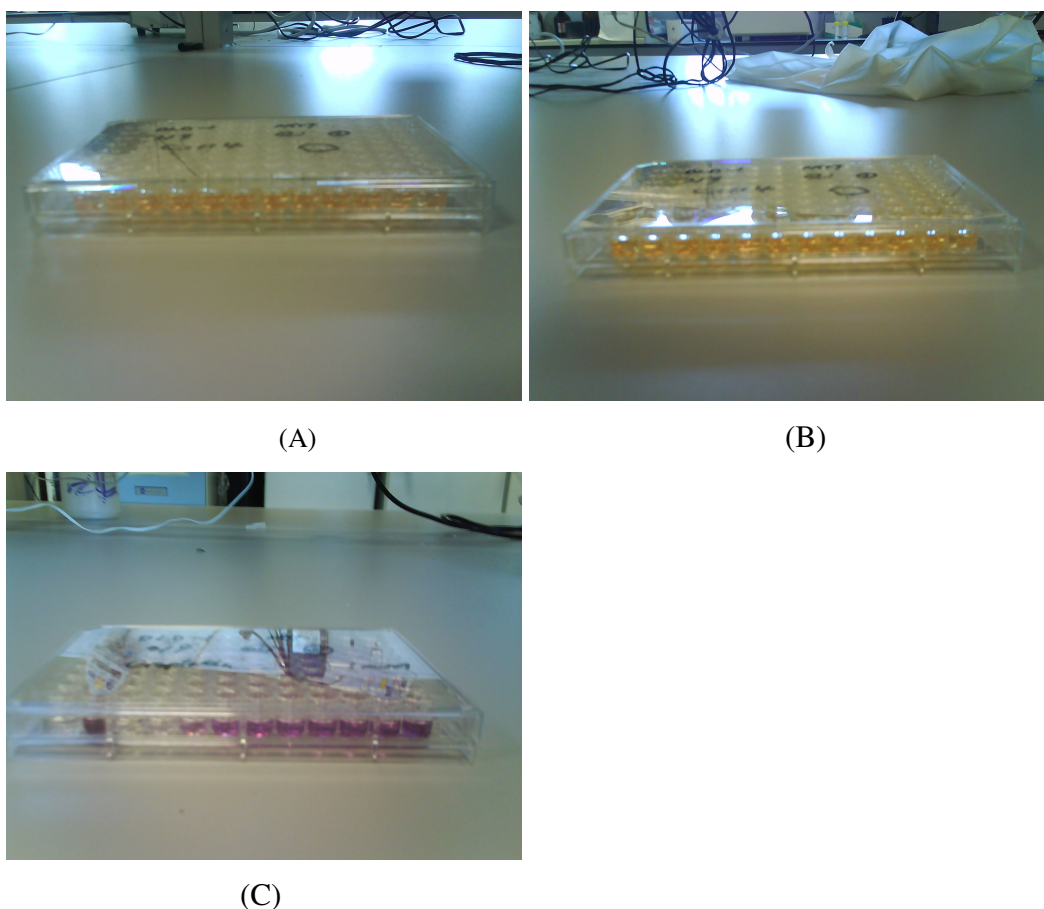


Figure 5-8. Pictures of conducting MTT assay, (A) after plating viable cells into 96-well plate; (B) after adding DMSO solution of drugs into plate; (C) complete conversion of MTT to formazan.

5.3.2 *In vitro* cytotoxicity tests

We chose human colon carcinoma cell line HT-29 and DLD-1, and human breast adenocarcinoma cell line MCF-7 to begin cytotoxicity tests with cyclopalladated complex **31** (chosen because of good solubility) and ruthenium complexes **38-42**. The IC_{50} values for those complexes are listed in Table 5-5. Complex **40** showed significantly lower IC_{50} values than those of other tested ruthenium complexes for all three cell lines in the similar magnitude. It is probably because the cyclohexyl ring of **40** increases the lipophilicity of **40** causing favorable penetration through the cell membrane. Compared to the standard drug *cis*-platin, **40** even showed higher cytotoxicity for DLD-1 and similar magnitude for HT-29, although the values we obtained for *cis*-platin are relatively higher than the previous results.⁶⁰ In order to confirm the real active species are related to the complex itself, *cis*-

$\text{RuCl}_2(\text{DMSO})_4$, neutral ligand **7** and protonated salt **43** were tested and showed non-cytotoxic activity within the tested concentration. Interestingly, complex **31** exhibited differential cytotoxicity effect against three cell lines with 64 μM for DLD-1. This unique result may lead to further development. Active dose-response curves are shown in Figure 5-9.

Table 5-5. IC_{50} values (μM) on the HT-29, MCF-7 and DLD-1 cell lines after 96 hr incubation.

Compounds	HT-29	MCF-7	DLD-1
<i>cis</i> -platin	61.5	10	~100
31	>100	>100	64.0 \pm 28.3
<i>cis</i> - $\text{RuCl}_2(\text{DMSO})_4$	>100	>100	>100
7	>100	>100	>100
38	>100	>100	>100
39	>100	>100	>100
40	71.5 \pm 9.2	58.2 \pm 30.6	86.4 \pm 17.8
41	>100	>100	>100
42	>100	>100	>100
43	>100	>100	>100

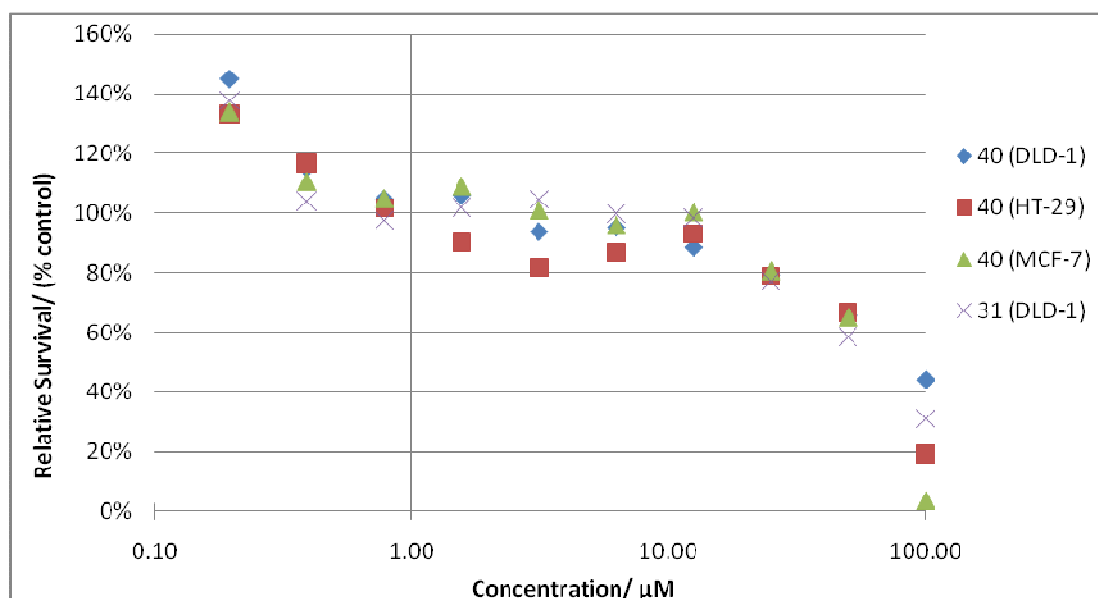
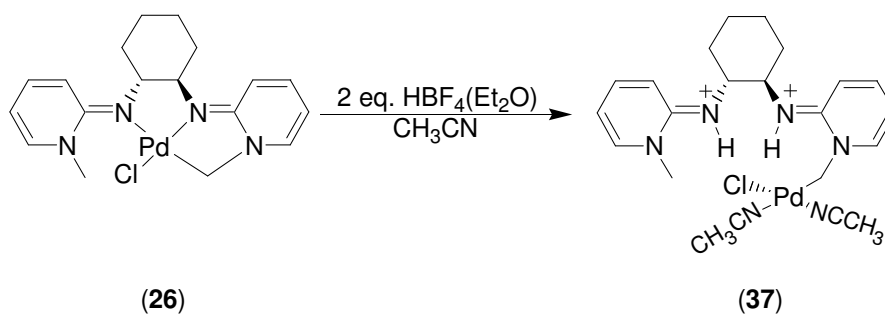


Figure 5-9. Cytotoxic activity of **31** on DLD-1 and **40** on various cell lines with a 4 days exposure.

5.4 Conclusions and future work

A series of ruthenium(II) complexes were synthesised in a straightforward method leading to two types of complexes, neutral type **38-39** and cationic type **40-42**. To the best of our knowledge, cationic ruthenium(II) complexes with chelating *N*-donor and three *S*-donor DMSO ligands have been synthesised and characterised for the first time. The contrasting speciation of the complexes formed from reaction between ligands **7** and **12** and *cis*-RuCl₂(DMSO)₄ is intriguing. One possible reason is due to a high *trans* effect caused by the strong σ donating ability of the PYE moiety, causing one chloride *trans* to coordinated nitrogen of **7** to be eliminated. In contrast, **12** can only form a typical neutral complex with *cis*-RuCl₂(DMSO)₄ because of a steric restriction caused by the aryl ring backbone. It is necessary to keep in mind that due to lack of X-ray and MS data the possibility of those ruthenium complexes described above being protonated form is not completely excluded.

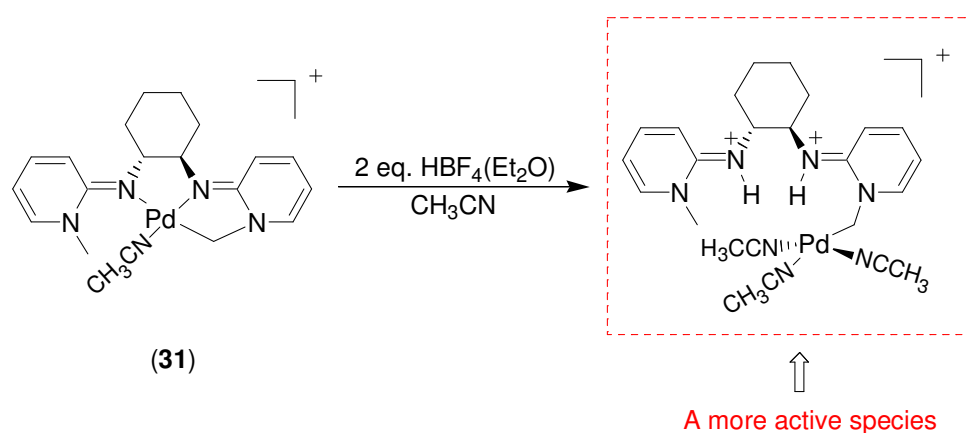
Nevertheless in cytotoxicity tests, **40** showed a better activity against cancer cell lines than other analogues, shedding light on structure/activity modification for future studies. The interesting differential response for various cell lines observed from palladacycle **31** suggests the effect of pH with respect to controlling and delivery of anticancer agents should be studied.



Scheme 5-5. Ring open of palladacycle **26** via protonation.

As described in section 4.4, the palladacycle ring of PYE palladacycle **26** can be opened in the presence of acid to give a new palladium species **37** (Scheme 5-5). Similarly, primary test has shown the palladacycle ring of acetonitrile adduct **31** can be also opened under low pH condition to provide a potentially more active species with two more binding

sites (similar function as hydrolysis process in anticancer mechanism of *cis*-platin) (Scheme 5-6). Two possible advantages for anticancer application of **31** are proposed below. First, as low extracellular pH is a unique character of the tumor microenvironment,⁶¹ the concentration of the more active species near tumor cells is higher than that near normal cells. Second, unlike some really active anticancer agents which lose their activity within the pathway to tumor cells, palladacycle **31** as a relatively stable prodrug could tolerate the general environment, before arriving at the target and then convert to the more active species.



Scheme 5-6. Formation of a proposed more active species from **31** under acidic condition.

5.5 References

1. B. Rosenberg, L. Vancamp and T. Krigas, *Nature*, 1965, **205**, 698.
2. Y. Jung and S. J. Lippard, *Chem. Rev.*, 2007, **107**, 1387-1407.
3. R. B. Weiss and M. C. Christian, *Drugs*, 1993, **46**, 360.
4. D. Lebwahl and R. Canetta, *Eur. J. Cancer*, 1998, **34**, 1522.
5. M. A. Fuertes, C. Alonso and J. M. Perez, *Chem. Rev.*, 2003, **103**, 645.
6. S. P. Fricker, *Dalton Trans.*, 2007, 4903.
7. O. R. Allen, L. Croll, A. L. Gott, R. J. Knox and P. C. McGowan, *Organometallics*, 2004, **23**, 288.
8. Y. K. Yan, M. Melchart, A. Habtemariam and P. J. Sadler, *Chem. Commun.*, 2005, 4764-4776.
9. C. G. Hartinger, S. Zorbas-Seifried, M. A. Jakupec, B. Kynast, H. Zorbas and B. K. Keppler, *J. Inorg. Biochem.*, 2006, **100**, 891-904.
10. E. Alessio, G. Mestroni, A. Bergamo and G. Sava, *Met. Ions Biol. Syst.*, 2004, **42**, 323-351.
11. C. Scolaro, A. Bergamo, L. Brescacin, R. Delfino, M. Cocchietto, G. Laurency, T. J. Geldbach, G. Sava and P. J. Dyson, *J. Med. Chem.*, 2005, **48**, 4161-4171.
12. J. E. Reed, A. A. Arnal, S. Neidle and R. Vilar, *J. Am. Chem. Soc.*, 2006, **128**, 5992-5993.
13. I. M. Dixon, F. Lopez, A. M. Tejera, J. P. Esteve, M. A. Blasco, G. Pratviel and B. Meunier, *J. Am. Chem. Soc.*, 2007, **129**, 1502-1503.
14. K. S. M. Smalley, R. Contractor, N. K. Haass, A. N. Kulp, G. E. Atilla-Gokcumen, D. S. Williams, H. Bregman, K. T. Flaherty, M. S. Soengas and E. Meggers, *Cancer Res.*, 2007, **67**, 209-217.
15. S. Urig, K. Fritz-Wolf, R. Reau, C. Herold-Mende, K. Toth, E. Davioud-Charvet and K. Becker, *Angew. Chem. Int. Ed.*, 2006, **45**, 1881-1886.
16. M. J. Clarke, *Coord. Chem. Rev.*, 2002, **232**, 69-93.
17. M. J. Clarke, *Met. Ions Biol. Syst.*, 1980, **11**, 231.
18. P. J. Dyson and G. Sava, *Dalton Trans.*, 2006, 1929-1933.
19. J. M. Rademaker-Lakhai, D. Bongard Van den, D. Pluim, J. H. Beijnen and J. H. Schellens, *Clin. Cancer Res.*, 2004, **10**, 3717-3727.

20. J. Dupont, C. S. Consorti and J. Spencer, *Chem. Rev.*, 2005, **105**, 2527-2571.
21. J. Spencer, R. P. Rathnam, M. Motukuri, A. K. Kotha, S. C. W. Richardson, A. Hazrati, J. A. Hartley, L. Male and M. B. Hursthouse, *Dalton Trans.*, 2009, 4299-4303.
22. J. D. Higgins III, L. Neely and S. Fricker, *J. Inorg. Biochem.*, 1993, **49**, 149.
23. A. C. F. Caires, E. T. Almeida, A. E. Mauro, J. P. Hemerly and S. R. Valentini, *Quim. Nova.*, 1999, **22**, 329.
24. E. G. Rodrigues, L. S. Silva, D. M. Fausto, M. S. Hayashi, S. Dreher, D. L. Santos, J. B. Pesquero, L. R. Travassos and A. C. F. Caires, *Int. J. Cancer*, 2003, **107**, 498.
25. C. Navarro-Ranninger, I. Lopez-Solera, J. M. Perez, J. Rodriguez, J. L. Garcia-Ruano, P. R. Raithby, J. R. Masaguer and C. Alonso, *J. Med. Chem.*, 1993, **36**, 3795.
26. X. Riera, A. Caubet, C. Lopez and V. Moreno, *Polyhedron*, 1999, **18**, 2549.
27. L. Tusek-Bozic, M. Komac, M. Curic, A. Lycka, V. M. D'Alpaos Scarcia and A. Furlani, *Polyhedron*, 2000, **19**, 937.
28. F. Zamora, V. M. Gonzalez, J. M. Perez, J. R. Masaguer, C. Alonso and C. Navarro-Ranninger, *Appl. Organomet. Chem.*, 1997, **11**, 659.
29. A. G. Quiroga, J. M. Perez, I. Lopez-Solera, J. R. Masaguer, A. Luque, P. Roman, A. Edwards, C. Alonso and C. Navarro-Ranninger, *J. Med. Chem.*, 1998, **41**, 1399.
30. A. G. Quiroga, J. M. Perez, E. I. Montero, D. X. West, C. Alonso and C. Navarro-Ranninger, *J. Inorg. Biochem.*, 1999, **75**, 293.
31. C. Bincoletto, I. L. S. Tersariol, C. R. Oliveria, S. Dreher, D. M. Fausto, M. A. Soufen, F. D. Nascimento and A. C. F. Caires, *Bioorg. Med. Chem.*, 2005, **13**, 3047-3055.
32. S. Guar, *Asian J. Chem.*, 2003, **15**, 250.
33. I. P. Evans, A. Spencer and J. Wilkinson, *J. Chem. Soc., Dalton Trans.*, 1973, **2**, 204-209.
34. E. Alessio, *Chem. Rev.*, 2004, **104**, 4203-4242.
35. G. Sava, S. Pacor, F. Bregant, V. Ceschia, E. Luxich, E. Alessio and G. Mestroni, *Pharmacol. (Life Sci. Adv.)*, 1990, **9**, 79-84.
36. V. Mahalingam, N. Chitrapriya, F. R. Fronczek and K. Natarajan, *Polyhedron*, 2008, **27**, 1917-1924.

37. V. Mahalingam, N. Chitrapriya, F. R. Fronczek and K. Natarajan, *Polyhedron*, 2008, **27**, 2743-2750.
38. C. Sens, M. Rodriguez, I. Romero, A. Llobet, T. Parella, B. P. Sullivan and J. Benet-Buchholz, *J. Inorg. Chem.*, 2003, **42**, 2040.
39. M. Toyama, R. Suganoya, D. Tsuduura and N. Nagao, *Bull. Chem. Soc. Jpn.*, 2007, **80**, 922-936.
40. E. Alessio, M. Calligaris, M. Iwamoto and L. G. Marzilli, *Inorg. Chem.*, 1996, **35**, 2538-2545.
41. M. M. Taqui Khan, N. H. Khan, R. I. Kureshy and K. Venkatasubramanian, *Polyhedron*, 1992, **11**, 431-441.
42. T. Toyama, K. Inoue, S. Iwamatsu and N. Nagao, *Bull. Chem. Soc. Jpn.*, 2006, **79**, 1525-1534.
43. M. Henn, E. Alessio, G. Mestroni, M. Calligaris and W. M. Attia, *Inorg. Chim. Acta.*, 1991, **187**, 39.
44. C. van der Drift, J. W. Sprengers, E. Bouwman, W. P. Mul, H. Kooijman, A. L. Spek and E. Drent, *Eur. J. Inorg. Chem*, 2002, 2147.
45. T. S. Akasheh, D. Marji and Z. M. Al-Ahmed, *Inorg. Chim. Acta.*, 1988, **141**, 125.
46. A. M. Saleem, H. A. Samha, H. A. Hodali and A. M. Seyam, *Synth. React. Inorg. Met.-Org. Chem.*, 1992, **22**, 805.
47. D. Ooyama, Y. Miura, Y. Kanazawa, F. S. Howell, N. Nagao, M. Mukaida, H. Nagao and K. Tanaka, *Inorg. Chim. Acta.*, 1995, **237**, 47.
48. S. M. Zakeeruddin, M. K. Nazeeruddin, R. Humphry-Baker and M. Gratzel, *Inorg. Chem.*, 1998, **37**, 5251.
49. W. Paw, W. B. Connick and R. Eisenberg, *Inorg. Chem.*, 1998, **37**, 3919.
50. T. Koizumi, T. Tomon and K. Tanaka, *Bull. Chem. Soc. Jpn.*, 2003, **76**, 1969.
51. W. F. Schmid, S. Zorbas-Seifried, R. O. John, V. B. Arion, M. A. Jakupec, A. Roller, M. Galanski, I. Chiorescu, H. Zorbas and B. K. Keppler, *Inorg. Chem.*, 2007, **46**, 3645.
52. T. Suzuki, T. Kuchiyama, S. Kishi, S. Kaizaki, H. D. Takagi and M. Kato, *Inorg. Chem.*, 2003, **42**, 785.

53. M. B. Cingi, M. Lanfranchi, M. A. Pellinghelli and M. Tegoni, *Eur. J. Inorg. Chem.*, 2000, 703.
54. J. L. Burmeister and N. J. De Stefano, *Inorg. Chem.*, 1969, **8**, 1546.
55. W. J. Geary, *Coord. Chem. Rev.*, 1971, **7**, 81-122.
56. R. Barbucci, G. Cialdi, G. Ponticelli and P. Paoletti, *J. Chem. Soc. A.*, 1969, 1775.
57. J. J. Rack and H. B. Gray, *Inorg. Chem.*, 1999, **38**, 2.
58. F. Wang, A. Habtemariam, E. P. L. van der Geer, R. Fernandez, M. Melchart, R. J. Deeth, R. Aird, S. Guichard, F. P. A. Fabbiani, P. Lozano-Casal, I. D. H. Oswald, D. I. Jodrell, S. Parsons and P. J. Sadler, *Proc. Natl Acad. Sci. USA*, 2005, **102**, 18269-18274.
59. T. Mosmann, *J. Immunol. Methods*, 1983, **65**, 55-63.
60. Y. Mizumura, Y. Matsumura, T. Hamaguchi, N. Nishiyama, K. Kataoka, T. Kawaguchi, W. J. M. Hrushesky, F. Moriyasu and T. Kakizoe, *Jpn. J. Cancer Res.*, 2001, **92**, 328-336.
61. S. L. Chi and S. V. Pizzo, *Cancer Res.*, 2006, **66**, 875.

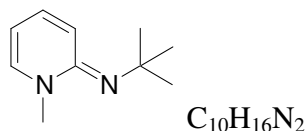
6.0 Experimental

6.1 General Procedures

Dioxygen and water sensitive reactions and manipulations were performed using Schlenk techniques under an argon atmosphere. All solvents were distilled under dinitrogen from a drying agent prior to use: calcium hydride (DCM and CH₃CN) or sodium benzophenone ketyl (diethyl ether, petroleum ether (40-60 °C), pentane, hexane, toluene and THF). All reagents were used as supplied (Aldrich or Alfa Aesar) except K₂CO₃, which was heated to 120 °C for at least 24 h prior to use. PdCl₂(NCMe)₂,¹ PdCl₂(COD),² N-benzyl-2-chloro pyridinium bromide,³ tetramethyldiamine,⁴ [RhCl(CO)₂]₂,⁵ and PdMe₂(pyd)⁶ were prepared using literatures procedure. NMR spectra were recorded at probe temperature on Joel JNM-EX 270, Joel ECX 400, Bruker AMX 400 or Bruker AMX 500 spectrometers. Chemical shifts are described in parts per million downfield shift from SiMe₄ and are reported consecutively as position (δ H or δ C), multiplicity (s = singlet, d = doublet, t = triplet, q = quartet, m = multiplet, dd = doublet of doublet, br = broad), coupling constant (*J*/Hz), relative integral and assignment. ¹H NMR spectra were referenced internally to the residual protio solvent resonances of CDCl₃ (δ 7.26), D₂O (δ 4.79), C₆D₆ (δ 7.16), CD₂Cl₂ (δ 5.33), CD₃CN (δ 1.94), CD₃OD (δ 3.31, 4.78), CD₅CD₃ (δ 2.09, 6.98, 7.00, 7.09), (CD₃)₂SO (δ 2.50). ¹³C{¹H} NMR PENDANT spectra were referenced to CDCl₃ (δ 77.0), C₆D₆ (δ 128.0), CD₂Cl₂ (δ 54.0), CD₃CN (δ 1.3, 118.3), CD₃OD (δ 49.2), CD₅CD₃ (δ 20.4, 125.5, 128.3, 129.2, 137.9), (CD₃)₂SO (δ 39.5). ¹H-¹H COSY, NoeSY, and ¹³C HSQC experiments were performed using standard Bruker pulse sequences. Fast Atom Bombardment (FAB+) mass spectra were recorded on a Micromass Autospec, using 3-nitrobenzyl alcohol as the matrix. Mass spectra were recorded on a Bruker Esquire 6000 ESI spectrometer and a Bruker microTOF instrument. Electrospray (ES) mass spectra were recorded by using methanol or acetonitrile as the mobile phase. Masses were analysed by Time Of Flight, (TOF). Elemental analyses were performed at the London Metropolitan University. Melting points are uncorrected. Electrical conductivity was recorded on a JENWAY Model 4310 Conductivity Meter.

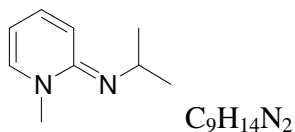
6.2 Compounds and complexes preparation and characterisation data

tert-Butyl-[1-methyl-1*H*-pyridin-(2*E*)-ylidene]-amine (^{Me}N^{tBu}) (1)



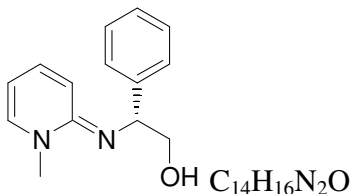
To an ampoule containing 2 - chloro-1-methyl-pyridinium iodide (7.83 mmol, 2.00 g), potassium carbonate (23.50 mol, 3.25 g) and acetonitrile (25 mL) was added tert-butylamine (8.65 mmol, 1 mL) and the mixture stirred for 4 h at 80 °C. After cooling to room temperature, the volatiles were removed under reduced pressure to give a yellow creamy solid that was washed with toluene (25 mL) and isolated by filtration. The solid was then dissolved in aqueous NaOH (5 M, 40 mL), extracted with toluene (3 x 20 mL) and dried over MgSO₄. On filtration, the volatiles of the filtrate were removed under reduced pressure to give **1** as yellow oil that can be distilled at 80 °C at 1 Torr (yield = 1.03 g, 80 %); ¹H NMR (270 MHz, CDCl₃) δ 1.27 (s, 12H, *t*Bu), 3.27 (s, 3H, NCH₃), 5.48 (m, 1H, py-*H*⁴), 6.42 (d, ³*J*_{H-H} = 10 Hz, 1H, py-*H*²), 6.73 (m, 1H, py-*H*³), 6.97 (d, ³*J*_{H-H} = 6 Hz, 1H, py-*H*⁵); ¹³C{¹H} NMR (67.9 MHz, CDCl₃) δ 30.4 (CCH₃), 39.6 (NCH₃), 51.4 (CCH₃), 99.0 (py-*C*⁴), 115.6 (py-*C*²), 133.1 (py-*C*³), 139.8 (py-*C*⁵), 150.4 (py-*C*¹); ¹H NMR (C₆D₆, 400 MHz) δ 1.48 (s, 12H, *t*Bu), 2.92 (s, 3H, NCH₃), 5.15 (m, 1H, py-*H*⁴), 6.26 (d, ³*J*_{H-H} = 7 Hz, 1H, py-*H*⁵), 6.35 (d, ³*J*_{H-H} = 10 Hz, 1H, py-*H*²), 6.45 (m, 1H, py-*H*³); ¹³C{¹H} NMR (100 MHz, C₆D₆) δ 30.2 (CCH₃), 39.0 (NCH₃), 51.1 (CCH₃), 98.1 (py-*C*⁴), 115.0 (py-*C*²), 132.7 (py-*C*³), 139.4 (py-*C*⁵), 149.6 (py-*C*¹); MS (ESI) *m/z* (%): 165.0 ([M+H]⁺, 100 %); Anal. [found(calc.)] for C₁₀H₁₆N₂: C 73.14 (73.13), H 9.76 (9.82), N 16.98 (17.06).

iso-Propyl-[1-methyl-1*H*-pyridin-(2*E*)-ylidene]-amine (^{Me}N^{iPr}) (2)



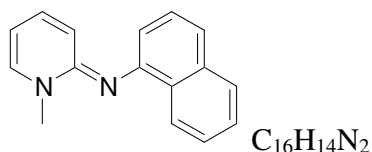
To an ampoule containing 2 - chloro-1-methyl-pyridinium iodide (7.83 mmol, 2.00 g), potassium carbonate (23.50 mol, 3.25 g) and acetonitrile (25 mL) was added isopropylamine (8.65 mmol, 0.74 mL) and the mixture stirred for 4 h at 80 °C. After cooling to room temperature, the volatiles were removed under reduced pressure to give a yellow creamy solid that was washed with toluene (25 mL) and isolated by filtration. The solid was then dissolved in aqueous NaOH (5 M, 40 mL), extracted with toluene (3 x 20 mL) and dried over MgSO₄. On filtration, the volatiles of the filtrate were removed under reduced pressure to give **2** as yellow oil that can be distilled at 80 °C at 1 Torr (yield = 0.88 g, 75 %); ¹H NMR (400 MHz, CDCl₃) δ 1.05 (d, ³J_{H-H} = 8 Hz, 6H, CH(CH₃)₂), 3.23 (s, 3H, NCH₃), 3.44 (m, 1H, CH(CH₃)₂), 5.45 (m, 1H, py-*H*⁴), 6.31 (d, ³J_{H-H} = 10 Hz, 1H, py-*H*²), 6.75 (m, 1H, py-*H*³), 6.87 (d, ³J_{H-H} = 6 Hz, 1H, py-*H*⁵); ¹³C{¹H} NMR (100 MHz, CDCl₃) δ 24.2 (CH(CH₃)₂), 39.0 (NCH₃), 46.8 (CH(CH₃)₂), 99.5 (py-*C*⁴), 112.1 (py-*C*²), 134.0 (py-*C*³), 139.0 (py-*C*⁵), 151.8 (py-*C*¹); MS (ESI) m/z (%): 151.0 ([M+H]⁺, 100 %); Anal. [found(calc.)] for C₉H₁₄N₂: C 71.99 (71.96), H 9.48 (9.39), N 18.56 (18.65).

(R)-2-(1-Methyl-1H-pyridin-(2E)-ylidene-amino]-2-phenyl-ethanol
($\text{MeN}^{\delta-}\text{CHPhCH}_2\text{OH}$) (**3**)



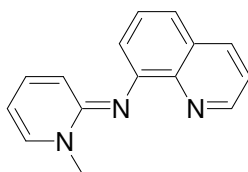
(R)-(-)-Phenylglycinol (2.68 g, 19.5 mmol) was added to an ampoule charged with 2-chloro-1-methyl-pyridinium iodide (5.0 g, 19.5 mmol), potassium carbonate (8.11 g, 58.8 mmol) in acetonitrile (25 mL) and the mixture was stirred for 12 h at 80 °C. After cooling to room temperature the volatiles were removed under reduced pressure to give a yellow creamy solid that was extracted with toluene (3×20 mL) and the filtrate was dried over MgSO_4 . The volatiles were removed under reduced pressure to give **3** as a waxy yellow solid (yield = 3.95 g, 89 %). ^1H NMR (400 MHz, CDCl_3) δ 3.49 (s, 3H, NCH_3), 3.60 (t, $^3J_{\text{H-H}} = 8$ Hz, 1H, NCH), 3.75 (m, 1H, CH_2OH), 4.36 (m, 1H, CH_2OH), 5.66 (m, 1H, py-H^4), 6.14 (d, $^3J_{\text{H-H}} = 8$ Hz, 1H, py-H^2), 6.79 (m, 1H, py-H^3), 7.05 (d, $^3J_{\text{H-H}} = 6$ Hz, 1H, py-H^5), 7.26 (m, 5H, PhCH); $^{13}\text{C}\{^1\text{H}\}$ NMR (100 MHz, CDCl_3) δ 39.7 (NCH_3), 62.0 (NCH), 68.8 (CH_2OH), 101.6 (py-C^4), 113.6 (py-C^2), 126.7 (PhCH), 127.0 (PhCH), 128.2 (PhCH), 135.3 (py-C^3), 138.9 (py-C^5), 142.8 (PhC_{ipso}), 155.2 (py-C^1); MS (ESI) m/z (%): 229.1 ($[\text{M}+\text{H}]^+$, 100%); Anal. [found(calc.)] for $\text{C}_{14}\text{H}_{16}\text{N}_2\text{O}$: C 73.63 (73.66), H 7.12 (7.06), N 12.17 (12.27).

1-Naphthyl-[1-methyl-1*H*-pyridin-(2*E*)-ylidene]-amine (^{Me}N^{Naph}) (4**)**



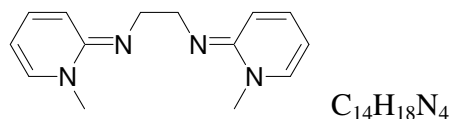
1-Naphthylamine (5.60 g, 39.2 mmol) was added to an ampoule charged with 2-chloro-1-methyl-pyridinium iodide (10.0 g, 39.2 mmol), triethylamine (11 mL, 79.1 mmol) in acetonitrile (25 mL) and the mixture was stirred for 19 h at 80 °C. The volatiles were removed under reduced pressure and the solid extracted with DCM (80 mL), filtered and the filtrate added into aqueous sodium hydroxide (50 mL, 5 M). Organic phase was extracted with DCM (50 mL × 3) and the volatiles were removed under reduced pressure to give **4** as a yellow solid (yield = 7.3 g, 80 %). ¹H NMR (400 MHz, CDCl₃) δ 3.68 (s, 3H, NCH₃), 5.76 (m, 1H, py-*H*⁴), 6.20 (d, ³*J*_{H-H} = 10 Hz, 1H, py-*H*²), 6.79 (m, 1H, py-*H*³), 6.93 (d, ³*J*_{H-H} = 7 Hz, 1H, CH_{naphthyl}), 7.12 (d, ³*J*_{H-H} = 7 Hz, 1H, py-*H*⁵), 7.35-7.51 (m, 4H, CH_{naphthyl}), 7.81 (d, ³*J*_{H-H} = 8 Hz, 1H, CH_{naphthyl}), 8.05 (d, ³*J*_{H-H} = 8 Hz, 1H, CH_{naphthyl}); ¹³C{¹H} NMR (100 MHz, CDCl₃) δ 40.2 (NCH₃), 103.4 (py-*C*⁴), 114.3 (py-*C*²), 116.9, 121.8, 123.7, 124.7, 125.7, 126.4, 127.8, 128.7, 134.7, 135.7 (py-*C*³), 138.8 (py-*C*⁵), 146.7, 153.0 (py-*C*¹); MS (ESI) *m/z* (%): 235.0 ([M+H]⁺, 100%); Anal. [found(calc.)] for C₁₆H₁₄N₂: C 81.97 (82.02), H 6.01 (6.02), N 11.89 (11.96).

8-Quinoliny[1-methyl-1*H*-pyridin-(2*E*)-ylidene]-amine (^{Me}N^{Quin}) (5**)**



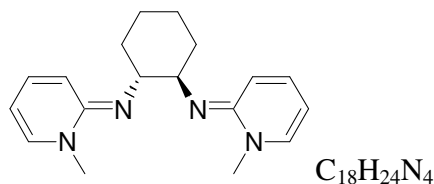
By using an analogues procedure to **4**, 8-aminoquinoline (2.0 g, 13.9 mmol) was added to an ampoule charged with 2-chloro-1-methyl-pyridinium iodide (3.54 g, 13.9 mmol), triethylamine (3.90 mL, 27.8 mmol) in acetonitrile (25 mL) and the mixture was stirred for 20 h at 80 °C to give **5** as a dark brown solid (yield = 3.26 g, 92 %). ¹H NMR (CDCl₃, 400 MHz) δ 3.78 (s, 3H, NCH₃), 5.94 (m, 1H, py-*H*⁴), 6.20 (d, ³J_{H-H} = 9 Hz, 1H, py-*H*²), 6.87 (m, 1H, py-*H*³), 7.26-7.32 (m, 3H, py-*H*⁵ + 2CH_{quinoliny}), 7.41 (m, 2H, CH_{quinoliny}), 8.04 (m, 1H, CH_{quinoliny}), 8.73 (m, 1H, CH_{quinoliny}); ¹³C{¹H} NMR (100 MHz, CDCl₃) δ 41.1 (NCH₃), 105.5 (py-*C*⁴), 115.1 (py-*C*²), 121.0, 121.6, 122.1, 127.2, 129.6, 136.3 (py-*C*³), 136.4, 139.2 (py-*C*⁵), 142.7, 145.6, 149.0, 153.4 (py-*C*¹); MS (ESI) m/z (%): 236.0 ([M+H]⁺, 100%); Anal. [found(calc.)] for C₁₅H₁₃N₃: C 76.59 (76.57), H 5.56 (5.57), N 17.71 (17.86).

***N,N'*-bis-[1-methyl-1*H*-pyridin-(2*E*)-ylidene]-ethane-1,2-diamine**
[^{Me}N(CH₂)₂N^{Me}] (**6**)



To an ampoule containing anhydrous potassium carbonate (6.9 g, 0.05 mol), 2-chloro-1-methyl pyridinium iodide (4.43 g, 0.017 mol) and acetonitrile (20 mL) was quickly added ethylene diamine (0.55 mL, 8.25 mmol) with stirring and the mixture heated at 80 °C with stirring for 16 hr. The volatiles were removed under reduced pressure and toluene (60 mL) and aqueous sodium hydroxide (90 mL, 0.475 mol) were added. Filtered and the filtrate left to stand at room temperature for 2 hr giving a yellow crystalline precipitate. The crystals were collected and dried under reduced pressure to give **6** as yellow microcrystals. Yield = 1.05 g, 50 %. ¹H (270 MHz, CDCl₃) δ 3.34 (s, 6H, NCH₃), 3.46 (s, 4H, CH₂), 5.65 (m, 2H, py-*H*⁴), 6.57 (d, ³J_{H-H} = 9 Hz, 2H, py-*H*²), 6.88 (m, 2H, py-*H*³), 7.03 (d, ³J_{H-H} = 5 Hz, 2H, py-*H*⁵); ¹³C{¹H} (67.9 MHz, CDCl₃) 39.9 (NCH₃), 48.9 (CH₂), 101.6 (py-*C*⁴), 112.6 (py-*C*²), 135.0 (py-*C*³), 139.0 (py-*C*⁵), 154.0 (py-*C*¹); MS (ESI) *m/z* (%): 243.1 ([M+H]⁺, 100 %); IR (KBr): 1641 s, 1569 s, 1535 s; Anal. [found(calc.)] for C₁₄H₁₈N₄: C 69.39 (69.28), H 7.49 (7.36), N 23.12 (22.93).

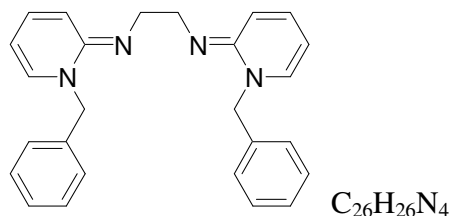
(1R,2R)-*N,N'*-bis-[1-methyl-1*H*-pyridin-(2*E*)-ylidene]-cyclohexane-1,2-diamine
[^{Me}N^{C6H10}N^{Me}] (**7**)



To an ampoule containing (1R, 2R)-cyclohexane-1,2-diammonium 2,3-dihydroxy succinate (2 g, 7.57 mmol), anhydrous potassium carbonate (6.28 g, 0.045 mol) and acetonitrile (30 mL), was added 2-chloro-1-methyl pyridinium iodide (4.06 g, 15.9 mmol) and the mixture heated at 80 °C with stirring for 40 hr. After cooling to 25 °C, the mixture was filtered and the filtrate was added aqueous sodium hydroxide (90 mL, 5 M). Organic phase was extracted with acetonitrile (50 mL × 3) and the volatiles were removed under reduced pressure. Recrystallize in acetone and diethyl ether at -30 °C. Crystals were collected to give **7** as a yellow solid. Yield = 1.12 g, 50 %. Mpt. 144 - 145 °C. ¹H NMR (400 MHz, CDCl₃) δ 1.29-1.49 (m, 4H, *c*-hex-CH₂), 1.66-1.68 (m, 4H, *c*-hex-CH₂), 3.08 (s, 6H, NCH₃), 3.24 (m, 2H, *c*-hex-CH), 5.31 (m, 2H, py-H⁴), 6.58 (m, 4H, py-H² and H³), 6.72 (d, ³J_{H-H} = 8.0 Hz, 2H, py-H⁵); ¹³C{¹H} NMR (100 MHz, CDCl₃) δ 25.3 (*c*-hex-CH₂), 33.8 (*c*-hex-CH₂), 39.5 (NCH₃), 61.8 (*c*-hex-CH), 99.5 (py-C⁴), 114.1 (py-C²), 132.7 (py-C³), 138.6 (py-C⁵), 152.3 (py-C¹); MS(CI⁺) *m/z*: 298.0 ([M+2H]⁺, 25 %), 297 (100, [M+H]⁺); Anal. [found(calc.)] for C₁₈H₂₄N₄: C 73.04 (72.94), H 8.19 (8.16), N 18.82 (18.90).

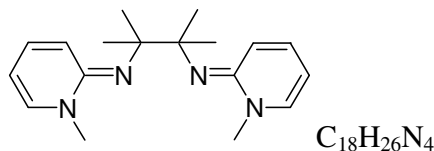
***N,N'*-bis-[1-benzyl-1*H*-pyridin-(2*E*)-ylidene]-ethane-1,2-diamine**

[^{Bn}N(CH₂)₂N^{Bn}] (8)



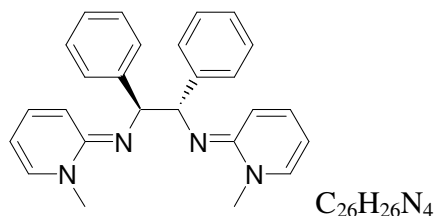
To an ampoule containing anhydrous potassium carbonate (0.41 g, 3 mmol), *N*-benzyl-2-chloro pyridinium bromide (0.3 g, 1.05 mmol) and acetonitrile (15 mL) was added ethylene diamine (0.033 mL, 0.5 mmol) with stirring and the mixture heated at 80 °C with stirring for 16 hr. The volatiles were removed under reduced pressure and toluene (20 mL) and aqueous sodium hydroxide (30 mL, 5 M) were added. The toluene phase was separated and the aqueous phase was washed with toluene (2 x 10 mL). The collected toluene extracts were concentrated to ca. 15 mL until a yellow precipitate began to form and diethyl ether (3 mL) added and the mixture cooled at -30 °C to give a yellow crystalline precipitate. The crystals were collected by filtration and dried under reduced pressure to give **8** as yellow microcrystals. Yield = 0.16 g, 81 %. Mpt. 127 - 131 °C. ¹H NMR (400 MHz, CDCl₃) δ 3.34 (s, 4H, CH₂CH₂), 4.98 (s, 4H, PhCH₂), 5.46 (m, 2H, py-*H*⁴), 6.45 (d, ³J_{H-H} = 8 Hz, 2H, py-*H*²), 6.70 (m, 2H, py-*H*³), 6.80 (d, ³J_{H-H} = 8 Hz, 2H, py-*H*⁵), 7.15-7.28 (m, 10H, C₆H₅); ¹³C{¹H} NMR (125 MHz, CDCl₃) δ 49.9 (CH₂CH₂), 52.4 (PhCH₂), 101.1 (py-*C*⁴), 113.6 (py-*C*²), 127.5 (C₆H₅), 128.5 (C₆H₅), 128.7 (C₆H₅), 134.3(py-*C*³), 137.6 (C₆H₅), 137.9 (py-*C*⁵), 153.3 (py-*C*¹); MS(TOF ES⁺) *m/z*: 396.2 ([M+2H]⁺, 25 %), 395.1 (100, [M+H]⁺); Anal. [found(calc.)] for C₂₆H₂₆N₄: C 79.16 (79.18), H 6.64 (6.75), N 14.20 (14.14).

2,3-bimethyl-*N,N'*-bis-[1-methyl-1*H*-pyridin-(2*E*)-ylidene]-butane-2,3-diamine
[$\text{MeN}^{\text{(C(Me)2)2N}^{\text{Me}}]$ (**9**)



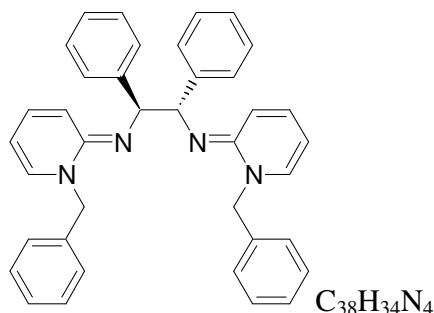
To an ampoule containing acetonitrile (80 mL) activated 5Å sieves (2 g), tetramethyldiamine (826 mg, 7.11 mmol) and 2-chloro-1-methyl pyridinium iodide (3.814 g, 14.93 mmol), was added triethylamine (3.60 g, 35.55 mmol) and the mixture stirred at 80 °C for 12 hr. The volatiles were removed under reduced pressure and the solid extracted with DCM (80 mL), filtered and the filtrate added into aqueous sodium hydroxide (50 mL, 5 M). Organic phase was extracted with DCM (50 mL × 3) and the volatiles were removed under reduced pressure. Recrystallize in acetone and diethyl ether at -30 °C give **9** as yellow microcrystals. Yield = 1.45 g, 66 %. ^1H NMR (400 MHz, CDCl_3) δ 1.23 (s, 12H, CCH_3), 3.20 (s, 6H, NCH_3), 5.35 (m, 2H, py-H^4), 6.42 (d, $^3J_{\text{H-H}} = 9$ Hz, 2H, py-H^2), 6.64 (m, 2H, py-H^3), 6.91 (d, $^3J_{\text{H-H}} = 6$ Hz, 2H, py-H^5); $^{13}\text{C}\{^1\text{H}\}$ NMR (100 MHz, CDCl_3) δ 20.9 (CCH_3), 42.0 (CCH_3), 62.1 (NCH_3), 107.4 (py-C^4), 113.7 (py-C^2), 139.1 (py-C^3), 142.4 (py-C^5), 153.0 (py-C^1); MS(TOF ES^+) m/z 299.2 ($[\text{M}+\text{H}]^+$, 40 %); Anal. [found(calc.)] for $\text{C}_{18}\text{H}_{26}\text{N}_4$: C 72.47 (72.44), H 8.69 (8.78), N 18.90 (18.77).

(1*S*,2*S*)-*N,N'*-Bis-[1-methyl-1*H*-pyridin-(2*E*)-ylidene]-1,2-diphenylethane-1,2-diamine
[^{Me}N^{(CHPh)₂N^{Me}] (10)}



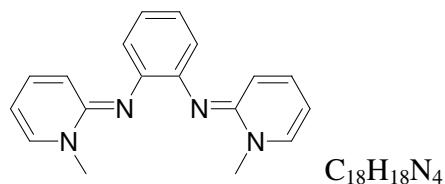
To an ampoule containing acetonitrile (40 mL) activated 5Å sieves (1 g), (1*S*,2*S*)-1,2-diphenylethane-1,2-diamine (500 mg, 2.36 mmol) and *N*-benzyl-2-chloro pyridinium bromide (1.264 g, 4.95 mmol), was added triethylamine (1.19g, 11.80 mmol) and the mixture stirred at 80 °C for 12 hr. The volatiles were removed under reduced pressure and the solid extracted with DCM (50 mL), filtered and the filtrate added into aqueous sodium hydroxide (50 mL, 5 M). The DCM phase was separated and dried over MgSO₄, filtered and removal of the volatiles gave **10** as a yellow solid. Yield = 0.75 g, 81 %. Mpt. 99 - 100 °C. ¹H NMR (270 MHz, CDCl₃) δ 3.26 (s, 6H, NCH₃), 4.57 (s, 2H, PhCH), 5.40 (t, ³J_{H-H} = 5 Hz, 2H, py-*H*⁴), 6.45 (d, ³J_{H-H} = 8 Hz, 2H, py-*H*²), 6.62 (m, 2H, py-*H*³), 6.85 (d, ³J_{H-H} = 5 Hz, 2H, py-*H*⁵), 6.90 - 7.10 (m, 10H, C₆H₅); ¹³C{¹H} NMR (100 MHz, CDCl₃) δ 35.1 (NCH₃), 65.0 (PhCH), 95.2 (py-*C*⁴), 109.5 (py-*C*²), 121.3 (C₆H₅), 122.5 (C₆H₅), 124.5 (C₆H₅), 128.9 (py-*C*³), 134.4(C₆H₅), 140.0 (py-*C*⁵), 148.1 (py-*C*¹); MS(TOF ES⁺) *m/z* 396.2 ([M+2H]⁺, 25%), 395.2 (100, [M+H]⁺); Anal. [found(calc.)] for C₂₆H₂₆N₄: C 79.03 (79.16), H 6.63 (6.64), N 14.03 (14.20).

(1*S*,2*S*)-*N,N'*-Bis-[1-benzyl-1*H*-pyridin-(2*E*)-ylidene]-1,2-diphenyl-ethane-1,2-diamine
[^{Bn}N^(CHPh)2^NBn] (11)



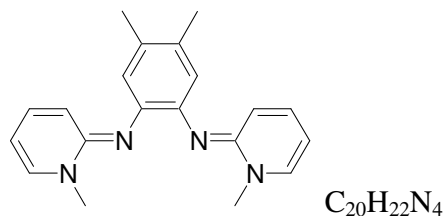
To an ampoule containing acetonitrile (40 mL) activated 5Å sieves (1 g), (1*S*,2*S*)-1,2-diphenylethane-1,2-diamine (533 mg, 2.51 mmol) and *N*-benzyl-2-chloro pyridinium bromide (1.5 g, 5.27 mmol), was added triethylamine (1.27 g, 12.55 mmol) and the mixture stirred at 80 °C for 12 hr. The volatiles were removed under reduced pressure and the solid extracted with DCM (50 mL), filtered and the filtrate added into aqueous sodium hydroxide (50 mL, 5 M). The DCM phase was separated and dried over MgSO₄, filtered and removal of the volatiles gave **11** as a yellow solid. Yield = 0.96 g, 70%. Mpt. 46 - 49 °C. ¹H NMR (270 MHz, CDCl₃) δ 4.47 (s, 2H, PhCH), 4.90 (d, ²J_{H-H} = 13 Hz, 2H, PhCH₂), 5.12 (d, ²J_{H-H} = 13 Hz, 2H, PhCH₂), 5.40 (m, 2H, py-*H*⁴), 6.40 (d, ³J_{H-H} = 8 Hz, 2H, py-*H*²), 6.60 (m, 2H, py-*H*³), 6.80-7.30 (m, 22H, C₆H₅ + py-*H*⁵); ¹³C{¹H} NMR (100 MHz, CDCl₃) δ 52.4 (PhCH₂), 69.5 (PhCH), 100.1 (py-*C*⁴), 114.3 (py-*C*²), 125.6 (C₆H₅), 126.8 (C₆H₅), 126.9 (C₆H₅), 127.9 (C₆H₅), 128.3(C₆H₅), 128.6(C₆H₅), 133.4(py-*C*³), 138.0(C₆H₅), 138.4 (C₆H₅), 144.1(py-*C*⁵), 151.5 (py-*C*¹); MS(TOF ES⁺) *m/z* 548.2 ([M+2H]⁺, 40%), 547.2 (100, [M+H]⁺); Anal. [found(calc.)] for C₃₈H₃₄N₄: C 83.36 (83.48), H 6.36 (6.27), N 10.22 (10.25).

***N,N'*-bis-[1-methyl-1*H*-pyridin-(2*E*)-ylidene]-phenyl-1,2-diamine**
[MeN^(C₆H₄)N^{Me}] (**12**)



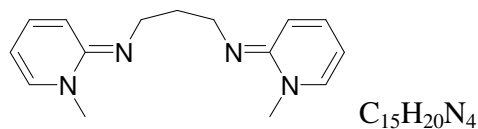
To an ampoule containing anhydrous potassium carbonate (10 g, 0.072 mol), 2-chloro-1-methyl pyridinium iodide (9.45 g, 0.037 mol) and acetonitrile (40 mL) was quickly added 1,2-phenyl diamine (2.0 g, 18.5 mmol) with stirring and the mixture heated at 80 °C with stirring for 16 hr. Filtered and the volatiles were removed under reduced pressure give **12** as a brown solid. Yield = 4.98 g, 93 %. 1H NMR (400 MHz, $CDCl_3$) δ 3.28 (s, 6H, NCH_3), 5.69 (m, 2H, py- H^4), 6.20 (d, $^3J_{H-H} = 9.2$ Hz, 2H, py- H^2), 6.88 (m, 2H, py- H^3), 6.94 (m, 6H, py- H^5 + C_6H_4); $^{13}C\{^1H\}$ NMR (100 MHz, $CDCl_3$) δ 39.5 (NCH_3), 102.4 (py- C^4), 116.2 (py- C^2), 122.5 (aryl-CH), 123.6 (aryl-CH), 133.8 (py- C^3), 137.8 (py- C^5), 142.0 (aryl-CN), 151.8 (py- C^1); MS (TOF EI^+) m/z : 291 ($[M+H]^+$, 20 %), 290 (100, $[M]^+$); Anal. [found(calc.)] for $C_{18}H_{18}N_4$: C 74.50 (74.46), H 6.17 (6.25), N 19.27 (19.30).

***N,N'*-bis-[1-methyl-1*H*-pyridin-(2*E*)-ylidene]-4,5-dimethyl-phenyl-1,2-diamine**
[$\text{MeN}^{(\text{C}_6\text{H}_2\text{Me}_2)\text{N}^{\text{Me}}]$ (**13**)



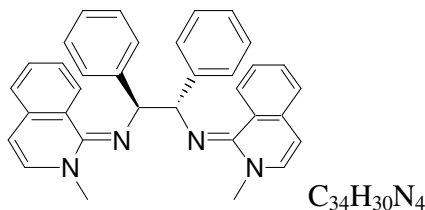
By using an analogous procedure to , 4,5-Dimethyl-1,2-phenylenediamine (2.0 g, 14.7 mmol) was added to an ampoule charged with 2-chloro-1-methyl-pyridinium iodide (7.50 g, 29.4 mmol), potassium carbonate (8.0 g, 57.9 mmol) in acetonitrile (25 mL) and the mixture was stirred for 16 h at 80 °C to give **13** as a yellow solid (yield = 4.0 g, 86 %). ^1H NMR (400 MHz, CDCl_3) δ 2.18 (s, 6H, CCH_3), 3.31 (s, 6H, NCH_3), 5.70 (m, 2H, py- H^4), 6.24 (d, $^3J_{\text{H-H}} = 9$ Hz, 2H, py- H^2), 6.73 (s, 2H, CH_{Ph}), 6.78 (m, 2H, py- H^3), 6.95 (d, 2H, $^3J_{\text{H-H}} = 6$ Hz, py- H^5); $^{13}\text{C}\{^1\text{H}\}$ NMR (100 MHz, CDCl_3) δ 19.1 (CCH_3), 39.7 (NCH_3), 102.6 (py- C^4), 116.5 (py- C^2), 125.0 (CH_{Ph}), 130.5 (CCH_3), 133.9 (py- C^3), 137.9 (py- C^5), 138.7 (aryl-CN), 151.9 (py- C^1); MS (ESI) m/z (%): 319.2 ($[\text{M}+\text{H}]^+$, 100%); Anal. [found(calc.)] for $\text{C}_{20}\text{H}_{22}\text{N}_4$: C 75.50 (75.44), H 6.91 (6.96), N 17.72 (17.60).

***N,N'*-bis-[1-methyl-1*H*-pyridin-(2*E*)-ylidene]-propane-1,2-diamine**
[MeN(CH₂)₃NMe] (**14**)

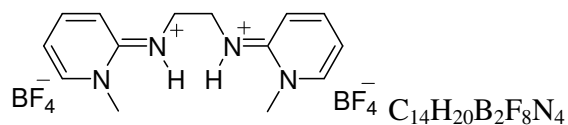


1,3-Diaminopropane (1.64 mL, 19.6 mmol) was added to an ampoule charged with 2-chloro-1-methyl-pyridinium iodide (10.0 g, 39.2 mmol), triethylamine (11 mL, 78.4 mmol) in acetonitrile (25 mL) and the mixture was stirred for 18 h at 80 °C. The volatiles were removed under reduced pressure and the solid extracted with acetonitrile (80 mL). Sodium hydride (1 g) was gradually added into the solution with vigorous stirring. Filtered and the volatiles were removed under reduced pressure to give **14** as a hygroscopic yellow solid (yield = 4.1 g, 82 %). ¹H NMR (400 MHz, CDCl₃) δ 1.85 (m, 2H, CH₂CH₂CH₂), 3.31 (t, ³J_{H-H} = 7 Hz, 4H, NCH₂), 3.34 (s, 6H, NCH₃), 5.57 (m, 2H, py-*H*⁴), 6.44 (d, ³J_{H-H} = 9 Hz, 2H, py-*H*²), 6.84 (m, 2H, py-*H*³), 6.96 (d, ³J_{H-H} = 5 Hz, 2H, py-*H*⁵); ¹³C{¹H} NMR (100 MHz, CDCl₃) δ 32.9 (CH₂CH₂CH₂), 39.4 (NCH₃), 46.4 (NCH₂), 100.2 (py-*C*⁴), 112.4 (py-*C*²), 134.4 (py-*C*³), 139.1 (py-*C*⁵), 153.7 (py-*C*¹); MS (ESI) m/z (%): 237.1 ([M+H]⁺, 100%); Anal. [found(calc.)] for C₁₅H₂₀N₄: C 70.27 (70.28), H 7.79 (7.86), N 21.82 (21.86).

(1*S*,2*S*)-*N,N'*-Bis-[1-methyl-1*H*-isoquinolin-(2*E*)-ylidene]-1,2-diphenyl-ethane-1,2-diamine
[^{Me}N_{isoquino}(^{CHPh})₂N_{isoquino}^{Me}] (**15**)

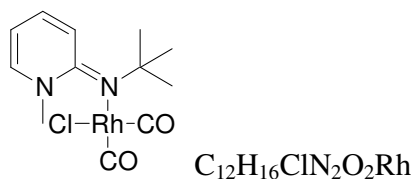


To an ampoule containing acetonitrile (20 mL) activated 5Å sieves (1 g), (1*S*,2*S*)-1,2-diphenylethane-1,2-diamine (347 mg, 1.63 mmol) and *N*-methyl-2-chloroisoquinolinium iodide (1.0 g, 3.27 mmol), was added triethylamine (1.14 mL, 8.18 mmol) and the mixture stirred at 80 °C for 12 hr. The volatiles were removed under reduced pressure and the solid extracted with DCM (50 mL), filtered and the filtrate added into aqueous sodium hydroxide (50 mL, 5 M). The DCM phase was separated and dried over MgSO₄, filtered and removal of the volatiles gave **15** as brown oil. Yield = 647 mg, 80 %. ¹H NMR (400 MHz, CDCl₃) δ 3.96 (s, 6H, NCH₃), 4.95 (d, ²J_{H-H} = 10 Hz, 2H), 5.08 (d, ²J_{H-H} = 10 Hz, 2H), 5.60 (s, 2H, PhCH), 5.96 (d, ³J_{H-H} = 8 Hz, 2H), 6.46 (d, ³J_{H-H} = 8 Hz, 2H), 6.49 (br, 2H), 7.10-7.50, 8.25 (m, 2H); MS (ESI) *m/z* (%): 495.2 ([M+H]⁺, 100%).



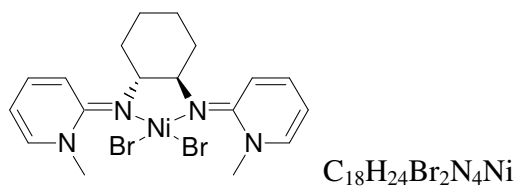
To a chloroform solution of **6** (200 mg, 0.83 mmol), was added $\text{HBF}_4 \cdot \text{Et}_2\text{O}$ (267 mg, 1.66 mmol). The suspension was stirred for 1 hr at room temperature. The volatiles were removed under reduced pressure to give **16** as a white solid. Yield = 343 mg, 99%. ^1H (400 MHz, D_2O) δ 3.60 (s, 4H, CH_2), 4.71 (s, 6H, NCH_3), 6.80 (m, 2H, py-H^4), 7.07 (d, $J = 9$ Hz, 2H, py-H^2), 7.80 (d, $J = 5$ Hz, 2H, py-H^5), 7.81 (m, 2H, py-H^3); $^{13}\text{C}\{^1\text{H}\}$ (100 MHz, D_2O) 41.1 (CH_2), 41.7 (NCH_3), 110.5 (py-C^2), 113.5 (py-C^4), 141.7 (py-C^5), 143.6 (py-C^3), 154.0 (py-C^1); MS (TOF ES^+) m/z (%): 331.2 ($[\text{M}-\text{BF}_4]^+$, 10%), 243.2 (100, $[\text{M}-2\text{BF}_4-\text{H}]^+$); Anal. [found(calc.)] for $\text{C}_{14}\text{H}_{20}\text{B}_2\text{F}_8\text{N}_4$: C 40.19 (40.23), H 4.79 (4.82), N 13.51 (13.41).

$[(^{\text{Me}}\text{N}^{\text{tBu}})\text{Rh}(\text{CO})_2\text{Cl}]$ (**17**)



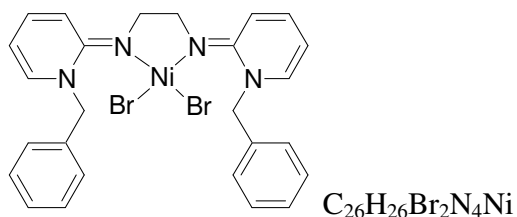
To a Schlenk tube containing a solution of **1** (0.104 mmol, 17 mg) in 2 mL of toluene was added $[\text{Rh}(\text{CO})_2(\mu\text{-Cl})]_2$ (0.051 mmol, 20 mg) and the solution stirred for 5 min at 25 °C. The volatiles were removed under reduced pressure to give **17** as a yellow-white powder. Yield = 35 mg, 95 %. ^1H NMR (500 MHz, $\text{C}_6\text{D}_5\text{CD}_3$) δ 1.50 (s, 9H, *t*Bu), 3.65 (s, 3H, NCH_3), 5.63 (m, 1H, $\text{py-}H^4$), 6.40 (d, $^3J_{\text{H-H}} = 6$ Hz, 1H, $\text{py-}H^5$), 6.58 (m, 1H, $\text{py-}H^3$), 6.81 (d, $^3J_{\text{H-H}} = 9$ Hz, 1H, $\text{py-}H^2$); $^{13}\text{C}\{^1\text{H}\}$ NMR (125 MHz, $\text{C}_6\text{D}_5\text{CD}_3$) δ 32.8 (CCH_3), 44.4 (NCH_3), 57.1 (CCH_3), 108.0 ($\text{py-}C^4$), 122.4 ($\text{py-}C^5$), 134.6 ($\text{py-}C^3$), 140.2 ($\text{py-}C^2$), 164.5 ($\text{py-}C^1$), 182.0 (d, $^1J_{\text{RhC}} = 78$ Hz, CO), 183.8 (d, $^1J_{\text{RhC}} = 66$ Hz, CO); IR (KBr) $\nu(\text{cm}^{-1})$: 2972, 2071, 1989, 1635, 1584, 1548, 1507; IR ($\text{C}_6\text{D}_5\text{CD}_3$) $\nu(\text{cm}^{-1})$: 2071, 1992; Anal. [found(calc.)] for $\text{C}_{12}\text{H}_{16}\text{ClN}_2\text{O}_2\text{Rh}$: C 40.11 (40.19), H 4.46 (4.50), N 7.73 (7.81).

$[\text{NiCl}_2(\text{Me}_2\text{N}^{\text{C}_6\text{H}_{10}}\text{N}^{\text{Me}_2})]$ (**18**)

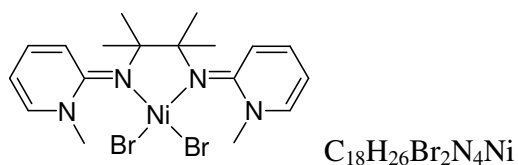
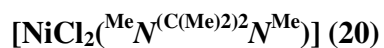


To a DCM (5 mL) solution of **7** (84.2 mg, 0.284 mmol) was added a DCM (5 mL) solution of Ni(DME)Br₂ (87.5 mg, 0.284 mmol) with string at 25 °C for 12 hr. The volatiles were removed under reduced pressure and the green solid extracted with DCM (10 mL) to give a green filtrate. Removal of the volatiles gave a green solid that was washed with diethyl ether (10 mL) to give **18** a dark green solid. Yield = 143 mg, 98 %. MS(TOF ES⁺) m/z (%): 435.0 ([M-Br+2H]⁺, 5 %), 297.2 (100, [M-2Br-Ni+H]⁺); Anal. [found(calc.)] for C₁₈H₂₄Br₂N₄Ni: C 41.99 (42.06), H 4.70 (4.78), N 10.88 (10.81).

$[\text{NiCl}_2(\text{BnN}(\text{CH}_2)_2\text{N}^{\text{Bn}})]$ (**19**)

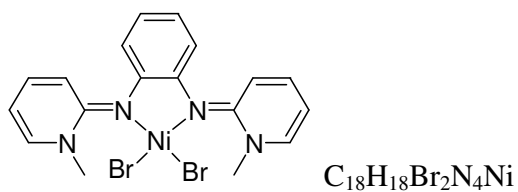


To a DCM (5 mL) solution of **8** (127 mg, 0.322 mmol) was added a DCM (5 mL) solution of Ni(DME)Br₂ (99.4 mg, 0.322 mmol) with stirring at 25 °C for 12 hr. The volatiles were removed under reduced pressure and the green solid extracted with DCM (20 mL) to give a green filtrate. Removal of the volatiles gave a green solid that was washed with diethyl ether (10 mL) to give **19** a dark green solid. Yield = 180 mg, 90 %. MS(TOF ES⁺) m/z (%): 613.0 ([M+3H]⁺, 20 %) 395.0 (75, [M-2Br-Ni+H]⁺); Anal. [found(calc.)] for C₂₆H₂₆Br₂N₄Ni: C 50.94 (51.03), H 4.28 (4.16), N 9.14 (9.16).



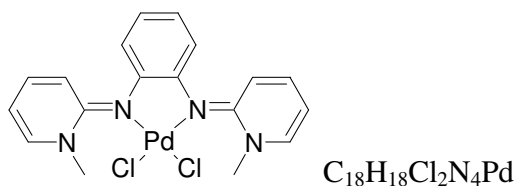
To a DCM (10 mL) solution of **9** (194 mg, 0.648 mmol) was added a DCM (10 mL) solution of Ni(DME)Br₂ (200 mg, 0.648 mmol) with stirring at 25 °C for 12 hr. The volatiles were removed under reduced pressure and the red solid extracted with DCM (20 mL) to give a red filtrate. Removal of the volatiles gave a red solid that was washed with diethyl ether (10 mL) to give **20** a red solid. Yield = 220 mg, 66 %. MS(TOF FD⁺) m/z (%): 516.0 ([M+2H]⁺, 25 %) 436.1 ([M-Br+H]⁺, 35%), 299.2 (100, [M-2Br-Ni+H]⁺); Anal. [found(calc.)] for C₁₈H₂₆Br₂N₄Ni: C 41.89 (41.82), H 5.14 (5.07), N 10.80 (10.84).

$[\text{NiCl}_2(\text{MeNC}_6\text{H}_4\text{NMe})]$ (**21**)

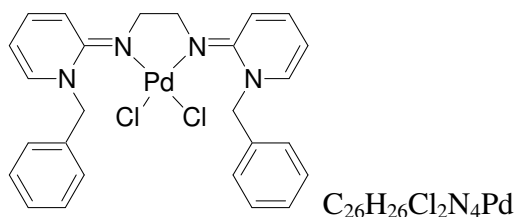
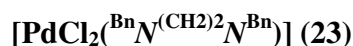


By using an analogous procedure to **19**, DCM solution of **12** (50.0 mg, 0.172 mmol) and $\text{Ni}(\text{DME})\text{Br}_2$ (53.0 mg, 0.172 mmol) were added in a Schlenk tube with stirring at 25 °C for 12 hr to give **21** a dark red solid. Yield = 83 mg, 95 %. MS (ESI) m/z (%): 428.8 ($[\text{M}-\text{Br}+\text{H}]^+$, 50%), 291 (100, $[\text{M}-2\text{Br}-\text{Ni}+\text{H}]^+$); Anal. [found(calc.)] for $\text{C}_{18}\text{H}_{18}\text{Br}_2\text{N}_4\text{Ni}$: C 42.41 (42.49), H 3.55 (3.57), N 10.97 (11.01).

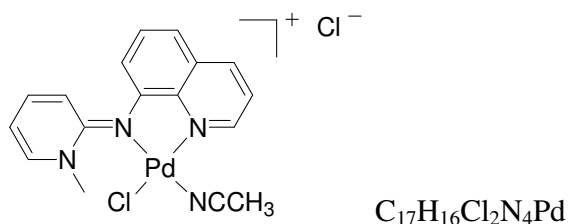
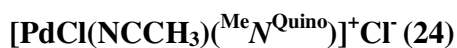
[PdCl₂(^{Me}N^{C₆H₄}N^{Me})] (**22**)



To a Schlenk containing Pd(CH₃CN)₂Cl₂ (45 mg, 0.17 mmol) and **12** (50 mg, 0.17 mmol) was added a acetonitrile (10 mL) with stirring for 12 hr at room temperature. The colour of solution became deep green. The volatiles were removed under reduce pressure and the solid residue washed with diethyl ether (2 × 15 mL) to give **22** as a dark green solid. Yield = 78 mg, 98 %. ¹H NMR (400 MHz, CDCl₃) δ 4.18 (s, 6H, NCH₃), 6.45 (m, 2H, aryl-CH), 6.58 (m, 2H, aryl-CH), 6.84 (m, 2H, py-H⁴), 7.64 (m, 2H, py-H³), 7.83 (d, ³J_{H-H} = 5 Hz, 2H, py-H⁵), 7.91 (d, ³J_{H-H} = 8 Hz, 2H, py-H²); ¹³C{¹H} NMR (100 MHz, CDCl₃) δ 42.0 (NCH₃), 114.6 (aryl-CH), 115.8 (py-C⁴), 119.6 (aryl-CH), 126.5 (py-C²), 139.9 (py-C³), 141.5 (py-C⁵), 147.8 (aryl-CN), 166.4 (py-C¹); MS(TOF EI⁺) m/z (%): 467.8 ([M+2H]⁺, 40%), 394.9 (100, [M-2Cl-H]⁺); Anal. [found(calc.)] for C₁₈H₁₈Cl₂N₄Pd: C 46.18 (46.23), H 3.81 (3.88), N 11.82 (11.98).

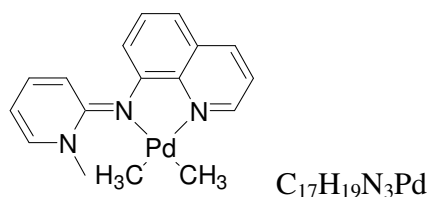


To a Schlenk containing $\text{Pd}(\text{COD})\text{Cl}_2$ (100 mg, 0.35 mmol) and **8** (138 mg, 0.35 mmol) was added a toluene (20 mL). Heated at 70°C with stirring for 2 hr over which time a red precipitate formed. The mixture was filtered and the solid residue washed with diethyl ether (2×20 mL) to give **23** as a dark red solid. Yield = 190 mg, 95%. ^1H NMR (400 MHz, CDCl_3 , 300 K) δ 3.67 (s, 4H, CH_2CH_2), 6.31 (m, 2H, H^4), 6.49 (s, 4H, PhCH_2), 6.95 (d, $^3J_{\text{H-H}} = 8$ Hz, 2H, H^2), 7.00 (d, $^3J_{\text{H-H}} = 7$ Hz, 4H, C_6H_5), 7.10 (m, 4H, C_6H_5), 7.16 (d, $^2J_{\text{H-H}} = 6$ Hz, 2H, C_6H_5), 7.24 (d, $^2J_{\text{H-H}} = 8$ Hz, 2H, H^5), 7.33 (m, 2H, H^3); $^{13}\text{C}\{^1\text{H}\}$ NMR (125 MHz, CDCl_3 , 298 K) δ 53.7 (CH_2CH_2), 57.9 (PhCH_2), 108.6 (py- C^4), 116.7 (py- C^2), 128.0 (C_6H_5), 128.1 (C_6H_5), 128.1 (C_6H_5), 136.1 (C_6H_5), 137.7 (py- C^5), 139.9 (py- C^3), 163.2 (py- C^1); MS(TOF ES+) m/z (%): 537.1 ($[\text{M}-\text{Cl}+2\text{H}]^+$, 25%), 499.1 (100, $[\text{M}-2\text{Cl}-\text{H}]^+$); Anal. [found(calc.)] for $\text{C}_{26}\text{H}_{26}\text{Cl}_2\text{N}_4\text{Pd}$: C 54.61 (54.56), H 4.58 (4.48), N 9.80 (9.74).

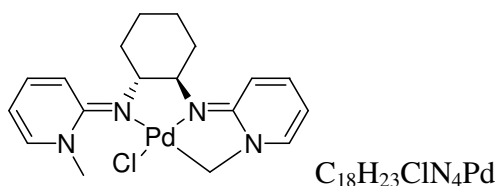
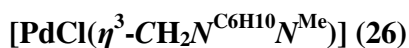


To a Schlenk containing $\text{Pd}(\text{CH}_3\text{CN})_2\text{Cl}_2$ (55 mg, 0.212 mmol) and **5** (50 mg, 0.212 mmol) was added a acetonitrile (5 mL) with stirring for 1 hr at room temperature. A deep red precipitate quickly formed. The volatiles were removed under reduce pressure and the solid residue washed with diethyl ether (2×10 mL) to give **24** as a deep red solid. Yield = 92 mg, 96 %. ^1H NMR (400 MHz, $(\text{CD}_3)_2\text{SO}$) δ 4.19 (s, 3 H, NCH_3), 6.74 (d, $^3J_{\text{H-H}} = 8$ Hz, 1H, CH_{quino}), 7.22 (d, $^3J_{\text{H-H}} = 8$ Hz, 1H, CH_{quino}), 7.35 (t, $^3J_{\text{H-H}} = 8$ Hz, 1H, CH_{quino}), 7.53 (m, 1H, py-H^4), 7.65 (m, 1H, CH_{quino}), 7.98 (d, $^3J_{\text{H-H}} = 8$ Hz, 1H, py-H^2), 8.24 (m, 1H, py-H^3), 8.56 (m, 1H, CH_{quino}), 8.73 (m, 1H, py-H^5), 9.00 (m, 1H, CH_{quino}); $^{13}\text{C}\{^1\text{H}\}$ NMR (100 MHz, $(\text{CD}_3)_2\text{SO}$) δ 43.4 (NCH_3), 111.2, 115.3, 120.1, 122.0, 126.7, 129.1, 130.7, 139.1, 143.9, 144.1, 144.2, 148.3, 152.7, 161.7; MS (ESI) m/z (%): 417.2 ($[\text{M-Cl}]^+$, 100%); Anal. [found(calc.)] for $\text{C}_{17}\text{H}_{16}\text{Cl}_2\text{N}_4\text{Pd}$: C 44.98 (45.01), H 3.49 (3.55), N 12.14 (12.35).

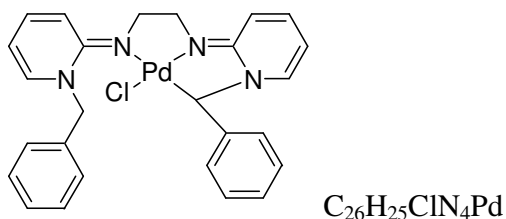
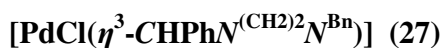
[Pd(CH₃)₂(^{Me}N^{Quin})] (**25**)



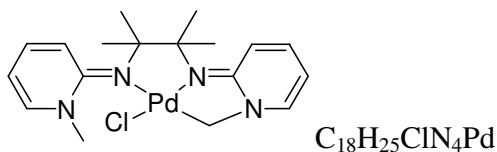
To a Schlenk tube containing **5** (30 mg, 0.127 mmol) and Pd(CH₃)₂(pyd) (27 mg, 0.127 mmol) was added toluene (5 mL) and mixture was stirred at room temperature for 30 min before leaving the tube into a fridge at -40 °C overnight. A red solid was formed and filtered quickly. The residual solid was washed with cold hexane (2 × 5 mL) and removal of volatiles under reduced pressure gave **25** as a red powder. Yield = 43 mg, 93 %. ¹H NMR (400 MHz, C₆D₆) δ 0.21 (s, 3H, PdCH₃), 1.31 (s, 3H, PdCH₃), 3.47 (s, 3H, NCH₃), 5.46 (m, 1H, py-H⁴), 6.36 (m, 1H, py-H⁵), 6.48 (m, 1H, py-H³), 6.58 (m, 1H, CH_{quino}), 6.89 (m, 2H, CH_{quino}), 6.97 (d, ³J_{H-H} = 9 Hz, 1H, CH_{quino}), 7.05 (m, 1H, CH_{quino}), 7.45 (m, 1H, py-H²), 8.82 (m, 1H, CH_{quino}); ¹H NMR (400 MHz, CD₃CN) δ -0.66 (s, 3 H, PdCH₃), 0.19 (s, 3H, PdCH₃), 3.93 (s, 3H, NCH₃), 6.64 (m, 1H, py-H⁴), 7.17 (m, 1H, CH_{quino}), 7.23 (m, 1H, CH_{quino}), 7.31 (m, 1H, CH_{quino}), 7.44 (m, 1H, CH_{quino}), 7.51 (d, ²J_{H-H} = 8 Hz, 1H, CH_{quino}), 7.62 (m, 1H, py-H³), 7.92 (m, 1H, py-H⁵), 8.25 (m, 1H, py-H²), 8.67 (m, 1H, CH_{quino}); ¹³C{¹H} NMR (100 MHz, C₆D₆) δ -10.1 (PdCH₃), -3.5 (PdCH₃), 42.5 (NCH₃), 110.4, 112.1, 117.4, 120.4, 122.0, 127.7, 131.2, 135.8, 138.3, 140.3, 145.4, 146.1, 151.3, 161.5; MS (ESI) m/z (%): 356.9 ([M-CH₃+H]⁺, 20 %), 236 (100, [M-Pd-2CH₃+H]⁺); Anal. [found(calc.)] for C₁₇H₁₉N₃Pd: C 54.89 (54.92), H 5.14 (5.15), N 11.26 (11.30).



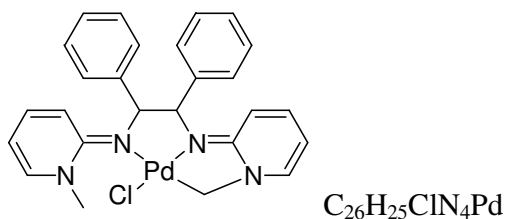
To a Schlenk containing **7** (1 g, 3.37 mmol), Pd[(CH₃CN)₂Cl₂] (875 mg, 3.37 mmol) and potassium carbonate (1 g), was added THF (60 mL) and the mixture stirred at 66 °C for 2 days. The volatiles were removed under reduced pressure and the solid extracted with DCM (60 mL). Filtered and removal of the volatiles gave a yellow solid that was washed with diethyl ether (30 mL) to give **26** a yellow solid. Yield = 1.18 g, 80 %. ¹H NMR (270 MHz, CD₂Cl₂) δ 1.04 (m, 1H, CCH₂), 1.15 (m, 1H, CCH₂), 1.30 (m, 2H, CCH₂), 1.66 (m, 2H, CCH₂), 1.91 (m, 1H, CCH₂), 2.55 (m, 1H, CCH₂), 3.47 (m, 2H, *c*-hexCH), 3.78 (s, 3H, NCH₃), 4.42 (d, ²J_{H-H} = 11 Hz, 1H, NCH₂), 4.66 (d, ²J_{H-H} = 11 Hz, 1H, NCH₂), 5.87 (m, 1H, *c*-metH⁴), 6.07 (m, 1H, H⁴), 6.42 (d, ³J_{H-H} = 8 Hz, 1H, *c*-metH²), 6.65 (d, ³J_{H-H} = 8 Hz, 1H, H²), 6.95 (m, 2H, *c*-metH³ + *c*-metH⁵), 7.24 (m, 1H, H³), 7.36 (m, 1H, H⁵); ¹³C{¹H} NMR (100 MHz, CD₂Cl₂) δ 25.1 (CCH₂), 30.7 (CCH₂), 31.2 (CCH₂), 42.2 (NCH₃), 46.2 (NCH₂), 66.3 (*c*-hexCH), 68.9 (*c*-hexCH), 105.6 (*c*-metC⁴), 106.3 (C⁴), 113.3(*c*-metC²), 114.8 (C²), 136.1 (*c*-metC³), 137.1 (C³), 140.8 (*c*-metC⁵), 141.2 (C⁵), 159.7 (*c*-metC¹), 162.9 (C¹); MS(TOF ES⁺) m/z (%): 438.3 ([M+2H]⁺, 10 %), 401.1 (100, [M-Cl]⁺); Anal. [found(calc.)] for C₁₈H₂₃ClN₄Pd: C 49.40 (49.44), H 5.26 (5.30), N 12.78 (12.81).



To a Schlenk containing **23** (414 mg, 0.72 mmol) and potassium carbonate (1 g, 7.24 mmol), was added THF (30 mL) and the mixture stirred at 66 °C for 2 days. The volatiles were removed under reduced pressure and the solid extracted with DCM (2 × 30 mL), filtered and removal of volatiles gave a yellow solid that was washed with toluene/hexane (1:2) to give **27** a yellow solid. Yield = 287 mg, 74 %. ^1H NMR (400 MHz, CDCl_3) δ 3.00 (m, 1H, CH_2CH_2), 3.20 (m, 3H, CH_2CH_2), 5.52 (d, $^2J_{\text{H-H}} = 16$ Hz, 1H, PhCH_2), 5.87 (m, 1H, $c\text{-met}H^4$), 5.95 (m, 2H, $H^4 + \text{PhCH}_2$), 6.06 (s, 1H, PhCH) 6.39 (d, $^3J_{\text{H-H}} = 8$ Hz, 1H, $c\text{-met}H^2$), 6.52 (d, $^2J_{\text{H-H}} = 8$ Hz, 1H, H^2), 6.88 (d, $^3J_{\text{H-H}} = 6$ Hz, 1H, $c\text{-met}H^5$), 7.03 - 7.25 (m, 13H, $\text{C}_6\text{H}_5 + c\text{-met}H^5 + H^3 + H^5$); $^{13}\text{C}\{^1\text{H}\}$ NMR (100 MHz, CDCl_3) δ 49.2 (CH_2CH_2), 54.7 (CH_2CH_2), 57.0 (PhCH_2), 66.9 (PhCH), 106.2 ($c\text{-met}C^4 + C^4$), 111.5 ($c\text{-met}C^2$), 115.1 (C^2), 124.2 (C_6H_5), 125.5 (2 x C_6H_5), 127.3 (C_6H_5), 128.2 (C_6H_5), 128.3 (C_6H_5), 137.0 ($c\text{-met}C^3$), 137.2 (ipsoPh), 137.4 (C^3), 139.7 ($c\text{-met}C^5$), 140.5 (C^5), 146.0 (ipsoPh), 160.0 ($c\text{-met}C^1$), 160.7 (C^1); MS(TOF ES⁺) m/z (%): 536.4 ($[\text{M}+2\text{H}]^+$, 10 %), 499.1 (100, $[\text{M}-\text{Cl}]^+$); Anal. [found(calc.)] for $\text{C}_{26}\text{H}_{25}\text{ClN}_4\text{Pd}$: C 58.28 (58.33), H 4.79 (4.71), N 10.37 (10.46).

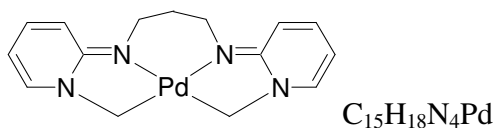


To a Schlenk containing **9** (500 mg, 1.68 mmol), $\text{Pd}[(\text{CH}_3\text{CN})_2\text{Cl}_2]$ (435 mg, 1.68 mmol) and potassium carbonate (1 g), was added THF (50 mL) and the mixture stirred at 66 °C for 2 days. The volatiles were removed under reduced pressure and the solid extracted with DCM (60 mL), filtered and hydrochloric acid solution (20 mL, 0.5 M) was added. DCM phase was extracted and MgSO_4 was added. Filtered and the volatiles were removed under reduced pressure to give **28** as a yellow solid. Yield = 346 mg, 47 %. ^1H NMR (400 MHz, CDCl_3) δ 1.18 (s, 3H, CCH_3), 1.36 (s, 3H, CCH_3), 1.37 (s, 3H, CCH_3), 1.84 (s, 3H, CCH_3), 4.03 (s, 3H, NCH_3), 4.38 (d, $^2J_{\text{H-H}} = 8$ Hz, 1H, CH_2), 4.64 (d, $^2J_{\text{H-H}} = 8$ Hz, 1H, CH_2), 5.87 (m, 1H, $_{\text{c-met}}\text{H}^4$), 6.03 (m, 1H, H^4), 6.55 (d, $^3J_{\text{H-H}} = 12$ Hz, 1H, $_{\text{c-met}}\text{H}^2$), 6.83 (d, $^3J_{\text{H-H}} = 12$ Hz, 1H, H^2), 6.97 (m, 2H, $_{\text{c-met}}\text{H}^3 +_{\text{c-met}}\text{H}^5$), 7.10 (m, 1H, H^3), 7.29 (m, 1H, H^5); $^{13}\text{C}\{^1\text{H}\}$ NMR (100 MHz, CDCl_3) δ 22.0 (CCH_3), 22.1 (CCH_3), 22.8 (CCH_3), 23.8 (CCH_3), 43.7 (NCH_3), 49.3 (NCH_2), 69.1 (CCH_3), 69.4 (CCH_3), 105.0 ($_{\text{c-met}}\text{C}^4$), 106.0 (C^4), 113.9 ($_{\text{c-met}}\text{C}^2$), 118.1 (C^2), 135.5 ($_{\text{c-met}}\text{C}^3$), 135.7 (C^3), 141.2 ($_{\text{c-met}}\text{C}^5$), 142.3 (C^5), 159.0 ($_{\text{c-met}}\text{C}^1$), 161.2 (C^1); MS(TOF ES⁺) m/z (%): 439.1 ($[\text{M}+\text{H}]^+$, 10 %), 403.1 (100, $[\text{M}-\text{Cl}]^+$); Anal. [found(calc.)] for $\text{C}_{18}\text{H}_{25}\text{ClN}_4\text{Pd}$: C 49.29 (49.21), H 5.91 (5.74), N 12.78 (12.75).

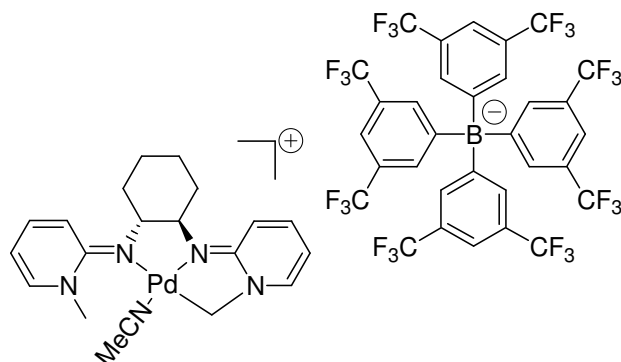


To a Schlenk containing **10** (200 mg, 0.51 mmol), $\text{Pd}[(\text{CH}_3\text{CN})_2\text{Cl}_2]$ (132 mg, 0.51 mmol) and potassium carbonate (350 mg, 2.53 mmol), was added THF (20 mL) and the mixture stirred at 66 °C for 12 hr. The volatiles were removed under reduced pressure and the solid extracted with DCM (30 mL). Filtered and the volatiles were removed under reduced pressure. The solid residue was washed with diethyl ether (20 mL) to give **29** as a yellow solid. Yield = 136 mg, 50 %. ^1H NMR (400 MHz, CDCl_3) δ 4.13 (s, 3H, NCH_3), 4.39 (s, 1H, CHCH), 4.54(s, 1H, CHCH), 4.71 (m, 2H, CH_2), 5.85 (m, 4H, $c\text{-met}H^4 + H^4 + c\text{-met}H^2 + H^2$), 6.75 (m, 2H, $c\text{-met}H^3 + H^3$), 6.90 (d, $^3J_{\text{H-H}} = 7.2$ Hz, 1H, $c\text{-met}H^5$), 7.08 (d, $^3J_{\text{H-H}} = 7.2$ Hz, 1H, H^5), 7.20 (m, 2H, aryl- H^{para}), 7.27 (t, $^3J_{\text{H-H}} = 6$ Hz, 2H, aryl- H^{meta}), 7.35 (t, $^3J_{\text{H-H}} = 6$ Hz, 2H, aryl- H^{meta}), 7.73 (d, $^3J_{\text{H-H}} = 7.2$ Hz, 2H, aryl- H^{ortho}), 8.01 (d, $^3J_{\text{H-H}} = 7.2$ Hz, 1H, aryl- H^{ortho}); $^{13}\text{C}\{^1\text{H}\}$ NMR (100 MHz, CDCl_3) δ 43.2 (NCH_3), 49.0 (NCH_2), 70.5 (CHCH), 77.2 (CHCH), 106.1, 106.3, 111.4, 116.3, 126.9, 127.0, 127.6, 128.2, 128.4, 136.4, 136.6, 140.0, 140.5, 142.1, 142.3, 160.0, 161.0; MS(TOF LIFDI $^+$) m/z (%): 536 (100, $[\text{M}+2\text{H}]^+$); Anal. [found(calc.)] for $\text{C}_{26}\text{H}_{25}\text{ClN}_4\text{Pd}$: C 58.25 (58.33), H 4.62 (4.71), N 10.38 (10.46).

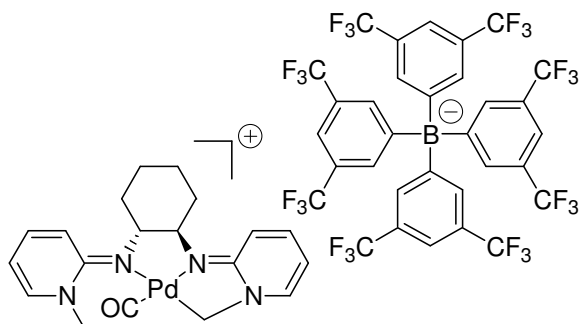
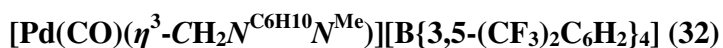
[Pd(η^4 -CH₂N^{(CH₂)₃}NCH₂)] (**30**)



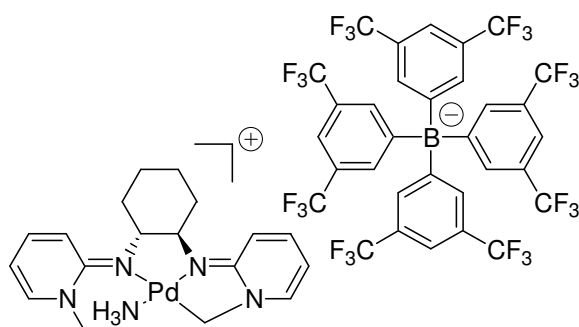
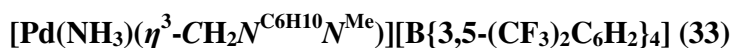
To a Schlenk containing **14** (300 mg, 1.17 mmol), Pd[(CH₃CN)₂Cl₂] (303 mg, 1.17 mmol) and potassium carbonate (356 mg, 2.56 mmol), was added acetonitrile (20 mL) and the mixture stirred at room temperature for 3 days. The volatiles were removed under reduced pressure and filtered with toluene (80 mL) to afford a yellow filtrate. Removed the volatiles to give **30** as a yellow creamy solid. Yield = 150 mg, 36 %. ¹H NMR (400 MHz, CDCl₃) δ 2.00 (m, 2H, CH₂CH₂CH₂), 3.25 (m, 4H, NCH₂CH₂), 4.20 (s, 4H, NCH₂Pd), 5.83 (m, 2H, py-*H*⁴), 6.40 (d, ³J_{H-H} = 9 Hz, 2H, py-*H*²), 7.00 (m, 2H, py-*H*³), 7.22 (m, 2H, py-*H*⁵); ¹³C{¹H} NMR (100 MHz, CDCl₃) δ 34.9 (CH₂CH₂CH₂), 45.7 (NCH₂CH₂), 46.4 (NCH₂Pd), 104.0 (py-*C*⁴), 110.7 (py-*C*²), 135.6 (py-*C*³), 143.3 (py-*C*⁵), 160.2 (py-*C*¹); MS (FD) m/z (%): 360 ([M]⁺, 100%); Anal. [found(calc.)] for C₁₅H₁₈N₄Pd: C 50.04 (49.94), H 5.15 (5.03), N 15.67 (15.53).



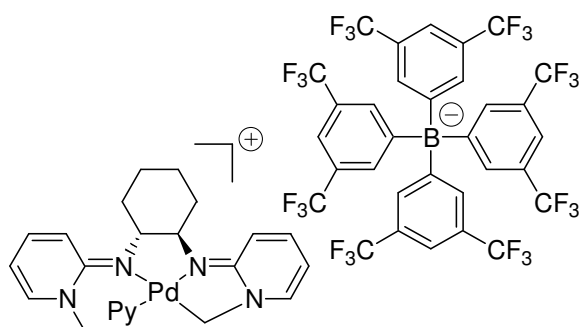
To a Schlenk containing **26** (100 mg, 0.23 mmol) and Na[B(3,5-(CF₃)₂C₆H₂)₄] (203 mg, 0.23 mmol), was added acetonitrile/DCM mix-solvent (1:1, 25 mL) and the mixture stirred at 25 °C for 16hr. The volatiles were removed under reduced pressure and the solid extracted with DCM (20 mL). Filtered and the volatiles of filtrate were removed under reduced pressure to give **31** a yellow solid. Yield = 255 mg, 85 %. ¹H NMR (400 MHz, CDCl₃) δ 1.05 (m, 1H, CCH₂), 1.13 (m, 1H, CCH₂), 1.29 (m, 2H, CCH₂), 1.67 (m, 2H, CCH₂), 1.77(s, 3H, CH₃CN), 1.91 (m, 1H, CCH₂), 2.54 (m, 1H, CCH₂), 3.41 (m, 2H, CH), 3.60 (s, 3H, NCH₃), 4.22 (d, ²J_{H-H} = 12 Hz, 1H, NCH₂), 4.55 (d, ²J_{H-H} = 12 Hz, 1H, NCH₂), 6.04 (m, 1H, *c*-metH⁴), 6.13 (m, 1H, H⁴), 6.49 (d, ³J_{H-H} = 8 Hz, 1H, *c*-metH²), 6.74 (d, ³J_{H-H} = 8 Hz, 1H, H²), 6.90 (d, ³J_{H-H} = 6 Hz, 1H, *c*-metH⁵), 7.09 (m, 1H, *c*-metH³), 7.18 (d, ²J_{H-H} = 6 Hz, 1H, H⁵), 7.32 (m, 1H, H³), 7.45 (Ar^FH, 4H), 7.62 (Ar^FH, 8H); ¹³C{¹H} NMR (100 MHz, CD₂Cl₂) δ 2.0 (CH₃CN), 24.7 (CCH₂), 30.8 (CCH₂), 41.7 (NCH₃), 48.0 (NCH₂), 67.2 (*c*-hexCH), 68.9 (*c*-hexCH), 107.8 (*c*-metC⁴), 108.2 (C⁴), 113.3 (*c*-metC²), 116.2 (C²), 117.5 (Ar^FCH), 125.9 (*ipso*-Ar^FCCF₃), 129.4 (q, ¹J_{C-F} = 273 Hz, CF₃), 134.8 (Ar^FCH), 137.4 (*c*-metC³), 138.2 (C³), 139.3 (*c*-metC⁵), 140.5 (C⁵), 160.4 (*c*-metC¹), 161.6 (m, ¹J_{B-C} = 51 Hz, *ipso*-Ar^FCB), 163.5 (C¹); MS(TOF ES⁺) m/z (%): 442.1 ([M-BAr^F₄]⁺, 20 %), 401.1 (100, [M-BAr^f-MeCN]⁺); Anal. [found(calc.)] for C₅₂H₃₈BF₂₄N₅Pd: C 47.94 (47.82), H 2.93 (2.93), N 5.26 (5.36).



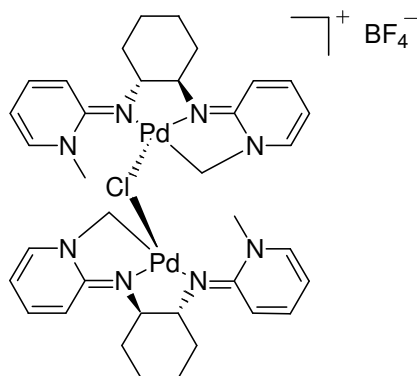
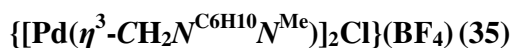
Dichloromethane (10 mL) was added to a Schlenk containing **31** (100 mg, 0.077 mmol) and the solution degassed before addition of carbon monoxide gas (1 atm) and the solution stirred at 25 °C for 5 min. The volatiles were removed under reduced pressure and the solid extracted with dichloromethane (10 mL), filtered and the volatiles removed under reduced pressure to give **32** as a dark green powder. Yield = 95 mg, 98 %. ^1H NMR (400 MHz, CDCl_3) δ 1.03 (m, 1H, CCH_2), 1.18 (m, 1H, CCH_2), 1.26 (m, 2H, CCH_2), 1.68 (m, 2H, CCH_2), 1.94 (m, 1H, CCH_2), 2.54 (m, 1H, CCH_2), 3.49 (m, 2H, CH), 3.71 (s, 3H, NCH_3), 4.36 (d, $^2J_{\text{H-H}} = 10$ Hz, 1H, NCH_2), 4.75 (d, $^2J_{\text{H-H}} = 10$ Hz, 1H, NCH_2), 6.22 (m, 1H, ${}_{\text{c-met}}\text{H}^4$), 6.40 (m, 1H, H^4), 6.59 (d, $^2J_{\text{H-H}} = 8$ Hz, 1H, ${}_{\text{c-met}}\text{H}^2$), 6.84 (d, $^3J_{\text{H-H}} = 8$ Hz, 1H, H^2), 6.99 (d, $^3J_{\text{H-H}} = 6$ Hz, 1H, ${}_{\text{c-met}}\text{H}^5$), 7.24 (m, 1H, ${}_{\text{c-met}}\text{H}^3$), 7.34 (d, $^3J_{\text{H-H}} = 6$ Hz, 1H, H^5), 7.44 ($\text{Ar}^{\text{F}}\text{H}$, 4H), 7.46 (m, 1H, H^3), 7.62 ($\text{Ar}^{\text{F}}\text{H}$, 8H); $^{13}\text{C}\{^1\text{H}\}$ NMR (100 MHz, CD_2Cl_2) δ 24.4 (2 x CCH_2), 30.7 (CCH_2), 31.0 (CCH_2), 42.0 (NCH_3), 50.4 (NCH_2), 67.7 (${}_{\text{c-hex}}\text{CH}$), 70.6 (${}_{\text{c-hex}}\text{CH}$), 109.9 (${}_{\text{c-met}}\text{C}^4$), 111.1 (C^4), 113.1 (${}_{\text{c-met}}\text{C}^2$), 116.6 (C^2), 117.5 ($\text{Ar}^{\text{F}}\text{CH}$), 125.8 (${}_{\text{ipso}}\text{Ar}^{\text{F}}\text{CCF}_3$), 129.0 (q, $^1J_{\text{C-F}} = 273$ Hz, CF_3), 134.7 ($\text{Ar}^{\text{F}}\text{CH}$), 139.2 (${}_{\text{c-met}}\text{C}^3$), 139.9 (C^3), 140.2 (${}_{\text{c-met}}\text{C}^5$), 140.5 (C^5), 161.5 (m, $^1J_{\text{B-C}} = 51$ Hz, ${}_{\text{ipso}}\text{Ar}^{\text{F}}\text{CB}$), 162.3 (${}_{\text{c-met}}\text{C}^1$), 165.7 (C^1), 177.5 (CO); IR(KBr, ν cm^{-1}): 2103 (s); MS (LIFDI $^+$) m/z (%): 429 (100, $[\text{M-BAr}^{\text{F}}_4]^+$); Anal. [found(calc.)] for $\text{C}_{51}\text{H}_{35}\text{BF}_{24}\text{N}_4\text{OPd}$: C 47.38 (47.37), H 2.80 (2.73), N 4.25 (4.33).



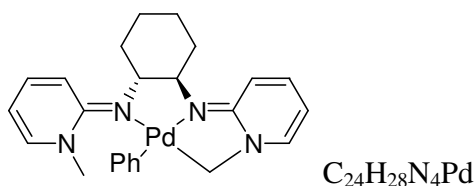
Dichloromethane (20 mL) was added to a Schlenk containing **31** (200 mg, 0.16 mmol) and the solution degassed before addition of ammonia gas (1 atm) and the solution stirred at 25 °C for 2 hr. The volatiles were removed under reduced pressure to give **33** as a yellow powder. Yield = 195 mg, 98 %. ^1H NMR (400 MHz, CDCl_3) δ 1.03 (m, 1H, CCH_2), 1.14 (m, 1H, CCH_2), 1.18 (bs, 3H, NH_3), 1.29 (m, 2H, CCH_2), 1.66 (m, 2H, CCH_2), 1.77 (s, 3H, CH_3CN), 1.91 (m, 1H, CCH_2), 2.53 (m, 1H, CCH_2), 3.38 (m, 2H, CH), 3.58 (s, 3H, NCH_3), 4.10 (d, $^2J_{\text{H-H}} = 9$ Hz, 1H, NCH_2), 4.59 (d, $^2J_{\text{H-H}} = 9$ Hz, 1H, NCH_2), 6.00 (m, 1H, $c\text{-met}H^4$), 6.19 (m, 1H, H^4), 6.49 (d, $^3J_{\text{H-H}} = 8$ Hz, 1H, $c\text{-met}H^2$), 6.76 (d, $^3J_{\text{H-H}} = 8$ Hz, 1H, H^2), 6.95 (d, $^3J_{\text{H-H}} = 6$ Hz, 1H, $c\text{-met}H^5$), 7.08 (m, 1H, $c\text{-met}H^3$), 7.29 (m, 1H, H^5), 7.31 (m, 1H, H^3), 7.48 ($\text{Ar}^{\text{F}}\text{H}$, 4H), 7.64 ($\text{Ar}^{\text{F}}\text{H}$, 8H); $^{13}\text{C}\{^1\text{H}\}$ NMR (100 MHz, CD_2Cl_2) δ 25.0 (CCH_2), 25.1 (CCH_2), 31.0 (CCH_2), 31.2 (CCH_2), 41.7 (NCH_3), 46.5 (NCH_2), 67.1 ($c\text{-hexCH}$), 69.4 ($c\text{-hexCH}$), 107.5 ($c\text{-met}C^4$), 108.8 (C^4), 113.7 ($c\text{-met}C^2$), 116.6 (C^2), 117.9 ($\text{Ar}^{\text{F}}\text{CH}$), 126.3 ($\text{ipsoAr}^{\text{F}}\text{CCF}_3$), 129.2 (q, $^1J_{\text{C-F}} = 273$ Hz, CF_3), 135.1 ($\text{Ar}^{\text{F}}\text{CH}$), 137.5 ($c\text{-met}C^3$), 139.0 (C^3), 140.1 ($c\text{-met}C^5$), 141.3 (C^5), 161.5 (m, $^1J_{\text{B-C}} = 51$ Hz, $\text{ipsoAr}^{\text{F}}\text{CB}$), 162.8 ($c\text{-met}C^1$), 163.5 (C^1); MS (ESI) m/z (%): 417.9 ($[\text{M-BAr}^{\text{F}}_4]^+$, 20 %), 400.9 (100, $[\text{M-Barf-NH}_3]^+$); Anal. [found(calc.)] for $\text{C}_{50}\text{H}_{38}\text{BF}_{24}\text{N}_5\text{Pd}$: C 46.84 (46.84), H 2.95 (2.99), N 5.50 (5.46).



Prydine (1.21 mg, 0.015 mmol) was added to a Young-type NMR tube containing a CD_2Cl_2 solution of **31** (20 mg, 0.015 mmol). The volatiles were removed under reduced pressure to give **34** as a yellow powder. Yield = 20 mg, 99 %. ^1H NMR (400 MHz, CD_2Cl_2) δ 1.05 (m, 1H, CCH_2), 1.18 (m, 1H, CCH_2), 1.19 (m, 1H, CCH_2), 1.33 (m, 2H, CCH_2), 1.68 (m, 2H, CCH_2), 1.94 (m, 1H, CCH_2), 2.58 (m, 1H, CCH_2), 3.19 (s, 3H, NCH_3), 3.43 (m, 1H, CH), 3.58 (m, 1H, CH), 4.09 (d, $^2J_{\text{H-H}} = 10$ Hz, 1H, NCH_2), 4.62 (d, $^2J_{\text{H-H}} = 10$ Hz, 1H, NCH_2), 6.03 (m, 2H, $c\text{-met}H^4 + H^4$), 6.56 (d, $^3J_{\text{H-H}} = 9$ Hz, 1H, $c\text{-met}H^2$), 6.62 (d, $^2J_{\text{H-H}} = 6$ Hz, 1H, $c\text{-met}H^5$), 6.87 (d, $^3J_{\text{H-H}} = 8$ Hz, 1H, H^2), 6.99 (d, $^3J_{\text{H-H}} = 6$ Hz, 1H, H^5), 7.12 (m, 3H, $c\text{-met}H^3 + \text{Py}$), 7.39 (m, 1H, H^3), 7.48 (s, 4H, $\text{Ar}^{\text{F}}H$), 7.65 (s, 9H, $\text{Ar}^{\text{F}}H + \text{Py}$), 8.10 (m, 2H, Py); $^{13}\text{C}\{^1\text{H}\}$ NMR (100 MHz, CD_2Cl_2) δ 25.3 (CCH_2), 25.4 (CCH_2), 31.3 (CCH_2), 31.6 (CCH_2), 41.8 (NCH_3), 50.6 (NCH_2), 67.3 ($c\text{-hexCH}$), 69.6 ($c\text{-hexCH}$), 107.6 ($c\text{-met}C^4$), 108.4 (C^4), 114.0 ($c\text{-met}C^2$), 117.0 (C^2), 118.0 ($\text{Ar}^{\text{F}}\text{CH}$), 126.1 ($\text{ipsoAr}^{\text{F}}\text{CCF}_3$), 126.5 (Py), 129.2 (q, $^1J_{\text{C-F}} = 273$ Hz, CF_3), 135.3 ($\text{Ar}^{\text{F}}\text{CH}$), 137.7 ($c\text{-met}C^3$), 138.6 (Py), 139.0 (C^3), 140.1 ($c\text{-met}C^5$), 141.5 (C^5), 151.8 (Py), 160.9 ($c\text{-met}C^1$), 161.5 (m, $^1J_{\text{B-C}} = 51$ Hz, $\text{ipsoAr}^{\text{F}}\text{CB}$), 163.8 (C^1), 177.5 (CO); IR(KBr, ν cm^{-1}): 2103 (s); MS(TOF ESI $^+$) m/z (%): 479.9 ($[\text{M-BAr}^{\text{F}}_4]^+$, 20 %), 401.0 (100, $[\text{M-BAr}^{\text{F}}\text{-Py}]^+$); Anal. [found(calc.)] for $\text{C}_{55}\text{H}_{40}\text{BF}_{24}\text{N}_5\text{Pd}$: C 49.23 (49.15), H 3.07 (3.00), N 5.14 (5.21).

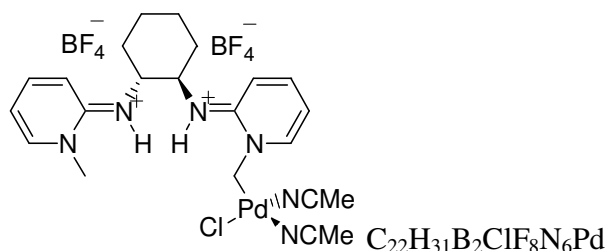


AgBF_4 (4.5 mg, 0.023 mmol) was added to a Schlenk containing a DCM (3 mL) solution of **26** (20 mg, 0.046 mmol). The mixture was stirred for 10 min at room temperature. The solid was filtered off and the volatiles were removed under reduced pressure to give **35** as a yellow solid. Yield = 15mg, 78 %. ^1H NMR (400 MHz, CD_2Cl_2) δ 0.94 (m, 1H, CCH_2), 1.15 (m, 1H, CCH_2), 1.30 (m, 2H, CCH_2), 1.63 (m, 2H, CCH_2), 1.91 (m, 1H, CCH_2), 2.53 (m, 1H, CCH_2), 3.31 (m, 2H, $c\text{-hexCH}$), 3.55 (s, 3H, NCH_3), 3.82 (d, $^2J_{\text{H-H}} = 9.6$ Hz, 1H, NCH_2), 4.61 (d, $^2J_{\text{H-H}} = 9.6$ Hz, 1H, NCH_2), 6.04 (m, 1H, $c\text{-metH}^4$), 6.19 (m, 1H, H^4), 6.46 (d, $^3J_{\text{H-H}} = 8$ Hz, 1H, $c\text{-metH}^2$), 6.67 (d, $^3J_{\text{H-H}} = 8$ Hz, 1H, H^2), 6.94 (m, 1H, $c\text{-metH}^5$), 7.08 (m, 1H, $c\text{-metH}^3$), 7.35 (m, 1H, H^3), 7.42 (m, 1H, H^5); $^{13}\text{C}\{^1\text{H}\}$ NMR (100 MHz, CD_2Cl_2) δ 25.2 (CCH_2), 31.1 (CCH_2), 31.2 (CCH_2), 42.1 (NCH_3), 48.2 (NCH_2), 67.2 ($c\text{-hexCH}$), 69.3 ($c\text{-hexCH}$), 107.1 ($c\text{-metC}^4$), 107.6 (C^4), 113.5 ($c\text{-metC}^2$), 116.2 (C^2), 137.1 ($c\text{-metC}^3$), 137.8 (C^3), 141.0 ($c\text{-metC}^5$), 141.3 (C^5), 160.6 ($c\text{-metC}^1$), 163.1 (C^1); MS(TOF ESI $^+$) m/z (%): 839.0 ($[\text{M}+2\text{H}]^+$, 15 %), 400.9 (100, $[\text{M}\text{-monomer-Cl}]^+$); HRMS calc. for $\text{C}_{36}\text{H}_{46}\text{ClN}_8\text{Pd}_2$: 837.1603, found 837.1598.



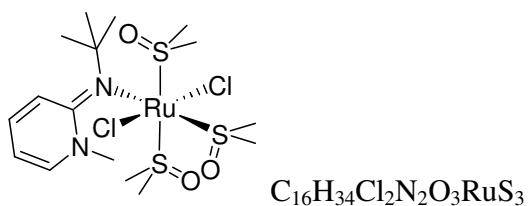
Phenyl Grignard (0.15 mL, 1M in THF) was dropwise added to a Schlenk containing a THF (15 mL) solution of **26** (65 mg, 0.15 mmol) at 0 °C. Then the Schlenk was warmed to room temperature with stirring for 12 hr. During the process, the suspension became a clear solution. The volatiles were removed under reduced pressure. The solid residue extracted with toluene (45 mL) and filtered. The removal of the volatiles under reduced pressure gave **36** as a yellow solid. Yield = 50 mg, 70 %. ^1H NMR (400 MHz, CD_2Cl_2) δ 1.01 (m, 1H, CCH_2), 1.18 (m, 1H, CCH_2), 1.31 (m, 2H, CCH_2), 1.63 (m, 2H, CCH_2), 1.91 (m, 1H, CCH_2), 2.54 (m, 1H, CCH_2), 3.37 (m, 2H, $_{\text{c-hex}}\text{CH}$), 3.68 (s, 3H, NCH_3), 4.25 (d, $^2J_{\text{H-H}} = 10$ Hz, 1H, NCH_2), 4.50 (d, $^2J_{\text{H-H}} = 10$ Hz, 1H, NCH_2), 5.89 (m, 1H, $_{\text{c-met}}\text{H}^4$), 6.07 (m, 1H, H^4), 6.40 (d, $^3J_{\text{H-H}} = 9$ Hz, 1H, $_{\text{c-met}}\text{H}^2$), 6.55 (m, 1H, $_{\text{c-met}}\text{H}^3$), 6.63 (d, $^3J_{\text{H-H}} = 10\text{Hz}$, 1 H, H^2), 6.73 (m, 1H, $_{\text{c-met}}\text{H}^5$), 6.95 (m, 2H, $\text{H}^3 + \text{H}^5$), 7.27 (m, 2H, Ph), 7.35 (m, 1H, Ph), 7.52 (d, $^3J_{\text{H-H}} = 8$ Hz, 2H, Ph); ^1H NMR (400 MHz, C_6D_6) δ 1.21 (m, 4H, CCH_2), 1.55 (m, 2H, CCH_2), 1.96 (m, 1H, CCH_2), 2.49 (m, 1H, CCH_2), 3.06 (s, 3H, NCH_3), 3.49 (m, 1H, $_{\text{c-hex}}\text{CH}$), 3.68 (m, 1H, $_{\text{c-hex}}\text{CH}$), 4.19 (d, $^2J_{\text{H-H}} = 11$ Hz, 1H, NCH_2), 4.91 (d, $^2J_{\text{H-H}} = 11$ Hz, 1H, NCH_2), 5.24 (m, 1H, $_{\text{c-met}}\text{H}^4$), 5.36 (m, 1H, H^4), 5.97 (d, $^2J_{\text{H-H}} = 6$ Hz, 1H, $_{\text{c-met}}\text{H}^2$), 6.05 (d, $^2J_{\text{H-H}} = 9$ Hz, 1H, H^2), 6.47 (m, 3H, $_{\text{c-met}}\text{H}^3 + _{\text{c-met}}\text{H}^5 + \text{H}^5$), 6.68 (m, 1H, H^3), 7.14 (m, 3H, Ph), 7.57 (m, 2H, Ph); $^{13}\text{C}\{^1\text{H}\}$ NMR (100 MHz, CD_2Cl_2) δ 25.5 (CCH_2), 31.2 (CCH_2), 31.7 (CCH_2), 42.6 (NCH_3), 46.6 (NCH_2), 66.8 ($_{\text{c-hex}}\text{CH}$), 69.4 ($_{\text{c-hex}}\text{CH}$), 106.1 ($_{\text{c-met}}\text{C}^4$), 106.8 (C^4), 113.7($_{\text{c-met}}\text{C}^2$), 115.3 (C^2), 127.6 (Ph), 127.8 (Ph), 129.3 (Ph), 136.6 ($_{\text{c-met}}\text{C}^3$), 137.6 (C^3), 139.2 (Ph), 141.3 ($_{\text{c-met}}\text{C}^5$), 141.7 (C^5), 159.9 ($_{\text{c-met}}\text{C}^1$), 163.4 (C^1); MS(TOF ESI $^+$) m/z (%): 479.0 ($[\text{M}+\text{H}]^+$, 100%).

[Pd(MeCN)₂Cl(η¹-CH₂N^{C₆H₁₀N^{Me})(H⁺)₂](BF₄)₂ (**37**)}

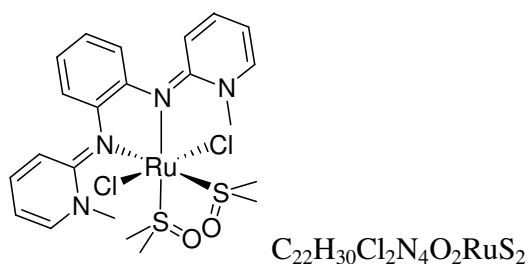
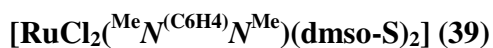


HBF₄.Et₂O (16.3 mg, 0.10 mmol) was added to a Schlenk containing a acetonitrile (3 mL) solution of **26** (22 mg, 0.05 mmol). The mixture was stirred for 1 hr at room temperature. The volatiles were removed under reduced pressure to give **37** as a yellow powder. Yield = 34 mg, 98 %. ¹H NMR (270 MHz, CD₃CN) δ 1.56 (m, 4H, CCH₂), 1.85 (m, 2H, CCH₂), 2.21 (m, 2H, CCH₂), 3.71 (s, 3H, NCH₃), 4.05 (m, 2H, *c*-hexCH), 4.11 (s, 2H, NCH₂), 6.51 (br, 1H, NH), 6.80 (m, 1H, *met*H⁴), 6.90 (m, 1H, H⁴), 7.25 (d, ³J_{H-H} = 8.9 Hz, 1H, *met*H²), 7.38 (d, ³J_{H-H} = 8.9 Hz, 1H, H²), 7.55 (br, 1H, NH), 7.88 (m, 4H, *met*H⁵ + *met*H³ + H³ + H⁵); ¹³C{¹H} NMR (67.9 MHz, CD₃CN) δ 25.3 (CCH₂), 32.2 (CCH₂), 32.5 (CCH₂), 33.4 (NCH₂), 43.6 (NCH₃), 57.4 (*c*-hexCH), 58.0 (*c*-hexCH), 112.2 (*c*-*met*C⁴), 112.4 (C⁴), 114.8 (*c*-*met*C²), 115.0 (C²), 141.5 (*c*-*met*C³), 144.0 (C³ + *c*-*met*C⁵), 144.9 (C⁵), 153.3 (*c*-*met*C¹), 154.4 (C¹); MS(TOF ESI⁺) *m/z* (%): 438.9 (100, [M-2BF₄-2CH₃CN]⁺); Anal. [found(calc.)] for C₂₂H₃₁B₂ClF₈N₆Pd: C 38.12 (38.02), H 4.57 (4.50), N 12.16 (12.09).

[RuCl₂(^{Me}N^tBu)(dmsO-S)₃] (38)

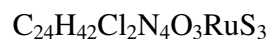
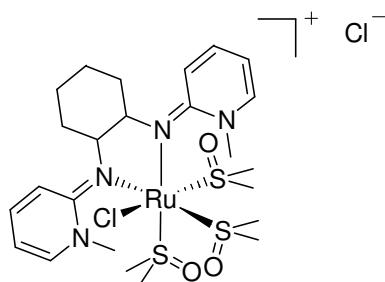


cis-[RuCl₂(dmsO)₄] (147 mg, 0.30 mmol) and the ligand **1** (50 mg, 0.30 mmol) were heated at 60 °C in methanol (5 mL) for 2 hr during which yellow suspension became red solution. The volatile was removed under reduced pressure. The product was washed with diethyl ether (3 x 10 mL) to give **38** as a red powder. Yield = 170 mg, 98 %. ¹H NMR (400 MHz, CD₃OD) δ 1.58 (s, 12H, *t*Bu), δ 3.10-3.50 (group of peaks, 18H, dmsO), 3.95 (s, 3H, NCH₃), 7.00 (m, 1H, py-*H*⁴), 7.49 (d, ³J_{H-H} = 9.2 Hz, 1H, py-*H*²), 8.02 (m, 1H, py-*H*³), 8.16 (m, 1H, py-*H*⁵); ¹³C{¹H} NMR (100 MHz, CD₃OD) δ 29.1 (CCH₃), 42.7 (NCH₃), 46.0 (dmsO), 46.3 (dmsO), 54.9 (CCH₃), 114.2 (py-*C*⁴), 114.4 (py-*C*²), 143.7 (py-*C*³), 143.8 (py-*C*⁵), 153.5 (py-*C*¹); IR (KBr, cm⁻¹), 1646 s, 1584 s, 1530 s, 1084 s, 1018 s; Anal. [found(calc.)] for C₁₆H₃₄Cl₂N₂O₃RuS₃: C 33.62 (33.68), H 6.07 (6.01), N 4.84 (4.91).

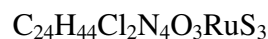
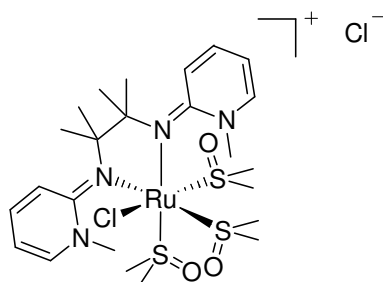


cis-[RuCl₂(dms_o)₄] (170 mg, 0.35 mmol) and the ligand **12** (102 mg, 0.35 mmol) were heated at 60 °C in methanol (10 mL) for 4 hr during which yellow suspension became red solution. The volatile was removed under reduced pressure. The product was washed with diethyl ether (3 x 15 mL) to give **39** as a red powder. Yield = 203 mg, 94 %. ¹H NMR (400 MHz, CD₃OD) δ 3.15-3.50 (group of peaks, 12H, dms_o), 3.46 (s, 6H, NCH₃), 6.30 (m, 2H, py-*H*⁴), 6.44 (d, ³J_{H-H} = 8.8 Hz, 2H, py-*H*²), 7.15 (m, 4H, C₆H₄), 7.28 (m, 2H, py-*H*³), 7.57 (m, 2H, py-*H*⁵); ¹³C{¹H} NMR (100 MHz, CD₃OD) δ 44.8 (NCH₃), dms_o peaks are in 46.2-48.2 region, 109.4 (py-*C*⁴), 115.8 (py-*C*²), 126.7 (aryl-CH), 126.9 (aryl-CH), 139.9 (py-*C*³), 140.1 (aryl-CN), 141.4 (py-*C*⁵), 154.7 (py-*C*¹); IR (KBr, cm⁻¹), 1641 s, 1552 s, 1093 s, 1017 s; Anal. [found(calc.)] for C₂₂H₃₀Cl₂N₄O₂RuS₂: C 42.66 (42.71), H 4.83 (4.89), N 8.87 (9.06).

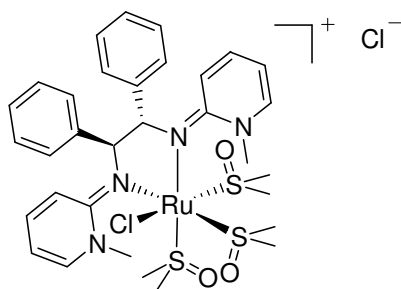
[RuCl(MeN^{C6H10}N^{Me})(dmsO-S)₃]Cl (40)



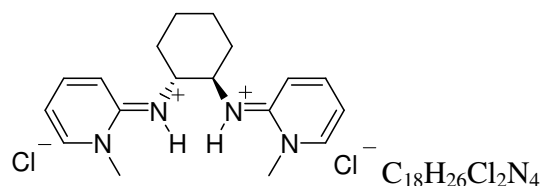
cis-[RuCl₂(dmsO)₄] (163 mg, 0.34 mmol) and the ligand **7** (100 mg, 0.34 mmol) were heated at 60 °C in methanol (5 mL) for 1 hr during which yellow suspension became red-orange solution. The volatile was removed under reduced pressure. The product was washed with diethyl ether (3 x 10 mL) to give **40** as a orange powder. Yield = 223 mg, 95 %. ¹H NMR (400 MHz, CD₃OD) δ 1.52-1.60 (m, 2H, *c*-hex-CH₂), 1.68-1.80 (m, 2H, *c*-hex-CH₂), 1.86-1.92 (m, 2H, *c*-hex-CH₂), 2.12-2.20 (m, 2H, *c*-hex-CH₂), 3.14-3.54 (group of peaks, 18H, dmsO), 3.74 (s, 6H, NCH₃), 4.08 (m, 2H, *c*-hex-CH), 6.81 (m, 2H, py-*H*⁴), 7.43 (d, ³J_{H-H} = 8.0 Hz, 2H, py-*H*²), 7.92 (m, 2H, py-*H*³ and py-*H*⁵); ¹³C{¹H} NMR (100 MHz, CD₃OD) δ 25.4 (*c*-hex-CH₂), 33.0 (*c*-hex-CH₂), 42.8 (NCH₃), 46.3 (dmsO), 54.9 (dmsO), 58.5 (*c*-hex-CH), 113.0 (py-*C*⁴), 113.4 (py-*C*²), 142.9 (py-*C*³), 143.8 (py-*C*⁵), 154.6 (py-*C*¹); IR (KBr, cm⁻¹), 1643 s, 1639 s, 1569 s, 1537 s, 1085 s, 1017 s; Anal. [found(calc.)] for C₂₄H₄₂Cl₂N₄O₃RuS₃: C 40.95 (41.02), H 5.96 (6.02), N 7.92 (7.97).



cis-[RuCl₂(dmsO)₄] (244 mg, 0.50 mmol) and the ligand **9** (150 mg, 0.50 mmol) were heated at 60 °C in methanol (10 mL) for 18 hr during which yellow suspension became deep red solution. The volatile was removed under reduced pressure. The product was washed with diethyl ether (3 x 15 mL) to give **41** as a red powder. Yield = 331 mg, 94 %. ¹H NMR (400 MHz, CD₃OD) δ 1.47 (s, 12H, CCH₃), 3.12-3.52 (group of peaks, 18H, dmsO), 3.63 (s, 6H, NCH₃), 6.38 (t, ³J_{H-H} = 6.4 Hz, 2H, py-H⁴), 7.07 (d, ³J_{H-H} = 8 Hz, 2H, py-H²), 7.53 (t, ³J_{H-H} = 8 Hz, 2H, py-H³), 7.76 (d, ³J_{H-H} = 6.4 Hz, 2H, py-H⁵); ¹³C{¹H} NMR (100 MHz, CD₃OD) δ 21.4 (CCH₃), 42.1 (NCH₃), 46.4 (dmsO), 50.1 (dmsO), 63.4 (CCH₃), 108.3 (py-C⁴), 115.4 (py-C²), 140.5 (py-C³), 142.9 (py-C⁵), 154.5 (py-C¹); IR (KBr, cm⁻¹), 1642 s, 1580 s, 1558 s, 1533 s, 1083 s, 1013 s; Anal. [found(calc.)] for C₂₄H₄₄Cl₂N₄O₃RuS₃: C 40.85 (40.90), H 6.17 (6.29), N 7.85 (7.95).



cis-[RuCl₂(dmsO)₄] (120 mg, 0.25 mmol) and the ligand **10** (98 mg, 0.25 mmol) were heated at 60 °C in methanol (5 mL) for 2 hr during which yellow suspension became red-orange solution. The volatile was removed under reduced pressure. The product was washed with diethyl ether (3 x 10 mL) to give **42** as a red powder. Yield = 190 mg, 95 %. ¹H NMR (400 MHz, CD₃OD) δ 3.15-3.50 (group of peaks, 18H, dmsO), 3.91 (s, 6H, NCH₃), 4.93 (s, 2H, PhCH), 6.37 (t, ³J_{H-H} = 8 Hz, 2H, py-H⁴), 6.45 (d, ³J_{H-H} = 8 Hz, 2H, py-H²), 7.24 (m, 2H, C₆H₅), 7.32 (m, 6H, py-H³ and C₆H₅), 7.49 (d, ³J_{H-H} = 4 Hz, 4H, C₆H₅), 7.77 (d, ³J_{H-H} = 6 Hz, 2H, py-H⁵); ¹³C{¹H} NMR (100 MHz, CD₃OD) δ 41.7 (NCH₃), 46.2 (dmsO), 46.5 (dmsO), 66.0 (PhCH), 110.0 (py-C⁴), 113.7 (py-C²), 128.3 (C₆H₅), 128.8 (C₆H₅), 129.7 (C₆H₅), 141.4 (py-C³), 142.1 (py-C⁵), 142.2 (C₆H₅), 154.9 (py-C¹); IR (KBr, cm⁻¹), 1642 s, 1588 s, 1560 s, 1538 s, 1077 s, 1015 s; Anal. [found(calc.)] for C₃₂H₄₄Cl₂N₄O₃RuS₃: C 47.95 (47.99), H 5.53 (5.54), N 6.93 (7.00).



To a water suspension of **7** (200 mg, 0.68 mmol), was added HCl (1.40 mmol). The suspension was stirred for 1 hr at room temperature. The volatiles were removed under reduced pressure to give **43** as a brown-orange solid. Yield = 250 mg, 99%. ^1H NMR (400 MHz, CD_3OD) δ 1.57 (m, 2H, *c*-hex- CH_2), 1.89 (m, 4H, *c*-hex- CH_2), 2.19 (m, 2H, *c*-hex- CH_2), 3.86 (s, 6H, NCH_3), 4.32 (m, 2H, *c*-hex- CH), 6.93 (m, 2H, py- H^4), 7.66 (d, $^3J_{\text{H-H}} = 8.0$ Hz, 2H, py- H^2), 8.03 (m, 4H, py- H^3 and H^5); $^{13}\text{C}\{^1\text{H}\}$ NMR (100 MHz, CD_3OD) δ 25.4 (*c*-hex- CH_2), 32.8 (*c*-hex- CH_2), 43.7 (NCH_3), 57.8 (*c*-hex- CH), 112.9 (py- C^4), 114.4 (py- C^2), 142.7 (py- C^3), 144.5 (py- C^5), 154.3 (py- C^1); MS(Cl^+) m/z 298.0 ($[\text{M}-2\text{Cl}]^+$, 20 %), 297 (100, $[\text{M}-(2\text{Cl}+\text{H})]^+$).

6.3 Suzuki-Miyaura cross-coupling catalysed by a Pd/PYE-ligand system

All aryl halides and phenylboronic acid (Aldrich or Alfa Aesar) were used as received. 1,4-Dioxane (anhydrous, Aldrich) was distilled under nitrogen from sodium benzophenone ketyl. Cesium carbonate (Aldrich) were stored in desiccators. Palladium acetate was purchased from Precious Metals. Flash chromatography was performed on silica gel 60 Å (230-400 mesh) (Aldrich).

Under an atmosphere of argon 1,4-dioxane (3 mL), aryl halide (1 mmol), Cs₂CO₃ (2.0 mmol) and arylboronic acid (1.5 mmol) were added in turn to a carousel tube charged with Pd(OAc)₂ (0.03 mmol), PYE ligand (0.03 mmol), and a magnetic stirring bar. Stirred at 80 °C for three hours. The mixture was then allowed to cool at room temperature. The mixture was purified either directly by flash chromatography, or filtered through a pad of celite, concentrated, and then purified by flash chromatography (ethyl acetate/hexane, 5: 95 per volume).

The identity of every product was confirmed by comparison with literature spectroscopic data: 4-methylbiphenyl,⁷ 2,4,6-trimethylbiphenyl,⁸ 3,5-bis(trifluoromethyl)-biphenyl⁹ and 4-Aminobiphenyl.¹⁰

6.4 Enantioselective addition of diethylzinc to aldehyde

Under argon to a predried vial were added PYE ligand (0.1 mmol), BINOL (0.1 mmol), CH₂Cl₂ (1 mL), and diethylzinc (2 mL of 1 M solution in hexane, 2 mmol) at room temperature. The vial was cooled to 0 °C, and then benzaldehyde (106 mg, 1 mmol) was introduced dropwise by a syringe. After stirring at 0 °C, water (2 mL) was added to quench the reaction. The aqueous layer was extracted with diethyl ether, and the combined organic phase was washed with brine and then dried over anhydrous MgSO₄. After removal of the solvent, the residue was analysed by ¹H NMR spectroscopy to determine the benzaldehyde conversion. The enantioselective excess (ee %) was determined by HPLC on Daicel OD column: hexane/2-propanol (99/1); flow rate 0.8 mL min⁻¹; UV detection at λ = 254 nm; retention time = 22.9 min (R), 26.0 (S).

6.5 Cell culture and MTT assay

MCF-7 (human breast adenocarcinoma cell line), HT-29 (human colon carcinoma cell line) and DLD-1 (human colon carcinoma cell line) were cultured at 37°C under humidified 95% air / 5% CO₂ in RPMI-1640 medium (Sigma) supplemented with 10% Fetal Bovine Serum (FBS, Sigma), 2 mM L-Glutamine (Sigma) and 0.11 mg/mL Sodium Pyruvate (Sigma). Cells from a confluent monolayer were removed from flasks by a 0.25% Trypsin-EDTA solution (Sigma).

The assay was carried out in 96 well plates with an average of 2×10^4 cells per mL with 100 μ L in each well. Treatment solution of all testing compounds with ten different concentrations (0.2-100 μ M) was prepared with culture medium. DMSO as co-solvent in solution of all compounds was limited to less than 1%. After an incubation of 96 hr, a 20 μ L aqua solution of MTT (5 mg mL⁻¹) was added to each well of the plate. The plate was further incubated for 4 hr at 37°C during which time purple formazan crystals formed at the bottom of the wells. The solution of each well was carefully removed leaving the formazan crystals which were dissolved in DMSO (150 μ L). The absorbance of each well was measured at 540 nm using a microplate reader (Multiskan Ex, Thermo Electron Corporation). The IC₅₀ was determined by plotting the percentage of cell viability vs. drug concentration (logarithmic scale) and finding the concentration at which 50% of the cells were viable relative to the control.

6.6 References

1. S. Komiya, *Synthesis of Organometallic Compounds: A Practice Guide*, 1997.
2. D. Drew and J. R. Doyle, *Inorg. Synth.*, 1990, **28**, 348.
3. Y. T. Park, C. H. Joo and L. H. Lee, *Bull. Korean Chem. Soc.*, 1990, **11**, 270-271.
4. C. Hirel, K. E. Vostrikova, J. Pecaut, V. I. Ovcharenko and P. Rey, *Chem. Eur. J.*, 2001, **7**, 2007-2014.
5. J. A. McCleverty and G. Wilkinson, *Inorg. Synth.*, 1990, **28**, 84.
6. P. K. Byers and A. J. Canty, *Organometallics*, 1990, **9**, 210-220.
7. M. S. C. Rao and G. S. K. Rao, *Synthesis*, 1987, 231.
8. J. C. Anderson, H. Namli and C. A. Roberts, *Tetrahedron*, 1997, **53**, 15123.
9. Z. Liu, T. Zhang and M. Shi, *Organometallics*, 2008, **27**, 2668-2671.
10. J. Zhou, X. M. Guo, C. Z. Tu, X. Y. Li and H. J. Sun, *J. Orgnomet. Chem*, 2009, **694**, 696-702.

Appendix 1

Single crystal X-ray structure data for [Me₂N⁺C₆H₁₀N⁻Me] (7)

Table 1. Crystal data and structure refinement for 7.

Identification code	7	
Empirical formula	C ₁₈ H ₂₄ N ₄	
Formula weight	296.41	
Temperature	110(2) K	
Wavelength	0.71073 Å	
Crystal system	Tetragonal	
Space group	P4(3)2(1)2	
Unit cell dimensions	a = 9.8908(4) Å	a = 90°.
	b = 9.8908(4) Å	b = 90°.
	c = 16.2853(8) Å	g = 90°.
Volume	1593.16(12) Å ³	
Z	4	
Density (calculated)	1.236 Mg/m ³	
Absorption coefficient	0.075 mm ⁻¹	
F(000)	640	
Crystal size	0.27 x 0.20 x 0.17 mm ³	
Theta range for data collection	2.41 to 30.05°.	
Index ranges	-13<=h<=13, -13<=k<=13, -22<=l<=22	
Reflections collected	21224	
Independent reflections	2316 [R(int) = 0.0355]	
Completeness to theta = 30.05°	99.9 %	
Absorption correction	Semi-empirical from equivalents	
Max. and min. transmission	0.990 and 0.807	
Refinement method	Full-matrix least-squares on F ²	
Data / restraints / parameters	2316 / 0 / 101	
Goodness-of-fit on F ²	1.134	
Final R indices [I>2sigma(I)]	R1 = 0.0386, wR2 = 0.0900	
R indices (all data)	R1 = 0.0397, wR2 = 0.0905	
Absolute structure parameter	-1(2)	
Largest diff. peak and hole	0.246 and -0.193 e.Å ⁻³	

Table 2. Atomic coordinates ($\times 10^4$) and equivalent isotropic displacement parameters ($\text{\AA}^2 \times 10^3$) for **7**. $U(\text{eq})$ is defined as one third of the trace of the orthogonalized U^{ij} tensor.

	x	y	z	$U(\text{eq})$
C(1)	330(1)	8648(1)	590(1)	17(1)
C(2)	713(1)	7889(1)	-135(1)	21(1)
C(3)	195(1)	6656(1)	-307(1)	24(1)
C(4)	-768(1)	6055(1)	223(1)	28(1)
C(5)	-1128(1)	6739(1)	907(1)	25(1)
C(6)	-1012(1)	8643(1)	1858(1)	27(1)
C(7)	1547(1)	10655(1)	285(1)	17(1)
C(8)	2461(1)	11564(1)	807(1)	20(1)
C(9)	3350(1)	12478(1)	282(1)	20(1)
N(1)	712(1)	9839(1)	827(1)	19(1)
N(2)	-592(1)	7966(1)	1102(1)	20(1)

Table 3. Bond lengths [\AA] and angles [$^\circ$] for **7**.

C(5)-C(4)	1.3509(17)	C(8)-H(8b)	0.9900
C(5)-N(2)	1.3628(14)	C(8)-H(8a)	0.9900
C(5)-H(5)	0.9500	C(9)-C(9)#1	1.528(2)
C(4)-C(3)	1.4162(17)	C(9)-H(9a)	0.9900
C(4)-H(4)	0.9500	C(9)-H(9b)	0.9900
C(3)-C(2)	1.3527(16)	C(6)-N(2)	1.4611(16)
C(3)-H(3)	0.9500	C(6)-H(6a)	0.9800
C(2)-C(1)	1.4496(16)	C(6)-H(6c)	0.9800
C(2)-H(2)	0.9500	C(6)-H(6b)	0.9800
C(1)-N(1)	1.2960(15)		
C(1)-N(2)	1.4078(14)	C(4)-C(5)-N(2)	122.44(11)
C(7)-N(1)	1.4542(14)	C(4)-C(5)-H(5)	118.8
C(7)-C(8)	1.5330(15)	N(2)-C(5)-H(5)	118.8
C(7)-C(7)#1	1.554(2)	C(5)-C(4)-C(3)	118.01(11)
C(7)-H(7)	1.0000	C(5)-C(4)-H(4)	121.0
C(8)-C(9)	1.5230(16)	C(3)-C(4)-H(4)	121.0

C(2)-C(3)-C(4)	120.46(11)	H(8b)-C(8)-H(8a)	107.9
C(2)-C(3)-H(3)	119.8	C(8)-C(9)-C(9)#1	110.29(8)
C(4)-C(3)-H(3)	119.8	C(8)-C(9)-H(9a)	109.6
C(3)-C(2)-C(1)	122.48(11)	C(9)#1-C(9)-H(9a)	109.6
C(3)-C(2)-H(2)	118.8	C(8)-C(9)-H(9b)	109.6
C(1)-C(2)-H(2)	118.8	C(9)#1-C(9)-H(9b)	109.6
N(1)-C(1)-N(2)	116.59(10)	H(9a)-C(9)-H(9b)	108.1
N(1)-C(1)-C(2)	129.59(10)	N(2)-C(6)-H(6a)	109.5
N(2)-C(1)-C(2)	113.83(10)	N(2)-C(6)-H(6c)	109.5
N(1)-C(7)-C(8)	108.86(9)	H(6a)-C(6)-H(6c)	109.5
N(1)-C(7)-C(7)#1	110.79(8)	N(2)-C(6)-H(6b)	109.5
C(8)-C(7)-C(7)#1	109.45(7)	H(6a)-C(6)-H(6b)	109.5
N(1)-C(7)-H(7)	109.2	H(6c)-C(6)-H(6b)	109.5
C(8)-C(7)-H(7)	109.2	C(5)-N(2)-C(1)	122.70(10)
C(7)#1-C(7)-H(7)	109.2	C(5)-N(2)-C(6)	119.62(10)
C(9)-C(8)-C(7)	112.13(9)	C(1)-N(2)-C(6)	117.64(9)
C(9)-C(8)-H(8b)	109.2	C(1)-N(1)-C(7)	119.29(9)
C(7)-C(8)-H(8b)	109.2		
C(9)-C(8)-H(8a)	109.2	Symmetry transformations used to generate	
C(7)-C(8)-H(8a)	109.2	equivalent atoms: #1 y-1,x+1,-z	

Table 4. Anisotropic displacement parameters ($\text{\AA}^2 \times 10^3$) for **7**. The anisotropic displacement factor exponent takes the form: $-2p^2 [h^2 a^{*2} U^{11} + \dots + 2 h k a^* b^* U^{12}]$

	U^{11}	U^{22}	U^{33}	U^{23}	U^{13}	U^{12}
C(1)	16(1)	18(1)	18(1)	2(1)	0(1)	1(1)
C(2)	20(1)	20(1)	23(1)	0(1)	2(1)	0(1)
C(3)	28(1)	20(1)	24(1)	-4(1)	1(1)	0(1)
C(4)	32(1)	20(1)	31(1)	-3(1)	1(1)	-9(1)
C(5)	26(1)	20(1)	28(1)	3(1)	4(1)	-6(1)
C(6)	36(1)	22(1)	23(1)	-1(1)	10(1)	-5(1)
C(7)	17(1)	15(1)	17(1)	-1(1)	0(1)	-2(1)
C(8)	22(1)	19(1)	19(1)	2(1)	-4(1)	-3(1)
C(9)	17(1)	19(1)	23(1)	0(1)	-3(1)	-4(1)

N(1)	20(1)	17(1)	19(1)	1(1)	1(1)	-2(1)
N(2)	22(1)	17(1)	21(1)	0(1)	3(1)	-2(1)

Table 5. Hydrogen coordinates ($\times 10^4$) and isotropic displacement parameters ($\text{\AA}^2 \times 10^{-3}$) for **7**.

	x	y	z	U(eq)
H(2)	1352	8273	-503	25
H(3)	479	6189	-787	29
H(4)	-1150	5196	101	33
H(5)	-1779	6349	1265	29
H(6a)	-1737	8122	2119	40
H(6c)	-1340	9553	1729	40
H(6b)	-240	8706	2233	40
H(7)	2121	10047	-60	20
H(8b)	1892	12130	1171	24
H(8a)	3043	10992	1159	24
H(9a)	3971	11918	-52	23
H(9b)	3902	13066	642	23

Table 6. Torsion angles [$^\circ$] for **7**.

N(2)-C(5)-C(4)-C(3)	-0.5(2)	N(1)-C(1)-N(2)-C(5)	176.61(11)
C(5)-C(4)-C(3)-C(2)	-1.2(2)	C(2)-C(1)-N(2)-C(5)	-3.43(16)
C(4)-C(3)-C(2)-C(1)	0.53(19)	N(1)-C(1)-N(2)-C(6)	-1.32(15)
C(3)-C(2)-C(1)-N(1)	-178.35(12)	C(2)-C(1)-N(2)-C(6)	178.65(11)
C(3)-C(2)-C(1)-N(2)	1.70(16)	N(2)-C(1)-N(1)-C(7)	-173.45(10)
N(1)-C(7)-C(8)-C(9)	-178.74(9)	C(2)-C(1)-N(1)-C(7)	6.60(18)
C(7)#1-C(7)-C(8)-C(9)	-57.51(13)	C(8)-C(7)-N(1)-C(1)	-149.62(10)
C(7)-C(8)-C(9)-C(9)#1	57.51(14)	C(7)#1-C(7)-N(1)-C(1)	89.98(13)
C(4)-C(5)-N(2)-C(1)	2.99(19)		
C(4)-C(5)-N(2)-C(6)	-179.12(13)		

Symmetry transformations used to generate equivalent atoms: #1 y-1,x+1,-z

Single crystal X-ray structure data for [MeN(C₆H₄)NMe] (12)

Table 1. Crystal data and structure refinement for **12**.

Identification code	12	
Empirical formula	C ₁₈ H ₁₈ N ₄	
Formula weight	290.36	
Temperature	110(2) K	
Wavelength	0.71073 Å	
Crystal system	Orthorhombic	
Space group	Pbca	
Unit cell dimensions	a = 8.7699(7) Å	a = 90°.
	b = 12.4164(10) Å	b = 90°.
	c = 27.659(2) Å	g = 90°.
Volume	3011.8(4) Å ³	
Z	8	
Density (calculated)	1.281 Mg/m ³	
Absorption coefficient	0.079 mm ⁻¹	
F(000)	1232	
Crystal size	0.12 x 0.12 x 0.08 mm ³	
Theta range for data collection	2.75 to 28.34°.	
Index ranges	-11 ≤ h ≤ 11, -16 ≤ k ≤ 16, -36 ≤ l ≤ 36	
Reflections collected	28903	
Independent reflections	3754 [R(int) = 0.0603]	
Completeness to theta = 28.34°	99.8 %	
Absorption correction	Semi-empirical from equivalents	
Max. and min. transmission	0.998 and 0.862	
Refinement method	Full-matrix least-squares on F ²	
Data / restraints / parameters	3754 / 0 / 201	
Goodness-of-fit on F ²	1.025	
Final R indices [I > 2σ(I)]	R1 = 0.0421, wR2 = 0.0886	
R indices (all data)	R1 = 0.0721, wR2 = 0.1000	
Largest diff. peak and hole	0.178 and -0.198 e.Å ⁻³	

Table 2. Atomic coordinates ($\times 10^4$) and equivalent isotropic displacement parameters ($\text{\AA}^2 \times 10^3$) for **12**. $U(\text{eq})$ is defined as one third of the trace of the orthogonalized U^{ij} tensor.

	x	y	z	$U(\text{eq})$
C(1)	13769(2)	4060(1)	3974(1)	28(1)
C(2)	14603(2)	4818(1)	4202(1)	33(1)
C(3)	13842(2)	5748(1)	4381(1)	33(1)
C(4)	12319(2)	5866(1)	4318(1)	26(1)
C(5)	11413(1)	5061(1)	4079(1)	20(1)
C(6)	9100(1)	5961(1)	4168(1)	21(1)
C(7)	8532(2)	5984(1)	4640(1)	26(1)
C(8)	7607(2)	6816(1)	4801(1)	29(1)
C(9)	7214(2)	7644(1)	4489(1)	25(1)
C(10)	7757(1)	7628(1)	4018(1)	23(1)
C(11)	8695(1)	6800(1)	3848(1)	20(1)
C(12)	8909(1)	6149(1)	3061(1)	23(1)
C(13)	7918(2)	5237(1)	3134(1)	26(1)
C(14)	7546(2)	4561(1)	2770(1)	38(1)
C(15)	8119(2)	4738(2)	2299(1)	46(1)
C(16)	9064(2)	5574(1)	2225(1)	40(1)
C(17)	11350(2)	3299(1)	3684(1)	29(1)
C(18)	10532(2)	7142(1)	2497(1)	37(1)
N(1)	12222(1)	4158(1)	3916(1)	23(1)
N(2)	9955(1)	5065(1)	4003(1)	23(1)
N(3)	9285(1)	6886(1)	3373(1)	23(1)
N(4)	9485(1)	6258(1)	2591(1)	28(1)

Table 3. Bond lengths [\AA] and angles [$^\circ$] for **12**.

C(1)-C(2)	1.347(2)	C(3)-C(4)	1.3547(19)
C(1)-N(1)	1.3716(17)	C(3)-H(3)	0.9500
C(1)-H(1)	0.9500	C(4)-C(5)	1.4371(18)
C(2)-C(3)	1.423(2)	C(4)-H(4)	0.9500
C(2)-H(2)	0.9500	C(5)-N(2)	1.2960(17)

C(5)-N(1)	1.4012(16)	C(1)-C(2)-C(3)	118.32(13)
C(6)-C(7)	1.3973(18)	C(1)-C(2)-H(2)	120.8
C(6)-C(11)	1.4109(18)	C(3)-C(2)-H(2)	120.8
C(6)-N(2)	1.4161(16)	C(4)-C(3)-C(2)	120.36(14)
C(7)-C(8)	1.3880(19)	C(4)-C(3)-H(3)	119.8
C(7)-H(7)	0.9500	C(2)-C(3)-H(3)	119.8
C(8)-C(9)	1.3848(19)	C(3)-C(4)-C(5)	121.94(13)
C(8)-H(8)	0.9500	C(3)-C(4)-H(4)	119.0
C(9)-C(10)	1.3874(18)	C(5)-C(4)-H(4)	119.0
C(9)-H(9)	0.9500	N(2)-C(5)-N(1)	116.82(12)
C(10)-C(11)	1.3981(17)	N(2)-C(5)-C(4)	128.11(12)
C(10)-H(10)	0.9500	N(1)-C(5)-C(4)	115.07(11)
C(11)-N(3)	1.4186(16)	C(7)-C(6)-C(11)	118.65(12)
C(12)-N(3)	1.2997(17)	C(7)-C(6)-N(2)	120.30(12)
C(12)-N(4)	1.4015(16)	C(11)-C(6)-N(2)	120.83(11)
C(12)-C(13)	1.4414(19)	C(8)-C(7)-C(6)	121.64(12)
C(13)-C(14)	1.3494(19)	C(8)-C(7)-H(7)	119.2
C(13)-H(13)	0.9500	C(6)-C(7)-H(7)	119.2
C(14)-C(15)	1.413(2)	C(9)-C(8)-C(7)	119.81(12)
C(14)-H(14)	0.9500	C(9)-C(8)-H(8)	120.1
C(15)-C(16)	1.344(2)	C(7)-C(8)-H(8)	120.1
C(15)-H(15)	0.9500	C(8)-C(9)-C(10)	119.30(12)
C(16)-N(4)	1.372(2)	C(8)-C(9)-H(9)	120.3
C(16)-H(16)	0.9500	C(10)-C(9)-H(9)	120.3
C(17)-N(1)	1.4609(17)	C(9)-C(10)-C(11)	121.83(12)
C(17)-H(17A)	0.9800	C(9)-C(10)-H(10)	119.1
C(17)-H(17B)	0.9800	C(11)-C(10)-H(10)	119.1
C(17)-H(17C)	0.9800	C(10)-C(11)-C(6)	118.76(12)
C(18)-N(4)	1.4542(19)	C(10)-C(11)-N(3)	118.08(11)
C(18)-H(18A)	0.9800	C(6)-C(11)-N(3)	122.99(11)
C(18)-H(18B)	0.9800	N(3)-C(12)-N(4)	117.11(12)
C(18)-H(18C)	0.9800	N(3)-C(12)-C(13)	127.85(12)
		N(4)-C(12)-C(13)	115.01(12)
C(2)-C(1)-N(1)	121.97(13)	C(14)-C(13)-C(12)	122.03(14)
C(2)-C(1)-H(1)	119.0	C(14)-C(13)-H(13)	119.0
N(1)-C(1)-H(1)	119.0	C(12)-C(13)-H(13)	119.0

C(13)-C(14)-C(15)	120.28(16)	N(4)-C(18)-H(18B)	109.5
C(13)-C(14)-H(14)	119.9	H(18A)-C(18)-H(18B)	109.5
C(15)-C(14)-H(14)	119.9	N(4)-C(18)-H(18C)	109.5
C(16)-C(15)-C(14)	118.63(15)	H(18A)-C(18)-H(18C)	109.5
C(16)-C(15)-H(15)	120.7	H(18B)-C(18)-H(18C)	109.5
C(14)-C(15)-H(15)	120.7	C(1)-N(1)-C(5)	122.32(12)
C(15)-C(16)-N(4)	122.18(15)	C(1)-N(1)-C(17)	120.29(11)
C(15)-C(16)-H(16)	118.9	C(5)-N(1)-C(17)	117.39(11)
N(4)-C(16)-H(16)	118.9	C(5)-N(2)-C(6)	118.25(11)
N(1)-C(17)-H(17A)	109.5	C(12)-N(3)-C(11)	118.00(11)
N(1)-C(17)-H(17B)	109.5	C(16)-N(4)-C(12)	121.79(13)
H(17A)-C(17)-H(17B)	109.5	C(16)-N(4)-C(18)	120.38(12)
N(1)-C(17)-H(17C)	109.5	C(12)-N(4)-C(18)	117.82(12)
H(17A)-C(17)-H(17C)	109.5		
H(17B)-C(17)-H(17C)	109.5		
N(4)-C(18)-H(18A)	109.5		

Symmetry transformations used to generate
equivalent atoms:

Table 4. Anisotropic displacement parameters ($\text{\AA}^2 \times 10^3$) **12**. The anisotropic displacement factor exponent takes the form: $-2p^2[h^2 a^{*2}U^{11} + \dots + 2 h k a^* b^* U^{12}]$

	U^{11}	U^{22}	U^{33}	U^{23}	U^{13}	U^{12}
C(1)	25(1)	32(1)	29(1)	7(1)	5(1)	9(1)
C(2)	20(1)	43(1)	37(1)	5(1)	1(1)	4(1)
C(3)	27(1)	36(1)	35(1)	0(1)	-2(1)	-6(1)
C(4)	26(1)	25(1)	27(1)	1(1)	0(1)	0(1)
C(5)	23(1)	21(1)	17(1)	4(1)	2(1)	3(1)
C(6)	17(1)	21(1)	25(1)	-3(1)	-3(1)	0(1)
C(7)	28(1)	30(1)	22(1)	2(1)	-3(1)	4(1)
C(8)	29(1)	36(1)	21(1)	-3(1)	1(1)	3(1)
C(9)	23(1)	25(1)	28(1)	-6(1)	0(1)	3(1)
C(10)	22(1)	18(1)	28(1)	0(1)	-1(1)	-1(1)
C(11)	18(1)	20(1)	23(1)	-2(1)	0(1)	-4(1)
C(12)	22(1)	25(1)	21(1)	2(1)	0(1)	8(1)
C(13)	23(1)	28(1)	27(1)	-2(1)	-5(1)	2(1)

C(14)	30(1)	39(1)	44(1)	-15(1)	-9(1)	0(1)
C(15)	41(1)	61(1)	37(1)	-23(1)	-10(1)	7(1)
C(16)	41(1)	58(1)	21(1)	-7(1)	-3(1)	21(1)
C(17)	32(1)	21(1)	34(1)	-2(1)	4(1)	1(1)
C(18)	43(1)	34(1)	35(1)	10(1)	18(1)	13(1)
N(1)	23(1)	22(1)	24(1)	3(1)	2(1)	3(1)
N(2)	23(1)	21(1)	24(1)	-1(1)	-1(1)	3(1)
N(3)	26(1)	20(1)	24(1)	1(1)	4(1)	1(1)
N(4)	31(1)	33(1)	22(1)	2(1)	3(1)	11(1)

Table 5. Hydrogen coordinates ($\times 10^4$) and isotropic displacement parameters ($\text{\AA}^2 \times 10^3$) for **12**.

	x	y	z	U(eq)
H(1)	14268	3440	3850	34
H(2)	15672	4733	4241	40
H(3)	14404	6290	4545	39
H(4)	11836	6500	4434	31
H(7)	8785	5416	4855	32
H(8)	7245	6819	5125	34
H(9)	6579	8215	4597	30
H(10)	7484	8197	3805	28
H(13)	7514	5108	3447	31
H(14)	6897	3964	2831	45
H(15)	7842	4275	2040	55
H(16)	9452	5695	1909	48
H(17A)	12050	2740	3568	43
H(17B)	10778	3595	3411	43
H(17C)	10639	2985	3918	43
H(18A)	10848	7124	2157	56
H(18B)	11431	7069	2705	56
H(18C)	10023	7828	2565	56

Table 6. Torsion angles [°] for **12**.

N(1)-C(1)-C(2)-C(3)	-0.7(2)	C(2)-C(1)-N(1)-C(17)	-177.61(13)
C(1)-C(2)-C(3)-C(4)	-0.7(2)	N(2)-C(5)-N(1)-C(1)	179.83(11)
C(2)-C(3)-C(4)-C(5)	1.2(2)	C(4)-C(5)-N(1)-C(1)	-1.01(17)
C(3)-C(4)-C(5)-N(2)	178.69(13)	N(2)-C(5)-N(1)-C(17)	-0.98(16)
C(3)-C(4)-C(5)-N(1)	-0.35(18)	C(4)-C(5)-N(1)-C(17)	178.18(11)
C(11)-C(6)-C(7)-C(8)	-1.1(2)	N(1)-C(5)-N(2)-C(6)	179.36(11)
N(2)-C(6)-C(7)-C(8)	-175.68(12)	C(4)-C(5)-N(2)-C(6)	0.33(19)
C(6)-C(7)-C(8)-C(9)	0.8(2)	C(7)-C(6)-N(2)-C(5)	-87.13(15)
C(7)-C(8)-C(9)-C(10)	-0.2(2)	C(11)-C(6)-N(2)-C(5)	98.38(14)
C(8)-C(9)-C(10)-C(11)	-0.05(19)	N(4)-C(12)-N(3)-C(11)	179.05(11)
C(9)-C(10)-C(11)-C(6)	-0.27(18)	C(13)-C(12)-N(3)-C(11)	1.37(19)
C(9)-C(10)-C(11)-N(3)	-175.68(12)	C(10)-C(11)-N(3)-C(12)	-118.44(13)
C(7)-C(6)-C(11)-C(10)	0.81(18)	C(6)-C(11)-N(3)-C(12)	66.35(16)
N(2)-C(6)-C(11)-C(10)	175.39(11)	C(15)-C(16)-N(4)-C(12)	-2.4(2)
C(7)-C(6)-C(11)-N(3)	175.98(12)	C(15)-C(16)-N(4)-C(18)	178.91(14)
N(2)-C(6)-C(11)-N(3)	-9.44(18)	N(3)-C(12)-N(4)-C(16)	-174.76(12)
N(3)-C(12)-C(13)-C(14)	175.97(14)	C(13)-C(12)-N(4)-C(16)	3.22(18)
N(4)-C(12)-C(13)-C(14)	-1.76(19)	N(3)-C(12)-N(4)-C(18)	3.95(17)
C(12)-C(13)-C(14)-C(15)	-0.6(2)	C(13)-C(12)-N(4)-C(18)	-178.07(11)
C(13)-C(14)-C(15)-C(16)	1.5(2)		
C(14)-C(15)-C(16)-N(4)	-0.1(2)		
C(2)-C(1)-N(1)-C(5)	1.6(2)		

Symmetry transformations used to generate equivalent atoms:

Single crystal X-ray structure data for [MeN(CH₂)₂NMe][H⁺]₂ (16)

Table 1. Crystal data and structure refinement for **16**.

Identification code	16	
Empirical formula	C ₁₆ H ₂₈ Br ₂ N ₄ O ₂	
Formula weight	468.24	
Temperature	383(2) K	
Wavelength	0.71073 Å	
Crystal system	Monoclinic	
Space group	P2(1)/n	
Unit cell dimensions	a = 4.8543(9) Å	a = 90°.
	b = 10.9428(19) Å	b = 90.032(4)°.
	c = 18.632(3) Å	g = 90°.
Volume	989.7(3) Å ³	
Z	2	
Density (calculated)	1.571 Mg/m ³	
Absorption coefficient	4.111 mm ⁻¹	
F(000)	476	
Crystal size	0.31 x 0.06 x 0.03 mm ³	
Theta range for data collection	1.09 to 28.33°.	
Index ranges	-5 ≤ h ≤ 6, -14 ≤ k ≤ 14, -24 ≤ l ≤ 18	
Reflections collected	7132	
Independent reflections	2463 [R(int) = 0.0374]	
Completeness to theta = 28.33°	99.4 %	
Absorption correction	Semi-empirical from equivalents	
Max. and min. transmission	0.880 and 0.568	
Refinement method	Full-matrix least-squares on F ²	
Data / restraints / parameters	2463 / 1 / 138	
Goodness-of-fit on F ²	0.997	
Final R indices [I > 2σ(I)]	R1 = 0.0321, wR2 = 0.0688	
R indices (all data)	R1 = 0.0398, wR2 = 0.0709	
Largest diff. peak and hole	0.574 and -0.448 e.Å ⁻³	

Table 2. Atomic coordinates ($\times 10^4$) and equivalent isotropic displacement parameters ($\text{\AA}^2 \times 10^3$) for **16**. $U(\text{eq})$ is defined as one third of the trace of the orthogonalized U^{ij} tensor.

	x	y	z	$U(\text{eq})$
Br(1)	772(1)	8525(1)	8508(1)	23(1)
C(1)	6820(7)	1481(3)	8884(2)	18(1)
C(2)	8246(7)	2249(3)	9368(2)	21(1)
C(3)	10108(7)	3079(3)	9115(2)	23(1)
C(4)	10663(9)	3159(3)	8373(2)	23(1)
C(5)	9298(9)	2418(3)	7927(1)	21(1)
C(6)	6067(8)	770(3)	7651(2)	24(1)
C(7)	4071(8)	465(3)	9820(1)	20(1)
N(1)	4882(5)	685(3)	9082(1)	19(1)
N(2)	7427(6)	1592(2)	8167(1)	18(1)
C(8A)	5580(20)	5983(18)	9197(7)	29(3)
O(1A)	3493(15)	5824(5)	8693(4)	40(2)
C(8B)	5250(30)	5830(40)	9095(18)	73(12)
O(1B)	2390(20)	5861(8)	9158(7)	41(4)

Table 3. Bond lengths [\AA] and angles [$^\circ$] for **16**.

C(1)-N(1)	1.334(4)	C(7)-H(7a)	0.9700
C(1)-N(2)	1.374(4)	C(7)-H(7b)	0.9700
C(1)-C(2)	1.413(4)	C(6)-N(2)	1.473(4)
C(2)-C(3)	1.366(5)	C(6)-H(6a)	0.9600
C(2)-H(2)	0.9300	C(6)-H(6b)	0.9600
C(3)-C(4)	1.412(4)	C(6)-H(6c)	0.9600
C(3)-H(3)	0.9300	N(1)-H(2)	0.90(4)
C(4)-C(5)	1.337(5)	C(8A)-O(1A)	1.393(10)
C(4)-H(4)	0.9300	C(8A)-H(8A1)	0.9600
C(5)-N(2)	1.358(4)	C(8A)-H(8A2)	0.9600
C(5)-H(5)	0.9300	C(8A)-H(8A3)	0.9600
C(7)-N(1)	1.451(4)	O(1A)-H(1A)	0.8200
C(7)-C(7)#1	1.515(6)	C(8B)-O(1B)	1.393(11)

C(8B)-H(8B1)	0.9600	C(7)#1-C(7)-H(7b)	109.3
C(8B)-H(8B2)	0.9600	H(7a)-C(7)-H(7b)	108.0
C(8B)-H(8B3)	0.9600	N(2)-C(6)-H(6a)	109.5
O(1B)-H(1B)	0.8200	N(2)-C(6)-H(6b)	109.5
		H(6a)-C(6)-H(6b)	109.5
N(1)-C(1)-N(2)	118.6(3)	N(2)-C(6)-H(6c)	109.5
N(1)-C(1)-C(2)	123.9(3)	H(6a)-C(6)-H(6c)	109.5
N(2)-C(1)-C(2)	117.5(3)	H(6b)-C(6)-H(6c)	109.5
C(3)-C(2)-C(1)	120.0(3)	C(5)-N(2)-C(1)	121.6(3)
C(3)-C(2)-H(2)	120.0	C(5)-N(2)-C(6)	119.4(3)
C(1)-C(2)-H(2)	120.0	C(1)-N(2)-C(6)	119.0(3)
C(2)-C(3)-C(4)	120.4(3)	C(1)-N(1)-C(7)	124.2(3)
C(2)-C(3)-H(3)	119.8	C(1)-N(1)-H(2)	126(2)
C(4)-C(3)-H(3)	119.8	C(7)-N(1)-H(2)	109(2)
C(5)-C(4)-C(3)	118.5(3)	O(1B)-C(8B)-H(8B1)	109.5
C(5)-C(4)-H(4)	120.8	O(1B)-C(8B)-H(8B2)	109.5
C(3)-C(4)-H(4)	120.8	H(8B1)-C(8B)-H(8B2)	109.5
C(4)-C(5)-N(2)	122.0(3)	O(1B)-C(8B)-H(8B3)	109.5
C(4)-C(5)-H(5)	119.0	H(8B1)-C(8B)-H(8B3)	109.5
N(2)-C(5)-H(5)	119.0	H(8B2)-C(8B)-H(8B3)	109.5
N(1)-C(7)-C(7)#1	111.6(3)	C(8B)-O(1B)-H(1B)	109.5
N(1)-C(7)-H(7a)	109.3		
C(7)#1-C(7)-H(7a)	109.3		
N(1)-C(7)-H(7b)	109.3		

Symmetry transformations used to generate
equivalent atoms: #1 -x+1,-y,-z+2

Table 4. Anisotropic displacement parameters ($\text{\AA}^2 \times 10^3$) for **16**. The anisotropic displacement factor exponent takes the form: $-2p^2 [h^2 a^{*2}U^{11} + \dots + 2 h k a^* b^* U^{12}]$

	U^{11}	U^{22}	U^{33}	U^{23}	U^{13}	U^{12}
Br(1)	22(1)	22(1)	27(1)	-3(1)	-1(1)	-2(1)
C(1)	19(2)	17(2)	18(1)	2(1)	-2(1)	3(1)
C(2)	28(2)	20(2)	16(1)	-1(1)	0(1)	2(1)
C(3)	27(2)	18(2)	25(2)	-2(1)	-7(1)	2(1)
C(4)	24(2)	20(1)	26(2)	8(1)	3(2)	0(2)

C(5)	27(2)	19(1)	16(1)	6(1)	-1(2)	1(2)
C(6)	35(2)	23(2)	13(1)	1(1)	-4(1)	-10(2)
C(7)	23(2)	20(1)	17(1)	1(1)	3(1)	-2(2)
N(1)	23(2)	19(1)	15(1)	0(1)	0(1)	-2(1)
N(2)	24(1)	17(1)	14(1)	2(1)	-3(1)	2(1)
C(8A)	37(5)	30(6)	19(3)	5(4)	2(5)	18(5)
O(1A)	42(3)	24(3)	55(5)	-9(2)	-15(3)	0(2)
C(8B)	70(20)	35(13)	110(30)	36(17)	36(19)	10(13)
O(1B)	33(5)	27(5)	62(8)	10(4)	-10(5)	-8(4)

Table 5. Hydrogen coordinates ($\times 10^4$) and isotropic displacement parameters ($\text{\AA}^2 \times 10^3$) for **16**.

	x	y	z	U(eq)
H(2)	7916	2189	9858	26
H(3)	11016	3595	9434	28
H(4)	11948	3715	8199	28
H(5)	9640	2471	7436	25
H(6a)	6606	987	7172	35
H(6b)	4105	845	7698	35
H(6c)	6603	-59	7748	35
H(7a)	2186	172	9831	24
H(7b)	4145	1227	10086	24
H(1)	4020(80)	140(30)	8793(17)	21(9)
H(8A1)	6581	6719	9091	43
H(8A2)	6814	5298	9180	43
H(8A3)	4792	6043	9668	43
H(1A)	2812	6490	8594	61
H(8B1)	5866	6559	8853	109
H(8B2)	5790	5127	8825	109
H(8B3)	6063	5799	9564	109
H(1B)	1792	6478	8963	61

Table 6. Torsion angles [°] for **16**.

N(1)-C(1)-C(2)-C(3)	-176.9(3)
N(2)-C(1)-C(2)-C(3)	1.2(5)
C(1)-C(2)-C(3)-C(4)	-1.3(5)
C(2)-C(3)-C(4)-C(5)	0.9(5)
C(3)-C(4)-C(5)-N(2)	-0.6(5)
C(4)-C(5)-N(2)-C(1)	0.6(5)
C(4)-C(5)-N(2)-C(6)	-177.7(3)
N(1)-C(1)-N(2)-C(5)	177.3(3)
C(2)-C(1)-N(2)-C(5)	-0.9(5)
N(1)-C(1)-N(2)-C(6)	-4.4(5)
C(2)-C(1)-N(2)-C(6)	177.4(3)
N(2)-C(1)-N(1)-C(7)	179.1(3)
C(2)-C(1)-N(1)-C(7)	-2.8(5)
C(7)#1-C(7)-N(1)-C(1)	-85.1(4)

Symmetry transformations used to generate equivalent atoms:

#1 -x+1,-y,-z+2

Table 7. Hydrogen bonds for **16** [Å and °].

D-H...A	d(D-H)	d(H...A)	d(D...A)	<(DHA)
N(1)-H(1)...Br(1)#2	0.90(4)	2.43(4)	3.273(3)	155(3)
O(1A)-H(1A)...Br(1)	0.82	2.44	3.255(6)	170.8
O(1B)-H(1B)...Br(1)	0.82	2.45	3.253(8)	168.4

Symmetry transformations used to generate equivalent atoms:

#1 -x+1,-y,-z+2 #2 x,y-1,z

Single crystal X-ray structure data for $[\text{NiCl}_2(\text{Me}_6\text{N}^{\text{C}_6\text{H}_{10}}\text{N}^{\text{Me}})]$ (**18**)

Table 1. Crystal data and structure refinement for **18**.

Identification code	18	
Empirical formula	C ₂₀ H ₂₇ Br ₂ N ₅ Ni	
Formula weight	556.00	
Temperature	110(2) K	
Wavelength	0.71073 Å	
Crystal system	Orthorhombic	
Space group	P2(1)2(1)2(1)	
Unit cell dimensions	a = 9.8785(6) Å	a = 90°.
	b = 11.1592(6) Å	b = 90°.
	c = 20.9780(12) Å	g = 90°.
Volume	2312.5(2) Å ³	
Z	4	
Density (calculated)	1.597 Mg/m ³	
Absorption coefficient	4.310 mm ⁻¹	
F(000)	1120	
Crystal size	0.25 x 0.15 x 0.15 mm ³	
Theta range for data collection	1.94 to 28.29°.	
Index ranges	-13 ≤ h ≤ 13, -14 ≤ k ≤ 14, -27 ≤ l ≤ 27	
Reflections collected	31966	
Independent reflections	5742 [R(int) = 0.0367]	
Completeness to theta = 28.29°	100.0 %	
Absorption correction	Semi-empirical from equivalents	
Max. and min. transmission	0.520 and 0.385	
Refinement method	Full-matrix least-squares on F ²	
Data / restraints / parameters	5742 / 0 / 256	
Goodness-of-fit on F ²	0.967	
Final R indices [I > 2σ(I)]	R1 = 0.0212, wR2 = 0.0442	
R indices (all data)	R1 = 0.0246, wR2 = 0.0447	
Absolute structure parameter	0.000(5)	
Largest diff. peak and hole	0.549 and -0.214 e.Å ⁻³	

Table 2. Atomic coordinates ($\times 10^4$) and equivalent isotropic displacement parameters ($\text{\AA}^2 \times 10^3$) for **18**. $U(\text{eq})$ is defined as one third of the trace of the orthogonalized U^{ij} tensor.

	x	y	z	$U(\text{eq})$
Br(1)	277(1)	-2224(1)	8950(1)	24(1)
Br(2)	-1387(1)	888(1)	8717(1)	28(1)
C(1)	802(2)	-1182(2)	10460(1)	18(1)
C(2)	1673(2)	-2069(2)	10723(1)	21(1)
C(3)	1194(2)	-3020(2)	11061(1)	26(1)
C(4)	-202(2)	-3141(2)	11171(1)	29(1)
C(5)	-1032(2)	-2295(2)	10927(1)	27(1)
C(6)	-1538(2)	-463(2)	10356(1)	31(1)
C(7)	2633(2)	18(2)	10090(1)	18(1)
C(8)	3167(2)	454(2)	10736(1)	24(1)
C(9)	4692(2)	652(2)	10701(1)	31(1)
C(10)	5075(2)	1511(2)	10162(1)	27(1)
C(11)	4437(2)	1134(2)	9533(1)	21(1)
C(12)	2898(2)	997(2)	9600(1)	18(1)
C(13)	2223(2)	1526(2)	8543(1)	21(1)
C(14)	2619(2)	2747(2)	8620(1)	25(1)
C(15)	2493(2)	3560(2)	8142(1)	33(1)
C(16)	1980(3)	3207(2)	7546(1)	37(1)
C(17)	1671(2)	2038(2)	7464(1)	32(1)
C(18)	1580(2)	-48(2)	7774(1)	30(1)
C(19)	5410(3)	1288(2)	7629(1)	42(1)
C(20)	6066(3)	2411(2)	7786(1)	40(1)
N(1)	1166(2)	-249(2)	10103(1)	17(1)
N(2)	-563(2)	-1343(2)	10588(1)	22(1)
N(3)	2210(2)	689(2)	8998(1)	19(1)
N(4)	1820(2)	1208(2)	7933(1)	24(1)
N(5)	4914(3)	412(2)	7510(2)	70(1)
Ni(1)	468(1)	-128(1)	9213(1)	19(1)

Table 3. Bond lengths [Å] and angles [°] for **18**.

Br(1)-Ni(1)	2.4106(4)	C(6)-H(6b)	0.9800
Br(2)-Ni(1)	2.3934(3)	C(6)-H(6c)	0.9800
C(7)-N(1)	1.480(2)	C(13)-N(3)	1.335(3)
C(7)-C(12)	1.522(3)	C(13)-N(4)	1.386(3)
C(7)-C(8)	1.534(3)	C(13)-C(14)	1.426(3)
C(7)-H(7)	1.0000	C(14)-C(15)	1.359(3)
C(8)-C(9)	1.524(3)	C(14)-H(14)	0.9500
C(8)-H(8a)	0.9900	C(15)-C(16)	1.404(4)
C(8)-H(8b)	0.9900	C(15)-H(15)	0.9500
C(9)-C(10)	1.529(3)	C(16)-C(17)	1.351(4)
C(9)-H(9a)	0.9900	C(16)-H(16)	0.9500
C(9)-H(9b)	0.9900	C(17)-N(4)	1.360(3)
C(10)-C(11)	1.521(3)	C(17)-H(17)	0.9500
C(10)-H(10b)	0.9900	C(18)-N(4)	1.461(3)
C(10)-H(10a)	0.9900	C(18)-H(18A)	0.9800
C(11)-C(12)	1.534(3)	C(18)-H(18B)	0.9800
C(11)-H(11b)	0.9900	C(18)-H(18C)	0.9800
C(11)-H(11a)	0.9900	N(1)-Ni(1)	1.9931(16)
C(12)-N(3)	1.476(2)	N(3)-Ni(1)	1.9990(16)
C(12)-H(12)	1.0000	C(19)-N(5)	1.122(3)
C(1)-N(1)	1.332(3)	C(19)-C(20)	1.448(4)
C(1)-N(2)	1.388(3)	C(20)-H(20A)	0.9800
C(1)-C(2)	1.424(3)	C(20)-H(20B)	0.9800
C(5)-C(4)	1.350(3)	C(20)-H(20C)	0.9800
C(5)-N(2)	1.360(3)		
C(5)-H(5)	0.9500	N(1)-C(7)-C(12)	108.96(16)
C(4)-C(3)	1.406(3)	N(1)-C(7)-C(8)	112.68(16)
C(4)-H(4)	0.9500	C(12)-C(7)-C(8)	108.02(17)
C(3)-C(2)	1.360(3)	N(1)-C(7)-H(7)	109.0
C(3)-H(3)	0.9500	C(12)-C(7)-H(7)	109.0
C(2)-H(2)	0.9500	C(8)-C(7)-H(7)	109.0
C(6)-N(2)	1.458(3)	C(9)-C(8)-C(7)	110.06(18)
C(6)-H(6a)	0.9800	C(9)-C(8)-H(8a)	109.6

C(7)-C(8)-H(8a)	109.6	C(3)-C(4)-H(4)	121.1
C(9)-C(8)-H(8b)	109.6	C(2)-C(3)-C(4)	120.1(2)
C(7)-C(8)-H(8b)	109.6	C(2)-C(3)-H(3)	119.9
H(8a)-C(8)-H(8b)	108.2	C(4)-C(3)-H(3)	119.9
C(8)-C(9)-C(10)	111.77(19)	C(3)-C(2)-C(1)	122.36(19)
C(8)-C(9)-H(9a)	109.3	C(3)-C(2)-H(2)	118.8
C(10)-C(9)-H(9a)	109.3	C(1)-C(2)-H(2)	118.8
C(8)-C(9)-H(9b)	109.3	N(2)-C(6)-H(6a)	109.5
C(10)-C(9)-H(9b)	109.3	N(2)-C(6)-H(6b)	109.5
H(9a)-C(9)-H(9b)	107.9	H(6a)-C(6)-H(6b)	109.5
C(11)-C(10)-C(9)	111.38(18)	N(2)-C(6)-H(6c)	109.5
C(11)-C(10)-H(10b)	109.4	H(6a)-C(6)-H(6c)	109.5
C(9)-C(10)-H(10b)	109.4	H(6b)-C(6)-H(6c)	109.5
C(11)-C(10)-H(10a)	109.4	N(3)-C(13)-N(4)	118.53(19)
C(9)-C(10)-H(10a)	109.4	N(3)-C(13)-C(14)	126.2(2)
H(10b)-C(10)-H(10a)	108.0	N(4)-C(13)-C(14)	115.32(19)
C(10)-C(11)-C(12)	110.99(18)	C(15)-C(14)-C(13)	122.0(2)
C(10)-C(11)-H(11b)	109.4	C(15)-C(14)-H(14)	119.0
C(12)-C(11)-H(11b)	109.4	C(13)-C(14)-H(14)	119.0
C(10)-C(11)-H(11a)	109.4	C(14)-C(15)-C(16)	120.2(2)
C(12)-C(11)-H(11a)	109.4	C(14)-C(15)-H(15)	119.9
H(11b)-C(11)-H(11a)	108.0	C(16)-C(15)-H(15)	119.9
N(3)-C(12)-C(7)	109.38(16)	C(17)-C(16)-C(15)	117.8(2)
N(3)-C(12)-C(11)	113.64(17)	C(17)-C(16)-H(16)	121.1
C(7)-C(12)-C(11)	107.68(17)	C(15)-C(16)-H(16)	121.1
N(3)-C(12)-H(12)	108.7	C(16)-C(17)-N(4)	122.7(2)
C(7)-C(12)-H(12)	108.7	C(16)-C(17)-H(17)	118.7
C(11)-C(12)-H(12)	108.7	N(4)-C(17)-H(17)	118.7
N(1)-C(1)-N(2)	118.20(18)	N(4)-C(18)-H(18A)	109.5
N(1)-C(1)-C(2)	126.86(18)	N(4)-C(18)-H(18B)	109.5
N(2)-C(1)-C(2)	114.93(19)	H(18A)-C(18)-H(18B)	109.5
C(4)-C(5)-N(2)	122.5(2)	N(4)-C(18)-H(18C)	109.5
C(4)-C(5)-H(5)	118.7	H(18A)-C(18)-H(18C)	109.5
N(2)-C(5)-H(5)	118.7	H(18B)-C(18)-H(18C)	109.5
C(5)-C(4)-C(3)	117.8(2)	C(1)-N(1)-C(7)	115.53(16)
C(5)-C(4)-H(4)	121.1	C(1)-N(1)-Ni(1)	119.12(13)

C(7)-N(1)-Ni(1)	107.96(12)	N(1)-Ni(1)-Br(1)	100.14(5)
C(13)-N(3)-C(12)	116.41(17)	N(3)-Ni(1)-Br(1)	117.27(5)
C(13)-N(3)-Ni(1)	119.27(13)	Br(2)-Ni(1)-Br(1)	107.433(12)
C(12)-N(3)-Ni(1)	108.00(12)	N(5)-C(19)-C(20)	179.2(3)
C(5)-N(2)-C(1)	122.26(19)	C(19)-C(20)-H(20A)	109.5
C(5)-N(2)-C(6)	118.43(18)	C(19)-C(20)-H(20B)	109.5
C(1)-N(2)-C(6)	119.31(18)	H(20A)-C(20)-H(20B)	109.5
C(17)-N(4)-C(13)	121.7(2)	C(19)-C(20)-H(20C)	109.5
C(17)-N(4)-C(18)	117.99(19)	H(20A)-C(20)-H(20C)	109.5
C(13)-N(4)-C(18)	120.28(18)	H(20B)-C(20)-H(20C)	109.5
N(1)-Ni(1)-N(3)	86.85(7)		
N(1)-Ni(1)-Br(2)	134.74(5)	Symmetry transformations used to generate	equivalent atoms:
N(3)-Ni(1)-Br(2)	110.17(5)		

Table 4. Anisotropic displacement parameters ($\text{\AA}^2 \times 10^3$) for **18**. The anisotropic displacement factor exponent takes the form: $-2p^2 [h^2 a^{*2} U^{11} + \dots + 2 h k a^* b^* U^{12}]$

	U^{11}	U^{22}	U^{33}	U^{23}	U^{13}	U^{12}
Br(1)	20(1)	23(1)	30(1)	-4(1)	-4(1)	-1(1)
Br(2)	22(1)	26(1)	35(1)	0(1)	-11(1)	5(1)
C(1)	16(1)	22(1)	18(1)	-6(1)	-3(1)	-1(1)
C(2)	18(1)	24(1)	21(1)	-1(1)	-3(1)	-2(1)
C(3)	31(1)	22(1)	24(1)	-1(1)	-4(1)	-1(1)
C(4)	36(1)	25(1)	25(1)	-2(1)	6(1)	-10(1)
C(5)	23(1)	33(1)	25(1)	-8(1)	7(1)	-11(1)
C(6)	18(1)	39(1)	35(1)	0(1)	2(1)	7(1)
C(7)	15(1)	17(1)	22(1)	0(1)	-2(1)	0(1)
C(8)	27(1)	25(1)	21(1)	1(1)	-6(1)	-5(1)
C(9)	25(1)	35(1)	31(1)	5(1)	-14(1)	-10(1)
C(10)	18(1)	27(1)	35(1)	0(1)	-4(1)	-7(1)
C(11)	16(1)	22(1)	26(1)	-1(1)	0(1)	-2(1)
C(12)	17(1)	16(1)	21(1)	-2(1)	-2(1)	0(1)
C(13)	16(1)	26(1)	20(1)	0(1)	2(1)	5(1)
C(14)	23(1)	27(1)	25(1)	4(1)	5(1)	4(1)

C(15)	32(1)	29(1)	37(1)	9(1)	14(1)	9(1)
C(16)	36(1)	45(2)	30(1)	18(1)	10(1)	17(1)
C(17)	27(1)	48(2)	22(1)	8(1)	2(1)	12(1)
C(18)	30(1)	39(1)	22(1)	-3(1)	-4(1)	1(1)
C(19)	31(1)	33(1)	61(2)	7(1)	12(1)	7(1)
C(20)	41(2)	34(1)	47(2)	9(1)	-7(1)	2(1)
N(1)	13(1)	19(1)	19(1)	-1(1)	-3(1)	1(1)
N(2)	16(1)	28(1)	22(1)	-4(1)	2(1)	-1(1)
N(3)	17(1)	22(1)	19(1)	2(1)	-1(1)	-1(1)
N(4)	21(1)	32(1)	19(1)	3(1)	1(1)	5(1)
N(5)	42(2)	39(2)	130(3)	-6(2)	18(2)	-3(1)
Ni(1)	15(1)	21(1)	21(1)	0(1)	-5(1)	0(1)

Table 5. Hydrogen coordinates ($\times 10^4$) and isotropic displacement parameters ($\text{\AA}^2 \times 10^{-3}$) for **18**.

	x	y	z	U(eq)
H(2)	2622	-1995	10662	25
H(3)	1805	-3604	11222	31
H(4)	-551	-3795	11410	34
H(5)	-1979	-2369	10995	33
H(6a)	-1744	-627	9907	46
H(6b)	-1153	343	10396	46
H(6c)	-2370	-515	10608	46
H(7)	3137	-721	9963	21
H(8a)	2713	1213	10854	29
H(8b)	2961	-149	11069	29
H(9a)	5149	-128	10631	37
H(9b)	5016	982	11111	37
H(10b)	4768	2330	10272	32
H(10a)	6072	1529	10115	32
H(11b)	4834	362	9394	26
H(11a)	4640	1742	9203	26
H(12)	2516	1767	9764	21

H(14)	2981	2999	9018	30
H(15)	2753	4370	8210	39
H(16)	1856	3771	7212	44
H(17)	1335	1785	7061	39
H(18A)	649	-264	7887	45
H(18B)	2213	-555	8011	45
H(18C)	1716	-167	7315	45
H(20A)	6182	2467	8249	60
H(20B)	5506	3079	7638	60
H(20C)	6954	2445	7579	60

Table 6. Torsion angles [°] for **18**.

N(1)-C(7)-C(8)-C(9)	177.13(17)	C(2)-C(1)-N(1)-C(7)	-13.1(3)
C(12)-C(7)-C(8)-C(9)	-62.5(2)	N(2)-C(1)-N(1)-Ni(1)	-60.8(2)
C(7)-C(8)-C(9)-C(10)	55.4(3)	C(2)-C(1)-N(1)-Ni(1)	118.0(2)
C(8)-C(9)-C(10)-C(11)	-51.2(3)	C(12)-C(7)-N(1)-C(1)	172.94(17)
C(9)-C(10)-C(11)-C(12)	54.5(2)	C(8)-C(7)-N(1)-C(1)	-67.2(2)
N(1)-C(7)-C(12)-N(3)	-48.5(2)	C(12)-C(7)-N(1)-Ni(1)	36.75(18)
C(8)-C(7)-C(12)-N(3)	-171.26(16)	C(8)-C(7)-N(1)-Ni(1)	156.62(14)
N(1)-C(7)-C(12)-C(11)	-172.48(16)	N(4)-C(13)-N(3)-C(12)	168.12(17)
C(8)-C(7)-C(12)-C(11)	64.8(2)	C(14)-C(13)-N(3)-C(12)	-11.8(3)
C(10)-C(11)-C(12)-N(3)	177.16(17)	N(4)-C(13)-N(3)-Ni(1)	-59.5(2)
C(10)-C(11)-C(12)-C(7)	-61.5(2)	C(14)-C(13)-N(3)-Ni(1)	120.5(2)
N(2)-C(5)-C(4)-C(3)	-0.6(3)	C(7)-C(12)-N(3)-C(13)	172.81(17)
C(5)-C(4)-C(3)-C(2)	0.7(3)	C(11)-C(12)-N(3)-C(13)	-66.8(2)
C(4)-C(3)-C(2)-C(1)	-1.3(3)	C(7)-C(12)-N(3)-Ni(1)	35.48(18)
N(1)-C(1)-C(2)-C(3)	-177.1(2)	C(11)-C(12)-N(3)-Ni(1)	155.84(14)
N(2)-C(1)-C(2)-C(3)	1.7(3)	C(4)-C(5)-N(2)-C(1)	1.1(3)
N(3)-C(13)-C(14)-C(15)	-174.5(2)	C(4)-C(5)-N(2)-C(6)	-178.7(2)
N(4)-C(13)-C(14)-C(15)	5.6(3)	N(1)-C(1)-N(2)-C(5)	177.35(18)
C(13)-C(14)-C(15)-C(16)	-1.0(3)	C(2)-C(1)-N(2)-C(5)	-1.6(3)
C(14)-C(15)-C(16)-C(17)	-2.3(4)	N(1)-C(1)-N(2)-C(6)	-2.9(3)
C(15)-C(16)-C(17)-N(4)	0.8(4)	C(2)-C(1)-N(2)-C(6)	178.20(18)
N(2)-C(1)-N(1)-C(7)	168.09(18)	C(16)-C(17)-N(4)-C(13)	4.1(3)

C(16)-C(17)-N(4)-C(18)	-174.2(2)
N(3)-C(13)-N(4)-C(17)	172.93(19)
C(14)-C(13)-N(4)-C(17)	-7.1(3)
N(3)-C(13)-N(4)-C(18)	-8.8(3)
C(14)-C(13)-N(4)-C(18)	171.17(19)
C(1)-N(1)-Ni(1)-N(3)	-148.31(15)
C(7)-N(1)-Ni(1)-N(3)	-13.96(13)
C(1)-N(1)-Ni(1)-Br(2)	96.11(15)
C(7)-N(1)-Ni(1)-Br(2)	-129.54(11)
C(1)-N(1)-Ni(1)-Br(1)	-31.17(15)

C(7)-N(1)-Ni(1)-Br(1)	103.19(12)
C(13)-N(3)-Ni(1)-N(1)	-148.12(16)
C(12)-N(3)-Ni(1)-N(1)	-12.21(13)
C(13)-N(3)-Ni(1)-Br(2)	-11.16(16)
C(12)-N(3)-Ni(1)-Br(2)	124.74(11)
C(13)-N(3)-Ni(1)-Br(1)	112.10(14)
C(12)-N(3)-Ni(1)-Br(1)	-112.00(12)

Symmetry transformations used to generate equivalent atoms:

Single crystal X-ray structure data for [NiCl₂(^{Me}N^{C6H4}N^{Me})] (21)

Table 1. Crystal data and structure refinement for **21**.

Identification code	21	
Empirical formula	C ₁₉ H ₂₀ Br ₂ Cl ₂ N ₄ Ni	
Formula weight	593.82	
Temperature	110(2) K	
Wavelength	0.71073 Å	
Crystal system	Orthorhombic	
Space group	Pmc2(1)	
Unit cell dimensions	a = 12.6621(6) Å	a = 90°.
	b = 8.0532(4) Å	b = 90°.
	c = 21.8322(10) Å	g = 90°.
Volume	2226.24(18) Å ³	
Z	4	
Density (calculated)	1.772 Mg/m ³	
Absorption coefficient	4.714 mm ⁻¹	
F(000)	1176	
Crystal size	0.21 x 0.20 x 0.02 mm ³	
Theta range for data collection	1.61 to 30.02°.	
Index ranges	-17<=h<=17, -11<=k<=11, -30<=l<=30	
Reflections collected	24637	
Independent reflections	6682 [R(int) = 0.0390]	
Completeness to theta = 30.02°	99.7 %	
Absorption correction	Semi-empirical from equivalents	
Max. and min. transmission	0.910 and 0.436	
Refinement method	Full-matrix least-squares on F ²	
Data / restraints / parameters	6682 / 1 / 292	
Goodness-of-fit on F ²	1.087	
Final R indices [I>2sigma(I)]	R1 = 0.0319, wR2 = 0.0782	
R indices (all data)	R1 = 0.0361, wR2 = 0.0796	
Absolute structure parameter	0.000(13)	
Largest diff. peak and hole	0.927 and -0.431 e.Å ⁻³	

Table 2. Atomic coordinates ($\times 10^4$) and equivalent isotropic displacement parameters ($\text{\AA}^2 \times 10^3$) for **21**. $U(\text{eq})$ is defined as one third of the trace of the orthogonalized U^{ij} tensor.

	x	y	z	$U(\text{eq})$
Br(1)	5000	4360(1)	7096(1)	21(1)
Br(2)	5000	8267(1)	8111(1)	23(1)
C(1)	6893(3)	3213(5)	8307(2)	18(1)
C(2)	7081(3)	1467(5)	8290(2)	21(1)
C(3)	7859(3)	840(6)	7947(2)	27(1)
C(4)	8540(4)	1868(5)	7607(2)	26(1)
C(5)	8383(3)	3521(5)	7644(2)	25(1)
C(6)	7495(3)	6000(5)	8021(2)	24(1)
C(7)	5554(3)	3055(4)	9063(2)	16(1)
C(8)	6101(3)	2294(5)	9547(2)	21(1)
C(9)	5546(3)	1485(5)	10011(2)	24(1)
N(1)	6061(2)	3942(4)	8592(1)	17(1)
N(2)	7582(2)	4180(4)	7993(2)	19(1)
Ni(1)	5000	5306(1)	8138(1)	16(1)
Br(3)	10000	2252(1)	2177(1)	22(1)
Br(4)	10000	6140(1)	1190(1)	21(1)
C(10)	8106(3)	1118(5)	946(2)	19(1)
C(11)	7933(3)	-623(5)	978(2)	23(1)
C(12)	7124(3)	-1265(6)	1332(2)	29(1)
C(13)	6450(4)	-187(6)	1656(2)	30(1)
C(14)	6598(3)	1473(6)	1598(2)	28(1)
C(15)	7448(3)	3920(5)	1178(3)	31(1)
C(16)	9443(3)	949(4)	191(2)	19(1)
C(17)	8905(3)	173(5)	-288(2)	24(1)
C(18)	9447(4)	-609(5)	-758(2)	24(1)
N(3)	8934(3)	1842(4)	665(2)	19(1)
N(4)	7391(2)	2121(4)	1245(2)	22(1)
Ni(2)	10000	3177(1)	1133(1)	18(1)
C(19)	5473(9)	7037(13)	9750(5)	42(2)
Cl(1)	4953(16)	6698(4)	10493(1)	55(1)
Cl(2)	6859(2)	7052(4)	9718(1)	56(1)

C(20)	9695(8)	5094(16)	9564(5)	47(3)
Cl(3)	10120(15)	4693(5)	8844(1)	87(3)
Cl(4)	8307(2)	5295(4)	9596(1)	55(1)

Table 3. Bond lengths [\AA] and angles [$^\circ$] for **21**.

Br(1)-Ni(1)	2.3988(9)	C(10)-N(4)	1.378(5)
Br(2)-Ni(1)	2.3853(8)	C(10)-C(11)	1.421(5)
C(1)-N(2)	1.355(5)	C(11)-C(12)	1.382(6)
C(1)-N(1)	1.357(5)	C(11)-H(11)	0.9500
C(1)-C(2)	1.427(5)	C(12)-C(13)	1.408(7)
C(2)-C(3)	1.337(6)	C(12)-H(12)	0.9500
C(2)-H(2)	0.9500	C(13)-C(14)	1.356(7)
C(3)-C(4)	1.407(6)	C(13)-H(13)	0.9500
C(3)-H(3)	0.9500	C(14)-N(4)	1.370(5)
C(4)-C(5)	1.349(6)	C(14)-H(14)	0.9500
C(4)-H(4)	0.9500	C(15)-N(4)	1.458(5)
C(5)-N(2)	1.375(5)	C(15)-H(15A)	0.9800
C(5)-H(5)	0.9500	C(15)-H(15B)	0.9800
C(6)-N(2)	1.470(5)	C(15)-H(15C)	0.9800
C(6)-H(6A)	0.9800	C(16)-C(17)	1.396(5)
C(6)-H(6B)	0.9800	C(16)-C(16)#2	1.411(8)
C(6)-H(6C)	0.9800	C(16)-N(3)	1.415(5)
C(7)-C(7)#1	1.402(7)	C(17)-C(18)	1.385(6)
C(7)-C(8)	1.404(5)	C(17)-H(17)	0.9500
C(7)-N(1)	1.407(5)	C(18)-C(18)#2	1.401(9)
C(8)-C(9)	1.395(6)	C(18)-H(18)	0.9500
C(8)-H(8)	0.9500	N(3)-Ni(2)	2.005(3)
C(9)-C(9)#1	1.382(9)	Ni(2)-N(3)#2	2.005(3)
C(9)-H(9)	0.9500	C(19)-Cl(2)	1.756(12)
N(1)-Ni(1)	1.998(3)	C(19)-Cl(1)	1.773(13)
Ni(1)-N(1)#1	1.998(3)	C(19)-H(19A)	0.9900
Br(3)-Ni(2)	2.3989(9)	C(19)-H(19B)	0.9900
Br(4)-Ni(2)	2.3894(8)	C(20)-Cl(3)	1.691(13)
C(10)-N(3)	1.347(5)	C(20)-Cl(4)	1.767(10)

C(20)-H(20A)	0.9900	C(1)-N(2)-C(5)	122.2(3)
C(20)-H(20B)	0.9900	C(1)-N(2)-C(6)	120.2(3)
		C(5)-N(2)-C(6)	117.6(3)
N(2)-C(1)-N(1)	118.9(3)	N(1)#1-Ni(1)-N(1)	84.49(18)
N(2)-C(1)-C(2)	116.5(3)	N(1)#1-Ni(1)-Br(2)	124.19(9)
N(1)-C(1)-C(2)	124.6(3)	N(1)-Ni(1)-Br(2)	124.19(9)
C(3)-C(2)-C(1)	120.7(4)	N(1)#1-Ni(1)-Br(1)	107.18(10)
C(3)-C(2)-H(2)	119.7	N(1)-Ni(1)-Br(1)	107.18(10)
C(1)-C(2)-H(2)	119.7	Br(2)-Ni(1)-Br(1)	107.10(3)
C(2)-C(3)-C(4)	121.6(4)	N(3)-C(10)-N(4)	118.2(3)
C(2)-C(3)-H(3)	119.2	N(3)-C(10)-C(11)	124.7(3)
C(4)-C(3)-H(3)	119.2	N(4)-C(10)-C(11)	117.0(3)
C(5)-C(4)-C(3)	117.3(4)	C(12)-C(11)-C(10)	120.7(4)
C(5)-C(4)-H(4)	121.3	C(12)-C(11)-H(11)	119.6
C(3)-C(4)-H(4)	121.3	C(10)-C(11)-H(11)	119.6
C(4)-C(5)-N(2)	121.5(4)	C(11)-C(12)-C(13)	119.9(4)
C(4)-C(5)-H(5)	119.2	C(11)-C(12)-H(12)	120.0
N(2)-C(5)-H(5)	119.2	C(13)-C(12)-H(12)	120.0
N(2)-C(6)-H(6A)	109.5	C(14)-C(13)-C(12)	118.5(4)
N(2)-C(6)-H(6B)	109.5	C(14)-C(13)-H(13)	120.7
H(6A)-C(6)-H(6B)	109.5	C(12)-C(13)-H(13)	120.7
N(2)-C(6)-H(6C)	109.5	C(13)-C(14)-N(4)	121.9(4)
H(6A)-C(6)-H(6C)	109.5	C(13)-C(14)-H(14)	119.0
H(6B)-C(6)-H(6C)	109.5	N(4)-C(14)-H(14)	119.0
C(7)#1-C(7)-C(8)	119.6(2)	N(4)-C(15)-H(15A)	109.5
C(7)#1-C(7)-N(1)	117.15(19)	N(4)-C(15)-H(15B)	109.5
C(8)-C(7)-N(1)	123.1(3)	H(15A)-C(15)-H(15B)	109.5
C(9)-C(8)-C(7)	120.1(4)	N(4)-C(15)-H(15C)	109.5
C(9)-C(8)-H(8)	119.9	H(15A)-C(15)-H(15C)	109.5
C(7)-C(8)-H(8)	119.9	H(15B)-C(15)-H(15C)	109.5
C(9)#1-C(9)-C(8)	120.3(2)	C(17)-C(16)-C(16)#2	119.2(2)
C(9)#1-C(9)-H(9)	119.9	C(17)-C(16)-N(3)	123.6(3)
C(8)-C(9)-H(9)	119.9	C(16)#2-C(16)-N(3)	117.1(2)
C(1)-N(1)-C(7)	118.0(3)	C(18)-C(17)-C(16)	121.2(4)
C(1)-N(1)-Ni(1)	122.2(2)	C(18)-C(17)-H(17)	119.4
C(7)-N(1)-Ni(1)	109.5(2)	C(16)-C(17)-H(17)	119.4

C(17)-C(18)-C(18)#2	119.7(2)	Cl(2)-C(19)-H(19A)	108.7
C(17)-C(18)-H(18)	120.2	Cl(1)-C(19)-H(19A)	108.7
C(18)#2-C(18)-H(18)	120.2	Cl(2)-C(19)-H(19B)	108.7
C(10)-N(3)-C(16)	117.8(3)	Cl(1)-C(19)-H(19B)	108.7
C(10)-N(3)-Ni(2)	121.6(3)	H(19A)-C(19)-H(19B)	107.6
C(16)-N(3)-Ni(2)	109.8(2)	Cl(3)-C(20)-Cl(4)	111.8(9)
C(14)-N(4)-C(10)	121.7(3)	Cl(3)-C(20)-H(20A)	109.3
C(14)-N(4)-C(15)	118.1(3)	Cl(4)-C(20)-H(20A)	109.3
C(10)-N(4)-C(15)	120.2(3)	Cl(3)-C(20)-H(20B)	109.3
N(3)#2-Ni(2)-N(3)	84.63(18)	Cl(4)-C(20)-H(20B)	109.3
N(3)#2-Ni(2)-Br(4)	124.20(9)	H(20A)-C(20)-H(20B)	107.9
N(3)-Ni(2)-Br(4)	124.20(9)		
N(3)#2-Ni(2)-Br(3)	108.52(10)	Symmetry transformations used to generate equivalent atoms:	
N(3)-Ni(2)-Br(3)	108.52(10)	#1	-x+1,y,z
Br(4)-Ni(2)-Br(3)	105.09(3)	#2	-x+2,y,z
Cl(2)-C(19)-Cl(1)	114.1(9)		

Table 4. Anisotropic displacement parameters ($\text{\AA}^2 \times 10^3$) for **21**. The anisotropic displacement factor exponent takes the form: $-2p^2[h^2 a^{*2}U^{11} + \dots + 2 h k a^* b^* U^{12}]$

	U^{11}	U^{22}	U^{33}	U^{23}	U^{13}	U^{12}
Br(1)	23(1)	21(1)	19(1)	-1(1)	0	0
Br(2)	22(1)	15(1)	32(1)	1(1)	0	0
C(1)	16(2)	20(2)	17(2)	1(1)	-2(1)	3(1)
C(2)	22(2)	20(2)	22(2)	1(2)	-3(2)	-1(2)
C(3)	29(2)	23(2)	28(2)	-5(2)	-6(2)	1(2)
C(4)	20(2)	33(2)	26(2)	-5(2)	0(2)	2(2)
C(5)	19(2)	31(2)	25(2)	1(2)	1(2)	1(2)
C(6)	20(2)	19(2)	34(2)	6(2)	4(2)	-1(2)
C(7)	19(2)	14(1)	14(2)	2(1)	-1(1)	1(1)
C(8)	19(2)	20(2)	23(2)	2(2)	-6(1)	-1(2)
C(9)	30(2)	25(2)	18(2)	1(2)	-4(2)	1(2)
N(1)	16(1)	17(1)	20(2)	2(1)	0(1)	-1(1)
N(2)	18(1)	19(1)	20(2)	4(1)	1(1)	-3(1)

Ni(1)	16(1)	15(1)	18(1)	3(1)	0	0
Br(3)	21(1)	21(1)	24(1)	2(1)	0	0
Br(4)	22(1)	16(1)	27(1)	-2(1)	0	0
C(10)	14(2)	23(2)	19(2)	-2(1)	-3(1)	4(1)
C(11)	21(2)	21(2)	26(2)	2(2)	0(2)	3(2)
C(12)	22(2)	31(2)	33(2)	7(2)	-1(2)	-3(2)
C(13)	18(2)	42(3)	31(2)	7(2)	-2(2)	-6(2)
C(14)	16(2)	41(2)	26(2)	-6(2)	2(2)	-2(2)
C(15)	20(2)	21(2)	51(3)	-13(2)	4(2)	0(2)
C(16)	19(2)	15(2)	21(2)	1(1)	-1(1)	4(1)
C(17)	21(2)	26(2)	26(2)	-2(2)	-5(2)	1(2)
C(18)	30(2)	26(2)	17(2)	-5(2)	-5(2)	-2(2)
N(3)	14(1)	19(1)	24(2)	-5(1)	-2(1)	1(1)
N(4)	14(1)	24(2)	26(2)	-3(1)	0(1)	-1(1)
Ni(2)	17(1)	16(1)	20(1)	-4(1)	0	0
C(19)	67(7)	32(5)	28(5)	-3(4)	7(4)	-8(4)
Cl(1)	55(3)	74(2)	34(1)	5(1)	13(4)	14(5)
Cl(2)	57(2)	69(2)	41(1)	-17(1)	9(1)	-27(2)
C(20)	52(7)	46(5)	41(5)	9(4)	-1(4)	1(5)
Cl(3)	106(8)	114(3)	43(1)	-29(2)	30(4)	-25(5)
Cl(4)	51(2)	75(2)	39(1)	16(1)	-5(1)	-23(2)

Table 5. Hydrogen coordinates ($\times 10^4$) and isotropic displacement parameters ($\text{\AA}^2 \times 10^3$) for **21**.

	x	y	z	U(eq)
H(2)	6648	743	8524	25
H(3)	7955	-330	7932	32
H(4)	9089	1416	7362	32
H(5)	8837	4248	7424	30
H(6A)	6927	6371	7749	36
H(6B)	8164	6500	7891	36
H(6C)	7337	6340	8442	36
H(8)	6851	2330	9558	25
H(9)	5920	932	10328	29

H(11)	8379	-1355	755	27
H(12)	7023	-2432	1355	34
H(13)	5904	-614	1910	36
H(14)	6138	2209	1809	33
H(15A)	7985	4362	1457	46
H(15B)	6760	4409	1277	46
H(15C)	7637	4198	755	46
H(17)	8155	181	-292	29
H(18)	9070	-1142	-1078	29
H(19A)	5207	6157	9473	51
H(19B)	5206	8114	9595	51
H(20A)	10026	6134	9711	56
H(20B)	9920	4183	9838	56

Table 6. Torsion angles [°] for **21**.

N(2)-C(1)-C(2)-C(3)	-4.1(6)	C(2)-C(1)-N(2)-C(6)	-175.6(3)
N(1)-C(1)-C(2)-C(3)	173.1(4)	C(4)-C(5)-N(2)-C(1)	-1.5(6)
C(1)-C(2)-C(3)-C(4)	2.0(6)	C(4)-C(5)-N(2)-C(6)	178.0(4)
C(2)-C(3)-C(4)-C(5)	0.5(6)	C(1)-N(1)-Ni(1)-N(1)#1	131.9(2)
C(3)-C(4)-C(5)-N(2)	-0.8(6)	C(7)-N(1)-Ni(1)-N(1)#1	-12.4(3)
C(7)#1-C(7)-C(8)-C(9)	2.6(5)	C(1)-N(1)-Ni(1)-Br(2)	-100.0(3)
N(1)-C(7)-C(8)-C(9)	177.6(4)	C(7)-N(1)-Ni(1)-Br(2)	115.7(2)
C(7)-C(8)-C(9)-C(9)#1	-2.6(5)	C(1)-N(1)-Ni(1)-Br(1)	25.6(3)
N(2)-C(1)-N(1)-C(7)	-160.4(3)	C(7)-N(1)-Ni(1)-Br(1)	-118.7(2)
C(2)-C(1)-N(1)-C(7)	22.4(5)	N(3)-C(10)-C(11)-C(12)	173.0(4)
N(2)-C(1)-N(1)-Ni(1)	58.2(4)	N(4)-C(10)-C(11)-C(12)	-4.4(6)
C(2)-C(1)-N(1)-Ni(1)	-119.0(3)	C(10)-C(11)-C(12)-C(13)	1.0(6)
C(7)#1-C(7)-N(1)-C(1)	-135.7(3)	C(11)-C(12)-C(13)-C(14)	1.8(7)
C(8)-C(7)-N(1)-C(1)	49.2(5)	C(12)-C(13)-C(14)-N(4)	-1.2(6)
C(7)#1-C(7)-N(1)-Ni(1)	10.3(2)	C(16)#2-C(16)-C(17)-C(18)	0.7(5)
C(8)-C(7)-N(1)-Ni(1)	-164.8(3)	N(3)-C(16)-C(17)-C(18)	176.5(4)
N(1)-C(1)-N(2)-C(5)	-173.5(4)	C(16)-C(17)-C(18)-C(18)#2	-0.7(5)
C(2)-C(1)-N(2)-C(5)	3.9(5)	N(4)-C(10)-N(3)-C(16)	-158.1(3)
N(1)-C(1)-N(2)-C(6)	7.0(5)	C(11)-C(10)-N(3)-C(16)	24.6(5)

N(4)-C(10)-N(3)-Ni(2)	61.1(4)
C(11)-C(10)-N(3)-Ni(2)	-116.2(4)
C(17)-C(16)-N(3)-C(10)	48.2(5)
C(16)#2-C(16)-N(3)-C(10)	-136.0(3)
C(17)-C(16)-N(3)-Ni(2)	-166.7(3)
C(16)#2-C(16)-N(3)-Ni(2)	9.1(3)
C(13)-C(14)-N(4)-C(10)	-2.3(6)
C(13)-C(14)-N(4)-C(15)	176.1(4)
N(3)-C(10)-N(4)-C(14)	-172.5(4)
C(11)-C(10)-N(4)-C(14)	5.0(5)
N(3)-C(10)-N(4)-C(15)	9.1(5)

C(11)-C(10)-N(4)-C(15)	-173.4(4)
C(10)-N(3)-Ni(2)-N(3)#2	132.5(2)
C(16)-N(3)-Ni(2)-N(3)#2	-11.0(3)
C(10)-N(3)-Ni(2)-Br(4)	-99.3(3)
C(16)-N(3)-Ni(2)-Br(4)	117.2(2)
C(10)-N(3)-Ni(2)-Br(3)	24.7(3)
C(16)-N(3)-Ni(2)-Br(3)	-118.8(2)

Symmetry transformations used to generate equivalent atoms:

#1	-x+1,y,z	#2	-x+2,y,z
----	----------	----	----------

Single crystal X-ray structure data for [PdCl₂(^{Me}N^{C6H4}N^{Me})] (22)

Table 1. Crystal data and structure refinement for **22**.

Identification code	22	
Empirical formula	C ₆₀ H ₆₆ Cl ₁₆ N ₁₂ O ₂ Pd ₃	
Formula weight	1519.15	
Temperature	110(2) K	
Wavelength	0.71073 Å	
Crystal system	Monoclinic	
Space group	C2/c	
Unit cell dimensions	a = 33.3939(12) Å	α = 90°.
	b = 10.4769(4) Å	β = 119.4090(10)°.
	c = 20.9116(8) Å	γ = 90°.
Volume	6373.4(4) Å ³	
Z	4	
Density (calculated)	1.583 Mg/m ³	
Absorption coefficient	1.141 mm ⁻¹	
F(000)	3064	
Crystal size	0.16 x 0.10 x 0.02 mm ³	
Theta range for data collection	1.97 to 30.00°.	
Index ranges	-46 ≤ h ≤ 46, -14 ≤ k ≤ 14, -28 ≤ l ≤ 29	
Reflections collected	35291	
Independent reflections	9214 [R(int) = 0.0468]	
Completeness to theta = 30.00°	99.1 %	
Absorption correction	Semi-empirical from equivalents	
Max. and min. transmission	0.9775 and 0.8385	
Refinement method	Full-matrix least-squares on F ²	
Data / restraints / parameters	9214 / 12 / 390	
Goodness-of-fit on F ²	1.063	
Final R indices [I > 2σ(I)]	R1 = 0.0388, wR2 = 0.0737	
R indices (all data)	R1 = 0.0547, wR2 = 0.0796	
Largest diff. peak and hole	0.920 and -0.532 e.Å ⁻³	

Table 2. Atomic coordinates ($\times 10^4$) and equivalent isotropic displacement parameters ($\text{\AA}^2 \times 10^3$) for **22**. $U(\text{eq})$ is defined as one third of the trace of the orthogonalized U^{ij} tensor.

	x	y	z	$U(\text{eq})$
C(1)	2036(1)	5222(2)	1695(2)	20(1)
C(2)	1981(1)	4466(3)	1099(2)	24(1)
C(3)	2352(1)	4056(3)	1048(2)	26(1)
C(4)	2795(1)	4364(3)	1602(2)	28(1)
C(5)	2846(1)	5068(3)	2183(2)	26(1)
C(6)	2556(1)	6206(3)	2891(2)	24(1)
C(7)	1295(1)	4992(3)	1579(1)	21(1)
C(8)	1305(1)	3666(3)	1647(2)	25(1)
C(9)	914(1)	2996(3)	1529(2)	27(1)
C(10)	514(1)	3653(3)	1362(2)	27(1)
C(11)	500(1)	4975(3)	1311(2)	23(1)
C(12)	887(1)	5663(2)	1409(1)	20(1)
C(13)	550(1)	7755(2)	1186(1)	20(1)
C(14)	146(1)	7601(3)	508(2)	23(1)
C(15)	-203(1)	8481(3)	270(2)	27(1)
C(16)	-162(1)	9530(3)	708(2)	25(1)
C(17)	225(1)	9652(3)	1376(2)	23(1)
C(18)	975(1)	8940(3)	2341(2)	24(1)
N(1)	2476(1)	5472(2)	2236(1)	20(1)
N(2)	1685(1)	5749(2)	1763(1)	21(1)
N(3)	930(1)	7005(2)	1449(1)	20(1)
N(4)	568(1)	8778(2)	1609(1)	21(1)
Cl(1)	2176(1)	8087(1)	1394(1)	22(1)
Cl(2)	1229(1)	9622(1)	993(1)	22(1)
Pd(1)	1513(1)	7601(1)	1453(1)	17(1)
C(19)	880(1)	4114(2)	3489(1)	21(1)
C(20)	1176(1)	4473(3)	3224(2)	29(1)
C(21)	1639(1)	4223(3)	3615(2)	38(1)
C(22)	1820(1)	3627(3)	4296(2)	39(1)
C(23)	1536(1)	3328(3)	4565(2)	33(1)
C(24)	789(1)	3326(3)	4517(2)	30(1)

C(25)	227(1)	5422(2)	2801(1)	20(1)
C(26)	443(1)	6579(3)	3089(2)	26(1)
C(27)	222(1)	7727(3)	2795(2)	32(1)
N(5)	1077(1)	3591(2)	4177(1)	23(1)
N(6)	412(1)	4229(2)	3114(1)	19(1)
Pd(2)	0	2766(1)	2500	16(1)
Cl(3)	539(1)	1212(1)	3172(1)	23(1)
C(28)	3695(1)	3092(4)	218(2)	51(1)
C(29)	3336(1)	3575(3)	396(2)	41(1)
C(30)	3270(2)	4977(4)	347(2)	58(1)
O(1)	3221(3)	2717(11)	661(8)	62(3)
O(1A)	3068(3)	2922(8)	506(6)	42(2)

Table 3. Bond lengths [\AA] and angles [$^\circ$] for **22**.

C(1)-N(2)	1.364(3)	C(9)-C(10)	1.386(4)
C(1)-N(1)	1.369(3)	C(9)-H(9)	0.9500
C(1)-C(2)	1.410(4)	C(10)-C(11)	1.388(4)
C(2)-C(3)	1.364(4)	C(10)-H(10)	0.9500
C(2)-H(2)	0.9500	C(11)-C(12)	1.403(4)
C(3)-C(4)	1.399(4)	C(11)-H(11)	0.9500
C(3)-H(3)	0.9500	C(12)-N(3)	1.412(3)
C(4)-C(5)	1.359(4)	C(13)-N(3)	1.357(3)
C(4)-H(4)	0.9500	C(13)-N(4)	1.372(3)
C(5)-N(1)	1.361(3)	C(13)-C(14)	1.407(4)
C(5)-H(5)	0.9500	C(14)-C(15)	1.373(4)
C(6)-N(1)	1.474(3)	C(14)-H(14)	0.9500
C(6)-H(6A)	0.9800	C(15)-C(16)	1.393(4)
C(6)-H(6B)	0.9800	C(15)-H(15)	0.9500
C(6)-H(6C)	0.9800	C(16)-C(17)	1.366(4)
C(7)-C(8)	1.395(4)	C(16)-H(16)	0.9500
C(7)-N(2)	1.409(3)	C(17)-N(4)	1.357(3)
C(7)-C(12)	1.415(4)	C(17)-H(17)	0.9500
C(8)-C(9)	1.394(4)	C(18)-N(4)	1.474(3)
C(8)-H(8)	0.9500	C(18)-H(18A)	0.9800

C(18)-H(18B)	0.9800	C(29)-O(1)	1.213(13)
C(18)-H(18C)	0.9800	C(29)-O(1A)	1.235(11)
N(2)-Pd(1)	2.037(2)	C(29)-C(30)	1.481(5)
N(3)-Pd(1)	2.041(2)	C(30)-H(30A)	0.9800
Cl(1)-Pd(1)	2.3319(7)	C(30)-H(30B)	0.9800
Cl(2)-Pd(1)	2.3260(7)	C(30)-H(30C)	0.9800
C(19)-N(6)	1.366(3)		
C(19)-N(5)	1.370(3)	N(2)-C(1)-N(1)	117.6(2)
C(19)-C(20)	1.403(4)	N(2)-C(1)-C(2)	124.9(2)
C(20)-C(21)	1.371(4)	N(1)-C(1)-C(2)	117.4(2)
C(20)-H(20)	0.9500	C(3)-C(2)-C(1)	121.2(3)
C(21)-C(22)	1.392(5)	C(3)-C(2)-H(2)	119.4
C(21)-H(21)	0.9500	C(1)-C(2)-H(2)	119.4
C(22)-C(23)	1.357(5)	C(2)-C(3)-C(4)	119.6(3)
C(22)-H(22)	0.9500	C(2)-C(3)-H(3)	120.2
C(23)-N(5)	1.365(4)	C(4)-C(3)-H(3)	120.2
C(23)-H(23)	0.9500	C(5)-C(4)-C(3)	118.8(3)
C(24)-N(5)	1.475(4)	C(5)-C(4)-H(4)	120.6
C(24)-H(24A)	0.9800	C(3)-C(4)-H(4)	120.6
C(24)-H(24B)	0.9800	C(4)-C(5)-N(1)	121.6(3)
C(24)-H(24C)	0.9800	C(4)-C(5)-H(5)	119.2
C(25)-C(26)	1.388(4)	N(1)-C(5)-H(5)	119.2
C(25)-N(6)	1.405(3)	N(1)-C(6)-H(6A)	109.5
C(25)-C(25)#1	1.416(5)	N(1)-C(6)-H(6B)	109.5
C(26)-C(27)	1.387(4)	H(6A)-C(6)-H(6B)	109.5
C(26)-H(26)	0.9500	N(1)-C(6)-H(6C)	109.5
C(27)-C(27)#1	1.388(6)	H(6A)-C(6)-H(6C)	109.5
C(27)-H(27)	0.9500	H(6B)-C(6)-H(6C)	109.5
N(6)-Pd(2)	2.038(2)	C(8)-C(7)-N(2)	124.1(2)
Pd(2)-N(6)#1	2.038(2)	C(8)-C(7)-C(12)	119.5(2)
Pd(2)-Cl(3)	2.3185(6)	N(2)-C(7)-C(12)	115.9(2)
Pd(2)-Cl(3)#1	2.3186(6)	C(9)-C(8)-C(7)	120.7(3)
C(28)-C(29)	1.506(5)	C(9)-C(8)-H(8)	119.6
C(28)-H(28A)	0.9800	C(7)-C(8)-H(8)	119.6
C(28)-H(28B)	0.9800	C(10)-C(9)-C(8)	119.8(3)
C(28)-H(28C)	0.9800	C(10)-C(9)-H(9)	120.1

C(8)-C(9)-H(9)	120.1	C(7)-N(2)-Pd(1)	111.71(17)
C(9)-C(10)-C(11)	120.5(3)	C(13)-N(3)-C(12)	120.3(2)
C(9)-C(10)-H(10)	119.8	C(13)-N(3)-Pd(1)	121.54(18)
C(11)-C(10)-H(10)	119.8	C(12)-N(3)-Pd(1)	111.92(16)
C(10)-C(11)-C(12)	120.5(3)	C(17)-N(4)-C(13)	122.2(2)
C(10)-C(11)-H(11)	119.8	C(17)-N(4)-C(18)	118.7(2)
C(12)-C(11)-H(11)	119.8	C(13)-N(4)-C(18)	119.1(2)
C(11)-C(12)-N(3)	125.4(2)	N(2)-Pd(1)-N(3)	80.23(9)
C(11)-C(12)-C(7)	119.0(2)	N(2)-Pd(1)-Cl(2)	173.07(7)
N(3)-C(12)-C(7)	115.0(2)	N(3)-Pd(1)-Cl(2)	94.73(6)
N(3)-C(13)-N(4)	117.0(2)	N(2)-Pd(1)-Cl(1)	95.57(6)
N(3)-C(13)-C(14)	125.9(2)	N(3)-Pd(1)-Cl(1)	174.15(6)
N(4)-C(13)-C(14)	117.1(2)	Cl(2)-Pd(1)-Cl(1)	89.09(2)
C(15)-C(14)-C(13)	120.8(3)	N(6)-C(19)-N(5)	117.6(2)
C(15)-C(14)-H(14)	119.6	N(6)-C(19)-C(20)	125.4(2)
C(13)-C(14)-H(14)	119.6	N(5)-C(19)-C(20)	117.0(3)
C(14)-C(15)-C(16)	119.9(3)	C(21)-C(20)-C(19)	121.3(3)
C(14)-C(15)-H(15)	120.0	C(21)-C(20)-H(20)	119.3
C(16)-C(15)-H(15)	120.0	C(19)-C(20)-H(20)	119.3
C(17)-C(16)-C(15)	118.9(3)	C(20)-C(21)-C(22)	119.5(3)
C(17)-C(16)-H(16)	120.5	C(20)-C(21)-H(21)	120.2
C(15)-C(16)-H(16)	120.5	C(22)-C(21)-H(21)	120.2
N(4)-C(17)-C(16)	120.9(3)	C(23)-C(22)-C(21)	119.1(3)
N(4)-C(17)-H(17)	119.6	C(23)-C(22)-H(22)	120.5
C(16)-C(17)-H(17)	119.6	C(21)-C(22)-H(22)	120.5
N(4)-C(18)-H(18A)	109.5	C(22)-C(23)-N(5)	121.2(3)
N(4)-C(18)-H(18B)	109.5	C(22)-C(23)-H(23)	119.4
H(18A)-C(18)-H(18B)	109.5	N(5)-C(23)-H(23)	119.4
N(4)-C(18)-H(18C)	109.5	N(5)-C(24)-H(24A)	109.5
H(18A)-C(18)-H(18C)	109.5	N(5)-C(24)-H(24B)	109.5
H(18B)-C(18)-H(18C)	109.5	H(24A)-C(24)-H(24B)	109.5
C(5)-N(1)-C(1)	121.4(2)	N(5)-C(24)-H(24C)	109.5
C(5)-N(1)-C(6)	118.6(2)	H(24A)-C(24)-H(24C)	109.5
C(1)-N(1)-C(6)	120.0(2)	H(24B)-C(24)-H(24C)	109.5
C(1)-N(2)-C(7)	118.1(2)	C(26)-C(25)-N(6)	124.0(2)
C(1)-N(2)-Pd(1)	118.40(17)	C(26)-C(25)-C(25)#1	119.16(17)

N(6)-C(25)-C(25)#1	116.59(14)	H(28A)-C(28)-H(28B)	109.5
C(27)-C(26)-C(25)	121.0(3)	C(29)-C(28)-H(28C)	109.5
C(27)-C(26)-H(26)	119.5	H(28A)-C(28)-H(28C)	109.5
C(25)-C(26)-H(26)	119.5	H(28B)-C(28)-H(28C)	109.5
C(26)-C(27)-C(27)#1	119.87(18)	O(1)-C(29)-O(1A)	23.6(7)
C(26)-C(27)-H(27)	120.1	O(1)-C(29)-C(30)	134.1(6)
C(27)#1-C(27)-H(27)	120.1	O(1A)-C(29)-C(30)	117.6(5)
C(23)-N(5)-C(19)	121.7(3)	O(1)-C(29)-C(28)	109.4(5)
C(23)-N(5)-C(24)	118.9(2)	O(1A)-C(29)-C(28)	126.7(5)
C(19)-N(5)-C(24)	119.5(2)	C(30)-C(29)-C(28)	115.3(3)
C(19)-N(6)-C(25)	117.6(2)	C(29)-C(30)-H(30A)	109.5
C(19)-N(6)-Pd(2)	121.53(17)	C(29)-C(30)-H(30B)	109.5
C(25)-N(6)-Pd(2)	111.68(16)	H(30A)-C(30)-H(30B)	109.5
N(6)-Pd(2)-N(6)#1	82.47(12)	C(29)-C(30)-H(30C)	109.5
N(6)-Pd(2)-Cl(3)	93.64(6)	H(30A)-C(30)-H(30C)	109.5
N(6)#1-Pd(2)-Cl(3)	172.86(7)	H(30B)-C(30)-H(30C)	109.5
N(6)-Pd(2)-Cl(3)#1	172.86(7)		
N(6)#1-Pd(2)-Cl(3)#1	93.64(6)	Symmetry transformations used to generate equivalent atoms:	
Cl(3)-Pd(2)-Cl(3)#1	90.83(3)	#1 -x,y,-z+1/2	
C(29)-C(28)-H(28A)	109.5		
C(29)-C(28)-H(28B)	109.5		

Table 4. Anisotropic displacement parameters ($\text{\AA}^2 \times 10^3$) for **22**. The anisotropic displacement factor exponent takes the form: $-2\pi^2 [h^2 a^{*2} U^{11} + \dots + 2 h k a^* b^* U^{12}]$

	U^{11}	U^{22}	U^{33}	U^{23}	U^{13}	U^{12}
C(1)	19(1)	17(1)	22(1)	3(1)	10(1)	2(1)
C(2)	22(1)	23(1)	22(1)	0(1)	9(1)	0(1)
C(3)	30(2)	26(1)	24(2)	-1(1)	14(1)	4(1)
C(4)	22(1)	35(2)	27(2)	3(1)	12(1)	10(1)
C(5)	16(1)	31(2)	27(2)	5(1)	8(1)	7(1)
C(6)	22(1)	26(1)	21(1)	-2(1)	8(1)	2(1)
C(7)	19(1)	22(1)	20(1)	-1(1)	10(1)	-2(1)
C(8)	26(1)	21(1)	29(2)	-2(1)	14(1)	0(1)

C(9)	32(2)	22(1)	29(2)	-3(1)	16(1)	-5(1)
C(10)	27(2)	30(2)	25(1)	-2(1)	13(1)	-10(1)
C(11)	19(1)	28(1)	20(1)	-1(1)	9(1)	-2(1)
C(12)	22(1)	21(1)	18(1)	-3(1)	11(1)	-2(1)
C(13)	16(1)	23(1)	20(1)	-1(1)	9(1)	-1(1)
C(14)	18(1)	29(1)	19(1)	-3(1)	8(1)	1(1)
C(15)	15(1)	38(2)	22(1)	0(1)	6(1)	1(1)
C(16)	19(1)	28(1)	27(2)	2(1)	11(1)	5(1)
C(17)	20(1)	23(1)	29(2)	0(1)	14(1)	3(1)
C(18)	17(1)	32(2)	21(1)	-5(1)	7(1)	-1(1)
N(1)	18(1)	21(1)	18(1)	0(1)	7(1)	3(1)
N(2)	18(1)	17(1)	28(1)	-1(1)	11(1)	1(1)
N(3)	14(1)	21(1)	23(1)	-1(1)	8(1)	1(1)
N(4)	15(1)	25(1)	21(1)	-1(1)	9(1)	2(1)
Cl(1)	17(1)	22(1)	26(1)	2(1)	10(1)	1(1)
Cl(2)	19(1)	22(1)	24(1)	4(1)	8(1)	4(1)
Pd(1)	13(1)	17(1)	17(1)	-1(1)	6(1)	1(1)
C(19)	27(1)	16(1)	17(1)	-2(1)	8(1)	-4(1)
C(20)	31(2)	30(2)	23(2)	2(1)	12(1)	-5(1)
C(21)	28(2)	46(2)	39(2)	1(2)	16(2)	-7(1)
C(22)	21(2)	46(2)	38(2)	0(2)	5(1)	-2(1)
C(23)	31(2)	32(2)	23(2)	3(1)	2(1)	1(1)
C(24)	36(2)	33(2)	20(1)	2(1)	14(1)	-1(1)
C(25)	29(1)	15(1)	21(1)	-1(1)	17(1)	-1(1)
C(26)	32(2)	19(1)	32(2)	-5(1)	19(1)	-5(1)
C(27)	45(2)	13(1)	49(2)	-4(1)	33(2)	-5(1)
N(5)	26(1)	22(1)	18(1)	0(1)	8(1)	-2(1)
N(6)	21(1)	16(1)	17(1)	-1(1)	7(1)	-3(1)
Pd(2)	18(1)	12(1)	18(1)	0	9(1)	0
Cl(3)	23(1)	15(1)	27(1)	1(1)	10(1)	3(1)
C(28)	46(2)	57(2)	48(2)	15(2)	22(2)	4(2)
C(29)	60(2)	38(2)	28(2)	-4(1)	24(2)	-9(2)
C(30)	73(3)	55(3)	53(3)	9(2)	35(2)	2(2)
O(1)	63(6)	55(5)	98(7)	37(4)	63(6)	24(4)
O(1A)	51(5)	28(4)	70(6)	-15(4)	48(5)	-12(4)

Table 5. Hydrogen coordinates ($\times 10^4$) and isotropic displacement parameters ($\text{\AA}^2 \times 10^3$) for **22**.

	x	y	z	U(eq)
H(2)	1681	4239	727	28
H(3)	2309	3563	637	32
H(4)	3057	4086	1573	34
H(5)	3146	5284	2560	31
H(6A)	2865	6020	3295	36
H(6B)	2327	5965	3032	36
H(6C)	2530	7120	2778	36
H(8)	1581	3215	1774	30
H(9)	921	2091	1564	33
H(10)	248	3196	1282	33
H(11)	227	5418	1208	28
H(14)	113	6878	212	27
H(15)	-472	8376	-193	32
H(16)	-400	10149	545	30
H(17)	254	10358	1681	28
H(18A)	1237	9214	2287	36
H(18B)	1047	8127	2607	36
H(18C)	910	9588	2616	36
H(20)	1054	4898	2764	34
H(21)	1834	4456	3423	46
H(22)	2138	3431	4568	47
H(23)	1659	2930	5032	40
H(24A)	597	4071	4460	44
H(24B)	987	3144	5041	44
H(24C)	592	2586	4277	44
H(26)	747	6585	3493	31
H(27)	375	8511	2997	38
H(28A)	3732	2168	302	77
H(28B)	3988	3519	533	77
H(28C)	3598	3273	-298	77
H(30A)	3006	5192	412	88
H(30B)	3212	5274	-135	88

Table 6. Torsion angles [°] for **22**.

N(2)-C(1)-C(2)-C(3)	175.0(3)	C(8)-C(7)-N(2)-C(1)	29.7(4)
N(1)-C(1)-C(2)-C(3)	-3.2(4)	C(12)-C(7)-N(2)-C(1)	-158.8(2)
C(1)-C(2)-C(3)-C(4)	1.4(4)	C(8)-C(7)-N(2)-Pd(1)	172.1(2)
C(2)-C(3)-C(4)-C(5)	0.1(4)	C(12)-C(7)-N(2)-Pd(1)	-16.3(3)
C(3)-C(4)-C(5)-N(1)	0.2(4)	N(4)-C(13)-N(3)-C(12)	136.5(2)
N(2)-C(7)-C(8)-C(9)	173.0(3)	C(14)-C(13)-N(3)-C(12)	-45.4(4)
C(12)-C(7)-C(8)-C(9)	1.7(4)	N(4)-C(13)-N(3)-Pd(1)	-73.4(3)
C(7)-C(8)-C(9)-C(10)	-1.7(4)	C(14)-C(13)-N(3)-Pd(1)	104.7(3)
C(8)-C(9)-C(10)-C(11)	0.0(4)	C(11)-C(12)-N(3)-C(13)	-19.4(4)
C(9)-C(10)-C(11)-C(12)	1.6(4)	C(7)-C(12)-N(3)-C(13)	169.3(2)
C(10)-C(11)-C(12)-N(3)	-172.6(3)	C(11)-C(12)-N(3)-Pd(1)	-172.1(2)
C(10)-C(11)-C(12)-C(7)	-1.5(4)	C(7)-C(12)-N(3)-Pd(1)	16.5(3)
C(8)-C(7)-C(12)-C(11)	-0.1(4)	C(16)-C(17)-N(4)-C(13)	1.6(4)
N(2)-C(7)-C(12)-C(11)	-172.1(2)	C(16)-C(17)-N(4)-C(18)	-178.7(3)
C(8)-C(7)-C(12)-N(3)	171.8(2)	N(3)-C(13)-N(4)-C(17)	174.5(2)
N(2)-C(7)-C(12)-N(3)	-0.1(3)	C(14)-C(13)-N(4)-C(17)	-3.7(4)
N(3)-C(13)-C(14)-C(15)	-174.5(3)	N(3)-C(13)-N(4)-C(18)	-5.1(4)
N(4)-C(13)-C(14)-C(15)	3.6(4)	C(14)-C(13)-N(4)-C(18)	176.6(2)
C(13)-C(14)-C(15)-C(16)	-1.4(4)	C(1)-N(2)-Pd(1)-N(3)	161.7(2)
C(14)-C(15)-C(16)-C(17)	-0.8(4)	C(7)-N(2)-Pd(1)-N(3)	19.42(18)
C(15)-C(16)-C(17)-N(4)	0.7(4)	C(1)-N(2)-Pd(1)-Cl(1)	-14.2(2)
C(4)-C(5)-N(1)-C(1)	-2.2(4)	C(7)-N(2)-Pd(1)-Cl(1)	-156.45(17)
C(4)-C(5)-N(1)-C(6)	178.5(3)	C(13)-N(3)-Pd(1)-N(2)	-172.0(2)
N(2)-C(1)-N(1)-C(5)	-174.8(2)	C(12)-N(3)-Pd(1)-N(2)	-19.58(18)
C(2)-C(1)-N(1)-C(5)	3.6(4)	C(13)-N(3)-Pd(1)-Cl(2)	3.2(2)
N(2)-C(1)-N(1)-C(6)	4.5(4)	C(12)-N(3)-Pd(1)-Cl(2)	155.63(17)
C(2)-C(1)-N(1)-C(6)	-177.1(2)	N(6)-C(19)-C(20)-C(21)	-174.4(3)
N(1)-C(1)-N(2)-C(7)	-138.8(2)	N(5)-C(19)-C(20)-C(21)	4.7(4)
C(2)-C(1)-N(2)-C(7)	42.9(4)	C(19)-C(20)-C(21)-C(22)	-1.4(5)
N(1)-C(1)-N(2)-Pd(1)	81.3(3)	C(20)-C(21)-C(22)-C(23)	-1.4(5)
C(2)-C(1)-N(2)-Pd(1)	-97.0(3)	C(21)-C(22)-C(23)-N(5)	0.7(5)

N(6)-C(25)-C(26)-C(27)	-173.7(3)
C(25)#1-C(25)-C(26)-C(27)	-0.1(5)
C(25)-C(26)-C(27)-C(27)#1	0.1(5)
C(22)-C(23)-N(5)-C(19)	2.9(5)
C(22)-C(23)-N(5)-C(24)	-175.9(3)
N(6)-C(19)-N(5)-C(23)	173.8(3)
C(20)-C(19)-N(5)-C(23)	-5.5(4)
N(6)-C(19)-N(5)-C(24)	-7.4(4)
C(20)-C(19)-N(5)-C(24)	173.3(3)
N(5)-C(19)-N(6)-C(25)	129.9(2)
C(20)-C(19)-N(6)-C(25)	-50.9(4)
N(5)-C(19)-N(6)-Pd(2)	-85.9(3)

C(20)-C(19)-N(6)-Pd(2)	93.3(3)
C(26)-C(25)-N(6)-C(19)	-30.1(4)
C(25)#1-C(25)-N(6)-C(19)	156.2(3)
C(26)-C(25)-N(6)-Pd(2)	-177.5(2)
C(25)#1-C(25)-N(6)-Pd(2)	8.7(4)
C(19)-N(6)-Pd(2)-N(6)#1	-149.0(2)
C(25)-N(6)-Pd(2)-N(6)#1	-2.99(12)

Symmetry transformations used to generate equivalent atoms:

#1 -x,y,-z+1/2

Single crystal X-ray structure data for [PdCl₂(^{Bn}N^{(CH₂)₂N^{Bn})] (23)}Table 1. Crystal data and structure refinement for **23**.

Identification code	23	
Empirical formula	C ₅₇ H _{59.50} Cl ₄ N _{10.50} Pd ₂	
Formula weight	1246.25	
Temperature	110(2) K	
Wavelength	0.71073 Å	
Crystal system	Triclinic	
Space group	P-1	
Unit cell dimensions	a = 11.0952(6) Å	α = 98.7810(10)°.
	b = 15.1574(8) Å	β = 94.8310(10)°.
	c = 17.8340(9) Å	γ = 110.6650(10)°.
Volume	2742.3(3) Å ³	
Z	2	
Density (calculated)	1.509 Mg/m ³	
Absorption coefficient	0.899 mm ⁻¹	
F(000)	1270	
Crystal size	0.18 x 0.16 x 0.05 mm ³	
Theta range for data collection	1.17 to 28.28°.	
Index ranges	-14 ≤ h ≤ 14, -18 ≤ k ≤ 20, -23 ≤ l ≤ 23	
Reflections collected	20439	
Independent reflections	13033 [R(int) = 0.0237]	
Completeness to theta = 28.28°	95.7 %	
Absorption correction	Semi-empirical from equivalents	
Max. and min. transmission	0.960 and 0.806	
Refinement method	Full-matrix least-squares on F ²	
Data / restraints / parameters	13033 / 6 / 680	
Goodness-of-fit on F ²	1.043	
Final R indices [I > 2σ(I)]	R1 = 0.0352, wR2 = 0.0806	
R indices (all data)	R1 = 0.0453, wR2 = 0.0891	
Largest diff. peak and hole	0.782 and -0.448 e.Å ⁻³	

Table 2. Atomic coordinates ($\times 10^4$) and equivalent isotropic displacement parameters ($\text{\AA}^2 \times 10^3$) for **23**. $U(\text{eq})$ is defined as one third of the trace of the orthogonalized U^{ij} tensor.

	x	y	z	$U(\text{eq})$
C(1)	8710(3)	1235(2)	1087(2)	22(1)
C(2)	9097(3)	487(2)	758(2)	26(1)
C(3)	10198(3)	383(2)	1077(2)	30(1)
C(4)	10967(3)	1026(2)	1730(2)	30(1)
C(5)	10609(3)	1753(2)	2036(2)	26(1)
C(6)	9349(3)	2771(2)	2031(2)	23(1)
C(7)	10161(3)	3570(2)	1669(2)	24(1)
C(8)	9871(4)	3565(3)	894(2)	37(1)
C(9)	10635(5)	4294(3)	567(2)	53(1)
C(10)	11682(5)	5038(3)	1002(3)	58(1)
C(11)	12000(4)	5051(3)	1777(2)	48(1)
C(12)	11245(3)	4315(2)	2109(2)	31(1)
C(13)	6988(3)	887(2)	48(2)	22(1)
C(14)	6024(3)	1330(2)	-189(2)	24(1)
C(15)	4508(3)	1934(2)	374(2)	21(1)
C(16)	3718(3)	1764(3)	-349(2)	33(1)
C(17)	2676(3)	2040(3)	-415(2)	37(1)
C(18)	2363(3)	2525(2)	229(2)	32(1)
C(19)	3157(3)	2737(2)	904(2)	26(1)
C(20)	5134(3)	2943(2)	1707(2)	22(1)
C(21)	5974(3)	3971(2)	1694(2)	23(1)
C(22)	7153(3)	4169(2)	1402(2)	31(1)
C(23)	7938(3)	5107(3)	1399(2)	39(1)
C(24)	7569(4)	5858(2)	1677(2)	39(1)
C(25)	6406(3)	5671(2)	1967(2)	32(1)
C(26)	5613(3)	4731(2)	1976(2)	24(1)
Cl(1)	6929(1)	548(1)	2333(1)	29(1)
Cl(2)	4037(1)	616(1)	1813(1)	21(1)
N(1)	7639(2)	1387(2)	826(1)	21(1)
N(2)	9529(2)	1864(2)	1720(1)	20(1)
N(3)	5448(2)	1605(2)	482(1)	20(1)

N(4)	4218(2)	2483(2)	980(1)	20(1)
Pd(1)	6065(1)	1128(1)	1395(1)	16(1)
C(1 [`])	5491(2)	3145(2)	4633(1)	15(1)
C(2 [`])	6875(2)	3605(2)	4871(2)	20(1)
C(3 [`])	7732(3)	3352(2)	4467(2)	21(1)
C(4 [`])	7279(3)	2615(2)	3811(2)	22(1)
C(5 [`])	5976(3)	2124(2)	3625(2)	20(1)
C(6 [`])	3750(2)	1621(2)	3887(2)	18(1)
C(7 [`])	3573(2)	905(2)	4413(2)	21(1)
C(8 [`])	3319(3)	1121(2)	5154(2)	24(1)
C(9 [`])	3122(3)	465(2)	5633(2)	34(1)
C(10 [`])	3166(3)	-428(3)	5366(2)	40(1)
C(11 [`])	3428(3)	-659(2)	4638(2)	40(1)
C(12 [`])	3636(3)	12(2)	4155(2)	30(1)
C(13 [`])	5051(2)	4073(2)	5708(2)	19(1)
C(14 [`])	4021(2)	4467(2)	5910(1)	16(1)
C(15 [`])	1723(2)	3837(2)	5905(1)	16(1)
C(16 [`])	1766(3)	4701(2)	6374(2)	20(1)
C(17 [`])	695(3)	4772(2)	6651(2)	26(1)
C(18 [`])	-496(3)	3980(2)	6488(2)	27(1)
C(19 [`])	-526(3)	3159(2)	6058(2)	22(1)
C(20 [`])	439(3)	2102(2)	5412(2)	19(1)
C(21 [`])	1503(3)	1948(2)	6676(2)	29(1)
C(22 [`])	1647(3)	1412(3)	7214(2)	36(1)
C(23 [`])	895(3)	439(3)	7091(2)	39(1)
C(24 [`])	-16(3)	15(2)	6436(2)	36(1)
C(25 [`])	-175(3)	557(2)	5899(2)	26(1)
C(26 [`])	592(3)	1528(2)	6017(2)	21(1)
cl(1 [`])	3393(1)	3430(1)	3235(1)	18(1)
cl(2 [`])	934(1)	3590(1)	4081(1)	24(1)
N(1 [`])	4622(2)	3439(2)	4940(1)	15(1)
N(2 [`])	5097(2)	2351(2)	4036(1)	16(1)
N(3 [`])	2731(2)	3708(2)	5617(1)	16(1)
N(4 [`])	549(2)	3076(2)	5777(1)	17(1)
pd(1 [`])	2878(1)	3448(1)	4475(1)	13(1)
C(27)	5905(4)	2265(3)	7182(2)	42(1)

C(28)	5305(5)	1796(4)	7770(3)	74(1)
N(5)	6423(4)	2619(3)	6722(2)	62(1)
C(29)	9147(4)	1920(3)	8387(2)	52(1)
C(30)	8472(4)	1481(3)	7625(2)	49(1)
N(6)	9683(5)	2233(4)	8984(3)	98(2)
C(31)	4756(7)	5811(6)	416(5)	46(2)
C(32)	4850(20)	4930(20)	30(17)	47(4)
N(7)	4461(7)	6394(6)	718(5)	62(2)

Table 3. Bond lengths [Å] and angles [°] for **23**.

C(13)-N(1)	1.465(3)	C(8)-C(9)	1.378(5)
C(13)-C(14)	1.514(4)	C(8)-H(8)	0.9500
C(13)-H(13a)	0.9900	C(9)-C(10)	1.370(6)
C(13)-H(13b)	0.9900	C(9)-H(9)	0.9500
C(14)-N(3)	1.476(3)	C(10)-C(11)	1.393(6)
C(14)-H(14b)	0.9900	C(10)-H(10)	0.9500
C(14)-H(14a)	0.9900	C(11)-C(12)	1.387(5)
C(1)-N(1)	1.348(3)	C(11)-H(11)	0.9500
C(1)-N(2)	1.377(4)	C(12)-H(12)	0.9500
C(1)-C(2)	1.414(4)	C(15)-N(3)	1.318(3)
C(2)-C(3)	1.373(4)	C(15)-N(4)	1.392(3)
C(2)-H(2)	0.9500	C(15)-C(16)	1.430(4)
C(3)-C(4)	1.390(5)	C(16)-C(17)	1.363(4)
C(3)-H(3)	0.9500	C(16)-H(16)	0.9500
C(4)-C(5)	1.354(4)	C(17)-C(18)	1.403(5)
C(4)-H(4)	0.9500	C(17)-H(17)	0.9500
C(5)-N(2)	1.355(3)	C(18)-C(19)	1.354(4)
C(5)-H(5)	0.9500	C(18)-H(18)	0.9500
C(6)-N(2)	1.489(3)	C(19)-N(4)	1.364(3)
C(6)-C(7)	1.505(4)	C(19)-H(19)	0.9500
C(6)-H(6b)	0.9900	C(20)-N(4)	1.484(3)
C(6)-H(6a)	0.9900	C(20)-C(21)	1.511(4)
C(7)-C(8)	1.390(4)	C(20)-H(20b)	0.9900
C(7)-C(12)	1.396(4)	C(20)-H(20a)	0.9900

C(21)-C(26)	1.387(4)	C(6`)-H(6`b)	0.9900
C(21)-C(22)	1.398(4)	C(7`)-C(8`)	1.389(4)
C(26)-C(25)	1.389(4)	C(7`)-C(12`)	1.389(4)
C(26)-H(26)	0.9500	C(8`)-C(9`)	1.380(4)
C(25)-C(24)	1.384(5)	C(8`)-H(8`)	0.9500
C(25)-H(25)	0.9500	C(9`)-C(10`)	1.384(5)
C(24)-C(23)	1.378(5)	C(9`)-H(9`)	0.9500
C(24)-H(24)	0.9500	C(10`)-C(11`)	1.375(6)
C(23)-C(22)	1.382(5)	C(10`)-H(10`)	0.9500
C(23)-H(23)	0.9500	C(11`)-C(12`)	1.402(5)
C(22)-H(22)	0.9500	C(11`)-H(11`)	0.9500
Cl(1)-Pd(1)	2.2944(7)	C(12`)-H(12`)	0.9500
Cl(2)-Pd(1)	2.3347(7)	C(15`)-N(3`)	1.332(3)
N(1)-Pd(1)	2.041(2)	C(15`)-N(4`)	1.374(3)
N(3)-Pd(1)	2.041(2)	C(15`)-C(16`)	1.425(4)
C(13`)-N(1`)	1.480(3)	C(16`)-C(17`)	1.357(4)
C(13`)-C(14`)	1.509(3)	C(16`)-H(16`)	0.9500
C(13`)-H(13a)	0.9900	C(17`)-C(18`)	1.407(4)
C(13`)-H(13b)	0.9900	C(17`)-H(17`)	0.9500
C(14`)-N(3`)	1.474(3)	C(18`)-C(19`)	1.346(4)
C(14`)-H(14b)	0.9900	C(18`)-H(18`)	0.9500
C(14`)-H(14a)	0.9900	C(19`)-N(4`)	1.370(3)
C(1`)-N(1`)	1.321(3)	C(19`)-H(19`)	0.9500
C(1`)-N(2`)	1.391(3)	C(20`)-N(4`)	1.479(3)
C(1`)-C(2`)	1.439(3)	C(20`)-C(26`)	1.519(4)
C(2`)-C(3`)	1.363(4)	C(20`)-H(20a)	0.9900
C(2`)-H(2`)	0.9500	C(20`)-H(20b)	0.9900
C(3`)-C(4`)	1.405(4)	C(26`)-C(25`)	1.388(4)
C(3`)-H(3`)	0.9500	C(26`)-C(21`)	1.388(4)
C(4`)-C(5`)	1.356(4)	C(25`)-C(24`)	1.393(4)
C(4`)-H(4`)	0.9500	C(25`)-H(25`)	0.9500
C(5`)-N(2`)	1.373(3)	C(24`)-C(23`)	1.383(5)
C(5`)-H(5`)	0.9500	C(24`)-H(24`)	0.9500
C(6`)-N(2`)	1.485(3)	C(23`)-C(22`)	1.385(5)
C(6`)-C(7`)	1.512(4)	C(23`)-H(23`)	0.9500
C(6`)-H(6`a)	0.9900	C(22`)-C(21`)	1.382(4)

C(22')-H(22')	0.9500	N(2)-C(1)-C(2)	115.8(2)
C(21')-H(21')	0.9500	C(3)-C(2)-C(1)	121.2(3)
cl(1')-pd(1')	2.3284(6)	C(3)-C(2)-H(2)	119.4
cl(2')-pd(1')	2.3057(7)	C(1)-C(2)-H(2)	119.4
N(1')-pd(1')	2.045(2)	C(2)-C(3)-C(4)	120.3(3)
N(3')-pd(1')	2.046(2)	C(2)-C(3)-H(3)	119.9
C(31)-N(7)	1.127(11)	C(4)-C(3)-H(3)	119.9
C(31)-C(32)	1.44(3)	C(5)-C(4)-C(3)	118.5(3)
C(32)-H(32a)	0.9800	C(5)-C(4)-H(4)	120.7
C(32)-H(32b)	0.9800	C(3)-C(4)-H(4)	120.8
C(32)-H(32c)	0.9800	C(4)-C(5)-N(2)	121.5(3)
C(29)-N(6)	1.119(5)	C(4)-C(5)-H(5)	119.2
C(29)-C(30)	1.433(5)	N(2)-C(5)-H(5)	119.2
C(30)-H(30c)	0.9800	N(2)-C(6)-C(7)	109.7(2)
C(30)-H(30a)	0.9800	N(2)-C(6)-H(6b)	109.7
C(30)-H(30b)	0.9800	C(7)-C(6)-H(6b)	109.7
C(27)-N(5)	1.134(5)	N(2)-C(6)-H(6a)	109.7
C(27)-C(28)	1.435(6)	C(7)-C(6)-H(6a)	109.7
C(28)-H(28b)	0.9800	H(6b)-C(6)-H(6a)	108.2
C(28)-H(28a)	0.9800	C(8)-C(7)-C(12)	119.3(3)
C(28)-H(28c)	0.9800	C(8)-C(7)-C(6)	121.0(3)
		C(12)-C(7)-C(6)	119.8(3)
N(1)-C(13)-C(14)	107.8(2)	C(9)-C(8)-C(7)	120.3(4)
N(1)-C(13)-H(13a)	110.2	C(9)-C(8)-H(8)	119.8
C(14)-C(13)-H(13a)	110.2	C(7)-C(8)-H(8)	119.8
N(1)-C(13)-H(13b)	110.2	C(10)-C(9)-C(8)	120.5(4)
C(14)-C(13)-H(13b)	110.2	C(10)-C(9)-H(9)	119.7
H(13a)-C(13)-H(13b)	108.5	C(8)-C(9)-H(9)	119.7
N(3)-C(14)-C(13)	109.8(2)	C(9)-C(10)-C(11)	120.1(4)
N(3)-C(14)-H(14b)	109.7	C(9)-C(10)-H(10)	119.9
C(13)-C(14)-H(14b)	109.7	C(11)-C(10)-H(10)	119.9
N(3)-C(14)-H(14a)	109.7	C(12)-C(11)-C(10)	119.7(4)
C(13)-C(14)-H(14a)	109.7	C(12)-C(11)-H(11)	120.1
H(14b)-C(14)-H(14a)	108.2	C(10)-C(11)-H(11)	120.1
N(1)-C(1)-N(2)	118.5(2)	C(11)-C(12)-C(7)	120.0(3)
N(1)-C(1)-C(2)	125.7(3)	C(11)-C(12)-H(12)	120.0

C(7)-C(12)-H(12)	120.0	C(22)-C(23)-H(23)	119.7
N(3)-C(15)-N(4)	120.7(2)	C(23)-C(22)-C(21)	120.3(3)
N(3)-C(15)-C(16)	124.1(3)	C(23)-C(22)-H(22)	119.9
N(4)-C(15)-C(16)	115.1(2)	C(21)-C(22)-H(22)	119.9
C(17)-C(16)-C(15)	121.7(3)	C(1)-N(1)-C(13)	117.1(2)
C(17)-C(16)-H(16)	119.1	C(1)-N(1)-Pd(1)	122.00(18)
C(15)-C(16)-H(16)	119.1	C(13)-N(1)-Pd(1)	100.09(16)
C(16)-C(17)-C(18)	120.6(3)	C(15)-N(3)-C(14)	118.4(2)
C(16)-C(17)-H(17)	119.7	C(15)-N(3)-Pd(1)	131.04(18)
C(18)-C(17)-H(17)	119.7	C(14)-N(3)-Pd(1)	109.25(17)
C(19)-C(18)-C(17)	117.6(3)	C(5)-N(2)-C(1)	122.6(2)
C(19)-C(18)-H(18)	121.2	C(5)-N(2)-C(6)	116.5(2)
C(17)-C(18)-H(18)	121.2	C(1)-N(2)-C(6)	120.5(2)
C(18)-C(19)-N(4)	122.7(3)	C(19)-N(4)-C(15)	121.7(2)
C(18)-C(19)-H(19)	118.6	C(19)-N(4)-C(20)	115.5(2)
N(4)-C(19)-H(19)	118.6	C(15)-N(4)-C(20)	122.2(2)
N(4)-C(20)-C(21)	111.2(2)	N(3)-Pd(1)-N(1)	79.18(9)
N(4)-C(20)-H(20b)	109.4	N(3)-Pd(1)-Cl(1)	173.14(6)
C(21)-C(20)-H(20b)	109.4	N(1)-Pd(1)-Cl(1)	94.44(7)
N(4)-C(20)-H(20a)	109.4	N(3)-Pd(1)-Cl(2)	94.70(7)
C(21)-C(20)-H(20a)	109.4	N(1)-Pd(1)-Cl(2)	168.35(7)
H(20b)-C(20)-H(20a)	108.0	Cl(1)-Pd(1)-Cl(2)	91.12(3)
C(26)-C(21)-C(22)	118.7(3)	N(1')-C(13')-C(14')	109.6(2)
C(26)-C(21)-C(20)	121.4(3)	N(1')-C(13')-H(13a)	109.8
C(22)-C(21)-C(20)	119.8(3)	C(14')-C(13')-H(13a)	109.8
C(21)-C(26)-C(25)	120.6(3)	N(1')-C(13')-H(13b)	109.8
C(21)-C(26)-H(26)	119.7	C(14')-C(13')-H(13b)	109.8
C(25)-C(26)-H(26)	119.7	H(13a)-C(13')-H(13b)	108.2
C(24)-C(25)-C(26)	120.1(3)	N(3')-C(14')-C(13')	108.4(2)
C(24)-C(25)-H(25)	120.0	N(3')-C(14')-H(14b)	110.0
C(26)-C(25)-H(25)	120.0	C(13')-C(14')-H(14b)	110.0
C(23)-C(24)-C(25)	119.7(3)	N(3')-C(14')-H(14a)	110.0
C(23)-C(24)-H(24)	120.2	C(13')-C(14')-H(14a)	110.0
C(25)-C(24)-H(24)	120.2	H(14b)-C(14')-H(14a)	108.4
C(24)-C(23)-C(22)	120.6(3)	N(1')-C(1')-N(2')	120.5(2)
C(24)-C(23)-H(23)	119.7	N(1')-C(1')-C(2')	124.1(2)

N(2 ['])-C(1 ['])-C(2 ['])	115.4(2)	C(11 ['])-C(12 ['])-H(12 ['])	120.0
C(3 ['])-C(2 ['])-C(1 ['])	121.4(3)	N(3 ['])-C(15 ['])-N(4 ['])	118.8(2)
C(3 ['])-C(2 ['])-H(2 ['])	119.3	N(3 ['])-C(15 ['])-C(16 ['])	125.2(2)
C(1 ['])-C(2 ['])-H(2 ['])	119.3	N(4 ['])-C(15 ['])-C(16 ['])	115.9(2)
C(2 ['])-C(3 ['])-C(4 ['])	120.5(3)	C(17 ['])-C(16 ['])-C(15 ['])	121.6(3)
C(2 ['])-C(3 ['])-H(3 ['])	119.7	C(17 ['])-C(16 ['])-H(16 ['])	119.2
C(4 ['])-C(3 ['])-H(3 ['])	119.7	C(15 ['])-C(16 ['])-H(16 ['])	119.2
C(5 ['])-C(4 ['])-C(3 ['])	118.1(2)	C(16 ['])-C(17 ['])-C(18 ['])	120.4(3)
C(5 ['])-C(4 ['])-H(4 ['])	120.9	C(16 ['])-C(17 ['])-H(17 ['])	119.8
C(3 ['])-C(4 ['])-H(4 ['])	120.9	C(18 ['])-C(17 ['])-H(17 ['])	119.8
C(4 ['])-C(5 ['])-N(2 ['])	122.2(2)	C(19 ['])-C(18 ['])-C(17 ['])	117.8(3)
C(4 ['])-C(5 ['])-H(5 ['])	118.9	C(19 ['])-C(18 ['])-H(18 ['])	121.1
N(2 ['])-C(5 ['])-H(5 ['])	118.9	C(17 ['])-C(18 ['])-H(18 ['])	121.1
N(2 ['])-C(6 ['])-C(7 ['])	111.5(2)	C(18 ['])-C(19 ['])-N(4 ['])	122.4(3)
N(2 ['])-C(6 ['])-H(6 ['] a)	109.3	C(18 ['])-C(19 ['])-H(19 ['])	118.8
C(7 ['])-C(6 ['])-H(6 ['] a)	109.3	N(4 ['])-C(19 ['])-H(19 ['])	118.8
N(2 ['])-C(6 ['])-H(6 ['] b)	109.3	N(4 ['])-C(20 ['])-C(26 ['])	110.5(2)
C(7 ['])-C(6 ['])-H(6 ['] b)	109.3	N(4 ['])-C(20 ['])-H(20a)	109.5
H(6 ['] a)-C(6 ['])-H(6 ['] b)	108.0	C(26 ['])-C(20 ['])-H(20a)	109.5
C(8 ['])-C(7 ['])-C(12 ['])	119.0(3)	N(4 ['])-C(20 ['])-H(20b)	109.5
C(8 ['])-C(7 ['])-C(6 ['])	120.6(2)	C(26 ['])-C(20 ['])-H(20b)	109.5
C(12 ['])-C(7 ['])-C(6 ['])	120.4(3)	H(20a)-C(20 ['])-H(20b)	108.1
C(9 ['])-C(8 ['])-C(7 ['])	121.2(3)	C(25 ['])-C(26 ['])-C(21 ['])	119.3(3)
C(9 ['])-C(8 ['])-H(8 ['])	119.4	C(25 ['])-C(26 ['])-C(20 ['])	119.2(3)
C(7 ['])-C(8 ['])-H(8 ['])	119.4	C(21 ['])-C(26 ['])-C(20 ['])	121.5(2)
C(8 ['])-C(9 ['])-C(10 ['])	119.3(3)	C(26 ['])-C(25 ['])-C(24 ['])	119.9(3)
C(8 ['])-C(9 ['])-H(9 ['])	120.3	C(26 ['])-C(25 ['])-H(25 ['])	120.1
C(10 ['])-C(9 ['])-H(9 ['])	120.3	C(24 ['])-C(25 ['])-H(25 ['])	120.1
C(11 ['])-C(10 ['])-C(9 ['])	120.7(3)	C(23 ['])-C(24 ['])-C(25 ['])	120.4(3)
C(11 ['])-C(10 ['])-H(10 ['])	119.6	C(23 ['])-C(24 ['])-H(24 ['])	119.8
C(9 ['])-C(10 ['])-H(10 ['])	119.6	C(25 ['])-C(24 ['])-H(24 ['])	119.8
C(10 ['])-C(11 ['])-C(12 ['])	119.8(3)	C(24 ['])-C(23 ['])-C(22 ['])	119.6(3)
C(10 ['])-C(11 ['])-H(11 ['])	120.1	C(24 ['])-C(23 ['])-H(23 ['])	120.2
C(12 ['])-C(11 ['])-H(11 ['])	120.1	C(22 ['])-C(23 ['])-H(23 ['])	120.2
C(7 ['])-C(12 ['])-C(11 ['])	120.0(3)	C(21 ['])-C(22 ['])-C(23 ['])	120.0(3)
C(7 ['])-C(12 ['])-H(12 ['])	120.0	C(21 ['])-C(22 ['])-H(22 ['])	120.0

C(23 ['])-C(22 ['])-H(22 ['])	120.0	N(3 ['])-pd(1 ['])-cl(1 ['])	168.92(6)
C(22 ['])-C(21 ['])-C(26 ['])	120.8(3)	cl(2 ['])-pd(1 ['])-cl(1 ['])	90.47(2)
C(22 ['])-C(21 ['])-H(21 ['])	119.6	N(7)-C(31)-C(32)	167.6(12)
C(26 ['])-C(21 ['])-H(21 ['])	119.6	N(6)-C(29)-C(30)	177.5(6)
C(1 ['])-N(1 ['])-C(13 ['])	117.0(2)	C(29)-C(30)-H(30c)	109.5
C(1 ['])-N(1 ['])-pd(1 ['])	131.82(17)	C(29)-C(30)-H(30a)	109.5
C(13 ['])-N(1 ['])-pd(1 ['])	109.61(15)	H(30c)-C(30)-H(30a)	109.5
C(15 ['])-N(3 ['])-C(14 ['])	116.4(2)	C(29)-C(30)-H(30b)	109.5
C(15 ['])-N(3 ['])-pd(1 ['])	125.38(17)	H(30c)-C(30)-H(30b)	109.5
C(14 ['])-N(3 ['])-pd(1 ['])	99.98(15)	H(30a)-C(30)-H(30b)	109.5
C(5 ['])-N(2 ['])-C(1 ['])	121.6(2)	N(5)-C(27)-C(28)	176.8(5)
C(5 ['])-N(2 ['])-C(6 ['])	115.9(2)	C(27)-C(28)-H(28b)	109.5
C(1 ['])-N(2 ['])-C(6 ['])	121.8(2)	C(27)-C(28)-H(28a)	109.5
C(19 ['])-N(4 ['])-C(15 ['])	121.8(2)	H(28b)-C(28)-H(28a)	109.5
C(19 ['])-N(4 ['])-C(20 ['])	116.9(2)	C(27)-C(28)-H(28c)	109.5
C(15 ['])-N(4 ['])-C(20 ['])	120.9(2)	H(28b)-C(28)-H(28c)	109.5
N(1 ['])-pd(1 ['])-N(3 ['])	79.93(8)	H(28a)-C(28)-H(28c)	109.5
N(1 ['])-pd(1 ['])-cl(2 ['])	173.13(6)		
N(3 ['])-pd(1 ['])-cl(2 ['])	94.21(6)	Symmetry transformations used to generate equivalent atoms:	
N(1 ['])-pd(1 ['])-cl(1 ['])	94.69(6)		

Table 4. Anisotropic displacement parameters ($\text{\AA}^2 \times 10^3$) for **23**. The anisotropic displacement factor exponent takes the form: $-2\pi^2 [h^2 a^{*2} U^{11} + \dots + 2 h k a^* b^* U^{12}]$

	U^{11}	U^{22}	U^{33}	U^{23}	U^{13}	U^{12}
C(1)	20(1)	30(2)	17(1)	4(1)	6(1)	11(1)
C(2)	27(2)	31(2)	24(1)	3(1)	10(1)	14(1)
C(3)	31(2)	36(2)	35(2)	15(1)	17(1)	21(1)
C(4)	19(1)	40(2)	39(2)	22(2)	10(1)	15(1)
C(5)	18(1)	33(2)	27(2)	15(1)	2(1)	6(1)
C(6)	25(1)	27(2)	16(1)	0(1)	2(1)	11(1)
C(7)	32(2)	27(2)	23(1)	8(1)	10(1)	21(1)
C(8)	60(2)	41(2)	26(2)	11(1)	13(2)	33(2)
C(9)	98(3)	52(2)	40(2)	26(2)	35(2)	52(3)

C(10)	92(3)	38(2)	71(3)	34(2)	54(3)	36(2)
C(11)	54(2)	30(2)	67(3)	16(2)	28(2)	17(2)
C(12)	35(2)	29(2)	37(2)	11(1)	14(1)	17(1)
C(13)	21(1)	33(2)	14(1)	-1(1)	3(1)	13(1)
C(14)	24(1)	36(2)	14(1)	2(1)	4(1)	14(1)
C(15)	26(1)	23(1)	18(1)	7(1)	5(1)	12(1)
C(16)	35(2)	51(2)	20(1)	8(1)	3(1)	25(2)
C(17)	37(2)	53(2)	31(2)	17(2)	2(1)	25(2)
C(18)	26(2)	36(2)	46(2)	17(2)	8(1)	20(1)
C(19)	23(1)	21(1)	39(2)	10(1)	11(1)	10(1)
C(20)	29(2)	22(1)	19(1)	5(1)	8(1)	14(1)
C(21)	30(2)	23(1)	16(1)	4(1)	5(1)	11(1)
C(22)	34(2)	32(2)	28(2)	7(1)	13(1)	10(1)
C(23)	38(2)	44(2)	32(2)	10(2)	12(2)	7(2)
C(24)	48(2)	29(2)	30(2)	11(1)	-2(2)	2(2)
C(25)	46(2)	23(2)	24(2)	2(1)	-3(1)	13(1)
C(26)	32(2)	25(2)	16(1)	2(1)	2(1)	12(1)
Cl(1)	34(1)	41(1)	25(1)	13(1)	7(1)	26(1)
Cl(2)	20(1)	24(1)	20(1)	2(1)	5(1)	8(1)
N(1)	18(1)	32(1)	14(1)	-1(1)	1(1)	13(1)
N(2)	18(1)	24(1)	21(1)	6(1)	3(1)	9(1)
N(3)	22(1)	27(1)	12(1)	4(1)	2(1)	13(1)
N(4)	20(1)	19(1)	23(1)	6(1)	6(1)	10(1)
Pd(1)	18(1)	21(1)	13(1)	1(1)	2(1)	11(1)
C(1 ^ˆ)	14(1)	16(1)	14(1)	7(1)	1(1)	6(1)
C(2 ^ˆ)	15(1)	23(1)	21(1)	4(1)	1(1)	6(1)
C(3 ^ˆ)	16(1)	24(1)	27(2)	11(1)	3(1)	9(1)
C(4 ^ˆ)	21(1)	25(1)	26(1)	11(1)	11(1)	13(1)
C(5 ^ˆ)	24(1)	20(1)	19(1)	5(1)	7(1)	12(1)
C(6 ^ˆ)	15(1)	17(1)	18(1)	0(1)	0(1)	4(1)
C(7 ^ˆ)	11(1)	17(1)	31(2)	3(1)	-1(1)	2(1)
C(8 ^ˆ)	17(1)	23(1)	30(2)	10(1)	3(1)	3(1)
C(9 ^ˆ)	21(2)	38(2)	40(2)	19(2)	2(1)	2(1)
C(10 ^ˆ)	19(2)	35(2)	64(2)	29(2)	-4(2)	4(1)
C(11 ^ˆ)	18(2)	16(2)	84(3)	10(2)	-6(2)	5(1)
C(12 ^ˆ)	15(1)	21(2)	48(2)	-1(1)	-1(1)	5(1)

C(13`)	16(1)	23(1)	16(1)	0(1)	1(1)	8(1)
C(14`)	16(1)	17(1)	13(1)	0(1)	2(1)	3(1)
C(15`)	18(1)	18(1)	14(1)	7(1)	2(1)	7(1)
C(16`)	22(1)	19(1)	20(1)	5(1)	5(1)	8(1)
C(17`)	31(2)	26(2)	25(1)	4(1)	8(1)	16(1)
C(18`)	23(1)	35(2)	29(2)	9(1)	12(1)	15(1)
C(19`)	16(1)	29(2)	24(1)	11(1)	6(1)	8(1)
C(20`)	18(1)	17(1)	19(1)	3(1)	0(1)	5(1)
C(21`)	26(2)	27(2)	29(2)	10(1)	-1(1)	5(1)
C(22`)	29(2)	47(2)	34(2)	20(2)	3(1)	13(2)
C(23`)	27(2)	49(2)	57(2)	38(2)	14(2)	19(2)
C(24`)	25(2)	26(2)	65(2)	27(2)	14(2)	10(1)
C(25`)	18(1)	24(2)	38(2)	7(1)	6(1)	8(1)
C(26`)	18(1)	21(1)	27(1)	9(1)	7(1)	8(1)
cl(1`)	16(1)	23(1)	14(1)	3(1)	4(1)	6(1)
cl(2`)	17(1)	41(1)	18(1)	8(1)	4(1)	16(1)
N(1`)	14(1)	16(1)	14(1)	0(1)	0(1)	5(1)
N(2`)	14(1)	16(1)	18(1)	3(1)	3(1)	6(1)
N(3`)	15(1)	17(1)	13(1)	2(1)	2(1)	4(1)
N(4`)	18(1)	19(1)	16(1)	6(1)	4(1)	8(1)
pd(1`)	11(1)	16(1)	12(1)	2(1)	2(1)	5(1)
C(27)	39(2)	36(2)	48(2)	11(2)	5(2)	8(2)
C(28)	65(3)	89(4)	80(4)	35(3)	31(3)	29(3)
N(5)	53(2)	62(2)	70(3)	33(2)	8(2)	13(2)
C(29)	34(2)	71(3)	41(2)	19(2)	6(2)	5(2)
C(30)	38(2)	68(3)	42(2)	16(2)	6(2)	19(2)
N(6)	78(3)	119(4)	55(3)	3(3)	-5(2)	-4(3)
C(31)	36(4)	42(4)	48(5)	28(4)	-8(3)	-5(3)
C(32)	50(9)	53(7)	33(5)	26(4)	6(6)	4(6)
N(7)	47(4)	47(4)	92(6)	26(4)	17(4)	11(3)

Table 5. Hydrogen coordinates ($\times 10^4$) and isotropic displacement parameters ($\text{\AA}^2 \times 10^3$) for **23**.

	x	y	z	U(eq)
H(2)	8586	48	308	31
H(3)	10434	-130	851	36
H(4)	11727	957	1956	36
H(5)	11126	2196	2483	31
H(6b)	9614	2940	2595	27
H(6a)	8419	2680	1922	27
H(8)	9142	3056	589	45
H(9)	10434	4281	36	63
H(10)	12191	5545	774	70
H(11)	12732	5563	2076	57
H(12)	11465	4318	2636	37
H(13a)	6529	193	38	27
H(13b)	7635	957	-311	27
H(14b)	6471	1905	-404	29
H(14a)	5327	862	-592	29
H(16)	3925	1451	-795	39
H(17)	2157	1902	-901	44
H(18)	1620	2699	192	39
H(19)	2968	3076	1343	31
H(20b)	5697	2574	1786	26
H(20a)	4633	2933	2142	26
H(22)	7415	3657	1206	38
H(23)	8740	5236	1203	47
H(24)	8111	6501	1669	46
H(25)	6149	6186	2161	38
H(26)	4816	4607	2177	29
H(2 ^ˆ)	7199	4095	5320	24
H(3 ^ˆ)	8642	3676	4630	25
H(4 ^ˆ)	7869	2466	3506	26
H(5 ^ˆ)	5660	1605	3197	24
H(6 ^ˆ a)	3556	1276	3347	21
H(6 ^ˆ b)	3127	1948	3964	21

H(8 [`])	3280	1732	5334	29
H(9 [`])	2958	625	6140	41
H(10 [`])	3013	-887	5690	47
H(11 [`])	3468	-1271	4463	48
H(12 [`])	3820	-144	3652	36
H(13a)	5881	4610	5708	23
H(13b)	5201	3705	6096	23
H(14b)	4113	4667	6473	20
H(14a)	4118	5035	5675	20
H(16 [`])	2565	5240	6497	24
H(17 [`])	749	5359	6957	31
H(18 [`])	-1254	4023	6675	32
H(19 [`])	-1322	2618	5944	27
H(20a)	1120	2151	5078	23
H(20b)	-421	1765	5087	23
H(21 [`])	2032	2612	6759	34
H(22 [`])	2263	1710	7667	43
H(23 [`])	1003	66	7455	47
H(24 [`])	-536	-651	6352	44
H(25 [`])	-808	263	5452	32
H(28b)	5764	1391	7925	112
H(28a)	4391	1395	7572	112
H(28c)	5350	2281	8214	112
H(30c)	9038	1257	7319	74
H(30a)	8235	1952	7390	74
H(30b)	7681	934	7646	74
H(32a)	4097	4383	97	71
H(32b)	5653	4881	247	71
H(32c)	4850	4942	-519	71

Table 6. Torsion angles [°] for **23**.

N(1)-C(13)-C(14)-N(3)	-35.4(3)	C(1)-C(2)-C(3)-C(4)	-0.9(5)
N(1)-C(1)-C(2)-C(3)	-178.8(3)	C(2)-C(3)-C(4)-C(5)	-0.4(4)
N(2)-C(1)-C(2)-C(3)	2.6(4)	C(3)-C(4)-C(5)-N(2)	-0.2(4)

N(2)-C(6)-C(7)-C(8)	67.7(3)	C(13)-C(14)-N(3)-Pd(1)	-6.2(3)
N(2)-C(6)-C(7)-C(12)	-110.5(3)	C(4)-C(5)-N(2)-C(1)	2.0(4)
C(12)-C(7)-C(8)-C(9)	-0.8(5)	C(4)-C(5)-N(2)-C(6)	-170.7(3)
C(6)-C(7)-C(8)-C(9)	-179.0(3)	N(1)-C(1)-N(2)-C(5)	178.1(3)
C(7)-C(8)-C(9)-C(10)	-0.6(5)	C(2)-C(1)-N(2)-C(5)	-3.1(4)
C(8)-C(9)-C(10)-C(11)	1.4(6)	N(1)-C(1)-N(2)-C(6)	-9.4(4)
C(9)-C(10)-C(11)-C(12)	-0.8(6)	C(2)-C(1)-N(2)-C(6)	169.3(2)
C(10)-C(11)-C(12)-C(7)	-0.7(5)	C(7)-C(6)-N(2)-C(5)	81.3(3)
C(8)-C(7)-C(12)-C(11)	1.5(4)	C(7)-C(6)-N(2)-C(1)	-91.6(3)
C(6)-C(7)-C(12)-C(11)	179.7(3)	C(18)-C(19)-N(4)-C(15)	-4.0(4)
N(3)-C(15)-C(16)-C(17)	173.4(3)	C(18)-C(19)-N(4)-C(20)	167.5(3)
N(4)-C(15)-C(16)-C(17)	-6.4(5)	N(3)-C(15)-N(4)-C(19)	-172.3(3)
C(15)-C(16)-C(17)-C(18)	1.6(5)	C(16)-C(15)-N(4)-C(19)	7.5(4)
C(16)-C(17)-C(18)-C(19)	2.3(5)	N(3)-C(15)-N(4)-C(20)	16.7(4)
C(17)-C(18)-C(19)-N(4)	-1.2(5)	C(16)-C(15)-N(4)-C(20)	-163.4(3)
N(4)-C(20)-C(21)-C(26)	92.3(3)	C(21)-C(20)-N(4)-C(19)	-77.1(3)
N(4)-C(20)-C(21)-C(22)	-88.6(3)	C(21)-C(20)-N(4)-C(15)	94.4(3)
C(22)-C(21)-C(26)-C(25)	0.1(4)	C(15)-N(3)-Pd(1)-N(1)	-162.1(3)
C(20)-C(21)-C(26)-C(25)	179.2(3)	C(14)-N(3)-Pd(1)-N(1)	31.42(18)
C(21)-C(26)-C(25)-C(24)	-0.1(4)	C(15)-N(3)-Pd(1)-Cl(2)	28.0(3)
C(26)-C(25)-C(24)-C(23)	-0.2(5)	C(14)-N(3)-Pd(1)-Cl(2)	-138.57(17)
C(25)-C(24)-C(23)-C(22)	0.5(5)	C(1)-N(1)-Pd(1)-N(3)	179.9(2)
C(24)-C(23)-C(22)-C(21)	-0.5(5)	C(13)-N(1)-Pd(1)-N(3)	-49.08(17)
C(26)-C(21)-C(22)-C(23)	0.2(5)	C(1)-N(1)-Pd(1)-Cl(1)	-2.7(2)
C(20)-C(21)-C(22)-C(23)	-179.0(3)	C(13)-N(1)-Pd(1)-Cl(1)	128.35(16)
N(2)-C(1)-N(1)-C(13)	163.6(2)	C(1)-N(1)-Pd(1)-Cl(2)	-121.0(3)
C(2)-C(1)-N(1)-C(13)	-15.0(4)	C(13)-N(1)-Pd(1)-Cl(2)	10.0(5)
N(2)-C(1)-N(1)-Pd(1)	-73.0(3)	N(1')-C(13')-C(14')-N(3')	37.3(3)
C(2)-C(1)-N(1)-Pd(1)	108.5(3)	N(1')-C(1')-C(2')-C(3')	-171.0(3)
C(14)-C(13)-N(1)-C(1)	-167.2(3)	N(2')-C(1')-C(2')-C(3')	8.5(4)
C(14)-C(13)-N(1)-Pd(1)	58.7(2)	C(1')-C(2')-C(3')-C(4')	-1.4(4)
N(4)-C(15)-N(3)-C(14)	-159.2(3)	C(2')-C(3')-C(4')-C(5')	-4.5(4)
C(16)-C(15)-N(3)-C(14)	21.0(4)	C(3')-C(4')-C(5')-N(2')	2.9(4)
N(4)-C(15)-N(3)-Pd(1)	35.3(4)	N(2')-C(6')-C(7')-C(8')	82.4(3)
C(16)-C(15)-N(3)-Pd(1)	-144.5(3)	N(2')-C(6')-C(7')-C(12')	-98.9(3)
C(13)-C(14)-N(3)-C(15)	-174.7(3)	C(12')-C(7')-C(8')-C(9')	-0.3(4)

C(6 [^])-C(7 [^])-C(8 [^])-C(9 [^])	178.3(2)	C(13 [^])-C(14 [^])-N(3 [^])-C(15 [^])	163.6(2)
C(7 [^])-C(8 [^])-C(9 [^])-C(10 [^])	-0.7(4)	C(13 [^])-C(14 [^])-N(3 [^])-pd(1 [^])	-58.4(2)
C(8 [^])-C(9 [^])-C(10 [^])-C(11 [^])	1.3(5)	C(4 [^])-C(5 [^])-N(2 [^])-C(1 [^])	4.8(4)
C(9 [^])-C(10 [^])-C(11 [^])-C(12 [^])	-0.9(5)	C(4 [^])-C(5 [^])-N(2 [^])-C(6 [^])	-166.0(3)
C(8 [^])-C(7 [^])-C(12 [^])-C(11 [^])	0.8(4)	N(1 [^])-C(1 [^])-N(2 [^])-C(5 [^])	169.4(2)
C(6 [^])-C(7 [^])-C(12 [^])-C(11 [^])	-177.9(3)	C(2 [^])-C(1 [^])-N(2 [^])-C(5 [^])	-10.2(4)
C(10 [^])-C(11 [^])-C(12 [^])-C(7 [^])	-0.2(4)	N(1 [^])-C(1 [^])-N(2 [^])-C(6 [^])	-20.4(4)
N(3 [^])-C(15 [^])-C(16 [^])-C(17 [^])	-179.4(3)	C(2 [^])-C(1 [^])-N(2 [^])-C(6 [^])	160.1(2)
N(4 [^])-C(15 [^])-C(16 [^])-C(17 [^])	-2.6(4)	C(7 [^])-C(6 [^])-N(2 [^])-C(5 [^])	89.4(3)
C(15 [^])-C(16 [^])-C(17 [^])-C(18 [^])	0.9(4)	C(7 [^])-C(6 [^])-N(2 [^])-C(1 [^])	-81.4(3)
C(16 [^])-C(17 [^])-C(18 [^])-C(19 [^])	0.5(4)	C(18 [^])-C(19 [^])-N(4 [^])-C(15 [^])	-1.6(4)
C(17 [^])-C(18 [^])-C(19 [^])-N(4 [^])	-0.2(4)	C(18 [^])-C(19 [^])-N(4 [^])-C(20 [^])	171.2(3)
N(4 [^])-C(20 [^])-C(26 [^])-C(25 [^])	141.6(2)	N(3 [^])-C(15 [^])-N(4 [^])-C(19 [^])	179.9(2)
N(4 [^])-C(20 [^])-C(26 [^])-C(21 [^])	-39.9(3)	C(16 [^])-C(15 [^])-N(4 [^])-C(19 [^])	2.9(4)
C(21 [^])-C(26 [^])-C(25 [^])-C(24 [^])	-0.7(4)	N(3 [^])-C(15 [^])-N(4 [^])-C(20 [^])	7.4(4)
C(20 [^])-C(26 [^])-C(25 [^])-C(24 [^])	177.9(3)	C(16 [^])-C(15 [^])-N(4 [^])-C(20 [^])	-169.7(2)
C(26 [^])-C(25 [^])-C(24 [^])-C(23 [^])	0.6(5)	C(26 [^])-C(20 [^])-N(4 [^])-C(19 [^])	-79.0(3)
C(25 [^])-C(24 [^])-C(23 [^])-C(22 [^])	0.3(5)	C(26 [^])-C(20 [^])-N(4 [^])-C(15 [^])	93.8(3)
C(24 [^])-C(23 [^])-C(22 [^])-C(21 [^])	-1.1(5)	C(1 [^])-N(1 [^])-pd(1 [^])-N(3 [^])	166.3(2)
C(23 [^])-C(22 [^])-C(21 [^])-C(26 [^])	1.1(5)	C(13 [^])-N(1 [^])-pd(1 [^])-N(3 [^])	-28.99(17)
C(25 [^])-C(26 [^])-C(21 [^])-C(22 [^])	-0.2(4)	C(1 [^])-N(1 [^])-pd(1 [^])-cl(1 [^])	-23.5(2)
C(20 [^])-C(26 [^])-C(21 [^])-C(22 [^])	-178.7(3)	C(13 [^])-N(1 [^])-pd(1 [^])-cl(1 [^])	141.24(16)
N(2 [^])-C(1 [^])-N(1 [^])-C(13 [^])	161.4(2)	C(15 [^])-N(3 [^])-pd(1 [^])-N(1 [^])	179.9(2)
C(2 [^])-C(1 [^])-N(1 [^])-C(13 [^])	-19.1(4)	C(14 [^])-N(3 [^])-pd(1 [^])-N(1 [^])	47.18(15)
N(2 [^])-C(1 [^])-N(1 [^])-pd(1 [^])	-34.7(4)	C(15 [^])-N(3 [^])-pd(1 [^])-cl(2 [^])	3.5(2)
C(2 [^])-C(1 [^])-N(1 [^])-pd(1 [^])	144.8(2)	C(14 [^])-N(3 [^])-pd(1 [^])-cl(2 [^])	-129.21(14)
C(14 [^])-C(13 [^])-N(1 [^])-C(1 [^])	170.6(2)	C(15 [^])-N(3 [^])-pd(1 [^])-cl(1 [^])	118.2(3)
C(14 [^])-C(13 [^])-N(1 [^])-pd(1 [^])	3.4(3)	C(14 [^])-N(3 [^])-pd(1 [^])-cl(1 [^])	-14.5(4)
N(4 [^])-C(15 [^])-N(3 [^])-C(14 [^])	-166.8(2)		
C(16 [^])-C(15 [^])-N(3 [^])-C(14 [^])	9.9(4)		
N(4 [^])-C(15 [^])-N(3 [^])-pd(1 [^])	67.1(3)		
C(16 [^])-C(15 [^])-N(3 [^])-pd(1 [^])	-116.2(3)		

Symmetry transformations used to generate equivalent atoms:

Single crystal X-ray structure data for [PdCl(η^3 -CH₂N^{C₆H₁₀}N^{Me})] (26)

Table 1. Crystal data and structure refinement for **26**.

Identification code	26	
Empirical formula	C ₁₈ H ₂₃ Cl N ₄ Pd	
Formula weight	437.25	
Temperature	110(2) K	
Wavelength	0.71073 Å	
Crystal system	Orthorhombic	
Space group	P2(1)2(1)2(1)	
Unit cell dimensions	a = 7.3789(11) Å	$\alpha = 90^\circ$.
	b = 11.5947(17) Å	$\beta = 90^\circ$.
	c = 20.367(3) Å	$\gamma = 90^\circ$.
Volume	1742.5(4) Å ³	
Z	4	
Density (calculated)	1.667 Mg/m ³	
Absorption coefficient	1.225 mm ⁻¹	
F(000)	888	
Crystal size	0.27 x 0.03 x 0.02 mm ³	
Theta range for data collection	2.00 to 25.09°.	
Index ranges	-8 ≤ h ≤ 8, -13 ≤ k ≤ 13, -24 ≤ l ≤ 24	
Reflections collected	13900	
Independent reflections	3081 [R(int) = 0.0623]	
Completeness to theta = 25.09°	99.7 %	
Absorption correction	Semi-empirical from equivalents	
Max. and min. transmission	0.980 and 0.854	
Refinement method	Full-matrix least-squares on F ²	
Data / restraints / parameters	3081 / 0 / 218	
Goodness-of-fit on F ²	1.032	
Final R indices [I > 2σ(I)]	R1 = 0.0294, wR2 = 0.0552	
R indices (all data)	R1 = 0.0414, wR2 = 0.0582	
Absolute structure parameter	0.00(3)	
Largest diff. peak and hole	0.872 and -0.509 e.Å ⁻³	

Table 2. Atomic coordinates ($\times 10^4$) and equivalent isotropic displacement parameters ($\text{\AA}^2 \times 10^3$) for **26**. $U(\text{eq})$ is defined as one third of the trace of the orthogonalized U^{ij} tensor.

	x	y	z	$U(\text{eq})$
C(1)	493(7)	8983(3)	1359(2)	15(1)
C(2)	565(6)	9918(3)	1823(2)	15(1)
C(3)	-634(6)	10796(4)	1783(2)	21(1)
C(4)	-1936(6)	10847(4)	1275(2)	20(1)
C(5)	-1995(5)	9970(3)	838(3)	17(1)
C(6)	-1014(6)	8040(4)	437(2)	22(1)
C(7)	2993(6)	7788(3)	1777(2)	14(1)
C(8)	4501(7)	8696(3)	1779(2)	17(1)
C(9)	5962(5)	8362(4)	2299(2)	20(1)
C(10)	6708(6)	7170(4)	2177(3)	20(1)
C(11)	5214(6)	6265(3)	2081(2)	16(1)
C(12)	3872(5)	6648(4)	1555(2)	16(1)
C(13)	3051(6)	4799(4)	1143(2)	14(1)
C(14)	4792(5)	4585(3)	849(2)	17(1)
C(15)	5199(6)	3555(3)	577(2)	22(1)
C(16)	3943(6)	2634(4)	578(2)	23(1)
C(17)	2312(6)	2841(3)	860(3)	20(1)
C(18)	154(6)	3970(4)	1503(2)	19(1)
Cl(1)	-942(1)	5403(1)	125(1)	19(1)
N(1)	1467(5)	8031(3)	1341(2)	14(1)
N(2)	-850(4)	9049(3)	887(2)	15(1)
N(3)	2457(5)	5767(3)	1412(2)	14(1)
N(4)	1874(5)	3862(3)	1140(2)	15(1)
Pd(1)	454(1)	6760(1)	813(1)	13(1)

Table 3. Bond lengths [\AA] and angles [$^\circ$] for **26**.

C(5)-C(4)	1.353(6)	C(15)-C(16)	1.414(6)
C(5)-N(2)	1.365(5)	C(15)-H(15)	0.9500
C(5)-H(5)	0.9500	C(16)-C(17)	1.355(6)
C(4)-C(3)	1.413(7)	C(16)-H(16)	0.9500
C(4)-H(4)	0.9500	C(17)-N(4)	1.353(5)
C(3)-C(2)	1.352(6)	C(17)-H(17)	0.9500
C(3)-H(3)	0.9500	C(6)-N(2)	1.491(6)
C(2)-C(1)	1.439(5)	C(6)-Pd(1)	1.990(4)
C(2)-H(2)	0.9500	C(6)-H(6b)	0.9900
C(1)-N(1)	1.318(5)	C(6)-H(6a)	0.9900
C(1)-N(2)	1.383(5)	C(18)-N(4)	1.473(6)
C(7)-N(1)	1.461(5)	C(18)-H(18a)	0.9800
C(7)-C(8)	1.532(6)	C(18)-H(18b)	0.9800
C(7)-C(12)	1.540(6)	C(18)-H(18c)	0.9800
C(7)-H(7)	1.0000	Cl(1)-Pd(1)	2.3457(12)
C(8)-C(9)	1.560(6)	N(1)-Pd(1)	1.972(3)
C(8)-H(8b)	0.9900	N(3)-Pd(1)	2.236(4)
C(8)-H(8a)	0.9900		
C(9)-C(10)	1.508(6)	C(4)-C(5)-N(2)	121.4(5)
C(9)-H(9b)	0.9900	C(4)-C(5)-H(5)	119.3
C(9)-H(9a)	0.9900	N(2)-C(5)-H(5)	119.3
C(10)-C(11)	1.534(6)	C(5)-C(4)-C(3)	118.2(4)
C(10)-H(10b)	0.9900	C(5)-C(4)-H(4)	120.9
C(10)-H(10a)	0.9900	C(3)-C(4)-H(4)	120.9
C(11)-C(12)	1.525(6)	C(2)-C(3)-C(4)	121.4(4)
C(11)-H(11a)	0.9900	C(2)-C(3)-H(3)	119.3
C(11)-H(11b)	0.9900	C(4)-C(3)-H(3)	119.3
C(12)-N(3)	1.490(5)	C(3)-C(2)-C(1)	120.2(4)
C(12)-H(12)	1.0000	C(3)-C(2)-H(2)	119.9
C(13)-N(3)	1.323(5)	C(1)-C(2)-H(2)	119.9
C(13)-N(4)	1.391(5)	N(1)-C(1)-N(2)	114.7(4)
C(13)-C(14)	1.439(6)	N(1)-C(1)-C(2)	128.9(4)
C(14)-C(15)	1.350(5)	N(2)-C(1)-C(2)	116.3(4)
C(14)-H(14)	0.9500	N(1)-C(7)-C(8)	115.4(3)

N(1)-C(7)-C(12)	108.2(3)	N(3)-C(13)-C(14)	127.9(4)
C(8)-C(7)-C(12)	106.6(3)	N(4)-C(13)-C(14)	114.9(4)
N(1)-C(7)-H(7)	108.9	C(15)-C(14)-C(13)	121.5(4)
C(8)-C(7)-H(7)	108.9	C(15)-C(14)-H(14)	119.3
C(12)-C(7)-H(7)	108.9	C(13)-C(14)-H(14)	119.3
C(7)-C(8)-C(9)	109.4(3)	C(14)-C(15)-C(16)	121.4(4)
C(7)-C(8)-H(8b)	109.8	C(14)-C(15)-H(15)	119.3
C(9)-C(8)-H(8b)	109.8	C(16)-C(15)-H(15)	119.3
C(7)-C(8)-H(8a)	109.8	C(17)-C(16)-C(15)	116.7(4)
C(9)-C(8)-H(8a)	109.8	C(17)-C(16)-H(16)	121.6
H(8b)-C(8)-H(8a)	108.2	C(15)-C(16)-H(16)	121.6
C(10)-C(9)-C(8)	111.6(4)	N(4)-C(17)-C(16)	123.1(4)
C(10)-C(9)-H(9b)	109.3	N(4)-C(17)-H(17)	118.5
C(8)-C(9)-H(9b)	109.3	C(16)-C(17)-H(17)	118.5
C(10)-C(9)-H(9a)	109.3	N(2)-C(6)-Pd(1)	107.7(3)
C(8)-C(9)-H(9a)	109.3	N(2)-C(6)-H(6b)	110.2
H(9b)-C(9)-H(9a)	108.0	Pd(1)-C(6)-H(6b)	110.2
C(9)-C(10)-C(11)	112.7(4)	N(2)-C(6)-H(6a)	110.2
C(9)-C(10)-H(10b)	109.1	Pd(1)-C(6)-H(6a)	110.2
C(11)-C(10)-H(10b)	109.1	H(6b)-C(6)-H(6a)	108.5
C(9)-C(10)-H(10a)	109.1	N(4)-C(18)-H(18a)	109.5
C(11)-C(10)-H(10a)	109.1	N(4)-C(18)-H(18b)	109.5
H(10b)-C(10)-H(10a)	107.8	H(18a)-C(18)-H(18b)	109.5
C(12)-C(11)-C(10)	110.9(3)	N(4)-C(18)-H(18c)	109.5
C(12)-C(11)-H(11a)	109.5	H(18a)-C(18)-H(18c)	109.5
C(10)-C(11)-H(11a)	109.5	H(18b)-C(18)-H(18c)	109.5
C(12)-C(11)-H(11b)	109.5	C(5)-N(2)-C(1)	122.4(4)
C(10)-C(11)-H(11b)	109.5	C(5)-N(2)-C(6)	121.3(4)
H(11a)-C(11)-H(11b)	108.0	C(1)-N(2)-C(6)	116.3(3)
N(3)-C(12)-C(11)	113.2(4)	C(1)-N(1)-C(7)	124.4(4)
N(3)-C(12)-C(7)	110.5(3)	C(1)-N(1)-Pd(1)	115.7(3)
C(11)-C(12)-C(7)	108.5(3)	C(7)-N(1)-Pd(1)	118.6(3)
N(3)-C(12)-H(12)	108.2	C(13)-N(3)-C(12)	115.5(3)
C(11)-C(12)-H(12)	108.2	C(13)-N(3)-Pd(1)	115.5(3)
C(7)-C(12)-H(12)	108.2	C(12)-N(3)-Pd(1)	102.5(2)
N(3)-C(13)-N(4)	117.2(4)	C(17)-N(4)-C(13)	122.4(4)

C(17)-N(4)-C(18)	119.4(4)	C(6)-Pd(1)-Cl(1)	91.79(13)
C(13)-N(4)-C(18)	118.0(3)	N(3)-Pd(1)-Cl(1)	105.69(10)
N(1)-Pd(1)-C(6)	81.92(17)		
N(1)-Pd(1)-N(3)	80.60(14)	Symmetry transformations used to generate	
C(6)-Pd(1)-N(3)	162.52(16)	equivalent	atoms:
N(1)-Pd(1)-Cl(1)	173.70(11)		

Table 4. Anisotropic displacement parameters ($\text{\AA}^2 \times 10^3$) for **26**. The anisotropic displacement factor exponent takes the form: $-2\pi^2 [h^2 a^{*2} U^{11} + \dots + 2 h k a^* b^* U^{12}]$

	U^{11}	U^{22}	U^{33}	U^{23}	U^{13}	U^{12}
C(1)	10(2)	20(2)	15(2)	5(2)	1(2)	1(2)
C(2)	13(2)	12(2)	20(2)	-1(2)	1(2)	-3(2)
C(3)	17(3)	18(2)	27(3)	-1(2)	4(2)	0(2)
C(4)	12(2)	15(2)	34(3)	3(2)	-2(2)	-2(2)
C(5)	9(2)	19(2)	23(2)	8(2)	0(2)	2(2)
C(6)	23(3)	23(3)	22(3)	0(2)	-5(2)	0(2)
C(7)	9(2)	12(2)	20(3)	4(2)	-3(2)	-3(2)
C(8)	13(2)	14(2)	23(2)	-2(2)	-1(2)	2(2)
C(9)	13(2)	22(3)	24(3)	-4(2)	-1(2)	-5(2)
C(10)	13(2)	22(3)	25(3)	0(2)	0(2)	1(2)
C(11)	14(2)	12(2)	20(2)	-1(2)	-1(2)	-2(2)
C(12)	15(2)	12(2)	22(2)	-6(2)	1(2)	1(2)
C(13)	14(2)	15(2)	11(2)	3(2)	-3(2)	-2(2)
C(14)	14(2)	19(2)	17(2)	0(2)	2(2)	-2(2)
C(15)	18(2)	25(3)	22(2)	-7(2)	0(2)	2(2)
C(16)	27(3)	16(2)	26(3)	-7(2)	-4(2)	3(2)
C(17)	24(2)	9(2)	25(3)	1(2)	-9(3)	-2(2)
C(18)	15(3)	15(2)	25(3)	2(2)	4(2)	-6(2)
Cl(1)	16(1)	20(1)	21(1)	-7(1)	0(1)	-4(1)
N(1)	13(2)	13(2)	15(2)	0(2)	-3(2)	-1(2)
N(2)	11(2)	15(2)	19(2)	0(2)	-3(2)	0(1)
N(3)	14(2)	9(2)	19(2)	-1(2)	-3(2)	-2(2)
N(4)	18(2)	13(2)	15(2)	-3(2)	2(2)	-2(2)

Pd(1) 11(1) 13(1) 16(1) -2(1) -1(1) -1(1)

Table 5. Hydrogen coordinates ($\times 10^4$) and isotropic displacement parameters ($\text{\AA}^2 \times 10^3$) for **26**.

	x	y	z	U(eq)
H(2)	1459	9918	2159	18
H(3)	-600	11392	2103	25
H(4)	-2749	11480	1242	24
H(5)	-2851	9995	490	20
H(6b)	-560	8244	-6	27
H(6a)	-2298	7803	397	27
H(7)	2527	7692	2235	17
H(8b)	3986	9462	1886	20
H(8a)	5063	8742	1339	20
H(9b)	6965	8929	2284	23
H(9a)	5417	8391	2743	23
H(10b)	7477	6941	2553	24
H(10a)	7483	7188	1780	24
H(11a)	5767	5522	1951	19
H(11b)	4565	6147	2501	19
H(12)	4563	6799	1142	20
H(14)	5676	5181	847	20
H(15)	6354	3447	380	26
H(16)	4229	1906	391	28
H(17)	1434	2241	861	23
H(18a)	-550	3259	1452	28
H(18b)	-540	4621	1327	28
H(18c)	409	4101	1969	28

Table 6. Torsion angles [$^\circ$] for **26**.

N(2)-C(5)-C(4)-C(3)	0.9(7)	C(4)-C(3)-C(2)-C(1)	-2.4(7)
C(5)-C(4)-C(3)-C(2)	2.1(7)	C(3)-C(2)-C(1)-N(1)	-175.8(4)

C(3)-C(2)-C(1)-N(2)	-0.1(6)	C(12)-C(7)-N(1)-Pd(1)	18.4(4)
N(1)-C(7)-C(8)-C(9)	176.2(4)	N(4)-C(13)-N(3)-C(12)	165.5(4)
C(12)-C(7)-C(8)-C(9)	-63.7(5)	C(14)-C(13)-N(3)-C(12)	-14.2(6)
C(7)-C(8)-C(9)-C(10)	56.2(5)	N(4)-C(13)-N(3)-Pd(1)	-74.9(4)
C(8)-C(9)-C(10)-C(11)	-49.8(5)	C(14)-C(13)-N(3)-Pd(1)	105.3(5)
C(9)-C(10)-C(11)-C(12)	52.5(5)	C(11)-C(12)-N(3)-C(13)	-65.8(5)
C(10)-C(11)-C(12)-N(3)	176.3(4)	C(7)-C(12)-N(3)-C(13)	172.3(4)
C(10)-C(11)-C(12)-C(7)	-60.6(5)	C(11)-C(12)-N(3)-Pd(1)	167.8(3)
N(1)-C(7)-C(12)-N(3)	-44.4(5)	C(7)-C(12)-N(3)-Pd(1)	45.9(4)
C(8)-C(7)-C(12)-N(3)	-169.0(3)	C(16)-C(17)-N(4)-C(13)	2.1(7)
N(1)-C(7)-C(12)-C(11)	-169.0(3)	C(16)-C(17)-N(4)-C(18)	-172.9(4)
C(8)-C(7)-C(12)-C(11)	66.4(4)	N(3)-C(13)-N(4)-C(17)	177.8(4)
N(3)-C(13)-C(14)-C(15)	-178.3(4)	C(14)-C(13)-N(4)-C(17)	-2.4(6)
N(4)-C(13)-C(14)-C(15)	2.0(6)	N(3)-C(13)-N(4)-C(18)	-7.1(6)
C(13)-C(14)-C(15)-C(16)	-1.2(7)	C(14)-C(13)-N(4)-C(18)	172.7(4)
C(14)-C(15)-C(16)-C(17)	0.7(7)	C(1)-N(1)-Pd(1)-C(6)	17.7(3)
C(15)-C(16)-C(17)-N(4)	-1.1(7)	C(7)-N(1)-Pd(1)-C(6)	-174.2(3)
C(4)-C(5)-N(2)-C(1)	-3.6(6)	C(1)-N(1)-Pd(1)-N(3)	-162.6(3)
C(4)-C(5)-N(2)-C(6)	175.1(4)	C(7)-N(1)-Pd(1)-N(3)	5.4(3)
N(1)-C(1)-N(2)-C(5)	179.4(4)	N(2)-C(6)-Pd(1)-N(1)	-15.3(3)
C(2)-C(1)-N(2)-C(5)	3.1(6)	N(2)-C(6)-Pd(1)-N(3)	-16.3(7)
N(1)-C(1)-N(2)-C(6)	0.7(5)	N(2)-C(6)-Pd(1)-Cl(1)	165.0(3)
C(2)-C(1)-N(2)-C(6)	-175.6(4)	C(13)-N(3)-Pd(1)-N(1)	-154.5(3)
Pd(1)-C(6)-N(2)-C(5)	-165.9(3)	C(12)-N(3)-Pd(1)-N(1)	-28.1(3)
Pd(1)-C(6)-N(2)-C(1)	12.8(4)	C(13)-N(3)-Pd(1)-C(6)	-153.5(5)
N(2)-C(1)-N(1)-C(7)	178.0(4)	C(12)-N(3)-Pd(1)-C(6)	-27.0(7)
C(2)-C(1)-N(1)-C(7)	-6.3(7)	C(13)-N(3)-Pd(1)-Cl(1)	25.1(3)
N(2)-C(1)-N(1)-Pd(1)	-14.7(5)	C(12)-N(3)-Pd(1)-Cl(1)	151.6(2)
C(2)-C(1)-N(1)-Pd(1)	161.0(4)		
C(8)-C(7)-N(1)-C(1)	-55.5(6)		
C(12)-C(7)-N(1)-C(1)	-174.7(4)		
C(8)-C(7)-N(1)-Pd(1)	137.6(3)		

Symmetry transformations used to generate equivalent atoms:

Single crystal X-ray structure data for [PdCl(η^3 -CH₂N^{C(Me)2}2N^{Me})] (28)

Table 1. Crystal data and structure refinement for **28**.

Identification code	28	
Empirical formula	C ₂₀ H _{29.19} Cl N ₄ O _{0.50} Pd	
Formula weight	475.52	
Temperature	110(2) K	
Wavelength	0.71073 Å	
Crystal system	Monoclinic	
Space group	C2/c	
Unit cell dimensions	a = 18.8784(9) Å	α = 90°.
	b = 9.0734(4) Å	β = 97.4930(10)°.
	c = 23.7087(11) Å	γ = 90°.
Volume	4026.4(3) Å ³	
Z	8	
Density (calculated)	1.569 Mg/m ³	
Absorption coefficient	1.069 mm ⁻¹	
F(000)	1953.4	
Crystal size	0.20 x 0.20 x 0.20 mm ³	
Theta range for data collection	1.73 to 30.00°.	
Index ranges	-26 ≤ h ≤ 25, -9 ≤ k ≤ 12, -33 ≤ l ≤ 32	
Reflections collected	15621	
Independent reflections	5785 [R(int) = 0.0233]	
Completeness to theta = 30.00°	98.5 %	
Absorption correction	Semi-empirical from equivalents	
Max. and min. transmission	0.810 and 0.740	
Refinement method	Full-matrix least-squares on F ²	
Data / restraints / parameters	5785 / 2 / 280	
Goodness-of-fit on F ²	1.024	
Final R indices [I > 2σ(I)]	R1 = 0.0260, wR2 = 0.0617	
R indices (all data)	R1 = 0.0326, wR2 = 0.0642	
Largest diff. peak and hole	0.612 and -0.362 e.Å ⁻³	

Table 2. Atomic coordinates ($\times 10^4$) and equivalent isotropic displacement parameters ($\text{\AA}^2 \times 10^3$) for **28**. U(eq) is defined as one third of the trace of the orthogonalized U^{ij} tensor.

	x	y	z	U(eq)
C(1)	1927(1)	10132(2)	2087(1)	20(1)
C(2)	2557(1)	10766(3)	2398(1)	30(1)
C(3)	2620(1)	10927(3)	2974(1)	33(1)
C(4)	2068(1)	10452(2)	3282(1)	28(1)
C(5)	1478(1)	9837(2)	2988(1)	22(1)
C(6)	731(1)	9083(2)	2106(1)	19(1)
C(7)	2229(1)	10242(2)	1090(1)	17(1)
C(8)	2816(1)	9067(2)	1115(1)	25(1)
C(9)	2567(1)	11786(2)	1163(1)	26(1)
C(10)	1723(1)	10155(2)	498(1)	16(1)
C(11)	2190(1)	10158(2)	11(1)	21(1)
C(12)	1216(1)	11489(2)	446(1)	21(1)
C(13)	1022(1)	8108(2)	42(1)	15(1)
C(14)	783(1)	8765(2)	-502(1)	19(1)
C(15)	462(1)	7967(2)	-948(1)	22(1)
C(16)	354(1)	6434(2)	-894(1)	23(1)
C(17)	578(1)	5802(2)	-385(1)	19(1)
C(18)	1185(1)	5790(2)	583(1)	18(1)
Cl(1)	-236(1)	7606(1)	1105(1)	18(1)
N(1)	1768(1)	9894(2)	1534(1)	16(1)
N(2)	1407(1)	9688(2)	2412(1)	19(1)
N(3)	1327(1)	8742(2)	512(1)	14(1)
N(4)	906(1)	6594(2)	67(1)	15(1)
Pd(1)	884(1)	8768(1)	1306(1)	13(1)
C(19)	405(2)	4883(5)	2509(2)	34(1)
C(20)	596(2)	3256(3)	2455(1)	37(1)
O(1)	-68(3)	2441(4)	2348(1)	34(1)
C(21)	558(10)	4460(20)	2369(7)	34(4)
C(22)	1127(8)	3398(17)	2190(7)	47(4)
O(2)	0	3615(16)	2500	42(4)

Table 3. Bond lengths [\AA] and angles [$^\circ$] for **28**.

C(10)-N(3)	1.487(2)	C(13)-N(3)	1.319(2)
C(10)-C(12)	1.539(2)	C(13)-N(4)	1.393(2)
C(10)-C(11)	1.541(2)	C(13)-C(14)	1.439(2)
C(10)-C(7)	1.593(2)	C(14)-C(15)	1.357(3)
C(7)-N(1)	1.484(2)	C(14)-H(14)	0.9500
C(7)-C(8)	1.533(3)	C(15)-C(16)	1.415(3)
C(7)-C(9)	1.540(3)	C(15)-H(15)	0.9500
C(11)-H(11a)	0.9800	C(16)-C(17)	1.352(3)
C(11)-H(11c)	0.9800	C(16)-H(16)	0.9500
C(11)-H(11b)	0.9800	C(17)-N(4)	1.369(2)
C(12)-H(12a)	0.9800	C(17)-H(17)	0.9500
C(12)-H(12c)	0.9800	C(18)-N(4)	1.463(2)
C(12)-H(12b)	0.9800	C(18)-H(18A)	0.9800
C(8)-H(8b)	0.9800	C(18)-H(18B)	0.9800
C(8)-H(8c)	0.9800	C(18)-H(18C)	0.9800
C(8)-H(8a)	0.9800	Cl(1)-Pd(1)	2.3550(4)
C(9)-H(9c)	0.9800	N(3)-Pd(1)	2.1560(14)
C(9)-H(9a)	0.9800	N(1)-Pd(1)	1.9714(14)
C(9)-H(9b)	0.9800	C(19)-C(19)#1	1.524(9)
C(1)-N(1)	1.325(2)	C(19)-C(20)	1.529(5)
C(1)-N(2)	1.384(2)	C(19)-H(19A)	0.9900
C(1)-C(2)	1.435(3)	C(19)-H(19B)	0.9900
C(2)-C(3)	1.364(3)	C(20)-O(1)#1	1.373(6)
C(2)-H(2)	0.9500	C(20)-O(1)	1.448(6)
C(3)-C(4)	1.415(3)	C(20)-H(20A)	0.987(5)
C(3)-H(3)	0.9500	C(20)-H(20B)	0.991(5)
C(4)-C(5)	1.355(3)	O(1)-O(1)#1	0.735(6)
C(4)-H(4)	0.9500	O(1)-C(20)#1	1.373(6)
C(5)-N(2)	1.363(2)	C(21)-O(2)	1.37(2)
C(5)-H(5)	0.9500	C(21)-C(22)	1.54(2)
C(6)-N(2)	1.487(2)	C(21)-H(20B)	1.47(3)
C(6)-Pd(1)	1.9781(17)	C(21)-H(21A)	0.9900
C(6)-H(6b)	0.9900	C(21)-H(21B)	0.9900
C(6)-H(6a)	0.9900	C(22)-H(20B)	0.76(4)

C(22)-H(22A)	0.9800	C(7)-C(9)-H(9a)	109.5
C(22)-H(22B)	0.9800	H(9c)-C(9)-H(9a)	109.5
C(22)-H(22C)	0.9800	C(7)-C(9)-H(9b)	109.5
O(2)-C(21)#1	1.37(2)	H(9c)-C(9)-H(9b)	109.5
		H(9a)-C(9)-H(9b)	109.5
N(3)-C(10)-C(12)	111.75(15)	N(1)-C(1)-N(2)	114.69(16)
N(3)-C(10)-C(11)	110.89(14)	N(1)-C(1)-C(2)	129.72(17)
C(12)-C(10)-C(11)	110.38(15)	N(2)-C(1)-C(2)	115.59(16)
N(3)-C(10)-C(7)	105.58(13)	C(3)-C(2)-C(1)	121.03(19)
C(12)-C(10)-C(7)	109.15(14)	C(3)-C(2)-H(2)	119.5
C(11)-C(10)-C(7)	108.93(14)	C(1)-C(2)-H(2)	119.5
N(1)-C(7)-C(8)	108.17(14)	C(2)-C(3)-C(4)	120.7(2)
N(1)-C(7)-C(9)	112.75(14)	C(2)-C(3)-H(3)	119.7
C(8)-C(7)-C(9)	109.98(16)	C(4)-C(3)-H(3)	119.7
N(1)-C(7)-C(10)	105.90(13)	C(5)-C(4)-C(3)	118.18(18)
C(8)-C(7)-C(10)	110.33(15)	C(5)-C(4)-H(4)	120.9
C(9)-C(7)-C(10)	109.63(14)	C(3)-C(4)-H(4)	120.9
C(10)-C(11)-H(11a)	109.5	C(4)-C(5)-N(2)	121.53(18)
C(10)-C(11)-H(11c)	109.5	C(4)-C(5)-H(5)	119.2
H(11a)-C(11)-H(11c)	109.5	N(2)-C(5)-H(5)	119.2
C(10)-C(11)-H(11b)	109.5	N(2)-C(6)-Pd(1)	107.29(11)
H(11a)-C(11)-H(11b)	109.5	N(2)-C(6)-H(6b)	110.3
H(11c)-C(11)-H(11b)	109.5	Pd(1)-C(6)-H(6b)	110.3
C(10)-C(12)-H(12a)	109.5	N(2)-C(6)-H(6a)	110.3
C(10)-C(12)-H(12c)	109.5	Pd(1)-C(6)-H(6a)	110.3
H(12a)-C(12)-H(12c)	109.5	H(6b)-C(6)-H(6a)	108.5
C(10)-C(12)-H(12b)	109.5	N(3)-C(13)-N(4)	116.56(15)
H(12a)-C(12)-H(12b)	109.5	N(3)-C(13)-C(14)	128.95(16)
H(12c)-C(12)-H(12b)	109.5	N(4)-C(13)-C(14)	114.50(15)
C(7)-C(8)-H(8b)	109.5	C(15)-C(14)-C(13)	122.21(17)
C(7)-C(8)-H(8c)	109.5	C(15)-C(14)-H(14)	118.9
H(8b)-C(8)-H(8c)	109.5	C(13)-C(14)-H(14)	118.9
C(7)-C(8)-H(8a)	109.5	C(14)-C(15)-C(16)	120.53(17)
H(8b)-C(8)-H(8a)	109.5	C(14)-C(15)-H(15)	119.7
H(8c)-C(8)-H(8a)	109.5	C(16)-C(15)-H(15)	119.7
C(7)-C(9)-H(9c)	109.5	C(17)-C(16)-C(15)	117.84(17)

C(17)-C(16)-H(16)	121.1	O(1)#1-C(20)-O(1)	30.0(3)
C(15)-C(16)-H(16)	121.1	O(1)#1-C(20)-C(19)	107.5(3)
C(16)-C(17)-N(4)	122.15(17)	O(1)-C(20)-C(19)	107.4(3)
C(16)-C(17)-H(17)	118.9	O(1)#1-C(20)-H(20A)	85(2)
N(4)-C(17)-H(17)	118.9	O(1)-C(20)-H(20A)	111(2)
N(4)-C(18)-H(18A)	109.5	C(19)-C(20)-H(20A)	115(2)
N(4)-C(18)-H(18B)	109.5	O(1)#1-C(20)-H(20B)	125(2)
H(18A)-C(18)-H(18B)	109.5	O(1)-C(20)-H(20B)	98(2)
N(4)-C(18)-H(18C)	109.5	C(19)-C(20)-H(20B)	107(2)
H(18A)-C(18)-H(18C)	109.5	H(20A)-C(20)-H(20B)	117(3)
H(18B)-C(18)-H(18C)	109.5	O(1)#1-O(1)-C(20)#1	80.7(7)
C(13)-N(3)-C(10)	121.52(14)	O(1)#1-O(1)-C(20)	69.3(7)
C(13)-N(3)-Pd(1)	124.47(11)	C(20)#1-O(1)-C(20)	108.4(3)
C(10)-N(3)-Pd(1)	105.28(10)	O(2)-C(21)-C(22)	107.0(15)
C(1)-N(1)-C(7)	126.10(15)	O(2)-C(21)-H(20B)	84.0(18)
C(1)-N(1)-Pd(1)	115.50(12)	C(22)-C(21)-H(20B)	29.0(14)
C(7)-N(1)-Pd(1)	118.00(11)	O(2)-C(21)-H(21A)	110.3
C(5)-N(2)-C(1)	122.99(16)	C(22)-C(21)-H(21A)	110.3
C(5)-N(2)-C(6)	119.40(15)	H(20B)-C(21)-H(21A)	136.7
C(1)-N(2)-C(6)	117.55(14)	O(2)-C(21)-H(21B)	110.3
C(17)-N(4)-C(13)	122.76(15)	C(22)-C(21)-H(21B)	110.3
C(17)-N(4)-C(18)	118.00(15)	H(20B)-C(21)-H(21B)	103.5
C(13)-N(4)-C(18)	119.11(14)	H(21A)-C(21)-H(21B)	108.6
N(1)-Pd(1)-C(6)	83.45(7)	C(21)-C(22)-H(20B)	70(3)
N(1)-Pd(1)-N(3)	80.45(6)	C(21)-C(22)-H(22A)	109.5
C(6)-Pd(1)-N(3)	163.88(7)	C(21)-C(22)-H(22B)	109.5
N(1)-Pd(1)-Cl(1)	173.24(4)	H(22A)-C(22)-H(22B)	109.5
C(6)-Pd(1)-Cl(1)	91.07(5)	C(21)-C(22)-H(22C)	109.5
N(3)-Pd(1)-Cl(1)	105.04(4)	H(22A)-C(22)-H(22C)	109.5
C(19)#1-C(19)-C(20)	104.2(2)	H(22B)-C(22)-H(22C)	109.5
C(19)#1-C(19)-H(19A)	110.9	C(21)-O(2)-C(21)#1	112(2)
C(20)-C(19)-H(19A)	110.9		
C(19)#1-C(19)-H(19B)	110.9		
C(20)-C(19)-H(19B)	110.9		
H(19A)-C(19)-H(19B)	108.9		

Symmetry transformations used to generate equivalent atoms:

#1 -x,y,-z+1/2

Table 4. Anisotropic displacement parameters ($\text{\AA}^2 \times 10^3$) for **28**. The anisotropic displacement factor exponent takes the form: $-2\pi^2 [h^2 a^{*2} U^{11} + \dots + 2 h k a^* b^* U^{12}]$

	U^{11}	U^{22}	U^{33}	U^{23}	U^{13}	U^{12}
C(1)	22(1)	19(1)	19(1)	0(1)	5(1)	-4(1)
C(2)	32(1)	37(1)	22(1)	-3(1)	3(1)	-15(1)
C(3)	36(1)	40(1)	23(1)	-4(1)	-1(1)	-16(1)
C(4)	42(1)	27(1)	15(1)	-3(1)	2(1)	-6(1)
C(5)	33(1)	20(1)	16(1)	0(1)	7(1)	-1(1)
C(6)	20(1)	20(1)	17(1)	-2(1)	6(1)	-4(1)
C(7)	17(1)	19(1)	17(1)	-1(1)	6(1)	-6(1)
C(8)	18(1)	31(1)	25(1)	3(1)	4(1)	3(1)
C(9)	32(1)	25(1)	23(1)	0(1)	4(1)	-14(1)
C(10)	18(1)	13(1)	17(1)	1(1)	6(1)	-2(1)
C(11)	25(1)	21(1)	20(1)	1(1)	11(1)	-4(1)
C(12)	27(1)	14(1)	24(1)	1(1)	5(1)	2(1)
C(13)	15(1)	14(1)	17(1)	0(1)	7(1)	0(1)
C(14)	21(1)	18(1)	19(1)	3(1)	4(1)	0(1)
C(15)	19(1)	29(1)	17(1)	1(1)	2(1)	1(1)
C(16)	20(1)	28(1)	21(1)	-5(1)	4(1)	-4(1)
C(17)	18(1)	19(1)	22(1)	-7(1)	7(1)	-5(1)
C(18)	21(1)	14(1)	19(1)	1(1)	4(1)	2(1)
Cl(1)	16(1)	17(1)	21(1)	-2(1)	4(1)	-3(1)
N(1)	17(1)	18(1)	15(1)	-1(1)	5(1)	-4(1)
N(2)	23(1)	18(1)	16(1)	-2(1)	6(1)	-3(1)
N(3)	16(1)	13(1)	14(1)	0(1)	6(1)	-1(1)
N(4)	17(1)	13(1)	16(1)	-1(1)	5(1)	0(1)
Pd(1)	14(1)	13(1)	13(1)	-1(1)	5(1)	-1(1)
C(19)	45(2)	24(2)	33(2)	-3(1)	3(2)	-6(2)
C(20)	42(2)	27(2)	39(2)	2(1)	-4(1)	6(1)
O(1)	49(3)	19(2)	35(3)	-6(1)	2(3)	0(2)
C(21)	40(10)	35(11)	21(8)	-1(6)	-17(7)	-14(7)
C(22)	28(7)	41(8)	71(11)	-33(7)	-1(7)	-7(6)
O(2)	44(9)	41(9)	37(7)	0	-13(6)	0

Table 5. Hydrogen coordinates ($\times 10^4$) and isotropic displacement parameters ($\text{\AA}^2 \times 10^{-3}$) for **28**.

	x	y	z	U(eq)
H(2)	2936	11077	2199	36
H(3)	3039	11363	3170	40
H(4)	2111	10561	3683	34
H(5)	1105	9502	3189	27
H(6b)	334	9785	2127	22
H(6a)	610	8140	2281	22
H(8b)	3058	8989	1506	37
H(8c)	3162	9345	860	37
H(8a)	2602	8114	996	37
H(9c)	2254	12437	1348	40
H(9a)	2631	12186	789	40
H(9b)	3033	11716	1398	40
H(11a)	2386	9170	-30	32
H(11c)	2582	10863	98	32
H(11b)	1898	10444	-344	32
H(12a)	833	11327	131	32
H(12c)	1483	12379	372	32
H(12b)	1008	11611	801	32
H(14)	853	9792	-551	23
H(15)	308	8443	-1300	26
H(16)	131	5867	-1204	27
H(17)	506	4775	-340	23
H(18A)	899	6027	887	27
H(18B)	1683	6076	700	27
H(18C)	1161	4728	507	27
H(19A)	639	5298	2872	41
H(19B)	551	5464	2190	41
H(20A)	908(14)	2850(30)	2783(9)	44
H(20B)	760(20)	3130(40)	2076(7)	44
H(21A)	760	5049	2704	41
H(21B)	393	5147	2054	41
H(22A)	1333	2821	2521	71

H(22B)	1505	3965	2043	71
H(22C)	904	2732	1894	71

Table 6. Torsion angles [°] for **28**.

N(3)-C(10)-C(7)-N(1)	-48.35(17)	C(2)-C(1)-N(1)-C(7)	0.2(3)
C(12)-C(10)-C(7)-N(1)	71.92(17)	N(2)-C(1)-N(1)-Pd(1)	-6.6(2)
C(11)-C(10)-C(7)-N(1)	-167.49(14)	C(2)-C(1)-N(1)-Pd(1)	172.75(18)
N(3)-C(10)-C(7)-C(8)	68.49(17)	C(8)-C(7)-N(1)-C(1)	76.6(2)
C(12)-C(10)-C(7)-C(8)	-171.24(15)	C(9)-C(7)-N(1)-C(1)	-45.3(2)
C(11)-C(10)-C(7)-C(8)	-50.65(18)	C(10)-C(7)-N(1)-C(1)	-165.15(17)
N(3)-C(10)-C(7)-C(9)	-170.25(14)	C(8)-C(7)-N(1)-Pd(1)	-95.83(15)
C(12)-C(10)-C(7)-C(9)	-49.98(19)	C(9)-C(7)-N(1)-Pd(1)	142.34(13)
C(11)-C(10)-C(7)-C(9)	70.61(18)	C(10)-C(7)-N(1)-Pd(1)	22.45(17)
N(1)-C(1)-C(2)-C(3)	179.7(2)	C(4)-C(5)-N(2)-C(1)	0.6(3)
N(2)-C(1)-C(2)-C(3)	-1.0(3)	C(4)-C(5)-N(2)-C(6)	-176.58(19)
C(1)-C(2)-C(3)-C(4)	1.0(4)	N(1)-C(1)-N(2)-C(5)	179.63(17)
C(2)-C(3)-C(4)-C(5)	-0.1(4)	C(2)-C(1)-N(2)-C(5)	0.2(3)
C(3)-C(4)-C(5)-N(2)	-0.7(3)	N(1)-C(1)-N(2)-C(6)	-3.1(2)
N(3)-C(13)-C(14)-C(15)	-178.61(18)	C(2)-C(1)-N(2)-C(6)	177.48(17)
N(4)-C(13)-C(14)-C(15)	1.0(3)	Pd(1)-C(6)-N(2)-C(5)	-171.95(14)
C(13)-C(14)-C(15)-C(16)	-0.5(3)	Pd(1)-C(6)-N(2)-C(1)	10.7(2)
C(14)-C(15)-C(16)-C(17)	0.2(3)	C(16)-C(17)-N(4)-C(13)	1.2(3)
C(15)-C(16)-C(17)-N(4)	-0.5(3)	C(16)-C(17)-N(4)-C(18)	-174.70(17)
N(4)-C(13)-N(3)-C(10)	156.54(15)	N(3)-C(13)-N(4)-C(17)	178.36(15)
C(14)-C(13)-N(3)-C(10)	-23.8(3)	C(14)-C(13)-N(4)-C(17)	-1.3(2)
N(4)-C(13)-N(3)-Pd(1)	-60.71(19)	N(3)-C(13)-N(4)-C(18)	-5.8(2)
C(14)-C(13)-N(3)-Pd(1)	118.93(17)	C(14)-C(13)-N(4)-C(18)	174.49(15)
C(12)-C(10)-N(3)-C(13)	81.42(19)	C(1)-N(1)-Pd(1)-C(6)	10.23(14)
C(11)-C(10)-N(3)-C(13)	-42.2(2)	C(7)-N(1)-Pd(1)-C(6)	-176.57(14)
C(7)-C(10)-N(3)-C(13)	-160.03(15)	C(1)-N(1)-Pd(1)-N(3)	-168.94(14)
C(12)-C(10)-N(3)-Pd(1)	-67.43(15)	C(7)-N(1)-Pd(1)-N(3)	4.25(12)
C(11)-C(10)-N(3)-Pd(1)	168.96(12)	N(2)-C(6)-Pd(1)-N(1)	-10.51(12)
C(7)-C(10)-N(3)-Pd(1)	51.12(14)	N(2)-C(6)-Pd(1)-N(3)	-7.6(3)
N(2)-C(1)-N(1)-C(7)	-179.13(16)	N(2)-C(6)-Pd(1)-Cl(1)	173.45(11)

C(13)-N(3)-Pd(1)-N(1)	-179.59(15)
C(10)-N(3)-Pd(1)-N(1)	-31.93(11)
C(13)-N(3)-Pd(1)-C(6)	177.5(2)
C(10)-N(3)-Pd(1)-C(6)	-34.9(3)
C(13)-N(3)-Pd(1)-Cl(1)	-3.61(14)
C(10)-N(3)-Pd(1)-Cl(1)	144.05(9)
C(19)#1-C(19)-C(20)-O(1)#1	-25.4(5)
C(19)#1-C(19)-C(20)-O(1)	6.1(5)

C(19)-C(20)-O(1)-O(1)#1	-95.0(5)
O(1)#1-C(20)-O(1)-C(20)#1	72.1(6)
C(19)-C(20)-O(1)-C(20)#1	-23.0(3)
C(22)-C(21)-O(2)-C(21)#1	-176.2(14)

Symmetry transformations used to generate
equivalent atoms:

#1 -x,y,-z+1/2

Single crystal X-ray structure data for $\{[\text{Pd}(\eta^3\text{-CH}_2\text{N}^{\text{C}_6\text{H}_{10}\text{N}^{\text{Me}})]_2\text{Cl}\}(\text{BF}_4)$ (**35**)

Table 1. Crystal data and structure refinement for **35**.

Identification code	35	
Empirical formula	C _{40.72} H _{48.96} B Cl _{1.76} F ₄ N ₈ Pd ₂	
Formula weight	1012.53	
Temperature	110(2) K	
Wavelength	0.71073 Å	
Crystal system	Orthorhombic	
Space group	P2(1)2(1)2(1)	
Unit cell dimensions	a = 9.974(2) Å	α = 90°.
	b = 18.827(4) Å	β = 90°.
	c = 22.628(5) Å	γ = 90°.
Volume	4249.3(17) Å ³	
Z	4	
Density (calculated)	1.583 Mg/m ³	
Absorption coefficient	1.014 mm ⁻¹	
F(000)	2049	
Crystal size	0.20 x 0.11 x 0.06 mm ³	
Theta range for data collection	1.41 to 25.05°.	
Index ranges	-11 ≤ h ≤ 11, -22 ≤ k ≤ 22, -26 ≤ l ≤ 26	
Reflections collected	44149	
Independent reflections	7521 [R(int) = 0.0789]	
Completeness to theta = 25.05°	100.0 %	
Absorption correction	Semi-empirical from equivalents	
Max. and min. transmission	0.941 and 0.790	
Refinement method	Full-matrix least-squares on F ²	
Data / restraints / parameters	7521 / 13 / 622	
Goodness-of-fit on F ²	1.038	
Final R indices [I > 2σ(I)]	R1 = 0.0512, wR2 = 0.1105	
R indices (all data)	R1 = 0.0741, wR2 = 0.1221	
Absolute structure parameter	-0.01(4)	
Largest diff. peak and hole	1.671 and -1.530 e.Å ⁻³	

Table 2. Atomic coordinates ($\times 10^4$) and equivalent isotropic displacement parameters ($\text{\AA}^2 \times 10^3$) for **35**. $U(\text{eq})$ is defined as one third of the trace of the orthogonalized U^{ij} tensor.

	x	y	z	$U(\text{eq})$
C(1)	13049(8)	10026(4)	6287(4)	38(2)
C(2)	12894(10)	8917(5)	5737(4)	44(2)
C(3)	12201(10)	8427(5)	5422(4)	44(2)
C(4)	10833(10)	8509(4)	5341(3)	44(2)
C(5)	10178(9)	9051(3)	5602(3)	30(2)
C(6)	10844(7)	9561(4)	5957(3)	28(2)
C(7)	8912(8)	10270(4)	6106(3)	33(2)
C(8)	8730(8)	10538(4)	5470(4)	41(2)
C(9)	7216(10)	10639(5)	5342(5)	59(3)
C(10)	6561(10)	11099(5)	5790(5)	59(3)
C(11)	6856(9)	10862(5)	6418(4)	51(2)
C(12)	8348(8)	10838(4)	6521(4)	36(2)
C(13)	8650(20)	11101(16)	7581(12)	44(5)
C(14)	7990(30)	11795(12)	7622(13)	56(7)
C(15)	7880(30)	12119(11)	8186(12)	74(8)
C(16)	8360(30)	11839(11)	8689(9)	64(6)
C(17)	9060(20)	11218(11)	8639(10)	61(7)
C(18)	9990(16)	10203(8)	8064(7)	29(3)
C(13A)	8140(40)	11010(30)	7610(20)	44(5)
C(14A)	7440(40)	11616(16)	7628(17)	44(9)
C(15A)	7130(50)	11908(16)	8141(14)	67(11)
C(16A)	7450(40)	11590(17)	8668(16)	72(11)
C(17A)	8300(50)	10988(19)	8648(16)	84(15)
C(18A)	9440(30)	9998(14)	8115(11)	29(3)
C(19)	9610(13)	8185(5)	6926(4)	72(3)
C(20)	8080(30)	7356(10)	6377(8)	68(7)
C(21)	7370(20)	6729(10)	6364(6)	56(4)
C(22)	7270(40)	6331(17)	6872(18)	79(11)
C(23)	7740(40)	6560(20)	7420(20)	53(10)
C(24)	8361(14)	7245(7)	7440(6)	21(3)
C(20A)	8750(50)	7140(20)	6385(17)	68(7)

C(21A)	8220(40)	6480(17)	6281(12)	56(4)
C(22A)	7850(80)	6140(30)	6850(40)	79(11)
C(23A)	8180(90)	6440(50)	7350(40)	53(10)
C(24A)	8870(20)	7092(12)	7381(11)	21(3)
C(25)	8807(8)	7303(4)	8503(3)	30(2)
C(26)	7377(8)	7144(4)	8709(4)	40(2)
C(27)	7371(11)	6864(5)	9336(4)	55(3)
C(28)	8019(10)	7402(5)	9752(4)	54(3)
C(29)	9428(8)	7603(4)	9547(3)	36(2)
C(30)	9393(7)	7876(4)	8904(3)	26(2)
C(31)	11301(8)	8639(4)	8961(3)	26(2)
C(32)	10701(7)	9150(4)	9340(3)	26(2)
C(33)	11374(8)	9701(4)	9569(3)	29(2)
C(34)	12749(9)	9787(4)	9436(3)	38(2)
C(35)	13353(8)	9300(4)	9090(3)	36(2)
C(36)	13403(8)	8186(4)	8540(4)	37(2)
N(1)	10713(5)	8099(3)	8692(2)	23(1)
N(2)	8944(8)	7547(4)	7897(3)	45(2)
N(3)	10323(6)	10100(3)	6258(2)	28(1)
N(4)	8782(8)	10676(4)	7116(3)	47(2)
N(5)	8605(19)	7585(9)	6899(8)	42(4)
N(6)	9186(18)	10880(9)	8123(8)	35(4)
N(8)	12675(6)	8726(3)	8865(3)	26(1)
N(9)	12232(7)	9484(3)	5993(3)	31(2)
N(5A)	9170(30)	7402(17)	6890(16)	42(4)
N(6A)	8600(30)	10683(14)	8103(12)	37(6)
Pd(1)	10229(1)	9988(1)	7226(1)	35(1)
Pd(2)	10311(1)	8268(1)	7742(1)	35(1)
Cl(1)	11867(2)	9146(1)	7464(1)	37(1)
B(2)	8667(10)	1470(5)	362(4)	41(2)
F(1)	9268(7)	1020(4)	-26(3)	89(2)
F(2)	9494(7)	2049(3)	448(3)	91(2)
F(3)	8544(7)	1128(3)	882(2)	71(2)
F(4)	7477(5)	1724(3)	150(2)	68(2)
C(38)	9662(11)	-147(6)	2867(4)	76(6)
C(39)	9457(12)	-572(5)	3361(5)	75(5)

C(40)	8683(11)	-324(6)	3828(4)	87(7)
C(41)	8114(9)	349(7)	3802(4)	57(5)
C(42)	8319(9)	774(5)	3308(5)	68(6)
C(43)	9093(11)	526(6)	2841(4)	22(4)
C(44)	9190(20)	1000(10)	2290(7)	78(6)
C(45)	8160(50)	1144(10)	2389(16)	250(50)
Cl(2)	9270(20)	453(9)	2771(9)	163(8)
Cl(3)	9436(8)	1888(5)	2271(4)	91(3)

Table 3. Bond lengths [Å] and angles [°] for **35**.

C(1)-N(9)	1.466(10)	C(9)-H(9B)	0.9900
C(1)-H(1A)	0.9800	C(10)-C(11)	1.518(13)
C(1)-H(1B)	0.9800	C(10)-H(10A)	0.9900
C(1)-H(1C)	0.9800	C(10)-H(10B)	0.9900
C(2)-C(3)	1.355(13)	C(11)-C(12)	1.507(12)
C(2)-N(9)	1.381(10)	C(11)-H(11A)	0.9900
C(2)-H(2)	0.9500	C(11)-H(11B)	0.9900
C(3)-C(4)	1.385(13)	C(12)-N(4)	1.447(10)
C(3)-H(3)	0.9500	C(12)-H(12)	1.0000
C(4)-C(5)	1.348(11)	C(13)-N(4)	1.33(3)
C(4)-H(4)	0.9500	C(13)-N(6)	1.40(3)
C(5)-C(6)	1.418(10)	C(13)-C(14)	1.47(4)
C(5)-H(5)	0.9500	C(14)-C(15)	1.42(4)
C(6)-N(3)	1.328(9)	C(14)-H(14)	0.9500
C(6)-N(9)	1.395(10)	C(15)-C(16)	1.34(3)
C(7)-N(3)	1.484(9)	C(15)-H(15)	0.9500
C(7)-C(12)	1.529(11)	C(16)-C(17)	1.36(3)
C(7)-C(8)	1.536(10)	C(16)-H(16)	0.9500
C(7)-H(7)	1.0000	C(17)-N(6)	1.34(3)
C(8)-C(9)	1.550(12)	C(17)-H(17)	0.9500
C(8)-H(8A)	0.9900	C(18)-N(6)	1.51(2)
C(8)-H(8B)	0.9900	C(18)-Pd(1)	1.953(15)
C(9)-C(10)	1.484(14)	C(13A)-C(14A)	1.34(6)
C(9)-H(9A)	0.9900	C(13A)-N(6A)	1.35(6)

C(13A)-N(4)	1.44(5)	C(24A)-N(5A)	1.29(4)
C(14A)-C(15A)	1.32(5)	C(24A)-N(2)	1.45(2)
C(14A)-H(14A)	0.9500	C(25)-N(2)	1.454(9)
C(15A)-C(16A)	1.37(4)	C(25)-C(30)	1.527(10)
C(15A)-H(15A)	0.9500	C(25)-C(26)	1.530(11)
C(16A)-C(17A)	1.42(4)	C(25)-H(25)	1.0000
C(16A)-H(16A)	0.9500	C(26)-C(27)	1.514(12)
C(17A)-N(6A)	1.39(5)	C(26)-H(26A)	0.9900
C(17A)-H(17A)	0.9500	C(26)-H(26B)	0.9900
C(18A)-N(6A)	1.53(4)	C(27)-C(28)	1.526(12)
C(18A)-Pd(1)	2.16(3)	C(27)-H(27A)	0.9900
C(19)-N(5)	1.51(2)	C(27)-H(27B)	0.9900
C(19)-N(5A)	1.54(4)	C(28)-C(29)	1.528(12)
C(19)-Pd(2)	1.982(9)	C(28)-H(28A)	0.9900
C(19)-H(19A)	0.9900	C(28)-H(28B)	0.9900
C(19)-H(19B)	0.9900	C(29)-C(30)	1.543(9)
C(20)-N(5)	1.36(3)	C(29)-H(29A)	0.9900
C(20)-C(21)	1.38(3)	C(29)-H(29B)	0.9900
C(20)-H(20)	0.9500	C(30)-N(1)	1.462(9)
C(21)-C(22)	1.37(4)	C(30)-H(30)	1.0000
C(21)-H(21)	0.9500	C(31)-N(1)	1.323(9)
C(22)-C(23)	1.39(6)	C(31)-N(8)	1.397(10)
C(22)-H(22)	0.9500	C(31)-C(32)	1.421(10)
C(23)-C(24)	1.44(5)	C(32)-C(33)	1.339(10)
C(23)-H(23)	0.9500	C(32)-H(32)	0.9500
C(24)-N(2)	1.316(14)	C(33)-C(34)	1.413(12)
C(24)-N(5)	1.40(2)	C(33)-H(33)	0.9500
C(20A)-N(5A)	1.31(5)	C(34)-C(35)	1.348(11)
C(20A)-C(21A)	1.37(5)	C(34)-H(34)	0.9500
C(20A)-H(20A)	0.9500	C(35)-N(8)	1.374(10)
C(21A)-C(22A)	1.49(9)	C(35)-H(35)	0.9500
C(21A)-H(21A)	0.9500	C(36)-N(8)	1.449(9)
C(22A)-C(23A)	1.30(12)	C(36)-H(36A)	0.9800
C(22A)-H(22A)	0.9500	C(36)-H(36B)	0.9800
C(23A)-C(24A)	1.40(10)	C(36)-H(36C)	0.9800
C(23A)-H(23A)	0.9500	N(1)-Pd(2)	2.211(5)

N(2)-Pd(2)	1.955(7)	C(2)-C(3)-C(4)	119.8(8)
N(3)-Pd(1)	2.202(5)	C(2)-C(3)-H(3)	120.1
N(4)-Pd(1)	1.954(7)	C(4)-C(3)-H(3)	120.1
Pd(1)-Cl(1)	2.340(2)	C(5)-C(4)-C(3)	120.2(8)
Pd(2)-Cl(1)	2.352(2)	C(5)-C(4)-H(4)	119.9
B(2)-F(3)	1.347(11)	C(3)-C(4)-H(4)	119.9
B(2)-F(1)	1.359(12)	C(4)-C(5)-C(6)	122.3(8)
B(2)-F(4)	1.366(11)	C(4)-C(5)-H(5)	118.8
B(2)-F(2)	1.382(12)	C(6)-C(5)-H(5)	118.8
C(38)-C(39)	1.3900	N(3)-C(6)-N(9)	116.0(7)
C(38)-C(43)	1.3900	N(3)-C(6)-C(5)	128.7(7)
C(38)-H(38)	0.9500	N(9)-C(6)-C(5)	115.3(7)
C(39)-C(40)	1.3900	N(3)-C(7)-C(12)	110.9(7)
C(39)-H(39)	0.9500	N(3)-C(7)-C(8)	113.5(6)
C(40)-C(41)	1.3900	C(12)-C(7)-C(8)	107.6(6)
C(40)-H(40)	0.9500	N(3)-C(7)-H(7)	108.2
C(41)-C(42)	1.3900	C(12)-C(7)-H(7)	108.2
C(41)-H(41)	0.9500	C(8)-C(7)-H(7)	108.2
C(42)-C(43)	1.3900	C(7)-C(8)-C(9)	109.3(7)
C(42)-H(43)	0.9500	C(7)-C(8)-H(8A)	109.8
C(43)-C(44)	1.53(2)	C(9)-C(8)-H(8A)	109.8
C(44)-H(44A)	0.9800	C(7)-C(8)-H(8B)	109.8
C(44)-H(44B)	0.9800	C(9)-C(8)-H(8B)	109.8
C(44)-H(44C)	0.9800	H(8A)-C(8)-H(8B)	108.3
C(45)-Cl(3)	1.91(3)	C(10)-C(9)-C(8)	111.9(8)
C(45)-Cl(2)	1.91(3)	C(10)-C(9)-H(9A)	109.2
		C(8)-C(9)-H(9A)	109.2
N(9)-C(1)-H(1A)	109.5	C(10)-C(9)-H(9B)	109.2
N(9)-C(1)-H(1B)	109.5	C(8)-C(9)-H(9B)	109.2
H(1A)-C(1)-H(1B)	109.5	H(9A)-C(9)-H(9B)	107.9
N(9)-C(1)-H(1C)	109.5	C(9)-C(10)-C(11)	112.5(8)
H(1A)-C(1)-H(1C)	109.5	C(9)-C(10)-H(10A)	109.1
H(1B)-C(1)-H(1C)	109.5	C(11)-C(10)-H(10A)	109.1
C(3)-C(2)-N(9)	120.1(9)	C(9)-C(10)-H(10B)	109.1
C(3)-C(2)-H(2)	119.9	C(11)-C(10)-H(10B)	109.1
N(9)-C(2)-H(2)	119.9	H(10A)-C(10)-H(10B)	107.8

C(12)-C(11)-C(10)	110.2(7)	C(16A)-C(15A)-H(15A)	119.1
C(12)-C(11)-H(11A)	109.6	C(15A)-C(16A)-C(17A)	117(3)
C(10)-C(11)-H(11A)	109.6	C(15A)-C(16A)-H(16A)	121.3
C(12)-C(11)-H(11B)	109.6	C(17A)-C(16A)-H(16A)	121.3
C(10)-C(11)-H(11B)	109.6	N(6A)-C(17A)-C(16A)	119(3)
H(11A)-C(11)-H(11B)	108.1	N(6A)-C(17A)-H(17A)	120.5
N(4)-C(12)-C(11)	116.5(7)	C(16A)-C(17A)-H(17A)	120.5
N(4)-C(12)-C(7)	108.2(6)	N(6A)-C(18A)-Pd(1)	100.9(16)
C(11)-C(12)-C(7)	106.8(7)	N(5)-C(19)-N(5A)	24.9(12)
N(4)-C(12)-H(12)	108.4	N(5)-C(19)-Pd(2)	109.3(8)
C(11)-C(12)-H(12)	108.4	N(5A)-C(19)-Pd(2)	103.1(13)
C(7)-C(12)-H(12)	108.4	N(5)-C(19)-H(19A)	109.8
N(4)-C(13)-N(6)	118(2)	N(5A)-C(19)-H(19A)	132.9
N(4)-C(13)-C(14)	129(2)	Pd(2)-C(19)-H(19A)	109.8
N(6)-C(13)-C(14)	112(2)	N(5)-C(19)-H(19B)	109.8
C(15)-C(14)-C(13)	118(3)	N(5A)-C(19)-H(19B)	90.5
C(15)-C(14)-H(14)	120.8	Pd(2)-C(19)-H(19B)	109.8
C(13)-C(14)-H(14)	120.8	H(19A)-C(19)-H(19B)	108.3
C(16)-C(15)-C(14)	124(2)	N(5)-C(20)-C(21)	119.1(17)
C(16)-C(15)-H(15)	117.8	N(5)-C(20)-H(20)	120.4
C(14)-C(15)-H(15)	117.8	C(21)-C(20)-H(20)	120.4
C(15)-C(16)-C(17)	116.8(19)	C(22)-C(21)-C(20)	119(2)
C(15)-C(16)-H(16)	121.6	C(22)-C(21)-H(21)	120.4
C(17)-C(16)-H(16)	121.6	C(20)-C(21)-H(21)	120.4
N(6)-C(17)-C(16)	122(2)	C(21)-C(22)-C(23)	123(4)
N(6)-C(17)-H(17)	119.1	C(21)-C(22)-H(22)	118.3
C(16)-C(17)-H(17)	119.1	C(23)-C(22)-H(22)	118.3
N(6)-C(18)-Pd(1)	109.0(10)	C(22)-C(23)-C(24)	117(4)
C(14A)-C(13A)-N(6A)	123(4)	C(22)-C(23)-H(23)	121.5
C(14A)-C(13A)-N(4)	129(4)	C(24)-C(23)-H(23)	121.5
N(6A)-C(13A)-N(4)	107(4)	N(2)-C(24)-N(5)	114.3(12)
C(15A)-C(14A)-C(13A)	120(4)	N(2)-C(24)-C(23)	127(2)
C(15A)-C(14A)-H(14A)	120.0	N(5)-C(24)-C(23)	117(2)
C(13A)-C(14A)-H(14A)	120.0	N(5A)-C(20A)-C(21A)	128(3)
C(14A)-C(15A)-C(16A)	122(3)	N(5A)-C(20A)-H(20A)	116.1
C(14A)-C(15A)-H(15A)	119.1	C(21A)-C(20A)-H(20A)	116.1

C(20A)-C(21A)-C(22A)	110(4)	C(28)-C(29)-C(30)	110.3(7)
C(20A)-C(21A)-H(21A)	125.2	C(28)-C(29)-H(29A)	109.6
C(22A)-C(21A)-H(21A)	125.2	C(30)-C(29)-H(29A)	109.6
C(23A)-C(22A)-C(21A)	120(7)	C(28)-C(29)-H(29B)	109.6
C(23A)-C(22A)-H(22A)	120.2	C(30)-C(29)-H(29B)	109.6
C(21A)-C(22A)-H(22A)	120.2	H(29A)-C(29)-H(29B)	108.1
C(22A)-C(23A)-C(24A)	124(8)	N(1)-C(30)-C(25)	110.6(6)
C(22A)-C(23A)-H(23A)	118.1	N(1)-C(30)-C(29)	112.6(6)
C(24A)-C(23A)-H(23A)	118.1	C(25)-C(30)-C(29)	109.5(6)
N(5A)-C(24A)-C(23A)	117(4)	N(1)-C(30)-H(30)	108.0
N(5A)-C(24A)-N(2)	114(2)	C(25)-C(30)-H(30)	108.0
C(23A)-C(24A)-N(2)	126(4)	C(29)-C(30)-H(30)	108.0
N(2)-C(25)-C(30)	107.5(6)	N(1)-C(31)-N(8)	116.9(6)
N(2)-C(25)-C(26)	115.9(7)	N(1)-C(31)-C(32)	127.7(7)
C(30)-C(25)-C(26)	108.3(6)	N(8)-C(31)-C(32)	115.4(7)
N(2)-C(25)-H(25)	108.3	C(33)-C(32)-C(31)	123.1(7)
C(30)-C(25)-H(25)	108.3	C(33)-C(32)-H(32)	118.4
C(26)-C(25)-H(25)	108.3	C(31)-C(32)-H(32)	118.4
C(27)-C(26)-C(25)	110.9(7)	C(32)-C(33)-C(34)	119.5(7)
C(27)-C(26)-H(26A)	109.5	C(32)-C(33)-H(33)	120.2
C(25)-C(26)-H(26A)	109.5	C(34)-C(33)-H(33)	120.2
C(27)-C(26)-H(26B)	109.5	C(35)-C(34)-C(33)	118.6(8)
C(25)-C(26)-H(26B)	109.5	C(35)-C(34)-H(34)	120.7
H(26A)-C(26)-H(26B)	108.0	C(33)-C(34)-H(34)	120.7
C(26)-C(27)-C(28)	110.2(7)	C(34)-C(35)-N(8)	122.0(7)
C(26)-C(27)-H(27A)	109.6	C(34)-C(35)-H(35)	119.0
C(28)-C(27)-H(27A)	109.6	N(8)-C(35)-H(35)	119.0
C(26)-C(27)-H(27B)	109.6	N(8)-C(36)-H(36A)	109.5
C(28)-C(27)-H(27B)	109.6	N(8)-C(36)-H(36B)	109.5
H(27A)-C(27)-H(27B)	108.1	H(36A)-C(36)-H(36B)	109.5
C(27)-C(28)-C(29)	111.6(7)	N(8)-C(36)-H(36C)	109.5
C(27)-C(28)-H(28A)	109.3	H(36A)-C(36)-H(36C)	109.5
C(29)-C(28)-H(28A)	109.3	H(36B)-C(36)-H(36C)	109.5
C(27)-C(28)-H(28B)	109.3	C(31)-N(1)-C(30)	117.9(6)
C(29)-C(28)-H(28B)	109.3	C(31)-N(1)-Pd(2)	114.6(4)
H(28A)-C(28)-H(28B)	108.0	C(30)-N(1)-Pd(2)	101.4(4)

C(24)-N(2)-C(24A)	24.4(8)	C(18)-Pd(1)-N(3)	161.9(4)
C(24)-N(2)-C(25)	124.3(8)	N(4)-Pd(1)-N(3)	80.9(2)
C(24A)-N(2)-C(25)	124.6(11)	C(18A)-Pd(1)-N(3)	160.1(8)
C(24)-N(2)-Pd(2)	117.9(7)	C(18)-Pd(1)-Cl(1)	90.1(4)
C(24A)-N(2)-Pd(2)	107.5(11)	N(4)-Pd(1)-Cl(1)	173.58(19)
C(25)-N(2)-Pd(2)	117.0(5)	C(18A)-Pd(1)-Cl(1)	92.7(7)
C(6)-N(3)-C(7)	114.6(6)	N(3)-Pd(1)-Cl(1)	105.33(17)
C(6)-N(3)-Pd(1)	117.0(4)	N(2)-Pd(2)-C(19)	82.3(3)
C(7)-N(3)-Pd(1)	102.1(4)	N(2)-Pd(2)-N(1)	81.5(2)
C(13)-N(4)-C(13A)	22(2)	C(19)-Pd(2)-N(1)	163.6(3)
C(13)-N(4)-C(12)	125.5(14)	N(2)-Pd(2)-Cl(1)	174.48(18)
C(13A)-N(4)-C(12)	120(2)	C(19)-Pd(2)-Cl(1)	92.3(3)
C(13)-N(4)-Pd(1)	111.8(13)	N(1)-Pd(2)-Cl(1)	104.00(15)
C(13A)-N(4)-Pd(1)	121(2)	Pd(1)-Cl(1)-Pd(2)	94.43(8)
C(12)-N(4)-Pd(1)	118.6(5)	F(3)-B(2)-F(1)	107.9(8)
C(20)-N(5)-C(24)	123.1(17)	F(3)-B(2)-F(4)	113.3(8)
C(20)-N(5)-C(19)	121.7(16)	F(1)-B(2)-F(4)	112.0(8)
C(24)-N(5)-C(19)	114.9(13)	F(3)-B(2)-F(2)	108.0(8)
C(17)-N(6)-C(13)	126(2)	F(1)-B(2)-F(2)	108.6(9)
C(17)-N(6)-C(18)	121.9(18)	F(4)-B(2)-F(2)	106.9(8)
C(13)-N(6)-C(18)	112.0(18)	C(39)-C(38)-C(43)	120.0
C(35)-N(8)-C(31)	121.1(6)	C(39)-C(38)-H(38)	120.0
C(35)-N(8)-C(36)	119.5(6)	C(43)-C(38)-H(38)	120.0
C(31)-N(8)-C(36)	119.3(6)	C(38)-C(39)-C(40)	120.0
C(2)-N(9)-C(6)	122.0(7)	C(38)-C(39)-H(39)	120.0
C(2)-N(9)-C(1)	117.6(7)	C(40)-C(39)-H(39)	120.0
C(6)-N(9)-C(1)	120.4(6)	C(41)-C(40)-C(39)	120.0
C(24A)-N(5A)-C(20A)	120(4)	C(41)-C(40)-H(40)	120.0
C(24A)-N(5A)-C(19)	117(3)	C(39)-C(40)-H(40)	120.0
C(20A)-N(5A)-C(19)	120(3)	C(42)-C(41)-C(40)	120.0
C(13A)-N(6A)-C(17A)	118(3)	C(42)-C(41)-H(41)	120.0
C(13A)-N(6A)-C(18A)	126(3)	C(40)-C(41)-H(41)	120.0
C(17A)-N(6A)-C(18A)	117(2)	C(43)-C(42)-C(41)	120.0
C(18)-Pd(1)-N(4)	84.0(5)	C(43)-C(42)-H(43)	120.0
C(18)-Pd(1)-C(18A)	18.2(7)	C(41)-C(42)-H(43)	120.0
N(4)-Pd(1)-C(18A)	80.9(7)	C(42)-C(43)-C(38)	120.0

C(42)-C(43)-C(44)	117.1(10)	
C(38)-C(43)-C(44)	122.7(10)	Symmetry transformations used to generate equivalent atoms:
Cl(3)-C(45)-Cl(2)	100(2)	

Table 4. Anisotropic displacement parameters ($\text{\AA}^2 \times 10^3$) for **35**. The anisotropic displacement factor exponent takes the form: $-2\pi^2 [h^2 a^{*2} U^{11} + \dots + 2 h k a^* b^* U^{12}]$

	U^{11}	U^{22}	U^{33}	U^{23}	U^{13}	U^{12}
C(1)	33(4)	28(4)	51(5)	10(4)	-1(4)	7(4)
C(2)	47(6)	42(5)	42(5)	15(4)	16(4)	11(4)
C(3)	64(7)	33(5)	36(5)	-4(4)	18(5)	-6(4)
C(4)	80(7)	29(4)	23(4)	1(3)	12(4)	-18(4)
C(5)	39(4)	27(4)	26(3)	5(3)	-3(3)	-4(4)
C(6)	27(4)	38(5)	20(3)	7(3)	3(3)	-3(3)
C(7)	27(4)	32(4)	40(5)	8(4)	0(3)	-1(3)
C(8)	46(5)	35(5)	44(5)	16(4)	-18(4)	-7(4)
C(9)	54(6)	34(5)	89(8)	24(5)	-35(6)	-10(5)
C(10)	42(6)	40(5)	95(8)	26(5)	-11(5)	-3(4)
C(11)	39(5)	38(5)	77(7)	26(5)	10(5)	5(4)
C(12)	41(5)	31(5)	37(5)	7(4)	7(4)	2(4)
C(13)	38(15)	50(10)	44(7)	17(6)	33(12)	14(13)
C(14)	84(18)	14(10)	70(14)	1(9)	27(13)	-18(9)
C(15)	102(18)	30(11)	91(18)	-25(11)	33(14)	-35(11)
C(16)	98(18)	47(12)	48(11)	-2(9)	35(12)	-6(12)
C(17)	93(17)	46(12)	44(10)	-19(8)	17(11)	-32(11)
C(18)	42(12)	18(8)	26(5)	8(5)	14(7)	2(6)
C(13A)	38(15)	50(10)	44(7)	17(6)	33(12)	14(13)
C(14A)	70(20)	13(17)	52(19)	12(14)	-9(18)	16(14)
C(15A)	130(30)	18(16)	53(18)	-24(13)	-10(20)	30(18)
C(16A)	80(30)	40(19)	90(30)	-8(17)	0(20)	34(18)
C(17A)	150(40)	50(20)	60(20)	-30(18)	-50(30)	50(20)
C(18A)	42(12)	18(8)	26(5)	8(5)	14(7)	2(6)
C(19)	118(10)	51(6)	47(5)	19(4)	-26(6)	-46(7)
C(20)	140(20)	41(12)	27(6)	21(8)	-51(12)	-13(11)

C(21)	88(15)	55(11)	26(6)	4(7)	-6(8)	-6(9)
C(22)	140(40)	37(19)	54(8)	14(13)	-40(20)	-34(16)
C(23)	100(30)	32(17)	27(12)	-2(10)	-6(16)	-21(16)
C(24)	24(6)	11(5)	28(4)	-2(4)	0(5)	7(5)
C(20A)	140(20)	41(12)	27(6)	21(8)	-51(12)	-13(11)
C(21A)	88(15)	55(11)	26(6)	4(7)	-6(8)	-6(9)
C(22A)	140(40)	37(19)	54(8)	14(13)	-40(20)	-34(16)
C(23A)	100(30)	32(17)	27(12)	-2(10)	-6(16)	-21(16)
C(24A)	24(6)	11(5)	28(4)	-2(4)	0(5)	7(5)
C(25)	36(5)	23(4)	31(4)	3(3)	-3(4)	-4(3)
C(26)	37(5)	32(4)	51(5)	-6(4)	4(4)	-8(4)
C(27)	75(7)	43(6)	49(5)	-8(4)	25(5)	-28(5)
C(28)	78(7)	43(5)	42(5)	-12(4)	25(5)	-29(5)
C(29)	53(6)	34(4)	21(4)	-3(3)	8(4)	-6(4)
C(30)	24(4)	20(4)	33(4)	-3(3)	1(3)	4(3)
C(31)	34(4)	23(4)	21(4)	2(3)	1(3)	2(3)
C(32)	29(4)	30(4)	20(3)	1(3)	2(3)	7(3)
C(33)	33(4)	32(4)	23(4)	-2(3)	-3(3)	2(4)
C(34)	48(5)	30(5)	37(4)	-2(4)	-8(4)	-4(4)
C(35)	30(4)	39(5)	39(4)	7(4)	-2(3)	-5(4)
C(36)	29(4)	38(5)	46(5)	3(4)	7(4)	10(4)
N(1)	22(3)	24(3)	23(3)	3(2)	7(2)	-5(3)
N(2)	74(5)	37(4)	25(4)	9(3)	-12(3)	-23(4)
N(3)	29(3)	27(3)	30(3)	-2(3)	-3(3)	4(3)
N(4)	82(6)	34(4)	24(4)	5(3)	10(3)	19(4)
N(5)	77(15)	25(9)	25(4)	14(6)	-21(9)	-3(7)
N(6)	52(11)	26(9)	29(7)	6(6)	5(7)	-9(6)
N(8)	21(3)	25(3)	33(3)	-2(3)	3(3)	3(3)
N(9)	37(4)	29(3)	27(3)	2(3)	3(3)	2(3)
N(5A)	77(15)	25(9)	25(4)	14(6)	-21(9)	-3(7)
N(6A)	60(20)	20(14)	34(12)	-3(10)	-7(14)	9(12)
Pd(1)	54(1)	28(1)	25(1)	3(1)	-1(1)	7(1)
Pd(2)	54(1)	28(1)	23(1)	6(1)	0(1)	-8(1)
Cl(1)	48(1)	30(1)	33(1)	12(1)	1(1)	-4(1)
B(2)	40(6)	41(6)	44(6)	8(5)	1(5)	2(5)
F(1)	106(6)	101(5)	61(4)	2(4)	0(4)	41(4)

F(2)	70(4)	53(3)	149(6)	41(4)	-23(4)	-15(3)
F(3)	105(5)	59(4)	48(3)	20(3)	-18(3)	-24(3)
F(4)	50(3)	88(4)	66(4)	28(3)	5(3)	14(3)
C(38)	104(14)	89(13)	34(8)	-34(8)	-18(9)	63(12)
C(39)	61(12)	90(13)	74(12)	-25(10)	9(10)	5(10)
C(40)	55(12)	130(20)	75(13)	-22(13)	14(10)	-49(12)
C(41)	19(7)	101(14)	50(9)	-47(10)	12(6)	6(8)
C(42)	19(8)	58(11)	126(17)	-39(11)	-31(9)	24(7)
C(43)	7(7)	29(8)	30(8)	3(7)	-6(6)	7(6)
C(44)	140(20)	57(11)	39(8)	-10(9)	13(12)	-12(11)
C(45)	70(30)	340(90)	340(90)	-320(80)	-30(40)	20(40)
Cl(2)	164(17)	141(16)	185(17)	-55(13)	-87(14)	-38(13)
Cl(3)	64(5)	142(8)	66(5)	5(5)	-6(4)	4(5)

Table 5. Hydrogen coordinates ($\times 10^4$) and isotropic displacement parameters ($\text{\AA}^2 \times 10^3$) for **35**.

	x	y	z	U(eq)
H(1A)	12777	10498	6149	56
H(1B)	13997	9948	6192	56
H(1C)	12920	9994	6715	56
H(2)	13836	8870	5783	53
H(3)	12652	8030	5257	53
H(4)	10355	8181	5100	53
H(5)	9238	9092	5546	36
H(7)	8365	9829	6155	40
H(8A)	9115	10190	5189	50
H(8B)	9207	10995	5419	50
H(9A)	7104	10855	4946	71
H(9B)	6770	10169	5338	71
H(10A)	5579	11093	5725	70
H(10B)	6875	11594	5737	70
H(11A)	6437	11197	6700	62
H(11B)	6467	10385	6486	62

H(12)	8736	11307	6405	43
H(14)	7639	12022	7280	67
H(15)	7431	12564	8211	89
H(16)	8229	12061	9061	77
H(17)	9473	11022	8981	73
H(14A)	7160	11835	7270	52
H(15A)	6673	12351	8145	80
H(16A)	7115	11767	9032	87
H(17A)	8667	10795	9001	101
H(19A)	9174	8636	6807	86
H(19B)	10356	8090	6649	86
H(20)	8211	7624	6026	81
H(21)	6947	6575	6010	68
H(22)	6862	5876	6847	94
H(23)	7651	6272	7762	64
H(20A)	8832	7443	6051	81
H(21A)	8114	6270	5902	68
H(22A)	7360	5706	6856	94
H(23A)	7954	6210	7705	64
H(25)	9355	6862	8551	36
H(26A)	6833	7583	8688	48
H(26B)	6967	6788	8442	48
H(27A)	7869	6410	9354	67
H(27B)	6436	6773	9463	67
H(28A)	8067	7198	10154	65
H(28B)	7455	7835	9769	65
H(29A)	10022	7183	9573	43
H(29B)	9795	7977	9809	43
H(30)	8784	8298	8890	31
H(32)	9779	9099	9436	32
H(33)	10930	10031	9819	35
H(34)	13238	10180	9588	46
H(35)	14277	9356	8999	43
H(36A)	13139	8201	8123	56
H(36B)	13195	7717	8704	56
H(36C)	14368	8276	8573	56

H(38)	10191	-316	2548	91
H(39)	9846	-1032	3379	90
H(40)	8543	-615	4166	104
H(41)	7585	518	4121	68
H(43)	7931	1234	3290	81
H(44A)	8500	1372	2312	118
H(44B)	9038	711	1936	118
H(44C)	10076	1219	2272	118

Table 6. Torsion angles [°] for **35**.

N(9)-C(2)-C(3)-C(4)	2.0(12)	C(14A)-C(15A)-C(16A)-C(17A)	9(7)
C(2)-C(3)-C(4)-C(5)	-3.7(12)	C(15A)-C(16A)-C(17A)-N(6A)	-10(7)
C(3)-C(4)-C(5)-C(6)	1.1(11)	N(5)-C(20)-C(21)-C(22)	-4(3)
C(4)-C(5)-C(6)-N(3)	-177.0(7)	C(20)-C(21)-C(22)-C(23)	7(4)
C(4)-C(5)-C(6)-N(9)	3.1(10)	C(21)-C(22)-C(23)-C(24)	-1(5)
N(3)-C(7)-C(8)-C(9)	175.4(7)	C(22)-C(23)-C(24)-N(2)	-176(2)
C(12)-C(7)-C(8)-C(9)	-61.5(9)	C(22)-C(23)-C(24)-N(5)	-8(3)
C(7)-C(8)-C(9)-C(10)	53.6(10)	N(5A)-C(20A)-C(21A)-C(22A)	14(6)
C(8)-C(9)-C(10)-C(11)	-50.7(10)	C(20A)-C(21A)-C(22A)-C(23A)	-8(7)
C(9)-C(10)-C(11)-C(12)	56.5(10)	C(21A)-C(22A)-C(23A)-C(24A)	2(10)
C(10)-C(11)-C(12)-N(4)	175.2(7)	C(22A)-C(23A)-C(24A)-N(5A)	0(9)
C(10)-C(11)-C(12)-C(7)	-63.8(9)	C(22A)-C(23A)-C(24A)-N(2)	161(5)
N(3)-C(7)-C(12)-N(4)	-42.3(8)	N(2)-C(25)-C(26)-C(27)	177.5(7)
C(8)-C(7)-C(12)-N(4)	-167.0(7)	C(30)-C(25)-C(26)-C(27)	-61.6(8)
N(3)-C(7)-C(12)-C(11)	-168.4(6)	C(25)-C(26)-C(27)-C(28)	58.3(10)
C(8)-C(7)-C(12)-C(11)	66.9(8)	C(26)-C(27)-C(28)-C(29)	-55.0(11)
N(4)-C(13)-C(14)-C(15)	174.6(19)	C(27)-C(28)-C(29)-C(30)	55.3(10)
N(6)-C(13)-C(14)-C(15)	-5(3)	N(2)-C(25)-C(30)-N(1)	-48.5(8)
C(13)-C(14)-C(15)-C(16)	1(3)	C(26)-C(25)-C(30)-N(1)	-174.5(6)
C(14)-C(15)-C(16)-C(17)	3(3)	N(2)-C(25)-C(30)-C(29)	-173.2(6)
C(15)-C(16)-C(17)-N(6)	-4(3)	C(26)-C(25)-C(30)-C(29)	60.9(8)
N(6A)-C(13A)-C(14A)-C(15A)	-2(6)	C(28)-C(29)-C(30)-N(1)	178.1(6)
N(4)-C(13A)-C(14A)-C(15A)	-167(4)	C(28)-C(29)-C(30)-C(25)	-58.4(8)
C(13A)-C(14A)-C(15A)-C(16A)	-3(7)	N(1)-C(31)-C(32)-C(33)	-176.6(7)

N(8)-C(31)-C(32)-C(33)	3.2(10)	C(12)-C(7)-N(3)-Pd(1)	46.1(6)
C(31)-C(32)-C(33)-C(34)	-0.3(11)	C(8)-C(7)-N(3)-Pd(1)	167.3(5)
C(32)-C(33)-C(34)-C(35)	-1.4(11)	N(6)-C(13)-N(4)-C(13A)	100(9)
C(33)-C(34)-C(35)-N(8)	-0.1(12)	C(14)-C(13)-N(4)-C(13A)	-80(8)
N(8)-C(31)-N(1)-C(30)	163.6(6)	N(6)-C(13)-N(4)-C(12)	-176.8(11)
C(32)-C(31)-N(1)-C(30)	-16.6(10)	C(14)-C(13)-N(4)-C(12)	4(3)
N(8)-C(31)-N(1)-Pd(2)	-77.2(7)	N(6)-C(13)-N(4)-Pd(1)	-20.0(19)
C(32)-C(31)-N(1)-Pd(2)	102.7(7)	C(14)-C(13)-N(4)-Pd(1)	160.8(16)
C(25)-C(30)-N(1)-C(31)	173.9(6)	C(14A)-C(13A)-N(4)-C(13)	88(9)
C(29)-C(30)-N(1)-C(31)	-63.3(8)	N(6A)-C(13A)-N(4)-C(13)	-79(8)
C(25)-C(30)-N(1)-Pd(2)	47.9(6)	C(14A)-C(13A)-N(4)-C(12)	-22(5)
C(29)-C(30)-N(1)-Pd(2)	170.7(5)	N(6A)-C(13A)-N(4)-C(12)	171(2)
N(5)-C(24)-N(2)-C(24A)	-83(3)	C(14A)-C(13A)-N(4)-Pd(1)	159(3)
C(23)-C(24)-N(2)-C(24A)	85(4)	N(6A)-C(13A)-N(4)-Pd(1)	-8(4)
N(5)-C(24)-N(2)-C(25)	178.2(10)	C(11)-C(12)-N(4)-C(13)	-69.7(15)
C(23)-C(24)-N(2)-C(25)	-14(2)	C(7)-C(12)-N(4)-C(13)	170.0(13)
N(5)-C(24)-N(2)-Pd(2)	-12.5(14)	C(11)-C(12)-N(4)-C(13A)	-44(2)
C(23)-C(24)-N(2)-Pd(2)	155.1(17)	C(7)-C(12)-N(4)-C(13A)	-164(2)
N(5A)-C(24A)-N(2)-C(24)	90(4)	C(11)-C(12)-N(4)-Pd(1)	135.0(7)
C(23A)-C(24A)-N(2)-C(24)	-72(5)	C(7)-C(12)-N(4)-Pd(1)	14.7(9)
N(5A)-C(24A)-N(2)-C(25)	-172.6(18)	C(21)-C(20)-N(5)-C(24)	-5(3)
C(23A)-C(24A)-N(2)-C(25)	26(5)	C(21)-C(20)-N(5)-C(19)	168.2(17)
N(5A)-C(24A)-N(2)-Pd(2)	-30(2)	N(2)-C(24)-N(5)-C(20)	-179.6(16)
C(23A)-C(24A)-N(2)-Pd(2)	169(5)	C(23)-C(24)-N(5)-C(20)	12(3)
C(30)-C(25)-N(2)-C(24)	-168.7(10)	N(2)-C(24)-N(5)-C(19)	6.5(17)
C(26)-C(25)-N(2)-C(24)	-47.3(13)	C(23)-C(24)-N(5)-C(19)	-162.4(18)
C(30)-C(25)-N(2)-C(24A)	161.6(13)	N(5A)-C(19)-N(5)-C(20)	-93(5)
C(26)-C(25)-N(2)-C(24A)	-77.1(15)	Pd(2)-C(19)-N(5)-C(20)	-172.1(14)
C(30)-C(25)-N(2)-Pd(2)	21.9(8)	N(5A)-C(19)-N(5)-C(24)	81(4)
C(26)-C(25)-N(2)-Pd(2)	143.3(6)	Pd(2)-C(19)-N(5)-C(24)	1.9(15)
N(9)-C(6)-N(3)-C(7)	166.7(6)	C(16)-C(17)-N(6)-C(13)	0(3)
C(5)-C(6)-N(3)-C(7)	-13.2(10)	C(16)-C(17)-N(6)-C(18)	178.3(17)
N(9)-C(6)-N(3)-Pd(1)	-73.8(7)	N(4)-C(13)-N(6)-C(17)	-175.2(17)
C(5)-C(6)-N(3)-Pd(1)	106.3(7)	C(14)-C(13)-N(6)-C(17)	4(3)
C(12)-C(7)-N(3)-C(6)	173.6(6)	N(4)-C(13)-N(6)-C(18)	7(2)
C(8)-C(7)-N(3)-C(6)	-65.2(8)	C(14)-C(13)-N(6)-C(18)	-174.0(13)

Pd(1)-C(18)-N(6)-C(17)	-168.4(14)	C(13)-N(4)-Pd(1)-C(18)	20.1(11)
Pd(1)-C(18)-N(6)-C(13)	9.8(16)	C(13A)-N(4)-Pd(1)-C(18)	-2(2)
C(34)-C(35)-N(8)-C(31)	3.3(11)	C(12)-N(4)-Pd(1)-C(18)	178.6(8)
C(34)-C(35)-N(8)-C(36)	-174.4(7)	C(13)-N(4)-Pd(1)-C(18A)	38.2(12)
N(1)-C(31)-N(8)-C(35)	175.2(6)	C(13A)-N(4)-Pd(1)-C(18A)	16(2)
C(32)-C(31)-N(8)-C(35)	-4.7(10)	C(12)-N(4)-Pd(1)-C(18A)	-163.3(10)
N(1)-C(31)-N(8)-C(36)	-7.1(10)	C(13)-N(4)-Pd(1)-N(3)	-149.9(11)
C(32)-C(31)-N(8)-C(36)	173.0(6)	C(13A)-N(4)-Pd(1)-N(3)	-172(2)
C(3)-C(2)-N(9)-C(6)	2.4(12)	C(12)-N(4)-Pd(1)-N(3)	8.6(6)
C(3)-C(2)-N(9)-C(1)	-175.1(7)	C(13)-N(4)-Pd(1)-Cl(1)	44(3)
N(3)-C(6)-N(9)-C(2)	175.2(6)	C(13A)-N(4)-Pd(1)-Cl(1)	22(3)
C(5)-C(6)-N(9)-C(2)	-4.8(10)	C(12)-N(4)-Pd(1)-Cl(1)	-157.2(17)
N(3)-C(6)-N(9)-C(1)	-7.3(10)	N(6A)-C(18A)-Pd(1)-C(18)	82(3)
C(5)-C(6)-N(9)-C(1)	172.6(6)	N(6A)-C(18A)-Pd(1)-N(4)	-16.7(14)
C(23A)-C(24A)-N(5A)-C(20A)	5(5)	N(6A)-C(18A)-Pd(1)-N(3)	-41(3)
N(2)-C(24A)-N(5A)-C(20A)	-159(3)	N(6A)-C(18A)-Pd(1)-Cl(1)	164.0(14)
C(23A)-C(24A)-N(5A)-C(19)	166(4)	C(6)-N(3)-Pd(1)-C(18)	170.5(17)
N(2)-C(24A)-N(5A)-C(19)	3(3)	C(7)-N(3)-Pd(1)-C(18)	-63.5(18)
C(21A)-C(20A)-N(5A)-C(24A)	-13(6)	C(6)-N(3)-Pd(1)-N(4)	-155.6(6)
C(21A)-C(20A)-N(5A)-C(19)	-174(4)	C(7)-N(3)-Pd(1)-N(4)	-29.6(5)
N(5)-C(19)-N(5A)-C(24A)	-83(5)	C(6)-N(3)-Pd(1)-C(18A)	-131(2)
Pd(2)-C(19)-N(5A)-C(24A)	25(3)	C(7)-N(3)-Pd(1)-C(18A)	-5(2)
N(5)-C(19)-N(5A)-C(20A)	78(4)	C(6)-N(3)-Pd(1)-Cl(1)	22.8(6)
Pd(2)-C(19)-N(5A)-C(20A)	-174(3)	C(7)-N(3)-Pd(1)-Cl(1)	148.8(4)
C(14A)-C(13A)-N(6A)-C(17A)	2(5)	C(24)-N(2)-Pd(2)-C(19)	10.9(9)
N(4)-C(13A)-N(6A)-C(17A)	169(3)	C(24A)-N(2)-Pd(2)-C(19)	35.0(11)
C(14A)-C(13A)-N(6A)-C(18A)	-179(3)	C(25)-N(2)-Pd(2)-C(19)	-179.0(7)
N(4)-C(13A)-N(6A)-C(18A)	-11(4)	C(24)-N(2)-Pd(2)-N(1)	-166.9(9)
C(16A)-C(17A)-N(6A)-C(13A)	5(6)	C(24A)-N(2)-Pd(2)-N(1)	-142.8(11)
C(16A)-C(17A)-N(6A)-C(18A)	-175(3)	C(25)-N(2)-Pd(2)-N(1)	3.2(6)
Pd(1)-C(18A)-N(6A)-C(13A)	21(3)	C(24)-N(2)-Pd(2)-Cl(1)	20(3)
Pd(1)-C(18A)-N(6A)-C(17A)	-159(3)	C(24A)-N(2)-Pd(2)-Cl(1)	44(3)
N(6)-C(18)-Pd(1)-N(4)	-15.8(9)	C(25)-N(2)-Pd(2)-Cl(1)	-170(2)
N(6)-C(18)-Pd(1)-C(18A)	-95(3)	N(5)-C(19)-Pd(2)-N(2)	-6.3(9)
N(6)-C(18)-Pd(1)-N(3)	18(2)	N(5A)-C(19)-Pd(2)-N(2)	-31.4(14)
N(6)-C(18)-Pd(1)-Cl(1)	166.9(9)	N(5)-C(19)-Pd(2)-N(1)	2(2)

N(5A)-C(19)-Pd(2)-N(1)	-24(2)	C(19)-Pd(2)-Cl(1)-Pd(1)	65.6(4)
N(5)-C(19)-Pd(2)-Cl(1)	174.5(9)	N(1)-Pd(2)-Cl(1)-Pd(1)	-116.40(16)
N(5A)-C(19)-Pd(2)-Cl(1)	149.4(14)	C(43)-C(38)-C(39)-C(40)	0.0
C(31)-N(1)-Pd(2)-N(2)	-156.2(6)	C(38)-C(39)-C(40)-C(41)	0.0
C(30)-N(1)-Pd(2)-N(2)	-28.0(4)	C(39)-C(40)-C(41)-C(42)	0.0
C(31)-N(1)-Pd(2)-C(19)	-164.0(14)	C(40)-C(41)-C(42)-C(43)	0.0
C(30)-N(1)-Pd(2)-C(19)	-35.9(16)	C(41)-C(42)-C(43)-C(38)	0.0
C(31)-N(1)-Pd(2)-Cl(1)	23.2(5)	C(41)-C(42)-C(43)-C(44)	175.3(13)
C(30)-N(1)-Pd(2)-Cl(1)	151.4(4)	C(39)-C(38)-C(43)-C(42)	0.0
C(18)-Pd(1)-Cl(1)-Pd(2)	78.7(5)	C(39)-C(38)-C(43)-C(44)	-175.0(14)
N(4)-Pd(1)-Cl(1)-Pd(2)	55(2)		
C(18A)-Pd(1)-Cl(1)-Pd(2)	60.7(8)		
N(3)-Pd(1)-Cl(1)-Pd(2)	-110.77(17)		
N(2)-Pd(2)-Cl(1)-Pd(1)	57(3)		

Symmetry transformations used to generate equivalent atoms:

Single crystal X-ray structure data for [Pd(C₆H₅)(η^3 -CH₂N^{C₆H₁₀}N^{Me})] (36)

Table 1. Crystal data and structure refinement for **36**.

Identification code	36	
Empirical formula	C ₂₄ H ₂₈ N ₄ Pd	
Formula weight	478.90	
Temperature	110(2) K	
Wavelength	0.71073 Å	
Crystal system	Orthorhombic	
Space group	P2(1)2(1)2(1)	
Unit cell dimensions	a = 10.4293(7) Å	$\alpha = 90^\circ$.
	b = 11.2250(8) Å	$\beta = 90^\circ$.
	c = 18.1758(13) Å	$\gamma = 90^\circ$.
Volume	2127.8(3) Å ³	
Z	4	
Density (calculated)	1.495 Mg/m ³	
Absorption coefficient	0.890 mm ⁻¹	
F(000)	984	
Crystal size	0.29 x 0.10 x 0.05 mm ³	
Theta range for data collection	2.13 to 28.30°.	
Index ranges	-13<=h<=13, -14<=k<=14, -24<=l<=24	
Reflections collected	29376	
Independent reflections	5282 [R(int) = 0.0277]	
Completeness to theta = 28.30°	100.0 %	
Absorption correction	Semi-empirical from equivalents	
Max. and min. transmission	0.9569 and 0.7825	
Refinement method	Full-matrix least-squares on F ²	
Data / restraints / parameters	5282 / 0 / 263	
Goodness-of-fit on F ²	1.068	
Final R indices [I>2sigma(I)]	R1 = 0.0197, wR2 = 0.0467	
R indices (all data)	R1 = 0.0208, wR2 = 0.0472	
Absolute structure parameter	-0.016(17)	
Largest diff. peak and hole	0.632 and -0.208 e.Å ⁻³	

Table 2. Atomic coordinates ($\times 10^4$) and equivalent isotropic displacement parameters ($\text{\AA}^2 \times 10^3$) for **36**. $U(\text{eq})$ is defined as one third of the trace of the orthogonalized U^{ij} tensor.

	x	y	z	$U(\text{eq})$
C(1)	7375(2)	4700(2)	8838(1)	19(1)
C(2)	7525(2)	3490(2)	9091(1)	24(1)
C(3)	6726(2)	2618(2)	8860(1)	29(1)
C(4)	5722(2)	2874(2)	8364(1)	28(1)
C(5)	5649(2)	3989(2)	8082(1)	25(1)
C(6)	6476(2)	6058(2)	7908(1)	22(1)
C(7)	8911(2)	5713(2)	9644(1)	21(1)
C(8)	8410(2)	5239(2)	10382(1)	29(1)
C(9)	9444(3)	5344(2)	10971(1)	38(1)
C(10)	9910(2)	6623(2)	11052(1)	31(1)
C(11)	10348(2)	7123(2)	10310(1)	25(1)
C(12)	9246(2)	7037(2)	9753(1)	20(1)
C(13)	9726(2)	8775(2)	9063(1)	20(1)
C(14)	9415(2)	9584(2)	9649(1)	24(1)
C(15)	9593(2)	10779(2)	9584(1)	29(1)
C(16)	10097(2)	11265(2)	8930(1)	30(1)
C(17)	10440(2)	10502(2)	8386(1)	26(1)
C(18)	10791(2)	8524(2)	7867(1)	27(1)
C(19)	7665(2)	8365(2)	7574(1)	18(1)
C(20)	7642(2)	8177(2)	6816(1)	25(1)
C(21)	7618(2)	9120(2)	6315(1)	30(1)
C(22)	7558(2)	10287(2)	6560(1)	32(1)
C(23)	7502(2)	10508(2)	7314(1)	28(1)
C(24)	7556(2)	9555(2)	7806(1)	23(1)
N(1)	6487(1)	4863(1)	8280(1)	20(1)
N(2)	7985(2)	5655(1)	9044(1)	19(1)
N(3)	9531(2)	7609(1)	9038(1)	20(1)
N(4)	10301(2)	9297(1)	8450(1)	21(1)
Pd(1)	7899(1)	7034(1)	8330(1)	17(1)

Table 3. Bond lengths [Å] and angles [°] for **36**.

C(1)-N(2)	1.301(2)	C(13)-N(4)	1.395(2)
C(1)-N(1)	1.386(2)	C(13)-C(14)	1.437(3)
C(1)-C(2)	1.442(3)	C(14)-C(15)	1.359(3)
C(2)-C(3)	1.352(3)	C(14)-H(14)	0.9500
C(2)-H(2)	0.9500	C(15)-C(16)	1.410(3)
C(3)-C(4)	1.411(3)	C(15)-H(15)	0.9500
C(3)-H(3)	0.9500	C(16)-C(17)	1.356(3)
C(4)-C(5)	1.354(3)	C(16)-H(16)	0.9500
C(4)-H(4)	0.9500	C(17)-N(4)	1.365(2)
C(5)-N(1)	1.362(2)	C(17)-H(17)	0.9500
C(5)-H(5)	0.9500	C(18)-N(4)	1.462(3)
C(6)-N(1)	1.502(2)	C(18)-H(18A)	0.9800
C(6)-Pd(1)	1.9986(19)	C(18)-H(18B)	0.9800
C(6)-H(6A)	0.9900	C(18)-H(18C)	0.9800
C(6)-H(6B)	0.9900	C(19)-C(20)	1.395(3)
C(7)-N(2)	1.459(2)	C(19)-C(24)	1.405(3)
C(7)-C(8)	1.535(3)	C(19)-Pd(1)	2.0437(18)
C(7)-C(12)	1.539(3)	C(20)-C(21)	1.397(3)
C(7)-H(7)	1.0000	C(20)-H(20)	0.9500
C(8)-C(9)	1.524(3)	C(21)-C(22)	1.384(3)
C(8)-H(8A)	0.9900	C(21)-H(21)	0.9500
C(8)-H(8B)	0.9900	C(22)-C(23)	1.395(3)
C(9)-C(10)	1.523(3)	C(22)-H(22)	0.9500
C(9)-H(9A)	0.9900	C(23)-C(24)	1.396(3)
C(9)-H(9B)	0.9900	C(23)-H(23)	0.9500
C(10)-C(11)	1.530(3)	C(24)-H(24)	0.9500
C(10)-H(10A)	0.9900	N(2)-Pd(1)	2.0213(15)
C(10)-H(10B)	0.9900	N(3)-Pd(1)	2.2287(16)
C(11)-C(12)	1.535(2)		
C(11)-H(11A)	0.9900	N(2)-C(1)-N(1)	115.30(16)
C(11)-H(11B)	0.9900	N(2)-C(1)-C(2)	129.19(17)
C(12)-N(3)	1.479(2)	N(1)-C(1)-C(2)	115.47(16)
C(12)-H(12)	1.0000	C(3)-C(2)-C(1)	121.02(18)
C(13)-N(3)	1.325(3)	C(3)-C(2)-H(2)	119.5

C(1)-C(2)-H(2)	119.5	C(11)-C(10)-H(10A)	109.5
C(2)-C(3)-C(4)	120.61(19)	C(9)-C(10)-H(10B)	109.5
C(2)-C(3)-H(3)	119.7	C(11)-C(10)-H(10B)	109.5
C(4)-C(3)-H(3)	119.7	H(10A)-C(10)-H(10B)	108.1
C(5)-C(4)-C(3)	118.06(18)	C(10)-C(11)-C(12)	109.61(16)
C(5)-C(4)-H(4)	121.0	C(10)-C(11)-H(11A)	109.7
C(3)-C(4)-H(4)	121.0	C(12)-C(11)-H(11A)	109.7
C(4)-C(5)-N(1)	122.01(18)	C(10)-C(11)-H(11B)	109.7
C(4)-C(5)-H(5)	119.0	C(12)-C(11)-H(11B)	109.7
N(1)-C(5)-H(5)	119.0	H(11A)-C(11)-H(11B)	108.2
N(1)-C(6)-Pd(1)	108.16(12)	N(3)-C(12)-C(11)	113.73(15)
N(1)-C(6)-H(6A)	110.1	N(3)-C(12)-C(7)	110.60(15)
Pd(1)-C(6)-H(6A)	110.1	C(11)-C(12)-C(7)	108.36(17)
N(1)-C(6)-H(6B)	110.1	N(3)-C(12)-H(12)	108.0
Pd(1)-C(6)-H(6B)	110.1	C(11)-C(12)-H(12)	108.0
H(6A)-C(6)-H(6B)	108.4	C(7)-C(12)-H(12)	108.0
N(2)-C(7)-C(8)	114.34(16)	N(3)-C(13)-N(4)	117.01(18)
N(2)-C(7)-C(12)	106.82(15)	N(3)-C(13)-C(14)	127.94(19)
C(8)-C(7)-C(12)	107.46(16)	N(4)-C(13)-C(14)	115.05(17)
N(2)-C(7)-H(7)	109.4	C(15)-C(14)-C(13)	122.0(2)
C(8)-C(7)-H(7)	109.4	C(15)-C(14)-H(14)	119.0
C(12)-C(7)-H(7)	109.4	C(13)-C(14)-H(14)	119.0
C(9)-C(8)-C(7)	110.22(18)	C(14)-C(15)-C(16)	120.4(2)
C(9)-C(8)-H(8A)	109.6	C(14)-C(15)-H(15)	119.8
C(7)-C(8)-H(8A)	109.6	C(16)-C(15)-H(15)	119.8
C(9)-C(8)-H(8B)	109.6	C(17)-C(16)-C(15)	117.94(19)
C(7)-C(8)-H(8B)	109.6	C(17)-C(16)-H(16)	121.0
H(8A)-C(8)-H(8B)	108.1	C(15)-C(16)-H(16)	121.0
C(10)-C(9)-C(8)	111.50(18)	C(16)-C(17)-N(4)	122.5(2)
C(10)-C(9)-H(9A)	109.3	C(16)-C(17)-H(17)	118.8
C(8)-C(9)-H(9A)	109.3	N(4)-C(17)-H(17)	118.8
C(10)-C(9)-H(9B)	109.3	N(4)-C(18)-H(18A)	109.5
C(8)-C(9)-H(9B)	109.3	N(4)-C(18)-H(18B)	109.5
H(9A)-C(9)-H(9B)	108.0	H(18A)-C(18)-H(18B)	109.5
C(9)-C(10)-C(11)	110.81(19)	N(4)-C(18)-H(18C)	109.5
C(9)-C(10)-H(10A)	109.5	H(18A)-C(18)-H(18C)	109.5

H(18B)-C(18)-H(18C)	109.5	C(5)-N(1)-C(6)	121.29(16)
C(20)-C(19)-C(24)	116.03(17)	C(1)-N(1)-C(6)	116.90(15)
C(20)-C(19)-Pd(1)	123.76(14)	C(1)-N(2)-C(7)	125.07(16)
C(24)-C(19)-Pd(1)	120.18(14)	C(1)-N(2)-Pd(1)	115.21(12)
C(19)-C(20)-C(21)	122.00(19)	C(7)-N(2)-Pd(1)	118.33(12)
C(19)-C(20)-H(20)	119.0	C(13)-N(3)-C(12)	115.43(17)
C(21)-C(20)-H(20)	119.0	C(13)-N(3)-Pd(1)	115.00(13)
C(22)-C(21)-C(20)	120.53(19)	C(12)-N(3)-Pd(1)	103.19(11)
C(22)-C(21)-H(21)	119.7	C(17)-N(4)-C(13)	121.98(17)
C(20)-C(21)-H(21)	119.7	C(17)-N(4)-C(18)	119.32(17)
C(21)-C(22)-C(23)	119.12(19)	C(13)-N(4)-C(18)	118.69(16)
C(21)-C(22)-H(22)	120.4	C(6)-Pd(1)-N(2)	81.87(7)
C(23)-C(22)-H(22)	120.4	C(6)-Pd(1)-C(19)	93.11(8)
C(22)-C(23)-C(24)	119.5(2)	N(2)-Pd(1)-C(19)	174.91(7)
C(22)-C(23)-H(23)	120.3	C(6)-Pd(1)-N(3)	161.33(7)
C(24)-C(23)-H(23)	120.3	N(2)-Pd(1)-N(3)	79.49(6)
C(23)-C(24)-C(19)	122.68(18)	C(19)-Pd(1)-N(3)	105.54(7)
C(23)-C(24)-H(24)	118.7		
C(19)-C(24)-H(24)	118.7	Symmetry transformations used to generate equivalent atoms:	
C(5)-N(1)-C(1)	121.80(16)		

Table 4. Anisotropic displacement parameters ($\text{\AA}^2 \times 10^3$) for **36**. The anisotropic displacement factor exponent takes the form: $-2\pi^2 [h^2 a^{*2} U^{11} + \dots + 2 h k a^* b^* U^{12}]$

	U^{11}	U^{22}	U^{33}	U^{23}	U^{13}	U^{12}
C(1)	19(1)	20(1)	19(1)	-2(1)	0(1)	2(1)
C(2)	26(1)	19(1)	26(1)	0(1)	-4(1)	1(1)
C(3)	34(1)	20(1)	35(1)	0(1)	-5(1)	-1(1)
C(4)	30(1)	22(1)	33(1)	-5(1)	-6(1)	-6(1)
C(5)	21(1)	27(1)	26(1)	-4(1)	-5(1)	-2(1)
C(6)	26(1)	20(1)	21(1)	-1(1)	-6(1)	2(1)
C(7)	21(1)	20(1)	22(1)	3(1)	-6(1)	-2(1)
C(8)	37(1)	28(1)	21(1)	5(1)	-6(1)	-12(1)
C(9)	55(2)	31(1)	27(1)	12(1)	-18(1)	-15(1)

C(10)	37(1)	32(1)	24(1)	6(1)	-14(1)	-9(1)
C(11)	26(1)	22(1)	27(1)	4(1)	-8(1)	-5(1)
C(12)	20(1)	21(1)	18(1)	3(1)	-3(1)	-3(1)
C(13)	16(1)	24(1)	20(1)	2(1)	-1(1)	-2(1)
C(14)	25(1)	22(1)	23(1)	0(1)	2(1)	-3(1)
C(15)	31(1)	23(1)	34(1)	-4(1)	3(1)	-2(1)
C(16)	29(1)	20(1)	42(1)	2(1)	5(1)	-3(1)
C(17)	24(1)	22(1)	33(1)	7(1)	3(1)	-4(1)
C(18)	27(1)	29(1)	26(1)	0(1)	8(1)	-2(1)
C(19)	12(1)	21(1)	22(1)	1(1)	-1(1)	3(1)
C(20)	23(1)	28(1)	24(1)	1(1)	0(1)	3(1)
C(21)	32(1)	40(1)	20(1)	4(1)	-1(1)	3(1)
C(22)	36(1)	30(1)	30(1)	12(1)	-1(1)	0(1)
C(23)	31(1)	21(1)	33(1)	4(1)	-2(1)	-1(1)
C(24)	23(1)	25(1)	21(1)	2(1)	0(1)	-1(1)
N(1)	21(1)	18(1)	20(1)	-2(1)	-2(1)	0(1)
N(2)	22(1)	18(1)	19(1)	1(1)	-4(1)	-3(1)
N(3)	20(1)	21(1)	19(1)	3(1)	-1(1)	-3(1)
N(4)	19(1)	21(1)	23(1)	1(1)	2(1)	-3(1)
Pd(1)	19(1)	17(1)	16(1)	0(1)	-1(1)	0(1)

Table 5. Hydrogen coordinates ($\times 10^4$) and isotropic displacement parameters ($\text{\AA}^2 \times 10^{-3}$) for **36**.

	x	y	z	U(eq)
H(2)	8195	3302	9426	29
H(3)	6842	1827	9032	35
H(4)	5114	2281	8231	34
H(5)	4994	4167	7736	30
H(6A)	5643	6458	7992	27
H(6B)	6598	5959	7372	27
H(7)	9702	5265	9502	25
H(8A)	7644	5700	10533	35
H(8B)	8154	4395	10327	35
H(9A)	9097	5065	11448	45

H(9B)	10177	4827	10839	45
H(10A)	10632	6650	11405	37
H(10B)	9207	7123	11250	37
H(11A)	11096	6666	10129	30
H(11B)	10610	7965	10368	30
H(12)	8481	7443	9969	23
H(14)	9074	9274	10094	28
H(15)	9376	11289	9982	35
H(16)	10195	12101	8872	36
H(17)	10788	10817	7944	31
H(18A)	10071	8153	7607	41
H(18B)	11334	7904	8083	41
H(18C)	11297	8999	7519	41
H(20)	7643	7383	6635	30
H(21)	7644	8960	5802	36
H(22)	7554	10928	6219	38
H(23)	7428	11301	7492	34
H(24)	7517	9717	8319	28

Table 6. Torsion angles [°] for **36**.

N(2)-C(1)-C(2)-C(3)	174.2(2)	N(2)-C(7)-C(12)-C(11)	-172.72(15)
N(1)-C(1)-C(2)-C(3)	-8.2(3)	C(8)-C(7)-C(12)-C(11)	64.2(2)
C(1)-C(2)-C(3)-C(4)	-0.1(3)	N(3)-C(13)-C(14)-C(15)	-175.7(2)
C(2)-C(3)-C(4)-C(5)	5.3(3)	N(4)-C(13)-C(14)-C(15)	4.2(3)
C(3)-C(4)-C(5)-N(1)	-1.9(3)	C(13)-C(14)-C(15)-C(16)	0.0(3)
N(2)-C(7)-C(8)-C(9)	-179.73(18)	C(14)-C(15)-C(16)-C(17)	-2.5(3)
C(12)-C(7)-C(8)-C(9)	-61.4(2)	C(15)-C(16)-C(17)-N(4)	0.6(3)
C(7)-C(8)-C(9)-C(10)	56.8(3)	C(24)-C(19)-C(20)-C(21)	5.0(3)
C(8)-C(9)-C(10)-C(11)	-54.1(3)	Pd(1)-C(19)-C(20)-C(21)	-172.99(15)
C(9)-C(10)-C(11)-C(12)	56.9(3)	C(19)-C(20)-C(21)-C(22)	-2.9(3)
C(10)-C(11)-C(12)-N(3)	174.17(18)	C(20)-C(21)-C(22)-C(23)	-0.9(3)
C(10)-C(11)-C(12)-C(7)	-62.4(2)	C(21)-C(22)-C(23)-C(24)	2.3(3)
N(2)-C(7)-C(12)-N(3)	-47.4(2)	C(22)-C(23)-C(24)-C(19)	0.0(3)
C(8)-C(7)-C(12)-N(3)	-170.56(16)	C(20)-C(19)-C(24)-C(23)	-3.6(3)

Pd(1)-C(19)-C(24)-C(23)	174.51(15)	C(16)-C(17)-N(4)-C(18)	-174.8(2)
C(4)-C(5)-N(1)-C(1)	-7.0(3)	N(3)-C(13)-N(4)-C(17)	173.79(18)
C(4)-C(5)-N(1)-C(6)	173.84(19)	C(14)-C(13)-N(4)-C(17)	-6.1(3)
N(2)-C(1)-N(1)-C(5)	-170.30(18)	N(3)-C(13)-N(4)-C(18)	-7.5(3)
C(2)-C(1)-N(1)-C(5)	11.7(3)	C(14)-C(13)-N(4)-C(18)	172.67(17)
N(2)-C(1)-N(1)-C(6)	8.9(2)	N(1)-C(6)-Pd(1)-N(2)	-9.08(12)
C(2)-C(1)-N(1)-C(6)	-169.11(16)	N(1)-C(6)-Pd(1)-C(19)	171.75(13)
Pd(1)-C(6)-N(1)-C(5)	-177.41(15)	N(1)-C(6)-Pd(1)-N(3)	-5.8(3)
Pd(1)-C(6)-N(1)-C(1)	3.43(19)	C(1)-N(2)-Pd(1)-C(6)	15.12(15)
N(1)-C(1)-N(2)-C(7)	176.66(17)	C(7)-N(2)-Pd(1)-C(6)	-177.61(15)
C(2)-C(1)-N(2)-C(7)	-5.7(3)	C(1)-N(2)-Pd(1)-N(3)	-163.83(15)
N(1)-C(1)-N(2)-Pd(1)	-17.0(2)	C(7)-N(2)-Pd(1)-N(3)	3.44(13)
C(2)-C(1)-N(2)-Pd(1)	160.59(17)	C(20)-C(19)-Pd(1)-C(6)	-52.55(17)
C(8)-C(7)-N(2)-C(1)	-54.0(3)	C(24)-C(19)-Pd(1)-C(6)	129.51(15)
C(12)-C(7)-N(2)-C(1)	-172.71(18)	C(20)-C(19)-Pd(1)-N(3)	126.65(15)
C(8)-C(7)-N(2)-Pd(1)	140.12(15)	C(24)-C(19)-Pd(1)-N(3)	-51.29(16)
C(12)-C(7)-N(2)-Pd(1)	21.39(19)	C(13)-N(3)-Pd(1)-C(6)	-157.8(2)
N(4)-C(13)-N(3)-C(12)	164.55(15)	C(12)-N(3)-Pd(1)-C(6)	-31.3(3)
C(14)-C(13)-N(3)-C(12)	-15.6(3)	C(13)-N(3)-Pd(1)-N(2)	-154.58(15)
N(4)-C(13)-N(3)-Pd(1)	-75.43(19)	C(12)-N(3)-Pd(1)-N(2)	-28.00(12)
C(14)-C(13)-N(3)-Pd(1)	104.4(2)	C(13)-N(3)-Pd(1)-C(19)	24.66(16)
C(11)-C(12)-N(3)-C(13)	-63.2(2)	C(12)-N(3)-Pd(1)-C(19)	151.23(12)
C(7)-C(12)-N(3)-C(13)	174.56(16)		
C(11)-C(12)-N(3)-Pd(1)	170.46(14)		
C(7)-C(12)-N(3)-Pd(1)	48.26(16)		
C(16)-C(17)-N(4)-C(13)	3.9(3)		

Symmetry transformations used to generate equivalent atoms:

Single crystal X-ray structure data for [Pd(MeCN)₂Cl(η^1 -CH₂N^{C₆H₁₀N^{Me})})(H⁺)₂](BF₄)₂ (37)

Table 1. Crystal data and structure refinement for **37**.

Identification code	37	
Empirical formula	C ₂₄ H ₃₄ B ₂ Cl F ₈ N ₇ Pd	
Formula weight	736.05	
Temperature	110(2) K	
Wavelength	0.71073 Å	
Crystal system	Monoclinic	
Space group	P2(1)	
Unit cell dimensions	a = 10.2938(8) Å	$\alpha = 90^\circ$.
	b = 8.3076(6) Å	$\beta = 90.084(2)^\circ$.
	c = 18.1884(13) Å	$\gamma = 90^\circ$.
Volume	1555.4(2) Å ³	
Z	2	
Density (calculated)	1.572 Mg/m ³	
Absorption coefficient	0.758 mm ⁻¹	
F(000)	744	
Crystal size	0.15 x 0.10 x 0.05 mm ³	
Theta range for data collection	1.98 to 28.29°.	
Index ranges	-13<=h<=13, -11<=k<=11, -24<=l<=24	
Reflections collected	21379	
Independent reflections	7674 [R(int) = 0.0254]	
Completeness to theta = 28.29°	99.7 %	
Absorption correction	Semi-empirical from equivalents	
Max. and min. transmission	0.963 and 0.891	
Refinement method	Full-matrix least-squares on F ²	
Data / restraints / parameters	7674 / 1 / 400	
Goodness-of-fit on F ²	1.083	
Final R indices [I>2sigma(I)]	R1 = 0.0301, wR2 = 0.0710	
R indices (all data)	R1 = 0.0319, wR2 = 0.0717	
Absolute structure parameter	-0.002(17)	
Largest diff. peak and hole	0.999 and -0.828 e.Å ⁻³	

Table 2. Atomic coordinates ($\times 10^4$) and equivalent isotropic displacement parameters ($\text{\AA}^2 \times 10^3$) for **37**. $U(\text{eq})$ is defined as one third of the trace of the orthogonalized U^{ij} tensor.

	x	y	z	$U(\text{eq})$
C(1)	6897(2)	3908(3)	8952(1)	15(1)
C(2)	6282(3)	5394(3)	9110(1)	19(1)
C(3)	6991(2)	6679(4)	9349(1)	21(1)
C(4)	8345(3)	6549(3)	9440(1)	22(1)
C(5)	8912(3)	5096(3)	9313(1)	20(1)
C(6)	8886(2)	2275(3)	8937(1)	18(1)
C(7)	4884(2)	2437(3)	8575(1)	14(1)
C(8)	4473(3)	754(3)	8821(2)	19(1)
C(9)	3017(3)	496(3)	8693(2)	25(1)
C(10)	2656(3)	751(3)	7892(2)	24(1)
C(11)	3072(3)	2421(3)	7635(2)	21(1)
C(12)	4530(2)	2702(3)	7759(1)	17(1)
C(13)	5835(2)	4851(3)	7117(1)	18(1)
C(14)	6806(3)	3821(3)	6831(1)	21(1)
C(15)	7783(3)	4448(4)	6404(2)	25(1)
C(16)	7830(3)	6111(4)	6250(2)	26(1)
C(17)	6893(3)	7065(3)	6534(1)	24(1)
C(18)	4906(3)	7558(3)	7232(2)	27(1)
C(19)	10300(3)	5269(3)	7618(1)	21(1)
C(20)	10680(3)	6920(5)	7465(2)	28(1)
C(21)	10246(3)	854(4)	6248(2)	26(1)
C(22)	10994(4)	495(5)	5591(2)	42(1)
N(2)	8206(2)	3793(3)	9079(1)	16(1)
N(1)	6288(2)	2620(3)	8678(1)	16(1)
N(3)	4846(2)	4355(3)	7540(1)	18(1)
N(4)	5906(2)	6457(2)	6958(1)	20(1)
N(5)	9978(2)	3976(3)	7739(1)	21(1)
N(6)	9695(2)	1141(3)	6769(1)	26(1)
Pd(1)	9145(1)	1783(1)	7864(1)	17(1)
Cl(1)	7913(1)	-509(1)	7999(1)	24(1)
B(1)	2560(3)	6055(4)	9240(2)	24(1)

F(1)	1472(1)	7037(2)	9266(1)	25(1)
F(2)	3086(2)	6080(2)	8525(1)	26(1)
F(3)	2194(3)	4495(3)	9403(2)	64(1)
F(4)	3484(2)	6628(5)	9712(1)	65(1)
B(2)	1968(4)	5270(5)	5581(2)	38(1)
F(5)	1654(3)	6758(5)	5357(3)	133(2)
F(6)	3043(3)	5340(4)	6026(1)	69(1)
F(7)	2217(3)	4352(4)	4967(2)	78(1)
F(8)	918(3)	4607(5)	5944(2)	82(1)
C(23)	5188(4)	2842(5)	5089(2)	40(1)
C(24)	4933(3)	1663(6)	5670(2)	35(1)
N(7)	4730(4)	771(4)	6124(2)	52(1)

Table 3. Bond lengths [\AA] and angles [$^\circ$] for **37**.

C(1)-N(1)	1.337(3)	C(8)-H(8A)	0.9900
C(1)-N(2)	1.370(3)	C(8)-H(8B)	0.9900
C(1)-C(2)	1.417(4)	C(9)-C(10)	1.517(4)
C(2)-C(3)	1.364(4)	C(9)-H(9A)	0.9900
C(2)-H(2)	0.9500	C(9)-H(9B)	0.9900
C(3)-C(4)	1.408(3)	C(10)-C(11)	1.525(4)
C(3)-H(3)	0.9500	C(10)-H(10A)	0.9900
C(4)-C(5)	1.361(4)	C(10)-H(10B)	0.9900
C(4)-H(4)	0.9500	C(11)-C(12)	1.536(3)
C(5)-N(2)	1.371(3)	C(11)-H(11A)	0.9900
C(5)-H(5)	0.9500	C(11)-H(11B)	0.9900
C(6)-N(2)	1.465(3)	C(12)-N(3)	1.467(3)
C(6)-Pd(1)	2.013(3)	C(12)-H(12)	1.0000
C(6)-H(6A)	0.9900	C(13)-N(3)	1.341(3)
C(6)-H(6B)	0.9900	C(13)-N(4)	1.368(3)
C(7)-N(1)	1.466(3)	C(13)-C(14)	1.416(4)
C(7)-C(8)	1.528(4)	C(14)-C(15)	1.373(4)
C(7)-C(12)	1.543(3)	C(14)-H(14)	0.9500
C(7)-H(7)	1.0000	C(15)-C(16)	1.410(4)
C(8)-C(9)	1.532(4)	C(15)-H(15)	0.9500

C(16)-C(17)	1.352(4)		
C(16)-H(16)	0.9500	N(1)-C(1)-N(2)	117.9(2)
C(17)-N(4)	1.372(3)	N(1)-C(1)-C(2)	124.3(2)
C(17)-H(17)	0.9500	N(2)-C(1)-C(2)	117.8(2)
C(18)-N(4)	1.465(3)	C(3)-C(2)-C(1)	120.5(2)
C(18)-H(18A)	0.9800	C(3)-C(2)-H(2)	119.8
C(18)-H(18B)	0.9800	C(1)-C(2)-H(2)	119.8
C(18)-H(18C)	0.9800	C(2)-C(3)-C(4)	120.5(3)
C(19)-N(5)	1.146(4)	C(2)-C(3)-H(3)	119.8
C(19)-C(20)	1.453(5)	C(4)-C(3)-H(3)	119.8
C(20)-H(20A)	0.9800	C(5)-C(4)-C(3)	118.2(3)
C(20)-H(20B)	0.9800	C(5)-C(4)-H(4)	120.9
C(20)-H(20C)	0.9800	C(3)-C(4)-H(4)	120.9
C(21)-N(6)	1.132(4)	C(4)-C(5)-N(2)	121.7(2)
C(21)-C(22)	1.453(4)	C(4)-C(5)-H(5)	119.1
C(22)-H(22A)	0.9800	N(2)-C(5)-H(5)	119.1
C(22)-H(22B)	0.9800	N(2)-C(6)-Pd(1)	114.11(16)
C(22)-H(22C)	0.9800	N(2)-C(6)-H(6A)	108.7
N(1)-H(1)	0.90(4)	Pd(1)-C(6)-H(6A)	108.7
N(3)-H(3A)	0.79(4)	N(2)-C(6)-H(6B)	108.7
N(5)-Pd(1)	2.026(2)	Pd(1)-C(6)-H(6B)	108.7
N(6)-Pd(1)	2.139(2)	H(6A)-C(6)-H(6B)	107.6
Pd(1)-Cl(1)	2.3010(7)	N(1)-C(7)-C(8)	109.3(2)
B(1)-F(4)	1.366(4)	N(1)-C(7)-C(12)	109.9(2)
B(1)-F(3)	1.382(4)	C(8)-C(7)-C(12)	110.3(2)
B(1)-F(1)	1.387(3)	N(1)-C(7)-H(7)	109.1
B(1)-F(2)	1.410(3)	C(8)-C(7)-H(7)	109.1
B(2)-F(5)	1.341(6)	C(12)-C(7)-H(7)	109.1
B(2)-F(6)	1.372(5)	C(7)-C(8)-C(9)	110.7(2)
B(2)-F(7)	1.377(5)	C(7)-C(8)-H(8A)	109.5
B(2)-F(8)	1.381(5)	C(9)-C(8)-H(8A)	109.5
C(23)-C(24)	1.464(5)	C(7)-C(8)-H(8B)	109.5
C(23)-H(23A)	0.9800	C(9)-C(8)-H(8B)	109.5
C(23)-H(23B)	0.9800	H(8A)-C(8)-H(8B)	108.1
C(23)-H(23C)	0.9800	C(10)-C(9)-C(8)	111.4(2)
C(24)-N(7)	1.129(5)	C(10)-C(9)-H(9A)	109.4

C(8)-C(9)-H(9A)	109.4	N(4)-C(17)-H(17)	119.1
C(10)-C(9)-H(9B)	109.4	N(4)-C(18)-H(18A)	109.5
C(8)-C(9)-H(9B)	109.4	N(4)-C(18)-H(18B)	109.5
H(9A)-C(9)-H(9B)	108.0	H(18A)-C(18)-H(18B)	109.5
C(9)-C(10)-C(11)	110.7(2)	N(4)-C(18)-H(18C)	109.5
C(9)-C(10)-H(10A)	109.5	H(18A)-C(18)-H(18C)	109.5
C(11)-C(10)-H(10A)	109.5	H(18B)-C(18)-H(18C)	109.5
C(9)-C(10)-H(10B)	109.5	N(5)-C(19)-C(20)	178.8(3)
C(11)-C(10)-H(10B)	109.5	C(19)-C(20)-H(20A)	109.5
H(10A)-C(10)-H(10B)	108.1	C(19)-C(20)-H(20B)	109.5
C(10)-C(11)-C(12)	111.6(2)	H(20A)-C(20)-H(20B)	109.5
C(10)-C(11)-H(11A)	109.3	C(19)-C(20)-H(20C)	109.5
C(12)-C(11)-H(11A)	109.3	H(20A)-C(20)-H(20C)	109.5
C(10)-C(11)-H(11B)	109.3	H(20B)-C(20)-H(20C)	109.5
C(12)-C(11)-H(11B)	109.3	N(6)-C(21)-C(22)	178.1(3)
H(11A)-C(11)-H(11B)	108.0	C(21)-C(22)-H(22A)	109.5
N(3)-C(12)-C(11)	108.6(2)	C(21)-C(22)-H(22B)	109.5
N(3)-C(12)-C(7)	110.0(2)	H(22A)-C(22)-H(22B)	109.5
C(11)-C(12)-C(7)	110.4(2)	C(21)-C(22)-H(22C)	109.5
N(3)-C(12)-H(12)	109.2	H(22A)-C(22)-H(22C)	109.5
C(11)-C(12)-H(12)	109.2	H(22B)-C(22)-H(22C)	109.5
C(7)-C(12)-H(12)	109.2	C(1)-N(2)-C(5)	121.2(2)
N(3)-C(13)-N(4)	117.5(2)	C(1)-N(2)-C(6)	120.1(2)
N(3)-C(13)-C(14)	124.2(3)	C(5)-N(2)-C(6)	118.7(2)
N(4)-C(13)-C(14)	118.3(2)	C(1)-N(1)-C(7)	126.4(2)
C(15)-C(14)-C(13)	119.7(3)	C(1)-N(1)-H(1)	123(2)
C(15)-C(14)-H(14)	120.1	C(7)-N(1)-H(1)	111(2)
C(13)-C(14)-H(14)	120.1	C(13)-N(3)-C(12)	127.8(2)
C(14)-C(15)-C(16)	120.6(3)	C(13)-N(3)-H(3A)	113(2)
C(14)-C(15)-H(15)	119.7	C(12)-N(3)-H(3A)	119(2)
C(16)-C(15)-H(15)	119.7	C(13)-N(4)-C(17)	121.2(2)
C(17)-C(16)-C(15)	118.3(3)	C(13)-N(4)-C(18)	119.9(2)
C(17)-C(16)-H(16)	120.8	C(17)-N(4)-C(18)	118.8(2)
C(15)-C(16)-H(16)	120.8	C(19)-N(5)-Pd(1)	170.8(2)
C(16)-C(17)-N(4)	121.8(3)	C(21)-N(6)-Pd(1)	165.2(3)
C(16)-C(17)-H(17)	119.1	C(6)-Pd(1)-N(5)	89.00(10)

C(6)-Pd(1)-N(6)	171.64(10)	F(5)-B(2)-F(6)	109.5(4)
N(5)-Pd(1)-N(6)	90.44(9)	F(5)-B(2)-F(7)	108.0(4)
C(6)-Pd(1)-Cl(1)	89.49(8)	F(6)-B(2)-F(7)	110.6(3)
N(5)-Pd(1)-Cl(1)	171.61(7)	F(5)-B(2)-F(8)	108.9(4)
N(6)-Pd(1)-Cl(1)	92.24(7)	F(6)-B(2)-F(8)	111.5(3)
F(4)-B(1)-F(3)	112.5(3)	F(7)-B(2)-F(8)	108.3(3)
F(4)-B(1)-F(1)	109.6(3)	N(7)-C(24)-C(23)	179.0(4)
F(3)-B(1)-F(1)	108.9(3)		
F(4)-B(1)-F(2)	107.9(2)	Symmetry transformations used to generate	
F(3)-B(1)-F(2)	108.5(3)	equivalent atoms:	
F(1)-B(1)-F(2)	109.5(2)		

Table 4. Anisotropic displacement parameters ($\text{\AA}^2 \times 10^3$) for **37**. The anisotropic displacement factor exponent takes the form: $-2\pi^2 [h^2 a^{*2} U^{11} + \dots + 2 h k a^* b^* U^{12}]$

	U^{11}	U^{22}	U^{33}	U^{23}	U^{13}	U^{12}
C(1)	14(1)	21(1)	11(1)	1(1)	2(1)	0(1)
C(2)	17(1)	19(1)	21(1)	-2(1)	1(1)	1(1)
C(3)	25(1)	17(1)	20(1)	-1(1)	3(1)	2(1)
C(4)	25(1)	18(2)	22(1)	-3(1)	0(1)	-8(1)
C(5)	16(1)	26(1)	19(1)	-1(1)	1(1)	-5(1)
C(6)	14(1)	22(1)	17(1)	0(1)	-1(1)	2(1)
C(7)	10(1)	16(1)	16(1)	-2(1)	1(1)	0(1)
C(8)	20(1)	16(1)	22(1)	2(1)	2(1)	-4(1)
C(9)	19(1)	20(1)	35(2)	0(1)	5(1)	-5(1)
C(10)	13(1)	19(1)	41(2)	-7(1)	0(1)	-4(1)
C(11)	12(1)	23(1)	29(1)	-4(1)	-5(1)	4(1)
C(12)	16(1)	15(1)	18(1)	0(1)	0(1)	1(1)
C(13)	17(1)	21(1)	16(1)	-2(1)	-3(1)	2(1)
C(14)	20(1)	22(1)	20(1)	2(1)	-1(1)	3(1)
C(15)	22(1)	29(1)	24(1)	-1(1)	3(1)	3(1)
C(16)	22(1)	36(1)	19(1)	2(1)	3(1)	-5(1)
C(17)	28(1)	23(2)	22(1)	2(1)	-1(1)	-3(1)
C(18)	29(2)	15(1)	37(2)	1(1)	11(1)	4(1)

C(19)	16(1)	28(1)	20(1)	0(1)	1(1)	1(1)
C(20)	27(1)	25(2)	33(1)	6(2)	-2(1)	-4(2)
C(21)	32(2)	27(2)	21(1)	-1(1)	2(1)	4(1)
C(22)	47(2)	52(2)	27(2)	-5(2)	17(1)	4(2)
N(2)	14(1)	18(1)	14(1)	-1(1)	1(1)	-1(1)
N(1)	13(1)	16(1)	19(1)	-2(1)	2(1)	2(1)
N(3)	18(1)	16(1)	21(1)	0(1)	4(1)	5(1)
N(4)	22(1)	19(2)	18(1)	0(1)	2(1)	1(1)
N(5)	15(1)	26(1)	22(1)	1(1)	3(1)	2(1)
N(6)	28(1)	26(1)	24(1)	1(1)	3(1)	3(1)
Pd(1)	15(1)	19(1)	18(1)	0(1)	2(1)	3(1)
Cl(1)	25(1)	19(1)	29(1)	-3(1)	5(1)	-1(1)
B(1)	21(2)	28(2)	23(2)	1(1)	6(1)	8(1)
F(1)	18(1)	20(1)	36(1)	0(1)	9(1)	1(1)
F(2)	26(1)	30(1)	22(1)	-1(1)	7(1)	4(1)
F(3)	73(2)	32(1)	87(2)	31(1)	47(1)	22(1)
F(4)	29(1)	127(2)	40(1)	-37(2)	-13(1)	25(2)
B(2)	35(2)	35(2)	42(2)	1(2)	6(2)	-1(2)
F(5)	103(2)	39(1)	258(5)	30(3)	-65(3)	-4(2)
F(6)	59(2)	91(2)	55(2)	4(1)	-13(1)	-18(2)
F(7)	57(2)	113(3)	64(2)	-33(2)	4(1)	12(2)
F(8)	60(2)	122(3)	64(2)	-9(2)	23(1)	-31(2)
C(23)	44(2)	44(2)	30(2)	10(2)	-2(1)	1(2)
C(24)	52(2)	30(2)	24(1)	-6(2)	-1(1)	-1(2)
N(7)	97(3)	32(2)	28(2)	-2(1)	6(2)	-8(2)

Table 5. Hydrogen coordinates ($\times 10^4$) and isotropic displacement parameters ($\text{\AA}^2 \times 10^{-3}$) for **37**.

	x	y	z	U(eq)
H(2)	5369	5495	9050	23
H(3)	6568	7669	9454	25
H(4)	8850	7452	9586	26
H(5)	9821	4981	9389	24
H(6A)	8387	1386	9164	21

H(6B)	9747	2314	9181	21
H(7)	4422	3256	8881	17
H(8A)	4674	615	9350	23
H(8B)	4971	-62	8542	23
H(9A)	2779	-612	8841	29
H(9B)	2519	1256	9003	29
H(10A)	1705	632	7831	29
H(10B)	3086	-77	7586	29
H(11A)	2571	3247	7907	26
H(11B)	2871	2540	7105	26
H(12)	5036	1932	7449	20
H(14)	6783	2700	6933	25
H(15)	8432	3756	6211	30
H(16)	8503	6548	5955	31
H(17)	6918	8189	6437	29
H(18A)	4874	7499	7770	41
H(18B)	4060	7250	7028	41
H(18C)	5115	8660	7081	41
H(20A)	9914	7617	7486	43
H(20B)	11066	6981	6973	43
H(20C)	11318	7275	7831	43
H(22A)	11709	1267	5546	63
H(22B)	10430	574	5158	63
H(22C)	11347	-598	5626	63
H(1)	6700(30)	1690(60)	8573(15)	20(7)
H(3A)	4460(30)	5070(40)	7718(17)	18(8)
H(23A)	4364	3300	4918	59
H(23B)	5628	2312	4678	59
H(23C)	5742	3703	5283	59

Table 6. Torsion angles [°] for **37**.

N(1)-C(1)-C(2)-C(3)	-176.1(2)	C(2)-C(3)-C(4)-C(5)	-2.6(4)
N(2)-C(1)-C(2)-C(3)	2.9(4)	C(3)-C(4)-C(5)-N(2)	2.1(4)
C(1)-C(2)-C(3)-C(4)	0.1(4)	N(1)-C(7)-C(8)-C(9)	-177.8(2)

C(12)-C(7)-C(8)-C(9)	-56.9(3)	Pd(1)-C(6)-N(2)-C(5)	-104.1(2)
C(7)-C(8)-C(9)-C(10)	57.3(3)	N(2)-C(1)-N(1)-C(7)	173.3(2)
C(8)-C(9)-C(10)-C(11)	-56.3(3)	C(2)-C(1)-N(1)-C(7)	-7.6(4)
C(9)-C(10)-C(11)-C(12)	55.9(3)	C(8)-C(7)-N(1)-C(1)	-137.2(2)
C(10)-C(11)-C(12)-N(3)	-176.8(2)	C(12)-C(7)-N(1)-C(1)	101.6(3)
C(10)-C(11)-C(12)-C(7)	-56.1(3)	N(4)-C(13)-N(3)-C(12)	177.2(2)
N(1)-C(7)-C(12)-N(3)	-63.3(3)	C(14)-C(13)-N(3)-C(12)	-3.1(4)
C(8)-C(7)-C(12)-N(3)	176.2(2)	C(11)-C(12)-N(3)-C(13)	-132.9(3)
N(1)-C(7)-C(12)-C(11)	176.8(2)	C(7)-C(12)-N(3)-C(13)	106.1(3)
C(8)-C(7)-C(12)-C(11)	56.3(3)	N(3)-C(13)-N(4)-C(17)	179.5(2)
N(3)-C(13)-C(14)-C(15)	-179.9(3)	C(14)-C(13)-N(4)-C(17)	-0.2(4)
N(4)-C(13)-C(14)-C(15)	-0.1(4)	N(3)-C(13)-N(4)-C(18)	-1.5(4)
C(13)-C(14)-C(15)-C(16)	0.2(4)	C(14)-C(13)-N(4)-C(18)	178.8(2)
C(14)-C(15)-C(16)-C(17)	0.1(4)	C(16)-C(17)-N(4)-C(13)	0.5(4)
C(15)-C(16)-C(17)-N(4)	-0.5(4)	C(16)-C(17)-N(4)-C(18)	-178.5(3)
N(1)-C(1)-N(2)-C(5)	175.7(2)	N(2)-C(6)-Pd(1)-N(5)	53.37(18)
C(2)-C(1)-N(2)-C(5)	-3.4(3)	N(2)-C(6)-Pd(1)-Cl(1)	-118.37(17)
N(1)-C(1)-N(2)-C(6)	-2.0(3)	C(21)-N(6)-Pd(1)-N(5)	60.7(10)
C(2)-C(1)-N(2)-C(6)	178.9(2)	C(21)-N(6)-Pd(1)-Cl(1)	-127.3(10)
C(4)-C(5)-N(2)-C(1)	0.9(4)		
C(4)-C(5)-N(2)-C(6)	178.7(2)		
Pd(1)-C(6)-N(2)-C(1)	73.7(2)		

Symmetry transformations used to generate equivalent atoms

Appendix 2

Compounds

